JOÃO PEDRO CARVALHO NUNES

VULNERABILITY OF MEDITERRANEAN WATERSHEDS TO CLIMATE CHANGE: THE DESERTIFICATION CONTEXT

Dissertação apresentada para obtenção do Grau de Doutor em Engenharia do Ambiente pela Universidade Nova de Lisboa, Faculdade de Ciências e Tecnologia.

LISBOA

2007

Ciência.Inovação 2010
Programa Operacional Ciência e Inovação 2010
MINISTÉRIO DA CIÊNCIA, TECNOLOGIA E ENSINO SUPERIOR
UNIÃO EUROPEIA
Fundo Social Europeu

Acknowledgments

Many people supported the work presented in this thesis – without their help, it's doubtful that my objectives would have been achieved.

First of all, I thank my supervisor, Júlia Seixas, for challenging me to do a PhD in her research group, encouraging me to explore and develop my ideas, thoroughly criticizing my work and above all keeping me focused on the main goals.

Second, I thank the people who contributed directly with their work to this thesis: Nuno Pacheco taught me the secrets of the SWAT model, António Ferreira brought his team to help me with my first (and only) fieldwork, and Gonçalo Vieira spent long hours with me programming the MEFIDIS model when it was in its infancy. Also, many ideas and developments in this work result from parallel research work: the post forest-fire erosion studies with Jan Jacob Keizer, the storm movement work with João Pedroso de Lima, and the erosion model intercomparison exercise coordinated by Mark Nearing.

Third, I thank the people who discussed these ideas and supported my work on this thesis. The original methodology for this thesis came from discussions with Peter Loucks and his research group; many technical details were discussed and perfected in international meetings with the people from the Soil Erosion Network and COST action 623, especially Victor Jetten. Also, issues from conceptual problems to minor details were thoroughly discussed with Carmona Rodrigues, Nuno Carvalhais, Nuno Grosso, Ana Nobre, Pedro Lourenço and other researchers at the New University of Lisbon.

Finally, I thank the people who helped me get started and gave me the mental tools to do this work: Pedro Gonçalves, who first introduced me to soil erosion modeling and all the possibilities of the field, and João Gomes Ferreira, who first taught me how the scientific world works in both the technical and the human dimensions.

This work was supported by the Portuguese Foundation for Science and Technology and the European Union under Operational Program "Science and Innovation" (POCI 2010), Ph.D. grant ref. SFRH/BD/5059/2001, co-sponsored by the European Social Fund. Further support for data acquisition and processing was given by the Portuguese Foundation for Science and Technology (FCT) under project GeneticLand, contract ref. POCTI/MGS/37970/2001.

Resumo

A desertificação é um problema crítico para as zonas secas do Mediterrâneo. Espera-se que as alterações climáticas agravem a sua extensão e severidade através do reforço dos processos biofísicos com impacto na desertificação: hidrologia, produtividade vegetal e erosão do solo. O principal objectivo desta tese é avaliar a vulnerabilidade de bacias hidrográficas Mediterrânicas às alterações climáticas, estimando os seus impactes nas forças motrizes da desertificação e a resiliência das bacias aos mesmos.

Para atingir este objectivo, desenvolve-se uma metodologia de modelação capaz de analizar os processos ligando o clima e as principais forças motrizes. A metodologia acopla modelos adaptados a diferentes escalas espaciais e temporais. É ainda desenvolvido um novo modelo à escala da tempestade – MEFIDIS – com o foco nos processos mais importantes em bacias Mediterrânicas. Os resultados dos modelos são comparados com limiares de desertificação para estimativas de resiliência. A metodologia é aplicada a duas áreas de estudo com climas contrastantes: o Guadiana, de clima semi-árido, e o Tejo, de clima húmido.

Resumidamente, as principais conclusões deste trabalho são:

- os processos hidrológicos mostram elevada sensibilidade às alterações climáticas, conduzindo à redução do escoamento de água e um aumento da sua variabilidade temporal;

- os processos associados à vegetação aparentam menor sensibilidade, com impactos negativos para espécies agrícolas e florestais, e positivos para espécies Mediterrânicas;

- os impactos nos processos erosivos aparentam depender do balanço entre alterações ao escoamento de água e coberto vegetal, determinado pela relação entre alterações à precipitação e temperatura;

- os limiares de desertificação são ultrapassados sequencialmente com a magnitude de alterações climáticas, começando pela capacidade de sustentação do consumo de água e seguido pela capacidade de suporte de vegetação;

- os limiares mais importantes aparentam ser um aumento de temperatura de +3.5 a +4.5 ºC, e um decréscimo da precipitação de -10 a -20 %;

- reduções da precipitação abaixo do limiar podem levar a pressões severas sobre os recursos hídricos mesmo com moderação nos consumos de água, com secas hidrológicas ocorrendo a cada 4 anos;

- subidas de temperatura acima do limiar podem levar à diminuição da produtividade agrícola e ao aumento da erosão do solo em campos cerealíferos;

- alterações à temperatura e precipitação para além dos limiares podem levar à transição dos sistemas para um estado de maior aridez, com pressões severas sobre os recusos hídricos e alterações significativas à capacidade de suporte das prácticas agrícolas e vegetação natural actualmente existentes.

Abstract

Desertification is a critical issue for Mediterranean drylands. Climate change is expected to aggravate its extension and severity by reinforcing the biophysical driving forces behind desertification processes: hydrology, vegetation cover and soil erosion. The main objective of this thesis is to assess the vulnerability of Mediterranean watersheds to climate change, by estimating impacts on desertification drivers and the watersheds' resilience to them.

To achieve this objective, a modeling framework capable of analyzing the processes linking climate and the main drivers is developed. The framework couples different models adapted to different spatial and temporal scales. A new model for the event scale is developed, the MEFIDIS model, with a focus on the particular processes governing Mediterranean watersheds. Model results are compared with desertification thresholds to estimate resilience. This methodology is applied to two contrasting study areas: the Guadiana and the Tejo, which currently present a semi-arid and humid climate.

The main conclusions taken from this work can be summarized as follows:

- hydrological processes show a high sensitivity to climate change, leading to a significant decrease in runoff and an increase in temporal variability;
- vegetation processes appear to be less sensitive, with negative impacts for agricultural species and forests, and positive impacts for Mediterranean species;
- changes to soil erosion processes appear to depend on the balance between changes to surface runoff and vegetation cover, itself governed by relationship between changes to temperature and rainfall;
- as the magnitude of changes to climate increases, desertification thresholds are surpassed in a sequential way, starting with the watersheds' ability to sustain current water demands and followed by the vegetation support capacity;
- the most important thresholds appear to be a temperature increase of +3.5 to +4.5 ºC and a rainfall decrease of -10 to -20 %;
- rainfall changes beyond this threshold could lead to severe water stress occurring even if current water uses are moderated, with droughts occurring in 1 out of 4 years;

- temperature changes beyond this threshold could lead to a decrease in agricultural yield accompanied by an increase in soil erosion for croplands;

- combined changes of temperature and rainfall beyond the thresholds could shift both systems towards a more arid state, leading to severe water stresses and significant changes to the support capacity for current agriculture and natural vegetation in both study areas.

Symbology and Notations

A – surface flow cross-sectional area

A_c – catchment area

A_s – surface area of a model grid cell

C_{sed} – sediment concentration

D – soil water deficit

d_{50} – soil median particle diameter

D_{max} – depression storage capacity

D_r – sediment delivery rate from rills

D_s – sediment delivery rate from interrill zones

dx – flow length

E – effective kinetic energy of rainfall

e_c – critical kinetic energy for soil detachment by a single raindrop

ET – accumulated evapotranspiration

F – infiltration rate

F_c – cumulative infiltration

I – interception storage rate

I_d – accumulated deep aquifer infiltration

I_{max} – interception storage capacity

K_p – soil detachability by a single raindrop

K_{sat} – saturated hydraulic conductivity of the soil

m – transmissivity decay with soil profile

M_s – suspended sediment

n – Manning's roughness coefficient

P – accumulated rainfall

P_0 – perimeter of the surface flow

P_{cv} – model cell paved fraction

Q – surface flow rate

Q_b – baseflow before storm

Q_i – inflow rate to model cell

Q_o – outflow rate from model cell

Q_{si} – sediment inflow rate to cell

Q_{so} – sediment outflow rate from cell

Q_{sub} – accumulated subsurface runoff through shallow aquifers

Q_{sup} – accumulated surface runoff

R – rainfall rate

R_c – threshold rainfall rate for soil detachment initiation

R_{cv} – fractional cover of vegetation and paved areas

R_h – dampening ratio due to surface water

S_0 – surface slope gradient

S_{clay} – clay mass fraction of the soil

S_{depth} – soil depth

S_i – soil moisture saturation ratio at the start of the event

SW – water content in the soil profile

t – temporal dimension

T_c – sediment transport capacity of the surface flow

u_{sed} – particle sedimentation velocity

V_{cv} – cell vegetation cover fraction

V_s – water storage volume within cell

w – flow width

$W_{channel}$ – channel width

x – spatial dimension

Y – detachment/deposition efficiency factor

γ – topographic wetness index value

θ – soil porosity fraction

ρ_p – soil particle density

σ_{oc} – soil shear strenght

ψ – soil matric potential

ω – stream power

ω_c –critical stream power for sediment transport

Table of Contents

Index of Figures

Index of Tables

1. Introduction

There is a growing consensus in Earth systems sciences that global temperatures are increasing and will continue during the next century, leading to changes in global climate patterns (IPCC, 2007). Different regions of the globe are expected to respond differently to global warming; the Mediterranean region has been identified as one of the Earth's primary "hot-spots" for climate change, due to the magnitude of expected changes to temperature and rainfall patterns (Giorgi, 2006), associated with an increase in extreme episodes such as heat waves and high-intensity storms (Räisänen et al., 2004).

The expected impacts of climate change on Mediterranean regions point to a trend of increased vulnerability of both natural and human systems due to the reduction of available water resources and increased land degradation (Schroter et al., 2005). This trend is expected to accelerate the process of desertification already occurring in these regions (Puigdefábregas, 1998). There is a need to quantify the impacts of climate change on the most important physical drivers of desertification – water resources, soil erosion and vegetation productivity – to estimate impacts and support the development of adequate adaptation measures (Huntingford et al., 2006).

These issues have been partly addressed in recent years, thanks to a significant research effort focusing on the regional impacts of climate change on hydrology (e.g. Xu and Singh, 2004) and vegetation productivity (e.g. Field et al., 2007). Research on the impacts on soil erosion has been more limited, although some work has been performed for North American regions (e.g. Nearing et al., 2004). However, these efforts have been conditioned by the large spatial and temporal scales at which climate change predictions are typically made, limiting impact studies for meso-scale and smaller watersheds, within-catchment dynamics, and temporal anomalies such as extreme floods and droughts (Bronstert, 2004). These problems have also significantly limited research on the impacts of climate change on soil erosion, due to the high variability in time and space of erosive processes (Michael et al., 2005).

These limitations are especially important for Mediterranean dryland catchments, which are characterized by a high spatial and temporal variability of hydrological and erosion processes when compared with humid catchments (e.g. Cammeraat, 2002). In particular, soil erosion is usually dominated by highly localized processes such as ephemeral gully erosion and occurs during a small number of high-intensity rainfall events (e.g. Boix-Fayos et al., 2006). Assessing the impacts of climate change on desertification biophysical drivers in these

regions therefore requires an analysis at multiple spatial and temporal scales, ranging from slope to catchment and taking localized storms into account, as issue which has been neglected in the recent literature (Imeson and Lavee, 1998; Boardman, 2006).

This thesis aims to take a further step towards analyzing and quantifying the impacts of climate change on the physical drivers for desertification processes in Mediterranean watersheds at multiple spatial and temporal scales, focusing on meso-scale catchments (c. 100 to 1000 Km^2). The main objective of this thesis is to **assess the vulnerability of hydrological, soil erosion and vegetation productivity patterns in Mediterranean watersheds to climate change, resulting from enhanced biophysical desertification processes**.

To achieve this goal, a vulnerability analysis framework is followed which focuses on: (i) the sensitivity of hydrological, vegetation and erosive patterns to changes in climate, (ii) the magnitude of the expected impacts, and (iii) the main biophysical components requiring adaptation, following the concepts exposed by Adger (2006). The analysis estimates seasonal, annual and long-term trends at the watershed scale, and uses these trends as boundary conditions to evaluate changes in within-catchment processes during extreme rainfall events in higher spatial and temporal detail. This allows an evaluation of the processes linking climate, hydrology, soil erosion and vegetation productivity operating at different spatial and temporal scales, taking into account cross-scale interactions.

This thesis is supported by a multi-scale modeling framework, using a seasonal-scale model to analyze long-term watershed trends and integrating these results into spatially detailed simulations at the extreme events scale. Models are currently the most appropriate tools to support climate change studies since they codify the existing knowledge on catchment processes and their response to meteorological forcing, allowing the quantification of the impacts of changed climate patterns in a feasible way (Bronstert, 2004).

The thesis is organized in 7 chapters, as follows:

Chapter 2 provides the conceptual background for this thesis. It begins with an overview of desertification processes in the northern Mediterranean and their link with physical drivers determined by the local climate. It follows with an overview on climate change science and scenarios for the northern Mediterranean, and a discussion on the relations between climate, hydrological and soil erosion processes, and the importance of vegetation biomass productivity. Current methods of climate change vulnerability assessment are then presented,

focusing on modeling tools; the current status of climate change impact assessment is then discussed, and the most important research gaps are identified.

Chapter 3 describes the main objectives of this thesis as well as the methodology used to achieve them. The methodological framework is based on a multi-scale, model-based vulnerability assessment, beginning with an analysis of the sensitivity of hydrological, vegetation and erosive processes to different degrees of change in climate parameters at multiple scales, followed by a cross-scale assessment of the resilience of these processes by analyzing the impacts of two climate change scenarios. The chapter then proceeds to present the modeling tools used in the two analysis scales. The spatially detailed, extreme event erosion model MEFIDIS – Physically-based Distributed Erosion Model (Modelo de Erosão FÍsico e DIStribuído – Nunes et al., 2006), optimized for Mediterranean watersheds, is developed within this thesis. MEFIDIS is evaluated using two well studied watersheds, and its sensitivity to changes in climate parameters is compared with other erosion models to evaluate the model's behavior as a tool for climate change response prediction. Finally, the seasonal scale SWAT model (Neitsch et al., 2002) is also briefly described.

Chapter 4 describes the implementation of the methodological framework in the study areas. Two Portuguese regions with Mediterranean climate were selected, one in a semi-arid climate and the other in a transitional dry to humid region; one watershed was selected inside each region to conduct a more detailed analysis. The application of the SWAT and MEFIDIS models to these areas is described, and their performance against measured data and current knowledge of hydrological, vegetation and erosion processes is assessed.

Chapter 5 presents the assessment of the impacts of climate change on hydrological, vegetation and erosive processes in the study areas. Firstly, a model-based sensitivity assessment to climate change is presented. The SWAT model is applied at the seasonal scale, providing results for average annual changes to water and sediment yield and vegetation biomass production in watersheds. The MEFIDIS model is applied at the extreme event scale, to analyze the impacts of changes in storm patterns, soil water content and vegetation cover to storm runoff, peak flow rates, hydrological and sediment connectivity and ephemeral gully distribution. Secondly, catchment response to two climate change scenarios for 2070-2100 is analyzed, based on results from the PROMES Regional Climate Model (Gallardo et al., 2001). The SWAT and MEFIDIS models are applied sequentially in order to obtain results at both the seasonal and extreme event scales; the extreme event assessment focuses on an

increase in seasonal storm variability and includes an analysis of changes to within-watershed hydrological and sediment connectivity and to gully erosion patterns.

Chapter 6 discusses the results of the previous chapter in light of the vulnerability assessment framework. The sensitivity of hydrological, vegetation and erosive patterns to climate change across scales is compared and discussed, together with an analysis of the resilience of catchment processes to climate change scenarios at multiple scales, using the PROMES impact assessment results as the basis for discussion. This is followed by a discussion of the implications of these results for the vulnerability of Mediterranean catchments to climate change, focusing on changes to desertification processes and pointing to the most important issues requiring adaptation measures. The discussion is completed by framing the results within the uncertainty caused by limitations in the methodology.

Finally, **chapter 7** concludes this thesis by synthesizing the main results and offering suggestions for further research.

1.1 References

Adger WN, 2006. Vulnerability. Global Environmental Change 16: 268–281.

Boardman J, 2006. Soil erosion science: reflections on the limitations of current approaches. Catena 68: 73-86.

Boix-Fayos C, Martínez-Mena M, Arnau-Rosalén E, Calvo-Cases A, Castillo V, Albaladejo J, 2006. Measuring soil erosion by field plots: Understanding the sources of variation. Earth-Science Reviews 78: 267-285.

Bronstert A, 2004. Rainfall-runoff modelling for assessing impacts of climate and land-use change. Hydrol. Process. 18, 567–570.

Cammeraat LH, 2002. A review of two strongly contrasting geomorphological systems within the context of scale. Earth Surf. Process. Landforms 27: 1201–1222.

Field CB, Lobell DB, Peters HA, Chiariello NR, 2007. Feedbacks of terrestrial ecosystems to climate change. Annual Review of Environment and Resources 32: 7.1-7.29.

Gallardo C, Arribas A, Prego JA, Gaertner MA, de Castro M, 2001. Multi-year simulations using a regional-climate model over the Iberian Peninsula: current climate and doubled CO_2 scenario. Quarterly Journal of the Royal Meteorological Society 127: 2740-2756.

Giorgi F, 2006. Climate change hot-spots. Geophys. Res. Lett. 33: L08707.

Huntingford C, Gash J, Giacomello AM, 2006. Climate change and hydrology: next steps for climate models. Hydrol. Process. 20: 2085-2087.

Imeson AC, Lavee H, 1998. Soil erosion and climate change: the transect approach and the influence of scale. Geomorphology 23: 219–227.

IPCC: Intergovernmental Panel on Climate Change, 2007. Climate Change 2007: The Physical Science Basis. Contribution of Working Group I to the Fourth Assessment Report of the Intergovernmental Panel on Climate Change. Solomon S, Qin D, Manning M, Chen Z, Marquis M, Averyt KB, Tignor M, Miller HL (Eds.). Cambridge University Press, Cambridge.

Michael A, Schmidt J, Enke W, Deutschländer Th, Malitz G, 2005. Impact of expected increase in precipitation intensities on soil loss – results of comparative model simulations. Catena 61: 155-164.

Nearing MA, Pruski FF, O'Neal MR, 2004. Expected climate change impacts on soil erosion rates: a review. Journal of Soil and Water Conservation 59 (1): 43-50.

Neitsch SL, Arnold JG, Kiniry JR, Williams JR, Kiniry KW, 2002. Soil and Water Assessment Tool theoretical documentation. TWRI report TR-191, Texas Water Resources Institute, College Station.

Nunes JP, Vieira GN, Seixas J, 2006. MEFIDIS – A Physically-based, Spatially-Distributed Runoff and Erosion Model for Extreme Rainfall Events. In: Singh VP, Frevert DK (Eds.), Watershed Models. CRC press, Boca Raton: 291-314.

Puigdefábregas J, 1998. Ecological impacts of global change on drylands and their implications for desertification. Land Degrad. Develop. 9: 393-406.

Räisänen J, Hansson U, Ullerstig A, Döscher R, Graham LP, Jones C, Meier HEM, Samuelsson P, Willén U, 2004. European climate in the late twenty-first century: regional simulations with two driving global models and two forcing scenarios. Climate Dynamics 22: 13–31.

Schroter D, Cramer W, Leemans R, Prentice IC, Araujo MB, Arnell NW, Bondeau A, Bugmann H, Carter TR, Gracia CA, de la Vega-Leinert AC, Erhard M, Ewert F, Glendining M, House JI, Kankaanpaa S, Klein RJT, Lavorel S, Lindner M, Metzger MJ, Meyer J, Mitchell TD, Reginster I, Rounsevell M, Sabate S, Sitch S, Smith B, Smith J, Smith P, Sykes MT, Thonicke K, Thuiller W, Tuck G, Zaehle S, Zierl B, 2005. Ecosystem service supply and vulnerability to global change in Europe. Science 310 (5752): 1333-1337.

Xu C-Y, Singh VP, 2004. Review on Regional Water Resources Assessment Models under Stationary and Changing Climate. Water Resources Management 18: 591–612.

2. Background

This chapter presents the background supporting the research presented in this thesis. The main focus is on the link between desertification and climate in the northern Mediterranean, the potential impacts of climate change on the physical drivers of desertification, and the current methods and tools used in their assessment.

The first part describes **The Mediterranean context**, the geographic framework embracing the conceptual issues of this thesis. After an exposition of the particular characteristics of the Mediterranean climate, the current understanding of the most pressing environmental problem in the region – desertification – is discussed.

The second part discusses **Climate change and the northern Mediterranean**, including the presentation of current climate change scenarios for the Mediterranean basin, particularly for the European rim, and the impacts of these changes on hydrological processes and soil erosion. The analysis focuses on the general processes operating in both cases, and on specific issues pertaining to Mediterranean semi-arid regions which could determine the potential response to future climate scenarios. Finally, the importance of vegetation biomass in soil protection is discussed and the potential impacts of climate change are analyzed.

The third part analyzes the methods for **Assessing vulnerability to climate change**, beginning with a discussion of the concepts and methods for vulnerability. Hydrological and erosion modeling is presented as a tool to support vulnerability assessments, including a review of modeling theory and currently existing models. Afterwards, existing model-based climate change impact studies are reviewed, focusing on studies for Mediterranean drylands. The discussion finishes with the major results from these studies and their limitations, leading to the final part presented in this chapter, **Current research needs**.

2.1 The Mediterranean context

The Mediterranean basin comprises the regions in Europe, Africa and Asia that surround the Mediterranean Sea. These regions have in common their climate, characterized by wet winters and dry, hot summers, which supports characteristic drought-adapted ecosystems. Mairota et al. (1998) have characterized the natural and human aspects of the Mediterranean rim of Europe, as well as the current environmental problems facing this region. Traditionally, humans in this region have adapted to the climate as well, relying on water-harvesting techniques, drought-resistant tree crops and rainfed cereal crops for sustenance. However, in

recent years there has been an increased pressure on local environmental resources, particularly due to urbanization, increased tourism and the spread of more intensive agricultural practices; problems such as water shortages, environmental pollution, and land degradation and abandonment followed. These problems are poised to continue in the future and be intensified if environmental changes turn the region towards a more arid climate.

2.1.1 The Mediterranean climate

The Mediterranean climate occurs in less than 1 % of the Earth's surface, more than half of which is located in the Mediterranean basin (Clark, 1996). Palutikof et al. (1996) have written an overview of this climate, pointing out its main characteristic: the pronounced seasonal cycle in all climate variables, particularly rainfall – typically, winter rainfall is at least three times greater than summer rainfall. The region experiences warm and dry conditions in July, August and September, linked to the presence of atmospheric high-pressure systems. The rainy season begins in mid-October and continues until around the end of May, with the maximum rainfall from December to February. Winter rainfall is mostly associated with cyclonic disturbances occurring over the Mediterranean itself, but in the Iberian Peninsula about half of the rain-producing depressions are originated over the Atlantic. The high temporal variability is also noticeable at the inter-annual and the sub-daily scale. At the inter-annual scale, the Mediterranean climate shows a frequent occurrence of abnormally dry years; these drought periods typically last several years in a row, and are characterized by rainfall decreases in only a part of the rainy season (Palutikof et al, 1996). At the sub-daily scale, the cyclonic nature of many rainfall episodes leads to the frequent occurrence of high-intensity storms (Thornes, 1998).

Climate patterns vary over the Mediterranean region. Palutikof et al. (1996) report that the annual average temperature shows an increasing N to S gradient, from around 12 ºC in the southern coast of France to over 18 ºC in Libya and Egypt. Mean annual rainfall is higher over the northern Mediterranean, ranging from 400 to 1200 mm per year, except over parts of SE Spain and W Turkey; in the south, annual rainfall averages drop below 200 mm per year. This spatial variability of temperature and rainfall leads to differing spatial patterns of climatic aridity. The average annual rainfall to Potential Evapotranspiration (PET) ratio is commonly used as an aridity index (UNEP, 1997); as shown in Figure 2.1, most of the northern Mediterranean is classified as humid, except for drylands (arid and semi-arid regions) located in the SE part of the Iberian Peninsula, Sicily, eastern Greece and central Turkey, while most of the south Mediterranean is dry.

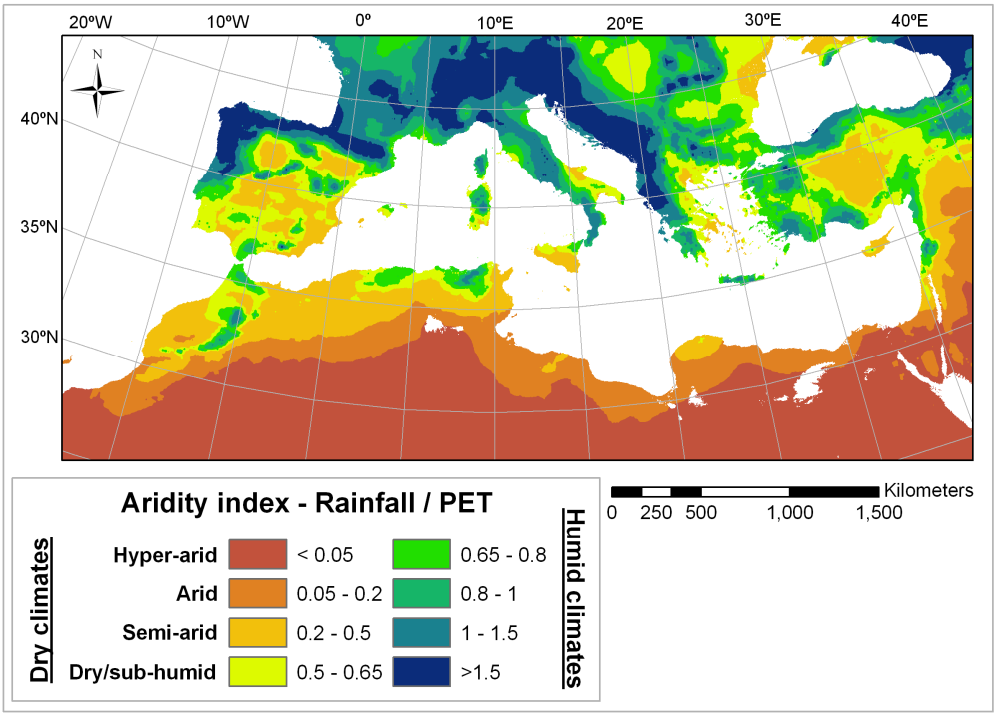

Figure 2.1 – Climatic aridity in the Mediterranean basin for 1961-1990; the map shows the UNEP aridity index (UNEP, 1997), calculated using the gridded climate datasets built by New et al. (2002).

2.1.2 Human occupation and desertification

The Mediterranean region is characterized by drought-adapted vegetation, capable of restricting water use during summer and drought years while maintaining vegetation productivity in winter, when more water is available (Clark, 1996). However, Grove and Rackham (1998) point to the long history of human occupation of the Mediterranean basin; the local environment is to a large extent human created or at least human managed.

Throughout the last 3000 years, natural areas have declined in periods of human expansion, only to recover in periods where human occupation receded; in the past, extensive land degradation in agricultural areas has been linked with the decline of ancient Mediterranean civilizations (Grove and Rackham, 1998; Toy et al., 2002). Currently, the Mediterranean rim of Europe appears to be on a cycle of expansion (Grove and Rackham, 1998). The twentieth century was characterized by increased urbanization, greater use of water resources, and the spread of intensive agriculture and forestry in most regions (Margaris et al., 1996), while traditional land management systems have been replaced by more intensive cultivation

practices (Margaris et al., 1998; Papadimitriou and Mairota, 1998; Puigdefábregas and Mendizabal, 1998). This has led to an increasing debate on the effect of the more intensive human occupation on the Mediterranean environments, which fuelled a research effort leading to a number of national and European research projects.

One research project which should be referred is MEDALUS – Mediterranean Desertification and Land-Use (Brandt and Thornes, 1996; Mairota et al., 1998), which focused on desertification processes in this region, particularly its causes, extent and severity. One of the overreaching conclusions of this project is that, while humans have impacted Mediterranean environments in the past, the impacts during the twentieth century were significantly more profound, pointing to the critical issue of these regions – the desertification of Mediterranean drylands. Current trends continue to support the driving forces behind this process, indicating an aggravation of its extension and severity.

Desertification can be defined as the degradation of biophysical and socio-economic conditions in dry regions, leading to land degradation, reduced vegetation productivity and human abandonment (Thornes, 1998; Fernández, 2002). While the debate over the global extent and causes is still ongoing, there is a consensus that desertification is driven by both physical and socio-economic factors (Puigdefábregas, 1998; Fernández, 2002; Herrmann and Hutchinson, 2005). In the northern Mediterranean, Thornes (1998) has described the hydrological cycle as the main physical driver: on one hand, the scarcity of water resources leads to limited vegetation growth and reduced water for agricultural irrigation, particularly in drought years; on the other, the variability of the hydrological cycle leads to an increased vulnerability to soil erosion, particularly in regions with reduced vegetation cover. Hydrological soil erosion also impacts directly on soil fertility, reducing agricultural productivity (Toy et al., 2002). While the natural ecosystems and many traditional agricultural methods evolved to minimize the impacts of this physical driver, the imposition of intensive-agricultural methods has increased the system's vulnerability and can therefore be considered one of the main socio-economic drivers (Puigdefábregas and Mendizabal, 1998; Vogiatzakis et al., 2006). When the socio-economic exploitation of natural systems surpasses their resilience threshold, either due to over-exploitation or climate changes reducing the natural systems' carrying capacity, desertification occurs (Puigdefábregas, 1998).

Martínez-Fernández and Esteve (2005) have provided a recent overview of how these two factors operate to increase the extent of desertification in southeast Spain, one of Europe's most vulnerable regions. Soil erosion and land degradation are linked mostly with the

expansion of agriculture to unsuitable regions, particularly marginal agricultural areas with steep slopes, and extensively irrigated regions. Vogiatzakis et al. (2006) report a similar interaction between socio-economic drivers and the climatic susceptibility of the landscape in the Mediterranean basin, and also in other regions with Mediterranean climate and vegetation in Chile and South Africa.

Land degradation and the consequential decrease in crop yield has often led to the abandonment of cultivated lands, which in many cases recover part of their vegetation cover and soil quality (Puigdefábregas and Mendizabal, 1998; Thornes,1998). However, external factors such as market prices and government subsidies can extend unsustainable agricultural practices (Audsley et al, 2006); the competition of Mediterranean farmers with those from more productive regions has led to the abandonment of marginal lands in some cases, while in others traditional land management systems were replaced by more intensive cultivation practices, leading to increased land degradation (Margaris et al., 1998; Papadimitriou and Mairota, 1998). In these cases, land degradation and desertification can be irreversible without extensive human intervention (Thornes, 1998), and many regions in the northern Mediterranean region are presently in this condition or approaching it (Puigdefábregas and Mendizabal, 1998). Furthermore, climate change could lead to decreased water availability and increased physical constraints on ecosystem productivity in the Mediterranean regions of Europe (Räisänen et al., 2004), therefore reducing the suitable regions for agriculture and increasing the number of areas exposed to desertification (Puigdefábregas, 1998).

Finally, Thornes (1998) notes that, while the recent development in Mediterranean regions has increased environmental pressures and the risks of desertification, it has also brought considerable socio-economic development to a traditionally poor region. Mediterranean societies are challenged with maintaining their socio-economic achievements while combating the environmental problems they created, adapting to the stringent constrains posed by the Mediterranean climate.

2.2 Climate change and the northern Mediterranean

Global warming, resulting from the anthropogenic emission of greenhouse gases, is expected to increase in the next century (IPCC, 2007). Global climate patterns are expected to change, and several regions are considered particularly vulnerable. Although the extent of these changes is still uncertain, General Circulation Models (GCMs) have commonly been used to develop plausible climate change scenarios. Giorgi (2006) compiled the results of 20 GCMs

for three CO_2 emission scenarios, and found that the Mediterranean region is one of the most vulnerable to climate change in terms of changes to mean air temperature and precipitation, as well as to the interannual variability of these parameters. Since the current climate in the northern Mediterranean already provides only marginal support for many of the region's economic activities, climate change could increase the conditions leading to desertification and land degradation (Palutikof et al., 1996).

The hydrological cycle in drylands is usually linked with two climate variables: rainfall, which determines the total water available to the system; and temperature, which determines the evapotranspiration rates, and therefore the water requirements by the vegetation (Xu and Singh, 2004). Soil erosion is also usually linked with rainfall, due to its erosive power and the generation of surface runoff; and with temperature and atmospheric CO_2 concentrations, due to their impacts on vegetation cover (Nearing et al., 2005). Therefore, and in the context of this work, the following analysis will focus on climate changes to rainfall, temperature and CO_2 concentrations.

2.2.1 Climate scenarios for the northern Mediterranean

In the past 15 years, several scenarios of climate change for Europe and the Mediterranean in particular have been published in the literature, usually obtained from GCM outputs. Prior to the publication of the Intergovernmental Panel on Climate Change (IPCC) of its Special Report on Emission Scenarios (SRES) in 2000 (IPCC, 2000), most scenarios assumed a doubling of CO_2 atmospheric concentration in 2100; Palutikof et al. (1996) and Goodess et al. (1998) have published scenarios for the Mediterranean region based on a compilation of GCM results operating under this assumption. Both studies agree on an increase of the mean annual temperature above the global temperature increase, particularly in inland regions, coupled with a decrease of the mean annual rainfall, with less pronounced changes during winter. This is predicted to cause a decrease of the rainfall to potential evapotranspiration ratio, leading to greater climate aridity over most of the region.

Recent estimates are based the in more complex socio-economic scenarios presented in the SRES, leading to new predictions of atmospheric CO_2 concentrations (shown in Table 2.1), coupled with more advanced GCMs and a new generation of Regional Climate Models (RCMs; IPCC, 2007). For example, Giorgi (2006) used the results from 20 GCMs for three CO_2 emission scenarios (A1B, A2 and B1) to develop a regional climate change index, based on changes to mean precipitation and surface air temperature, as well as changes to the interannual variability of these variables. In global terms, the Mediterranean emerged as one

of the regions with the highest index values. Trends point to a temperature increase and precipitation decrease, as in previous results; but they also point to an increase in the interannual variability of both variables, leading to a more frequent occurrence of extreme weather years.

Table 2.1 – Description and predicted atmospheric CO_2 concentrations for the SRES emission scenarios and the antecedent IS92 scenarios, based on the SRES report (IPCC, 2001); concentrations in 2000 were estimated at c. 370 ppm.

Scenario family	**Economic orientation**	**Globalization / regionalization**	**Atmospheric CO_2 concentration in 2100 (ppm)**
A1B	Development and growth	Global convergence	710[a]
A2	Development and growth	Regional heterogeneity	845
B1	Sustainability and social equity	Global convergence	545
B2	Sustainability and social equity	Regional heterogeneity	615
IS92a	"Business as usual" – average of the IS92 scenario families		715

a – CO2 concentrations for the A1 scenario family vary from 582 to 970 ppm, depending on the use of nuclear and renewable energy sources or carbon-intensive sources; A1B assumes a balanced mix.

Another example is the research effort in RCM analysis, in international research projects such as PRUDENCE (Prediction of Regional scenarios and Uncertainties for Defining EuropeaN Climate change risks and Effects; Déqué et al., 2005); the work by Räisänen et al. (2004) can be referred as a sample of research results. The authors analyzed a sample of the predictions for European climate in 2070-2100 obtained from one RCM forced by two different GCMs and based on two CO_2 emission scenarios, B2 and A2, with the latter representing the greatest changes to atmospheric CO_2 concentrations (Table 2.1). For the northern Mediterranean, the model predictions show:

- a similar trend for the results of the B2 and A2 emission scenarios, with greater changes for the latter due to the greater atmospheric forcing with CO_2;
- an increase of mean annual temperature, particularly in the western regions, of 2-6 ºC for the B2 scenario and 4-8 ºC for the A2 scenario, above the average global increases of c. 2.5 ºC (B2) and c. 3.3 ºC (A2);

- a trend for temperature increases occurring mostly during the summer months, with values reaching 4-8 ºC (B2) and 4-12 ºC (A2);

- an increase of annual maximum temperatures above the average annual increase, of 3-8 ºC (B2) and 4-10 ºC (A2), suggesting an increase in heat wave episodes;

- a maintenance or decrease of mean annual rainfall of +10 % to -20 % (B2) and 0 to -60 % (A2), with the greatest decreases in the western Mediterranean regions, associated with a reduction in the number of rain days rather than reduced precipitation intensity;

- a trend for greater decreases in summer months, with smaller changes but also slightly decreasing in winter months, increasing the seasonal variability of climate;

- changes to the yearly maximum daily rainfall of -20 % to +30 % in both scenarios, with maximum rainfall rates decreasing less than the average annual rainfall, or even increasing where mean annual rainfall decreases;

- increased winter and spring evaporation due to higher temperatures associated with reduced cloudiness, leading to reduced soil moisture.

Once more, these results point to a very significant increase in climate aridity over the Mediterranean by reducing the rainfall to potential evapotranspiration ratio; an example for the A2 emission scenario is shown in Figure 2.2. The changes to climatic extremes are also very significant, with an increased probability of occurrence of heat waves and heavy rainfall episodes. These results for climatic extremes agree well with the ones reported by Sanchéz et al. (2004) for the Mediterranean region, which used one RCM for 2070-2100 considering the A2 emission scenario. The authors also point to the greater intensity and duration of heat waves, coupled with the longer duration of cold waves in the western Mediterranean, indicating an increase in climatic extremes. They also predict no changes or a slight increase in daily rainfall rates, this despite a reduction of average winter rainfall of up to 25 %, albeit with a very high spatial variability, pointing to a broadening of the rainfall variability, with greater frequency of dry and wet extremes when compared with average conditions. The results of this project are further explored in projects MICE (Modeling the Impacts of Climate Extremes; Hanson et al., 2007) and STARDEX (STAtistical and Regional dynamical Downscaling of EXtremes for European regions; Beniston et al., 2006).

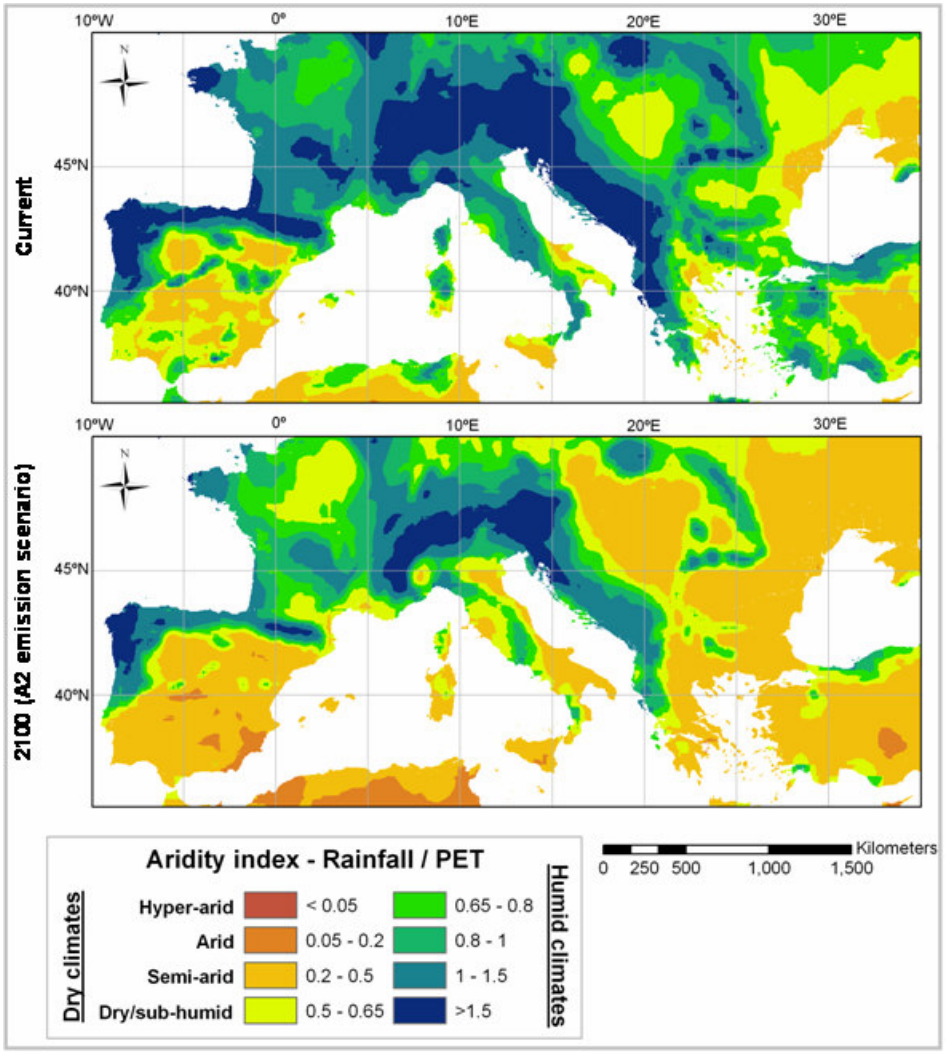

Figure 2.2 – Climatic aridity in the northern Mediterranean basin under current (1961-1990) and changed climate (2071-2100, A2 emission scenario), using the UNEP aridity index (UNEP, 1997); the current map is based on the climate data by New et al. (2002), while the climate change map is based on results from the HADRM3 RCM (PRUDENCE, 2007).

The results presented above are a sample of the available literature; similar results for the average annual, seasonal and extreme trends of precipitation and temperature were published by several authors, using different methods – from GCM and RCM analysis to statistical downscaling of GCM results – and for different CO_2 emission scenarios. Similar overall assessments of climate change scenarios for the Mediterranean were published by Gibelin and Déqué (2003) and Giorgi et al. (2004); the latter authors also report an increase in the interannual variability of rainfall for Mediterranean Europe of around 20 to 40 %, coupled by an increase of summer temperature variability in the Iberian peninsula. Other authors have

published similar results for increasing temperatures (e.g. Sanchéz et al., 2007), decreasing rainfall (e.g. Gao et al., 2006) and increased climate extremes (e.g. Good et al., 2006; Lionello et al., 2002). A number of regional analysis have completed the larger picture for the Mediterranean (e.g. Trigo and Palutikof, 2001 and Sumner et al., 2003 for Iberia; Boroneant et al., 2006 for the Maritime Alps; or Knippertz et. al, 2003 for North Africa).

In conclusion, a large consensus appears to exist that climate change in the Mediterranean region will lead to a very significant temperature increase coupled with lower rainfall rates. This is likely to be accompanied by an increase in climate extremes, with greater seasonal variability of rainfall and temperature, namely longer and more frequent heat waves and frequent extreme rainfall episodes. In the European rim of the Mediterranean, the most affected regions are expected to be the southeastern Iberian Peninsula and the regions around the Aegean Sea. These trends point to an increase of climate aridity, and on the climatic drivers for desertification, over most of the Mediterranean basin. This is particularly worrying given the already large extent of dry climates in the region.

2.2.2 Impacts of climate change on hydrological processes

As previously stated, the hydrological cycle is one of the main physical drivers for desertification, and impacts resulting from climate change could therefore enhance or mitigate this process. The analysis of hydrological processes usually focuses on the most important water fluxes in the hydrological cycle, which can be divided in three main hydrological systems according to the medium through which water flows: (i) the atmospheric water system, consisting of rainfall and evapotranspiration from surface water bodies, soil surfaces and through plants; (ii) the surface water system, consisting of overland and channel water flows; and (iii) the subsurface water system, consisting of water flows through the soil (Chow et al., 1988). These fluxes have been schematized and characterized into a perceptual model by hydrologists, and the most common process definitions can be found in e.g. Chow et al. (1988) or Beven (2000).

The relationship between these systems is highly non-linear (Bronstert et al., 2002), and therefore changes to surface and subsurface water cannot be assessed by direct relationship with changes to the atmospheric water system. The IPCC's fourth assessment report summarized the potential impacts of climate change on these processes at the global scale, following an analysis of the scientific literature (Kundzewicz et al., 2007), including:

- an increase of potential evapotranspiration, due to an increase in the atmosphere's vapor pressure deficit caused by rising temperatures;

- changes to actual evapotranspiration varying with available soil water storage, with less increases in dryer catchments;

- a possible reduction of soil moisture, with a high degree of spatial variability depending on changes to evapotranspiration and soil hydraulic properties, but with a trend of greater climate change impacts on soils with low water storage capacity;

- positive or negative trends for total stream flow, following changes in precipitation, with a trend of greater climate change impacts on drylands;

- decreasing stream flow during low flow periods, due to less subsurface runoff caused by increased evapotranspiration;

- increased flood magnitude and frequency, following a more vigorous hydrological cycle with rainfall concentrated in extreme weather events.

For the Mediterranean rim of Europe, Alcamo et al. (2007) point to a reduction of stream flow following rainfall decreases, with a considerable increase in the difference between winter and summer flows and an increase in the frequency of droughts. These changes will likely have impacts on water resources for human use. In particular, Kundzewicz et al. (2007) point to the interaction between climate change impacts and human water management systems. The impacts of climate change on stream flow can be mitigated in systems with large reservoir capacity, at least in terms of water resources reliability; on the other hand, climate change will have greater impacts in systems that are currently highly stressed in terms of climate and human water demands, such as Mediterranean systems in general and especially Mediterranean drylands.

These impacts, however, are expected to vary significantly in time and space, even within particular physiographic and climatic regions. These differences result from the interaction of spatial variability in catchment characteristics, variability of rainfall inputs and surface and subsurface hydrological processes, leading to different catchment responses to climate. Understanding and predicting this variability requires the understanding of scale issues in hydrological processes, particularly the drivers for spatial and temporal variability at different scales and their cross-scale interaction.

Scale issues in hydrological processes

Some work has been done in recent years in defining and characterizing the scale issues surrounding hydrological processes. Blöschl and Sivapalan (1995) described the characteristic length and scale of the most important hydrological processes, and their schematization is shown in Figure 2.3; Skøien and Blöschl (2003) have confirmed the scales in this figure using a comprehensive dataset for hydrological processes in Austria and Australia. This schematization describes the scale of a process as its order of magnitude, a combination of process lifetime and return period. Two important scale characteristics of hydrological processes can be taken from the scheme.

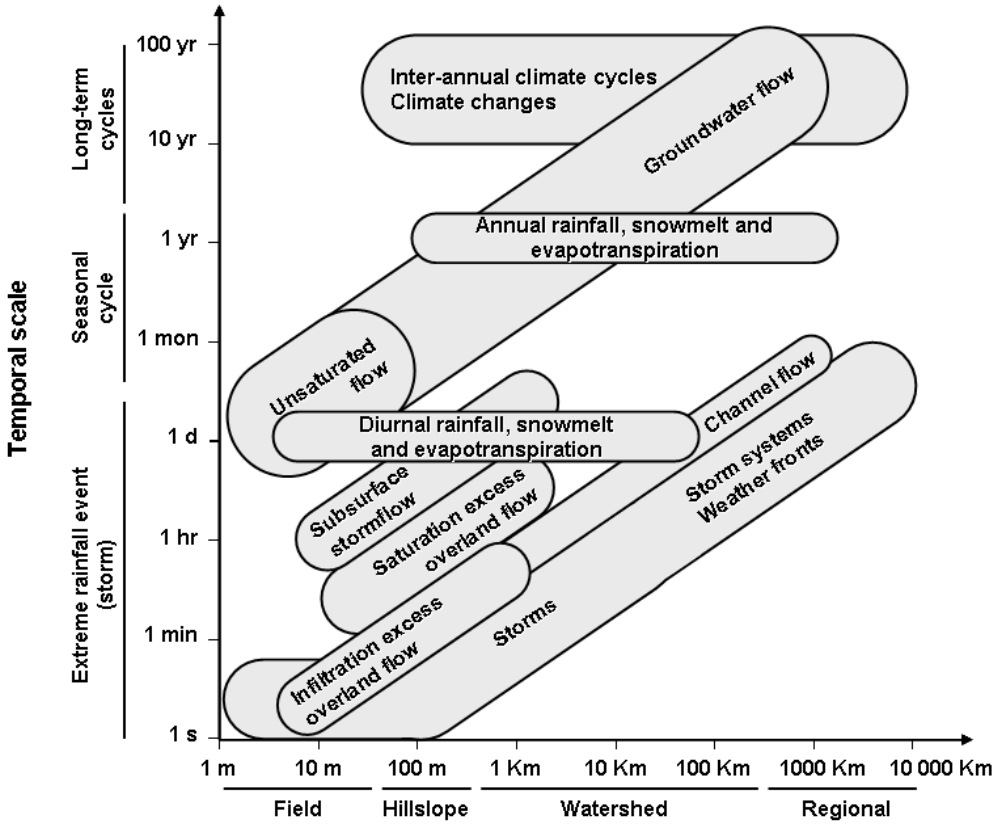

Figure 2.3 – Characteristic time-length combinations of climatic and hydrological processes, adapted from Blöschl and Sivapalan (1995), with inter-annual climate cycles and climate changes added over original picture; scale denominators indicate typical working and modeling scales.

First, the scheme shows a relationship between the spatial and temporal scales of a given hydrological process, with a roughly constant ratio of characteristic length and time scales, defined as the characteristic velocity of each process. This is due to the impact of the transport medium: larger-scale processes require a minimum catchment area for process initiation, but a temporal delay is added due to the friction of the transport medium. As a result, large-scale spatial processes also have a large temporal scale. However, some processes do not fit the spatial and temporal velocity characteristics defined above. These processes are governed by diurnal and annual solar cycles, and include seasonal and daily patterns of rainfall, evapotranspiration and snowmelt. This implies that some longer-term processes can have impacts at a range of spatial scales.

Second, the scheme shows a reduction of characteristic velocity from atmospheric processes to surface processes, with subsurface processes being the slowest, due to a reduction of spatial characteristic scales coupled with a large increase of temporal characteristic scales. Characteristic velocities are in the order of 10 $m.s^{-1}$ for atmospheric processes, 1 $m.s^{-1}$ for surface processes and 0.1 $m.s^{-1}$ for subsurface processes. Skøien and Blöschl (2003) suggest that the reduction of spatial characteristic scales is due to superimposing the small-scale variability of channel networks and soil moisture patterns (via aquifers and lateral channel flows) over rainfall patterns, which appear to be scale-invariant and possess multi-fractal properties. The authors also suggest that the increase of temporal characteristic scales from rainfall to surface processes is due to delays related with runoff generation (dealing with soil moisture accumulation and subsurface flow), while the reduction from surface to subsurface processes is due to velocity constraints imposed by the soil on water flows. Again, this points to cross-scale interactions between processes; e.g. where there is an interaction between subsurface and surface processes, the former could act at a significantly longer temporal scale than the latter.

The smaller the characteristic scale of a given hydrological process, the higher spatial and temporal variability occurs. The scale characteristics of hydrological processes shown in Figure 2.3 imply that, except for the cross-scale interactions described above, large-scale hydrological processes will show considerably less spatial and temporal variability than that of smaller-scale processes; hydrological storm response presents the higher variability in space and time (Woods and Sivapalan, 1999). Skøien and Blöschl (2003) also report a difference in variability between atmospheric, surface and subsurface processes. As water flows from the atmosphere to the surface and then to the soil, spatial variability is added while

temporal variability is removed. Spatial variability is added since the properties of the water storing and routing media (soil, vegetation, channels, etc.) are more variable in space than rainfall. Temporal variability is removed since there are delays associated with water storage in these media; the greater the storage space, the more temporal variability will be filtered.

The driving forces behind the **spatial variability** of hydrological processes have been studied by several authors. Cameraat (2002) presents a review of surface runoff controls in both humid regions and drylands, at multiple spatial scales, and Kirkby et al. (2002) complete the review specifically for drylands, while Blöschl and Sivapalan (1995) have listed the major controls for subsurface processes; these are shown in Table 2.2. Channel flow variability appears to exhibit scale-invariant characteristics depending on channel network patterns, operating above a specific drainage area threshold (Veitzer and Gupta, 2001). It should be noted that subsurface storm flow doesn't appear to be an important process in drylands (Beven, 2000; Kirkby et al., 2002), and therefore most of the spatial variability is linked with surface processes, at least at the storm scale. One of the conclusions that can be taken from Table 2.2 is that the nature of water flow through hillslopes to streams differs significantly between drylands and humid regions, a conclusion also reached by Kirkby et al. (2002).

Table 2.2 – Spatial controls on surface and subsurface flow at multiple scales, with characteristic lengths similar to those shown in Figure 2.3.

	Field	**Hillslope**	**Watershed**	**Regional**
Overland flow controls[a]	Soil drainage structure, vegetation structure, slope gradient	Soil saturation patterns, vegetation type patterns, slope gradient	Channel network, soil types	Channel network, geological patterns
Subsurface flow controls[b]	Macropores	Preferential flowpaths	Soil types	Geological patterns

a – Cameraat, 2002 ; Kirkby et al., 2002.
b – Blöschl and Sivapalan, 1995.

Boix-Fayos et al. (2006) present a review of surface runoff controls in Mediterranean regions, at multiple spatial scales, focusing on the contrast between humid and dryland processes at the field and hillslope scales. In humid regions, the spatial variability of runoff generation and overland flow is driven by the contrast between the "wet" and "dry" areas, i.e. areas where the soil is saturated with water or not; these areas are related with soil biological activity and its effect on hydraulic properties. In drylands, the coarsening of vegetation cover leads to

different runoff generation processes. The spatial variability in drylands is driven by the contrast between vegetated and bare areas; vegetated areas tend to be runoff sinks, while bare areas tend to be runoff sources, especially after soil crusting during high-intensity rainstorms.

The influence of vegetation on the spatial patterns of runoff generation is connected with the dryness of the environment due to the increasing heterogeneity of vegetation cover; the degree of organization of the vegetation spatial structure is also linked with higher runoff rates. At larger scales, Cameraat (2002) notes that similar channel processes operate in both humid and dryland regions. In transitional climatic regions such as those with a dry/sub-humid and semi-arid climate, catchments may exhibit humid controls in the wet season and dryland controls in the dry season (Kirkby et al., 2002).

The **temporal variability** drivers for surface and subsurface flows, represented by the channel hydrograph at the catchment scale, are shown in Table 2.3, following the characterization by Blöschl and Sivapalan (1995) and Boix-Fayos et al. (2006). One interesting phenomena is the strong link between the spatial and temporal variability of overland flow generation at the extreme event scale through spatial connectivity – the capacity of water to move inside a watershed. In both humid systems and drylands, a number of runoff generation areas must be connected for runoff to reach from fields to hillslopes and onwards to the channel network (Boix-Fayos et al., 2006).

Table 2.3 - Temporal controls on catchment flow at multiple scales, with characteristic times similar to those shown in Figure 2.3.

	Event	**Seasonal**	**Long-term**
Catchment flow controls	Storm and catchment characteristics[a, b], spatial connectivity[b]	Physioclimatic characteristics[a]	Climatic variability[a], anthropogenic disturbances[a], geomorphological processes[a]

a – Blöschl and Sivapalan, 1995.
b – Boix-Fayos et al., 2006.

Hydrological connectivity is linked with the intensity-duration-frequency characteristics of rainfall, and with critical rainfall intensity and magnitude thresholds that must be surpassed for connectivity to occur; these thresholds increase with spatial scale and are controlled by physical and biological properties (Cammeraat, 2002). Therefore, the larger the spatial scale, the greater rainfall intensity is required for overland flow initiation. Boix-Fayos et al. (2006)

describe the different controls on runoff generation thresholds according to storm and soil properties. High-intensity rainstorms usually surpass the thresholds and generate runoff; runoff from low and medium intensity storms is dependent on soil moisture conditions before storms, which vary with seasonal soil storage levels. The consequence is that, in summer, the critical rainfall intensity required for runoff initiation is usually higher than in winter. Another important property is soil permeability; in regions with less permeable soils, runoff response shows less dependency on antecedent soil moisture patterns. Finally, the variability of within-storm rainfall intensity is also linked with connectivity (Puigdefabregas et al., 1999).

The typical rainfall and soil properties of Mediterranean regions lead to specific characteristics of the spatial and temporal variability of overland flow generation. In particular, the low hydrological connectivity of Mediterranean watersheds leads to a high variability in storm response (Puigdefabregas et al., 1998; Cammeraat, 2002; Kirkby et al., 2002). Kirkby et al. (2002) point to a seasonal humid and dry behavior, leading to runoff generation driven by soil moisture patterns in the wet season. The importance of antecedent soil moisture for rainfall-runoff response, at least for low and medium intensity storms, has been observed in multiple Mediterranean catchments (e.g. Cerdà, 1998; Castillo et al., 2003; Garcia-Ruiz et al., 2005). Castillo et al. (2003) establish the threshold for high intensity storms as being above 60 $mm.h^{-1}$ during 30 minutes. García-Ruiz et al. (2005) reports that this dependency on antecedent soil moisture has been observed under a number of typical Mediterranean land uses: dehesa (sparse cork or holm oak forest), forests, open shrubs, and abandoned farmlands. Boix-Fayos et al. (2005) report that this process is more common in less degraded regions. Yair and Kossovsky (2002) link this with the gravelly soils and vegetation cover associated with semi-arid regions, which if dry have a high capacity for water absorption; in contrast, arid rocky areas have a low water absorption capacity and therefore rainfall generation is independent of soil moisture. Typical rainfall thresholds for runoff generation appear to be around 10 $mm.h^{-1}$ during 30 min (Boix-Fayos et al., 2005; Kirkby et al., 2005). Subsurface storm flow appears to represent a small part of total storm flow (Ribolzi et al., 2000; Kirkby et al., 2002).

Several efforts have been made to formalize the drivers for spatial and temporal variability of hydrological processes. In spatial terms, regions with similar hydrological characteristics in terms of topography, land use and soil properties have been proposed; these are termed Hydrological Response Units (HRUs) and are usually considered as subdivisions of catchments, although their existence at multiple scales has been proposed (Beven, 2000;

Grayson and Blöschl, 2001a). Kirkby et al. (2002) propose to subdivide HRU's into Hydrologically Similar Surfaces (HYSS), consisting of regions with similar point responses to runoff generation, and a spatial connectivity factor linked with topography via slope gradient and distance. In temporal terms, the rainfall threshold required for runoff generation, for different HRU's, can be made a function of soil moisture status using methods such as the curve number method (SCS, 1972) or more sophisticated approaches combining rainfall intensity and duration with soil moisture status and runoff travel times (Kirkby et al., 2005). These methods present an effort to quantify the impacts of different spatial and temporal variability drivers on runoff generation, thus generalizing studies made for specific catchments or storms. There is still a need, however, to study the impacts of climate on runoff at a sufficiently detailed scale where the impacts of varying HRUs, storm types and soil moisture conditions can be assessed.

Implications for climate change impacts

The spatial and temporal variability of hydrological processes informs and limits our predictions on the possible impacts of climate change for the Mediterranean region. Comparing the probable impacts outlined in the beginning of this section with the characteristic times and lengths of processes shown in Figure 2.1, as well as the characteristics of hydrological processes referred above, a number of spatial and temporal issues in assessing the impacts of climate change on hydrological processes can be inferred:

- the increase of evapotranspiration and the decrease of channel flow in mean annual and seasonal terms can probably be assessed at the regional scale, allowing for changes to water balance estimates being made for the Mediterranean region following climate change patterns;

- changes to channel flow behavior at smaller timescales, particularly scales associated with floods (hourly and daily flows), should be studied at the watershed scale;

- decreases to soil moisture should be assessed with the help of HRU classifications, possibly at the sub-watershed scale.

Furthermore, considering the processes governing runoff generation in Mediterranean regions outlined above, changes to extreme floods should take into account changes to soil moisture. The increase in the frequency and intensity of extreme rainfall events described above could have its impact attenuated by the decrease in winter soil moisture values, at least for the most

frequent floods. Furthermore, regions with thinner soils could show greater responses to climate change due to the low capacity to store rainfall from stronger storms (van den Hurk et al., 2005). This implies the need for a coupled study at different time scales: a seasonal study of changes to soil moisture patterns combined with an event-scale study of runoff generation, taking soil moisture into account, conducted for different HRUs and possibly at the sub-watershed scale.

Finally, it should be noted that the spatial and temporal variability of hydrological processes for the Mediterranean region can be generalized using concepts such as HRUs and rainfall-runoff response curves, with the goal of assessing typical responses at the sub-watershed scale to climate change patterns. However, watershed responses will still be a function of particular combinations of HRU patterns superimposed over climate patterns, and should be assessed in this regard, perhaps using some type of watershed typology study.

2.2.3 Impacts of climate change on soil erosion processes

As stated above, one of the key physical drivers for desertification is soil erosion which must therefore be studied to understand the impacts of climate change in this process. The analysis of erosion processes is usually focused on hydrological soil erosion, which is the dominant process in most of the world, including Mediterranean regions (Thornes, 1998; Toy et al., 2002). Toy et al. (2002) describe a number of erosive processes, from erosion due to rain splash to concentrated flow erosion operating in rills, ephemeral and permanent gullies, and channels, to mass-movements such as landslides. These processes have been characterized and described in a number of geomorphology and soil erosion publications, e.g. Foster (1982), Harmon and Doe (2001) or Toy et al. (2002). One important issue is that, although soil erosion depends mostly on hydrological drivers, the relationship between rainfall, runoff generation, and soil detachment and transport is highly non-linear and dependent on a number of thresholds (Brown et al., 1999; Salles et al., 2000; Tucker and Bras, 2000; Morgan and Quinton, 2001). Therefore, soil erosion changes cannot be assessed from hydrological changes alone.

As seen in the previous section, climate change is expected to be accompanied by an increase in climatic variability, probably resulting in a higher frequency and intensity of extreme weather events (Milly et al., 2002; Senior et al., 2002). Since these events are usually the determinant factor in hydrological soil erosion (Brown et al., 1999; Tucker and Bras, 2000), one potential consequence is expected to be the acceleration of soil erosion rates, responding to changes both in rainfall volume and intensity, with consequences for topsoil degradation,

loss of agricultural productivity and increased export of sediment and contaminants from agricultural fields (Toy et al., 2002; SWCS, 2003). In a recent review conducted for the IPCC's fourth assessment report, Kundzewicz et al. (2007) list the possible consequences of climate change for hydrological soil erosion rates at the global scale:

- an increase of soil erosion rates in regions where rainfall is expected to increase;
- uncertainty in regions where rainfall is expected to decrease, due both to changes in extreme event intensity and to system feedbacks related to decreased biomass production which could increase the soil's susceptibility to eroding forces;
- additional impacts due to shifts in land use necessary to accommodate new climate regimes, which can increase or decrease the soil vegetation cover.

In Mediterranean regions, the report points to the impacts of greater wildfire frequency, which could increase erosion risk due to reduced vegetation cover (Alcamo et al., 2007); other disturbances such as grazing and tillage could have the same impact (Imeson and Lavee, 1998). These issues highlight the uncertainty surrounding the consequences of climate change for soil erosion in Mediterranean regions, and the likelihood of high spatial heterogeneity. Furthermore, soil erosion in semi-arid Mediterranean watersheds appears to be extremely sensitive to small changes in extreme event characteristics, making them particularly vulnerable to the intensification of the hydrological cycle (Puigdefabregas et al., 1999; Maas and Macklin, 2002).

Understanding and predicting the variability of these impacts within the Mediterranean region requires knowledge of scale issues in erosion processes, especially the drivers for spatial and temporal variability at different scales. In particular, the links between hydrological and erosion processes at different scales should be understood, so that the impacts of changes to hydrology can be properly assessed.

Scale issues in erosion processes

The characterization of scale issues surrounding erosive processes has received less attention than that of hydrological processes. Soil erosion presents a problem in terms of temporal scale characterization, since soil erosion occurs during one or several short rainfall events but accumulates over time to produce significant changes (Toy et al., 2002). Both Favis-Mortlock et al. (2001) and Imeson and Lavee (1998) have correlated the spatial and temporal characteristic scales of erosive processes, the former in terms of the period during which

processes are active, and the latter in terms of the process lifetime, i.e. the time during which they operate changes in the landscape; a schematization of this work is given in Table 2.4.

Table 2.4 – Characteristic time-length combinations of erosive processes, adapted from Favis-Mortlock et al. (2001) and Imeson and Lavee (1998); sample processes are taken from Imeson and Lavee (1998).

			Spatial scale			
	Active period	**Process lifetime**	**Patch (< 1 m)**	**Field**	**Hillslope**	**Watershed Regional**
Temporal scale	Multiple storms	Centuries				Geomorphological adjustments
	Storm	Decades			Rill and gully erosion	
	Within storm	Years		Interill erosion		
		Months	Soil degradation			

As for hydrological processes, there appears to be a relationship between the spatial and temporal scales of a given erosive process. This can also be attributed to the fact that larger-scale processes require a minimum drainage area for activation, but there are time delays as eroded soil moves through the watershed (Favis-Mortlock et al., 2001). Therefore, large-scale spatial processes also have a large temporal scale.

Soil erosion can also be characterized as the result of erosion, transport and sedimentation processes occurring at all scales. In spatial terms, Lane et al. (1997) characterize erosion as a sediment source-transport-sink continuum that operates at most spatial scales, from 1 m^2 plots to large-scale river systems. The different erosion and sedimentation processes are shown in Table 2.5; note that, although different processes dominate at different scales, erosion, transport and deposition are present at all scales. It should be noted that the spatial scale of rill processes in Table 2.5 are different from those reported by Imeson and Lavee (1998), shown in Table 2.4. This is indicative of a larger problem with the definition of rill, gully and channel bank erosion. According to Raff et al. (2003), the three processes are differentiated using a functional definition; rills are small channels that can be destroyed by tillage, while gullies are channels that can be crossed over by a tractor. However, the authors point out that these appear to be different designations for a single process of concentrated flow erosion,

which appears to be scale-invariant above the 1 m scale. The difference of erosion and deposition rates between rills, gullies and channels appear to be linked mostly with the sediment transport capacity of flow, which itself is controlled by flow volume and terrain slope (Govers, 1990). It should also be noted that splash erosion and mass movements are dominated by different processes (Toy et al., 2002), although Favis-Mortlock et al. (2000) have suggested that splash and rill erosions could be linked through a positive feed-back, self-organizing process in which the former eventually leads to the latter.

Table 2.5 – Characteristic spatial scales of erosion and sedimentation processes, associated with erosion, transport or deposition dominance, with characteristic lengths similar to those shown in Figure 2.3.

	Field	**Hillslope**	**Small watershed (< 1 Km)**	**Large watershed (> 1 Km)**
Erosion processes	Splash erosion[a, b, c], rill erosion[b, c]	Gully erosion[a, b, c]	Channel bank erosion[a, b], mass movements[b]	
Sedimentation processes	Depression storage[b], parcel boundary storage[b]	Footslope storage[b]	Floodplain storage[b]	
Dominant processes	Soil erosion[a, c]	Soil erosion, transport and sedimentation[a, c]	Soil erosion, transport and sedimentation[a, c]	Soil transport and sedimentation[a, c]

a – Lane et al., 1997.
b – de Vente and Poesen, 2005.
c – Boix-Fayos et al., 2006.

De Vente and Poesen (2005) point to an increase of sediment yield rates (the net result of soil erosion and sedimentation processes) with larger spatial scale, up to a threshold. Sediment yield due to splash and rill erosion processes is relatively low in most conditions, averaging 0.9 $ton.ha^{-1}.y^{-1}$. However, as catchment area increases, gully erosion processes begin to occur, greatly increasing sediment yield rates. Peak sediment yield is associated with a spatial scale in the order of 0.1-3 Km, which can also be inferred from the dominant processes shown in Table 2.5, and referred by Lane et al. (1997). Above this scale, erosion ceases to be limited by the soil detachment capacity of river flows, and instead becomes limited by the sediment transport capacity of water; the opportunities for sediment deposition increase with spatial scale, leading to a gradual decrease of sediment yield, which eventually becomes smaller than that observed at the field scale.

Furthermore, De Vente and Poesen (2005) also point that these values are average, and can suffer significant deviations due to differences in vegetation cover, lithology and topography. The increase of sediment yield with gully erosion processes is strongly dependent on whether local conditions favor gully formation, as occurs in most Mediterranean semi-arid regions (Boix-Fayos et al.; 2006). Gully and rill/interill erosion rates are similar in humid climates, but in Mediterranean semi-arid climates, gully erosion rates can represent a five-fold increase over rill/interill rates (Vandaele et al., 1997; Toy et al., 2002). These differences are also noticeable at larger spatial scales, as the characteristics of floodplain sediments can lead to increased sediment yield rates (de Vente and Poesen, 2005). Therefore, the relationship between erosion processes, sediment yield and spatial scale is subject to a very significant degree of spatial variability. It should be noted that the sediment yield increase, peak and decrease with length is also present at smaller spatial scales; for example, Toy et al. (2002) refer a similar evolution of sediment yield ratios along the length of gullies.

The spatial and temporal variability of a given erosion process increases with smaller characteristic scales; the relationship between space and time scales shown in Table 2.4 implies that large-scale erosive processes tend to show considerably less spatial and temporal variability than smaller-scale processes. However, this conclusion has to be weighted with the fact that the activity period of erosive processes is much smaller than their lifetime, and therefore erosion will always show a high degree of temporal variability. At the field scale, Silva et al. (1998) observed that, over a period of three decades, 1 % of extreme events was responsible for 64 % of soil loss in a number of semi-arid Mediterranean wheat fields; they conclude that extreme events with return periods of over two years dominate erosion in that region. This observation exemplifies why a process with a lifetime of years should still be studied taking the extreme event scale into account.

The driving forces behind the **spatial variability** of erosion processes have been studied by several authors. According to Toy et al. (2002), the original formulation of the problem in the Universal Soil Loss Equation (USLE) is still valid, even if the actual calculation method for USLE parameters is questionable. Erosion varies with climate (represented as rainfall erosivity), topographical factors – slope gradient and length, soil erodibility, vegetation cover and erosion control practices.

Lane et al. (1997) and Boix-Fayos et al. (2006) present a review of erosion constraints at multiple spatial scales, mostly focused on dryland watersheds. Lane et al. (1997) note a strong link between runoff and erosion patterns, meaning that processes driving the spatial variability

of overland flow (Table 2.2) are also drivers for varying erosive processes. In particular, runoff sources tend to be erosion sources, and the previously referred contrasts between "wet" and "dry" areas in humid catchments, and vegetated and bare areas in dry catchments, are also verified for erosion patterns (Boix-Fayos et al., 2006). However, as shown in Table 2.6, other spatial factors control soil erosion in conjunction with hydrological response. They increase the spatial variability of soil erosion by superimposing factors such as soil structural strength, vegetative protection of the soil, and topographical slope controls on the sediment transport capacity of surface runoff (Lane et al., 1997).

Table 2.6 – Spatial constraints on erosion processes at multiple scales, following Lane et al. (1997), with characteristic lengths similar to those shown in Figure 2.3.

	Field	**Hillslope**	**Small watershed (< 1 Km)**	**Large watershed (> 1 Km)**
Scale-variant	Vegetation cover, soil properties, topography	Vegetation cover, soil properties, topography	Vegetation type, soil type	Rainfall partial cover patterns, channel properties, soil type
All scales	Rainfall intensity patterns, runoff generation and routing patterns			

The **temporal variability** drivers for soil erosion, following Boix-Fayos et al. (2006) and Imeson and Lavee (1998), are shown in Table 2.7. Like in hydrological processes, there is a strong link between the spatial and temporal variability of soil erosion at the extreme event scale through spatial connectivity – in this case, the capacity of sediment to move inside a watershed. According to Favis-Mortlock et al. (2001), sediment connectivity is linked with hydrological connectivity; a number of sediment generation areas must be connected through surface runoff for eroded sediment to reach from fields and gullies to the channel network. It is linked with the magnitude of the erosive event but, in contrast with hydrological connectivity, it usually increases from the field to the hillslope scale due to active gully erosion processes; however, the magnitude of hydrological response has a significant impact on sediment connectivity, as sedimentation-dominated regions in a low runoff event can become dominated by soil detachment in a high runoff event, bringing sediment eroded during previous storms in the channel network (Boix-Fayos et al., 2006). This phenomena is therefore dependent on thresholds for runoff generation, with the characteristics and variability described above, and thresholds for gully formation.

Table 2.7 – Temporal constraints on erosion processes at multiple scales, with characteristic times similar to those shown in Figure 2.3.

	Event	**Seasonal**	**Long-term**
Scale-variant	Catchment characteristics[a], spatial connectivity[a]	Soil aggregation status[b]	Soil stability and resilience[b], vegetation stability and resilience[b], frequency and severity of vegetation and soil disturbances[b]
All scales	Rainfall intensity patterns[b], runoff generation patterns[a]		

a – Boix-Fayos et al., 2006.
b – Imeson and Lavee, 1998.

Over time periods longer than one extreme event, erosion is driven to a number of processes which have a slower timescale. Imeson and Lavee (1998) note that, beyond seasonal and interannual climate and runoff patterns, soil erosion is linked with seasonal and multi-annual changes to the soil physical status, particularly its aggregation. Over longer periods, erosion is also dependent on the stability and resilience of existing soil and vegetation patterns, and the frequency and severity of existing disturbances such as fires, grazing and tillage.

The typical processes associated with overland flow generation in Mediterranean regions, combined with rainfall, vegetation and soil properties, lead to specific characteristics of the spatial and temporal variability of erosive processes. Puigdefabregas et al. (1999) point to the importance of vegetation for erosion heterogeneity at the field scale. In regions with sparse vegetation cover, a range of positive feedback mechanisms leads to the concentration of soil beneath plant clusters at the expense of the neighboring bare ground. This interaction is designed to create a mosaic of bare and vegetated patches with patterns that minimize the redistribution length of sediments. This process occurs mainly in natural vegetation fields, and cultivated patches will be therefore more exposed to soil erosion.

At the hillslope scale, most rainfall showers have insufficient duration for surface runoff to become concentrated and transfer sediments to channels (Puigdefabregas et al., 1999; Yair and Raz-Yassif, 2004; Boix-Fayos et al., 2006). During most low- and medium-intensity storms, soil erosion is transport-limited and soil loss occurs only in regions of concentrated flow such as existing gullies (Wijdenes et al., 2000; Cammeraat, 2002; Boix-Fayos et al., 2005). Significant soil erosion and sediment export at the hillslope scale is usually dominated by a small number of high-intensity rainfall events, normally occurring during winter (Cerdà, 1998; Kirkby et al., 2002; Maas and Macklin, 2002). However, gully formation conditions are more favorable in this region, leading to higher rates of gully erosion processes – when they

occur – than of rill and interill processes (Vandaele et al., 1997; Boix-Fayos et al., 2006). Consequentially, numerous studies have observed a high degree of spatial and temporal heterogeneity in soil erosion rates, with soil loss concentrated in small areas and occurring in small periods of time (e.g. Cerdà, 1998; Imeson and Lavee, 1998; Martinez-Mena et al., 1998; Cammeraat, 2002; Kirkby et al., 2002). Overall, this leads to smaller field erosion rates for Mediterranean regions when compared with more humid climates, but with a much greater temporal variability and a trend for more active gully erosion processes.

The formulation of the drivers for spatial variability of erosion processes has suffered little changes since the formulation of the USLE (Toy et al., 2002). Concepts combining several USLE factors, such as the HRU and HYSS concepts discussed in the previous section, are also applicable within the soil erosion context. Furthermore, a number of gully erosion indexes have been proposed and validated for Mediterranean regions (Vandaele et al., 1997). The analysis of the temporal variability of soil erosion still appears to be limited to observations and complex erosion models, although attempts have been made to estimate annual erosion rates based on simple assumptions of rainfall erosivity and runoff thresholds such as the Morgan-Morgan-Finney (MMF) model (Morgan, 2001). Again, these methods intend to generalize observations made for specific catchments or storms of the spatial and temporal variability drivers on soil erosion. There is still a need, however, to study the impacts of climate on soil erosion at a sufficiently detailed scale where changes to interill/rill erosion, gully formation, sediment connectivity and yield can be analyzed.

Implications for climate change impacts

Predicting the possible impacts of climate change on soil erosion in the Mediterranean region is limited by the spatial and temporal variability of erosive processes. Moreover, the link between soil erosion and overland runoff at the event scale requires a combined analysis of both parameters, as well as others associated with them, at appropriate spatial scales. This would require a combination of soil erosion studies with the seasonal/extreme event study of surface runoff at the HRU scale, proposed in the previous section.

Additionally, the importance of gully erosion outlined above requires their explicit inclusion in climate change studies. Gully erosion rates are highly sensitive to changes in storm intensity (Kirkby et al., 2003; Vandekerckhove et al., 2003), and gully erosion has been suggested as a key process in desertification by Avni (2005). It is possible that the increase in the frequency and intensity of extreme events would also increase gully erosion rates, but this

study would have to be conducted for extreme events at a scale close to that of hillslopes, allowing for the identification of gully erosion-prone regions and their characteristics.

Furthermore, the long-term changes associated with soil and vegetation cover should also be analyzed in conjunction with changes to soil erosion at all rates. This would require a long-term seasonal or decadal analysis of changes to vegetation cover, coupled with the event-scale studies of changes to erosion rates proposed above, to locate regions prone to increased soil erosion due to the loss of vegetation cover as described in the beginning of this section. Land-use changes would also be required in conjunction with soil erosion changes, although this study is beyond the scope of this thesis.

Finally, typical responses at the sub-watershed scale to climate change patterns can be assessed using concepts such as HRUs and erosion response curves to rainfall and runoff rates. It should be taken into consideration, however, that watershed responses will still be a function of particular combinations of HRU patterns superimposed over climate patterns, and that gully responses will depend of topography at a finer scale.

2.2.4 Impacts of climate change on vegetation productivity

As the previous sections have shown, vegetation patterns are often linked with hydrological and erosion patterns; an explicit link between ecological and hydrological landscape characterization has been suggested by Schröder (2006). This is one of the reasons why vegetation cover is an important physical driver for desertification, as previously stated. Vegetation is usually well-adapted to climate (Salisbury and Cross, 1991), and is therefore also vulnerable to climate changes; one common prediction is an increase in vegetation biomass productivity and evapotranspiration due to greater atmospheric CO_2 concentrations (Rosenzweig and Hillel, 1998). Potential vulnerabilities and impacts were summarized in the IPCC's fourth assessment report (Fischlin et al., 2007), and include:

- changes to vegetation productivity patterns, resulting from the interaction between increased atmospheric CO_2 concentrations – generally leading to increased vegetation productivity – and rising temperatures – whose effect on productivity depends on vegetation species and current adaptability to the local climate;

- ecosystems appear to dampen the impacts of modest amounts of climate change, but changes above a certain threshold can lead to major transitions or productivity collapses – enhanced in agricultural regions by human-driven adaptation;

- for Mediterranean ecosystems, the increase in disturbances – particularly wildfires and droughts – could trigger a shift to ecosystems adapted to this condition, coupled with a general decrease in biomass productivity and vegetation cover.

The report also notes that the distribution of vegetation types in biogeographical regions is driven by climate thresholds which are not fully understood, and climate changes could alter the relevant thresholds and lead to shifts in vegetation occupying a certain region. For example an increase in climate aridity in drylands, coupled with severe vegetation disturbances leading to extreme mortality, such as droughts and grazing, could lead to the northwards expansion of deserts. Droughts could also offset the effects of higher CO_2 concentrations in this region and lead to long-term decreases in vegetation productivity due to increased land degradation. As an example, Boix-Fayos et al. (2005) report how thresholds linked with increased climate aridity can affect the organic feedback cycle between soil and vegetation, decreasing the water retention capacity and leading to higher sediment yield.

The report's assessment for the Mediterranean rim of Europe (Alcamo et al., 2007) points to different impacts according to vegetation type. Agricultural productivity for most annual crops, particularly wheat, is expected to decrease due to rising temperatures shifting away from the optimum, while forests could be exposed to an increase in fire frequency. In contrast, arid and semi-arid environments such as steppes, shrubs and schlerophyllous forests, are expected to suffer fewer impacts and even expand in area, although an increase in wildfire frequency could be prejudicial to ecosystems with dense vegetation cover. Field work carried out with native Mediterranean vegetation species – such as schlerophyllous oaks, olive trees and native shrubs – confirm these results experimentally, showing a positive response to increased CO_2 concentrations with few negative effects from higher temperatures (Llorens et al., 2004; Tognetti et al., 1998, 2000, 2001). However, these benefits could be negated by a significant increase in hydrological stress caused by lower rainfall (Cheddadi et al., 2001).

The variability of vegetation responses to climate change can be expected to superimpose additional heterogeneity on the response of hydrology and soil erosion. This can be expected to occur in the spatial domain, due to the mosaic of different vegetation types usually occurring on a given landscape; and in the temporal domain, due to changes in the frequency and severity of vegetation disturbance processes, and the response of different vegetation types to these processes. This implies that the response of hydrological, erosive and vegetation growth processes to climate change should be assessed simultaneously, and at

similar spatial and temporal scales. A possible generalization unit for this analysis could be the concept of HRU, as long as vegetation species is a factor in delineating the units.

2.3 Assessing vulnerability to climate change

The previous section showed how climate change can impact the biophysical drivers for desertification in Mediterranean regions. The subsequent questions are: how will these impacts affect existing socio-economic systems? How can these systems adapt in order to mitigate these impacts?

These issues have been addressed by a number of authors in recent years under the general designation of vulnerability assessment (e.g. Adger, 2006; Folke, 2006; Gallopín, 2006; Smit and Wandel, 2006; Young et al., 2006). Gallopín (2006) discusses the general terms associated with the study of this problem:

- **socio-ecological systems** are the result of mutual interactions between socio-economic and biophysical sub-systems, and have been proposed as the analytical unit for sustainable development research;

- **impacts** are the results of short-term perturbations and long-term pressures on socio-ecological systems, capable of inducing a significant transformation;

- **sensitivity** is the degree to which a socio-ecological system will respond to perturbations or pressures, while the response capacity is the systems' ability to cope with the consequences of a transformation that occurs;

- **vulnerability** to a given impact is a measure of the systems' sensitivity to that impact and its response capacity (or lack thereof).

In this context, the Mediterranean landscape can be seen as a socio-ecological system, shaped by centuries of interactions between humans and the natural world. The impacts of climate change can be described as changes in the socio-ecological system resulting from pressures and perturbations caused by climatic shifts. The magnitude of these changes refers to the system's sensitivity to climate change, and the system's response capacity is its ability to endure or adapt to any transformation that occurs. Assessing the system's vulnerability to climate change therefore requires an evaluation of both its sensitivity to climate change and its response capacity.

As described in the previous sections, desertification is the critical issue for Mediterranean socio-ecological systems. Assessing vulnerability of this system to climate change requires the measurement of the sensitivity of the biophysical drivers of desertification to changes in climate, as well as the response capacity of the socio-ecological systems to an exacerbation of the desertification process. This vulnerability can be analyzed in terms of socio-economic and biophysical drivers for desertification, debated in the previous sections; if the existing socio-ecological systems are unable to withstand the perturbations and pressures caused by the enhancement of these drivers, then the desertification process will become more intense.

Although climate change can condition and drive both biophysical and socio-economic systems (Adger, 2006), this thesis focuses on the biophysical component supporting Mediterranean socio-ecological systems.

2.3.1 Vulnerability assessment methods

Vulnerability to climate change has been assessed in recent years using the concepts described above. One example was performed under the context of the Terrestrial Ecosystem Analysis and Modelling (ATEAM) project, described by Metzger et al. (2005). Overall, the frameworks proposed for vulnerability assessment have in common their analysis of the sensitivity of socio-ecological systems to an external perturbation – climate change – and their response capacity. The theoretical framework for vulnerability assessment has been described by Gallopín (2006); a schematic version is shown in Figure 2.4.

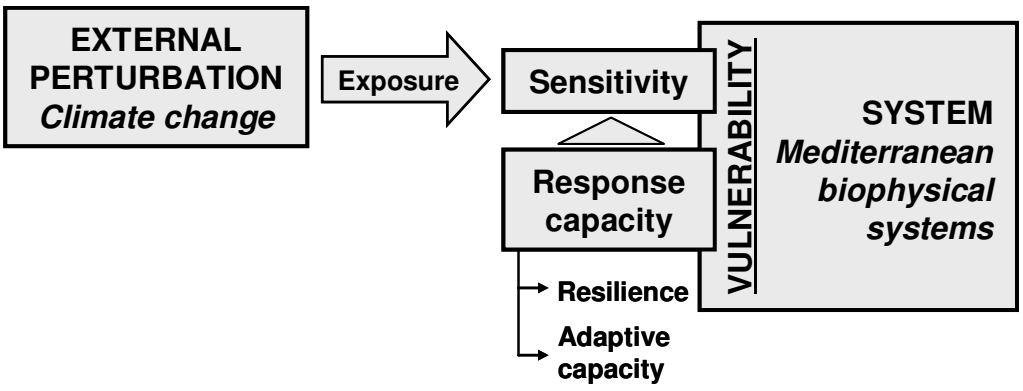

Figure 2.4 – Theoretical framework for vulnerability assessment, adapted from Gallopín (2006) with items relevant to this thesis in italic.

Following the vulnerability assessment process described by Adger (2006), the first step is the evaluation of the probability of **exposure** of a system to a perturbation by an external process. Within the context of this thesis, this is the probability of exposure of biophysical systems to significant climate shifts (Figure 2.4), which is currently assessed using GCMs and RCMs, as described in the previous section.

The second step is the assessment of the **sensitivity** of a system to the perturbations (Adger, 2006), which in the context of this thesis means assessing the response of the main biophysical patterns to changes in climate (Figure 2.4). The response to climate shifts is usually assessed by using a number of hypothetical or GCM/RCM-based scenarios, as inputs to biophysical models (i.e. models simulating components of the biophysical system such as hydrological processes and vegetation growth) to obtain changes to the main patterns (e.g. Metzger et al., 2005). Modeling is currently the best available tool for this purpose due to the complexity and non-linearity of processes involved (Bronstert, 2004). This approach has been successfully applied for hydrology (as reviewed by e.g. Xu and Singh, 2004) and vegetation processes (as reviewed by e.g. Olesen and Bindi, 2002). The approach has also been proposed for soil erosion by Imeson and Lavee (1998), although the scope for the application of erosion models is limited by the poor description of interactions between biological and physical processes; some of the first steps on this research are reviewed by Nearing et al. (2004).

The final step is the assessment of the system's **response capacity** to the perturbations and comparing it with sensitivity (Adger, 2006). Gallopín (2006) assesses this capacity as a function of (i) the system's resilience, i.e. the capacity to maintain its present state in face of perturbations and pressures, and (ii) its adaptability, i.e. the ability to maintain or improve its condition, transforming the present state if necessary (Figure 2.4). In the context of this thesis, the analysis of a system's response capacity requires the answers to two questions:

- is the system resilient to climate change, i.e. is the system able to endure climate shifts without any further enhancement of desertification?

- if not, is the system capable of adapting to climate change, or is there a need for measures to mitigate the effects of desertification drivers, take advantage of new opportunities and cope with the consequences?

As discussed earlier, desertification is manifested when socio-economic exploitation of the biophysical system surpasses their resilience threshold, considering e.g. a certain vegetation

productivity level (Puigdefábregas, 1998). The system's **resilience** can therefore be assessed by determining the current position of the system to thresholds of desertification, and by assessing whether the expected climate shifts are capable of moving the system beyond these thresholds. A major limitation of resilience analysis is the difficulty in establishing thresholds; research on this issue has been hampered by the lack of long-term data for vegetation, land degradation, water resources and soil quality in drylands (Herrmann and Hutchinson, 2005).

One approach to determine resilience consists in evaluating the level of the natural system's goods and services provided to socio-economic systems, using it as a threshold, and assess if climate shifts are sufficient to reduce good and services below that level. The IPCC's fourth assessment report (Fischlin et al., 2007) lists a number of services provided by ecosystems; these include human provisioning services such as water resources and food production, and secondary services supporting the former such as soil fertility primary productivity. Resilience has been analyzed using the biophysical modeling approach described above (e.g. Arnell, 2004; Metzger et al., 2005), usually focusing on human provisioning thresholds. The assessment of secondary services can also be performed using modeling, whose results for biophysical desertification indexes such as vegetation cover or land degradation (e.g. Field et al., 2007) can give an idea of the degree of transformation that is expected to occur under climate shifts. However, the current lack of knowledge on the interactions between some biophysical drivers, particularly land degradation and vegetation cover, poses a very important limitation to this approach (Boardman, 2006). An alternative approach for resilience analysis consists on observing regions where desertification is most intense, registering the state of its biophysical drivers, and evaluating how far other regions are from biophysical thresholds; this is called the climatic transect approach, and has been applied in Mediterranean regions by several authors (e.g. Imeson and Lavee, 1998; Fleischer and Sternberg, 2006).

The socio-ecological system's **adaptive capacity** is usually evaluated through relative indexes, built with a number of surrogate variables obtained from regions with different levels of vulnerability and subjectively evaluated by researchers (e.g. the examples by Smit and Wandel, 2006). This capacity usually refers to measures adopted at the socio-economic level. Gallopín (2006) points to the dynamic nature of a system's adaptive capacity, particularly in the long term, where new strategies can be adopted that increase the system's ability to cope with the consequences of climate change. To take this dynamic into account, researchers have often used model results to hypothesize on a range of possible adaptation measures that can be

adopted by a particular socio-ecological system. Afterwards, he relative merits of each option are assessed in order to recommend some of them (Smit and Wandel, 2006). Instead of assessing the adaptability of the system, this approach highlights methods to improve it.

Overall, biophysical modeling appears as a key tool for vulnerability assessment in climate change studies, as it is the best available tool to assess the magnitude of climate change, evaluate the response of biophysical systems to these changes, assess degrees of transformation, and test solutions to improve the adaptive capacity of the socio-ecological system as a whole. In the desertification context, where the hydrological cycle is considered a major biophysical driver, climate change vulnerability assessment requires the use of models which simulate the impacts of climate change on hydrological variables as well as on processes driven by hydrology, particularly soil erosion and vegetation growth. Given the scope of this thesis, the following section shows a detailed presentation on modeling methods.

2.3.2 Modeling hydrology, soil erosion and vegetation productivity

The predictive ability of hydrological variables, soil loss and vegetation productivity rates has improved steadily in recent decades. Recent models incorporate components both for hydrological and soil erosion prediction, attesting the fact that an accurate estimate of runoff depth and velocity is at least as important as the correct estimation of other soil erosion parameters (Aksoy and Kavvas, 2005). Furthermore, erosion models designed for long-term prediction of erosion rates usually include a vegetation growth modeling component (Morgan and Quinton, 2001). This section will focus on current methods for the coupled simulation of hydrology, soil erosion and (at the long-term scale) vegetation productivity.

The drive for this type of coupled models has been caused in a large part by the uncertainties associated with methods to estimate erosion only, such as the Universal Soil Loss Equation (USLE) approach (Wischmeier and Smith, 1978). The USLE appears to be particularly fallible in Mediterranean regions, where erosion is irregular and depended on a few extreme rainfall and runoff events (Boix-Fayos et al., 2005). Morgan and Quinton (2001) also point to the non-linear relationship between rainfall, runoff generation and soil detachment and transport as a driving force for the creation of complex models capable of simulating the impact of a number of parameters and thresholds associated with these processes. This has led to the development of a number of models in recent decades.

However, these models usually represent the same hydrological and erosion processes; their diversity is mostly due to the method in which they are represented (Favis-Mortlock et al.,

2001). Process representation follows the conceptual models for hydrology and soil erosion described in the previous section; the most common processes and mathematical representations still follow the descriptions made by Huggins and Burney (1982) for hydrological modeling, and Foster (1982) for soil erosion modeling. It is therefore possible to make a comparative analysis of coupled hydrological and soil erosion models, and classify them on the methods used to represent these processes.

Model classification

In a review of recent soil erosion models, Aksoy and Kavvas (2005) summarize a classification system based on different criteria that encompass process description and scale, following earlier work (e.g. Chow et al., 1988). This system is adopted for model classification throughout this section.

In terms of **process description**, the authors differentiate between models based on empirical relationships using observed data, and models based on a conceptual description of water and sediment sources and sinks (also called process-based models). When the latter is formulated using mass conservation equations for water and sediment, it can be classified as physically-based. It should be noted, however, that many process-based models include a number of empirical equations in their framework.

Scale issues in modeling are more complex, and have been discussed by Blöschl and Sivapalan (1995) in terms of observation scales, and by Favis-Mortlock et al. (2001) specifically for hydrological-erosion models. Both authors agree that models usually describe hydrological and erosion processes inside a range of scales. The upper limit of this scale is the model's extent; processes existing above this scale are introduced in the model as constants. The lower scale limit is the model's resolution; processes below this scale are lumped together into either a constant value or a statistical distribution of values. Models are usually classified in terms of both extent and resolution in the spatial and temporal domains.

In terms of **spatial extent**, the authors describe models as (i) hillslope-scale, representing hillslope processes only, and (ii) catchment-scale, representing both hillslope processes and larger-scale gully and channel processes. These scales follow those referred in sections 2.2.2 and 2.2.3, for hydrological and soil erosion processes respectively. It should be noticed that both types of models can be applied to larger areas; in this case, a hillslope-scale model applied to one or several watersheds, but it will only represent hillslope processes.

In terms of **spatial resolution**, the same authors describe the models as (i) lumped, where the resolution is the same as the extent, with no spatial variability allowed, and (ii) spatially distributed, where the spatial variability within the model representation area is simulated. Jetten et al. (2003) further divide spatially-distributed models into grid-based models, dividing the modeling area into a grid of regular cells, and cascade-based models, dividing the area into a cascade of planes and channels, with homogenous areas with different sizes. Key parameters that are usually inserted into these models in a spatially-distributed form are topography (Wollock and Price, 1994; Schoorl et al., 2000; Horritt and Bates, 2001), soil hydraulic properties (Binley et al., 1989 a and b; Fisher et al., 1997) and vegetation cover (Lane et al., 1995). Describing the spatial patterns of these parameters might be as important as estimating their actual values (Grayson and Blöschl, 2001b), and therefore parameters are often aggregated in one easily measurable surrogate parameter (e.g., soil type serving as surrogate for soil hydraulic properties; Refsgaard, 2001). It should be noted that all physically-based models are also spatially-distributed due to the nature of the mass conservation equations (Aksoy and Kavvas, 2005).

One further class found mostly in hydrological models is represented by semi-distributed models (Beven, 2000), where simulation is performed in a lumped fashion but results can be mapped using statistical functions. While there are examples of attempts to use similar methods in erosion modeling (e.g. Vigiak et al., 2006), they remain incipient. It should be noted that, with Geographical Information Systems (GIS), many lumped hillslope-scale models such as the USLE have been applied to larger areas in a spatially-distributed format (De Roo, 1998); remaining lumped models usually predict sediment yield at the watershed scale (van Rompaey et al., 2001).

For the temporal domain and in terms of **temporal extent**, Aksoy and Kavvas (2005) describe models as (i) event-based, if the model is applied to a single rainfall event, and (ii) continuous, if the model is applied to consecutive rainfall events, occurring during a season or longer period. In terms of **temporal resolution**, models can be described as (i) steady-state, if the resolution is the same as the extent, i.e. the model predicts only an average soil erosion rate for the duration of the simulation, and (ii) dynamic, if the temporal variability of hydrological and soil erosion processes is simulated.

Dynamic models pose a problem related with the temporal extent, as the variables governing the long-term temporal variability of hydrological and erosion processes are quite different from those operating within an extreme event (see Table 2.3 and Table 2.7). Morgan and

Quinton (2001) consider that the most important distinction for process-based dynamic models is between the continuous and event-based scale; the former usually incorporate some sort of vegetation modeling component superimposed over the hydrological-erosion model, while the latter consider vegetation cover as a constant value. This scale difference means that continuous models usually do not simulate at the within-event scale, as the inclusion of these processes would make a model too cumbersome; extreme events are often lumped together. In other words, the temporal resolution of continuous hydrological-erosion models usually corresponds to the temporal extent of single-event models, and almost no models currently simulate both scales simultaneously.

While these are the most important distinctions for current models, Aksoy and Kavvas (2005) propose other classification categories. Process description can also be classified into deterministic, when the equations provide for a single prediction for a certain set of input parameters; and stochastic, where one input parameter set leads to a suite of results according to a probabilistic distribution. Current hydrological-erosion models are usually deterministic. There are also differences related with the technique of solution, related with the number of spatial dimensions considered (fully 2-D or 1-D approximations), the incorporation of fixed rill structures, or the inclusion of multiple sediment size classes in the simulations.

Table 2.8 shows a representative sample of current hydrological-erosion models, classified according to the criteria defined above. The large amount of combinations between process description methods and spatio-temporal representations stands out, reflecting the diversity of research and practical problems for which these models were developed. Hydrological-erosion models are usually adapted for a particular scale, outside of which their performance is uncertain or their applications is difficult, hence this diversity in process representation (Blöschl and Sivapalan, 1995; Favis-Mortlock et al., 2001). It should also be noted that, as stated above, all the 3 referred dynamic continuous models incorporate vegetation cover dynamics via a biomass growth modeling component.

Furthermore, several models present additional advantages and limitations not shown in the table and often not explicitly referred in the literature (Favis-Mortlock et al., 2001), such as:

- different design options can lead to different advantages and disadvantages – e.g. cascade models require less computational power than grid-based models, but erosion patterns inside each plane element are not simulated and problems may arise when applied to regions with high spatial heterogeneity of erosion rates (Jetten et al., 2003);

- some models are designed for the processes occurring in a determined region and could be difficult to apply elsewhere – e.g. the STREAM model is designed for the loess soils of northwestern Europe and therefore puts a high emphasis on soil crusting processes for runoff generation while disregarding others (Cerdan et al., 2002);

- particular research questions have guided the design of some models, and their applicability to other questions could suffer – e.g. the LISEM model is explicitly designed to simulate well-studied catchments smaller than 50 km^2 in high detail, leading to a complex description of erosion processes which can be a hindrance when applying the model to larger, poorly-studied catchments (Jetten and De Roo, 2001).

Table 2.8 – Representative sample of current hydrological-erosion models.

Model	**Process description**	**Spatial extent**	**Spatial resolution**	**Temporal extent**	**Temporal resolution**	**Reference**
RUSLE[a]	Empirical	Hillslope	Lumped	Continuous	Steady-state	Renard et al., 1997
STREAM	Empirical	Watershed	Distributed (grid-based)	Single event	Steady-state	Cerdan et al., 2002
SEDEM	Empirical	Watershed	Distributed (grid-based)	Continuous	Steady-state	Van Rompaey et al., 2001
MMF	Empirical	Watershed	Distributed (cascade)	Continuous	Steady-state	Morgan, 2001
PESERA[b]	Process-based	Hillslope	Distributed (grid-based)	Continuous	Dynamic	Mantel et al., 2003
WEPP[b]	Process-based	Hillslope	Distributed (cascade)	Continuous	Dynamic	Flanagan and Nearing, 1995
SWAT[b]	Process-based	Watershed	Distributed (cascade)	Continuous	Dynamic	Neitsch et al., 2002
EROSION3D	Process-based	Watershed	Distributed (grid-based)	Single event	Dynamic	Schmidt et al., 1999
LISEM	Process-based	Watershed	Distributed (grid-based)	Single event	Dynamic	De Roo et al., 1996a and b
ANSWERS	Process-based	Watershed	Distributed (cascade)	Single event	Steady-state	Beasley et al., 1980
EUROSEM	Process-based	Watershed	Distributed (cascade)	Single event	Dynamic	Morgan et al., 1998
KINEROS2	Process-based	Watershed	Distributed (cascade)	Single event	Dynamic	Smith et al., 1995

a – hydrological processes not represented.
b – vegetation biomass growth component included.

These issues require the attention of hydrology and erosion modelers. Favis-Mortlock et al. (2001) recommend a careful analysis of the research area and problem to be studied before selecting a particular erosion model. In the particular case of vulnerability assessment for Mediterranean regions, the recommendations and restrictions described in the previous section should be carefully taken into account.

Model intercomparison and selection

The performance and capabilities of different hydrological and erosion models has been compared in a number of recent works. One of the most comprehensive was performed under the International Geosphere–Biosphere Programme (IGBP), inserted in the Global Change and Terrestrial Ecosystems (GCTE) project. The GCTE's Soil Erosion Network held two model comparison workshops in 1995 and 1997 under the title "Global Change: Modelling Soil Erosion by Water"; the first workshop focused on the application of hillslope-scale models, while the second focused on modeling at the watershed scale. The main results of these workshops were synthesized by Jetten et al. (1999, 2003).

The evaluations involved the joint application of a number of models referred in Table 2.8, including RUSLE and WEPP at the hillslope scale, and EROSION3D, LISEM, EUROSEM and KINEROS2 at the catchment scale, as well as other models. Participants were modelers with a high experience in applying one or more of the referred models. They were given a common dataset, split into a "training set" and a "testing set" of data; for the "testing set", measured values of runoff and erosion were withheld from the modelers, to be used in the final model evaluation. The hillslope scale workshop used 73 plot-years from seven sites in three countries; the catchment scale workshop used data for 10 events on a 40 ha agricultural catchment in the Netherlands. Jetten et al. (1999) list the main conclusions from both workshops in terms of model performance, as follows:

- model performance depends on both the quality of numerical input data and the availability of "soft" (qualitative) information such as existing agricultural practices and their impacts on soil structure, as well as the modeler's familiarity with the model and study area;

- the performance of most tested models is greatly improved by calibration, particularly if it is done for a wide range of rainfall conditions, with most of the calibration effort focusing on soil water content and associated hydrological parameters;

- most models predict total runoff discharge better than peak runoff discharges, with the worst performance for sediment detachment and transport, and relative model results – the correlation between observed and predicted values – are usually better than absolute results;

- the quality of model results decreases with increasing temporal scale: models perform better for longer time periods, and continuous models in particular perform best in simulating long-term averages;

- similarly, the quality of model results decreases with increasing spatial scale: models perform better for catchment outlet prediction than for within-catchment runoff and erosion patterns.

Overall, the performance of hydrological and erosion models appears to decrease with the increase in complexity of the simulated processes, independent of the model being studied. This could reflect the uncertainty in the mathematical description of erosion processes, as well as the non-linear nature of soil erosion, as significant differences can even be found in erosion measurements from apparently identical test plots (Nearing, 2000; Jetten et al., 2003). Jetten et al. (1999) point out that input data quality, calibration procedures and the knowledge of modelers can be more important than model structure for successful hydrological and erosion model application. Furthermore, increased model structure complexity – in terms of both process description and spatial and temporal discretization – does not lead to improved model performance. Jetten et al. (2003) link this with the uncertainty associated with the input parameters required by complex models, which propagate through the model calculations and often lead to a greater uncertainty in the results without providing additional predictive power.

This assessment raises the issue of the need to accommodate complexity in physically-based models, which is determined by the requirements of model application, i.e. the questions for which answers are needed (Jetten at al., 1999), such as:

- spatial and temporal scale studies – models usually perform better at the scale they were designed for, e.g. event-scale models give better peak discharge predictions than continuous models simulating events as a lumped phenomena, but perform worse in estimating long-term averages;

- analysis for changing conditions – process-based models can accommodate process changes that do not currently occur, while simple empirical models are constrained by current processes.

These issues were discussed by Jetten et al. (2003) using the spatial prediction of erosion patterns as an example. Complex spatially-distributed models might perform as well as lumped models for predicting sediment export from a watershed, but they also provide information on the spatial patterns of erosion and sedimentation, which is arguably more important since it allows the effective design and implementation of erosion control measures. In this regard, grid-based models are potentially more effective than models using other spatial discretization schemes (see the previous section) due to the spatial heterogeneity associated with erosion rates. Despite the failings of current grid models in predicting erosion patterns, particularly at finer scales, these results represent a significant added value over hillslope-scale or cascade-based models, even if they can at best represent an assessment of relative erosion risk.

Overall, these results indicate that it is difficult to point to the superiority of one or a few of the existing hydrological and erosion models. Model selection criteria include the research questions being asked, the characteristics of the study area, and the research data available to carry out the study. Selecting models with parameterization requirements which largely exceed available data could result in additional uncertainty instead of additional predictive ability. On the other hand, modelers should make an effort to select a model structure which represents the processes operating in the catchment; Jetten et al. (1999) provide an example of catchments dominated by slow throughfall mechanisms which cannot be adequately simulated by most of the currently existing runoff and erosion models.

In some cases, the cross-scale nature of the processes dominating a watershed could point to the use of a multi-scale modeling framework, where appropriate models are used to represent different processes with appropriate degrees of complexity. Some existing modeling studies have used this approach; for example, Boulain et al. (2006) coupled an extreme event and a seasonal-scale model to study the impacts of short-term hydrological variability, typical of semi-arid environments, in vegetation biomass productivity, and Panagoulia and Dimou (1997a and b) used a similar approach to study relationships between short-term processes such as runoff and soil moisture, and longer-term processes such as snowmelt. While there is a lack of these studies incorporating soil erosion processes, this approach could be useful in e.g. studying be the interaction between vegetation growth – operating at the seasonal scale –

and soil erosion at the extreme event scale. It could also be facilitated due to the already widespread distinction between extreme-event and long-term hydrological-erosion models (Morgan and Quinton; 2001).

In the scope of this thesis, the description of hydrological and erosion processes in Mediterranean regions (described in section 2.2), the interactions with vegetation cover, and the potential impacts of climate change will inform the selection of models to carry out the analysis. In this context, it should be noted that, for rainfall-runoff simulation, spatially-distributed models with physically-based equations have been shown to have better overall accuracy than models with either a lumped or an empirical approach in regions with high climatic variability, possibly due to the high spatial and temporal variability of the processes involved (Wu et al., 1993; Lidén and Harlin, 2000).

2.3.3 Recent modeling studies of climate change impacts

There has been a significant research effort in recent years to estimate the impacts of climate change on hydrological processes and vegetation biomass growth. This effort has often been done under international cooperation processes such as the IGBP-GCTE, often in a larger context of vulnerability studies. Overall, most of the modeling studies analyze Mediterranean regions in the context of European and Global scale studies; few efforts have focused on the regional and local scale. Furthermore, few studies of any kind have been performed for soil erosion, possibly because of the uncertainty related with the processes driving soil erosion coupled with the limited amount of information on the consequences of climate change for extreme weather events (Michael et al., 2005). This results in a poor understanding and quantification of the consequences of climate change for desertification drivers in Mediterranean regions, particularly at the smaller spatial and temporal scales.

Nevertheless, existing results can provide a picture of the general trend for these variables as well as indicate the response magnitude, with the possible exception of soil erosion. Recent examples of climate change impact studies were described by Xu and Singh (2004) for water resources and Nearing et al. (2005) for soil erosion and vegetation interactions. In most cases, they are restricted to a number of scenarios supported by GCM results, overlooking the uncertainty associated with them and therefore subordinating the validity of their results to the validity of the climate scenario assumptions (Beven, 2000; Bronstert, 2004). However, some studies have approached the uncertainty in climatic predictions by assessing the sensitivity of watersheds to gradual changes in climate parameters. While this method has focusing mostly in hydrology (Xu and Singh, 2004), its use for integrated hydrology, soil erosion and

vegetation productivity studies have been less common. One study of this kind was performed by Pruski and Nearing (2002), who simulated the response of hillslopes with different soil types and vegetation covers to changed rainfall intensities and amounts. Their results showed that surface runoff and soil erosion are, in most cases, highly sensitive to changes in rainfall, changing by up to 2.5 % per 1 % change in rainfall. These studies applied a number of different methods for impact assessment; the following section systematizes the most common approaches used in modeling studies.

Modeling analysis methods

The number of climate change modeling studies in recent years has allowed for the emergence and consolidation of standard methodologies, at least for hydrological predictions. According to a recent review performed by Xu and Singh (2004), a common problem is the mismatch between the processes and scales where GCMs provide better results, and those which are more important for water resources assessment; typical gaps are shown in Table 2.9. A comparison of this data with the description provided in the previous section, and in particular with Figure 2.3, shows that GCM performance is worse for the processes occurring at the catchment scale, particularly for surface processes.

Table 2.9 – Mismatch between the capabilities of current GCMs and hydrological assessment requirements (adapted from Xu and Singh, 2004).

GCM ability	**Best**	**Intermediate**	**Worst**
Hydrological importance	**Lesser**	**Intermediate**	**Greater**
Spatial scales	Global 500 × 500 Km	Regional 50 × 50 Km	Local 0-50 Km
Temporal scales	Mean annual and seasonal	Mean monthly	Mean daily
Vertical scales	500 hPa	800 hPa	Earth surface
Hydrological parameters	Wind Temperature Air pressure	Cloudiness Precipitation Humidity	Evapotranspiration Runoff Soil moisture

To surpass these gaps, a number of methods have been applied in climate change assessment analysis, as schematized in Figure 2.5 following Xu and Singh (2004). One method is to directly use hydrological outputs from GCMs, which usually results in very significant problems associated with the incomplete description of surface hydrology by these models.

However, there are some encouraging experiments with Macroscale Hydrological Models (MHMs) coupled with GCMs, and the next generation of climate models is expected to be more accurate in hydrological simulation (Huntingford et al., 2006). According to Xu and Singh (2004), the remaining methods downscale GCM results and transform these into climate scenarios to input in hydrological models. Downscaling methods include:

- dynamic downscaling using RCMs – where GCM results are used to force regional simulations of climate change at finer spatial and temporal scales, the results of this simulations being subsequently used to force hydrological models;

- statistical downscaling – where GCM results are downscaled using a statistical analysis of the relationship between GCM "control" runs (for current conditions) and the observed climate patterns in a given location;

- hypothetic – where GCM results are used to provide a range of possible changes to climate variables, with a subsequent perturbation of current climate conditions with several degrees of change in order to obtain a response function of hydrological variables to changes in climate parameters, in effect studying the hydrological sensitivity to changes in climate given a reasonable interval.

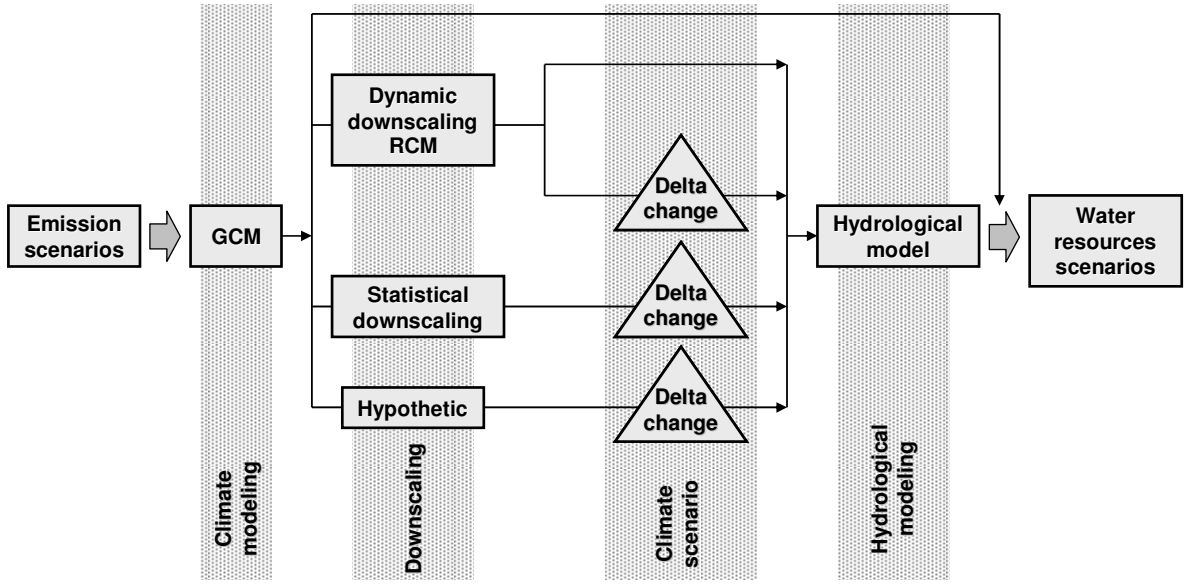

Figure 2.5 – Schematic representation of methods to assess the impacts of climate change on water resources (adapted from Xu and Singh, 2004).

Figure 2.5 also shows methods to transform GCM results into climate scenarios, either by directly using GCM or RCM outputs (constrained by the quality of model results, usually assessed by comparing "control" run results with current climate patterns) or by calculating the degree of change (i.e. "delta change") in climate parameters estimated by the downscaled GCM results and applying this change to current climate datasets, thereby reducing the impact of GCM model uncertainty in the design of future climate scenarios.

These methods have also been applied to analyze the impacts of climate change on soil erosion, although the literature on this subject is still scarce. Examples of dynamic downscaling studies for soil erosion include the work by Mantel et al. (2003), who used the results for Europe of the HadRM3 RCM for one climate change scenario to force the PESERA erosion model. For statistical downscaling studies, Zhang and Nearing (2005) applied climate changes predicted for Oklahoma by a GCM to a stochastic weather generator, using the results to drive the WEPP erosion model. A different statistical method – focusing on extreme events – was applied by Michael et al. (2005), downscaling GCM rainfall predictions to a time series with 5 min resolution for the most significant extreme events, which was used to force the EROSION3D event erosion model for a catchment in Germany. Finally, the hypothetic method was applied by Pruski and Nearing (2002) for slopes in three regions of the USA; a stochastical weather generator was used to perturb current rainfall patterns in 10 % increments (positive and negative) with the resulting climate series used to force the WEPP model, obtaining a measure of the sensitivity of soil erosion to changes in rainfall patterns. It should be noted that all of the above studies also simulated changes to vegetation biomass production (albeit only superficially in the case of Michael et al., 2005).

Modeling studies for impacts on hydrological processes

The study of climate change impacts on hydrology in the Mediterranean has been given some attention in recent years, particularly in studies dealing with the region as a whole or as a subset of a wider study area – usually Europe or the world. As described in section 2.2, the expected reduction in rainfall coupled with higher average temperatures is expected to reduce runoff rates in the Mediterranean region. Nohara et al. (2006) studied the impacts of the A1B climate change scenario (Table 2.1) on surface runoff and river discharge at the global scale, applying the climate predictions of 19 GCMs to a MHM and constructing predictions from a weighted model result average in order to take into account uncertainties in climate prediction. Starting from an estimated rainfall reduction in the Mediterranean region of c. 360 $mm.y^{-1}$, their main results suggest:

- a decrease in evapotranspiration of 30 to 70 mm.y^{-1}, due to less water availability in the soil;

- a decrease in surface runoff of 70 to 180 mm.y^{-1}, particularly in the northern Mediterranean regions;

- a decrease in river flow of 10 to 40 %, particularly in the northern Mediterranean regions, due both to reduced surface runoff and surface water retention in river reservoirs.

One important impact of climate changes in the Mediterranean is a shift in the allocation of available rainwater to replenish soil water storage at the expense of surface runoff. Therefore, the results predict an increase of the importance of evapotranspiration in the hydrological balance, and therefore proportionally larger impacts in surface water resources. The authors also point out that the Mediterranean regions are expected to suffer the greatest reductions of surface runoff at the global scale, together with southwestern regions of north and south America, where Mediterranean climates are dominant. These results for the Mediterranean region agree with those reported by Wetherald and Manabe (2002), who used an ensemble of 8 GCMs to provide climate forcing for a MHM based on the IS92a emission scenario (roughly equivalent to the B2 scenario; Table 2.1). The results point to a decrease of surface runoff in the Mediterranean rim of c. 40 mm.y^{-1}; the smaller rate when compared with the results by Nohara et al. (2006) can be attributed to the smaller magnitude of climate change. Wetherald and Manabe (2002) also suggest a reduction of soil moisture in the northern Mediterranean of 10 to 20 % during spring and summer, with the Iberian peninsula experiencing the greatest rates of decrease which extend over most of the year. Finally, the authors also point out to a shift in the allocation of rainfall towards evapotranspiration.

These results point to an increase of water stresses in Mediterranean regions. This increase appears to be directly dependent on the magnitude of climate change, with greater changes leading to a reduction of surface runoff soil moisture during most of the year to levels which could induce the outward expansion of deserts to the surrounding regions (Manabe et al., 2004). Arnell (2004) has used the results of 6 GCMs, coupled with a MHM to predict the impacts of climate change on water stress. Using a threshold of 1000 m^3.hab^{-1}.y^{-1} for water stress, the author predicts an increasing trend for people living in water-stressed regions in western Europe (mostly located in the Mediterranean rim), with an increase above current numbers of 90 % in the B2 emission scenario and of 130 % in the A2 scenario.

The research cited above, however, was conducted mostly at a coarse spatial and temporal scale. Regional and local studies, particularly those focusing on extreme weather events, remain scarcer. Avila et al. (1996) applied the MAGIC hydrochemical model to a small forested catchment in northeast Spain using a hypothetical scenario with a 4 ºC increase and a 10 % rainfall decrease, leading to a shift in the hydrological balance towards more evapotranspiration and a sharp concentration increase in stream water chemistry. Bathurst et al. (1996) used downscaled results from a GCM, considering a doubled concentration of atmospheric CO_2, to force the SHETRAN hydrological model which was applied to two semi-arid catchments in the Iberian peninsula. For a rainfall reduction of 10 to 17 %, the authors report a reduction in runoff of 15 to 55 % accompanied with a significant shift of rainfall allocation to evapotranspiration. These results indicate that those obtained for the Mediterranean region as a whole will be reproduced at the medium catchment scale.

More recently, Cunha et al. (2002 and 2006) analyzed the impacts of a number of downscaled climate change scenarios from the HadCM3 GCM, for surface runoff in 62 Portuguese catchments. The catchments represent a large variety of Mediterranean climates, ranging from humid to semi-arid; a simplified version of the Stanford Watershed Model was used to estimate changes to hydrological parameters. The scenarios consider an overall temperature increase coupled with a decrease in rainfall which is greater in the semi-arid regions, following a doubling of atmospheric CO_2 concentration (Cunha et al., 2002) and the A2 and B2 emission scenarios (Cunha et al., 2006; Table 2.1). The main results were:

- for the double CO_2 scenario, runoff decreases from 10 % in the humid region to 50 % in the semi-arid region;
- for the B2 scenario, runoff increases of 10 to 20 % due to larger winter rainfall;
- for the A2 scenario, larger runoff reductions, going down by 15 % in the humid region to 80 % in the semi-arid region;
- changes occurring mostly from spring to autumn, with smaller changes in winter where, in the humid region, runoff could remain at current levels or increase slightly.

These changes are coupled with a significant drop in groundwater recharge even where runoff increases (Cunha et al., 2006). The results also exemplify the uncertainty associated with different climate change scenarios, with runoff predictions ranging from an increase of 20 % to a decrease of 80 %. Furthermore, while the authors refer a probable maintenance or

increase of current flood risks, no modeling analysis has been made. This lack of analysis of changes to Mediterranean river flow regimes, particularly to extreme flows, represents a major gap in modeling studies. Overall, the work by Cunha et al. (2002 and 2006) highlights the impact of climate change at the regional and local catchment scale. The main additional result is a prediction of increasing spatial and temporal variability of runoff within Mediterranean regions and seasons.

Impacts on soil erosion

In contrast with hydrology, there have been few soil erosion modeling studies both at the global scale and for Mediterranean regions. Michael et al. (2005) point to the high spatial and temporal variability of soil erosion processes, when compared with the low spatial and temporal resolution of GCMs and current climate downscaling approaches, as a major obstacle preventing the realization of these studies. One European-wide approach was performed by Mantel et al. (2003), who applied the PESERA soil erosion model using a climate scenario based on the HadRM3 RCM considering the A2b emissions scenario (Table 2.1). Their results for the semi-arid southern part of the Iberian peninsula point to an overall decrease in soil erosion rates. However, this is coupled with a change in erosion patterns, leading to an increase in the area for which significant erosion risk is expected, coupled with a great decrease in soil erosion rates for the rest of the study area. Nevertheless, the overall erosion rates remain low, in the order of 0.5 to 1 $ton.ha^{-1}.y^{-1}$.

The results of this study must be analyzed in light of the model's poor performance for Mediterranean regions. In a study of the PESERA model performance, Van Rompaey et al. (2003) report that the model results for sediment yield in Italy and Spain have a poor correlation with observed values, which is underestimated by a factor of two; this contrasts with the acceptable model results for agricultural areas in northern and central Europe. The authors attribute these errors to the low resolution of altimetry used in the study, coupled with errors in the climate and land-use databases used to run the model. For the Mediterranean region in particular, the authors point to another problem in assessing the role of large-scale processes such as gully and channel erosion and deposition, which are the dominant processes in this region (an issue previously discussed in section 2.2). Nevertheless, the study results point to an increase in erosion heterogeneity at the hillslope scale, revealing the need of local studies for climate change impact assessment.

At the catchment scale, one of the few published studies was performed by Bathurst et al. (1996) who used downscaled results from a GCM, considering a doubling of CO_2

concentrations, to force the SHETRAN model. The model was applied to two semi-arid catchments in the Iberian peninsula, with the results point to a reduction of 25 to 50 % in soil erosion rates. However, this study also did not consider changes to gully erosion rates; furthermore, changes in vegetation cover were not taken into account. The impact of these changes can be illustrated by the results reported by Nearing et al. (2004) for the USA, who suggest that lower rainfall rates can lead to increased soil erosion through a reduction of vegetation cover. Overall, the low number of modeling studies prevents an assessment of the impact of climate change on soil erosion rates in Mediterranean regions. In particular, and considering the potential impacts of climate change discussed in section 2.2, there is a lack of integrated studies of impacts in vegetation cover and soil erosion at all levels, as well as detailed studies on the impacts of changes to the frequency and intensity of extreme events, particularly for gully erosion rates.

Impacts on vegetation biomass productivity

As stated in the previous sections, the assessment of changes to vegetation cover is essential when studying changes to soil erosion rates, which makes a review of existing studies pertinent even if the detailed prediction of this phenomena falls beyond the scope of this thesis. While there have also been a number of studies of the impacts of climate change on vegetation biomass productivity in recent years, they have focused both on the European and Mediterranean scale, and on the very small scale considering a single or limited number of plants. As referred in section 2.2, climate change is expected to impact vegetation productivity in the Mediterranean due to increased atmospheric CO_2, rising temperatures and lower water resources, with greater changes for cultivated species. An example of modeling studies of these effects is given by Morales et al. (2007). The authors applied the LPJ-GUESS ecosystem model using a suit of RCM-based scenarios for Europe in 2100, aiming to predict the balance of impacts between changes in temperature, rainfall and atmospheric CO_2 concentrations on ecosystem productivity. Their results indicate that:

- rising temperatures and CO_2 concentrations will increase Net Primary Production (NPP) throughout Europe, but with significant spatial variability, with the Mediterranean region registering the smallest increases;
- many ecosystems in the Mediterranean are expected to suffer a decrease in NPP under climate change, with some switching from carbon sinks to sources;

- this NPP decrease can be mostly attributed to a deteriorating water balance, resulting from a decrease in rainfall.

The authors also point out to the great uncertainty in scenario estimates, with the most significant differences attributable to different GCM results (being greater than differences attributable to emission scenarios). Other authors have looked separately at impacts on cultivated species and rangelands. Olesen and Bindi (2002) reviewed the impacts of climate change on agriculture throughout Europe, concluding that NPP is dependent on the balance between advantages and disadvantages caused by climate change (as described in section 2.2), but with the disadvantages will predominate in southern Europe. The increase in extreme weather events and water shortages is expecting to lead to a 16 % drop in wheat productivity and a 36 % drop in maize productivity, for a double CO_2 scenario, leading to an expected trend of agricultural extensification in the Mediterranean rim. Metzger et al. (2005), in the context of a vulnerability assessment analysis, obtained similar results for crop production and showed an significant negative impact on the livelihood of Mediterranean farmers. In contrast, Cheddadi et al. (2001) used the BIOME3 model to predict the distribution of rangelands in the Mediterranean, and found a trend for the increase in the regions dominated by xeric woodlands and scrub, particularly when considering a drop in rainfall.

Morales et al. (2007) point to the need of regional studies to assess the full scope of regional variability on the climate change impacts on NPP. In a recent work on the impact of climate changes for Portugal, Pinto et al. (2006) studied impacts on agricultural productivity, while Pereira et al. (2006) assessed impacts on forests. Pinto et al. (2006) considered two climate scenarios based on the A2 and B2 emissions scenario (Table 2.1), using predictions by the HadRM3 RCM to force the models CERES and CROPGRO for four cultures – wheat, maize, rice and pastures. The results are similar to those reported by Olesen and Bindi (2002); generally speaking, they point to a decrease in crop productivity of 11 % for wheat, 26 % for maize and 70 % for rice, considering the A2 scenario, with less severe changes for the B2 scenario. Furthermore, the impacts on wheat productivity – the most important culture in the dry regions of Portugal – are more severe in drylands than in the humid climates. As for pastures (which can be considered a kind of managed rangeland), the authors predict an increase in productivity of 10 to 13 % in both scenarios. For forests, Pereira et al. (2006) used a climate scenario based on double CO_2 concentrations downscaled with the HadRM2 RCM, the results of which were used to force the GOTILWA+ vegetation growth model for eucalyptus, pine and cork oak in several Portuguese regions. The impacts also show a great

heterogeneity between humid and dry regions, with productivity tending to increase in the former while tending towards decrease in the latter, mostly due to lower water availability. These impacts are expected to be less severe for cork oaks, which are more adapted to low water availability environments.

Overall, the work by Pinto et al. (2006) and Pereira et al. (2006) confirm the impacts of climate change at the local scale, but also reveals an increase in spatial heterogeneity for vegetation productivity such as the one predicted for hydrological parameters (as previously discussed). The general trend appears to be an increased climate aridity in the semi-arid regions. Arribas et al. (2003) studied the impacts of a decrease on vegetation cover for climate using the PROMES RCM; their results suggest that a reduction in vegetation productivity could increase temperature and decrease rainfall, particularly in summer, pointing to a positive feedback loop in which the reduction in vegetation NPP due to greater climate aridity would reinforce arid conditions. Furthermore, the more arid conditions could also increase the risk of vegetation disturbances such as droughts and forest fires, with a positive feedback for reducing vegetation productivity. Mouillot et al. (2002) simulated the impacts of climate change in the vegetation dynamics of Mediterranean shrublands and forests, applying the SIERRA model with hypothetical scenarios based on GCM results. Assuming an increase in drought and wildfire frequency, the model results point to increased drought adaptability by reduced productivity and water use during drought periods, coupled with an increase in the shrubland vs. forest ratio as a strategy for wildfire adaptation, with a consequential loss in the ecosystem's productivity.

The regional studies have been coupled with a number of in-depth modeling studies focusing on single plants or vegetation clumps, often driven by the need to quantify future changes to the carbon balance in Europe. Pinto and Brandão (2002) used the CERES crop model to predict the impacts of a double CO_2 climate change scenario on wheat and maize productivity in a semi-arid Portuguese cropland; while productivity was expected to drop by c. 30 %, these conditions could be mitigated using irrigation, and an adaptation of cultivation practices to take advantage of increased winter temperatures could lead to higher crop productivity (if irrigation could be sustained). Martínez-Vilalta et al. (2002) used a hydraulic model with hypothetic climate scenarios to study the impacts of climate change on Mediterranean trees and shrubs; their results indicate that, while sclerophyllous trees appear to be more resistance to water stress than shrubs under current climate conditions, they also appear to be near the limit of their water stress tolerance, and an increase in drought frequency and severity due to

changes in climate could lead to an increase in tree mortality and consequentially a dominance is sparser shrub communities. On the other hand, Davi et al. (2006) suggest a better climate change response of sclerophyllous trees when compared with evergreen pines. The authors used the CASTANEA model coupled with the ARPEGE GCM for the B2 emission scenario (Table 2.1) to simulate changes in the NPP of several Mediterranean forest sites, with results pointing to an increase of NPP for sclerophyllous trees and an NPP decrease for evergreen pines due to the former's advantages caused by the lengthening of the foliated period. The results by these authors illustrate the level of detail on which current impact studies are focused.

Overall, modeling studies of vegetation dynamics for the Mediterranean appear to cover most of the expected impacts of climate change at the regional scale, but there is a lack of smaller-scale studies on the variability of these impacts. Furthermore, there are still gaps in the studies of native Mediterranean species, particularly permanent agricultural species such as vines and olive trees.

2.3.4 Limits of modeling approaches

The limits of modeling studies in estimating the impact of climate changes have received some attention in the recent literature, resulting in part from the effort to evaluate model capacities for climate change science. Criticism has focused on the models themselves, the way they are parameterized and assessed, and their applicability under changed boundary conditions. Alternative methods for impact assessment have been suggested, but they have not proven to have the same predictive capacities and usefulness as models when applied in a correct way (Bronstert, 2004). However, modeling studies must be designed taking limitations into account. This section focuses on the coupled simulation of hydrology and erosion.

Model limitations

The performance of current erosion hydrological and models suffers from a number of limitations. Traditional approaches such as the USLE and its revised version (RUSLE) are not capable of accurately estimating soil erosion rates, particularly for regions outside the original application domain in the eastern USA (Boardman, 2006). However, more recent models also suffer from a number of inadequacies. In a recent review of the status of soil erosion science, Boardman (2006) reports that the development of complex process-based models has not yielded significant improvements in the predictive capacity of soil erosion.

One problem is related with the lack of knowledge on erosion processes, and their representation in erosion models. Jetten et al. (2003) point to the high temporal and spatial variability of soil erosion processes, which is insufficiently described by the parameters commonly used in erosion assessment. This poses a fundamental limit on the expected accuracy of erosion models built using current knowledge. Nearing et al. (1999) and Nearing (2000) analyzed this problem with an evaluation of erosion measurements taken from replicate plots, i.e. erosion plots located side by side which are considered identical in terms of the parameters driving soil erosion. They found significant differences between plots, averaging 50 % for the whole data set but rising significantly (up to more than 100 %) when considering the smaller events. This value can be taken as an empirically-based limit on the capacity of current models for erosion prediction at the field scale. Similarly, De Vente and Poesen (2005) point to the complex interactions between different hydrological and erosion processes at the catchment scale that are often poorly understood and difficult to model.

This problem is even more significant in Mediterranean watersheds, due to a lack of representation of significant processes by current models. Boardman (2006) point to two significant problems:

- the common representation of runoff generation through infiltration excess, whereas in Mediterranean catchments the role of saturation excess is very significant;

- most erosion models were developed based on data collected from experimental plots and therefore focus on rill/interill erosion processes, whereas gully erosion processes can be responsible for most of soil erosion processes in Mediterranean environments.

The role of saturation excess runoff generation and gully erosion processes in Mediterranean catchments was discussed in detail in section 2.2. In particular, misrepresentation of gully erosion has prevented accurate estimates of catchment scale erosion rates (De Vente and Poesen, 2005), and current gully erosion modeling technology is still not capable of making useful predictions (Jetten et al., 1999; Nachtergaele at al., 2001). De Vente et al. (2006) have linked this problem with a wider failure of current erosion models to accurately represent sediment sources and connectivity in Mediterranean basins.

Another problem pointed by Boardman (2006) and several other authors (e.g. Favis-Mortlock et al., 2001; Morgan and Quinton, 2001; Jetten et al., 2003) is the mismatch between the data requirements and complexity of process based models, and their capacity to answer the

questions posed by model users. Despite improved spatial and temporal discretization and more complex process description, the results of the more complex models are highly variable and very sensitive to input parameters (Wu et al., 1993; Jetten et al., 1999, 2003). Jetten et al. (2003) describe this problem as overparameterization; model performance decreases significantly with uncertainty in defining key parameters, either because of sampling errors or difficulties in estimation, up to the point where uncertainty in parameterization overshadows the greater predictive power of these models. The non-linear nature of runoff and erosion processes themselves and their mathematical descriptions further exacerbates this problem by propagating input data errors throughout the model (Morgan and Quinton, 2001; Jetten et al., 2003). Overparameterization appears to be a common problem of complex models and has also been observed in stand-alone hydrological models (Jakeman and Hornberger, 1993; Thiemann et al., 2001).

As described previously, these limitations should be taken into account during model selection for a particular study. Jetten et al. (2003) recommend achieving a balance between model complexity and available data; models should limit themselves to describing the most significant erosive processes in their intended region of application, making the most of existing data and knowledge to avoid parameterization uncertainty. However, Boardman (2006) reports that these problems which are perceived and discussed by modeling experts are often not appreciated by users, leading to a major problem in model misapplication. Recent models often provide convincing map outputs which may mislead users as to their accuracy; Favis-Mortlock et al. (2001) refer the risk in believing that an erosion model can be used for assessing erosion rates, while in fact it is only capable of screening a region for the relative risk of erosion. However, and in spite of recent proposals for substantial changes to the framework behind most catchment models (e.g. Beven, 2002; Sivapalan et al., 2003), the models described above still represent the best available technology for hydrological and erosion prediction in watersheds.

Calibration and validation for climate change scenarios

As described above, models generally require improvement via calibration of input parameters, and results must be assessed through a validation procedure. Calibration and validation is difficult for current conditions, particularly for complex process-based models requiring large amounts of input data. One typical problem is the lack of measured data at the appropriate scale used by the model; for example, in many cases the only available data for validating spatially distributed models is collected at the catchment's outlet, with no

additional information of within-basin runoff and erosion processes. Models validated in these conditions often fail to reasonably reproduce within-catchment patterns of runoff and erosion, providing correct results at the larger scale through an incorrect simulation of smaller-scale processes (Beven, 2000; Boardman, 2006). Another common problem in calibrating complex models is parameter equifinality, where different sets of model parameters provide equally good results, making the selection of a unique parameter set that best describe the catchment dynamics difficult (Beven, 2000; De Vente and Poesen, 2005). A final problem is over-calibration; Quinton (1997) suggests that methods to reduce model predictive uncertainty for a number of measurements, e.g. through better parameterization, may actually reduce model performance for the remaining measurements as model calibration can become excessively conditioned by a small sample of observations.

Insufficient calibration and validation of models can have a direct impact in their robustness. Toy et al. (2002) define a robust model as a model able to reasonably perform with similar parameter values, including highly dynamic ones, for the widest possible range of conditions. Models usually perform best for the range of conditions for which they were calibrated (Favis-Mortlock et al.; 2001); therefore, calibrating and validating a model for future conditions presents a number of additional problems. Apaydin et al. (2006) refer that calibrated model parameters can have limited transferability in time, particularly in face of significant changes to climate parameters or watershed conditions. Furthermore, Wilby (2005) refers the problems associated with parameter equifinality, where parameter sets performing equally well for current conditions can lead to significant differences in climate change predictions. These calibration and validation problems for uncertain future conditions call into question the robustness of runoff and erosion models for climate change analysis (Beven, 2000; Morgan and Quinton, 2001).

Xu and Singh (2004) propose that models used for climate change studies must demonstrate an increased degree of robustness considering both current conditions and those closer to possible changes. For example, a model intended to simulate stream flows in a dryer climate scenario should be calibrated using a wet set of rainfall records and validated for a dry set, thus demonstrating its ability to handle the wet/dry transition. Further validity can be demonstrated by calibrating the model for one catchment and validating it for another. Similarly, Bronstert (2004) proposes that the model must demonstrate their ability to represent both current and altered internal dynamics of the catchments. This can be achieved by multi-catchment validation, i.e. validating the model for several catchments with different

internal dynamics and dominant processes, thus increasing confidence in its ability to represent changes in these systems. A further option is multi-process validation, i.e. to validate the model for the highest possible number of catchment variables such as soil moisture or the different runoff components. This final approach has also been proposed by Ebel and Loague (2006) to tackle the problem of parameter equifinality.

These solutions to improve model robustness require an increase in the data used for the calibration and validation process. Unfortunately, this contrasts with the generally poor availability of data; hydrological data is often only available for catchment outlets, while erosion data is often not available at all, which could prevent a calibration and validation study of this kind in most catchments (Beven, 2000; Morgan and Quinton, 2001). To overcome this problem, Favis-Mortlock et al. (2001) suggests a qualitative evaluation of model performance when quantitative data is not available. This approach consists in comparing model outputs with expected results in terms of process knowledge to assert the rationality of model behavior, and therefore the model's capacity to simulate responses to change in environmental conditions. Ebel and Loague (2006) also propose this approach to derive unique parameter sets when parameter equifinality is a problem. In this regard, soft knowledge on the impacts of climate change – coming from observations in different sites, laboratory experimentation or extrapolation from observations in different climatic regions – can be useful to judge model performance under changed climates.

Alternatives to modeling

To circumvent the difficulties in performing meaningful simulation analysis of the impacts of climate change, a number of alternative methods have been proposed in recent years. While modeling is still the best available tool for quantitative impact assessment (Bronstert, 2004), qualitative impact assessment can be useful in complementing model studies or replacing them where they are not feasible. In particular, these studies can provide a good assessment to combined changes in ecohydrological systems, highlighting interactions and processes which might not be described by models. While they point to general trends instead of quantitative impacts, their results could be used in modeling studies to confer the advantages provided by the availability of "soft" information for calibration and validation described previously, as well as qualify and complement the results of these studies.

One such alternative approach is to use a data-driven approach, where changes to the spatial distribution of simple indicators of climatic characteristics, well-known and well-correlated with ecohydrological regimes, are used to estimate a corresponding change in ecohydrological

systems. One example of these studies was performed by Arora (2002), based on the relationship between an aridity index (the ratio of annual evapotranspiration to precipitation) and the partitioning of rainfall into evaporation and runoff. Using the results of one GCM to compute changes to the aridity index, the author was able to estimate changes in surface runoff which compared well with the GCM's hydrological outputs. Berry et al. (2006) used a similar approach to evaluate the vulnerability of European farmers and agricultural crops to climate change based on climate-productivity relations and socio-economic indexes. Results from GCMs under several different emission scenarios for 2050 suggest that the distribution of crops will be determined mostly by climate change, while farming patterns (intensive or extensive agriculture and land abandonment) will be mostly dependent on socio-economic scenarios, framed by the potential for crop growth (determined by climate change) which defines available agricultural options.

Another, more detailed approach is represented by "space-for-time" studies, where the consequences of future climate change are studied using a comparative analysis between a study area and another with climatic characteristics resembling GCM predictions. One example is the report by Imeson and Lavee (1998) on monitoring studies for different sites across a climate transect, which ranged from humid to dry regions over similar limestone rocks across the Mediterranean. The monitoring results have been used to analyze the impacts of climate on several erosion processes and patterns at different spatial and temporal scales, providing indicators of the long-term resilience of ecosystems subjected to erosion, along with the response of these indicators to changes in climate. A similar approach has been used by Fleischer and Sternberg (2006) to study the combined impact of grazing and climate change on the economical value of rangeland ecosystems in Israel.

Overall, these approaches provide an insight on the major processes linking climate with hydrology, erosion and vegetation at different spatial and temporal scales, particularly when the mechanism underlying these processes is also understood (Helmuth et al., 2005). This information can be used to improve the calibration and validation of models for climate change studies by establishing guidelines for the major expected trends and responses.

2.4 Current research needs

The analysis presented on the previous section about the expected impacts of climate change for hydrological and erosion processes in Mediterranean, compared with the currently available modeling studies aimed at estimating them, highlights a number of research gaps.

First, there is a degree of uncertainty in estimating the actual degree of climate change that is seldom incorporated in modeling studies. The non-linear nature of the climate system and natural forcings, compounded with differences in the formulation of different GCMs, causes an intrinsic level of uncertainty to GCM-based climate change predictions (Stott and Kettleborough, 2002; Giorgi, 2005). An example of this problem is given by Cunha et al. (2002), who compiled a wide range of GCM and RCM predictions for Portugal; they report a trend of increasing temperatures reaching c. 5 ºC by 2100, with an uncertainty of c. +/- 1 ºC between predictions. The uncertainty is also high in rainfall predictions, with a predicted decrease of c. 12 % by 2100 and an uncertainty of c. +/- 24 % between predictions, meaning that in some scenarios rainfall is expected to increase. Furthermore, the estimated changes of temperature and rainfall are not always correlated; some extreme temperature change scenarios reported by these authors predict small changes in rainfall, and vice-versa. This issue is illustrated in Figure 2.6, which shows RCM results for central and southern Portugal from a more recent climate change prediction exercise (PRUDENCE, 2007). The data shows predictions for temperature change ranging from 2 to 4 ºC coupled with rainfall decreases from 5 to 30 %; even when considering a single emission scenario there is a great degree of uncertainty, particularly for rainfall estimates (decreases from 5 to 20 % for scenario B2 and from 10 to 30 % for scenario A2, in both regions). The magnitude of changes to rainfall and temperature appears to have some correlation but the uncertainty in rainfall change estimates for a given change in temperature is large (c. 10 %) and appears to increase with climate change magnitude.

This level of uncertainty points to the unreliability of impact assessment studies based on few scenarios of climate change. However, many model-based studies (particularly those aiming at local scale predictions) are restricted to a small number of scenarios supported by GCM results, overlooking the uncertainty associated with them; in consequence, the validity of the results is subordinated to the validity of the climate scenario assumptions (Bronstert, 2004). Several methods have been proposed to overcome this research gap, such as the use of multi-model ensemble from GCM predictions to generate climate change scenarios; an example of this method was given in the previous section. Moreover, Phillips (2006) found that the combined results from multiple GCMs are often closer to observed climate statistics than that of any single GCM, leading to the suggestion that the use of multi-model ensemble averages would better represent future climate scenarios. However, Bronstert (2004) proposes that this technique is insufficient to fully consider the uncertainty associated with climate change prediction. One more complete approach could be the use of hypothetical climate scenarios

based on the full range of GCM predictions, reported by Xu and Singh (2004) and also described in the previous section.

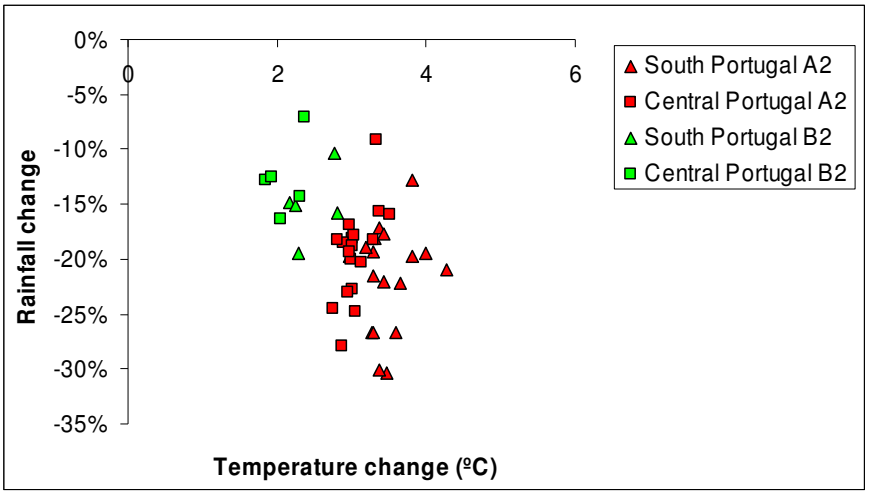

Figure 2.6 – Climate change estimates for central and south Portugal for 2071-2100 considering the A2 and B2 emission scenarios, resulting from 3 GCM estimates downscaled using 13 different RCMs to a resolution of 50×50 Km; model results were obtained in the PRUDENCE project (PRUDENCE, 2007).

While the uncertainty issue applies to most model studies, other research gaps are present in studies focusing specifically on hydrological processes. The major ones can be assessed by comparing the expected impacts outlined in section 2.2.2 and the model studies discussed in section 2.3.3; this comparison is summarized in Table 2.10, with particularly importance given to the appropriated scale for assessment. Overall, a number of significant research gaps can be identified:

- the long-term impact assessment on hydrological variables at the Mediterranean scale appears to have been well studied, but only a few catchments were studied at the local scale, which is particularly important for heterogeneous landscapes;

- there is a significant lack of studies of stream flow regime changes, particularly for changes to flood magnitude and frequency;

- there are few studies concerned with within-catchment variability of soil moisture patterns, which can severely impact predictions for surface runoff and stream flow partitioning due to the great degree of interaction between these processes (as discussed in section 2.2.2).

Table 2.10 – Comparison between estimated climate change impacts on hydrological processes and existing impact assessment studies.

Expected climate change impact	**Existing assessment studies for Mediterranean regions**
Long-term changes to evapotranspiration, runoff and soil moisture	Multi-model ensemble studies performed at the Mediterranean scale, including seasonal changes
	Lack of soil moisture studies at smaller spatial scales
Changes to stream flow regimes	Some catchment-scale studies for changes to seasonal flow patterns
	Lack of catchment-scale studies for changes to stream flow partitioning
Changes on flood magnitude and frequency	Lack of catchment-scale studies on the impact of changes in storm patterns for flood magnitude
	Lack of catchment-scale studies on the interaction between changes in patterns of storm and soil moisture, and the consequences for runoff generation and flood magnitude

Xu and Singh (2004) report other research gaps in hydrological impact assessment studies. There is a lack of integration of hydrological processes across multiple spatial and temporal scales, and across the surface/soil boundary. There is also a need for more research on calibration and validation methods that address uncertainty for unknown boundary conditions, particularly in terms of changes to climate and land use. Finally, the modeling of water quality processes is still limited in model studies. These research gaps should be addressed in some fashion when studying the impacts of climate change on hydrological processes for Mediterranean regions.

A similar analysis can be performed for soil erosion impact assessment studies. A comparison between the expected impacts of climate change discussed in section 2.2.3 and the assessment studies described in section 2.3.3 can be performed to identify the major research gaps in this area; Table 2.11 summarizes the results with a focus on the appropriate assessment scale. This highlights a number of research gaps:

- the only significant studies concern long-term changes to erosion rates at the field and hillslope scale, focusing on rill and interill erosion and neglecting changes to gully erosion rates, which could be more important in Mediterranean studies (as discussed in section 2.2.3);

- few studies include multiple climate change scenarios or focus on catchments in different regions throughout the Mediterranean;

- few studies focus on changes due to the most extreme events or in the interactions between changes to soil moisture patterns, vegetation cover and soil erosion rates.

Table 2.11 – Comparison between estimated climate change impacts on soil erosion processes and existing impact assessment studies.

Expected climate change impact	**Existing assessment studies for Mediterranean regions**
Long-term changes to erosion rates at the field and hillslope scale	Transect-based studies on changes to erosion drivers performed across Mediterranean environments
	Single climate change scenario studies performed at the regional scale and for selected catchments
	Lack of multi-scenario studies at any scale
	Lack of studies focusing on changes to gully erosion patterns
Long-term changes to sediment yield from catchments	Lack of catchment-scale studies focusing on changes to sediment yield
Changes to erosion rates during extreme events	Lack of within-catchment studies linking changes in storm patterns, soil moisture patterns and erosion rates
	Lack of within-catchment studies on the spatial patterns on soil erosion, including changes to gully erosion patterns
Interactions between changes to vegetation cover and soil erosion	Lack of studies on the interactions between climate change, vegetation cover and soil erosion rates at any scale

Several of the research gaps described above derived from gaps in hydrological impact assessment, particularly the lack of studies at the extreme event scale. Furthermore, these gaps can be attributed also to the general lack of erosion impact assessment studies at the global scale or for regions other than the Mediterranean. In a critical review and assessment of the current status of soil erosion science, Boardman (2006) refers the lack of capacity to assess the current importance of soil erosion and associated problems, particularly during extreme events, as a major hindrance in projecting this knowledge into the future. This problem is worsened by the limited value of current erosion modeling techniques, both in terms of low

predictive ability and inadequate model application. Major issues to be addressed in soil erosion science include lack of data at multiple spatial and temporal scales and lack of prediction and assessment capacity, issues which also need to be addressed when making climate change impact assessments on soil erosion. For this particular case, Poesen et al. (2003) identify the response of gully erosion to changes in climate, hydrology and land use as a research issue requiring urgent attention.

Overall, it can be stated that most of the research gaps in assessing the impacts of climate change on soil erosion are due to the lack of appropriate data, process knowledge and modeling tools; this contrasts with research gaps in hydrological studies, where impact assessment methods are well developed but their application in the Mediterranean region is lacking. Despite these failings, however, several techniques applied in recent years show some promise in solving these research gaps. For example, Pruski and Nearing (2002) used hypothetical climate scenarios to simulate the response of long-term soil erosion rates in hillslopes located in the USA, with different soil types and vegetation covers, to changed rainfall intensities and amounts. Their results showed that surface runoff and soil erosion are, in most cases, highly sensitive to changes in rainfall, changing by up to 2.5 % per 1 % change in rainfall. More recently, Nearing et al. (2005) performed a similar study for catchments in Belgium and the USA, considering how within-storm rainfall patterns can interact with changes to vegetation cover in order to modify soil erosion rates. Finally, Michael et al. (2005) took advantage of statistical downscaling techniques to simulate the impacts of changes in storm patterns and vegetation cover for a German catchment, also considering the impact of agricultural management changes caused by climate change adaptation. These methodologies can be combined and adapted to consider the most important erosion processes in Mediterranean regions and thus serve as a basis for assessing the impacts of climate change on soil erosion in the northern Mediterranean.

Finally, it should be noted that other authors refer more significant limitations to current climate change impact assessment studies linked with the misrepresentation of feedback between different systems. For example, Huntingford et al. (2006) refer that the poor representation of hydrological processes in current GCMs prevents the proper estimation of the consequences of climate change on surface-atmosphere interactions. Another problem, noted both by Huntingford et al. (2006) and Simonovic and Davies (2006), is the lack of the coupled simulation of physical and socio-economic processes, which prevents the accurate estimation of feedbacks and interactions within the so-called socio-ecological system. For soil

erosion studies, Boardman (2006) refers the lack of knowledge on interactions and feedbacks between soil erosion and vegetation growth processes. While these represent major gaps in the current methods for climate change impact assessment, they fall outside the scope of this thesis. Nevertheless, these problems should be addressed when discussing the results of impact assessment studies.

2.5 References

Adger WN, 2006. Vulnerability. Global Environmental Change 16: 268–281.

Aksoy H, Kavvas ML, 2005. A review of hillslope and watershed scale erosion and sediment transport models. Catena 64: 247–271.

Alcamo J, Moreno JM, Nováky B, Bindi M, Corobov R, Devoy RJN, Giannakopoulos C, Martin E, Olesen JE, Shvidenko A, 2007. Europe. In: Parry ML, Canziani OF, Palutikof JP, van der Linden PJ, Hanson CE (Eds.), Climate Change 2007: Impacts, Adaptation and Vulnerability. Contribution of Working Group II to the Fourth Assessment Report of the Intergovernmental Panel on Climate Change. Cambridge University Press, Cambridge: 541-580.

Apaydin H, Anli AS, Ozturk A, 2006. The temporal transferability of calibrated parameters of a hydrological model. Ecological modelling 195: 307–317.

Arnell N, 2004. Climate change and global water resources: SRES emissions and socio-economic scenarios. Global Environmental Change 14: 31–52.

Arora VK, 2002. The use of the aridity index to assess climate change effect on annual runoff. J. Hydrol. 265 (1-4): 164-177.

Arribas A, Gallardo C, Gaertner MA, Castro M, 2003. Sensitivity of the Iberian Peninsula climate to a land degradation. Climate Dynamics 20: 477–489.

Audsley E, Pearn KR, Simota C, Cojocaru G, Koutsidou E, Rounsevell MDA, Trnka M, Alexandrov V, 2006. What can scenario modelling tell us about future European scale agricultural land use, and what not? Environmental science & policy 9: 148-162.

Avila A, Neal C, Terradas J, 1996. Climate change implications for streamflow and streamwater chemistry in a Mediterranean catchment. J. Hydrol. (1-2): 99-116.

Avni Y, 2005. Gully incision as a key factor in desertification in an arid environment, the Negev highlands, Israel. Catena 63: 185–220.

Bathurst JC, Kilsby C, White S, 1996. Modeling the impacts of climate and land-use change on basin hydrology and soil erosion in Mediterranean Europe. In: Brandt CJ, Thornes JB (Eds.), Mediterranean desertification and land use. John Wiley and sons, Chichester: 355-388.

Beasley DB, Huggins LF, Monke EJ, 1980. ANSWERS: a model for watershed planning. Transactions of the ASAE: 938– 944.

Beniston M, Stephenson DB, Christensen OB, Ferro CAT, Frei C, Goyette S, Halsnaes K, Holt T, Jylhä K, Koffi B, Palutikof J, Schöll R, Semmler T, Woth K, 2006. Future extreme events in European climate: An exploration of regional climate model projections. Climatic Change 81: 71-95.

Berry PM, Rounsevell MDA, Harrison PA, Audsley E, 2006. Assessing the vulnerability of agricultural land use and species to climate change and the role of policy in facilitating adaptation. Environmental Science and Policy 9: 189-204.

Beven K, 2000. Rainfall-Runoff Modelling – The Primer. John Wiley & Sons, Chichester.

Beven K, 2002. Towards an alternative blueprint for a physically based digitally simulated hydrologic response modelling system. Hydrol. Process. 16: 189–206.

Binley A, Elgy J, Beven K, 1989a. A Physically Based Model of Heterogeneous Hillslopes - 1. Runoff Production. Water Resour. Res. 25 (6): 1219-1226.

Binley A, Elgy J, Beven K, 1989b. A Physically Based Model of Heterogeneous Hillslopes - 2. Effective Hydraulic Conductivities. Water Resour. Res. 25 (6): 1227-1233.

Blöschl G, Sivapalan M, 1995. Scale issues in hydrological modeling: a review. In: Kalma JD, Sivapalan M (Eds.), Scale issues in hydrological modeling. John Wiley & Sons, Chichester: 9-48.

Boardman J, 2006. Soil erosion science: reflections on the limitations of current approaches. Catena 68: 73-86.

Boix-Fayos C, Martínez-Mena M, Calvo-Cases A, Castillo V, Albaladejo J, 2005. Concise review of interrill erosion studies in SE Spain (Alicante and Murcia): erosion rates and progress of knowledge from the 1980s. Land Degrad. Develop. 16: 517–528.

Boix-Fayos C, Martínez-Mena M, Arnau-Rosalén E, Calvo-Cases A, Castillo V, Albaladejo J, 2006. Measuring soil erosion by field plots: Understanding the sources of variation. Earth-Science Reviews 78: 267-285.

Boroneant C, Plaut G, Giorgi F, Bi X, 2006. Extreme precipitation over the Maritime Alps and associated weather regimes simulated by a regional climate model: Present-day and future climate scenarios. Theoretical and Applied Climatology 86 (1-4): 81-99.

Boulain N, Cappelaere B, Séguis L, Gignoux J, Peugeot C, 2006. Hydrologic and land use impacts on vegetation growth and NPP at the watershed scale in a semi-arid environment. Reg Environ Change 6: 147–156.

Brandt CJ, Thornes JB (Eds.), 1996. Mediterranean desertification and land use. John Wiley and sons, Chichester.

Bronstert A, Niehoff D, Bürger G, 2002. Effects of climate and land-use change on storm runoff generation: present knowledge and modelling capabilities. Hydrol. Process. 16: 509-529.

Bronstert A, 2004. Rainfall-runoff modelling for assessing impacts of climate and land-use change. Hydrol. Process. 18, 567–570.

Brown VA, McDonnell JJ, Burns DA, Kendall C, 1999. The role of event water, a rapid shallow flow component, and catchment size in summer stormflow. J. Hydrol. 217: 171-190.

Cammeraat LH, 2002. A review of two strongly contrasting geomorphological systems within the context of scale. Earth Surf. Process. Landforms 27: 1201–1222.

Castillo VM, Gómez-Plaza A, Martínez-Mena M, 2003. The role of antecedent soil water content in the runoff response of semiarid catchments: a simulation approach. J. Hydrol. 284:114–130.

Cerdà A, 1998. The influence of geomorphological position and vegetation cover on the erosional and hydrological processes on a Mediterranean hillslope. Hydrol. Process. 12: 661-671.

Cerdan O, Le Bissonnais Y, Couturier A, Saby N, 2002. Modelling interrill erosion in small cultivated catchments. Hydrological Processes, 16 (16): 3215-3226.

Cheddadi R, Guiot J, Jolly D, 2001. The Mediterranean vegetation: what if the atmospheric CO_2 increased? Landscape Ecol. 16: 667-675.

Chow VT, Maidment DR, Mays LW, 1988. Applied Hydrology. McGraw-Hill, New York.

Clark SC, 1996. Mediterranean ecology and an ecological synthesis of the field sites. In: Brandt CJ, Thornes JB (Eds.), Mediterranean desertification and land use. John Wiley and sons, Chichester: 271-302.

Cunha LV, Oliveira R, Nunes V, 2002. Water Resources. In: Santos FD, Forbes K, Moita R (Eds.), Climate change in Portugal: scenarios, impacts and adaptation measures – project SIAM. Gradiva – Publicações, Lisbon: 23-83.

Cunha LV, Ribeiro L, Oliveira RP, Nascimento J, 2006. Recursos hídricos. In: Santos FD, Miranda P (Eds.), Alterações climáticas em Portugal: cenários, impactos e medidas de adaptação – projecto SIAM II. Gradiva – Publicações, Lisbon: 115-168.

Davi H, Dufrêne E, Francois C, Le Maire G, Loustau D, Bosc A, Rambal S, Granier A, Moors E, 2006. Sensitivity of water and carbon fluxes to climate changes from 1960 to 2100 in European forest ecosystems. Agricultural and Forest Meteorology 141: 35–56.

De Roo APJ, Wesseling CG, Ritsema CJ, 1996a. LISEM: a single event physically-based hydrological and soil erosion model for drainage basins: I – theory, input and output. Hydrol. Process. 10 (8): 1107-1117.

De Roo APJ, Offermans RJE, Cremers NHTD, 1996b. LISEM: a single event physically-based hydrological and soil erosion model for drainage basins: II – sensitivity analysis, validation and application. Hydrol. Process. 10 (8): 1119-1126.

De Roo APJ, 1998. Modelling runoff and sediment transport in catchments using GIS. Hydrol. Process. 12: 905-922.

de Vente J, Poesen J, 2005. Predicting soil erosion and sediment yield at the basin scale: scale issues and semi-quantitative models. Earth-Science Reviews 71: 95–125.

de Vente J, Poesen J, Bazzoffi P, Van Rompaey A, Verstraeten G, 2006. Predicting catchment sediment yield in Mediterranean environments: the importance of sediment sources and connectivity in Italian drainage basins. Earth Surf. Process. Landforms 31: 1017–1034.

Déqué M, Jones RG, Wild M, Giorgi F, Christensen JH, Hassell DC, Vidale PL, Rockel B, Jacob D, Kjellström E, de Castro M, Kucharski F, van den Hurk B, 2005. Global high resolution versus Limited Area Model climate change projections over Europe: quantifying confidence level from PRUDENCE results. Climate Dynamics 25: 653–670.

Ebel BA, Loague K, 2006. Physics-based hydrologic-response simulation: seeing through the fog of equifinality. Hydrol. Process. 20: 2887–2900.

Favis-Mortlock D, Boardman J, MacMillan V, 2001. The limits of erosion modeling: why we should proceed with care. In: Harmon RS, Doe WW (Eds.), Landscape Erosion and Evolution Modeling. Kluwer Academic/Plenum Publishers, New York: 477-516.

Fernández RJ, 2002. Do humans create deserts? TRENDS in Ecology & Evolution 17 (1): 6-7.

Field CB, Lobell DB, Peters HA, Chiariello NR, 2007. Feedbacks of terrestrial ecosystems to climate change. Annual Review of Environment and Resources 32: 7.1-7.29.

Fischlin A, Midgley GF, Price JT, Leemans R, Gopal B, Turley C, Rounsevell MDA, Dube OP, Tarazona J, Velichko AA, 2007. Ecosystems, their properties, goods, and services. In: Parry ML, Canziani OF, Palutikof JP, van der Linden PJ, Hanson CE (Eds.), Climate Change 2007: Impacts, Adaptation and Vulnerability. Contribution of Working Group II to the Fourth Assessment Report of the Intergovernmental Panel on Climate Change. Cambridge University Press, Cambridge: 211-272.

Fisher P, Abrahart RJ, Herbinger W, 1997. The sensitivity of two distributed non-point source pollution models to the spatial arrangement of the landscape. Hydrol. Process. 11: 241-252.

Flanagan DC Nearing MA, 1995. USDA-Water Erosion Prediction project: Hillslope profile and watershed model documentation. NSERL Report No. 10. USDA-ARS National Soil Erosion Research Laboratory, West Lafayette.

Fleischer A, Sternberg M, 2006. The economic impact of global climate change on Mediterranean rangeland ecosystems: A Space-for-Time approach. Ecological Economics 59 (3): 287-295.

Folke C, 2006. Resilience: the emergence of a perspective for social–ecological systems analyses. Global Environmental Change 16: 253–267.

Foster GR, 1982. Modeling the erosion process. In: Haan CT, Johnson HP, Brakensiek DL (Eds.), Hydrologic Modeling of Small Watersheds. American Society of Agricultural Engineers, St. Joseph: 295-380.

Gallopín GC, 2006. Linkages between vulnerability, resilience, and adaptive capacity. Global Environmental Change 16: 293–303.

Gao XJ, Pal JS, Giorgi F, 2006. Projected changes in mean and extreme precipitation over the Mediterranean region from a high resolution double nested RCM simulation. Geophysical Research Letters 33 (3): Art. No. L03706.

García-Ruiz JM, Arnaéz J, Beguería S, Seeger M, Martí-Bono C, Regüés D, Lana-Renault N, White S, 2005. Runoff generation in an intensively disturbed, abandoned farmland catchment, Central Spanish Pyrenees. Catena 59: 79–92.

Gibelin AL, Déqué M, 2003. Anthropogenic climate change over the Mediterranean region simulated by a global variable resolution model. Climate Dynamics 20 (4): 327-339.

Giorgi F, Bi XQ, Pal J, 2004. Mean, interannual variability and trends in a regional climate change experiment over Europe. II: climate change scenarios (2071-2100). Climate Dynamics 23 (7-8): 839-858.

Giorgi F. 2005. Climate change prediction. Climatic Change 73 (3): 239-265.

Giorgi F, 2006. Climate change hot-spots. Geophys. Res. Lett. 33: L08707.

Good P, Barring L, Giannakopoulos C, Holt T, Palutikof J, 2006. Non-linear regional relationships between climate extremes and annual mean temperatures in model projections for 1961-2099 over Europe. Climate Research 31 (1): 19-34.

Goodess CM, Mariani L, Palutikof JP, Menichini V, Minardi GP, 1998. Estimating future climates in the Mediterranean. In: Mairota P, Thornes JB, Geeson N (Eds.), Atlas of Mediterranean environments in Europe. John Wiley and Sons, Chichester: 38-43.

Govers G, 1990. Empirical relationships for the transporting capacity of overland flow. International Association of Hydrological Sciences Publication 189: 45-63.

Grayson R, Blöschl G, 2001a. Spatial modelling of catchment dynamics. In: Grayson R, Blöschl G (Eds.), Spatial Patterns in Catchment Hydrology – Observations and Modelling. Cambridge University Press, Cambridge: 51-81.

Grayson R, Blöschl G, 2001b. Summary of Pattern Comparison and Concluding Remarks. In: Grayson R, Blöschl G (Eds.), Spatial Patterns in Catchment Hydrology – Observations and Modelling. Cambridge University Press, Cambridge: 355-367.

Grove AT, Rackham O, 1998. History of Mediterranean land-use. In: Mairota P, Thornes JB, Geeson N (Eds.), Atlas of Mediterranean environments in Europe. John Wiley and Sons, Chichester: 76-79.

Hanson CE, Palutikof JP, Livermore MTJ, Barring L, Bindi M, Corte-Real J, Durao R, Giannakopoulos C, Good P, Holt T, Kundzewicz Z, Leckebusch GC, Moriondo M, Radziejewski M, Santos J, Schlyter P, Schwarb M, Stjernquist I, Ulbrich U, 2007. Modelling the impact of climate extremes: an overview of the MICE project. Climatic Change 81: 163-177.

Harmon RS, Doe WW (Eds.), 2001. Landscape erosion and evolution modeling. Kluwer Academic /Plenum Publishers, New York.

Helmuth B, Kingsolver JG, Carrington E, 2005. Biophysics, physiological ecology, and climate change: does mechanism matter? Annual Review of Physiology 67: 177-201.

Herrmann SM, Hutchinson CF, 2005. The changing contexts of the desertification debate. J. Arid Environments 63: 538–555.

Horritt MS, Bates PD, 2001. Effects of spatial resolution on a raster based model of flood flow. J. Hydrol. 253: 239-249.

Huggins LF, Burney JR, 1982. Surface runoff, storage, and routing. In: Haan CT, Johnson HP, Brakensiek DL (Eds.), Hydrologic Modeling of Small Watersheds. American Society of Agricultural Engineers, St. Joseph: 167-226.

Huntingford C, Gash J, Giacomello AM, 2006. Climate change and hydrology: next steps for climate models. Hydrol. Process. 20: 2085–2087.

Imeson AC, Lavee H, 1998. Soil erosion and climate change: the transect approach and the influence of scale. Geomorphology 23: 219–227.

IPCC: Intergovernmental Panel on Climate Change, 2000. Special Report on Emissions Scenarios. A Special Report of Working Group III of the Intergovernmental Panel on Climate Change. Nakićenović N, Swart R (Eds.). Cambridge University Press, Cambridge.

IPCC: Intergovernmental Panel on Climate Change, 2001. Climate Change 2001: The Scientific Basis. Houghton JT, Ding Y, Griggs DJ, Noguer M, van der Linden PJ, Dai X, Maskell K, Johnson CA (Eds.). Cambridge University Press: Cambridge.

IPCC: Intergovernmental Panel on Climate Change, 2007. Climate Change 2007: The Physical Science Basis. Contribution of Working Group I to the Fourth Assessment Report of the Intergovernmental Panel on Climate Change. Solomon S, Qin D, Manning M, Chen Z, Marquis M, Averyt KB, Tignor M, Miller HL (Eds.). Cambridge University Press, Cambridge.

Jakeman AJ, Hornberger GM, 1993. How Much Complexity Is Warranted in a Rainfall-Runoff Model? Water Resour. Res. 29 (8): 2673-2649.

Jetten V, de Roo A, Favis-Mortlock D, 1999. Evaluation of field-scale and catchment-scale soil erosion models. Catena 37 (4): 521-541.

Jetten V, de Roo APJ, 2001. Spatial analysis of erosion conservation measures with LISEM. In: Harmon RS, Doe WW (Eds.), Landscape Erosion and Evolution Modeling. Kluwer Academic/Plenum Publishers. New York: 117-144.

Jetten V, Govers J, Hessel R, 2003. Erosion models: quality of spatial predictions. Hydrol. Process. 17: 887-900.

Kirkby M, Bracken L, Reaney S, 2002. The influence of land use, soils and topography on the delivery of hillslope runoff to channels in SE Spain. Earth Surf. Process. Landforms 27: 1459–1473.

Kirkby MJ, Bull LJ, Poesen J, Nachtergaele J, Vandekerckhove L, 2003. Observed and modelled distributions of channel and gully heads – with examples from SE Spain and Belgium. Catena 50 (2-4): 415-434.

Kirkby MJ, Bracken LJ, Shannon J, 2005. The influence of rainfall distribution and morphological factors on runoff delivery from dryland catchments in SE Spain. Catena 62: 136–156.

Knippertz P, Christoph M, Speth P, 2003. Long-term precipitation variability in Morocco and the link to the large-scale circulation in recent and future climates. Meteorology and Atmospheric Physics 83 (1-2): 67-88.

Kundzewicz ZW, Mata LJ, Arnell NW, Döll P, Kabat P, Jiménez B, Miller KA, Oki T, Sen Z, Shiklomanov IA, 2007. Freshwater resources and their management. In: Parry ML, Canziani OF, Palutikof JP, van der Linden PJ, Hanson CE (Eds.), Climate Change 2007: Impacts, Adaptation and Vulnerability. Contribution of Working Group II to the Fourth Assessment Report of the Intergovernmental Panel on Climate Change. Cambridge University Press, Cambridge: 173-210.

Lane LJ, Nichols MH, Simanton JR, 1995. Spatial variability of cover affecting erosion and sediment yield in overland flow. In: Osterkamp WR (Ed.), Effects of Scale on Interpretation and Management of Sediment and Water Quality. IAHS Publication No. 226: 147-152.

Lane LJ, Hernandez M, Nichols M, 1997. Processes controlling sediment yield from watersheds as functions of spatial scale. Environmental Modelling & Software 12 (4): 355-369.

Lidén R, Harlin J, 2000. Analysis of conceptual rainfall-runoff modelling performance in different climates. J. Hydrol. 238: 231-247.

Lionello P, Dalan F, Elvini E, 2002. Cyclones in the Mediterranean region: the present and the doubled CO_2 climate scenarios. Climate Research 22 (2): 147-159.

Llorens L, Penuelas J, Estiarte M, Bruna P, 2004. Contrasting growth changes in two dominant species of a Mediterranean shrubland submitted to experimental drought and warming. Annals of Botany 94 (6): 843-853.

Maas GS, Macklin MG, 2002. The Impact of Recent Climate Change on Flooding and Sediment Supply Within a Mediterranean Mountain Catchment, Southwestern Crete, Greece. Earth Surf. Process. Landforms 27: 1087-1105.

Mairota P, Thornes JB, Geeson N (Eds.), 1998. Atlas of Mediterranean environments in Europe. John Wiley and Sons, Chichester.

Manabe S, Wetherald RT, Milly PCD, Delworth TL, Stouffer RJ, 2004. Century-scale change in water availability: CO2-quadrupling experiment. Climatic Change 64: 59–76.

Mantel S, Van Lynden GJ, Huting J, 2003. PESERA, Work package 6: Scenario analysis. Final report: April 2003 - September 2003, ISRIC – World Soil Information, Wageningen.

Margaris NS, Koustidou E, Giourga Ch, 1996. Changes in traditional Mediterranean land-use systems. In: Brandt CJ, Thornes JB (Eds.), Mediterranean desertification and land use. John Wiley and sons, Chichester: 29-42.

Margaris NS, Koustidou E, Giourga CE, 1998. Agricultural transformations. In: Mairota P, Thornes JB, Geeson N (Eds.), Atlas of Mediterranean environments in Europe. John Wiley and Sons, Chichester: 82-85.

Martínez-Fernández JM, Esteve MA, 2005. A critical view of the desertification debate in southeastern Spain. Land Degrad. Develop. 16: 529-539.

Martinez-Mena M, Albaladejo J, Castillo VM, 1998. Factors influencing surface runoff generation in a Mediterranean semi-arid environment: Chicamo watershed, SE Spain. Hydrol. Process. 12: 741-754.

Martínez-Vilalta J, Piñol J, Beven K, 2002. A hydraulic model to predict drought-induced mortality in woody plants: an application to climate change in the Mediterranean. Ecological Modelling 155 (2-3): 127-147.

Metzger MJ, Leemans R, Schröter D, 2005. A multidisciplinary multi-scale framework for assessing vulnerabilities to global change. International Journal of Applied Earth Observation and Geoinformation 7: 253–267.

Michael A, Schmidt J, Enke W, Deutschländer Th, Malitz G, 2005. Impact of expected increase in precipitation intensities on soil loss – results of comparative model simulations. Catena 61: 155-164.

Milly PCD, Wetherald RT, Dune KA, Delworth TL, 2002. Increasing risk of great floods in a changing climate. Nature 415: 514-617.

Morales P, Hickler T, Rowell DP, Smith B, T Sykes M, 2007. Changes in European ecosystem productivity and carbon balance driven by regional climate model output. Global Change Biology 13 (1): 108-122.

Morgan RPC, Quinton JN, Smith RE, Govers G, Poesen JWA, Chisci G, Torri D, 1998. The EUROSEM model. In: Boardman J, Favis-Mortlock DT (Eds.), Modeling soil erosion by water. NATO-ASI Series I-55, Springer, Berlin: 389-398.

Morgan RPC, 2001. A simple approach to soil loss prediction: a revised Morgan–Morgan–Finney model. Catena 44: 305–322.

Morgan RPC, Quinton JN, 2001. Erosion Modeling. In: Harmon RS, Doe WW (Eds.), Landscape Erosion and Evolution Modeling. Kluwer Academic/Plenum Publishers. New York: 117-144.

Mouillot F, Rambal S, Joffre R, 2002. Simulating climate change impacts on fire frequency and vegetation dynamics in a Mediterranean-type ecosystem. Global Change Biology 8 (5): 423-437.

Nachtergaele J, Poesen J, Vandekerckhove L, Wijdenes DO, Roxo M, 2001. Testing the ephemeral gully erosion model (EGEM) for two Mediterranean environments. Earth Surf. Process. Landf. 26 (1): 17-30.

Nearing MA, Govers G, Norton LD, 1999. Variability in soil erosion data from replicated plots. Soil Sci. Soc. Am. J. 63: 1829-1835.

Nearing MA, 2000. Evaluating soil erosion models using measured plot data: accounting for variability in the data. Earth Surf. Process. Landforms 25: 1035-1043.

Nearing MA, Pruski FF, O'Neal MR, 2004. Expected climate change impacts on soil erosion rates: A review. Journal of Soil and Water Conservation 59 (1): 43-50.

Nearing MA, Jetten V, Baffaut C, Cerdan O, Couturier A, Hernandez M, Le Bissonnais Y, Nichols MH, Nunes JP, Renschler CS, Souchère V, van Oost K, 2005. Modeling response of soil erosion and runoff to changes in precipitation and cover. Catena 61 (2-3): 131-154.

Neitsch SL, Arnold JG, Kiniry JR, Williams JR, Kiniry KW, 2002. Soil and Water Assessment Tool theoretical documentation. TWRI report TR-191, Texas Water Resources Institute, College Station.

New M, Lister D, Hulme M, Makin I, 2002. A high-resolution data set of surface climate over global land areas. Clim. Res. 21: 1-25.

Nohara D, Kitoh A, Hosaka M, Oki T, 2006. Impact of Climate Change on River Discharge Projected by Multimodel Ensemble. Journal of Hydrometeorology 7 (5): 1076-1089.

Olesen JE, Bindi M, 2002. Consequences of climate change for European agricultural productivity, land use and policy. European Journal of Agronomy 16: 239–262.

Palutikof JP, Conte M, Casimiro Mendes J, Goodess CM, Espirito Santo F, 1996. Climate and climate change. In: Brandt CJ, Thornes JB (Eds.), Mediterranean desertification and land use. John Wiley and sons, Chichester: 43-86.

Panagoulia D, Dimou G, 1997a. Linking space-time scale in hydrological modelling with respect to global climate change part 1: models, model properties, and experimental design. J. Hydrol. 194: 15-37.

Panagoulia D, Dimou G, 1997b. Linking space-time scale in hydrological modelling with respect to global climate change part 2: hydrological response for alternative climates. J. Hydrol. 194: 38-63.

Papadimitriou F, Mairota P, 1998. Agriculture. In: Mairota P, Thornes JB, Geeson N (Eds.), Atlas of Mediterranean environments in Europe. John Wiley and Sons, Chichester: 86-91.

Pereira JS, Correia AV, Correia AC, Ferreira MT, Onofre N, Freitas H, Godinho F, 2006. Florestas e biodiversidade. In: Santos FD, Miranda P (Eds.), Alterações climáticas em Portugal: cenários, impactos e medidas de adaptação – projecto SIAM II. Gradiva – Publicações, Lisbon: 301-344.

Phillips TJ, 2006. Evaluation of continental precipitation in 20th century climate simulations: The utility of multimodel statistics. Water Resources Research 42: W03202.

Pinto PA, Brandão AP, 2002. Agriculture. In: Santos FD, Forbes K, Moita R (Eds.), Climate change in Portugal: scenarios, impacts and adaptation measures – project SIAM. Gradiva – Publicações, Lisbon: 133-171.

Pinto PA, Braga R, Brandão AP, 2006. Agricultura. In: Santos FD, Miranda P (Eds.), Alterações climáticas em Portugal: cenários, impactos e medidas de adaptação – projecto SIAM II. Gradiva – Publicações, Lisbon: 209-232.

Poesen J, Nachtergaele J, Verstraeten G, Valentin C, 2003. Gully erosion and environmental change: importance and research needs. CATENA 50 (2-4): 91-133.

PRUDENCE: Prediction of Regional scenarios and Uncertainties for Defining EuropeaN Climate change risks and Effects, 2007. PRUDENCE data archive. Available online in prudence.dmi.dk (accessed in January 2007). The PRUDENCE project (EU contract EVK2-CT2001-00132).

Pruski FF, Nearing MA, 2002. Runoff and soil-loss responses to changes in precipitation: A computer simulation study. J. Soil Water Conserv. 57 (1): 7-16.

Puigdefábregas J, 1998. Ecological impacts of global change on drylands and their implications for desertification. Land Degrad. Develop. 9: 393-406.

Puigdefábregas J, Mendizabal T, 1998. Perspectives on desertification: western Mediterranean. J. Arid Environments 39: 209-224.

Puigdefabregas J, del Barrio G, Boer MM, Gutiérrez L, Solé B, 1998. Differential responses of hillslope and channel elements to rainfall events in a semi-arid area. Geomorphology 23: 337-351.

Puigdefabregas J, Sole A, Gutierrez L, del Barrio G, Boer M, 1999. Scales and processes of water and sediment redistribution in drylands: results from the Rambla Honda field site in Southeast Spain. Earth-Science Reviews 48: 39–70.

Quinton JN, 1997. Reducing predictive uncertainty in model simulations: a comparison of two methods using the European Soil Erosion Model (EUROSEM). Catena 30: 101-117.

Raff DA, Smith JL, Trlica MJ, 2003. Statistical descriptions of channel networks and their shapes on non-vegetated hillslopes in Kemmerer, Wyoming. Hydrol. Process. 17: 1887–1897.

Räisänen J, Hansson U, Ullerstig A, Döscher R, Graham LP, Jones C, Meier HEM, Samuelsson P, Willén U, 2004. European climate in the late twenty-first century: regional simulations with two driving global models and two forcing scenarios. Climate Dynamics 22: 13–31.

Refsgaard JC, 2001. Towards a formal approach to calibration and validation of models using spatial data. In: Grayson R, Blöschl G (Eds.), Spatial Patterns in Catchment Hydrology – Observations and Modelling. Cambridge University Press, Cambridge: 329-354.

Renard KG, Foster GR, Weesies GA, McCool DK, Yoder DC, 1997. Predicting soil erosion by water – a guide to conservation planning with the revised universal soil loss equation (RUSLE). Agricultural Handbook No. 703, US Government Printing Office, Washington DC.

Ribolzi O, Andrieux P, Valles V, Bouzigues R, Bariac T, Voltz M, 2000. Contribution of groundwater and overland flows to storm flow generation in a cultivated Mediterranean catchment. Quantification by natural chemical tracing. Journal of Hydrology 233: 241-257.

Rosenzweig C, Hillel D. 1998. Climate change and the global harvest. Potential impacts of the greenhouse effect on agriculture. Oxford University Press, New York.

Salisbury FW, Ross CW, 1991. Plant Physiology, 2nd ed. Wadsworth Inc., Belmont.

Salles C, Poesen J, Govers G, 2000. Statistical and physical analysis of soil detachment by raindrop impact: Rain erosivity indices and threshold energy. Water Resour. Res 36 (9): 2721-2729.

Sanchéz E, Gallardo C, Gaertner MA, Arribas A, Castro M, 2004. Future climate extreme events in the Mediterranean simulated by a regional climate model: a first approach . Global and Planetary Change 44 (1-4): 163-180.

Sanchez E, Yague C, Gaertner MA, 2007. Planetary boundary layer energetics simulated from a regional climate model over Europe for present climate and climate change conditions. Geophysical Research Letters 34 (1): Art. No. L01709.

Schoorl JM, Sonneveld MPW, Veldkamp A, 2000. Three-dimensional landscape process modelling: the effect of DEM resolution. Earth Surf. Process. Landforms 25: 1025-1034.

Schmidt J,Werner MV, Michael A, 1999. Application of the EROSION 3D model to the CATSOP watershed, The Netherlands. Catena 37: 449– 456.

SCS: Soil Conservation Service, 1972. Section 4: Hydrology. In: National Engineering Handbook. Soil Conservation Service.

Schröder B, 2006. Pattern, process, and function in landscape ecology and catchment hydrology – how can quantitative landscape ecology support predictions in ungauged basins? Hydrol. Earth Syst. Sci. 10: 967–979.

Senior CA, Jones RG, Lowe JA, Durman CF, Hudson D, 2002. Predictions of extreme precipitation and sea-level rise under climate change. Philos. Trans. R. Soc. Lond. Ser. A – Math. Phys. Eng. Sci. 360 (1796): 1301-1311.

Silva JRM, Ferreira AG, Tomás PMPP, 1998. Rainfall Characteristics and Soil Erosion in Alentejo. Geoökodynamik XIX: 249-255.

Simonovic SP, Davies EGR, 2006. Are we modelling impacts of climatic change properly? Hydrol. Process. 20: 431–433.

Sivapalan M, Blöschl G, Zhang L, Vertessy R, 2003. Downward approach to hydrological prediction. Hydrol. Process. 17: 2101–2111.

Skøien JO, Blöschl G, 2003. Characteristic space scales and timescales in hydrology. Water Resources Research 39 (10): 1304.

Smit B, Wandel J, 2006. Adaptation, adaptive capacity and vulnerability. Global Environmental Change 16: 282–292.

Smith RE, Goodrich DC, Quinton JN, 1995. Dynamic, distributed simulation of watershed erosion: the KINEROS2 and EUROSEM models. J. Soil and Water Conservation 50 (5): 517-520.

Stott PA, Kettleborough JA, 2002. Origins and estimates of uncertainty in predictions of twenty-first century temperature rise. Nature 416 (6882): 723-726.

Sumner GN, Romero R, Homar V, Ramis C, Alonso S, Zorita E, 2003. An estimate of the effects of climate change on the rainfall of Mediterranean Spain by the late twenty first century. Climate Dynamics 20 (7-8): 789-805.

SWCS: Soil and Water Conservation Society, 2003. Conservation implications of climate change: soil erosion and runoff from cropland. Soil and Water Conservation Society, Ankeny.

Thiemann M, Trosset M, Gupta H, Sorooshian S, 2001. Bayesian recursive parameter estimation for hydrologic models. Water Resour. Res. 37 (10): 2521-2535

Thornes JB, 1998. Mediterranean desertification. In: Mairota P, Thornes JB, Geeson N (Eds.), Atlas of Mediterranean environments in Europe. John Wiley and Sons, Chichester: 2-5.

Tognetti R, Johnson JD, Michelozzi M, Raschi A, 1998. Response of foliar metabolism in mature trees of Quercus pubescens and Quercus ilex to long-term elevated CO2. Environ. Exp. Bot. 39: 233-245.

Tognetti R, Minnocci A, Peñuelas J, Raschi A, Jones MB, 2000. Comparative field water relations of three Mediterranean shrub species co-occuring at a natural CO2 vent. J. Exp. Bot. 51 (347): 1135-1146.

Tognetti R, Sebastiani L, Vitagliano C, Raschi A, Minnocci A, 2001. Responses of two olive tree (Olea europaea L.) cultivars to elevated CO2 concentration in the field. Photosynthetica 39 (3): 403-410.

Toy TJ, Foster GR, Renard KG, 2002. Soil erosion: processes, prediction, measurement, and control. John Wiley and Sons, New York.

Trigo RM, Palutikof JP, 2001. Precipitation Scenarios over Iberia: A Comparison between Direct GCM Output and Different Downscaling Techniques. J. Climate 14: 4422-4446.

Tucker GE, Bras RL, 2000. A stochastic approach to modeling the role of rainfall variability in drainage basin evolution. Water Resour. Res. 36 (7): 1953-1964.

UNEP: United Nations Environment Program, 1997. World Atlas of Desertification, 2nd ed. Middleton N, Thomas D (Eds.), UNEP, London.

van den Hurk B, Hirscho M, Schär C, Lenderink G, van Meijgaard E, van Ulden A, Rockel B, Hagemann S, Graham P, Kjellström E, Jones R, 2005. Soil control on runoff response to climate change in regional climate model simulations. Journal of Climate 18 (17): 3536-3551.

van Rompaey AJJ, Verstraeten G, van Oost K, Govers G, Poesen J, 2001. Modelling mean annual sediment yield using a distributed approach. Earth Surf. Process. Landforms 26: 1221–1236.

van Rompaey AJJ, Vieillefont V, Jones RJA, Montanarella L, Verstraeten G, Bazzoffi P, Dostal T, Krasa J, de Vente J, Poesen J, 2003 Validation of soil erosion estimates at European scale. European Soil Bureau Research Report No. 13, EUR 20827 EN, Office for Official Publications of the European Communities, Luxembourg.

Vandaele K, Poesen J, Marques de Silva JR, Govers G, Desmet P, 1997. Assessment of factors controlling ephemeral gully erosion in Southern Portugal and Central Belgium using aerial photographs. Zeitschrift fur Geomorphologie 41 (3): 273-287.

Vandekerckhove L, Poesen J, Govers G, 2003. Medium-term gully headcut retreat rates in Southeast Spain determined from aerial photographs and ground measurements. Catena 50 (2-4): 329-352.

Veitzer SA, Gupta VK, 2001. Statistical self-similarity of width function maxima with implications to floods. Advances in Water Resources 24: 955-965.

Vigiak O, Sterk G, Romanowicz RJ, Beven KJ, 2006. A semi-empirical model to assess uncertainty of spatial patterns of erosion. Catena 66 : 198 – 210.

Vogiatzakis IN, Mannion AM, Griffiths GH, 2006. Mediterranean ecosystems: problems and tools for conservation. Progress in Physical Geography 30 (2): 175–200.

Wetherald RT, Manabe S, 2002. Simulation of hydrologic changes associated with global warming. J. Geophys. Res. 107 (D19): 4379-4393.

Wijdenes DJO, Poesen J, Vandekerckhove L, Ghesquiere M, 2000. Spatial distribution of gully head activity and sediment supply along an ephemeral channel in a Mediterranean environment. CATENA 39 (3): 147-167.

Wilby RL, 2005. Uncertainty in water resource model parameters used for climate change impact assessment. Hydrol. Process. 19: 3201–3219.

Wischmeier WH, Smith DD, 1978. Predicting Rainfall Erosion Losses, a Guide to Conservation Planning. United States Department of Agriculture, Agriculture Handbook no. 282.

Wollock DM, Price CV, 1994. Effects of Digital Elevation Model Map Scale and Data Resolution on a Topography-based Watershed Model. Water Resour. Res. 30 (11): 3041-3052.

Woods R, Sivapalan M, 1999. A synthesis of space-time variability in storm response: rainfall, runoff generation, and routing. Water Resour. Res. 35 (8): 2469-2485.

Wu TH, Hall JA, Bonta JV, 1993. Evaluation of Runoff and Erosion Models. J. Irrig. Drainage Eng. – ASCE 119 (4): 364-381.

Xu C-Y, Singh VP, 2004. Review on Regional Water Resources Assessment Models under Stationary and Changing Climate. Water Resources Management 18: 591–612.

Yair A, Kossovsky A, 2002. Climate and surface properties: hydrological response of small arid and semi-arid watersheds. Geomorphology 42: 43– 57.

Yair A, Raz-Yassif N, 2004. Hydrological processes in a small arid catchment: scale effects of rainfall and slope length. Geomorphology 61: 155–169.

Young OR, Berkhout F, Gallopin GC, Janssen MA, Ostrom E, van der Leeuw S, 2006. The globalization of socio-ecological systems: an agenda for scientific research. Global Environmental Change 16 (2006) 304–316.

Zhang XC, Nearing MA, 2005. Impact of climate change on soil erosion, runoff, and wheat productivity in central Oklahoma. Catena 61: 185–195.

3. Objectives and Methodology

The previous chapter described the current knowledge on climate change, hydrology and soil erosion in Mediterranean regions, and presented the major gaps in the current research efforts. This chapter defines the thesis **Objectives and methodological framework**. It describes the modeling tools used to support the methodology, both at the seasonal and the extreme event scale. At the extreme event scale, a new model is presented, **MEFIDIS – a modeling tool for extreme rainfall events**, followed by a section on **MEFIDIS evaluation**, assessing its capacity to support the methodology used in this thesis using data from two well-studied watersheds. The final section presents a **Seasonal scale modeling tool – the SWAT model**.

3.1 Objectives and methodological framework

As discussed in chapter 1, the main motivation for this thesis is to analyze the vulnerability of Mediterranean watersheds to climate change, focusing on the physical drivers for desertification. The broad objectives of this analysis are:

- proposing and evaluating a modeling framework to study the processes linking climate and the main biophysical drivers for desertification: hydrology, vegetation cover and soil erosion, by coupling different modeling tools adapted to different spatial and temporal scales, focusing on the particularities of Mediterranean watershed processes;

- assessing the sensitivity of Mediterranean watersheds to changes in climate, as well as their resilience to a range of magnitudes of change;

- identifying possible adaptation measures to counteract the expected negative impacts of climate change, from biophysical and socio-economic perspectives.

The thesis also aims to contribute to closing some research gaps in this field, as identified in section 2.4, particularly within model-based vulnerability assessment studies. Given the importance of analyzing the impacts of climate change in these studies, i.e. the implications of climate pressures capable of inducing a significant transformation in watershed processes, the thesis presents a modeling framework to:

- estimate the impacts of climate change at the regional, catchment and Hydrological Response Unit (HRU) scales;

- estimate impacts at the interannual, seasonal and extreme event scales, with a particular focus on soil saturation patterns, stream flow partitioning and floods;
- differentiate between impacts on rill/interill erosion patterns, gully erosion patterns and sediment yield rates;
- study the interaction between changes to rainfall, soil moisture and vegetation cover patterns and the consequence for changes to soil erosion rates;
- provide an impact assessment for multiple climate change scenarios.

The novelty of this work lies on explicitly integrating different spatial and temporal scales in the vulnerability assessment, focusing on detailed spatial and temporal analysis which has so far been neglected in these studies, although it is determinant to understand watershed processes in Mediterranean climates. This integration is supported by the development of an innovative modeling analysis framework which couples models operating at two distinct spatial and temporal scales, using coarse-scale model results to frame boundary conditions when applying the fine-scale model. Moreover, this framework is supported by a new model (MEFIDIS) at the extreme event scale, built under the context of this thesis, which takes into account runoff generation and soil erosion processes for Mediterranean watersheds. Finally, this work also presents new results for the impacts of climate change on desertification drivers, particularly in terms of erosion processes and in tremors of impacts specifically related with Mediterranean climates (see section 2.4).

3.1.1 Modeling analysis framework

A vulnerability assessment analysis could potentially be performed using measurements of multiple climate, hydrological, vegetation and soil erosion variables at multiple spatial and temporal scales to derive empirical relationships between these parameters. However, these relationships are difficult to determine for Mediterranean regions due to the complex nature of hydrological and erosive processes and the non-linear relationships between them, especially in climates driven by extreme weather conditions (Morgan and Quinton, 2001). Furthermore, there is a lack of long-term data on soil erosion, particularly noticeable for gully erosion processes and in Mediterranean regions (Boardman, 2006). Finally, climate change is expected to drive climate extremes beyond their current limits, thus changing the nature of hydrological and erosive processes and possibly limiting the applicability of empirical knowledge derived from data measured with current climate conditions (Beven, 2000).

This thesis adopts modeling as a tool to circumvent these problems. Models, when based on physical relations and properly calibrated and validated for the selected range of applications, allow the simulation of the complex response patterns of hydrological and erosive processes to changes in climate characteristics (Favis-Mortlock et al., 2001). A further advantage of the modeling approach is its capacity for controlled experiments difficult to achieve under natural conditions (Xu and Singh, 2004). Changes in one climate factor while maintaining all others constant rarely occurs in the field, but this condition can be studied by designing model experiments for this effect.

This thesis presents a modeling framework that explicitly integrates processes at several scales in such a way that they can be studied separately while still taking into account cross-scale interactions. However, the complexity of the biophysical processes underlying desertification and the practical constraints imposed by limits in modeling technology present several challenges and limitations which must also be addressed. The first step in building the modeling framework is therefore defining a practical **analysis scope**, i.e. lower and upper boundaries for its application. The lower boundary can be considered as this study's resolution and the upper boundary as the study's extent, following the definitions given by Blöschl and Sivapalan (1995).

For spatial scales, the selected resolution is the field/hillslope scale, at which many hydrological and erosion processes have been analyzed and described (e.g. Blöschl and Sivapalan, 1995; Favis-Mortlock et al., 2001; see also sections 2.2.2 and 2.2.3). The results will be upscaled to the watershed scale. The selected extent consists of two regions in the northern Mediterranean with an area of c. 2000 Km^2, each comprising several large watersheds; the task of upscaling results to the entire northern Mediterranean, with its characteristic heterogeneity in topography, climate aridity, soil type and vegetation, is beyond the scope of this thesis.

For temporal scales, the selected resolution is the extreme event scale, at which the most important erosion processes are active (Favis-Mortlock et al., 2001; see also section 2.2.3). The results will be upscaled to the seasonal scale, where vegetation processes are best described and analyzed (Morgan and Quinton, 2001); this analysis is particularly important in Mediterranean climates given their characteristic seasonal variability of Mediterranean climates (Palutikof et al., 1996). The selected extent is three decades, to account for the long lifetime of erosive processes and the importance of years with extreme rainfall characteristics

(Imeson and Lavee; 1998); an analysis of geomorphological adjustments over longer time scales is beyond the scope of this thesis.

Finally, it should be noted that the complexity associated with modeling extreme weather events, particularly when performed in a spatially-distributed format, limits the applicability of this analysis to a small sample of catchments for which enough parameter information can be collected. Therefore, the spatial extent of the analysis for extreme rainfall events is limited to a subset of each region defined above, comprising one meso-scale watershed per region with an area of c. 150 Km^2 each.

The second step in building the modeling framework is the selection of appropriate **modeling tools**, capable of operating within the full extent of the scope defined above. In practical terms, the complexity of processes occurring at the extreme event scale often prevents their simulation with models operating for longer timescales, especially if they are performed in a spatially-distributed format which takes the field/hillslope scale into account (Morgan and Quinton, 2001). However, as discussed in sections 2.2.2 and 2.2.3, large-scale processes often frame the boundary conditions for those occurring at a smaller scale, and temporal scales are usually associated with spatial scales. The modeling framework takes advantage of these factors by using different models for different scales:

- vulnerability is analyzed at two distinct temporal scales: the seasonal and the single extreme event;

- the temporal scale is associated with a spatial scale: the seasonal assessment focuses on changes to the full extent of the study areas, with a resolution of individual HRUs, while the extreme event analysis focuses on one individual catchment in each study area, with a hillslope-scale resolution;

- the seasonal scale assessment is performed using a model capable of continuously simulating several watersheds for long periods of time, providing results with a daily resolution;

- the extreme event scale assessment is performed using a model capable of detailed prediction of conditions within extreme weather events, operating for a single storm;

- the results of the seasonal scale assessment are integrated into the extreme-event assessment as boundary conditions.

The SWAT model (Neitsch et al., 2002a) was selected as a tool for seasonal scale assessment, due to its combination of multi-process analysis (including hydrology, vegetation growth and sediment yield) with relatively light data requirements, and its proven applicability for climate change studies at this scale (e.g. Chaplot, 2007; see section 3.4 for further details). At the extreme event scale, current modeling tools have proven unsuitable for this framework due mostly to their simplified representation of saturation-excess runoff generation processes, which are determinant in Mediterranean watersheds (as previously detailed), coupled with the large complexity which could pose parameterization and data gathering problems when simulating meso-scale watersheds (>100 Km^2). These facts led to the development of a new extreme event hydrological-erosion model, MEFIDIS, within the context of this thesis; the model is capable of a spatially-distributed simulation of the most important within-storm processes occurring in a meso-scale watershed (Nunes et al., 2005 and 2006a; see section 3.2 for further details).

3.1.2 Vulnerability assessment overview

This thesis uses the modeling framework described in the previous section to support a broader vulnerability assessment analysis. The theoretical framework proposed by Adger (2006) is applied to the context of climate change and desertification (see section 2.3.1 for a further discussion). In this context, and after assessing the exposure of Mediterranean watersheds to climate change, vulnerability is assessed by evaluating:

- the **sensitivity** of the physical drivers for desertification to changes in climate;
- the **response capacity** of Mediterranean watersheds to climate change, measured both by their resilience – the capacity to endure climate shifts without further desertification, and their adaptive capacity – the availability of adaptation options to the impacts of climate change.

The framework to evaluate these parameters is shown schematically in Figure 3.1, superimposed over the modeling framework described above, inspired by the theoretical framework shown in Figure 2.4. Both parameters are evaluated independently, since each provide complementary results: the sensitivity analysis provides information on the processes affected by climate change, while the response capacity analysis provides as estimate on the importance of these changes for Mediterranean watersheds. This section provides a brief overview of the methodology used in this thesis; a detailed discussion is given in chapter 5.

As the scheme shows, the first step is to evaluate the **probability of exposure** of Mediterranean watersheds to climate change by using Global Circulation Model (GCM) and Regional Climate Model (RCM) scenarios. Two approaches are used for scenario building:

- hypothetical scenarios (Xu and Singh, 2004) are used for sensitivity analysis, exploring and quantifying the response of hydrology, vegetation growth and soil erosion to changes in single climate parameters as well as multiple change permutations;

- GCM/RCM-based climate change scenarios are used for response capacity analysis, evaluating the impact of several types of changes to climate variables, including changes to extreme event patterns, selected to coincide with the most frequent GCM/RCM predictions for the study area (Figure 2.6).

The adoption of different scenario building methods is justified by the capacities and limitations of each method for the purposes of this thesis. Hypothetical scenarios allow the exploration of the consequences of multiple changes to climate parameters, but still present limitations due to a lack of internal coherence and inadequate representation of extreme event changes (Yu, 2005). RCM scenarios offer a good degree of internal spatial and temporal coherence, with the reproduction of phenomena such as changes to drought and storm patterns not achievable through the stochastic method, therefore presenting a more comprehensive picture of changed climate patterns.

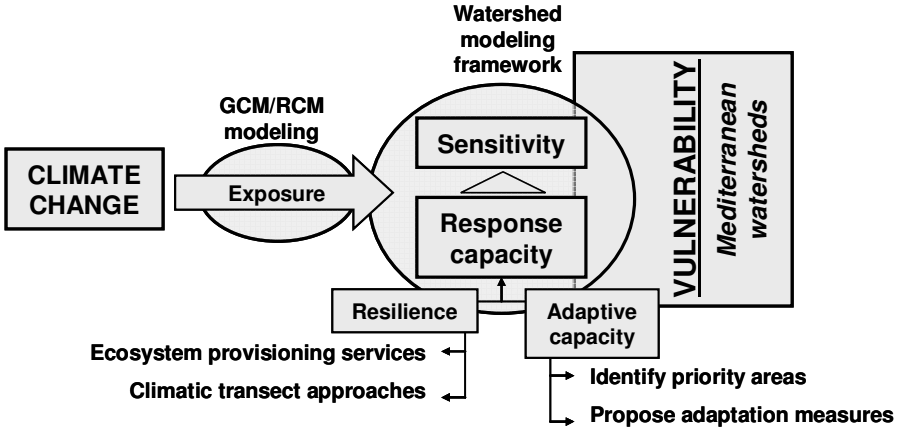

Figure 3.1 – Framework for vulnerability assessment, adapted from Gallopín (2006), superimposed over the modeling framework.

The following step is the assessment of the **sensitivity** to climate change (Figure 3.1). Sensitivity is assessed by quantifying the response of hydrological, vegetation and erosion processes to different magnitudes of climate change (represented by hypothetical climate change scenarios). This is achieved using the watershed modeling framework detailed above: the SWAT and MEFIDIS models are used for controlled experiments, where a single climate parameter is changed in increasing steps and the correspondent changes to hydrological, vegetation and erosion parameters is registered, therefore providing data points for a change/response curve. Combined parameter changes are also made to study the existence of positive and negative feedbacks. Figure 3.2 illustrates the framework used in this analysis.

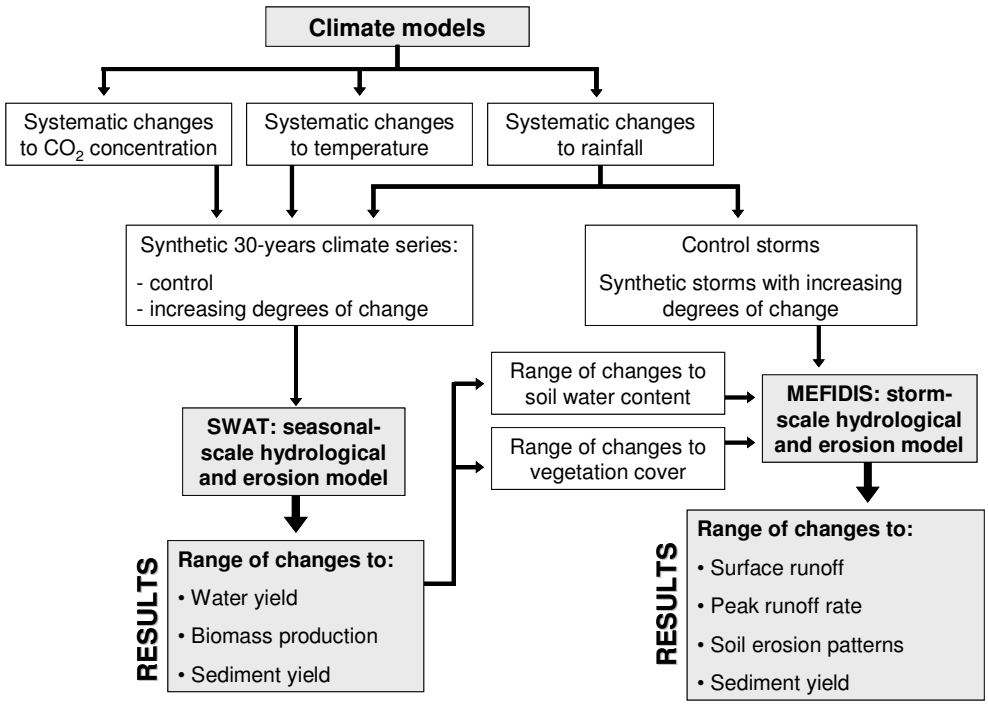

Figure 3.2 – Framework for a multi-scale analysis of the sensitivity of hydrological, vegetation and erosion processes to climate changes.

The sensitivity analysis begins by identifying the predicted range of changes to three key variables: rainfall, temperature and atmospheric CO_2 concentration (Xu and Singh, 2004), taken from GCM and RCM climate scenarios. This range is then applied to both the seasonal and extreme event scale in sequence. At the seasonal scale, the following steps are taken:

- apply the SWAT model for a control run with a synthetic 30-year climate series, stochastically generated with similar statistical characteristics to the 1961-90 climatic normal;

- change the average annual rainfall, temperature and atmospheric CO_2 concentration in increasing degrees of severity, and use these changes to stochastically generate synthetic 30-year climate series (hypothetical scenarios) used to force the model;

- compare model results for the control run and the climate change runs in order to quantify changes to surface and subsurface water yield, sediment yield and biomass production.

At the extreme event scale, the following steps are taken:

- apply the MEFIDIS model for a control run using observed present-day storms in each study area and current soil water content and vegetation cover conditions;

- use a range of possible changes to storm patterns to modify the present-day storms, creating synthetic storms with increasing degrees of change (hypothetical scenarios) to force the model;

- use a range of changes to soil water content and vegetation cover, and run the model for the present-day and synthetic storms with these changes;

- compare model results for the control run and the climate change runs in order to quantify impacts on surface runoff rate, peak runoff rate, within-watershed soil erosion patterns and sediment yield.

It should be noted that, while event-scale changes to rainfall can be simulated directly, the impacts of seasonal changes to rainfall, temperature and CO_2 concentration need be simulated using event-scale parameters which are affected by these changes. Two intermediate parameters were selected, soil water content at the start of the storm and vegetation cover, since they depend on seasonal-scale climate and have direct impact on storm runoff and erosion. Trends for these parameters are evaluated using the seasonal-scale sensitivity results.

The final step for vulnerability analysis, shown in Figure 3.1, is to assess the **response capacity** to climate change of Mediterranean watersheds. Response capacity is assessed in two phases, by evaluating the system's resilience and adaptive capacity.

Resilience is evaluated by (i) estimating the impacts of both the hypothetical scenarios described above, and an RCM-based climate change scenario on hydrological, vegetation and erosion processes, and (ii) evaluating if these impacts cross existing desertification thresholds. The RCM-based scenario combines a range of changes to multiple climate parameters at several scales, from inter-annual to seasonal variability, with coherent relationships between them. RCM-generated control runs (for a reference climate for 1961-1990) and climate change scenarios are used to force the catchment models, in order to evaluate the changes to hydrological, vegetation and erosion processes. Resilience is further analyzed using the results from the sensitivity analysis, coupled with "soft" information in terms of watershed provisioning services and vegetation support capacity. The framework used in this case is illustrated in Figure 3.3.

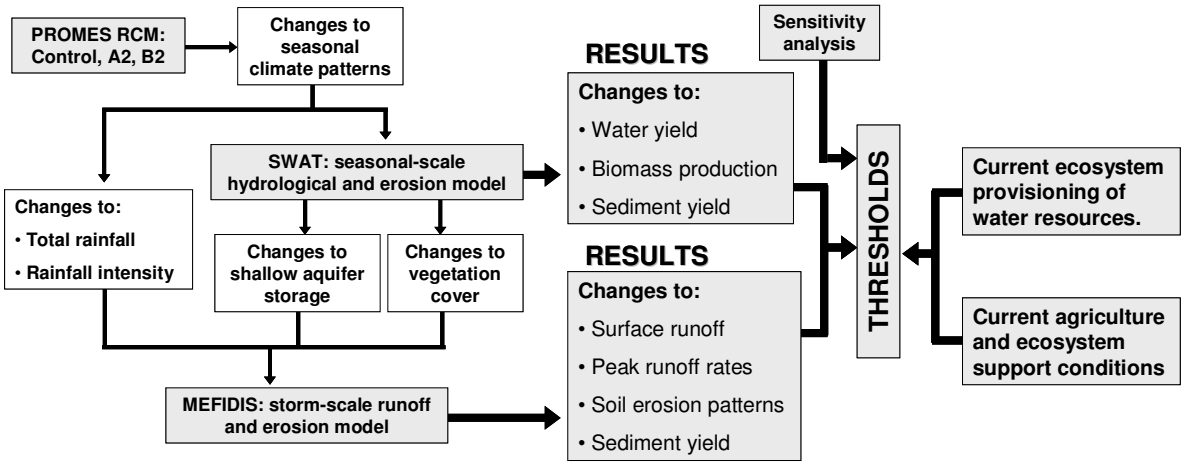

Figure 3.3 – Framework used for a multi-scale analysis of the resilience of hydrological, vegetation and erosion processes to RCM-based climate change scenarios.

The starting point of the resilience analysis is the results of the PROMES RCM (Gallardo et al., 2001) for two CO_2 emission scenarios, A2 and B2 (IPCC, 2000; see section 2.2.1 for a further discussion). The seasonal and extreme event models are applied sequentially, with the results from the former for soil water content and vegetation cover used as parameters in the latter. As in the previous case, surface and subsurface water yield, sediment yield and biomass production are analyzed at the seasonal scale, while surface runoff rate, peak runoff rate, within-watershed soil erosion patterns and sediment yield are analyzed at the extreme event scale. The following steps are taken:

- apply the SWAT model for a control run using the RCM results for the current climate (1960-90);

- apply the SWAT model using the RCM results for the A2 and B2 emission scenarios, for 2070-2100, and compare them with the control run to estimate inter-annual and seasonal changes;

- apply the MEFIDIS model for a control run using present-day storms observed in each study area and current soil water content and vegetation cover conditions;

- use changes to storm event intensity, as predicted by the RCM, to create synthetic storms used to force the extreme event model;

- run the MEFIDIS model using the synthetic storms coupled with the SWAT results for soil water content and vegetation cover;

- compare model results for the control run and the climate change runs in order to estimate changes.

The change estimates are used to assess the long-term impacts of soil erosion on fertility (following Bakker et al., 2004). These results are then compared with existing thresholds for desertification. As discussed in section 2.3.1, thresholds are difficult to quantify; in the context of this work, they are identified using additional "soft" information. Two desertification thresholds are evaluated:

- ecosystem provisioning of water resources, evaluated through water stress thresholds defined by Alcamo et al. (2003) and Arnell (2004);

- capacity to support current agricultural patterns and ecosystems, evaluated through a comparison between current and changed climate aridity and taking into account aridity thresholds for vegetation estimated with a "space for time" approach (Imeson and Lavee, 1998).

Finally, the **adaptive capacity** of Mediterranean watersheds to changes in climate is assessed using the method proposed by Smit and Wandel (2006). The results from the sensitivity and resilience analysis described above are used to identify and prioritize areas requiring adaptation, and to suggest measures to promote adaptation (Figure 3.1).

3.2 MEFIDIS – a modeling tool for extreme rainfall events

The MEFIDIS model – the Portuguese acronym for Spatially-Distributed Physical Erosion Model (Modelo de Erosão FÍsico e DIStribuído) – was developed in the context of this thesis, to assess the risk posed by unusually intense storm events for flooding and land degradation in medium-sized watersheds, in particular due to climate and land-use changes. The model was designed with the following capabilities:

- predict the impacts of extreme rainfall events on water flow and soil erosion;
- predict erosion patterns with a high degree of spatial discretization by using a raster-based approach to spatial distribution (Jetten et al., 2003);
- predict time-variable hydrographs using a fully dynamic approach, in order to estimate peak flow and hydrograph growth and decline during floods.

MEFIDIS is based on physical equations, allowing greater confidence on model results under changed climate and vegetation conditions (Beven, 2000; Grayson and Blöschl, 2001a). It was designed to use commonly available data in terms of geographical information, vegetation and soil parameters, and rainfall datasets.

MEFIDIS was built to adapt to the problems faced by modelers in Mediterranean watersheds. As discussed in section 2.3, a number of spatially-distributed, physically based erosion models are currently available, and have been recently evaluated with similar datasets (Jetten et al., 2003). KINEROS2 (Smith et al., 1995) and EUROSEM (Morgan et al., 1998) are representative of a sub-class of models which divide a catchment in a cascade of planes and channels. Although they require less computational ability than grid-based models, erosion patterns inside each plane element are not simulated (Jetten et al., 2003), limiting their applicability to Mediterranean regions where erosion patterns are heterogeneous and gully erosion plays a significant role (see section 2.2). LISEM (de Roo et al., 1996a and b) is a good example of a sub-class of models that are grid-based, able to fully integrate GIS input data and simulate erosion patterns with the same resolution. However, LISEM is highly detailed in the erosion processes described; available field measurements for most Mediterranean watersheds fall short of the level of parameter detail required by the model. Furthermore, LISEM is explicitly designed to simulate catchments smaller than 50 km^2 in high detail (Jetten and de Roo, 2001), making its validation difficult for poorly instrumented Mediterranean watersheds; for example, in Portugal instrumented watersheds are usually

larger than 100 km^2. KINEROS2 and EUROSEM are also difficult to apply to large watersheds due to the large number of plane and channel elements involved in the simulation, a characteristic which also hinders their capability for fine-scale erosion pattern prediction (Jetten et al., 2003). Finally, as described in section 2.2, runoff generation processes in Mediterranean watersheds are often more correlated with pre-storm soil moisture patterns than with storm intensity and duration, and therefore an extreme-event model should explicitly incorporate a method to estimate these patterns in face of scarce soil moisture data.

MEFIDIS was built to address these issues, aiming to make full use of available spatial and field data for Mediterranean watersheds to widen its applicability as much as possible. Model complexity was kept low, trading process description for ease of parameterization. The following sections describe the model's structure, equations, data requirements and results, with work which was published by Nunes et al. (2005 and 2006a).

3.2.1 Model description

MEFIDIS simulates erosion patterns inside watersheds caused by single rainfall events. Following the classification system described by Aksoy and Kavvas (2005) and discussed in section 2.3, the modeling approach can be classified as physically-based, spatially distributed and dynamical in time, focusing on medium-sized watersheds and single weather events. The finest spatial resolution tested so far was 5 × 5m, using 1s time-steps; the larger spatial extent tested so far was 290 Km^2, and the longest time period was six days.

The approach to spatially distributed modeling is shown in Figure 3.4 The simulation area is divided into an orthogonal matrix of square cells, assumed to represent homogenous conditions (1); runoff generation and soil detachment are computed for each cell (2). Resulting overland flow and suspended sediment are routed between cells following the steepest slope (3). Spatial dynamics are handled with a finite difference scheme, while temporal dynamics are handled by solving the model's governing equations in discrete, successive time-steps.

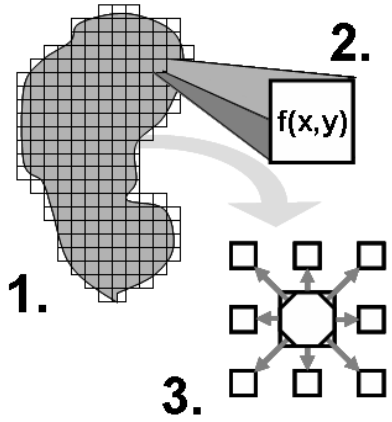

Figure 3.4 – Spatial distribution approach used by MEFIDIS: 1. division of target watershed into a matrix of orthogonal grid cells, 2. computation of runoff generation and detachment for each grid cell, 3. routing overland flow and suspended sediment following the steepest slope.

Erosion simulation can be divided in two parallel phases: runoff generation and soil detachment (Wu et al., 1993). Figure 3.5 shows the processes taken into account by MEFIDIS, following Chow et al. (1988) and Foster (1982). Both Hortonian and saturation excess runoff generation processes are taken into account. Soil detachment is simulated for interrill and rill areas as, respectively, rain splash and flow erosion. Runoff flow is computed as a kinematic wave (Chow et al., 1988); suspended sediment flow is calculated using the transport capacity approach (Foster, 1982).

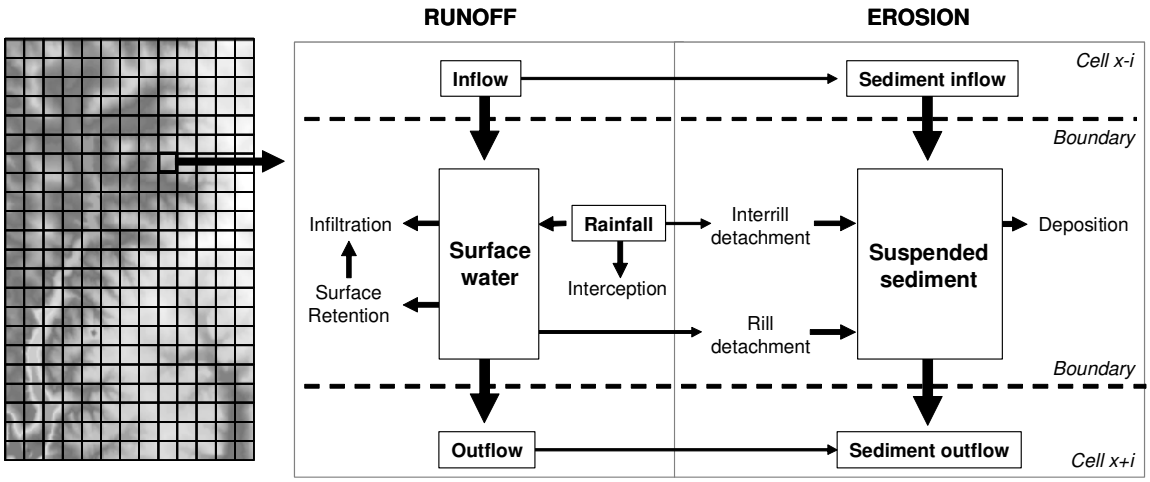

Figure 3.5 – Processes simulated by the model within each cell and at the boundaries between grid cells.

Mathematical formulation – hydrological model

MEFIDIS uses the St. Venant equations to simulate runoff generation and routing (Chow et al., 1988). The continuity equation takes into account interception and infiltration, using the following form:

$$\frac{\partial Q}{\partial x} + \frac{\partial A}{\partial t} = R - I - F \qquad 3.1$$

Where:
Q – surface flow rate ($m^3.s^{-1}$)
A – surface flow cross-sectional area (m^2)
R – rainfall rate per unit length of flow ($m^3.m^{-1}.s^{-1}$)
I – interception storage rate per unit length of flow ($m^3.m^{-1}.s^{-1}$)
F – infiltration rate per unit length of flow ($m^3.m^{-1}.s^{-1}$)
x and t – spatial (m) and temporal (s) dimensions.

Evapotranspiration and subsurface lateral flow are not simulated as in most cases they occur on a time-scale greater than a single event (Chow et al., 1988). Equation 3.1 is solved with a finite difference approximation using a Forward-Time Backward-Space (FTBS) explicit scheme (Huggins and Burney, 1982; Chapra, 1997), assuming that the cell size equals flow length, shown in Equation 3.2. This method requires the use of very short time-steps in order to insure the stability of the results.

$$\frac{\Delta V_s}{\Delta t} = Q_i + R \cdot A_{cell} - I \cdot V_{cv} - F \cdot (1 - P_{cv}) - Q_o \qquad 3.2$$

Where:
V_s – water storage volume within cell (m^3);
t – time (s)
Q_i – inflow rate to cell ($m^3.s^{-1}$)
R – rainfall rate ($m.s^{-1}$)
A_s – surface area of a single model grid cell (m^2)
I – interception rate ($m.s^{-1}$)
V_{cv} – fraction of cell covered by vegetation
F – infiltration rate ($m.s^{-1}$)
P_{cv} – fraction of cell covered by pavement
Q_o – outflow rate from cell ($m^3.s^{-1}$).

The interception rate is calculated following Linsley et al. (1975) as a function of the maximum interception storage capacity and the vegetation cover fraction. The infiltration rate for each time-step is calculated using the Green-Ampt method (Chow et al., 1988):

$$F = K_{sat} \cdot \left(\frac{\psi \cdot (1 - S_i) \cdot \theta}{F_c} + 1 \right) \qquad 3.3$$

Where:
F – infiltration rate (mm.h^{-1})
K_{sat} – saturated hydraulic conductivity of the soil (mm.h^{-1})
ψ – soil matric potential (mm)
S_i – soil moisture saturation ratio at the start of the event
θ – soil porosity fraction
F_c – cumulative infiltration (mm).

Equation 3.3 is solved by iteration with an initial value of $F = K \cdot \Delta t$. Saturation excess runoff is simulated by stopping infiltration if the water in the soil reaches the maximum storage capacity, calculated by comparing cumulative infiltration with soil depth.

A fraction of surface runoff is held in depression storage, estimated from the maximum surface storage capacity and the lateral inflow rate ($R - I - F$ in equation 3.1) following Linsley et al. (1975). The outflow rate for the remaining surface runoff is calculated using a kinematic wave approach (Chow et al., 1988):

$$Q = \frac{A^{5/3} \cdot S_0^{1/2}}{n \cdot P_0^{2/3}} \qquad 3.4$$

Where:
S_0 – surface slope gradient (m.m^{-1})
n – Manning's roughness coefficient
P_0 – perimeter of the surface flow (m)
Q and A – as defined for equation 3.1.

Flow width is calculated from the fraction of the cell covered by water, which is approximated by the relationship between surface runoff height and the maximum depression storage capacity. Since the model calculates the outflow rate for each cell, inflow rates become the outflow rates from neighboring upstream cells, which results in a one-dimensional approximation of two-dimensional flow (Chow et al., 1988).

Mathematical formulation – erosion model

Soil detachment and transport is handled with the continuity equation described by Foster (1982) and Chapra (1997), taking into account interrill and rill sediment delivery rates, inflow and outflow. Sedimentation occurs when the rill sediment delivery rate is negative. The equation is:

$$\frac{\partial(A \cdot C_{sed})}{\partial t} + \frac{\partial(Q \cdot C_{sed})}{\partial x} = D_s + D_r \qquad 3.5$$

Where:
C_{sed} – sediment concentration in the flow (Kg.m^{-3})
D_s and D_r – interrill and rill sediment delivery rates per unit length of flow (Kg.m^{-1}.s^{-1})
A, Q, t and x – as defined for equation 3.1.

Gully erosion processes are not simulated due to the uncertainty associated with current models (Nachtergaele et al., 2001; Jetten et al., 2003). Equation 3.5 is solved with a finite-difference approximation, using a FTBS explicit scheme:

$$\frac{\Delta M_s}{\Delta t} = Q_{si} + D_s + D_r - Q_{so} \qquad 3.6$$

Where:
M_s – suspended sediment (Kg)
t – time (s)
Q_{si} – sediment inflow rate (Kg.s^{-1})
D_s – sediment delivery rate from interrill zones (Kg.s^{-1})
D_r – sediment delivery rate from rills (Kg.s-1)
Q_{so} – sediment outflow rate (Kg.s^{-1}).

Sediment delivery from interrill zones is assumed to be entirely from rainfall splash erosion (Foster, 1982; Toy et al., 2002). The splash detachment rate is calculated following Sharma et al. (1991, 1993 and 1995):

$$D_s = K_P \cdot E \cdot (R - R_c) \cdot R_h \cdot R_{cv} \cdot A_s \qquad 3.7$$

With:

$$K_P = 0.001 \cdot \sigma_{oc}^{-0.35} \cdot \exp(3.88 - 3.7 \cdot S_{clay}) \qquad 3.8$$

$$E = 33 - 853 \cdot \sqrt{e_c} \quad 3.9$$

$$i_c = \frac{5.5 + 763.4 \cdot \sqrt{e_c}}{3.6 \cdot 10^6} \quad 3.10$$

$$e_c = 1.3 \cdot 10^{-5} \cdot \sigma_{oc} + 5 \cdot 10^{-4} \cdot S_{clay} \quad 3.11$$

Where:
K_p – soil detachability by a single raindrop (Kg.J^{-1})
E – effective kinetic energy of rainfall (J.m^{-3})
R and R_c – rainfall rate and the threshold rainfall rate for soil detachment initiation (m.s^{-1})
R_h – dampening ratio due to surface water
R_{cv} – fractional cover of vegetation and paved areas
σ_{oc} – soil shear strength (kPa)
S_{clay} – clay mass fraction of the soil
e_c – critical kinetic energy for soil detachment by a single raindrop (J)
A_s – as described for equation 3.2
D_s – as described for equation 3.6.

Dampening by surface water is related with raindrop diameter following the work of Ferreira and Singer (1985); splash erosion occurs only inside the limits of ponded water height equaling one-third and three times the average raindrop diameter, which is correlated with rainfall intensity following Lencastre and Franco (1992).

Soil detachment and deposition in rills are simulated as a result of runoff flow, following the sediment transport capacity approach: if suspended sediment is lower than this capacity, detachment occurs, otherwise excess soil sediments (Foster, 1982; Govers, 1990). The equation is:

$$D_r = Y \cdot (T_c - C_{sed}) \cdot u_{sed} \cdot w \cdot dx \quad 3.12$$

Where:
Y – detachment/deposition efficiency factor
T_c – sediment transport capacity of the surface flow (Kg.m^{-3})
u_{sed} – particle sedimentation velocity (m.s^{-1})
w and dx – flow width and length (m)
C_{sed} – as described for equation 3.5
D_s – as described for equation 3.6.

Particle sedimentation velocity is related with particle diameter following Stoke's Law (Chapra, 1997). Detachment rate efficiency is calculated from a relationship with the soil shear strength; complete efficiency is considered in the case of sediment deposition (Rauws and Govers, 1988):

$$Y = \frac{1}{0.89 + 0.56 \cdot \sigma_{oc}} \qquad 3.13$$

Where:
σ_{oc} – as described for equation 3.8
Y – as described for equation 3.12.

Transport capacity is calculated from the stream power and the sediment mean particle diameter following Govers (1990):

$$T_c = \rho_p \cdot c \cdot (\omega - \omega_c)^d \qquad 3.14$$

With:

$$c = \left[\frac{(d_{50} \cdot 10^3 + 5)}{0.32} \right]^{-0.6} \qquad 3.15$$

$$d = \left[\frac{(d_{50} \cdot 10^3 + 5)}{300} \right]^{0.25} \qquad 3.16$$

Where:
ρ_p – soil particle density (2650 Kg.m^{-3})
ω and ω_c – stream power and critical stream power for sediment transport (cm.s^{-1})
d_{50} – soil median particle diameter (mm)
T_c – as described for equation 3.12.

Stream power is calculated from outflow velocity and local slope. Critical stream power for soil transport is calculated using Neill's equation (Lencastre & Franco, 1992). MEFIDIS assumes that rills form over the entire length of the cell, with widths totaling the total flow width (calculated as described above).

Channel processes

In grid cells containing channels, MEFIDIS separates overland and channel flow and erosion processes. In equation 3.4, the variable rill width is replaced by a fixed channel width, and a channel Manning's roughness coefficient replaces the one for overland flow. Each channel section can also be designated as impermeable – where infiltration does not occur – or as unerodible – where only sediments brought from upstream and deposited in the channel bed can be ressuspended. All the overland flow in a channel cell is considered to drain into the channel.

3.2.2 Data requirements and model outputs

The MEFIDIS model is implemented as a Windows^{TM}-based program, using the inovaGIS package for direct interaction with Geographical Information Systems (inovaGIS, 2001). MEFIDIS requires storm data to provide the boundary conditions which force the model. It also requires static spatial parameters for topography, soils and vegetation, and initial conditions for soil moisture at the beginning of a storm.

Storm data

The model is forced by rainfall, ideally representing a single storm or a series of storms occurring in short succession. Since evapotranspiration and subsurface flow are not simulated by the model, it should not be applied for time periods much larger than the storm event and the subsequent flow peak in the catchment's main outlet.

The spatial distribution of rainfall is represented directly. As acquiring data with the spatial and temporal resolution required by MEFIDIS is difficult, the model also accepts as input data time-series of precipitation for several points within the watershed; values for each point in the watershed are interpolated with the with the Inverse Distance Weight (IDW) method (Isaaks and Srivastava, 1989) at each time step. MEFIDIS also has a number of functions to generate synthetic storms; Nunes et al. (2006b) provide an example of synthetic circular storms used in MEFIDIS to study the consequences of storm movement direction for peak flow rates and sediment yield.

Fixed spatial parameters

Altimetry and flow direction maps must be supplied to the model; channel location can also be used, along with specific width and Manning roughness values for any number of channel sections. Table 3.1 shows the parameters required by MEFIDIS in a spatially-distributed form; spatial information can be given directly or supplied by appropriate surrogate maps, such as soil maps for texture and hydraulic properties, and land use maps for the remaining parameters (Grayson and Blöschl, 2001b). Care should be taken to represent the spatial information at a high resolution to insure good model performance (e.g. Braun et al., 1997; Schoorl et al., 2000); for example, Walker & Wilgoose (1999) suggest a minimum resolution of 100 × 100m for altimetry to capture local topographic details. Canfield and Goodrich (2006) have suggested that this minimum is more important for the accurate representation of soil erosion and sediment yield, while the accurate representation of runoff processes appears to be less affected by parameter lumping in space. Temporal resolution should be related with

the spatial resolution, not only to ensure model stability but also to minimize numerical dispersion (Chapra, 1997).

Table 3.1 – Spatially-distributed parameters required by MEFIDIS.

Class	**Symbol**	**Units**	**Description**
Soil texture	d_{50}	mm	Median particle diameter
	S_{clay}	-	Mass fraction of clay
	σ_{oc}	kPa	Soil shear strenght
Soil hydraulic properties	K_{sat}	$mm.h^{-1}$	Saturated hydraulic conductivity
	θ	-	Porosity
	ψ	mm	Matric potential
	S_{depth}	mm	Depth
Land cover	D_{max}	mm	Depression storage capacity
	I_{max}	mm	Interception capacity
	n	-	Manning's roughness coefficient
	P_{cv}	-	Pavement cover
	V_{cv}	-	Vegetation canopy cover
Channel properties	n	-	Manning's roughness coefficient
	$W_{channel}$	m	Channel width

Soil moisture parameterization

The soil water content at the beginning of a storm is an initial condition required by the model. This can be provided either as a basin-average parameter, or in a spatially-distributed format. Since spatially-distributed information on soil moisture is difficult to obtain and regular spatial interpolation techniques are not useful for the adequate representation of this information (Blöschl and Grayson, 2001), MEFIDIS integrates a soil water deficit map generator based on both topography and initial base flow at the cacthment's outlet using a TOPMODEL-based approach (Beven, 2000). This approach is based in the spatial distribution of the topographic wetness index, which estimates relative values of soil moisture for a particular point *i* within the watershed, as follows:

$$\gamma_i = \ln\left(\frac{A_{ci}}{S_{0i}}\right) \qquad 3.17$$

Where:
γ_i – topographic wetness index value for point i
A_{ci} – catchment area draining to point i per unit contour length ($m^2.m^{-1}$)
S_{0i} – slope gradient at point i ($m.m^{-1}$).

The wetness index can be used to determine local values of soil moisture deficit when the average soil moisture deficit for the watershed is known, by using a parameter (m) representing the decay of hydraulic transmissivity with soil profile depth:

$$D_i = D + m \cdot (\gamma - \gamma_i) \qquad 3.18$$

Where:
D and D_i – soil moisture deficit for the watershed and at point i (m)
m – transmissivity decay with soil profile (m)
γ – average topographic wetness index value for the watershed
γ_i – as defined for equation 3.17.

The average soil moisture deficit at the beginning of each storm (D) can be estimated from the average wetness index value and the river flow in the beginning of each storm (Beven, 2000). After determining D_i, soil moisture at the beginning of each event is divided in two classes: when $D_i = 0$, the soil is assumed to be saturated with water, while for the other cases soil moisture is assumed to be at field capacity in the top layers and saturated at a depth equal to D_i / θ (soil porosity).

Model results

MEFIDIS provides spatial results for runoff generation (in mm) and accumulated soil loss per unit area (in $Kg.m^{-2}$) at the end of the storm event, in the form of grid-based maps. The model also generates time-series of averaged results for the entire watershed; the parameters are shown in Table 3.2. Finally, the user can obtain time-series for the parameters detailed in the table for selected points within the watershed. In this case, the model also provides time-series for instant flow velocity (in $mm.s^{-1}$) and solid flow (in $Kg.m^{-2}.s^{-1}$).

Table 3.2 - Results provided by MEFIDIS as time-series for the entire watershed.

Output parameter	Output units
Instant surface runoff height	mm
Accumulated interception	mm
Accumulated infiltration	mm
Accumulated runoff outflow from the watershed	mm
Instant suspended sediment	$Kg.m^{-2}$
Accumulated interill erosion	$Kg.m^{-2}$
Accumulated rill erosion	$Kg.m^{-2}$
Accumulated sedimentation	$Kg.m^{-2}$
Accumulated sediment outflow from the watershed	$Kg.m^{-2}$

3.2.3 Sensitivity analysis

The process conceptualization behind the MEFIDIS model was tests by performing a sensitivity analysis, which analyzed model response to changes in single and multiple parameters. While a sensitivity analysis for complex models has indicative value only, it is useful to judge model rationality in responding to the different drivers for runoff and soil erosion (Morgan and Quinton, 2001). It can also improve model application by determining the most important parameters to adjust in different contexts, which is particularly important for parameters that cannot be measured in a spatially distributed fashion, and must therefore be estimated and adjusted by modelers (Beven, 2000). Evaluating the sensitivity of a spatially distributed model at the catchment scale is difficult due to the computational requirements of single model runs coupled with the difficulty of evaluating the sensitivity to some basin-scale parameters (such as basin shape and average slope; Morgan and Quinton, 2001). A sensitivity analysis at the single cell scale, while less complex to perform, is still able to provide a general overview of the parameters dominating field-scale responses in most applications.

The method selected for this analysis is based on Monte Carlo sampling, as described by Loucks and van Beek (2005). Two cell sizes were selected for sampling: 0.5 × 0.5 m, equivalent to the patch scale where splash erosion processes dominate; and 90 × 90 m, equivalent to the field and hillslope scales and dominated by flow erosion processes (Favis-Mortlock et al., 2001; see also section 2.2.3). These sizes were selected as they represent resolution boundaries at which MEFIDIS is expected to operate. In both cases, the model was run for 25 combinations of rainfall and slope, since both these parameters are usually not calibrated; data in the form of e.g. raingauge measurements or topographic maps is used

directly. Five 60 min rainfall showers with 10, 25, 50, 75 and 100 $mm.h^{-1}$ were combined with five slope classes: 0.05, 0.1, 0.2, 0.3 and 0.4 $m.m^{-1}$. This resulted in a total of 50 tests: 25 rainfall-slope combinations applied to two sites. The model was run 10 000 times per test, for a total of 500 000 model runs. In each test, the parameters described in Table 3.1 for soil texture, hydraulic properties and landcover, plus initial soil moisture, were selected randomly from a range, assuming a uniform distribution within this range as suggested by Beven (2000). The minimum and maximum values delimiting this range, per parameter, are shown in Table 3.3. Parameter limits for landcover were taken from the literature; for soil properties, the values represent the percentile 5 and 95 of all soil samples in the Portuguese soil database published by Cardoso (1965). Soil moisture was selected based on soil porosity, to allow for near-saturation soils.

Table 3.3 – Parameter range used in the MEFIDIS sensitivity analysis.

Class	**Symbol**	**Units**	**Description**	**Minimum value**	**Maximum value**
Soil properties[a]	d_{50}	mm	Median particle diameter[b]	0.001	0.6
	S_{clay}	-	Mass fraction of clay	0.03	0.56
	σ_{oc}	kPa	Soil shear strenght[c]	6	26
	K_{sat}	$mm.h^{-1}$	Saturated hydraulic conductivity[d]	1	120
	θ	-	Porosity[e]	0.18	0.56
	ψ	mm	Matric potential[f]	60	820
	S_{depth}	mm	Soil depth	150	1290
Land cover	D_{max}	mm	Depression storage capacity[g]	1	42
	I_{max}	mm	Interception capacity[h]	0.5	2.5
	n	-	Manning's roughness coefficient[i]	0.05	0.8
	P_{cv}	-	Pavement cover	0.05	0.95
	V_{cv}	-	Vegetation canopy cover	0.05	0.95
Soil moisture	S_i	-	Soil volume occupied by water	0	0.56

a – Cardoso (1965).
b – calculated following Bittelli et al. (1999) and Skaggs et al. (2001).
c – calculated following Lencastre and Franco (1992) and Rachman et al. (2003).
d – missing values estimated using Saxton et al. (1986).
e – missing values estimated using Botelho da Costa (1995) and Saxton et al. (1986).
f – calculated following Rawls et al. (1983).
g – Onstad (1984) and Ludwig et al. (1995).
h – Beasley and Huggins (1981).
i – USDA (1986).

A comparison of the results for the different rainfall/slope combinations for both scales (Figure 3.6) shows that rainfall amount and intensity controls runoff, while soil erosion is controlled both by rainfall characteristics and slope; this is consistent with the current knowledge on runoff and erosion controls (Lane et al., 1997; Cameraat, 2002; see also section 2.2). It should be noted that soil erosion appears to be much more sensitive to slope at the patch scale.

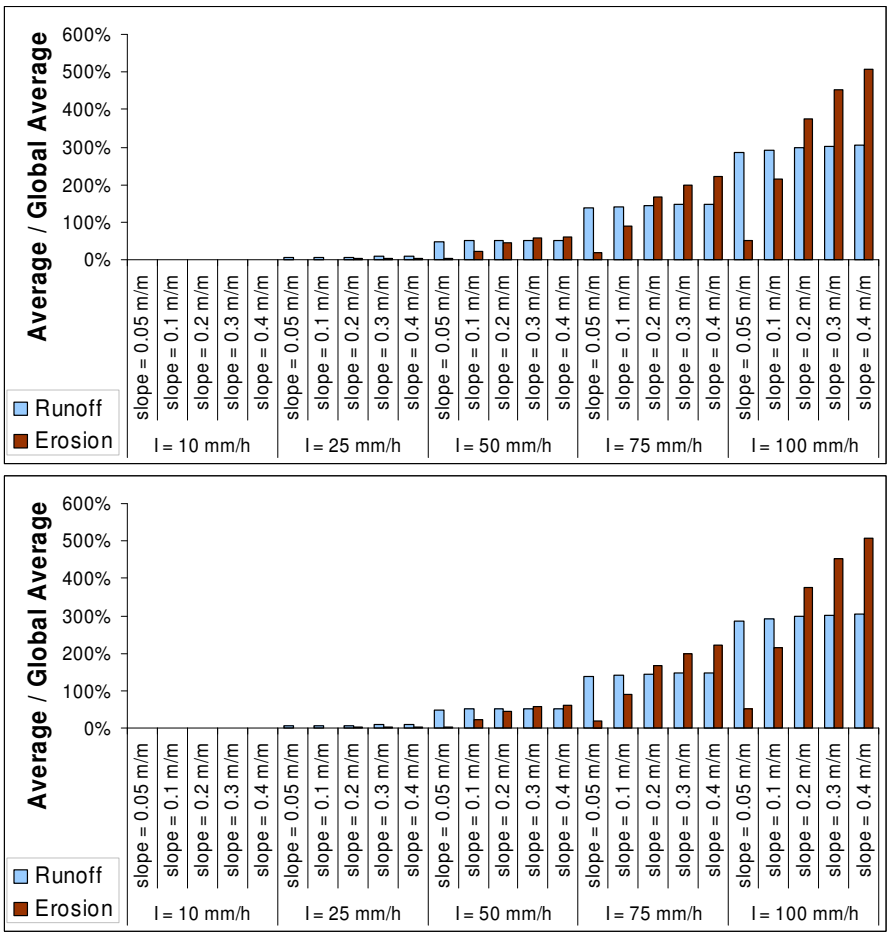

Figure 3.6 – Average runoff and erosion estimates for the different sensitivity tests, expressed as test average divided by the overall average for all tests, for the patch scale (top) and field/hillslope scale (bottom).

In terms of land use and soil parameters, the tests show that runoff generation is mostly sensitive to soil depth, moisture and porosity, as shown in Figure 3.7, although with low correlation values; there are no significant differences between spatial scales. In effect, the

model is more sensitive to the parameters which determine the soil's water holding capacity; this sensitivity increases with the total amount of rainfall, as the probability of achieving soil saturation increases. The sensitivity to soil depth appears to be dependent on the total amount of rainfall, and is only significant for very low values (below 800 mm) which are common in Mediterranean regions (Cardoso, 1965). Above these values, runoff is dominated by soil moisture and porosity only. The correlation with other parameters is not significant; however, saturated hydraulic conductivity and surface depression storage capacity impose a lower and upper limit (respectively) on runoff generation, as can be seen in Figure 3.8; this limit appears to be dependent on rainfall intensity. Furthermore, it should be noted the low importance of interception capacity; this is due both to the model formulation for interception storage, which is a product of capacity and canopy cover, and the low maximum interception values used in the test when compared with rainfall and depression storage. MEFIDIS could still be sensitive to interception capacity when simulating low-intensity storms in vegetated areas. Overall, the results show that MEFIDIS is sensitive to the formulation of soil water holding capacity for high-intensity storms, with results framed between the parameters chosen for K_{sat} and maximum depression storage.

Soil erosion estimates appear to be somewhat sensitive to runoff estimates, especially for higher slopes, as can be seen in Figure 3.9, albeit with relatively low correlation values; this is common to most erosion model formulations, as rill erosion and sediment transport is usually parameterized as depending on runoff velocity and depth (Jetten et al., 1999). This dependency could be linked with the relationship between the sediment transport capacity of runoff and slope in the formulation developed by Govers (1990) and used in the MEFIDIS model; at lower slopes, the low sediment transport capacity implies that other parameters control soil erosion estimates. Furthermore, the model is particularly sensitive to runoff estimates for low rainfall intensities, possibly since in these conditions the presence or absence of runoff conditions the existence of soil export. Finally, the model behaves differently at different scales for intermediate slope values; in this case, erosion estimates are more sensitive to runoff estimates at the field/hillslope scale, possibly due to the added importance of re-sedimentation. It should be noted that erosion estimates are also sensitive to the main parameters influencing runoff, such as soil depth, moisture and porosity.

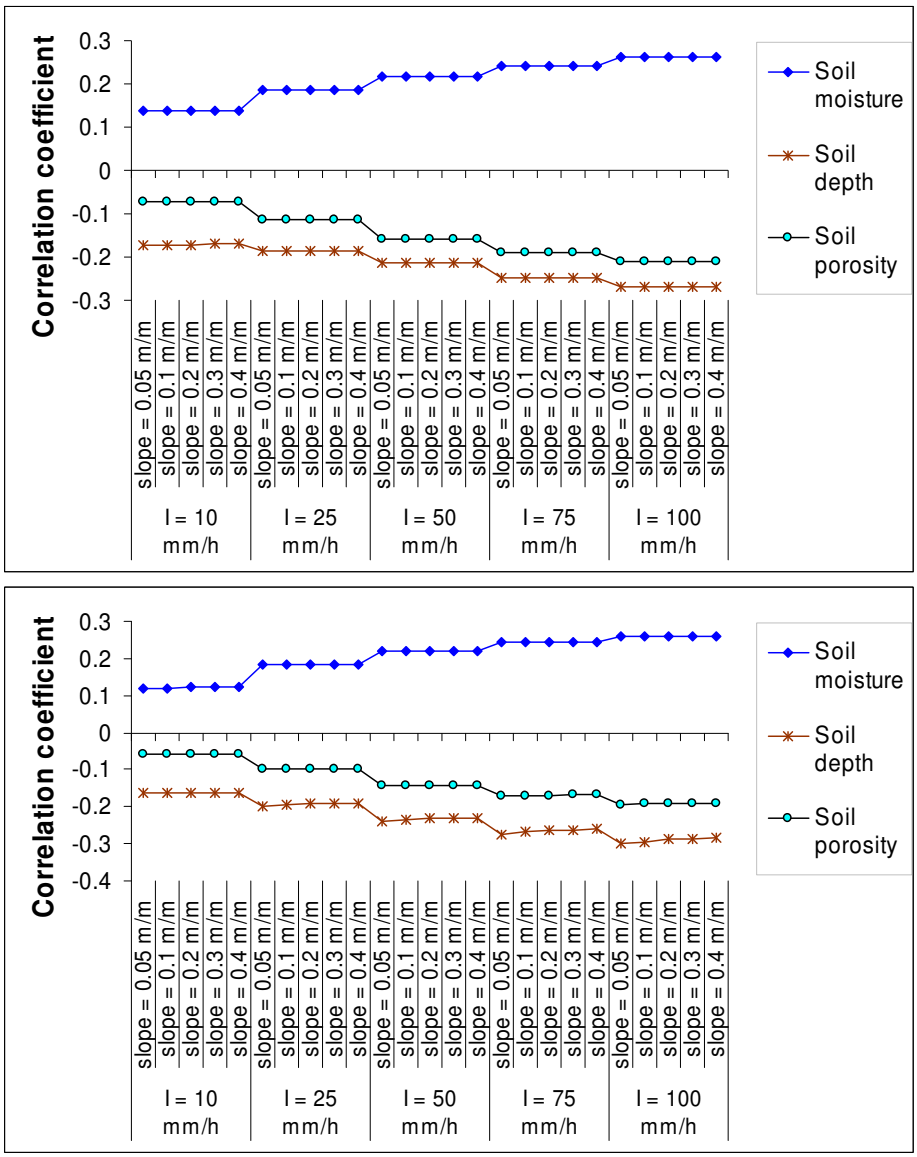

Figure 3.7 – Correlation coefficient between runoff and soil moisture, depth and porosity, for the different sensitivity tests at the patch scale (top) and field/hillslope scale (bottom).

In this case, however, model estimates are also sensitive to a number of other parameters besides runoff, as shown in Figure 3.10, albeit with low correlations. The sensitivity to the median particle diameter (d_{50}) of the soil appears to be inversely proportional to the sensitivity to runoff, albeit at a much larger scale; this could reflect the importance of particle diameter in sediment transport and deposition, which appears to be more important than runoff height for lower slope rates. In contrast, the importance of parameters which directly affect splash erosion, such as pavement and vegetation cover, clay mass fraction and depression storage (due to dampening the erosive power of raindrops; Ferreira and Singer, 1985), appears to be

directly proportional to the importance of runoff for soil erosion estimates, particularly at high rainfall rates with greater erosive power. Flow roughness, which impacts runoff velocity and therefore its sediment transport capacity, also has a similar importance for intermediate slopes, possibly since higher slopes have greater impact over velocity. These results indicate that, for low slopes and rainfall rates, MEFIDIS is sensitive to parameters governing sediment transport, while for high slopes and rainfall rates the model becomes sensitive to parameters governing sediment detachment. This is in accordance with current field observations and process knowledge (Boix-Fayos et al., 2005). Finally, it should be noted that, although the model is not very sensitive to soil shear strength, this parameter imposes an upper limit on possible soil erosion rates, much like previously described for the impacts of saturated hydraulic conductivity and depression storage capacity on runoff.

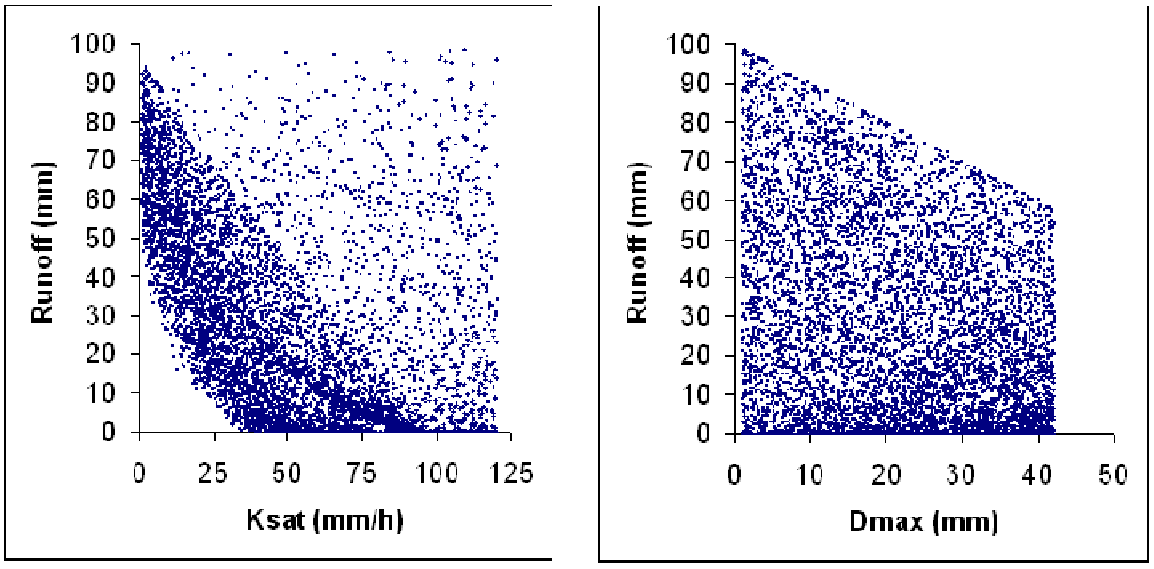

Figure 3.8 – Runoff estimates per saturated hydraulic conductivity (left) and depression storage capacity (right) for the hillslope/field scale test, 100 $mm.h^{-1}$ rainfall intensity and 0.4 $m.m^{-1}$ slope.

Overall, the sensitivity analysis shows that, at the single cell scale, the runoff and erosion estimates by MEFIDIS are somewhat sensitive to a number of parameters, but not dominated by any single parameter other than measured rainfall rates and surface slopes. Furthermore, different rainfall and slope conditions cause sensitivity to shift between different parameter subsets. These results indicate that the model is sensitive to particular combinations of

parameters, which can vary with storm and study area conditions, as often happens in complex physically-based models (Jetten et al., 1999, 2003). This implies that MEFIDIS can suffer parameterization problems such as equifinality (Beven, 2000). Furthermore, the analysis also shows that erosion estimates are sensitive to runoff estimates, implying that errors can propagate from one estimate to the other, as also often happens in erosion models (Morgan and Quinton, 2001; Jetten et al., 2003). Nevertheless, the dominance of rainfall rates and slope gradient on runoff and erosion estimates is encouraging, as these parameters are usually measured in the field with a good degree of precision.

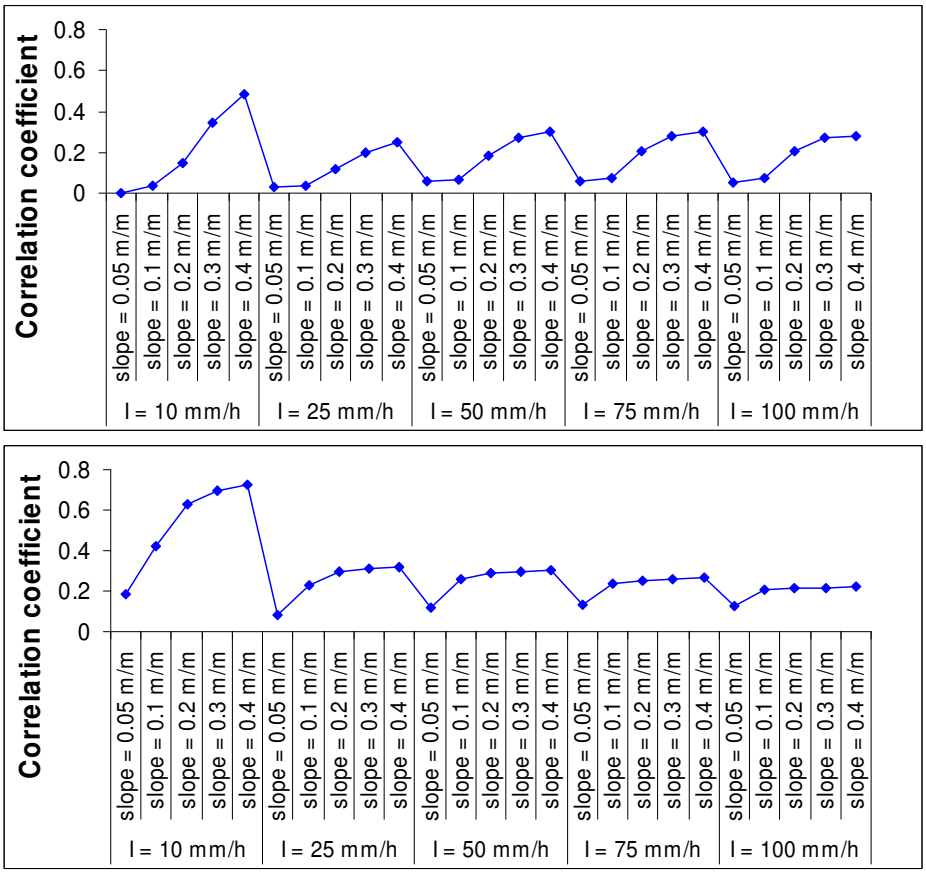

Figure 3.9 – Correlation coefficient between erosion and runoff, for the different sensitivity tests at the patch scale (top) and field/hillslope scale (bottom).

Finally, while model sensitivity was not evaluated at the catchment scale using this procedure, the application of MEFIDIS to several catchments within the context of this thesis allowed for a number of experiments to be conducted in this regard. Sections 3.3 and 4.4 provide further

information on this subject; overall, it appears that the runoff predictions by MEFIDIS are significantly sensitive to the parameterization of soil moisture at the catchment scale regardless of the method used, as is usually the case for event-scale runoff and erosion models (Jetten et al., 1999, 2003); the simulation of peak runoff rates and their location in time is also sensitive to channel roughness parameterization. Sediment yield predictions appear to be more dependent on the quality of total and peak runoff simulations, which was also observed by Jetten et al. (1999) in other models.

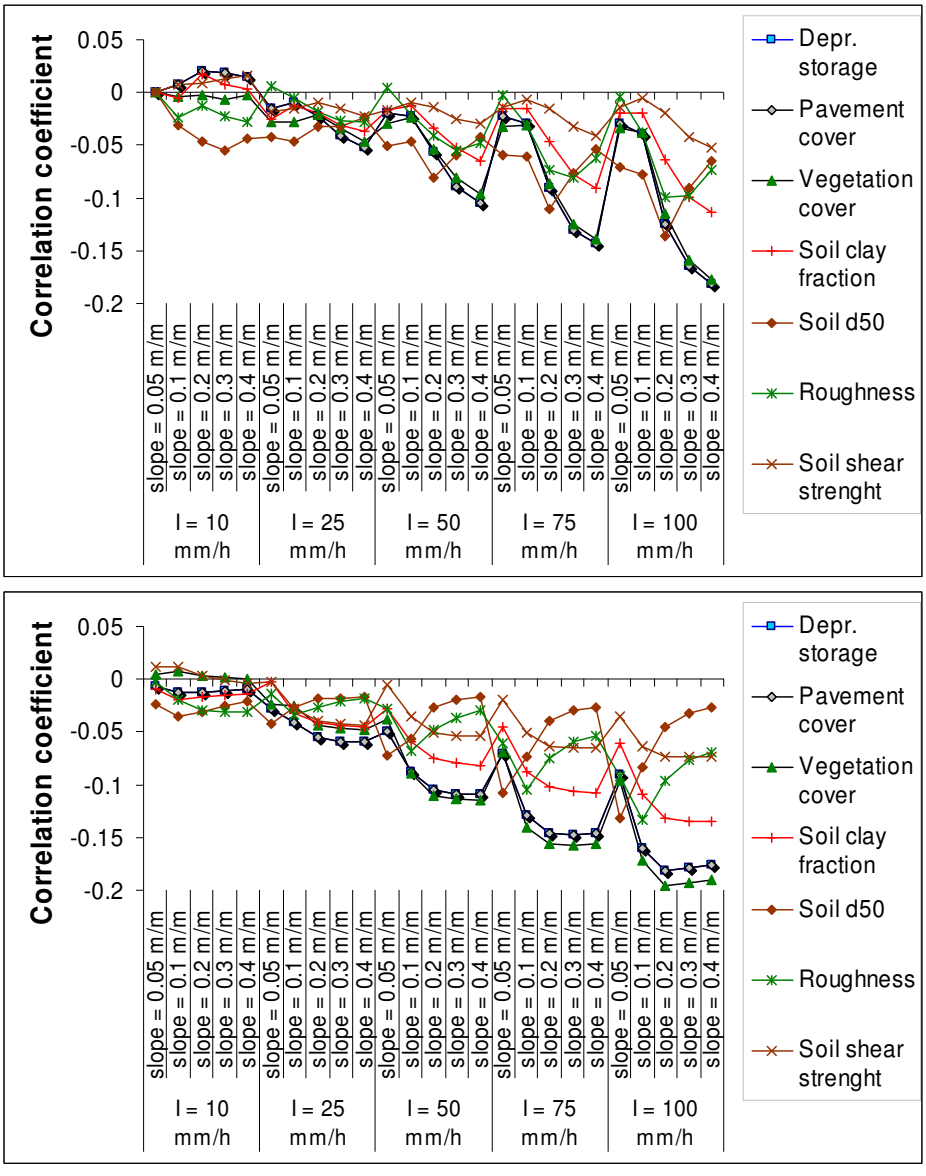

Figure 3.10 – Correlation coefficient between erosion and model landcover and soil parameters, for the different sensitivity tests at the patch scale (top) and field/hillslope scale (bottom).

3.3 MEFIDIS evaluation

Since MEFIDIS was specifically developed for this work, an evaluation of the model's robustness for climate and land use change assessment was required. This was performed using data from two well-studied catchments: a semi-arid natural catchment, Lucky Hills 103 (U.S.A.), and a humid agricultural catchment, Ganspoel (Belgium). The model's response to changes in climate parameters was also assessed by comparing its results with that of other event-scale models.

The following results were, for the most part, obtained under the Soil Erosion Network's model intercomparison exercise, which was carried out in Tucson, Arizona, in 2003. Several event models, including MEFIDIS, were applied to the Lucky Hills 103 and Ganspoel watersheds by a team of experts, and the results used to evaluate the sensitivity of hydrological and erosion parameters to climate change (Nearing et al., 2005a). The results from this exercise, including the two references mentioned above, can be found on Catena's special issue on "soil erosion under climate change: rates, implications and feedbacks", described by Nearing et al. (2005b). The results for the model robustness assessment were previously published in Nunes et al. (2005); the full results for the model intercomparison exercise are reported by Nearing et al. (2005a). The following section presents a brief summary focusing on the MEFIDIS model performance.

3.3.1 Model robustness

The quality of predictions made by physically-based watershed models such as MEFIDIS is very sensitive to input parameters (Wu et al., 1993; Jetten et al., 1999, 2003). Model results can generally be improved by adjusting the parameters through calibration, but an excessive calibration for a small collection of events does not imply that the model will perform well for events whose characteristics differ from those used in the calibration exercise (Favis-Mortlock et al., 2001). Furthermore, models used for prediction and management purposes are usually applied to simulate conditions which do not exist and therefore cannon be accounted for during calibration (Beven, 2000; Morgan and Quinton, 2001). A model used for these purposes must be assessed in terms of robustness, i.e. its capacity to reasonably perform with similar parameter values, including highly dynamic ones, for the widest possible range of conditions (Toy et al., 2002).

This section assesses the robustness of MEFIDIS for two well studied catchments: a semi-arid natural catchment, Lucky Hills 103 (U.S.A.), and a humid agricultural catchment, Ganspoel

(Belgium). The model was run using a single parameter set for each catchment and simple assumptions on soil moisture content (dry or wet), and was applied to a variable set of events. The focus on soil moisture assumptions follows the model's sensitivity to this parameter, as discussed in section 3.2.3. The quality of within-watershed predictions were also evaluated using runoff measurements at a point inside Lucky Hills 103 and observed erosion and deposition patterns in Ganspoel.

Study sites

Lucky Hills 103 (Figure 3.11, top) is a small (3.7 ha) instrumented catchment inside the Walnut Gulch test watershed, Arizona. A small nested catchment, Lucky Hills 101 (1.3 ha), is also instrumented for runoff measurement. This area represents a semi-arid rangeland with a gravelly sandy-loam soil, covered with rocks and shrub vegetation. The Lucky Hills 103 dataset has been described in detail by Ritchie et al. (2005).

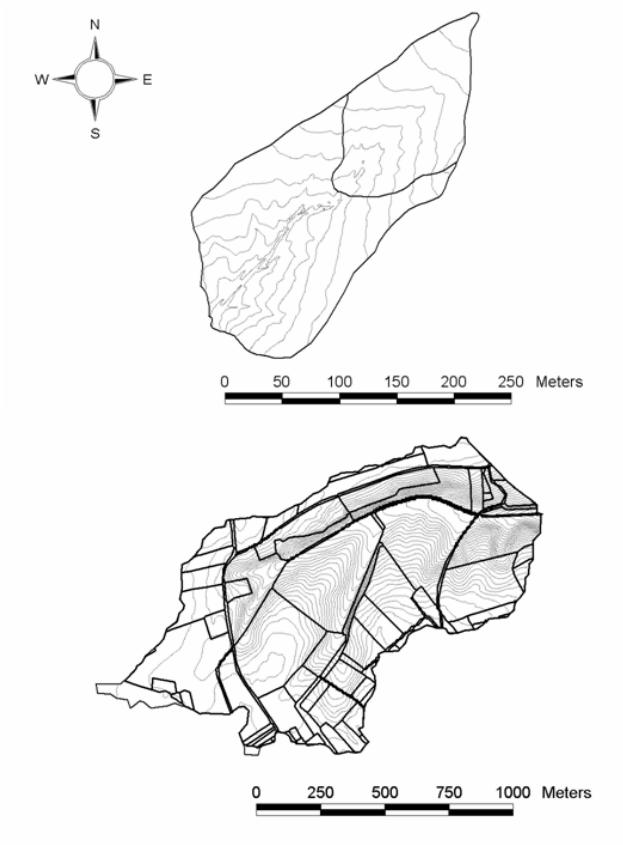

Figure 3.11 – The Lucky Hills 103 (top) and Ganspoel (bottom) catchments, with 5 m contour lines; darker lines represent the Lucky Hills 101 nested catchment (top) and field boundaries in Ganspoel (bottom).

The Ganspoel watershed (Figure 3.11, bottom) is a larger catchment (111 ha), representative of a temperate agricultural area over the European loess belt. Soils in this region are very prone to crusting, a condition which leads to decreased permeability and increased runoff and erosion (Cerdan et al., 2001). The catchment is subdivided into c. 80 fields with crops varying with season: typical crops are winter cereals followed by maize or a root crop, such as beet or potatoes. Four land use cases were studied: May 1997, dominated by beet, winter cereals and summer cereals; July 1997, with the same occupation as in May but with crops in a latter stage of development; August 1998, dominated by beet, potatoes and winter cereals; and September 1998, with the same occupation as in August except that winter cereals were harvested. The Ganspoel watershed has been described in detail by Van Oost et al. (2005).

Evaluation Method

The evaluation of MEFIDIS was performed using seven rainfall events for the Ganspoel catchment and nine events for the Lucky Hills 103 catchment; event rainfall, runoff and erosion characteristics are shown in Table 3.4. The model was applied using a spatial resolution of 5×5m and a temporal resolution of 1 second. A split-sample calibration/validation test was performed using data collected at the outlet, taking three events for calibration and the remaining ones for validation. Calibration events were selected to represent the largest possible range of measured conditions, as model performance usually diminishes for events outside the calibration interval (Favis-Mortlock et al., 2001).

The objective of this exercise was to assess model performance using a single set of calibrated parameters and general assumptions of initial soil moisture; in this case, soil moisture was considered at full capacity when an event equal or greater than 10 mm occurred in the six hours prior to the event, and at field capacity in the remaining cases. Since runoff and erosion models are usually very sensitive to the assumed initial soil moisture at the beginning of each event (Jetten et al., 1999, 2003), this test was conducted to evaluate whether simplified assumptions such as the one described in section 3.2.2 lead to satisfactory simulation results. Test variables were total runoff, peak runoff rates, and net erosion.

Model agreement with outlet measurements does not necessarily mean that results within the watershed are adequately simulated (Jetten et al., 2003). To assess within-catchment model performance for Lucky Hills 103, available runoff measurements for the nested 101 sub-basin (Figure 3.11) were evaluated in the same way as the outlet measurements. For Ganspoel, a spatial comparison between simulated and mapped patterns of erosion and deposition was performed for the events that occurred in May 1997. These maps indicate the location of

erosion features (rills and gullies) and deposition as observed in this period. Although these features might reflect the consequences of all erosive storms since the previous tillage operations, spatial patterns were considered to remain stable throughout the period.

Table 3.4 – Characteristics of events used in the model evaluation exercise.

	Event date	Rainfall (mm)	Mean rainfall intensity (mm.h^{-1})	Runoff (mm)	Peak runoff rate (mm.h^{-1})	Net soil loss (ton.ha^{-1})
Ganspoel	19-May-1997[a]	10.0	25.0	0.23	0.33	0.082
	21-May-1997[b]	3.0	25.7	0.16	0.18	0.025
	11-Jul-1997	19.5	33.4	2.15	2.79	0.387
	23-Aug-1998[a, c]	22.5	2.9	0.47	0.15	0.007
	24-Aug-1998[b, d]	10.0	10.9	0.13	0.12	0.006
	9-Sep-1998	10.5	9.8	0.31	0.22	0.013
	14-Sep-1998[a, b, c]	41.0	5.3	9.19	3.3	0.595
Lucky Hills 103	12-Aug-1982[a]	6.6	32.0	0.34	2.98	0.082
	23-Aug-1982	30.7	19.2	5.12	12.03	0.913
	10-Sep-1982	18.8	12.6	3.38	9.02	0.721
	10-Sep-1983	26.7	20.3	6.55	15.94	0.878
	20-Sep-1983[a]	18.5	34.8	2.09	6.02	1.145
	1-Sep-1984[a]	32.8	33.0	15.55	47.67	3.075
	14-Jul-1985	13.7	16.3	0.38	1.87	0.101
	14-Jul-1985[b]	10.7	20.0	1.18	5.68	0.374
	2-Aug-1985	5.9	42.0	0.58	4.35	0.137

a – event used for calibration.
b – 100 % soil water saturation assumed.
c – 0.1 mm baseflow not considered.
d – 0.2 mm baseflow not considered.

Calibration procedure

The calibration storms were used to derive a best fit parameter set, used subsequently in model validation. Initial values for the parameters described in Table 3.1 were taken from measurements; rock fragment cover in Lucky Hills 103 was represented by P_{cv}. Measurements were not available for D_{max}, I_{max} and d_{50} in both cases; θ, ψ and n values were also lacking for Lucky Hills 103. D_{max} was calculated from random roughness following Kamphorst et al. (2000). I_{max} was calculated from Leaf Area Index values compiled by Scurlock et al. (2001), using the method described by Hoyningen-Huene (1983). Values for d_{50} were calculated from soil texture measurements using a fractal approach (Bittelli et al.,

1999). Soil texture was used to estimate θ and ψ for Lucky Hills 103 following Chow et al. (1988), while n was selected based on land cover (USDA, 1986). Calibration focused on the saturated hydraulic conductivity K_{sat} and the depression storage capacity D_{max}; a comparison between calibrated and measured values for these parameters is shown in Table 3.5.

Table 3.5 – Calibrated hydraulic conductivity and depression storage capacity compared with measured values.

		Sat. hydraulic conductivity (mm.h^{-1})		**Depression storage capacity (mm)**	
	Land use	**Calibrated**	**Measured**	**Calibrated**	**Estimated[a]**
Ganspoel	Beet[b]	38	37.6 – 540.3	2	2.5 – 3.1
	(crusted)[c]	4.2	4.2 – 32.1	1.8	
	Forest	35	3.4 – 362.6	2.5	2.8
	Meadow	15	2.7 – 151.1	2	2.8
	Fallow (crusted)[b]	1.5	1.1 – 25.3	3	5.6
	Maize[b]	18	17.3 – 120	1.8	2
	(crusted)[c]	4.5	4.2 – 32.1		
	Potatoes[b]	38	37.6 – 540.3	2.5	2.5
	(crusted)[c]	7.5	1.1 – 25.3		
	Summer Cereals[c]	8	1.9 – 319.9	2.4	2.2 – 3.4
	Winter Cereals	8	1.9 – 319.9	2	2.5
	Track	–	–	1.4	1.4
	Road	–	–	1.4	1.4
	Building	–	–	1.4	1.4
Lucky Hills 103	Shrub[d]	8	9.8	7.5	5.6

a – D_{max} values estimated following Kamphorst et al. (2000), with an error of 3 mm.
b – values calibrated and validated for 1998 only.
c – values calibrated and validated for 1997 only.
d – D_{max} values estimated for California shrub.

It should be noted that, for both catchments but especially for Ganspoel, calibrated K_{sat} values are significantly lower than the average measurements. An explanation can be found in the fact that MEFIDIS uses the Green-Ampt method to calculate infiltration rates; Chow et al. (1988) refer that the K_{sat} parameter used in this method is a "field" parameter, significantly lower than the hydraulic conductivity for saturated soil. Soil erosion was calibrated by

changing d_{50} from 0.022 mm to 0.02 mm for Ganspoel and from 0.11 mm to 0.1 mm for Lucky Hills 103.

One difficulty in estimating a common parameter set for the Ganspoel catchment is the significant variation in vegetation cover with season, with consequences for surface roughness. Four V_{cv} and n parameter sets were estimated, one for each month when simulated events occurred; V_{cv} was taken directly from measured values, and n was estimated using a regression with random roughness and vegetation cover. Another difficulty in Ganspoel is the difference in surface crusting conditions observed during the simulated events; this impacts soil infiltration rates (Cerdan et al., 2001) and surface storage (Darboux et al., 2001). For half of the analyzed land cover types, two sets of parameters were calibrated for K_{sat} and D_{max}, but one set was validated for 1997 only and the other for 1998 only; the effects of crusting on soil erodibility were not taken into account. Overall, it was impossible to find a common parameter set for every storm in Ganspoel due to the variable conditions; this would require a significant number of additional storm events for calibration and validation.

Watershed results

Table 3.6 shows the model results for both watersheds, compared with measured values at the outlet for runoff, peak runoff and net erosion; Figure 3.12 compares the results for net erosion with the 1:1 line of agreement. The correlation between the simulated and observed results after normalization (Table 3.7) is quite good, showing that MEFIDIS performs well in predicting the relative consequences of storms. The Nash-Sutcliffe efficiency index (Beven, 2000) is also widely used as an indicator of model performance; the index measures the variance of the simulated results from the 1:1 prediction line, with values above 0.5 considered to be satisfactory (Morgan and Quinton, 2001). In this case (Table 3.7), this index indicates a good agreement between simulated and observed results, with values ranging between 0.61 and 0.87.

An analysis of the average unsigned error (Table 3.7) shows a significant dispersion around the 1:1 line of agreement, with values ranging from 37 % to 47 %; in other words, MEFIDIS performs better in terms of accuracy than in terms of precision. However, this error must be compared with variability in erosion measurements; Nearing et al. (1999) found that the variability in measured soil erosion from replicated plots, under similar rainfall, soil and surface conditions, decreased with increasing magnitude of soil loss, from 150 % for a measured soil loss of 0.1 ton.ha^{-1} to 14 % for measured soil loss of 200 ton.ha^{-1}. Although extrapolation of plot values for watersheds is difficult, this implies that at least a part of the

model error can be explained due to variability in net erosion measurements and surface condition factors which are difficult to estimate with precision. This conclusion is supported by the fact that the relative difference between simulated and measured results (calculated following Nearing et al., 1999) for Lucky Hills 103 significantly decreases with soil loss magnitude (Figure 3.13; the correlation coefficient between measured erosion and relative difference is -0.77). This fact also helps to explain the high values for the Nash-Sutcliffe index, when considering that values above 0.7 are not expected due to the uncertainty inherent to field measurements (Morgan and Quinton, 2001). Not only is there large variance between measurements due to the selected range of events, but this index is biased towards model performance for the larger magnitudes (Beven, 2000), where it is significantly better.

Table 3.6 – Measured and simulated results for the events detailed in Table 3.4.

		Runoff		**Peak Runoff**		**Net Erosion**	
	Event date	**Measured (mm)**	**Simulated (mm)**	**Measured ($mm.h^{-1}$)**	**Simulated ($mm.h^{-1}$)**	**Measured ($ton.ha^{-1}$)**	**Simulated ($ton.ha^{-1}$)**
Ganspoel	19-May-1997[a]	0.23	0.29	0.33	0.45	0.082	0.084
	21-May-1997	0.16	0.11	0.18	0.14	0.025	0.008
	11-Jul-1997	2.15	2.00	2.79	2.13	0.387	0.303
	23-Aug-1998[a]	0.47	0.17	0.15	0.12	0.007	0.008
	24-Aug-1998	0.13	0.14	0.12	0.15	0.006	0.012
	09-Sep-1998[a]	0.31	0.47	0.22	0.79	0.013	0.162
	14-Sep-1998	9.19	4.10	3.30	2.03	0.595	0.409
Lucky Hills 103	12-Aug-1982[a]	0.34	0.11	2.98	0.55	0.082	0.013
	23-Aug-1982	5.12	6.16	12.03	9.78	0.913	1.377
	10-Sep-1982	3.38	0.91	9.02	1.53	0.721	0.171
	10-Sep-1983	6.55	9.62	15.94	22.01	0.878	1.941
	20-Sep-1983[a]	2.06	3.65	6.02	8.71	1.145	0.819
	01-Sep-1984[a]	15.55	16.17	47.67	38.05	3.075	3.377
	14-Jul-1985	0.39	2.00	1.87	5.72	0.101	0.437
	14-Jul-1985	1.18	3.00	5.69	7.15	0.374	0.671
	02-Aug-1985	0.58	0.15	4.35	0.66	0.137	0.023

a – event used for calibration.

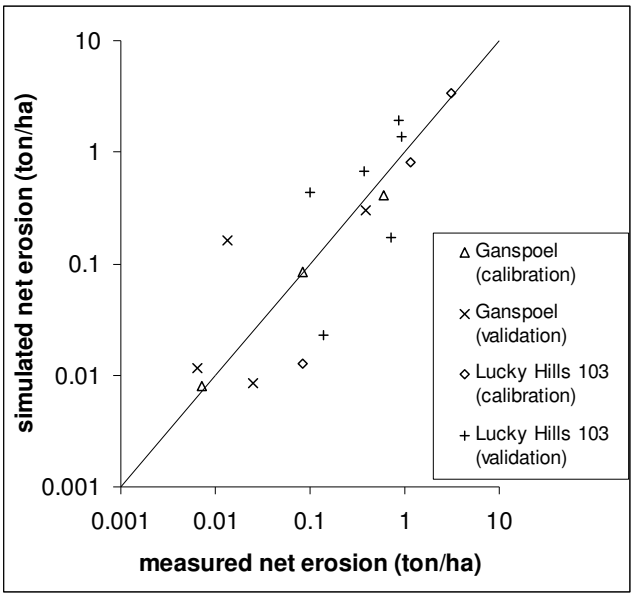

Figure 3.12 – Measured and simulated results for net erosion in Ganspoel and Lucky Hills 103, compared with the 1:1 agreement line (logarithmic scale).

Table 3.7 – Overall correlation coefficient, Nash-Sutcliffe efficiency index and average unsigned error for the results shown in Table 3.6.

		Runoff	Peak Runoff	Net Erosion
Ganspoel	**Correlation coefficient** [a]	0.96 (p = 0.01)	0.93 (p = 0.01)	0.88 (p = 0.01)
	Nash-Sutcliffe efficiency index	0.61	0.80	0.81
	Average unsigned error (%)	46	38	40
Lucky Hills 103	**Correlation coefficient** [a]	0.89 (p = 0.01)	0.85 (p = 0.01)	0.86 (p = 0.01)
	Nash-Sutcliffe efficiency index	0.87	0.85	0.7
	Average unsigned error (%)	37	37	47

a – correlation between the squared roots of measured and observed values.

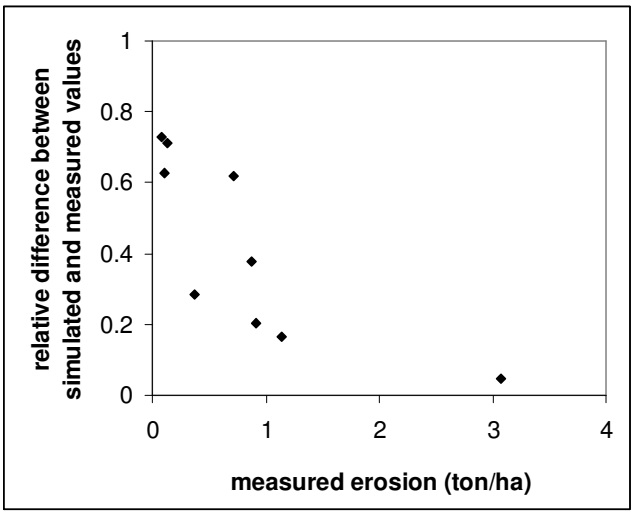

Figure 3.13 – Relationship between erosion magnitude and relative difference between measured and simulated values (the error divided by the sum of measured and simulated values).

For the Ganspoel catchment, average unsigned error values do not vary significantly with storm magnitude. One cause for this may be that the observed event magnitude in Ganspoel is smaller than that observed for Lucky Hills 103. However, a more likely explanation might rest with the propensity of loess soils to crusting; when crusting is not dynamically simulated (as is the case for MEFIDIS), the model error may increase with event magnitude (Jetten et al., 2003). When the model was calibrated individually for each event by adjusting only K_{sat} and D_{max} to reflect the possible crusting effects of previous rainfall conditions and within-event storm magnitude, i.e. lowering both to represent increased soil crusting (Cerdan et al., 2001; Darboux et al., 2001) down to the lowest measured values (Table 3.5), model results improved substantially (Figure 3.14). The average unsigned error dropped to 14-15 % for runoff, peak runoff and net erosion. These results indicate that the model could be improved by a better description of the crusting effects, at least in the case of the Ganspoel catchment, or in alternative, different soil parameterizations depending on event intensity.

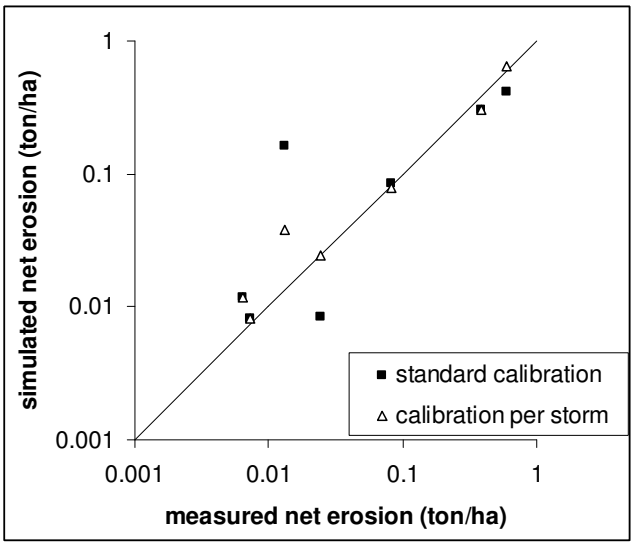

Figure 3.14 – Comparison of simulated and measured net erosion in Ganspoel, with MEFIDIS using a standard calibration for all storms and a unique calibration per storm.

Finally, one significant factor for the lack of model precision can be the simplified assumptions taken for initial soil moisture, a parameter to which most runoff and erosion models are highly sensitive (Jetten et al., 1999, 2003). The percent error margin, however, is still small compared with the variability within measured conditions for both watersheds (one order of magnitude for peak runoff rates and two orders of magnitude for both runoff and net erosion; see Table 3.4), which shows that the model performs well for the selected catchments and land use conditions.

Within-watershed runoff rates

Simulated values for runoff and peak runoff for the Lucky Hills 101 sub-watershed were also compared with measured values (Table 3.8). Lucky Hills 101 represents around 35 % of the Lucky Hills 103 catchment area (Figure 3.11). A comparison of model results shows that there is a slight increase in the average unsigned error when compared with the simulations for the entire catchment (Table 3.6); in relative terms, the errors are higher for total runoff (40 %) and lower for peak runoff (30 %). While the smaller number of events measured at Lucky Hills 101 might explain the differences in error, these results indicate that MEFIDIS has a good performance in simulating runoff rates within the Lucky Hills 103 watershed.

Table 3.8 – Measured and simulated results for the events detailed in Table 3.4, for Lucky Hills 101.

	Runoff		Peak Runoff	
Event date	**Measured (mm)**	**Simulated (mm)**	**Measured ($mm.h^{-1}$)**	**Simulated ($mm.h^{-1}$)**
12-Aug-1982	0.18	0.06	3.20	0.23
23-Aug-1982	5.59	7.04	22.92	15.06
10-Sep-1982	2.94	0.92	10.25	2.31
20-Sep-1983	2.65	4.25	18.04	15.04
01-Sep-1984	14.70	17.83	54.85	65.58
14-Jul-1985	0.36	2.58	-	-
02-Aug-1985	0.14	0.07	1.36	0.81

Spatial patterns of erosion and deposition

Observed areas of rill/gully erosion and sedimentation in Ganspoel for May 1997 were compared with the simulated results for the two events occurring in that month (Table 3.4). The simulated erosion map was calculated by adding the spatially-distributed model results for erosion and deposition for both events.

Figure 3.15 compares simulated and observed erosion and deposition areas. A direct comparison is difficult since the threshold erosion rate above which these areas are mapped is not known; an arbitrary threshold of 5 $ton.ha^{-1}$ was selected for both erosion and deposition to create the map showing simulated patterns. The Figure shows that MEFIDIS was capable of locating the main sediment sources and sinks within the Ganspoel catchment during this period. The model was also able to assign major erosion features to the appropriate fields.

These results also show that the simulated maps of erosion and deposition are not reliable when considering a resolution of 5 × 5 m. One source of errors appears to be the fact that roads were not taken into account when building the flow directions map, leading to significant areas of erosion and deposition at roadsides. Another problem is that observed erosion areas represent only 1.7 % of the total catchment area, while deposition areas represent only 0.4 % of the total. Significant erosion patterns are more likely to occur on regions of concentrated flow (Foster, 1982); errors in flow routing when considering only eight possible directions, as is the case of MEFIDIS, can cause significant errors in locating these areas (Costa-Cabral and Burges, 1994). This can be seen in Figure 3.15, where the

simulated erosion patters are much more dispersed than the observed patterns; the latter either occur uniformly over slopes or along flow lines.

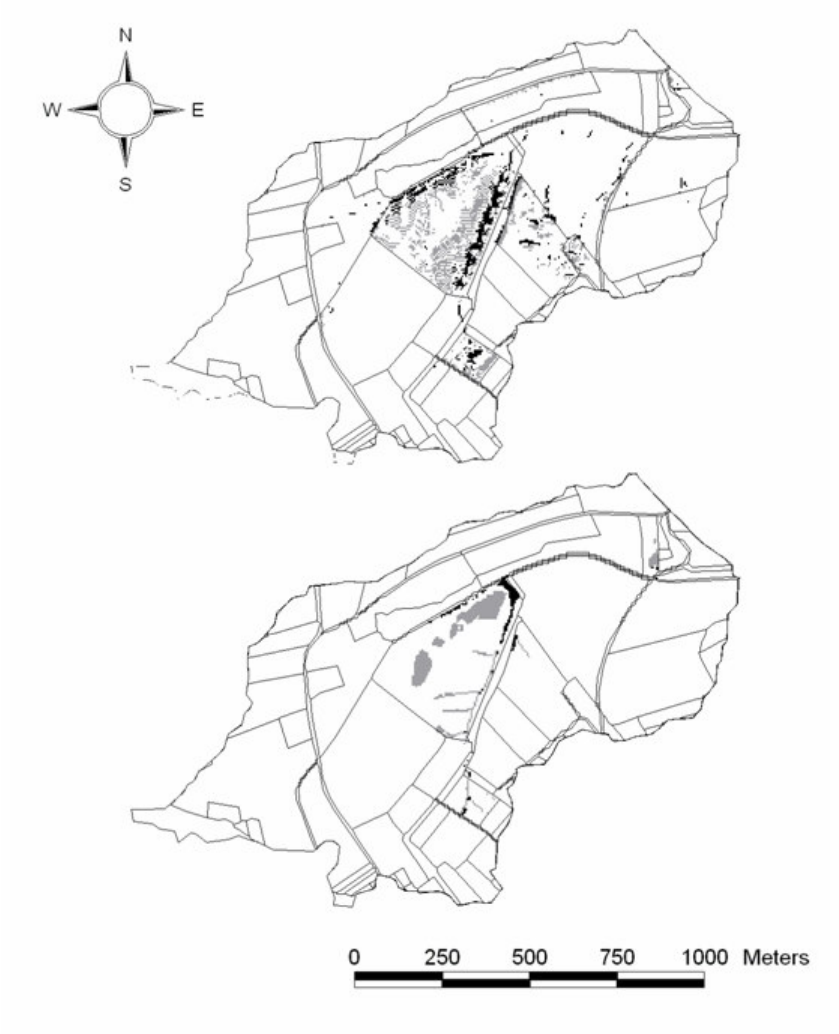

Figure 3.15 – Simulated (top) and observed (bottom) patterns of erosion (grey) and deposition (black) in Ganspoel, for May 1997; lines represent field boundaries.

Similar results were obtained by Jetten et al. (2003) for the LISEM erosion model, where flow routing determination is done in a similar way to the MEFIDIS approach (Jetten and De Roo, 2001); in that case, simulated erosion rates with a 10 × 10 m resolution were only correlated with observed values when the resolution was resampled to 50 × 50 m. Jetten et al. (2003) indicate that one source of this positional error might lie with flow path delineation; another source of uncertainty referred is the high spatial variability of parameters assumed constant by

the model. The latter case appears to be a common problem of spatially distributed models (Morgan and Quinton, 2001).

The displacement error of simulated erosion and deposition patterns was estimated by calculating average erosion and deposition rates according to their distance to observed features. This was done by creating a map representing this distance in 5 m increments, and calculating the average model results for erosion and deposition inside each class; the results are shown in Figure 3.16. In both cases, simulated rates decrease sharply with distance to the mapped areas. Beyond a distance of c. 75 m for erosion and c. 60 m for deposition, both erosion and deposition rates remain constant and below a threshold of c. 0.5 ton.ha^{-1}. When considering this threshold, MEFIDIS accuracy in classifying regions without erosion or deposition (the largest part of the catchment) is 85.2 %. In absolute terms, 75 % of the mass of eroded soil came from within 65 m of mapped soil erosion regions, and 75 % of the mass of deposited soil occurred within 105 m of mapped deposition regions. These results show that MEFIDIS was able to reasonably locate sediment sources and sinks inside Ganspoel for May 1997, although with a low precision.

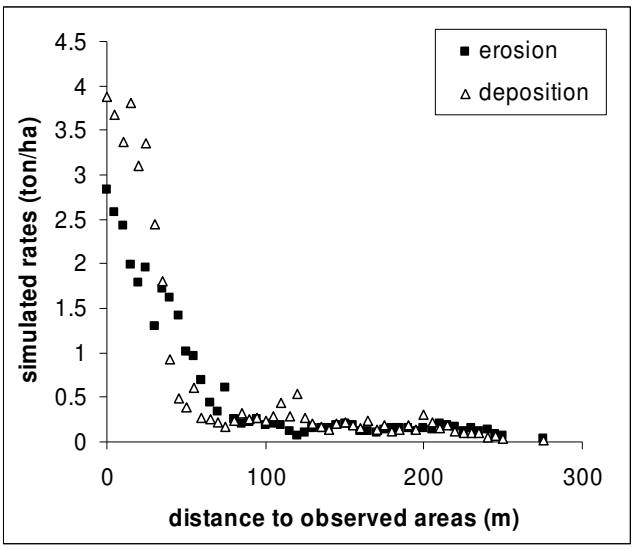

Figure 3.16 – Variation of average simulated erosion and deposition rates with distance to observed erosion and deposition features in Ganspoel, for May 1997.

Discussion

Overall, the results of this simulation exercise show that MEFIDIS can be applied to watersheds using common calibrated parameter sets and simplified assumptions on soil moisture with good accuracy; model precision is less satisfactory, although it is in part related to the uncertainty surrounding erosion measurements and improves with event magnitude. The precision of the results is still sufficient to estimate runoff and soil erosion rates when considering the range of events selected for the evaluation exercise. For the Lucky Hills 103 test site, a single parameter set could be defined that provided good results for all analyzed events, including the Lucky Hills 101 nested watershed. For Ganspoel, however, different parameter sets were required to reflect changes in land-use, vegetation growth and surface conditions. This indicates that in complex watersheds, model calibration and validation must rely on measured events for several land use scenarios; similar results have been found for other models (e.g. Morgan and Quinton, 2001).

The performance of MEFIDIS in detecting soil erosion patterns for Ganspoel was difficult to evaluate due to the nature of the observations, but it is clear that small-scale precision should not be expected. The main factor is apparently the algorithm used to delineate flow routing paths; these results are comparable to those of Jetten et al. (2003) for LISEM. Improved performance could come from designing flow paths taking into account roads (Duke et al., 2003) or tillage direction (Takken et al., 1999). Another possibility is taking into account two-dimensional flow paths instead of limiting them to a single direction (Costa-Cabral and Burges, 1994; Liu et al., 2004); however, this would require a significant shift in the conceptualization of MEFIDIS, and possibly a revision of the one-dimensional flow equations (Chow et al., 1988).

One way to improve model precision for Ganspoel appears to be a better estimation of surface crusting conditions and their reflection on surface properties. Simple assumptions per land-cover type and condition can be established using data from remote sensing (e.g. Baghdadi et al., 2002; Oh, 2004) or laboratory studies (e.g. Assouline and Mualem, 2000); an example of this approach can be found in Cerdan et al. (2001).

Overall, the results show that MEFIDIS can be a robust tool for predicting the effects of change in storm characteristics for runoff, peak runoff rates and soil erosion, for the same watershed and land use conditions. The model also performed well in predicting the general location of significant erosion features, indicating its usefulness as a spatially-distributed risk assessment tool. However, the potential to simulate changes in land use patterns and

vegetation properties requires further analysis with more extensive datasets both for calibration and validation. The capacity to simulate within-catchment erosion and deposition rates also requires further evaluation.

3.3.2 Model intercomparison exercise

There is always a level of uncertainty in interpreting the results of model-based studies of the climatic sensitivity of soil erosion, since each erosion model has limitations in terms of its representation of erosion processes (Jetten et al., 1999, 2003). The Soil Erosion Network's model intercomparison exercise was carried out in Tucson, Arizona, in 2003 (Nearing et al., 2005a), as a follow-up to other exercises as described in section 2.3; the objective was to investigate the response of a variety of different soil erosion models to key variables expected to be impacted by climate change: precipitation and vegetation. The models were calibrated using data for the Lucky Hills 103 and Ganspoel watersheds described in section 3.3.1. Perturbations were then made to rainfall intensities and amounts, and to plant cover in order to assess and compare the sensitivities of simulated storm runoff and erosion rates. The following sections briefly present the results reported by Nearing et al. (2005a), focusing on the performance of MEFIDIS compared with that of other models used in the exercise.

Models and methods

For this exercise, a representative sample of currently existing erosion models was selected. The sample included:

- the Physically-Based Distributed Erosion Model (MEFIDIS), described in section 3.2;
- the Limburg Soil Erosion Model (LISEM), a process-based model designed for extreme events in small watersheds, using a grid-based runoff and sediment routing algorithm (de Roo et al., 1996a and b);
- the Revised Universal Soil Loss Equation (RUSLE), an upgrade from the empirically based USLE (Renard et al., 1997);
- the Sealing and Transfer by Runoff and Erosion related to Agricultural Management model (STREAM), a non-dynamic model combining an empirically-based approach to derive runoff generation and erosion with a grid-based runoff and sediment routing algorithm based on topography and agricultural features such as furrows or ditches (Cerdan et al., 2002);

- the Kinematic Erosion model (KINEROS), a process-based model designed for extreme events, using a runoff and sediment routing algorithm based on representing a catchment as a cascade of planes and channels (Smith et al., 1995);

- the Soil and Water Assessment Tool (SWAT), a process based model running continuously with a daily time-step, representing spatial variability by dividing a watershed into Hydrological Response Units (HRUs) with similar vegetation and soil characteristics (Neitsch et al., 2002a; see also section 3.4);

- the Water Erosion Prediction Project (WEPP), a process based model running continuously, representing spatial variability by simulating representative hillslopes inside a watershed (Flanagan and Nearing, 1995).

Further information on the classification of these models is found in section 2.3 (Table 2.8). As can be seen from the list, the selected models are quite heterogeneous. They combine different approaches to process description – empirical or physical; temporal description – dynamical simulation within events, lumped simulation of events or non-dynamic representation of average conditions; and spatial description – based on a topographical grid, on a cascade of planes and channels, or on representative areas. Consequentially, not all models were applied in the same way or to the same exercises. For example, LISEM required a separate calibration for each event due to its detailed description of many processes, while RUSLE required the adjustment of a long-term rainfall erodibility factor for each storm. Vegetation process description in SWAT is too complex to allow tests of variable vegetation cover, while in STREAM vegetation cover is described with a simple class method which was ill-suited for the vegetation cover change tests. In terms of spatial scale, both WEPP and RUSLE had problems in adequately representing the larger Ganspoel catchment, and the latter wasn't applied to this dataset. Finally, lack of suitable data meant that SWAT was not applied to the Ganspoel catchment, while STREAM's application to Lucky Hills suffered from a number of parameter estimation problems. All these examples show how models suffered different limitations in the exercise which were unrelated with the method of process representation or with the degree of model complexity.

The basic methodology for this exercise was to calibrate the models to measured data for the two watersheds, and to then superimpose change scenarios on those baseline simulations. A sample of storms were selected from each of the data sets to serve as baseline scenarios, represented in Table 3.4; for Ganspoel they are the events which occurred in 19 and 21 May

1997, 11 July 1997, and 14 September 1998, while for Lucky Hills the event dates are 12 August and 10 September 1982, and 1 September 1984. The sensitivity of runoff and sediment yield was assessed relative to changes in rainfall and vegetation parameters, relative to unchanged (baseline) conditions; the specific parameters and test characteristics are described in Table 3.9. Each test consisted of changing the parameters by -20 %, -10 %, +10 % and +20 %; the ratios of predicted runoff and sediment yield versus corresponding values for the zero change condition were calculated for each model, each storm and each change test. This was done in order to compare changes in model response as a function of storm and cover inputs, ignoring absolute estimates of runoff and erosion.

Table 3.9 – Characteristics of the rainfall and vegetation cover change tests.

Test	Parameters
1A	Rainfall amount and intensity (keeping duration constant)
1B	Rainfall amount and duration (keeping intensity constant)
2	Rainfall intensity only (reducing duration to keep rainfall amount constant)
3A	Ground cover (or Manning's roughness coefficient)
3B	Canopy cover
3C	Ground and canopy cover

Results and discussion

The results were interpreted using linear sensitivity analysis, with values calculated using linear regression between the percent change of response variable to the percent change of input variable for each model and each test. The median values of sensitivities between the models were used as an index to represent the sample set of model responses for each test. Coefficients of variation (standard deviation divided by the mean) were used to quantify differences in variability between model responses for each test.

The sensitivity of runoff to parameter changes is shown in Figure 3.17 for Ganspoel and Figure 3.18 for Lucky Hills 103. It is apparent that the relative sensitivity to each test is coherent irrespective of the model, e.g. all models have greater responses to tests 1A and 1B than to test 2, and all respond positively to tests 1 and 2 while responding negatively to test 3. This indicates that each one of the tested models can be used to assess the relative impacts of different changes in parameters. The coefficients of variation between models are significant

but most models responded inside a similar range, implying that the uncertainty in runoff process representation does not prevent the use of a single model to evaluate the responses of runoff to parameter changes. The MEFIDIS response is similar to the median of model sensitivities. Finally, it should be noted that the difference between models varies with catchment, e.g. MEFIDIS is less sensitive than LISEM for Ganspoel but more sensitive for Lucky Hills 103, implying that different models could be better suited to represent a certain type of watersheds.

The sensitivity of sediment yield to parameter changes is shown in Figure 3.19 for Ganspoel, and Figure 3.20 for Lucky Hills 103. The sensitivity of sediment yield is generally greater that that of runoff. The results follow a similar pattern to those obtained for runoff, with models showing a coherent response, but with higher coefficients of variation between models, particularly for the Lucky Hills watershed where more models were used. Nevertheless, the MEFIDIS results are comparable to that of other models for Ganspoel, and also for Lucky Hills 103 in most scenarios except 1A, indicating that process uncertainty does not prevent its use to evaluate the responses of sediment yield to parameter changes.

The implications of these results are discussed in depth by Nearing et al. (2005a), but they can be summarized in the conclusion that runoff and erosion appear to be very sensitive to changes in rainfall and cover. Soil erosion appears to be more sensitive than runoff, and rainfall changes appear to have greater impacts than vegetation cover changes. While these values are only indications and further work comparing more storms and including the effects of the consequences of climate change at coarser scales should be taken into account, the response trends are clear and significant. A further discussion of these results, compared with others obtained in this study for Mediterranean watersheds, is presented in section 5.2.

Overall, it can be concluded that erosion models can be used to study the complex responses to changes in climate parameters. The models studied in this work have different process descriptions, and were applied with different data requirements and calibration methods and criteria. Nevertheless, their responses to changes in rainfall and vegetation cover parameters were similar, which indicates that the relative results of model responses are credible. It should be noted that model response was more coherent for the stronger storms.

MEFIDIS responded in a similar way as other erosion models, and therefore its process representation can be considered suitable for climate change studies at this scale. This, coupled with its capacity to provide robust results shown in the previous section, indicates the

model's suitability for application in this thesis. The added value that MEFIDIS brings to this work is the focus on processes occurring in Mediterranean watersheds, particularly saturation excess runoff generation, and the spatially-distributed simulation of erosion patterns.

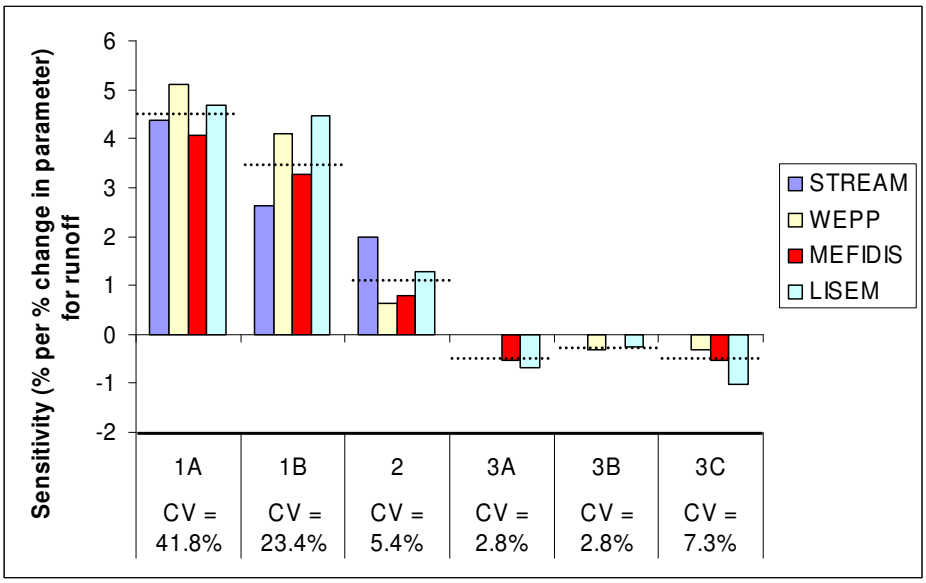

Figure 3.17 – Sensitivities of model runoff predictions relative to changes in inputs for the Ganspoel watershed, for the tests described in Table 3.9, with the dotted lines showing the median of model sensitivities and CV representing the coefficients of variation.

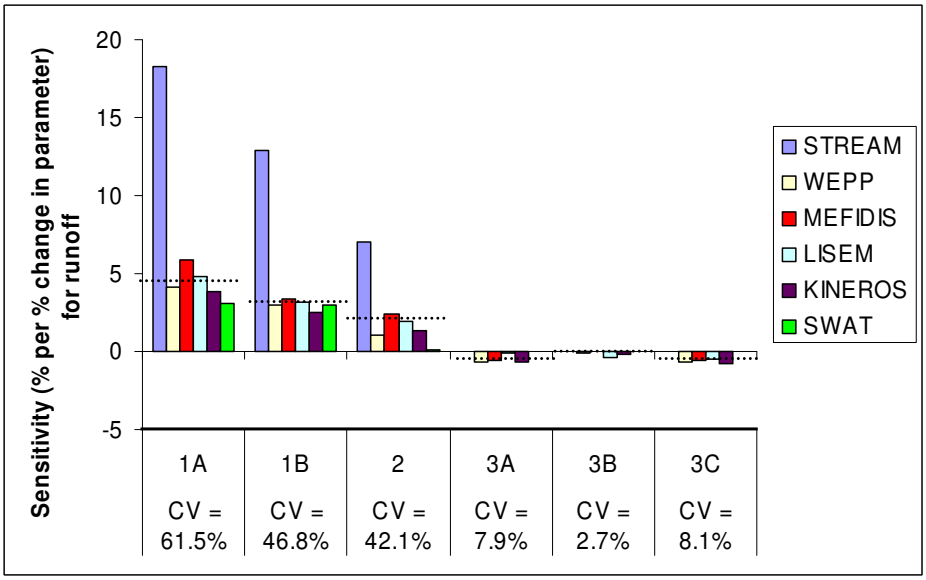

Figure 3.18 – Sensitivities of model runoff predictions relative to changes in inputs for the Lucky Hills 103 watershed, for the tests described in Table 3.9, with the dotted lines showing the median of model sensitivities and CV representing the coefficients of variation.

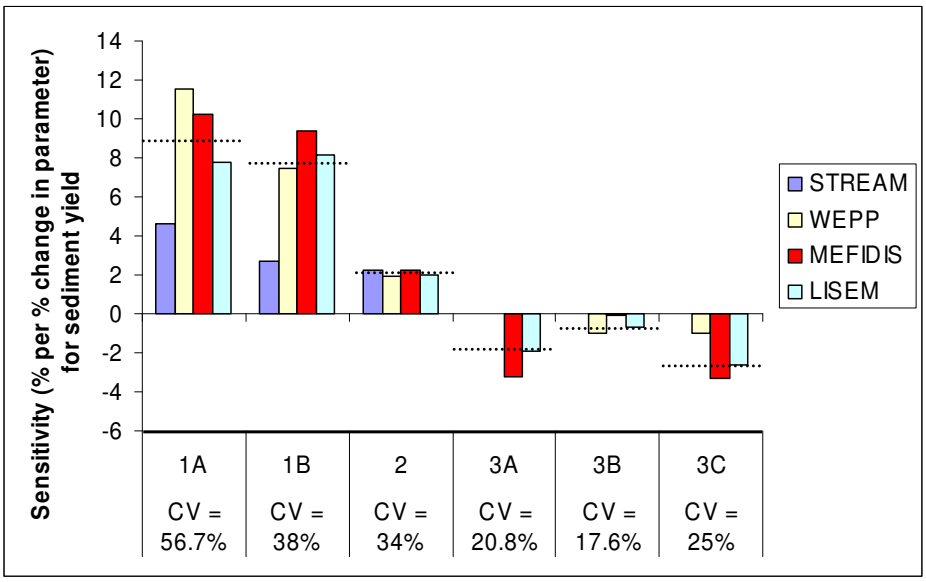

Figure 3.19 – Sensitivities of model sediment yield predictions relative to changes in inputs for the Ganspoel watershed, for the tests described in Table 3.9, with the dotted lines showing the median of model sensitivities and CV representing the coefficients of variation.

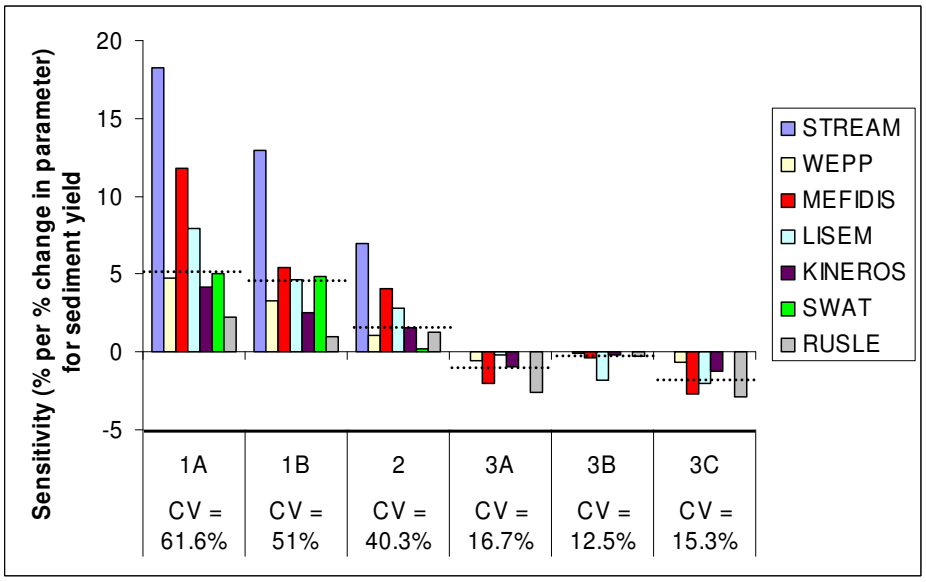

Figure 3.20 – Sensitivities of model sediment yield predictions relative to changes in inputs for the Lucky Hills 103 watershed, for the tests described in Table 3.9, with the dotted lines showing the median of model sensitivities and CV representing the coefficients of variation.

3.4 Seasonal scale modeling tool – the SWAT model

The SWAT model (Neitsch et al., 2002a) – short for Soil and Water Assessment Tool – was developed for the Agricultural Research Service of the United States Department of Agriculture as a tool for analysis of the impacts of human intervention in the hydrological and chemical processes of watersheds. The model was selected for seasonal scale modeling due to its major capabilities, namely:

- designed to predict the impacts of climate and human intervention on vegetation growth, water flow and soil erosion;
- capable of simulating large groups of watersheds with complex land uses and soil types, while providing results with a high degree of spatial discretization;
- provides continuous results for long time periods (one or more years), allowing the extraction of average annual and seasonal patterns from simulations with variable climatic conditions from year to year.

The versatility of the SWAT model is demonstrated by its wide range of applications in watershed studies. Examples include scientific studies in modeling processes (e.g. Cao et al., 2006), model application practices (e.g. Di Luzio and Arnold, 2004), watershed management practices assessment (e.g. Santhi et al., 2006), and climate change impact assessment (e.g. Gosain et al., 2006; Chaplot, 2007). Two of the model's characteristics make it particularly useful for this study. First, the model is based on physical equations rather than empirical relations. Despite requiring more base information, this allows greater confidence on model results both for unmonitored watersheds and under changed climate conditions (Beven, 2000; Grayson and Blöschl, 2001a). Second, the model was designed to use easily available data, particularly geographical information and daily climate datasets. Most of this data is freely available for Portugal, either in the National Hydrological Resources Information System (SNIRH) or in other online data repositories. The following sections provide a brief description of SWAT's structure, data requirements and results. Neitsch et al. (2002a) provide a more complete description of the theory and equations supporting the model, while Neitsch et al. (2002b) provide detailed information on the parameters required to apply the model, as well as the main model results.

3.4.1 Model description

Following the classification of Aksoy and Kavvas (2005), SWAT can be defined as a process-based, spatially distributed and continuous model. In other words, the model is based on hydrological and soil erosion process descriptions, takes inputs and provides results in a spatially-distributed way inside a particular watershed, and makes continuous simulations in time by taking into account the results of multiple rainfall events. Further information on the classification of SWAT can be found in section 2 (Table 2.8).

Representation of spatial heterogeneity

SWAT was designed to be applied to an entire watershed; however, the study area can be divided in sub-basins in order to refine the spatial resolution of model results. Sub-basins are linked in a cascade structure following the river network, where upstream basin discharge into the ones located downstream, and so on until the final outlet of the watershed. Each sub-basin is considered to have homogenous climatic and physiographic characteristics and a single main channel through which runoff and sediments flow towards the channels of sub-basins located further downstream.

SWAT also divides each sub-basin into Hydrological Response Units (HRUs) in order to simulate complex geographical patterns. Inside each basin, each combination of one land use, soil type and agricultural practice in considered as a separate HRU. The model considers each HRU as homogenous, with similar vegetation growth, runoff generation and soil erosion processes. HRUs are useful to discriminate the major water and sediment sources inside each sub-basin. The concept of HRU is described in detail by Beven (2000) and Grayson and Blöschl (2001a).

Within-watershed hydrological and erosion modeling

The central component of the SWAT model is the daily calculation of the hydrological balance for each sub-basin; the fraction of rainfall reaching the river network is then routed to downstream basins. The amount of runoff and drainage direction and time are used to estimate the amount of sediments carried by the river towards the outlet. The simulation of the hydrological cycle is divided in two phases, with the first dealing with overland runoff generation. The mass balance equation for this phase is (Neitsch et al., 2001a):

$$SW_t = SW_0 + \left(P - Q_{\text{sup}} - ET - I_d - Q_{sub}\right) \quad 3.19$$

Where:
SW_t – water content in the soil profile at the end of time-step t (mm)
t – simulation time-step (days)
SW_0 – water content in the soil profile at the beginning of time-step t (mm)
P – accumulated rainfall during time-step t (mm)
Q_{sup} – accumulated surface runoff during time-step t (mm)
ET – accumulated evapotranspiration during time-step t (mm)
I_d – deep aquifer infiltration during time-step t (mm)
Q_{sub} – total subsurface runoff through shallow aquifers during time-step t (mm).

Rainfall is the model's forcing function in this equation, provided by the user; the remaining parameters are simulated by the model. The fraction of surface runoff is simulated using the Curve Numbers method developed by the Soil Conservation Service (SCS, 1972), which separates rainfall into surface runoff and infiltration, or computing infiltration using the Green and Ampt method (Chow et al., 1998). Peak surface runoff is calculated using the rational method (Lencastre and Franco, 1992), where the maximum 30-min rainfall rate is estimated from the daily rainfall rate and observed 30-min maximum values for the model application area. Evapotranspiration includes soil water evaporation through open-air surfaces and plant transpiration; both are calculated as a fraction of potential evapotranspiration (following Ritchie, 1972), which can be calculated using the methods proposed by Thornthwaite (1948), Penman and Monteith (Monteith, 1965), Priestley and Taylor (1972) or Hargreaves et al. (1985). Subsurface runoff is simulated using a kinematic soil water flow model developed by Sloan and Moore (1984).

Soil erosion is simulated using the Modified Universal Soil Loss Equation (MUSLE; Williams, 1975) according to rainfall, surface runoff, vegetation cover factors (calculated with the vegetation growth sub-model) and other parameters related with topography, soil erodibility and agricultural practices. The vegetation growth sub-model is a simplified of the EPIC plant growth model (Williams, 1995). Phenological plant development is based on daily accumulated heat units. The potential biomass production is then modeled using a method developed by Monteith which simulates leaf area development (according to the phenological stage), light interception and conversion of intercepted light into biomass, including the consequences of atmospheric CO_2 concentrations on the efficiency of this conversion. Actual plant growth can be inhibited by temperature, water and nutrient stress. Finally, agricultural practices such as irrigation, fertilization, and planting and harvesting dates are simulated by a management sub-model.

Water and sediment routing

The second phase of the hydrological cycle is the drainage phase, where runoff and suspended sediments are routed through the river channels. SWAT uses Manning's equation to define the rate and velocity river flow; water is then routed through the channel network using the variable storage routing method or the Muskingum river routing method, which are both variations of the kinematic wave model (Chow et al., 1988).

Sediment transport in the channel network is a function of two processes, suspended sediment deposition and channel degradation. The maximum amount of suspended sediment that may be transported in the stream is calculated using a simplified version of the stream power concept (Arnold et al., 1995). If suspended sediments are in excess of the current's transport capacity sediment deposition occurs, otherwise the channel is eroded and the sediments are added to those already being carried by the stream.

3.4.2 Data requirements and model outputs

The SWAT version used in this view is AVSWAT2000, which operates inside the ArcView Geographical Information System in order to facilitate geographical data manipulation and calculations. To apply SWAT to a watershed, the following information is required:

- Digital Elevation Model (DEM) of the watershed, used to delineate the sub-basins and the drainage network;
- Cartography describing land use and soil type, used to delineate HRUs;
- Physical parameters for each soil type, used mostly to calculate surface and subsurface runoff;
- Biophysical parameters for the vegetation associated which each land use type, used mostly by the vegetation growth sub-model;
- Information on the agricultural management practices associated with the various land uses, used by the vegetation growth sub-model;
- Daily meteorological data (rainfall, maximum and minimum temperature, solar radiation, relative humidity and wind speed) for the study period, used as forcing functions for the hydrological cycle and vegetation growth calculations.

In alternative to the meteorological data, SWAT can generate stochastic climate series using a weather generator based on the WXGEN weather generator model (Sharpley and Williams, 1990). Rainfall is generated using a Markov chain skewed or exponential model, with the probability of occurrence of a rain day based on the occurrence of rainfall in the previous day. Solar radiation and temperature values are generated together by a weakly stationary generating process based on the previous day's values. Relative humidity is generated from temperature values and average dew point temperatures using a triangular distribution. All these parameters are afterwards adjusted for the presence or absence of rainfall. Finally, wind speed is generated from average monthly values using a modified exponential distribution. To implement the weather generator, SWAT requires long-term monthly statistical information (e.g. average and standard deviation) for rainfall, maximum and minimum temperature, dew point temperature, solar radiation and wind speed.

SWAT provides results for both the overland flow and channel routing components. For each sub-basin, the model provides daily values for (i) hydrological balance components – evapotranspiration, deep aquifer infiltration, and surface and subsurface runoff, (ii) upslope soil erosion, and (iii) vegetation biomass production and agricultural yields. The model also provides annual results for these parameters for each HRU within each sub-basin, as well as overall temperature, water and nutrient stress results for the entire watershed. Finally, SWAT provides daily results for water and sediment yield for each channel inside each sub-basin.

3.5 References

Adger WN, 2006. Vulnerability. Global Environmental Change 16: 268–281.

Aksoy H, Kavvas ML, 2005. A review of hillslope and watershed scale erosion and sediment transport models. Catena 64: 247–271.

Alcamo J, Doll P, Henrichs T, Kaspar F, Lehner B, Rosch T, Siebert S, 2003. Global estimates of water withdrawals and availability under current and future "business-as-usual" conditions. Hydrological Sciences Journal – Journal Des Sciences Hydrologiques 48 (3): 339-348.

Arnell N. 2004. Climate change and global water resources: SRES emissions and socio-economic scenarios. Global Environmental Change 14: 31–52.

Arnold JG, Williams JR, Maidment DR, 1995. Continuous-time water and sediment-routing model for large basins. Journal of Hydraulic Engineering 121: 171-183.

Assouline S, Mualem Y, 2000. Modeling the dynamics of soil seal formation: analysis of the effect of soil and rainfall properties. Water Resour. Res. 36 (8): 2341-2349.

Baghdadi N, King C, Bourguignon A, Remond A, 2002. Potential of ERS and Radarsat data for surface roughness monitoring over bare agricultural fields: application to catchments in Northern France. Int. J. Remote Sens. 23 (17): 3427-3442.

Bakker MM, Govers G, Rounsevell MDA, 2004. The crop productivity–erosion relationship: an analysis based on experimental work. Catena 57: 55–76.

Beasley DB, Huggins LF, 1981. ANSWERS User's Manual. USDA Report No. EPA-905/9-82-01, United States Department of Agriculture.

Beven K, 2000. Rainfall-Runoff Modelling – The Primer. John Wiley & Sons, Chichester.

Bittelli M, Campbell GS, Flury M, 1999. Characterization of Particle-Size Distribution in Soils with a Fragmentation Model. Soil Sci. Soc. Am. J. 63(4): 782-788.

Blöschl G, Sivapalan M, 1995. Scale issues in hydrological modeling: a review. In: Kalma JD, Sivapalan M (Eds.), Scale issues in hydrological modeling. John Wiley & Sons, Chichester: 9-48.

Blöschl G, Grayson R, 2001. Spatial observation and interpolation. In: Grayson R, Blöschl G (Eds.), Spatial Patterns in Catchment Hydrology – Observations and Modelling. Cambridge University Press, Cambridge: 17-50.

Botelho da Costa J, 1995. Caracterização e constituição do solo (soil characterization and constitution), 5th ed. Calouste Gulbenkian Foundation, Lisbon.

Boardman J, 2006. Soil erosion science: reflections on the limitations of current approaches. Catena 68: 73-86.

Boix-Fayos C, Martínez-Mena M, Calvo-Cases A, Castillo V, Albaladejo J, 2005. Concise review of interrill erosion studies in SE Spain (Alicante and Murcia): erosion rates and progress of knowledge from the 1980s. Land Degrad. Develop. 16: 517–528.

Braun P, Molnar T, Kleeberg H-B, 1997. The problem of scaling in grid-related hydrological process modelling. Hydrol. Process. 11 : 1219-1230.

Cammeraat LH, 2002. A review of two strongly contrasting geomorphological systems within the context of scale. Earth Surf. Process. Landforms 27: 1201–1222.

Canfield HE, Goodrich DC, 2006. The impact of parameter lumping and geometric simplification in modelling runoff and erosion in the shrublands of southeast Arizona. Hydrol. Process. 20: 17–35.

Cardoso JVJC, 1965. Os solos de Portugal, sua classificação, caracterização e génese: 1- a sul do rio Tejo (Portuguese soils, their classification, characterization and genesis: 1- south from the Tagus river). General-Directorate for Agricultural Services, Lisbon.

Cao W, Bowden WB, Davie T, Fenemor A, 2006. Multi-variable and multi-site calibration and validation of SWAT in a large mountainous catchment with high spatial variability. Hydrol. Process. 20: 1057–1073.

Cerdan O, Souchère V, Lecomte V, Couturier A, Le Bissonais Y, 2001. Incorporating soil surface crusting processes in an expert-based runoff model: Sealing and Transfer by Runoff and Erosion related to Agricultural Management. Catena 46: 189-205.

Cerdan O, Le Bissonnais Y, Couturier A, Saby N, 2002. Modelling interrill erosion in small cultivated catchments. Hydrological Processes, 16 (16): 3215-3226.

Chaplot V, 2007. Water and soil resources response to rising levels of atmospheric CO_2 concentration and to changes in precipitation and air temperature. Journal of Hydrology 337: 159-171.

Chapra SC, 1997. Surface water-quality modeling. McGraw-Hill, New York.

Chow VT, Maidment DR, Mays LW, 1988. Applied Hydrology. McGraw-Hill, New York.

Costa-Cabral MC, Burges SJ, 1994. Digital elevation model networks (DEMON): a model of flow over hillslopes for computation of contributing and dispersal areas. Water Resour. Res. 30 (6) : 1681-1692.

Darboux F, Davy P, Gascuel-Odoux C, Huang C, 2001. Evolution of soil surface roughness and flowpath connectivity in overland flow experiments. Catena 46: 125-139.

de Roo APJ, Wesseling CG, Ritsema CJ, 1996a. LISEM: a single event physically-based hydrological and soil erosion model for drainage basins: I – theory, input and output. Hydrol. Process. 10 (8): 1107-1117.

de Roo APJ, Offermans RJE, Cremers NHTD, 1996b. LISEM: a single event physically-based hydrological and soil erosion model for drainage basins: II – sensitivity analysis, validation and application. Hydrol. Process. 10 (8): 1119-1126.

Di Luzio M, Arnold JG, 2004. Formulation of a hybrid calibration approach for a physically based distributed model with NEXRAD data input. Journal of Hydrology 298: 136–154.

Duke GD, Kienzle SW, Johnson DL, Byrne JM, 2003. Improving overland flow routing by incorporating ancillary road data into Digital Elevation Models. J. Spatial Hydrology 3 (2): 1-27.

Favis-Mortlock DT, Boardman J, Parsons AJ, Lascelles B, 2000. Emergence and erosion: a model for rill initiation and development. Hydrol. Process. 14: 2173-2205.

Favis-Mortlock D, Boardman J, MacMillan V, 2001. The limits of erosion modeling: why we should proceed with care. In: Harmon RS, Doe WW (Eds.), Landscape Erosion and Evolution Modeling. Kluwer Academic/Plenum Publishers, New York: 477-516.

Ferreira AG, Singer MJ, 1985. Energy dissipation for water drop impact into shallow pools. Soil Sci. Soc. Am. J. 49 (6): 1537-1542.

Flanagan DC Nearing MA, 1995. USDA-Water Erosion Prediction project: Hillslope profile and watershed model documentation. NSERL Report No. 10. USDA-ARS National Soil Erosion Research Laboratory, West Lafayette.

Foster GR, 1982. Modeling the erosion process. In: Haan CT, Johnson HP, Brakensiek DL (Eds.), Hydrologic Modeling of Small Watersheds. American Society of Agricultural Engineers, St. Joseph: 295-380.

Gallardo C, Arribas A, Prego JA, Gaertner MA, de Castro M, 2001. Multi-year simulations using a regional-climate model over the Iberian Peninsula: current climate and doubled CO_2 scenario. Quarterly Journal of the Royal Meteorological Society 127: 2740-2756.

Gallopín GC, 2006. Linkages between vulnerability, resilience, and adaptive capacity. Global Environmental Change 16: 293–303.

Gosain AK, Rao S, Basuray D, 2006. Climate change impact assessment on hydrology of Indian river basins. Current Science 90 (3): 346-353.

Govers G, 1990. Empirical relationships for the transporting capacity of overland flow. International Association of Hydrological Sciences Publication 189: 45-63.

Grayson R, Blöschl G, 2001a. Spatial modelling of catchment dynamics. In: Grayson R, Blöschl G (Eds.), Spatial Patterns in Catchment Hydrology – Observations and Modelling. Cambridge University Press, Cambridge: 51-81.

Grayson R, Blöschl G, 2001b. Summary of Pattern Comparison and Concluding Remarks. In: Grayson R, Blöschl G (Eds.), Spatial Patterns in Catchment Hydrology – Observations and Modelling. Cambridge University Press, Cambridge: 355-367.

Hargreaves GL, Hargreaves GH, Riley JP, 1985. Agricultural benefits for Senegal River Basin. J. Irrig. and Drain. Engr. 111 (2): 113-124.

Hoyningen-Huene Jv, 1983. Die Interzeption des Niederschlages in landwirtschaftlichen Pflanzenbeständen (rainfall interception in agricultural plants). DVWK-Schrift Nr. 57, Verlag Paul Parey, Hamburg / Berlin.

Huggins LF, Burney JR, 1982. Surface runoff, storage, and routing. In: Haan CT, Johnson HP, Brakensiek DL (Eds.), Hydrologic Modeling of Small Watersheds. American Society of Agricultural Engineers, St. Joseph: 167-226.

Imeson AC, Lavee H, 1998. Soil erosion and climate change: the transect approach and the influence of scale. Geomorphology 23: 219–227.

inovaGIS, 2001. Geographical Information Interoperable Technology. Published online at http://www.inovagis.org.

IPCC: Intergovernmental Panel on Climate Change, 2000. Special Report on Emissions Scenarios. A Special Report of Working Group III of the Intergovernmental Panel on Climate Change. Nakićenović N, Swart R (Eds.). Cambridge University Press, Cambridge.

Isaaks EH, Srivastava RM, 1989. An Introduction to Applied Geostatistics. Oxford University Press, New York.

Jetten V, de Roo A, Favis-Mortlock D, 1999. Evaluation of field-scale and catchment-scale soil erosion models. Catena 37 (4): 521-541.

Jetten VG, de Roo APJ, 2001. Spatial analysis of erosion conservation measures with LISEM. In: Harmon RS, Doe WW (Eds.), Landscape Erosion and Evolution Modeling. Kluwer Academic/Plenum Publishers, New York: 429-445.

Jetten V, Govers G, Hessel R, 2003. Erosion models: quality of spatial predictions. Hydrol. Process. 17: 887-900.

Kamphorst EC, Jetten V, Guerif J, Pitkanen J, Iversen BV, Douglas JT, Paz A, 2000. Predicting depressional storage from soil surface roughness. Soil Sci. Soc. Am. J. 64 (5): 1749-1758.

Lane LJ, Hernandez M, Nichols M, 1997. Processes controlling sediment yield from watersheds as functions of spatial scale. Environmental Modelling & Software 12 (4): 355-369.

Lencastre A, Franco FM, 1992. Lições de hidrologia (lessons in hydrology), 2nd ed. New University of Lisbon Editorial Services, Lisbon.

Linsley RK, Kohler MA, Paulhus JLH, 1975. Hydrology for Engineers, 2nd ed. McGraw-Hill, New York.

Liu QQ, Chen L, Li JC, Singh VP, 2004. Two-dimensional kinematic wave model of overland flow. J. Hydrol. 291 (1-2): 28-41.

Loucks DP, van Beek E, 2005. Water resources systems planning and management: an introduction to methods, models and applications. UNESCO, Paris.

Ludwig B, Boiffin J, Chadoeuf J, Auzet AV, 1995. Hydrological structure and erosion damage caused by concentrated flow in cultivated catchments. CATENA 25: 227-252.

Monteith JL, 1965. Evaporation and the environment. In: The state and movement of water in living organisms, XIXth Symposium. Soc. for Exp. Biol., Swansea. Cambridge University Press, Cambridge: 205-234.

Morgan RPC, Quinton JN, 2001. Erosion Modeling. In: Harmon RS, Doe WW (Eds.), Landscape Erosion and Evolution Modeling. Kluwer Academic/Plenum Publishers. New York: 117-144.

Nachtergaele J, Poesen J, Vandekerckhove L, Wijdenes DO, Roxo M, 2001. Testing the ephemeral gully erosion model (EGEM) for two Mediterranean environments. Earth Surf. Process. Landf. 26 (1): 17-30.

Nearing MA, Govers G, Norton LD, 1999. Variability in soil erosion data from replicated plots. Soil Sci. Soc. Am. J. 63: 1829-1835.

Nearing MA, Jetten V, Baffaut C, Cerdan O, Couturier A, Hernandez M, Le Bissonnais Y, Nichols MH, Nunes JP, Renschler CS, Souchère V, van Oost K, 2005a. Modeling response of soil erosion and runoff to changes in precipitation and cover. CATENA 61 (2-3): 131-154.

Nearing MA, Jetten V, Stone J, 2005b. Introduction. Catena 61 (2-3): 103-104.

Neitsch SL, Arnold JG, Kiniry JR, Williams JR, Kiniry KW, 2002a. Soil and Water Assessment Tool theoretical documentation. TWRI report TR-191, Texas Water Resources Institute, College Station.

Neitsch SL, Arnold JG, Kiniry JR, Srinivasan R, Williams JR, 2002b. Soil and Water Assessment Tool user's manual. TWRI report TR-192, Texas Water Resources Institute, College Station.

Nunes JP, Vieira G, Seixas J, Gonçalves P, Carvalhais N, 2005. Evaluating the MEFIDIS model for runoff and soil erosion prediction during rainfall events. Catena 61 (2-3): 210-228.

Nunes JP, Vieira GN, Seixas J, 2006a. MEFIDIS - A Physically-based, Spatially-Distributed Runoff and Erosion Model for Extreme Rainfall Events. In: Singh VP, Frevert DK (Eds.), Watershed Models. CRC press, Boca Raton: 291-314.

Nunes JP, de Lima JLMP, Singh VP, de Lima MIP, Vieira GN, 2006b. Numerical modelling of surface runoff and erosion due to moving rainstorms at the drainage basin scale. J. Hydrol. 330 (3-4): 709-720.

Oh Y, 2004. Quantitative Retrieval of Soil Moisture Content and Surface Roughness From Multipolarized Radar Observations of Bare Soil Surfaces. IEEE Trans. Geosci. Remote Sensing 42 (3): 596-601.

Onstad CA, 1984. Depressional storage on tilled soil surfaces. T. ASAE 27 (3): 729-732.

Palutikof JP, Conte M, Casimiro Mendes J, Goodess CM, Espirito Santo F, 1996. Climate and climate change. In: Brandt CJ, Thornes JB (Eds.), Mediterranean desertification and land use. John Wiley and sons, Chichester: 43-86.

Priestley CHB, Taylor RJ, 1972. On the assessment of surface heat flux and evaporation using large-scale parameters. Mon. Weather. Rev. 100: 81-92.

Rachman A, Anderson SH, Gantzer CJ, Thompson AL, 2003. Influence of Long-term Cropping Systems on Soil Physical Properties Related to Soil Erodibility. Soil Sci. Soc. Am. J. 67: 637-644.

Rauws G, Govers G, 1988. Hydraulic and soil mechanical aspects of rill generation on agricultural soils. J. Soil Sci. 39: 111-124.

Rawls WJ, Brakensiek DL, Miller N, 1983. Green-ampt infiltration parameters from soils data. Journal of Hydraulic Engineering-ASCE 109 (1): 62-70.

Renard KG, Foster GR, Weesies GA, McCool DK, Yoder DC, 1997. Predicting soil erosion by water – a guide to conservation planning with the revised universal soil loss equation (RUSLE). Agricultural Handbook No. 703, US Government Printing Office, Washington DC.

Ritchie JT, 1972. Model for predicting evaporation from a row crop with incomplete cover. Water Resour. Res. 8: 1204-1213.

Ritchie JC, Nearing MA, Nichols MH, Ritchie CA, 2005. Patterns of Soil Erosion and Redeposition on Lucky Hills Watershed, Walnut Gulch Experimental Watershed, Arizona. Catena 61 (2-3): 122-130.

Santhi C, Srinivasan R, Arnold JG, Williams JR, 2006. A modeling approach to evaluate the impacts of water quality management plans implemented in a watershed in Texas. Enbironmental Modeling & Software 21: 1141-1157.

Saxton KE, Rawls WJ, Romberger JS, Papendick RL, 1986. Estimating generalized soil-water characteristics from texture. Soil Sci. Soc. Am. J. 50(4): 1031-1036.

Schoorl JM, Sonneveld MPW, Veldkamp A, 2000. Three-dimensional landscape process modelling: the effect of DEM resolution. Earth Surf. Process. Landf. 25: 1025-1034.

SCS: Soil Conservation Service, 1972. Section 4: Hydrology. In: National Engineering Handbook. Soil Conservation Service.

Scurlock JMO, Asner GP, Gower ST, 2001. Worldwide Historical Estimates and Bibliography of Leaf Area Index, 1932-2000. ORNL Technical Memorandum TM-2001/268, Oak Ridge National Laboratory, Oak Ridge.

Sharma PP, Gupta SC, Rawls WJ, 1991. Soil detachment by single raindrops of varying kinetic-energy. Soil Sci. Soc. Am. J. 55 (2): 301-307.

Sharma PP, Gupta SC, Foster GR, 1993. Predicting soil detachment by raindrops. Soil Sci. Soc. Am. J. 57 (3): 674-680.

Sharma PP, Gupta SC, Foster GR, 1995. Raindrop-induced soil detachment and sediment transport from interrill areas. Soil Sci. Soc. Am. J. 59: 727-734.

Sharpley AN, Williams JR (Eds.), 1990. EPIC – Erosion Productivity Impact Calculator, 1. model documentation. USDA Agricultural Research Service, Washington DC.

Skaggs TH, Arya LM, Shouse PJ, Mohanty BP, 2001. Estimating Particle-Size Distribution from Limited Soil Texture Data. Soil Sci. Soc. Am. J. 65: 1038-1044.

Sloan PG, Moore ID, 1984. Modeling subsurface stormflow on steeply sloping forested watersheds. Water Resources Research. 20 (12): 1815-1822.

Smit B, Wandel J, 2006. Adaptation, adaptive capacity and vulnerability. Global Environmental Change 16: 282–292.

Smith RE, Goodrich DC, Quinton JN, 1995. Dynamic, distributed simulation of watershed erosion: the KINEROS2 and EUROSEM models. J. Soil and Water Conservation 50 (5): 517-520.

Takken I, Beuselinck L, Nachtergaele J, Govers G, Poesen J, Degraer G, 1999. Spatial evaluation of a physically-based distributed erosion model (LISEM). Catena 37: 431-447.

Thornthwaite CW, 1948. An approach toward a rational classification of climate. Geographical Review 38: 55-94.

Toy TJ, Foster GR, Renard KG, 2002. Soil erosion: processes, prediction, measurement, and control. John Wiley and Sons, New York.

USDA – United States Department of Agriculture, 1986. Urban Hydrology for Small Watersheds. Natural Resources Conservation Service, Conservation Engineering Division, Technical Release 55.

Van Oost K, Govers G, Cerdan O, Thaure D, Van Rompaey A, Steegen A, Nachtergaele J, Takken I, Poesen J, 2005. Spatially distributed data for erosion model calibration and validation: The Ganspoel and Kinderveld datasets. Catena 61 (2-3): 105-121.

Walker JP, Wilgoose GR, 1999. On the Effect of Digital Elevation Model Accuracy on Hydrology and Geomorphology. Water Resour. Res. 35 (7): 2259-2268.

Williams JR, 1975. Sediment-yield prediction with universal equation using runoff energy factor. In: Present and prospective technology for predicting sediment yield and sources: Proceedings of the sediment yield workshop, USDA Sedimentation Lab., Oxford, MS, November 28-30, 1972. Publ. ARS-S-40, USDA Agricultural Research Service, Washington DC: 244-252.

Williams JR, 1995. Chapter 25: The EPIC model. In: Singh VP (Ed.), Computer models of watershed hydrology. Water Resources Publications, Highlands Ranch: 909-1000.

Wu TH, Hall JA, Bonta JV, 1993. Evaluation of Runoff and Erosion Models. J. Irrig. Drainage Eng. – ASCE 119 (4): 364-381.

Xu C-Y, Singh VP, 2004. Review on Regional Water Resources Assessment Models under Stationary and Changing Climate. Water Resources Management 18: 591–612.

Yu B, 2005. Adjustment of CLIGEN parameters to generate precipitation change scenarios in southeastern Australia. Catena 61: 196–209.

4. Study areas

The previous chapter described the objectives proposed by this thesis, as well as the methodology and tools used to achieve them. This chapter describes the application of the modeling framework to two study areas, used to assess the vulnerability of Mediterranean catchments to climate change. It begins with a brief **Overview** of the selected study areas; both experience typical Mediterranean climatic conditions and land uses, but contrast in terms of climate aridity. A discussion of the **Physical description and data gathering** in the study areas follows, focusing on the processes requiring modeling and data useful model parameterization, calibration and validation. The methods for both **SWAT application and evaluation** and **MEFIDIS application and evaluation** are presented next, focusing on model calibration and validation strategies and presenting a full evaluation of each model's performance. Finally, the section concludes with a discussion over **Scale issues in storm rainfall representation** in the MEFIDIS model.

4.1 Overview

The methodology developed in this thesis is designed for application in Mediterranean catchments. The process of selecting a study area involved a number of considerations:

- presence of different levels of climate aridity, in order to study catchments with different degrees of ongoing desertification processes;
- availability of climate, hydrological, soil and other data for system analysis and model parameterization, calibration and validation;
- presence of different Mediterranean landcover types, such as olive and vine cultivation, sclerophyllous forests and shrubs;
- diversity of topography and soils;
- availability of other scientific studies and background information.

These criteria led to the selection of catchments located in two different climatic regions of Portugal, shown in Figure 4.1. The option for Portuguese catchments presents three advantages: easy access to the study sites, access to scientific information available only in Portuguese, and free access to a vast repository of climate and hydrological data via the National Hydrological Resources Information System (SNIRH, 2006). The SNIRH is a

consistent database with a good spatial and temporal resolution, including daily records of variables such as rainfall and river discharge since the 1980s or earlier, measured in a network covering the entire country. Access to this data allowed the analysis of multiple catchments with contrasting physiographic characteristics and landcover patterns, as well as of multiple years with different rainfall and temperature conditions.

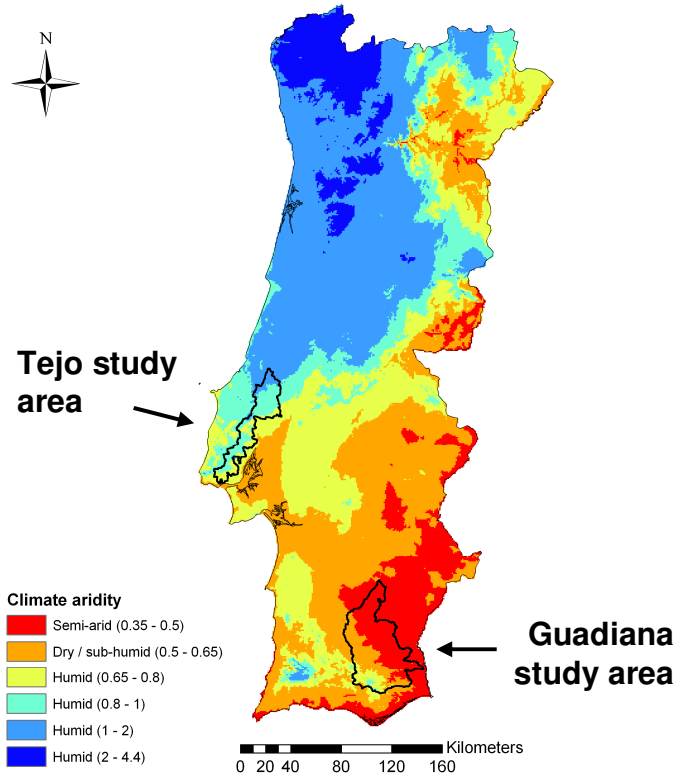

Figure 4.1 – Map of Portugal showing the location of the study areas superimposed over the climate aridity index (UNEP, 1997), calculated using the spatial datasets for long-term average rainfall and potential evapotranspirations available in SNIRH (2006).

The Guadiana study area is located in the southwestern end of the Guadiana catchment, on a plain with rocky and shallow lithosols. It is characterized by a semi-arid climate which only allows the development of extensive agriculture, including semi-natural cork oak forests. Furthermore, this area is suffering an ongoing process of biophysical and human desertification and many former agricultural areas are now covered by shrubs and steppelands. The Tejo study area is located in the west of the Tejo catchment, on the slopes of the Montejunto mountain range. It is characterized by a humid Mediterranean climate,

allowing for the development of intensive agriculture and forestry. The selection of humid catchments for this analysis makes possible a study of the impacts of a transition towards a drier climate, which could be a consequence of climate change.

Both study areas have received some attention in recent scientific studies. The Guadiana study area was one of the European Union's MEDALUS project sites, and an extensive analysis of hydrological and erosion processes coupled with other information was published by authors such as Brandt and Thornes (1996) or Mairota et al. (1998). The Tejo study area received some research attention from the Portuguese Water Institute (Instituto da Água – INAG), resulting in a more dense gauging network and publications in the Portuguese literature such as the work by de Macedo (1996). This allowed the use of a number of additional information beyond that present in the SNIRH network, including qualitative catchment information used to improve the quality of model applications (Jetten et al., 1999; see also section 2.3.2).

As described in section 3.1, one meso-scale watershed was selected in each study area to conduct event-scale modeling and analysis. In the Guadiana, the selected watershed is Odeleite, which has suffered significant land abandonment and natural re-vegetation in the past decades; in the Tejo, the Alenquer watershed was selected, an intensively agricultural catchment experiencing significant flood and erosion problems.

4.1.1 Guadiana and the Odeleite watershed

The Guadiana study area is located in a dry region, mostly with sub-humid and semi-arid climate (Figure 4.1). Figure 4.2 represents the study area, showing 8 watersheds draining to the Guadiana river in a SE-NW direction, comprising a total area of 2778 Km^2. Most of the area is composed by low-sloped plains with a dry climate, while the southwestern hills have steeper slopes and a more humid climate. The average slope is of c. 8 %. The Portuguese Meteorological Institute (Instituto de Meteorologia – IM) climate normals for 1961-1990 show an average temperature of c. 16 ºC and annual rainfall of c. 550 $mm.y^{-1}$. Lithosols, with very little depth and low fertility, dominate the area; the intensive agriculture performed in the last decades has caused severe problems of land degradation, leading to the abandonment of unproductive lands and consequently to desertification (Roxo, 1994; Vandaele et al., 1997). About half of the area is still used for annual rainfed crops, with the remainder either used for cork oak cultivation or covered with natural shrublands. Sustained research on erosion and land degradation processes in this region has recently been undertaken under the MEDALUS European projects (Roxo, 1994; Roxo et al., 1996; Roxo and Cortesão Casimiro, 1999), spawning a number of additional research work (e.g. Vandaele et al., 1997; Seixas, 2000).

The Odeleite catchment is located near the southern end of the study area, draining 290 Km^2. The basin's climate is more humid than that of the remaining area, particularly in the western part where it drains the Caldeirão mountain range. This region has suffered significant land abandonment in the past decades, and Mediterranean shrub vegetation has covered most of the former agricultural fields. The study of hydrological and soil erosion patterns in this site is particularly important due to the Odeleite reservoir, located downstream from the catchment's outlet, which supplies water for urban consumption and 81 Km^2 of irrigated farmland.

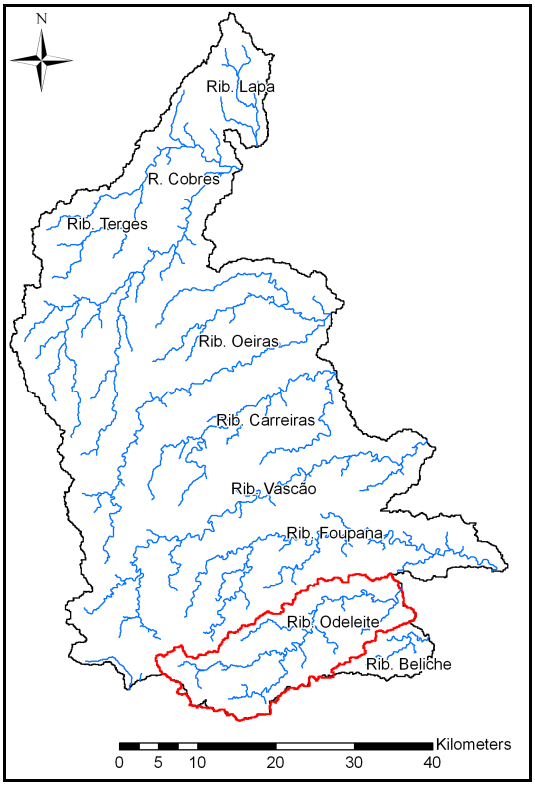

Figure 4.2 – Guadiana study area, showing major rivers and the Odeleite watershed (in red).

4.1.2 Tejo and the Alenquer watershed

In contrast, the Tejo study area is in a transitional region between sub-humid and humid climates (Figure 4.1). The area is represented in Figure 4.3, and includes 11 watersheds draining rainwater from the Montejunto mountain range to the Tagus river in a NW-SE direction, with a total area of 1252 Km^2. This results in an average slope of c. 10 %, greater in the headwater catchments. According to the IM climate normals for 1961-1990, the average annual temperature is c. 16 ºC, coupled with an average annual of c. 810 $mm.y^{-1}$. The

combination of these climatic parameters leads to a climatic aridity classification of humid. Cambisols are the dominant soil type and the major land use is annual crops, with smaller but significant areas of commercial forestry (especially pine forests), vine cultivation and urbanization. The most significant environmental problems include floods and soil erosion.

The Alenquer catchment is located in the middle of the Tejo study area, and has an area of 115 Km^2. De Macedo (1996) provides a concise description of the catchment; the main characteristics include a greater slope that the surrounding area (c. 15 %), and a propensity for flooding, particularly in the city of Alenquer, located on a narrow valley near the catchment's outlet.. The climate and soil are similar to those of the surrounding region, but the landcover has a greater domination of arboreal vegetation such as commercial forestry and vineyards. Due to the flood propensity and the availability of climatic and hydrological data on the catchment, INAG has declared Alenquer as a test watershed for hydrological modeling.

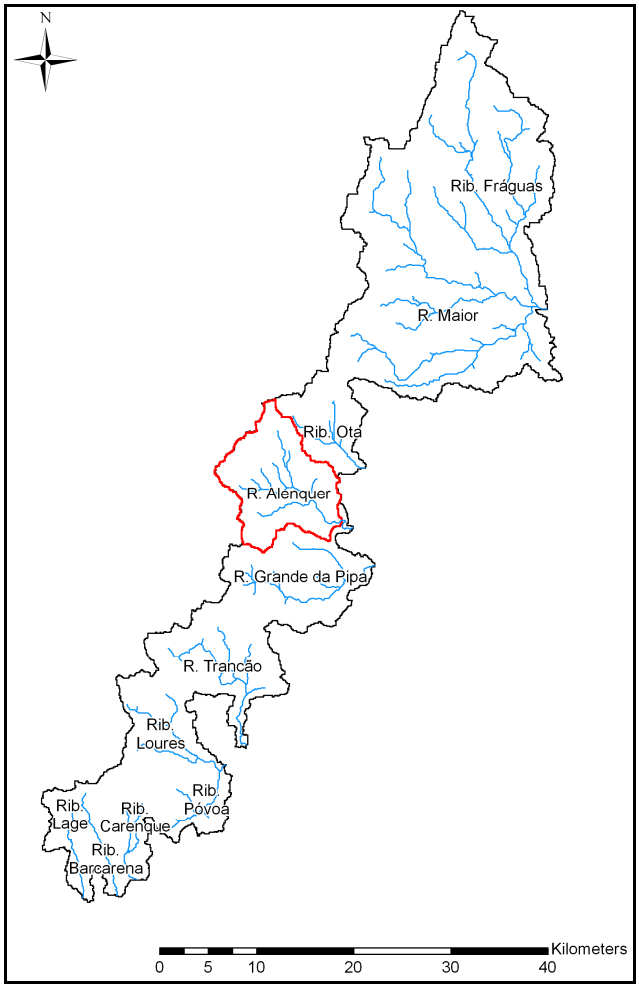

Figure 4.3 – Tejo study area, showing major rivers and the Alenquer watershed (in red).

4.2 Physical description and data gathering

The following sections present a detailed description of the study area. This description is framed by the data requirements of both modeling tools, MEFIDIS and SWAT, as described in section 3; the SWAT model was applied for the Guadiana and Tejo areas, while the MEFIDIS model was applied to the Odeleite and Alenquer watersheds. Therefore, this section also reports the process of data collection and analysis for model application. The model parameter requirements, particularly those for the SWAT model, are quite complete and provide a good picture of the study area's climate, hydrological regime, physiography, land use and soil patterns, and major erosion processes.

4.2.1 Climate

The climate in both study areas can be characterized as Mediterranean with dry characteristics in the Guadiana area, and humid in the Tejo area. The meteorological sampling network in the study area is operated by INAG (mostly for rainfall) and IM (for rainfall and other climate variables, such as maximum and minimum daily temperature, solar radiation, relative humidity and wind speed); data from the INAG stations is available via SNIRH. The location of the sampling stations is shown in Figure 4.4. The average distance between udometric stations is 10 to 20 Km, while for climate stations it is c. 50 Km. This results in c. 25 udometric stations in both study areas, coupled with 2 climatic stations for the Guadiana and 3 for the Tejo. As stated above, the average temperature for both regions is c. 16 ºC, with the average annual rainfall ranging from 550 $mm.y^{-1}$ in the Guadiana to 810 $mm.y^{-1}$ in the Tejo.

Seasonal, decadal and long-term climate

Average monthly values for the measured parameters in the climate stations were collected from the 1961-90 climate normals, supplied by the IM, which were used to parameterize the stochastic weather generator used by the SWAT model (Neitsch et al., 2002; see section 3.4 for details). The values for rainfall and average temperature, for the four IM climate stations, is visible in Figure 4.5; the high seasonal climatic variability can be seen, with most of the rainfall concentrating on the wet season from October to April and a dry summer season from May to September coinciding with the highest temperatures. The average daily rainfall is 5.5 to 7.5 mm (considering rain days only). However, the number of rainfall days (with rainfall above 0.1 mm) also drops from the wet season maximum of 11 to 15 per month (in February) to the dry season minimum of 1 or 2 per month (in July); therefore the reduction in daily rainfall intensity from dry to wet season is proportionally smaller than the reduction in monthly rainfall.

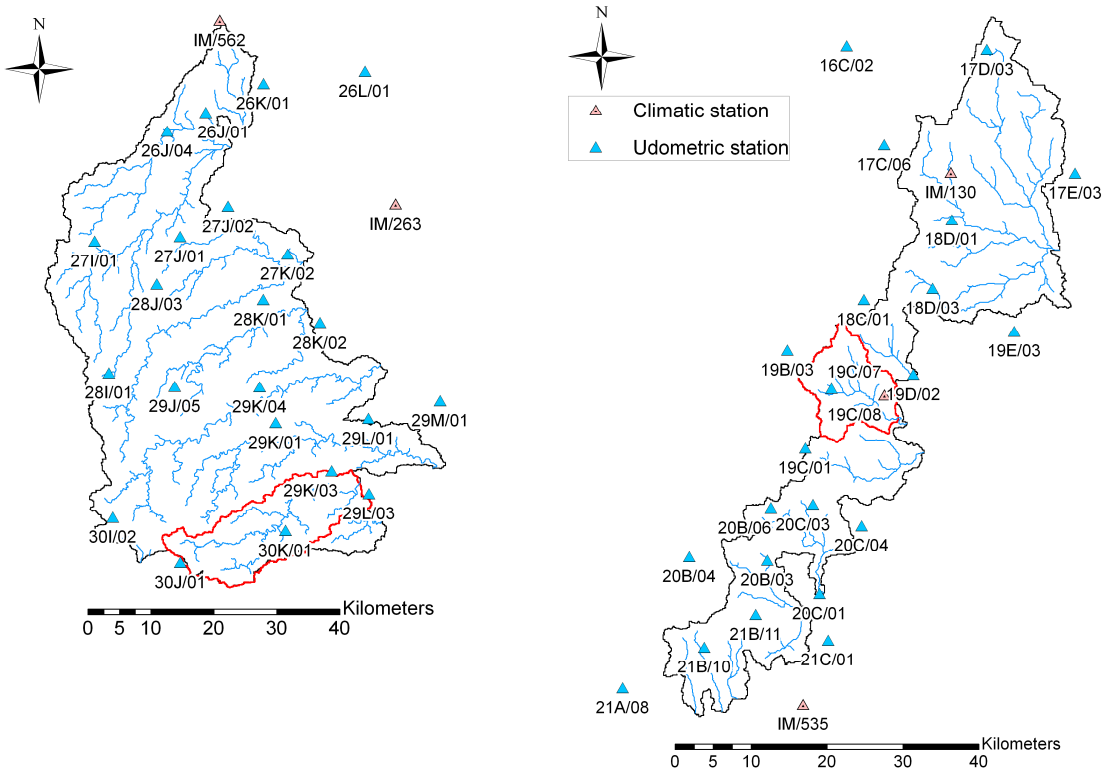

Figure 4.4 – Meteorological sampling network in the Guadiana (left) and Tejo (right) study areas; station codes follow the SNIRH system for classification except when beginning by IM, in which case they refer to stations operating by the Portuguese Meteorological Institute.

Daily climate data for all the stations shown in Figure 4.4 was also collected to force the SWAT model for the 1980s. The annual values for this data, for rainfall and temperature, are shown in Figure 4.6. The data is aggregated per hydrological year, a common practice in Mediterranean regions due to the seasonal climate variability; one hydrological year is considered to begin in October, at the start of the wet season, and last to September of the following year as the dry season ends (Palutikof et al., 1996). As the figure shows, the rainfall in the 1980s showed a high interannual variability, particularly due to the drought beginning in 1979/80 and lasting until 1982/83, during which rainfall dropped by -55 % in the Guadiana area and by -40 % in the Tejo area from average annual values. In other years, rainfall was rarely close to the average, surpassing it by up to 30 % in the Tejo and 75 % in the Guadiana. This represents a range from 244 to 808 mm in the driest catchments of the Guadiana, compared with a range from 387 to 995 in the mid-Tejo catchments. Note that the interannual variability of rainfall is significantly greater in the drier Guadiana catchments. These values, especially for drought years, are close to those predicted under climate change scenarios (as

discussed in section 2.2.1), allowing a test of the SWAT model under average conditions close to those expected under climate change. Interannual variations of temperature, however, were much smaller than the magnitude of changes predicted in climate scenarios.

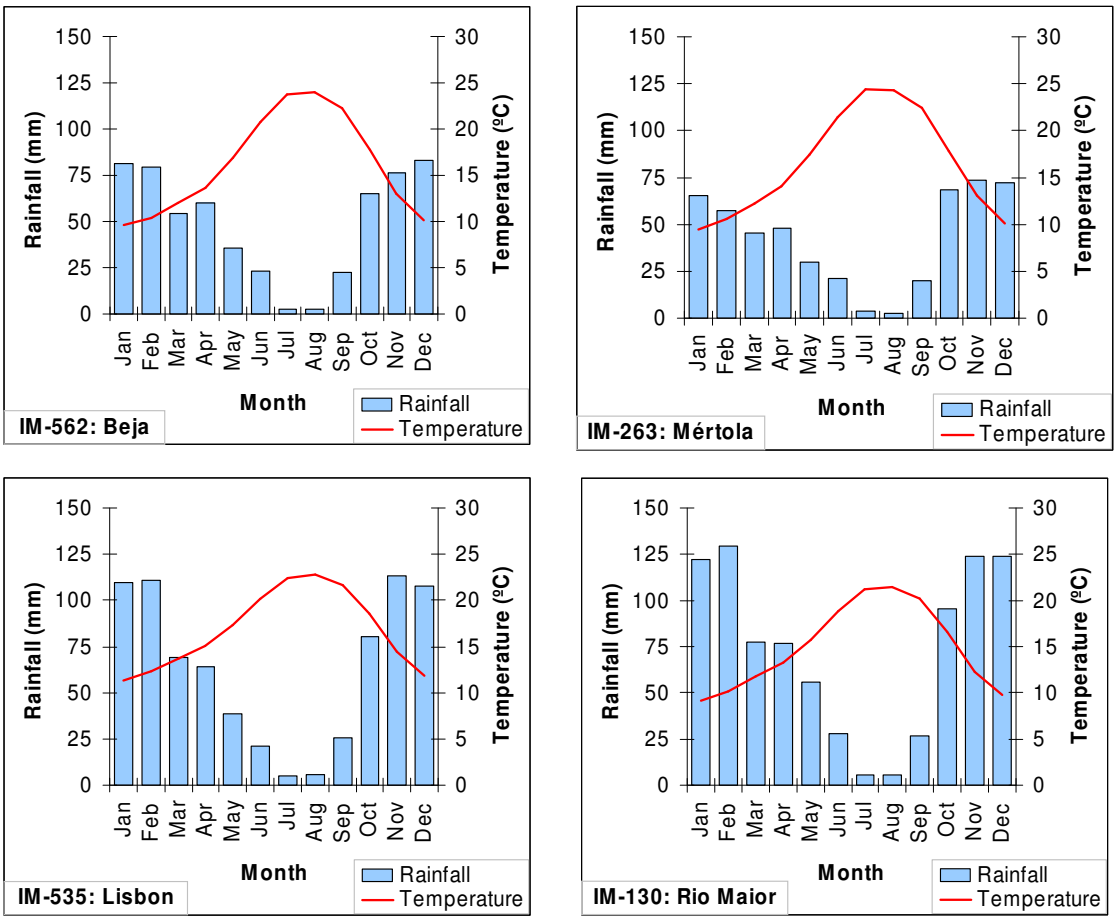

Figure 4.5 – 1961-1990 climate normals for rainfall and temperature for climate stations in the Guadiana (top) and Tejo (bottom); location is shown in Figure 4.4.

The variability between observed monthly rainfall for this period and the one shown in Figure 4.5 was also very significant; rainfall in some winter months was above 350 mm in both study areas, compared with the average of 75 to 125 mm observed in the 1961-1990 period (Figure 4.7). This variability is also characteristic of Mediterranean climates (Palutikof et al., 1996). The variability in daily rainfall was also high, with the highest extreme rainfall episodes reaching 50 mm in Guadiana and 100 mm in Tejo (Figure 4.7). This also allowed the test of the SWAT model under highly variable conditions, both in terms of total monthly rainfall

rates (with implications for soil water balance) and extreme rainfall episodes (with implications for maximum flood rates).

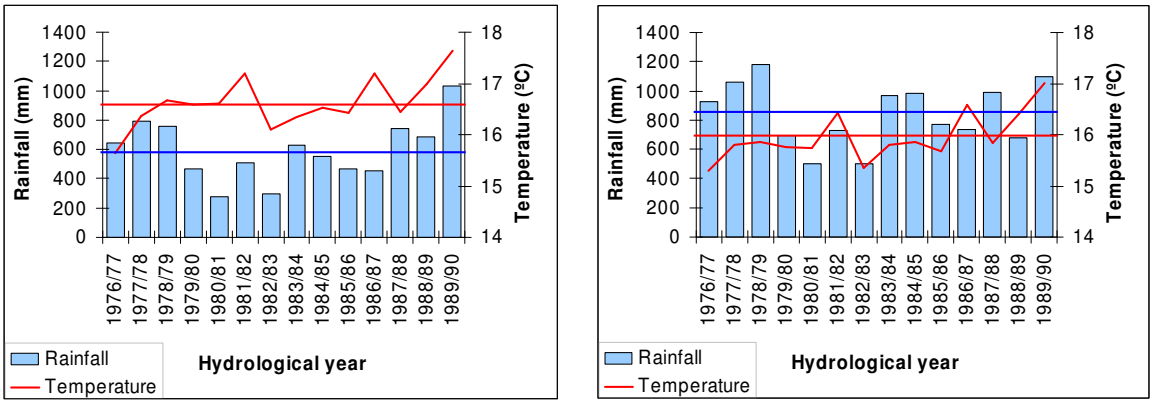

Figure 4.6 – Annual rainfall and mean temperature for the Guadiana (left) and Tejo (right), for the hydrological years from 1976/77 to 1989/90 (SNIRH, 2006); horizontal lines represent average rainfall (blue) and temperature (red) for the sampling period.

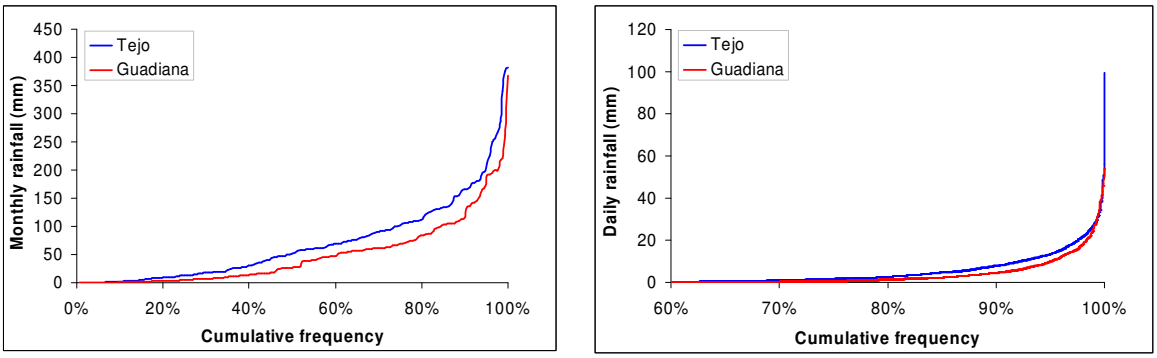

Figure 4.7 – Cumulative histogram for the distribution of monthly (left) and daily (right) rainfall in both study areas, for the period from 1976/77 to 1989/90 (SNIRH, 2006).

Extreme rainfall events

High-resolution rainfall data was collected for a number of extreme rainfall events in both the Odeleite and Alenquer watersheds, for a number of stations shown in Figure 4.4. Data from stations 30J/03 (Feiteira, close to station 30J/01), 30K/01 (Mercador) and 29K03 (Malefrades) was used for Odeleite; the data was collected in SNIRH (2006) and consisted of hourly rainfall measurements for 13 storms, shown in Table 4.1. Peak rainfall resolution was downscaled to 15 minutes using average hourly-to-subhourly rainfall relationships for this region, calculated by Brandão et al. (2001).

Table 4.1 – Characteristics for the selected storms in the Odeleite watershed, calculated from data collected via SNIRH (2006).

Storm beginning	Total rainfall (mm)	Duration[a] (min)	Intensity[a] ($mm.h^{-1}$)	Maximum 10 min intensity ($mm.h^{-1}$)
18-Oct-01 01:00	37.8	2745	0.8	12.8
4-Nov-01 03:00	59.6	3300	1.0	19.4
10-Dec-01 22:00	72.3	1875	2.2	14.8
1-Jan-02 17:00	55.1	1958	1.6	25.4
23-Jan-02 04:00	10.8	480	1.3	10.7
3-Mar-02 00:00	38.7	1718	1.3	20.9
12-Mar-02 01:00	49.9	3540	0.8	22.3
15-Mar-02 16:00	12.7	420	1.7	14.2
17-Mar-02 10:00	9.8	938	0.6	3.2
5-Apr-02 09:00	47.9	5985	0.5	12.1
30-Oct-05 03:00	25.7	780	1.9	19.3
22-Nov-05 00:00	32.0	735	2.5	16.2
1-Dec-05 16:00	15.6	5760	0.2	3.9

a – considering the period corresponding to 95 % of total storm rainfall.

Data for Alenquer came from station 19C/07 (Merceana), and consisted of 15 INAG udographs which were digitized to obtain rainfall breakpoint data; the major storm characteristics are shown in Table 4.2. As the tables show, the collected storms present a wide range of intensities and durations. Figure 4.8 shows the relationship between these characteristics and the most likely return period as determined from Intensity-Duration-Frequency (IDF) curves for both watersheds. As could be expected from the 5 to 7 years sampling period used in both stations, the return period of all storms is under five years; one further problem for the Alenquer was to avoid storms with peak flow rates above 100 $m^3.s^{-1}$, which overflow the river banks and are therefore not measurable (de Macedo, 1996). Nevertheless, the selected storms represent a good combination between short and intense storms, and lower intensity but longer storms.

Table 4.2 – Characteristics for the selected storms in the Alenquer watershed, calculated from udographs supplied by INAG.

Storm beginning	Total rainfall (mm)	Duration[a] (min)	Intensity[a] ($mm.h^{-1}$)	Maximum 10 min intensity ($mm.h^{-1}$)
1-Nov-95 03:20	16.4	130	7.3	37.8
28-Nov-95 15:40	34	450	4.4	31.8
9-Jan-96 07:00	2.5	120	1.2	3.0
1-Nov-97 23:50	47	490	5.7	33.0
2-Nov-97 18:30	20.8	775	1.5	28.8
23-Nov-97 22:40	26.8	450	3.4	39.0
1-Feb-98 15:20	24.8	690	2.1	10.8
2-Feb-98 16:10	31.6	760	2.4	22.2
16-May-99 19:35	34.1	910	2.1	26.4
28-Apr-00 21:40	60	2480	1.4	14.4
3-May-00 17:00	25.1	165	8.7	40.8
1-Mar-01 19:50	25.3	490	3.0	22.2
4-Mar-01 00:00	26.7	585	2.6	19.2
6-Mar-01 10:20	6.4	140	2.7	6.0
11-Mar-02 17:00	9.91	550	1.1	7.9

a – considering the period corresponding to 95 % of total storm rainfall.

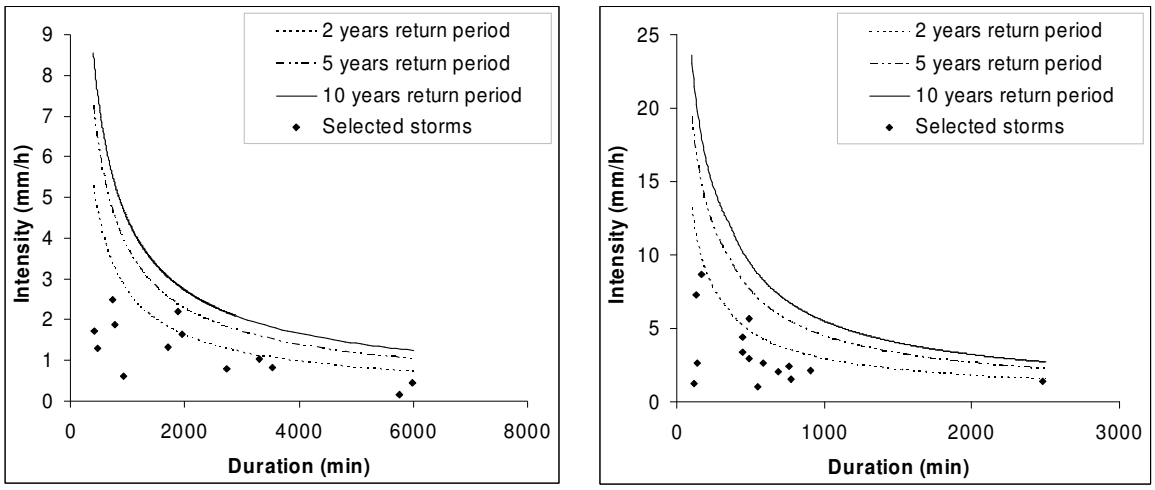

Figure 4.8 – Comparison between selected storms and Intensity-Duration-Frequency (IDF) curves for the Odeleite (left) and Alenquer (right) watersheds, determined by Brandão et al. (2001).

4.2.2 Hydrology and sediment yield

Data on surface hydrology and watershed sediment yield for both study areas was collected from the river sampling network, operated by INAG and available via SNIRH, with the spatial distribution shown in Figure 4.9. The network consists of 9 hydrometric stations for the Guadiana area, 5 of which also possess sediment sampling, and 15 hydrometric stations for the Tejo area, 9 of which with sediment sampling records. The selection criteria for these stations was data availability for the study period, and the absence of major reservoirs and water abstraction systems upstream from the stations, to facilitate the analysis of rainfall-runoff data in terms of natural hydrological processes.

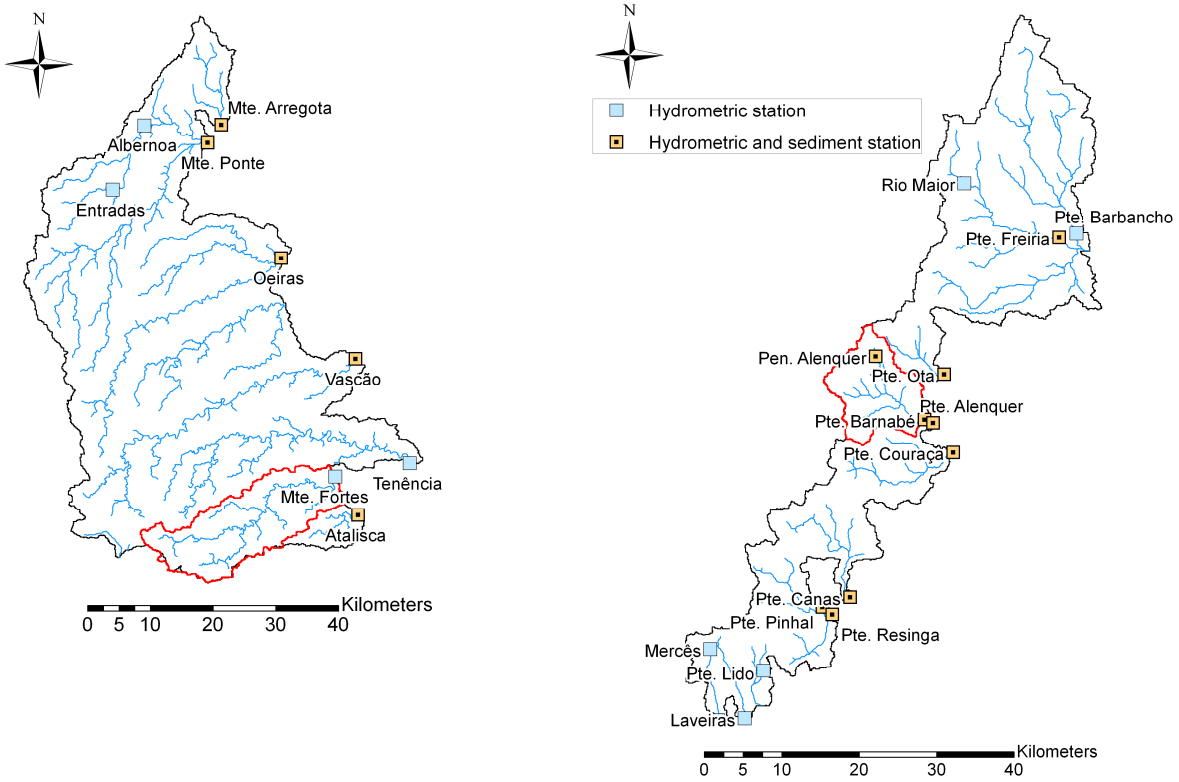

Figure 4.9 – Hydrometric and sediment sampling network in the Guadiana (left) and Tejo (right) study areas; station names correspond to the SNIRH designation.

The average drained area for each station is 296 Km^2 in the Guadiana area and 86 Km^2 in the Tejo, with significant differences between stations due in part to the gauging of nested catchments. Hydrometric stations measure river stage, transformed into river discharge using stage-discharge relationships calculated by INAG (SNIRH, 2006); for the period before 2001, only daily data is available in the information system. The average annual runoff for the

1980s ranged from 159 mm.y^{-1} in the Guadiana to 257 mm.y^{-1} in the Tejo, respectively representing c. 28 % and 32 % of the total rainfall in this period. Daily runoff data was also used to estimate the baseflow fraction by hydrograph separation analysis, using the automated method described by Arnold et al. (1995) and Arnold and Allen (1999).

The data available for sediment stations includes a series of simultaneous water and sediment flow measurements for a very small period of the hydrographic record. While this is insufficient to estimate daily sediment discharge rates directly, the data can be used to derive a sediment rating curve for each station. These curves calculate sediment discharge from water discharge usually via a power function; they are applicable at a range of scales, from hourly to annual, and provide good estimates for both perennial and intermittent streams (Lane et al., 1997). Sediment rating curves were derived for all the sediment stations represented in Figure 4.9, plus the Monte dos Fortes station in the Odeleite watershed. For this station, an alternative sediment sampling dataset from the Portuguese General-Directorate for the Environment (DGA) was used, valid for 2000 to 2005 (SNIRH, 2006); this dataset was also used for the Pte. Barnabé station in the Tejo area in order to obtain valid results for 2000 to 2005. The sediment rating curve formula used has the form:

$$Q_s = a \cdot Q^b \qquad 4.1$$

Where:
Qs – sediment flow rate (Kg.s^{-1})
Q – surface flow rate (m^3.s^{-1})
a and b – equation parameters

The parameters for the curves, together with the minimum and maximum sampled sediment flow, the number of samples, and the correlation coefficient and significance of the curves are shown in Table 4.3; in general, there are more samples for curves in the Guadiana study area, which is reflected in better correlation coefficients and wider Q_s range. In fact, the poor r^2 and significance of some curves for the Tejo area prevents their use for sediment yield estimation. Figure 4.10 shows the sediment rating curves for the Odeleite and Alenquer watersheds; the lower sediment flow values observed in Odeleite reflects lower sediment concentrations, as can be inferred by comparing the surface flow values for both watersheds. It should also be noted that, in this case, the curve appears to underestimate the largest sediment flow rates, although it is difficult to ascertain this due to the lack of measured data for higher values. The median sediment yield in the 1980s ranged from 0.2 ton.ha^{-1}.y^{-1} in the Guadiana to 0.5 ton.ha^{-1}.y^{-1} in the Tejo area.

Table 4.3 – Sediment rating curve (equation 4.1) parameters for sampling stations in the Guadiana and Tejo study areas, together with range of application, number of samples, correlation coefficient and level of significance, calculated using data from SNIRH (2006).

	Sampling station	a	b	r^2	Qs min. ($Kg.s^{-1}$)	Qs max. ($Kg.s^{-1}$)	Samples	Significance level
Guadiana	26K/01S – Monte da Arregota	0.1635	1.3199	0.88	0.0001	6.0	35	0.005
	27J/01S – Monte da Ponte	0.0823	1.3668	0.92	0.0004	243.6	26	0.005
	28K/02S – Oeiras	0.0548	1.4167	0.96	0.001	221.1	48	0.005
	28L/02S – Vascão	0.0287	1.2939	0.94	0.0001	57.0	43	0.005
	30L/04S – Atalisca	0.0281	1.4018	0.95	0.0002	5.4	26	0.005
	29L/01 – Monte dos Fortes	0.0017	1.294	0.90	0.000	8.1	22	0.005
Tejo	18E/01S – Ponte Freira	0.0415	1.2914	0.74	0.003	7.0	15	0.005
	19C/01S – Penedos de Alenquer	0.8058	1.4458	0.80	0.0002	2.7	37	0.005
	19C/02S – Ponte Barnabé	0.3885	1.6921	0.81	0.004	252.8	53	0.005
	19C/03S – Ponte Alenquer	0.2154	2.8792	0.56	0.005	0.8	8	> 0.05
	19D/04S – Ponte Ota	0.4651	2.0906	0.96	0.0002	10.5	9	0.005
	19D/05S – Ponte Couraça	0.1692	0.6309	0.99	0.03	0.2	3	0.05
	20C/01S – Ponte Canas	0.0513	1.4763	0.64	0.009	0.4	9	0.05
	21C/01S – Ponte Pinhal	0.0559	1.3063	0.54	0.005	0.7	9	> 0.05
	21C/02S – Ponte Resinga	0.2658	1.3223	0.44	0.07	2.1	7	> 0.05

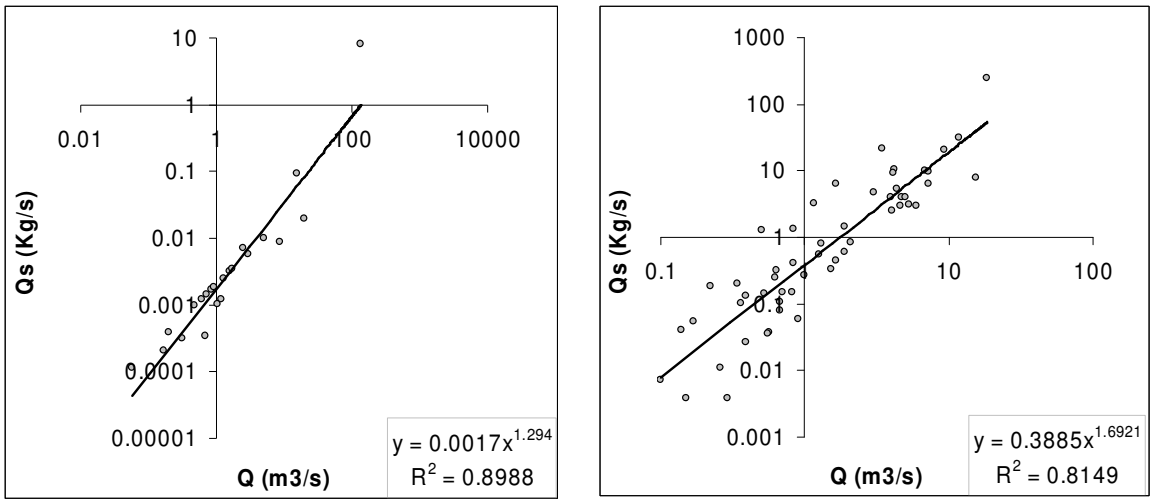

Figure 4.10 – Comparison between sediment-discharge measurements (SNIRH, 2006) and sediment rating curves for the Odeleite (left) and Alenquer (right) watersheds, in logarithmic scale.

Seasonal, decadal and long-term hydrology and sediment yield

Daily runoff data for all the stations shown in Figure 4.9 was collected to calibrate and validate the SWAT model for the 1980s. These values were used together with the sediment rating curves shown in Table 4.3 to estimate daily sediment yield values. The sampling period and drained area for each sampling station is shown in Table 4.4 for the Guadiana area and Table 4.5 for the Tejo area, together with the average annual flow and sediment yield, as well as the baseflow fraction. The Tejo area is characterized by a higher annual runoff and sediment yield, which can be expected from the rainfall characteristics. There is also a contrast in the baseflow fraction, which averages 0.3 in the Guadiana watersheds and 0.6 in the Tejo watersheds. This shows that runoff in the Guadiana is much more irregular in terms of daily variability, which is related with the low water holding capacity of most soils in this region (see section 4.2.4 for details).

Table 4.4 – Sampling period, drained area and hydrological and sediment yield characteristics for watersheds in the Guadiana study area (SNIRH, 2006).

Sampling station	**Sampling start**	**Data years**	**Drained area (Km^2)**	**Average annual runoff ($mm.y^{-1}$)**	**Baseflow fraction**	**Average annual sediment yield ($ton.ha^{-1}.y^{-1}$)**
26K/01 – Monte da Arregota	1981/82	2	96.0	41.2	0.30	0.1
27I/01 – Entradas	1976/77	14	48.3	163.0	0.23	–
27J/01 – Monte da Ponte	1976/77	13	709.4	147.0	0.24	0.6
28K/02 – Oeiras	1981/82	6	481.5	142.6	0.24	0.4
28L/02 – Vascão	1976/77	12	412.1	232.9	0.31	0.2
29L/01 – Monte dos Fortes	1976/77	14	288.8	268.5	0.33	–
29M/01 – Tenência (Porto Areias)	1979/80	4	397.8	94.5	0.40	–
30L/04 – Atalisca	1986/87	3	53.2	300.9	0.28	0.2
26J/01 – Albernoa	1976/77	14	173.7	136.6	0.25	–

Table 4.5 – Sampling period, drained area and hydrological and sediment yield characteristics for watersheds in the Tejo study area (SNIRH, 2006).

Sampling station	Sampling start	Data years	Drained area (Km^2)	Average annual runoff ($mm.y^{-1}$)	Baseflow fraction	Average annual sediment yield ($ton.ha^{-1}.y^{-1}$)
17E/01 – Rio Maior	1978/79	11	36.0	660.0	0.64	–
18E/01 – Ponte Freiria	1976/77	13	187.1	311.1	0.53	0.2
18E/06 – Ponte Barbancho	1981/82	9	251.2	215.2	0.64	–
19C/01 – Penedos de Alenquer	1980/81	9	5.8	235.1	0.67	1.1
19C/02 – Ponte Barnabé	1979/80	10	115.4	161.6	0.56	1.8
19C/03 – Ponte Alenquer	1981/82	2	119.1	288.8	0.55	7.3[a]
19D/04 – Ponte Ota	1979/80	11	59.0	132.5	0.53	13.0[b]
19D/05 – Ponte Couraça	1980/81	4	116.7	125.3	0.79	0.2
20C/01 – Ponte Canas	1979/80	9	104.8	280.9	0.40	0.3
21B/01 – Mercês	1985/86	3	6.1	613.2	0.41	–
21B/02 – Estação Agronómica Nacional	1985/86	5	36.5	575.5	0.62	–
21B/03 – Laveiras	1987/88	2	33.6	686.8	0.69	–
21B/05 – Ponte Lido (Amadora)	1988/89	2	10.5	586.3	0.78	–
21C/01 – Ponte Pinhal	1977/78	10	78.3	407.5	0.60	0.4
21C/02 – Ponte Resinga	1977/78	9	126.6	203.0	0.58	0.7[a]

a – low correlation coefficient in the sediment rating curve.
b – biased towards one extreme flow event on 19-Nov-1983, with 183 mm flow and 90.6 $ton.ha^{-1}$ sediment yield.

Monthly values for rainfall and runoff for 1976 to 1990 were averaged to highlight seasonal behavior patterns, as shown in Figure 4.11. The highest contrast between the Guadiana and Tejo areas is in the amount of rainfall and runoff for this period. However, the figure also shows the impact of the low water holding capacity of the Guadiana soils. While runoff follows rainfall in both systems, there is a period of soil water recharge in the beginning of the rain season (October) where runoff generation is much lower than in the other months. In the Tejo, runoff peaks in December and again in February, probably owing to the wet conditions of the soil; after March, the soil water is slowly drained into the river network, leading to

permanent, if low, river flows throughout the dry season; the rivers are perennial in nature, although with much larger flow rates during the wet season.

In the Guadiana, however, there is less water stored in the soils available for drainage, and soil water is usually exhausted by the end of May, leading to almost no river flow in the dry season (June to September). Many of the rivers, particularly in the northern part of the study area, can therefore be considered intermittent. It should be noted, however, that this period includes a severe drought (as previously referred) which could lead to an under-representation of average runoff rates.

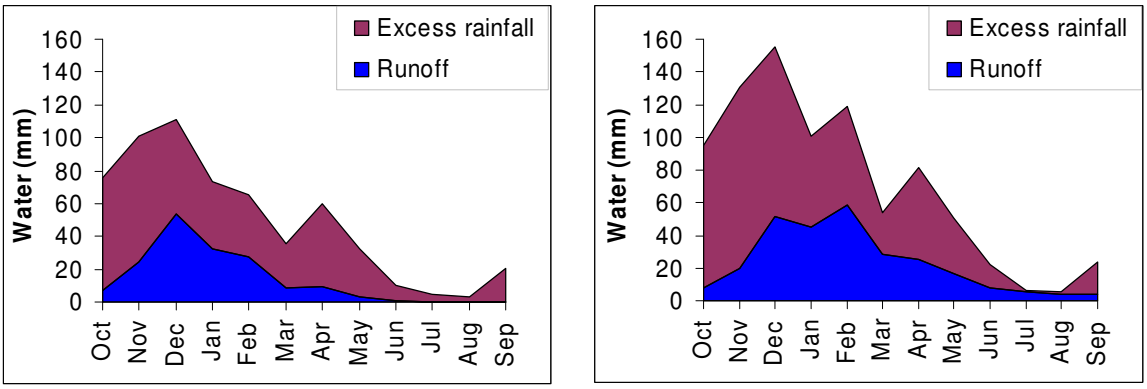

Figure 4.11 – Average monthly estimates for rainfall and runoff in the Guadiana (left) and Tejo (right) study areas, using data from the stations shown in Table 4.5 and Table 4.4 (SNIRH, 2006).

The annual values for runoff from 1976 to 1990 (the same period for which daily climate data was collected), broken down into surface flow and baseflow, are shown in Figure 4.12, again aggregated by hydrological year (Palutikof et al., 1996). Runoff during the 1980s showed a high interannual variability, following the variability in rainfall; the drought lasting from 1979/80 to 1982/93 is visible in the figure. Runoff showed a higher trend for variability than rainfall, ranging from c. -80 to -90 % in both study areas during the worst drought years to c. +190 to +200 % in the wettest years. This represents a range from 19 to 478 mm in the Guadiana catchments, compared with 52 to 752 mm in the more humid Tejo catchments; in 1980/81 there was virtually no runoff measured in most rivers in the Guadiana. These values show the non-linear relationship between rainfall and runoff rates in the study areas, as described by numerous authors (e.g. Kirkby et al., 2002; see section 2.2.2 for a full discussion

of this subject). This range of annual and seasonal runoff rates allows a comparison of the SWAT model results with a wide range of runoff conditions, including several drought years which could represent the dryer conditions expected under climate change in these regions.

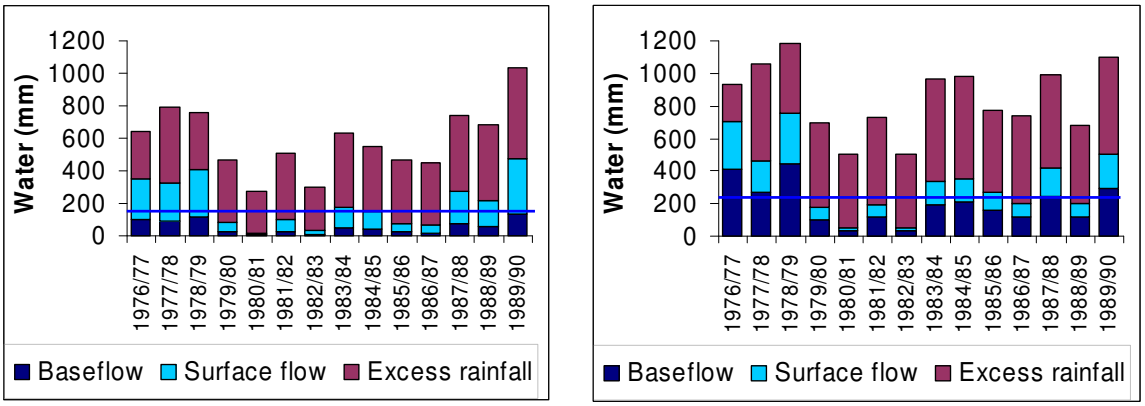

Figure 4.12 – Annual estimates for rainfall subsurface and surface runoff in the Guadiana (left) and Tejo (right) study areas, using data from the stations shown in Table 4.4 and Table 4.5 for the hydrological years from 1976/77 to 1989/90 (SNIRH, 2006); the horizontal blue lines show the average annual runoff within this period.

Extreme rainfall events

High-resolution runoff data was collected for the period during and immediately following the extreme rainfall events shown in Table 4.1 and Table 4.2. Data for Odeleite came from station 29L/01 (Monte dos Fortes), while data for Alenquer came from station 19C/02 (Ponte Barnabé), both represented in Figure 4.9. The Alenquer data consisted of 15 INAG hydrographs which were digitized to obtain breakpoint values; the Odeleite data consisted of hourly discharge measurements for 13 storms. Sediment discharge was estimated for these values using the sediment rating equations shown in Figure 4.10. The data for the selected storms are shown in Table 4.6 and Table 4.7 for the Odeleite and Alenquer watersheds, respectively.

Table 4.6 – Hydrological characteristics and sediment yield for the selected storms in the Odeleite watershed, calculated from data collected via SNIRH (2006).

Storm beginning	Baseflow ($mm.h^{-1}$)	Surface runoff[a] (mm)	Surface runoff duration[b] (min)	Peak runoff rate[c] ($mm.h^{-1}$)	Sediment yield ($ton.ha^{-1}$)
18-Oct-01 01:00	0.0009	3.1	4320	0.18	0.00005
4-Nov-01 03:00	0.002	13.7	5400	0.42	0.0004
10-Dec-01 22:00	0.002	25.8	4200	0.93	0.004
1-Jan-02 17:00	0.02	22.7	2760	1.48	0.007
23-Jan-02 04:00	0.01	2.9	3360	0.14	0.00004
3-Mar-02 00:00	0.004	3.2	3780	0.21	0.00006
12-Mar-02 01:00	0.01	11.1	4500	0.54	0.0006
15-Mar-02 16:00	0.18	1.4	2340	0.12	0.0001
17-Mar-02 10:00	0.18	1.5	3420	0.23	0.0002
5-Apr-02 09:00	0.009	14.8	8640	0.24	0.0003
30-Oct-05 03:00	0.00	0.8	5100	0.03	0.00001
22-Nov-05 00:00	0.29	18.0	2160	1.61	0.010
1-Dec-05 16:00	0.006	2.1	6480	0.05	0.00003

a – not considering total baseflow.
b – considering the period from the storm start to the inflexion period of the hydrograph's descending limb.
c – not considering baseflow rate.

The tables show that the collected storms present a wide range of hydrological and sediment yield characteristics. One particular note is the difference in rainfall-runoff generation ratios between both watersheds; they average 26.6 % in Odeleite but only 12.6 % in Alenquer. Considering that the IDF characteristics for the selected storms in both catchments are not significantly different (as shown in Figure 4.8), this can possibly be attributed to the shallower soils in Odeleite with a significantly lower water holding capacity (see section 4.2.4 for more details). This is concurrent with the observation of a lower baseflow fraction in Odeleite when compared with Alenquer for the 1980s (0.33 and 0.55 respectively; see Table 4.4 and Table 4.5), as more rainfall appears to be diverted for surface runoff in the former watershed.

Another note is that, although typical rainfall thresholds for runoff generation in Mediterranean watersheds usually range around 10 $mm.h^{-1}$ during 30 min (Boix-Fayos et al., 2005; Kirkby et al., 2005), several storms shown in Table 4.1 and Table 4.2 had significantly lower peak rainfall intensities which still resulted in surface runoff generation. This is due to the importance of saturation excess rainfall generation processes common in Mediterranean watersheds, as reported by García-Ruiz et al. (2005) and other authors; see section 2.2.2 for a full discussion on this subject. Considering antecedent baseflow as an indicator of antecedent

soil moisture conditions in a watershed, particularly in terms of saturated area (Beven, 2000), the importance of soil moisture for runoff generation can be seen in Figure 4.13. While rainfall appears to govern surface runoff in both watersheds, there is a clear difference between the response for low and high baseflow storms, with the latter producing considerably more runoff for a similar amount of rainfall. In Odeleite, this phenomena appears to lose importance with the total rainfall amount, possibly due to the low water holding capacity of soils referred above; this data indicates that, after a certain rainfall threshold is reached – possibly enough to saturate a large part of the Odeleite watershed – the remaining rainfall is mostly transformed into surface runoff.

Table 4.7 – Hydrological characteristics and sediment yield for the selected storms in the Alenquer watershed, calculated from hydrographs supplied by INAG.

Storm beginning	**Baseflow ($mm.h^{-1}$)**	**Surface runoff[a] (mm)**	**Surface runoff duration[b] (min)**	**Peak runoff rate[c] ($mm.h^{-1}$)**	**Sediment yield ($ton.ha^{-1}$)**
1-Nov-95 03:20	0.0002	0.1	400	0.03	0.0003
28-Nov-95 15:40	0.001	0.7	750	0.11	0.006
9-Jan-96 07:00	0.46	0.4	300	0.14	0.01
1-Nov-97 23:50	0.002	2.6	1090	0.65	0.05
2-Nov-97 18:30	0.03	1.1	935	0.20	0.02
23-Nov-97 22:40	0.02	6.2	750	1.22	0.20
1-Feb-98 15:20	0.06	4.8	1070	0.89	0.09
2-Feb-98 16:10	0.21	8.8	1260	1.15	0.31
16-May-99 19:35	0.005	0.8	1290	0.09	0.007
28-Apr-00 21:40	0.02	12.8	2130	1.34	0.36
3-May-00 17:00	0.07	3.7	425	1.00	0.11
1-Mar-01 19:50	0.04	2.2	800	0.39	0.04
4-Mar-01 00:00	0.05	6.9	1445	1.46	0.22
6-Mar-01 10:20	0.31	1.0	710	0.23	0.02
11-Mar-02 17:00	0.009	0.1	970	0.02	0.0007

a – not considering total baseflow.
b – considering the period from the storm start to the inflexion period of the hydrograph's descending limb.
c – not considering baseflow rate.

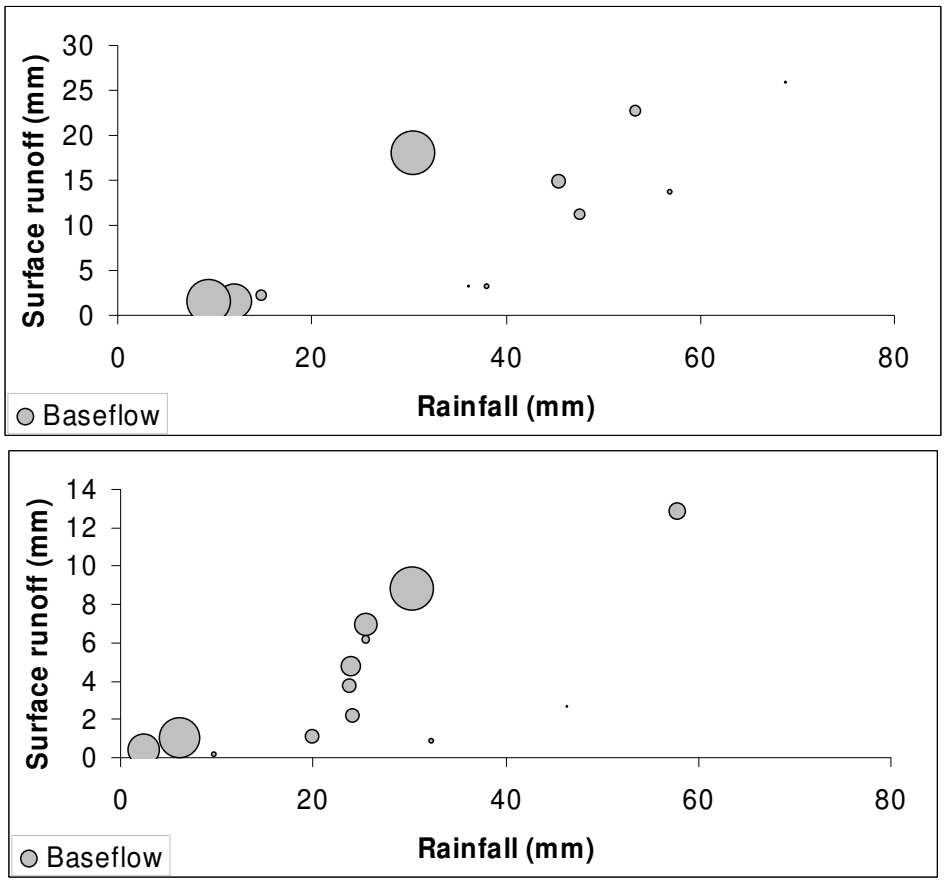

Figure 4.13 – Relationship between rainfall and surface runoff for the Odeleite (top) and Alenquer (bottom) watersheds, for the storms represented in Table 4.6 and Table 4.7 respectively; symbol size represents the storm baseflow in proportion to the average baseflow for the entire dataset.

This observation is confirmed with the correlation between surface runoff, rainfall and antecedent baseflow. For Odeleite the correlation values are 0.57 for rainfall ($p < 0.05$) and 0.32 ($p > 0.1$) for baseflow, indicating both the importance of rainfall for runoff generation and also that the correlation with antecedent baseflow might not exist for part of the dataset. In contrast, the correlation values for Alenquer are 0.47 for rainfall ($p < 0.1$) and 0.53 for baseflow ($p < 0.05$). Overall, these observations point to the importance of antecedent baseflow and pre-storm soil moisture for runoff generation in both watersheds; in Odeleite, however, this phenomena can be eclipsed by the amount of rainfall during large storms.

Finally, the results for sediment yield (Table 4.6 and Table 4.7) show a difference between observations in Odeleite and Alenquer of almost two orders of magnitude, with the storms averaging a yield of c. 0.002 ton.ha^{-1} in the former and 0.1 ton.ha^{-1} in the latter. Part of this

difference can be explained by the shrublands covering most of Odeleite, which in Mediterranean regions present soil erosion rates of c. 0.5 ton.ha^{-1}.y^{-1}, c. one to two orders of magnitude lower than those usually observed for the most common landcovers in Alenquer, wheat and vineyards, with 3.6 and 13.5 ton.ha^{-1}.y^{-1} respectively (Poesen and Hooke, 1997; Wainwright and Thornes, 2004). Another difference can be attributed to the lower sediment delivery ratio in Odeleite, as discussed in detail in the next section. Some of the values for Odeleite shown in Table 4.6 are very low, and given the errors associated with the sediment rating curve (equation 4.1) they can be taken as representing virtually no sediment yield.

There is also a significant variability for this parameter within storms, of c. 3 orders of magnitude in Odeleite (Table 4.6) and c. 4 orders of magnitude in Alenquer (Table 4.7). This variability is associated with the variability of runoff and in particular peak runoff rates between storms. However, this could be considered as an artifact of the sediment rating curves described in the previous section. Nevertheless, it is important to note that this dataset shows peak runoff rates as being more important than total runoff for sediment yield.

4.2.3 Topography and watershed characterization

The study areas show contrasting topographic profiles The Guadiana watersheds are composed of rivers crossing the Alentejo plain towards the incised valley of the Guadiana river (with the exception of watersheds draining from the Caldeirão mountain range in the southwest), while the Tejo watersheds are mostly composed of rivers draining from the Montejunto mountain range to the Tejo river floodplain, with quick changes in altitude. The topographic information used in this work consists of a Digital Elevation Model (DEM) shown in Figure 4.14; the data source is NASA's Shuttle Radar Topography Mission (SRTM) 90×90 m dataset, with data gaps filled using a contour-based interpolation method (Jarvis et al., 2006). Typical slope and watershed characteristics are visible from the figure: the Guadiana watersheds show an elongated shape (see also Figure 4.2) and an average slope of 8 %, evenly distributed throughout the watershed, while the Tejo watersheds are heart-shaped (see also Figure 4.3) and show an average slope of 10 %, but much higher in the headwater catchments.

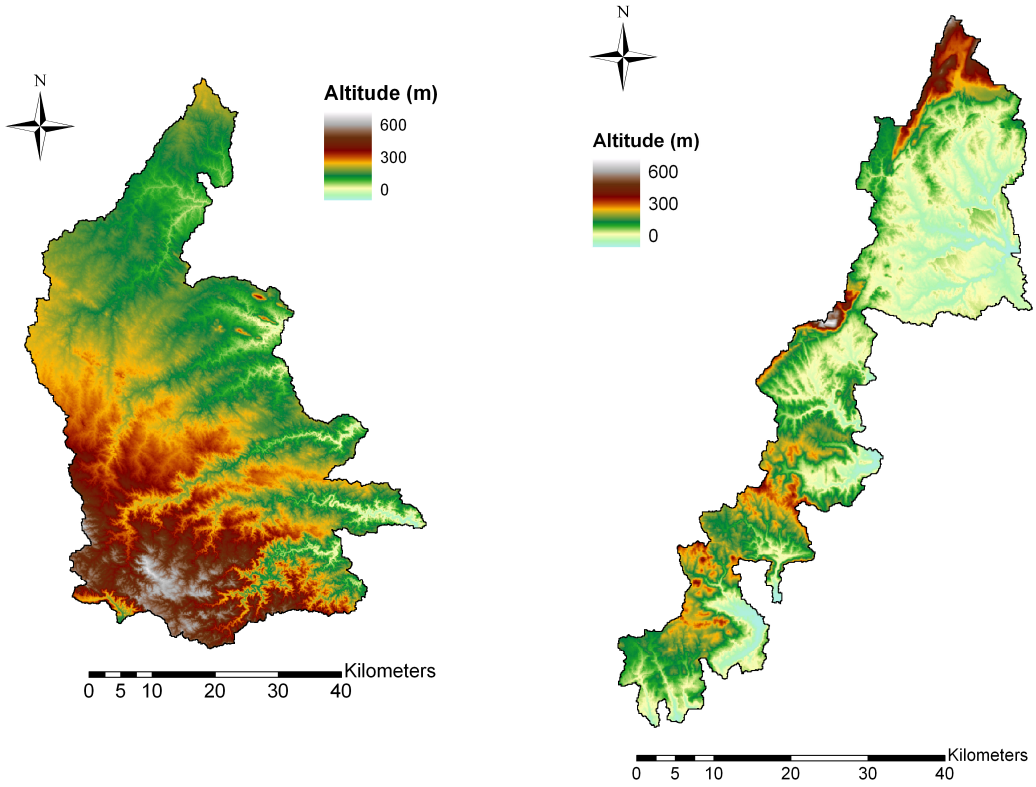

Figure 4.14 – Topography for the Guadiana (left) and Tejo (right) study areas; the dataset was produced by Jarvis et al. (2006) from the SRTM 90×90 m DEM, and cut using watershed limits.

The MEFIDIS model application required additional topographic characterization for the Odeleite and Alenquer watersheds, in terms of channel network description and soil moisture patterns estimation (see section 3.2); this was performed using the DEMs described above. The model requires the description of each watershed's channel network; this analysis required the construction of a drainage map using the flow direction map described above. An arbitrary drainage area of 5 Km^2 (similar to that used for the SWAT model) was selected as a threshold for permanent channel initiation; cells with drainage areas above the threshold were considered to have permanent channels. A channel width for each channel section was then estimated using the drainage area – width relationships described by Veitzer and Gupta (2001). The authors report that maximum channel width can usually be considered a power function of the catchment drainage area, with exponents between 0.42 and 0.51. This assumption was tested for both catchments by measuring of channel widths at several points, which were then compared with the local drained area using the map described above. In the Odeleite region 20 measurements were made in the field, while in Alenquer 21 measurements were made using a high-resolution (3 × 3 m) aerial photograph. Figure 4.15 shows the results,

as well as the power function derived from the measurements; the exponent falls within the values proposed by the authors. This relationship was used to parameterize channel width for the MEFIDIS model; widths ranged from 1 to 13 m in the Odeleite watershed, and 1 to 9 m in the Alenquer watershed.

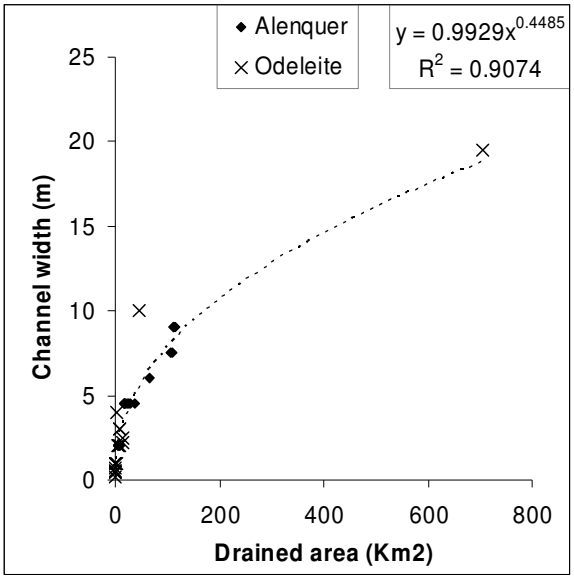

Figure 4.15 – Comparison between observed channel width and drained area for points within the Odeleite and Alenquer catchments (and in catchments neighboring Odeleite).

The river network extracted in this fashion, together with the DEM, allowed for the calculation of the sediment delivery ratio in both catchments. Although this parameter is not used by the MEFIDIS model, it is useful for model validation purposes since it correlates soil erosion in the outlet with that found at the field and hillslope scale (represented by single model cells). A large number of methods to estimate sediment delivery ratio based on watershed morphological parameters have been proposed by several authors, usually taking catchment area into account; Lane et al. (1997) provide a discussion of different methods. The Roehl method (Ponce Álvares and Pimenta, 1998) was selected for this estimation since it takes into account not only catchment area but also the different shapes of the Odeleite and Alenquer watersheds. This is achieved by taking into account both the rate between catchment height difference and axial length, and by including the bifurcation ratio of first order channels in the calculation. The results are 0.04 for Odeleite and 0.18 for Alenquer, indicating that a very low fraction of sediment eroded in the Odeleite hillslopes reaches the catchment

outlet. This concurs with the observed low sediment concentrations observed in Odeleite (as previously discussed, and shown in Figure 4.10), and the low sediment yields during extreme events (Table 4.6).

The model also requires a number of topographic parameters in order to estimate the spatial distribution of soil moisture deficits before a storm. The method used by MEFIDIS is based in the TOPMODEL approach (Beven, 2000), described in section 3.2.2 and in equations 3.17 and 3.18. Although there is no available soil moisture data to validate this index for the watersheds, the existence of expanding saturated areas in both humid and semi-arid catchments during the wet season has been observed (Kirkby, 2002); during this season, several authors (e.g. Puigdefabregas et al., 1998; Gómez-Plaza et al., 2000) have reported topographic controls on soil moisture patterns, therefore indicating the potential reliability of topographic wetness indexes in Mediterranean catchments. The first step consists in the calculation of the topographic wetness index (equation 3.17), using the drainage area map, and a DEM-derived slope map. The results are shown in Figure 4.16, one important difference between catchments being the existence of saturation-prone plains in Alenquer. The average wetness index (γ in equation 3.18) is 7.4 for Odeleite and 7.9 for Alenquer.

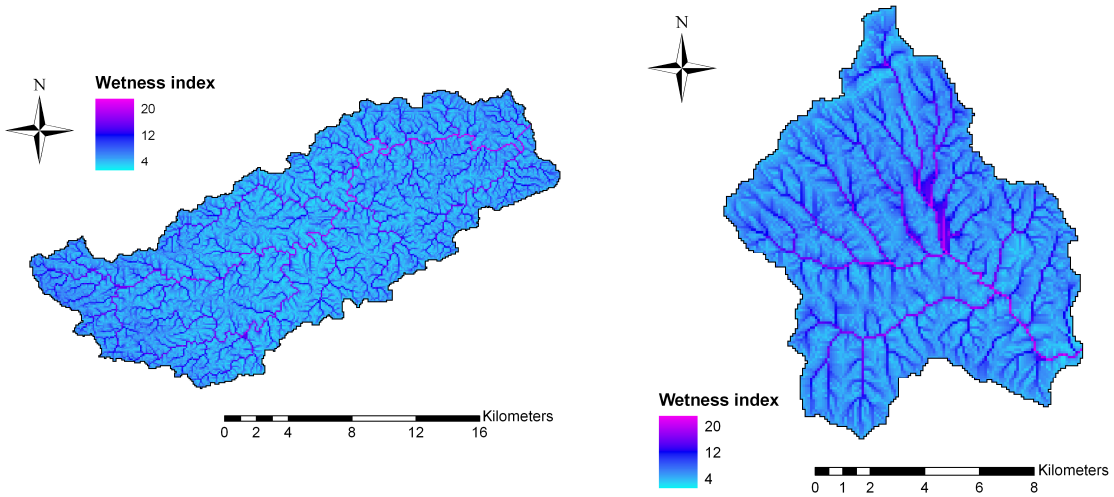

Figure 4.16 – Topographic wetness index distribution for Odeleite (left) and Alenquer (right), calculated following equation 3.17.

The estimation of soil moisture patterns using equation 3.18 requires one further parameter, the rate of decay of transmissivity in the soil profile (m). Beven (2000) links this parameter

with the active water storage capacity of the soil profile, and provides a simple estimation method using measured recession curves and assuming negligible recharge. 13 post-storm daily hydrograph recession curves, for days with no rainfall, were collected for Odeleite, and 5 for Alenquer; the smaller number of curves for Alenquer is due to the rainfall characteristics in the catchment during the wet season, where it is uncommon for a strong rainfall event to be followed by consecutive days without rainfall. Figure 4.17 shows three curves per catchment, highlighting the differences in catchment behavior during the hydrograph recession phase: water stored in the soil profile drains more rapidly in Odeleite, indicating a much lower soil water storage capacity (this issue was discussed previously and is elaborated in section 4.2.4).

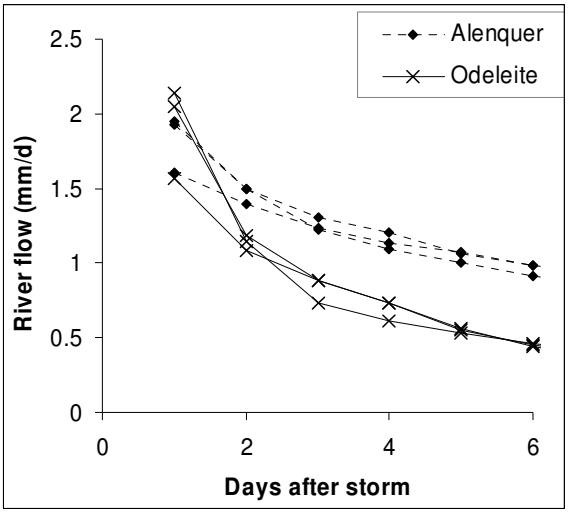

Figure 4.17 – Measured daily recession curves after 3 storms for Odeleite and Alenquer.

Using the methodology described by Beven (2000), the *m* parameter was estimated to fall between 0.7 and 3.4 mm in Odeleite, and between 8.3 and 13.3 mm in Alenquer. Beven (1997) has listed typical TOPMODEL *m* values in different model applications; they usually range between 3 and 100 mm, with most being between 15 and 30 mm. While the estimated values for Odeleite are below those reported by the author, lower *m* values represent soils with a lower active water storage capacity (Beven, 2000). Since the water storage capacity of soils in Odeleite is very small (see section 4.2.4), the estimated values appear to accurately represent soil transmissivity decay characteristics. However, it should be noted that the recession curves for Odeleite spanned between 10 and 20 days, and therefore evapotranspiration processes could be contributing to soil water depletion; it is therefore

expected that calibrated *m* values in the model belong to the higher end of the estimated range or surpass it slightly.

4.2.4 Soils

The Guadiana and Tejo study areas present contrasting soil distributions resulting both from climatic characteristics and past land uses. The Guadiana area is mostly occupied by Lithosols, characterized by their shallow depths (usually under 250 mm) and unsuitability for agriculture, coupled with a propensity for soil erosion when cultivated (Driessen et al., 2001); their extensive presence in this region has been attributed to extensive human agricultural practices by Cardoso (1965). In contrast, Tejo area is mostly occupied by Cambisols, an incipient soil type which is nevertheless very suitable for agriculture (Driessen et al., 2001). These differences, coupled with different climate and aridity patterns, partly explain the marked contrast in hydrological processes and land cover patterns between both study areas.

Soil mapping and characterization is a necessary step to apply both the SWAT and the MEFIDIS models. However, the different scales at which the models operate required the use of data sources with different levels of detail. For SWAT, soil parameterization was based on the global-scale survey performed by the United Nations' Food and Agriculture Organization (FAO), while MEFIDIS used the more detailed national-scale survey performed by Cardoso (1965) and maintained and updated by the General-Directorate for Agriculture and Rural Development (DGADR). These data sources were used respectively for the entire study areas and for the Odeleite and Alenquer catchments.

Soil characterization for the Guadiana and Tejo

The soil distribution in the Guadiana and Tejo study areas was characterized using the 1978 FAO soil map, with a scale of 1:1,000,000, shown in Figure 4.18; the Portuguese contribution for the world map was described by Cardoso et al. (1973). The Guadiana study area is dominated by eutric Lithosols (82 % of the total area), although Luvisols (18 %) are also present, particularly of the ferric and orthic suborders. The Tejo study area is dominated by Cambisols (75 % of the total area), mostly of the calcic, chromic and eutric suborders, although important patches of Luvisols (17 %) and Vertisols (7 %) are also present.

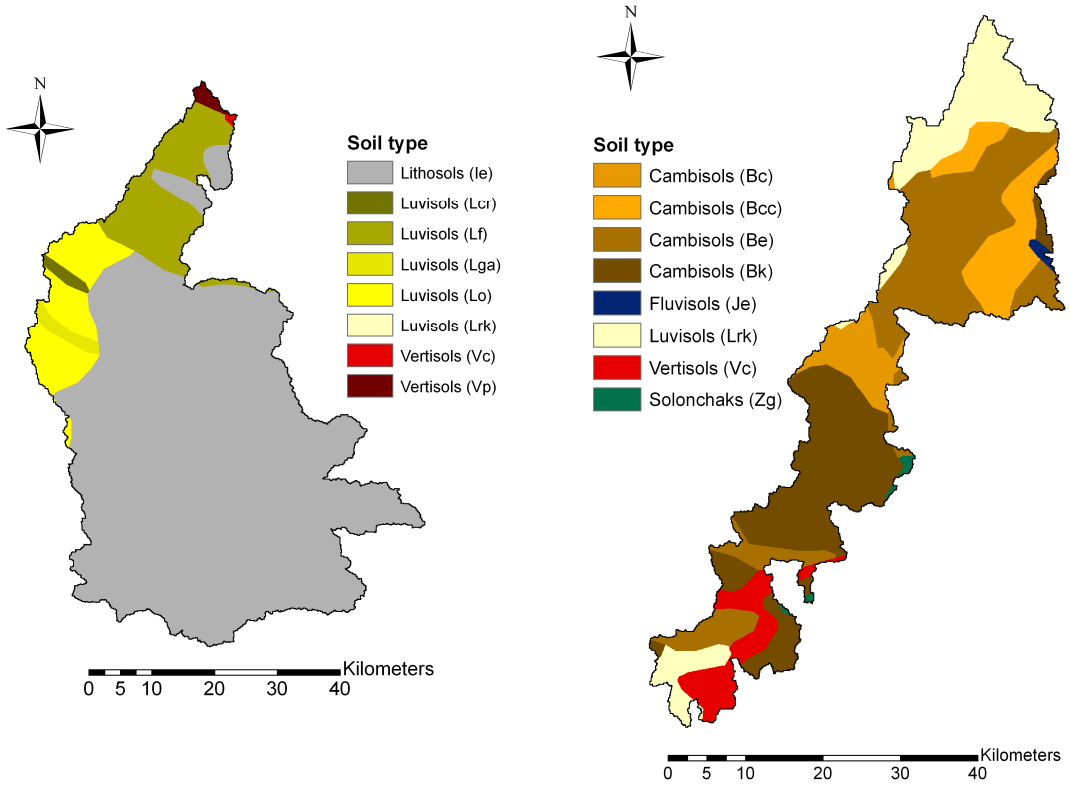

Figure 4.18 – Soil types in the Guadiana (left) and Tejo (right) study areas, classified according to the 1990 FAO soil classification (Driessen et al., 2001), following the 1978 1:1,000,000 FAO soil map (Cardoso et al., 1973).

The physical characterization of these soils focused on the main soil parameters required by the SWAT model, described by Neitsch et al. (2002) and discussed in section 3.4; it followed the database published by the International Soil Reference and Information Centre (ISRIC; Batjes, 2002), which contains information taken from an analysis of global soil profiles for two generic soil depths, surface (0 to 300 mm) and subsurface (> 300 mm). Table 4.8 shows the main soil types and properties for the entire profile. The Soil Conservation Service (SCS) hydrological group was determined according to soil depth and the hydraulic conductivity of all soil layers, following Neitsch et al. (2002). One further parameter, soil albedo, was given the value of 0.11 for all soil types suggested by Lencastre and Franco (1992). It should be noted that the soil depth for Lithosols given in the table is significantly larger than the depth of c. 100 mm measured by Cardoso (1965) for these soils in the Guadiana.

Table 4.8 – Main soil types shown in Figure 4.18 and physical properties for the entire profile, following Batjes (2002).

FAO classification		**Soil properties**		
Order	**Code**	**Texture**	**Depth (mm)**	**SCS hydrological group[a]**
Cambisols	Bc	Clay loam	1150	C
	Be	Loam	1100	B
	Bk	Loam	1200	B
Lithosols	Ie	Loam	240	D
Fluvisols	Je	Loam	1200	B
Luvisols	Lc	Sandy clay loam	1170	C
	Lf	Sandy loam	1300	C
	Lg	Sandy clay loam	1200	C
	Lo	Sandy loam	1200	C
	Lr	Sandy loam	1200	C
Vertisols	Vc	Clay	1500	C
	Vp	Clay	1200	C
Solonchaks	Zg	Clay loam	1100	C

a – calculated following Neitsch et al. (2002).

Table 4.9 and Table 4.10 present the soil physical and hydraulic parameters for different layers. The saturated hydraulic conductivity (K_{sat}) was not available in the original dataset; the values were estimated using the Pedo-Transfer Functions (PTFs) developed by Saxton et al. (1996) and considered by Ferrer-Julià et al. (2004) as appropriate to estimate this parameter for soils in the Iberian Peninsula. Soil erodibility, corresponding to the Universal Soil Loss Equation (USLE) K factor, was estimating using the formulation proposed by Williams (1995). Both methods require soil texture parameters as input data, which are present in the ISRIC database and are shown in Table 4.11 and Table 4.12.

An analysis of the data presented in these tables shows that Lithosols, which dominate the Guadiana study area, have a much lower soil water holding capacity than the major soils in the Tejo area. This is the result of a low soil depth – 240 mm on average, compared with more than 1 m for other soil types (Table 4.8), coupled with a similar bulk density and water holding capacity to that of other soils (Table 4.9). Furthermore, Lithosols have a significantly higher percentage of rock fragments, further reducing the available water storage space (Table 4.11). These characteristics can explain the low baseflow fraction found in the river flow of Guadiana watersheds, as discussed in section 4.2.2.

Table 4.9 – Soil physical and hydraulic parameters for the surface layer (Batjes, 2002).

FAO classification		Max. Depth	Bulk density	Available water capacity for plants	K_{sat}[a]	
Order	**Code**	**(mm)**	**($g.cm^{-3}$)**	**(fraction)**	**($mm.h^{-1}$)**	**Erodibility[b]**
Cambisols	Bc	300	1.29	0.12	3.33	0.30
	Be	300	1.37	0.11	6.11	0.30
	Bk	300	1.40	0.12	4.83	0.35
Lithosols	Ie	240	1.35	0.13	4.27	0.30
Fluvisols	Je	300	1.35	0.13	7.34	0.31
Luvisols	Lc	300	1.45	0.10	4.17	0.28
	Lf	300	1.50	0.05	12.58	0.24
	Lg	300	1.40	0.17	4.76	0.27
	Lo	300	1.42	0.11	8.60	0.26
	Lr	300	1.43	0.10	7.24	0.26
Vertisols	Vc	300	1.65	0.12	2.10	0.36
	Vp	300	1.30	0.13	1.81	0.32
Solonchaks	Zg	300	1.39	0.14	3.71	0.33

a – calculated following Saxton et al. (1986).
b – calculated following Williams (1995).

Table 4.10 – Soil physical and hydraulic parameters for the subsurface layer (Batjes, 2002).

FAO classification		Max. Depth	Bulk density	Available water capacity for plants	Ksat[a]	
Order	**Code**	**(mm)**	**($g.cm^{-3}$)**	**(fraction)**	**($mm.h^{-1}$)**	**Erodibility[b]**
Cambisols	Bc	1150	1.40	0.11	2.21	0.31
	Be	1100	1.38	0.12	4.58	0.31
	Bk	1200	1.40	0.11	4.24	0.35
Lithosols	Ie	–	–	–	–	–
Fluvisols	Je	1200	1.41	0.12	6.97	0.31
Luvisols	Lc	1170	1.48	0.13	2.13	0.29
	Lf	1300	1.49	0.05	2.65	0.25
	Lg	1200	1.55	0.14	2.23	0.28
	Lo	1200	1.48	0.11	2.79	0.26
	Lr	1200	1.50	0.11	2.52	0.27
Vertisols	Vc	1500	1.75	0.12	2.16	0.37
	Vp	1200	1.39	0.14	1.83	0.33
Solonchaks	Zg	1100	1.57	0.14	2.97	0.30

a – calculated following Saxton et al. (1986).
b – calculated following Williams (1995).

Table 4.11 – Soil texture parameters for the surface layer (Batjes, 2002).

FAO classification Order	Code	Clay (% fines)	Silt (% fines)	Sand (% fines)	Rock fragments (%)	Organic carbon (%)
Cambisols	Bc	29.59	26.53	43.88	4.00	1.12
	Be	22.68	30.93	46.39	10.00	1.05
	Bk	26.88	38.71	34.41	8.00	0.79
Lithosols	Ie	26.90	30.46	42.64	28.00	2.18
Fluvisols	Je	21.05	33.68	45.26	4.50	0.98
Luvisols	Lc	25.77	21.65	52.58	6.50	0.91
	Lf	15.31	12.24	72.45	6.00	0.75
	Lg	23.96	18.75	57.29	4.00	0.94
	Lo	18.32	16.75	64.92	4.00	0.89
	Lr	19.79	16.67	63.54	5.00	0.81
Vertisols	Vc	56.54	28.80	14.66	4.50	0.85
	Vp	55.67	23.71	20.62	2.00	1.25
Solonchaks	Zg	29.35	32.61	38.04	4.00	0.49

Table 4.12 – Soil texture parameters for the subsurface layer (Batjes, 2002).

FAO classification Order	Code	Clay (% fines)	Silt (% fines)	Sand (% fines)	Rock fragments (%)	Organic carbon (%)
Cambisols	Bc	36.56	24.73	38.71	4.00	0.48
	Be	25.91	30.05	44.04	13.00	0.40
	Bk	28.57	37.76	33.67	10.00	0.41
Lithosols	Ie	–	–	–	–	–
Fluvisols	Je	21.28	30.85	47.87	8.00	0.39
Luvisols	Lc	35.57	20.10	44.33	8.00	0.40
	Lf	29.90	11.34	58.76	8.00	0.33
	Lg	34.34	19.19	46.46	6.00	0.30
	Lo	29.79	14.89	55.32	5.00	0.35
	Lr	31.41	15.71	52.88	7.00	0.34
Vertisols	Vc	57.89	28.42	13.68	5.00	0.46
	Vp	57.95	21.54	20.51	4.00	0.63
Solonchaks	Zg	31.11	25.56	43.33	4.00	0.30

Soil characterization for Odeleite and Alenquer

The soil distribution in the Odeleite and Alenquer watersheds was derived from the DGADR 1:50,000 soil maps, described in detail by Gonçalves et al. (2005). The original maps were classified in the Portuguese system used by DGADR and developed by Cardoso (1965); soil types were translated into the 1990 FAO classification system following the correspondence tables published by Pimenta (1998), shown in Table 4.13. Figure 4.19 shows the maps. The map for Odeleite is very similar at both scales, with the watershed dominated by eutric Lithosols; little information is added at the 1:50,000 scale. In contrast, the map for Alenquer is significantly more detailed than the one used for the Tejo study area; the calcic Cambisols are further discretized, and important patches of Luvisols, Vertisols, and Fluvisols are shown, the latter along the banks of the Alenquer river and tributaries. However, there are also significant differences in soil classification for the northwestern part of the watershed, identified as Cambisols in the FAO map and as Luvisols in the DGADR map; this can be attributed to the different criteria for soil classification used by the FAO and DGADR schemes, leading to a non-unique relationship between designations and making correspondence tables merely indicative (Pimenta, 1998).

The physical characterization of these soils focused on the main soil parameters required by the MEFIDIS model, discussed in section 3.2.2 and shown in Table 3.1. It used the soil database published by Cardoso (1965) for the most common Portuguese soil profiles. Several of the soil types shown in Figure 4.19 were not sampled by the author and, for this case, a representative sample for a similar soil profile was used. The selected soil profile for each case is shown in Table 4.13.

The first step in this characterization involved the conversion of soil texture data from the original Atterberg texture classes into the more commonly used United States Department of Agriculture (USDA) classes, usually required as input parameters in many PTFs. This was achieved using a log-normal approach proposed by Skaggs et al. (2001). The second step involved the collection of data from Cardoso (1965), using PTFs to estimate missing values; some parameters such as soil matric potential (Ψ) or median particle diameter (d_{50}) were not present in the database and had to be estimated. The soil shear strength (σ_{oc}) was also not present in the database, but several measurements were made in the Alenquer watershed using a Torvane (see section 4.2.6 for details). Furthermore, while most parameters were taken from all soil profile layers sampled in the database, the soil's particle diameter, shear strength and clay mass fraction (S_{clay}) were taken only from the topmost layer, as these are textural

parameters directly related with soil erodibility. The parameters are shown in Table 4.14 for soils in Odeleite, and in Table 4.15 for soils in Alenquer; when multiple soil samples and/or layers were used in the estimate, the median parameter value is shown followed by the minimum and maximum values. It should be noted that measured saturated hydraulic conductivity (K_{sat}) values were halved in order to transform them into the K_{sat} parameter required by the MEFIDIS Green-Ampt infiltration equation (equation 3.3), following the recommendation made by Chow et al. (1988).

Table 4.13 – Correspondence between the 1990 FAO soil classification (Driessen et al., 2001) and the Portuguese soil classification, used by DGADR (Cardoso, 1965), for soils occurring in the Odeleite and Alenquer watersheds, according to Pimenta (1998); the DGADR soil sample data used to extract physical soil parameters for each soil patch is also shown.

	FAO order	**FAO suborder and code**	**DGADR order**	**DGADR suborder and code**	**DGADR soil sample used[a]**
Alenquer	Fluvisols	Eutric Fluvisols (Je)	Incipient Soils	Colluvial Soils (Sbc)	Alluvial Soils (A)
	Vertisols	Pellic Vertisols (Vp)	Vertisols	Black Vertisols (Bc)	Black Vertisols (Cp)
	Cambisols	Chromic Calcic Cambisols (Bkc)	Calcareous Soils	Brown Calcareous Soils, normal (Pcst)	Brown Calcareous Soils, normal (Pc)
		Vertic Calcic Cambisols (Bkv)		Brown Calcareous Soils, para-vertisols (Pcst')	Brown Calcareous Soils, para-vertisols (Pc')
		Chromic Cambisols (Bcc)		Red Calcareous Soils, normal (Vcst)	Red Calcareous Soils, normal (Vcs)
		Dystric Cambisols (Bd)	Litholic Soils	Non-Humic Litholic Soils (Vto)	Non-Humic Litholic Soils (Pt)
	Luvisols	Vertic Calcic Luvisols (Lkv)	Mediterranean Soils	Brown Mediterranean Soils (Pato)	Brown Mediterranean Soils (Pac)
		Rhodo-chromic Calcic Luvisols (Lrk)		Red/Yellow Mediterranean Soils (Vato)	Red/Yellow Mediterranean Soils (Vcc)
Odeleite	Lithosols	Eutric Lithosols (Ie)	Incipient Soils	Lithosols (Ex)	Lithosols (Ex)
	Fluvisols	Eutric Fluvisols (Je)		Alluvial Soils (A)	Alluvial Soils (A)
	Luvisols	Orthic Luvisols (Lo)	Mediterranean Soils	Brown Mediterranean Soils (Px)	Brown Mediterranean Soils (Px)

a – Samples published by Cardoso (1965).

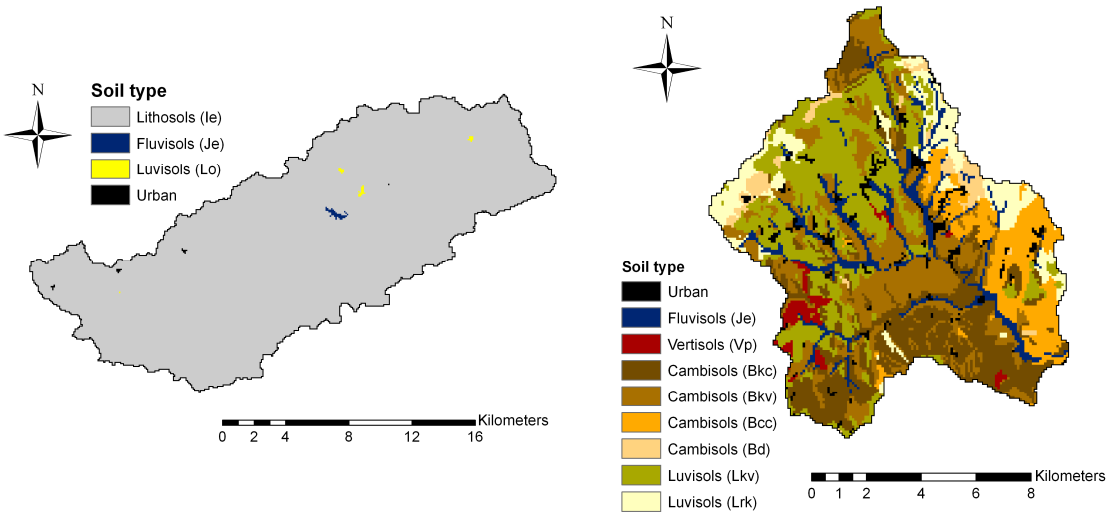

Figure 4.19 – Soil types in the Odeleite (left) and Alenquer (right) watersheds, classified according to the 1990 FAO soil classification (Driessen et al., 2001), following the 1:50,000 DGADR soil map (Gonçalves et al., 2005).

Table 4.14 – Soil hydraulic and texture parameters for the Odeleite watershed, showing median values followed by parameter range where multiple samples are present; parameters are identified in Table 3.1.

FAO code	S_{depth} **(mm)**	θ	Ψ **(mm)**	K_{sat} **(mm.h^{-1})**	d_{50} **(mm)**	σ_{oc} **(kPa)**	S_{clay}
Ie	100	0.43 (0.38 to 0.48)[a]	126 (93 to 159)[b]	27.6 (4.8 to 50.4)[c]	0.092 (0.020 to 0.163)[d]	14.03 (10.47 to 17.58)[e]	0.158 (0.061 to 0.256)
Je	1300	0.45 (0.41 to 0.48)[a]	230 (132 to 292)[b]	16.9 (8.9 to 32.7)[c]	0.027[d]	11.02 (3.89 to 18.16)	0.144
Lo	475 (350 to 600)	0.41 (0.27 to 0.54)	977 (143 to 1811)	5.5 (2.2 to 8.9)	0.040 (0.016 to 0.066)	23.82 (22.40 to 25.24)[e]	0.165 (0.163 to 0.167)

a – estimated using Botelho da Costa (1995) and Saxton et al. (1986).
b – calculated following Rawls et al. (1983).
c – estimated using Saxton et al. (1986).
d – calculated following Bittelli et al. (1999) and Skaggs et al. (2001).
e – estimated following Rachman et al. (2003).

Table 4.15 – Soil hydraulic and texture parameters for the Alenquer watershed, showing median values followed by parameter range where multiple samples are present; parameters are identified in Table 3.1.

FAO code	S_{depth} (mm)	θ	Ψ (mm)	K_{sat} (mm.h^{-1})	d_{50} (mm)	σ_{oc} (kPa)	S_{clay}
Je	1300	0.45 (0.41 to 0.48)[a]	230 (132 to 292)[b]	16.9 (8.9 to 32.7)[c]	0.027[d]	11.02 (3.89 to 18.16)	0.144
Vp	1400	0.50 (0.38 to 0.51)	772 (511 to 4020)[b]	1.8 (0.85 to 10.7)	0.002[d]	10.93[e]	0.496
Bkc	800 (600 to 1000)	0.40 (0.34 to 0.47)	239 (82 to 846)[b]	8.9 (4.2 to 14.8)	0.028 (0.007 to 0.049)[d]	21.80 (9.86 to 33.75)	0.210 (0.171 to 0.248)
Bkv	525 (500 to 550)	0.57 (0.48 to 0.65)	186 (107 to 463)[b]	16.7 (1.1 to 89.2)	0.010 (0.003 to 0.016)[d]	8.58 (1.86 to 22.05)	0.334 (0.262 to 0.406)
Bcc	1100	0.28 (0.26 to 0.28)	228 (201 to 258)[b]	12.4 (11.9 to 18.6)	0.038[d]	14.7 (8.96 to 20.44)	0.106
Bd	450	0.35 (0.34 to 0.35)	82 (82 to 83)[b]	71.6 (65.2 to 78.0)	0.066[d]	21.25[e]	0.101
Lkv	1150	0.35 (0.34 to 0.39)	291 (132 to 543)[b]	14.2 (5.9 to 24.4)	0.060[d]	14.70 (8.67 to 20.73)	0.248
Lrk	500 (400 to 600)	0.47 (0.37 to 0.62)	308 (206 to 1093)[b]	44.9 (7.5 to 88.5)	0.011 (0.004 to 0.018)[d]	17.65 (12.60 to 34.30)	0.239 (0.221 to 0.257)

a – estimated using Botelho da Costa (1995) and Saxton et al. (1986).
b – calculated following Rawls et al. (1983).
c – estimated using Saxton et al. (1986).
d – calculated following Bittelli et al. (1999) and Skaggs et al. (2001).
e – estimated following Rachman et al. (2003).

The difference in soil properties between Odeleite and Alenquer mirrors the contrast found between the Guadiana and Tejo study areas, discussed above. Lithosols, which dominate the Odeleite watershed, have a much lower soil water holding capacity than those present in the Alenquer watershed. This can be calculated from the low soil depth – 100 mm on average, compared with 500 to 1500 mm in Alenquer – coupled with a similar porosity (see Table 4.14 and Table 4.15). The higher hydraulic conductivity could lead to greater infiltration rates but only when rainfall does not exceed the soil's water holding capacity. This contrast can explain the higher surface runoff generation ratio for Odeleite, as discussed in section 4.2.2. It also confirms the low soil water capacity which was already indicated by the very low rate of

decay of transmissivity in the soil profile (*m*) estimated from baseflow recession, as discussed in section 4.2.3. The agreement between soil hydraulic properties estimated from hydrological measurements and measured in the field is a good indicator of the reliability of these soil parameters, increasing the confidence in their application for the MEFIDIS model.

4.2.5 Land use and vegetation productivity

The contrasting climate, topographic and soil characteristics in the Guadiana and Tejo areas have led to significant differences in land use. The Guadiana study area presents a homogenous landscape of wheat croplands, replaced by sparse schlerophyllous oak forests (the "montado" land cover) in the southwest, where the climate is more amenable for this vegetation type, and by extensive shrublands occupying abandoned agricultural fields in the southern mountain range and some of the areas with greatest slopes. In contrast, the Tejo area is characterized by a heterogeneous agricultural landscape, mixing annual crops (mostly wheat), vineyards and olive groves, with commercial pine and eucalyptus forests in the highlands; the proximity of the southwestern part of the study area to Lisbon has led to extensive urbanization.

The application of the MEFIDIS and SWAT models require the mapping and parameterization of land cover and land use. Land use for SWAT was based on the CORINE landcover maps for the Guadiana and Tejo study areas, parameterized through an extensive literature survey. More detailed maps were built using remote sensing techniques for Odeleite and Alenquer, to be inputted in the MEFIDIS model.

Land use characterization for the Guadiana and Tejo

Land cover in the Guadiana and Tejo study areas was mapped using the 1990 CORINE Land Cover (CLC) dataset (EEA, 1995), with a scale of 1:100,000. The survey for Portugal was carried out between 1985 and 1987, coinciding with the period for which climate and hydrological data was collected (as discussed above). The CLC legend was condensed and reclassified, both to correlate the map with the vegetation cover types present in the SWAT database (see Neitsch et al., 2002), and to limit model parameterization to the most important vegetation types. For artificial surfaces, CLC class 11 (urban fabric) was classified as generic urban while the remaining classes were classified as industrial. The reclassification criteria for vegetated land covers are shown in Table 4.16; note that some Mediterranean agricultural and natural vegetation cover types were not present in the SWAT database and had to be created and parameterized.

Table 4.16 – Correspondence table between CLC classes and the land cover classes used by the SWAT model, for vegetated land covers.

CORINE Land Cover	Code	Identification	SWAT land cover
Agricultural areas	211	Non-irrigated arable land	Winter wheat croplands
	212	Permanently irrigated land	Corn croplands
	213	Rice fields	Rice croplands
	221	Vineyards	Vineyards[a]
	222	Fruit trees and berry plantations	Apple orchards
	223	Olive groves	Olive groves[a]
	231	Pastures	Bermudagrass pastures
	241 to 243	Heterogeneous agricultural areas	Winter wheat croplands
	244	Agro-forestry areas	Schlerophyllous oak forest[a]
Forest and semi-natural areas	3111 to 3113	Broad-leaved forest, cork and holm oak forest	Schlerophyllous oak forest[a]
	3114 and 3115	Chesnut and oak forest	Oak forest
	3116	Eucalyptus forest	Eucalyptus forest[a]
	312 and 313	Coniferous and mixed forest	Pine forest
	321	Natural grasslands	Little bluestem grasslands
	322 and 323	Moors and heathland and sclerophyllous vegetation	Mediterranean shrublands[a]
	324	Transitional woodland-shrub	Pine forest[b]
	331 to 333	Open spaces with little or no vegetation	Little bluestem steppelands
	334	Burnt areas	Pine forest[b]
	4	Wetlands	Alamo switchgrass wetlands

a – land cover type not present in the SWAT database.
b – SWAT land cover type modified to take into account a reduction in vegetation cover density.

The reclassified land cover map is shown in Figure 4.20. As stated above, the Guadiana is mostly occupied by wheat fields (48 %) in the northern half, while most of the southern half is either occupied by cork oak "montado" (32 %) or Mediterranean shrublands (18 %), with other land covers occupying only 2 %. In contrast, the Tejo region presents a heterogeneous land cover composed by 34 % wheat croplands, 22 % vineyards, 21 % forests, 10 % shrublands, 6 % urban areas and 4 % olive groves, with the remaining 3 % divided between other land uses.

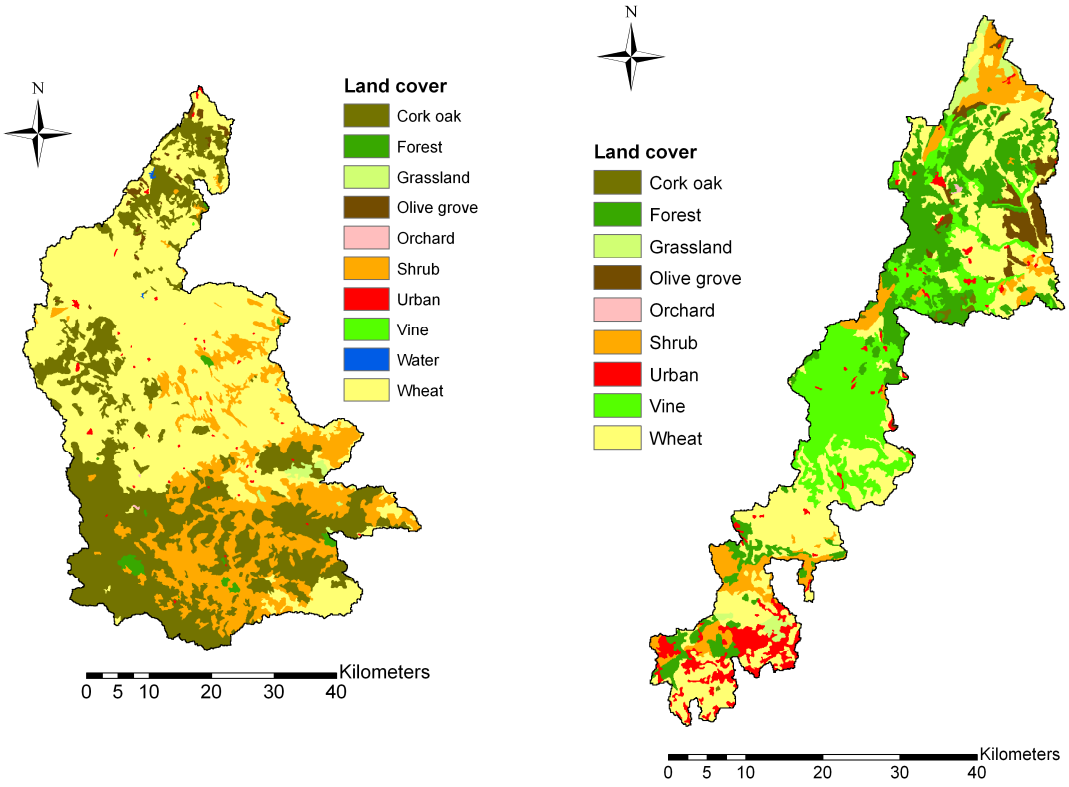

Figure 4.20 – Land cover in the Guadiana (left) and Tejo (right) study areas, from the 1:100,000 1990 CORINE Land Cover map (EEA, 1995).

The biophysical parameterization of the land uses shown in Table 4.16 focused on the main vegetation parameters required by the SWAT model, described by Neitsch et al. (2002) and discussed in section 3.4. Most vegetation types were parameterized according to the model's database (also described by the author), with the exceptions shown in Table 4.17. The biophysical parameters for these landcover types were taken from a literature survey, including:

- radiation-use efficiency and phenology (Table 4.18);
- physical characteristics, response to temperature and nutrient contents of biomass (Table 4.19);
- response to changes in atmospheric vapor pressure deficit and CO_2 concentration (Table 4.20);
- other parameters related with harvesting, soil protection and runoff generation (Table 4.21).

Table 4.22 lists the references used in the parameterization of these characteristics for each vegetation type. Agricultural landcovers were further parameterized in terms of management practices, such as planting and harvesting dates or fertilizer application, following recommended practices for Portugal (INIA-LQARS, 2000).

Table 4.17 – Land cover types not present in the SWAT database, and the vegetation species used to parameterize the land cover type.

Land cover type	**Major vegetation species**
Vineyards	Vine (*Vitis vinifera*)
Olive groves	Olive tree (*Olea europaea*)
Schlerophyllous oak forest	Holm oak (*Quercus ilex rotundifolia*) Cork oak (*Quercus suber*)
Eucalyptus forest	Eucalyptus (*Eucalyptus globulus*)
Mediterranean shrublands	Rock-rose (*Cistus ladanifer*) Heath (*Erica sp.*)

Table 4.18 – Radiation-use efficiency and phenology parameters for Mediterranean vegetation; references are shown in Table 4.22.

Parameter		**Vineyard**	**Olive Grove**	**Schlerophyllous oak forest**	**Eucalyptus forest**	**Mediterranean shrubland**
Radiation-use efficiency ($kg.ha^{-1}$)/($MJ.m^{-2}$)		15	15	15	22	15
Maximum potential Leaf Area Index (LAI) ($m.m^{-1}$)		3	4	2	5	2.5
1st point in the optimal LAI curve	Fraction of growing season	0.05	0.05	0.05	0.15	0.05
	LAI fraction	0.05	0.75	0.75	0.8	0.75
2nd point in the optimal LAI curve	Fraction of growing season	0.55	0.27	0.2	0.25	0.2
	LAI fraction	0.8	0.95	0.95	0.99	0.99
LAI decline: fraction of growing season		0.8	0.99	0.99	0.99	0.4

Table 4.19 – Parameters for Mediterranean vegetation physical characteristics, response to temperature and biomass nutrient content; references are shown in Table 4.22.

Parameter		Vineyard	Olive Grove	Schlerophyllous oak forest	Eucalyptus forest	Mediterranean shrubland
Max. canopy height (m)		1.75	6	6	25	2
Max. root depth (m)		2	9	9	12	2
Optimal temperature for plant growth (ºC)		20	30	30	22	22.5
Minimum temperature for plant growth (ºC)		10	9	9	8	15
Nitrogen fraction (kg N.kg biomass^{-1})	Emergence	0.041	0.006	0.006	0.006	0.006
	50 % maturity	0.026	0.002	0.002	0.002	0.002
	Maturity	0.011	0.0015	0.0015	0.0015	0.0015
	Harvested yield	0.03	0.0015	0.0015	0.0015	0.0015
Phosphorus fraction (kg P.kg biomass^{-1})	Emergence	0.0055	0.0007	0.0007	0.0007	0.0007
	50 % maturity	0.0041	0.0004	0.0004	0.0004	0.0004
	Maturity	0.0013	0.0003	0.0003	0.0003	0.0003
	Harvested yield	0.004	0.0003	0.0003	0.0003	0.0003

Table 4.20 – Parameters for Mediterranean vegetation response to vapor pressure deficit and atmospheric CO_2 concentration; references are shown in Table 4.22.

Parameter		Vineyard	Olive Grove	Schlerophyllous oak forest	Eucalyptus forest	Mediterranean shrubland
Max. stomatal conductance in optimal conditions (m.s^{-1})		0.005	0.004	0.003	0.003	0.005
2nd point in the stomatal cond. curve	Vapor pressure deficit (kPa)	4	4	4	4	4
	Fraction of max. stomatal conductance	0.4	0.5	0.3	0.2	0.25
Rate of decline in radiation use efficiency per unit increase in vapor pressure deficit (g.MJ^{-1}.kPa^{-1})		7	7	6.5	8	10
2nd point in the radiation-use eff. curve	CO_2 atm. conc. (uL CO_2 .L air^{-1})	660	560	700	660	700
	Radiation-use efficiency (kg.ha^{-1}) /(MJ.m^{-2})	18.75	19	20	24	18

Table 4.21 – Other Mediterranean vegetation parameters; references are shown in Table 4.22.

Parameter		Vineyard	Olive Grove	Schlerophyllous oak forest	Eucalyptus forest	Mediterranean shrubland
Harvest index for optimal growing conditions		0.5	0.1	0.1	0.76	0.76
Lower limit of harvest index		0.1	0.01	0.01	0.6	0.01
Annual USLE landcover factor (*C*)		0.2	0.1	0.1	0.2	0.02
Minimum USLE landcover factor (*C*)		0.1	0.04	0.04	0.1	0.004
Plant residue decomposition coefficient		0.05	0.05	0.05	0.05	0.05
Manning's *n* for overland flow		0.15	0.15	0.1	0.1	0.1
SCS runoff curve number for moisture condition II	Soil type A	43	45	57	45	35
	Soil type B	65	66	73	66	56
	Soil type C	76	77	82	77	70
	Soil type D	82	83	86	83	77

Table 4.22 – References for SWAT land cover parameters for Mediterranean vegetation.

Vegetation type	References
Vineyard	Castelan-Estrada, 2001[1, 2, 4]; Cook et al., 1983[5]; Correia et al., 1995[6]; Flanagan and Nearing, 1995[1-4, 8]; Jacobs et al., 1996[6]; Johnson, 2003[2]; Klein et al., 2000[5]; Lebon et al., 2003[2, 6]; Lu et al., 2003[6]; Moutinho-Pereira et al., 2004[6]; Nelson, 2003[2-5, 7, 8]; Salisbury and Ross, 1991[5]; Williams et al., 1985[2, 4]
Olive grove	Bussoti et al., 2003[2]; de Melo-Abreu, 2004[2, 4]; Giorio et al., 1999[6]; Hoff et al., 2002[4]; Infante et al., 1999[2]; Korner, 1994[6]; Lhomme et al., 2001[2]; Mariscal et al., 2000a[2, 3], 2000b[1]; Martínez-Vilalta et al., 2002[3]; Neitsch et al., 2002[8]; Rapp et al., 1999[5]; Tognetti et al., 1998[5], 2001[7]; Villalobos et al., 1995[2]
Schlerophyllous oak forest	Bombelli and Gratani, 2003[6]; Bussoti et al., 2003[2]; David et al., 2004[2, 3, 6]; García-Mozo et al., 2002[2, 4]; Hoff et al., 2002[2, 4]; Infante et al., 1999, 2003[2, 6]; Lhomme et al., 2001[2, 3, 6]; Maroco et al., 2002[7]; Medlyn et al., 2001[6]; Neitsch et al., 2002[2, 4, 5, 8]; Peñuelas et al., 1997[1, 3]; Rapp et al., 1999[5]; Sala and Tenhunen, 1996[2, 6]; Tognetti et al., 1998[3, 5, 7]
Eucalyptus forest	Almeida et al., 2004[4]; David et al., 1997[3, 6], 2004[2, 3]; Korner, 1994[6]; Landsberg and Hingston, 1996[1-3]; Neitsch et al., 2002[2, 5, 7, 8]; Schulze et al., 1994[6]; Scurlock et al., 2001[2]; Whitehead and Beadle, 2004[1-4, 6]
Mediterranean shrubland	Bombelli and Gratani, 2003[6]; Fillela et al., 2004[1]; Hoff et al., 2002[2]; Korner, 1994[6]; Llorens i Guasch, 2003[1-4, 6]; Medlyn et al., 2001[6, 7]; Neitsch et al., 2002[5, 8]; Perez-Latorre and Cabezudo, 2002[2, 3]; Schulze et al., 1994[6]; Scurlock et al., 2001[2]; Tognetti et al., 2000[6, 7]

Parameter class:
1 – Radiation use efficiency.
2 – Phenology.
3 – Physical characteristics.
4 – Response to temperature.
5 – Nutrient content.
6 – Response to vapor pressure deficit.
7 – Response to CO_2.
8 – Others.

Finally, data on agricultural productivity in both study areas was compiled to complete the land cover and vegetation biophysical dataset. This data was collected to allow an evaluation of the vegetation productivity component of the SWAT model. The Portuguese Statistics Institute (INE) collects annual production data for the most important crops in several districts of Portugal; however, annual data does not reflect actual agricultural productivity since it does not take into account the setting-aside of fields, variation in agricultural practices, or the suspension of planting and harvesting when agricultural production is too poor. Nevertheless, this data is a good indicator of average annual productivity of crops in both study areas. The values are shown in Table 4.23, converted into dry weight (INE statistics are given in fresh weight). Many of the differences in productivity between both areas can be attributed to climatic and soil differences, as described previously; the only crop without significant differences in behavior is olives, as could be expected from the adaptation of olive trees to drier Mediterranean climates.

Table 4.23 – Average annual dry weight yield for major crops in the Guadiana and Tejo study areas, averaged from statistics between 1985 and 2000 (INE, 2006).

	Yield – dry weight ($ton.ha^{-1}.y^{-1}$)	
Crop	**Guadiana**	**Tejo**
Winter wheat[a]	1.45	1.96
Olives[b]	0.33	0.20
Grapes[c]	0.80	1.40

a – dry weight estimated following Nielsen et al. (2002).
b – dry weight estimated following Proietti and Antognozzi (1996).
c – dry weight estimated following Gardea et al. (1994).

Land use characterization for Odeleite and Alenquer

Land use in the Odeleite and Alenquer watersheds was mapped using remote sensing data through a supervised classification (Lillesand and Kiefer, 2000); the resulting maps are shown in Figure 4.21. The Odeleite dataset was a Landsat ETM+ image for February 2003, with a resolution of 25 × 25 m; images for Alenquer were acquired with a survey flight made in February 1998, using an airborne Daedalus TMS radiometer with a resolution of 3 × 3 m and 11 spectral bands. The images were selected to derive land cover prevailing in the rainy

season. A comparison between the resulting land cover maps and field areas presented an overall accuracy ratio of 0.83 for Odeleite and 0.81 for Alenquer.

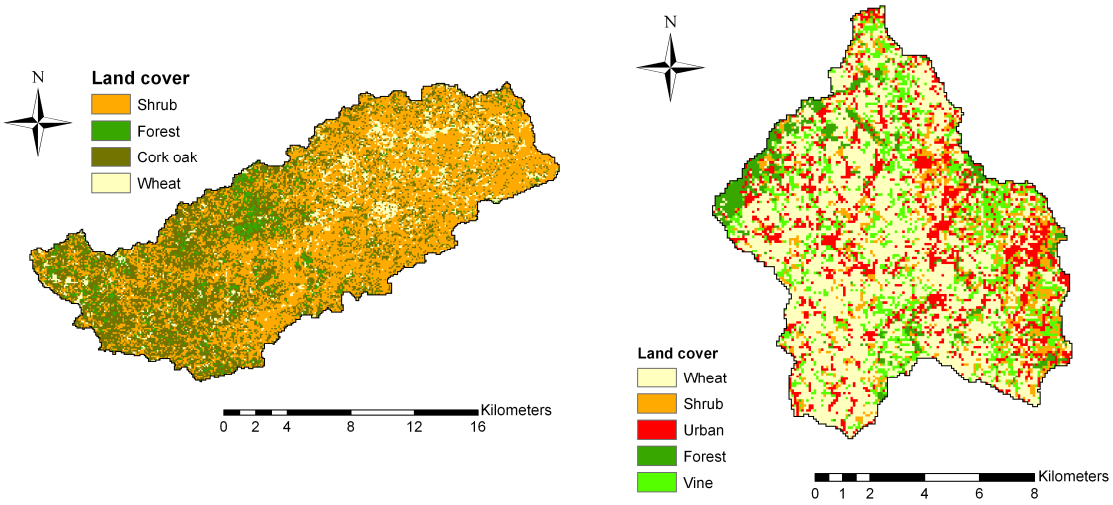

Figure 4.21– Land cover in the Odeleite (left) and Alenquer (right) watersheds, obtained using remote sensing data.

As in the case of soil type, the map for Odeleite is very similar at both scales, with Mediterranean shrublands and schlerophyllous oak forests dominating the watershed; the higher-resolution map adds the presence of wheat cultivation along the river banks. In contrast, the Alenquer map shows significantly more detail than the one used for the Tejo study area; it also shows a significant land cover difference, with many of the CLC vineyards classified as wheat croplands in this map, and a significant increase in urban areas. While local farmers refer to a trend of vineyard abandonment and increasing urbanization since the 1990s, part of this difference can be attributed to the CLC classification method, as combined vineyard and wheat croplands can be classified as the former class (dos Santos, 2003). To confirm this, the maps shown in Figure 4.20 and Figure 4.21 were compared with the Portuguese 1:25,000 land occupation map for 1990 (COS 90; IGP, 1990). The annual "croplands + vineyards" class occupies 61 % of the COS 90 map for Alenquer, indicating that the vineyards shown in Figure 4.20 represent in fact a combination of vineyards and wheat croplands; these landcovers are disaggregated in the higher resolution Daedalus-based map.

The physical characterization of these land covers focused on the parameters required by the MEFIDIS model as discussed in section 3.2.2 and shown in Table 3.1. The parameterization

was done through a literature survey of typical values; when values were not commonly available (such as interception capacity), estimations were made using surrogate parameters (in this case, using Leaf Area Index values and the Hoyningen-Huene formulation). Table 4.24 shows the model parameters for land cover classes in both watersheds. It should be noted that these parameters are expected to represent wet season conditions; since this is the growth season for winter wheat, most land cover parameters vary significantly during this period, which caused a problem in deriving a single parameter set for MEFIDIS.

Table 4.24 – Land use parameters for the Odeleite and Alenquer watersheds, showing the most common values followed by parameter range where multiple samples are present; parameters are identified in Table 3.1.

Land cover	**Manning's roughness coefficient** n	**Vegetation canopy cover** V_{cv}	**Pavement cover** P_{cv}	**Depression storage capacity** D_{max} **(mm)**	**Interception capacity** I_{max} **(mm)**
Urban	0.014 (0.01 to 0.02)[a]	0.0	1.00	1	0
Mediterranean Shrubland	0.17 (0.13 to 0.24)[a]	0.9 (0.5 to 0.95)[b]	0.00	10.0 (5.0 to 15.0)[f]	3.7 (2.6 to 4.8)[h]
Forest	0.5 (0.4 to 0.8)[a]	0.8[c]	0.00	10.0 (5.0 to 15.0)[f]	3.3 (2.5 to 4.1)[h]
Schlerophyllous oak forest	0.21 (0.15 to 0.41)[a]	0.35 (0.1 to 0.4)[d]	0.00	12.6 (1.0 to 25.8)[f]	3.0 (2.5 to 3.8)[h]
Vineyard	0.05 (0.05 to 0.06)[a]	0.5[e]	0.00	12.6 (1.0 to 25.8)[f]	3.3 (2.5 to 4.1)[h]
Winter wheat croplands	0.09 (0.06 to 0.17)[a]	0.4 (0.1 to 0.7)[c]	0.00	34.6 (10.7 to 58.5)[g]	2.9 (1.4 to 4.4)[h]

a – USDA (1986).
b – Llorens i Guasch (2003).
c – Deguchi et al. (2006).
d – David et al. (2004).
e – Johnson (2003).
f – estimated from surface roughness data reported by USDA (1986) following Kamphorst et al. (2000).
g – Beasley and Huggins (1981).
h – estimated from LAI data reported by Scurlock et al. (2001) and Johnson (2003) following Hoyningen-Huene (1983).

4.2.6 Field- and hillslope-scale hydrological and erosion processes

The hydrological and sediment yield data described in section 4.2.2 represents watershed outlet measurements. However, outlet data alone cannot be used to successfully evaluate model performance in terms of describing hydrological and erosion processes occurring

within a watershed (Jetten et al., 2003). While spatially-distributed data for both study areas is currently unviable, a number of field experiments have been conducted in the Guadiana which provide a good representation of rill/interill and gully erosion processes in the region. This information was collected and complemented with a number of field experiments on rainfall-runoff-erosion relationships in both study areas, in order to provide data for model calibration and evaluation.

Vale Formoso experimental erosion center

In the Guadiana study area, research on hillslope and field scale hydrological and erosion processes has focused on the Mértola region, particularly in the Vale Formoso experimental erosion center. The location of the station is close to the Mértola/Vale Formoso climate station shown on the right side of Figure 4.4 (coded IM/263). The center, research objectives and overall collected data has been described in several publications (e.g. Roxo, 1994; Roxo et al., 1996; Roxo and Cortesão Casimiro, 1998). The research infrastructure consists of 16 Wischmeyer plots (20 × 8.33 m) and one half-plot (20 × 4.15 m), running continuously since 1961. They are located in a hillslope with a grade of 10 to 20 %, over rhodo-chromic Calcic Luvisols with up to 50 % rock cover. The plots present several agricultural crop rotation schemes (in space): wheat and fallow, wheat and legumes (for sideration), and wheat and legumes (for sideration) followed by wheat and legumes (for grain); in 1989, a number of permanently ploughed plots were introduced, as well as a permanent pasture plot and one supporting Mediterranean shrublands. Table 4.25 shows the average annual erosion values in the plots; they can be considered relatively low, particularly when compared with the threshold of 2 to 12 ton.ha^{-1}.y^{-1}, below which normal soil regeneration is sufficient to compensate for soil losses (Romero-Díaz et al., 1999).

Table 4.25 – Average annual observations for soil erosion in the Vale Formoso center for different agricultural land use types, after 22 years of observations, following Tomás and Coutinho (1993).

Land use	**Annual soil erosion (ton.ha^{-1})**
Wheat + fallow	0.8 (0.4 to 1.3)
Wheat + legumes (sideration)	0.5 (0.3 to 0.6)
Wheat + legumes (sideration) + wheat + legumes (grain)	0.5 (0.2 to 0.8)

These low values hide the great variability in soil erosion rates between events; after analyzing the data for plots with wheat-fallow rotation, Silva et al. (1998) found that 2.3 % events (11 in 471) were responsible for 73.5 % of the soil loss. The authors conclude that the threshold for significant erosion rates (> 1 ton.ha^{-1}) consists of rainfall intensities above 20 mm.h^{-1}, falling for at least one hour; storms with these conditions have a return period of over two years. This has led to significant problems when applying the USLE to this data, particularly since the annual rainfall erosivity index appears not to adequately represent the heterogeneous nature of rainfall in this region (Coutinho and Tomás, 1995).

Furthermore, observations for the erosion plots are not necessarily representative of soil erosion rates in the region. Vandaele et al. (1997) used aerial photographs from 1970 to 1985 to estimate ephemeral gully erosion rates in the Mértola region surrounding the Vale Formoso center. The authors estimate erosion rates of 0.9 to 6.8 ton.ha^{-1}.y^{-1}; when compared with the plot values – representing estimates of rill and interill erosion rates – this implies a ratio of gully to rill/interill erosion ranging from 4.5 to 5.2. These results imply that average erosion rates in this region are closer to 4 ton.ha^{-1}.y^{-1}. These results are concurrent with other observations of soil erosion in Mediterranean regions (Boix-Fayos et al., 2006; see also section 2.2.3). Vandaele et al. (1997) also proposed a method to map probable gully location, based on the importance of flow concentration and subsurface saturation in the appearance of ephemeral gullies. These factors can be described by the streampower index (the product of accumulated drainage area and local slope gradient) and the wetness index (see equation 3.17, above). For gully formation, the authors suggest thresholds above 40 and 9.8, respectively.

Rainfall simulation campaigns

In order to complement the Vale Formoso dataset, two field rainfall simulation campaigns were conducted in the study areas to analyze rainfall-runoff-erosion relationships. These tests were selected due to the difficulty in obtaining meaningful relationships using natural rainfall experiments, due to the irregular nature of rainfall in Mediterranean regions (Cerdà, 1998). In the Guadiana area, the campaign was conducted in the Portel region, which shows similar characteristics to the Odeleite watershed; in terms of climate patterns, dominant soil type (Lithosol), and land cover ("montado" – schlerophyllous cork oak forests – and Mediterranean shrublands. The campaign for the Tejo area was conducted in 2000, inside the Alenquer watershed.

The campaigns included a number of tests using a rainfall simulator similar to the one described by Cerdà (1998). Each test was performed over a small area (a circle with c. 0.5 m

diameter); in Portel the tests used a rainfall intensity of c. 45 $mm.h^{-1}$ and lasted for 60 min, while in Alenquer, the tests were conducted for a rainfall with c. 50 $mm.h^{-1}$ intensity lasting for 45 min. For each test, runoff and soil moisture at 60 mm depth were measured each minute, the latter using a TDR probe; a number of runoff samples were also collected for later laboratory measurement of sediment transport. In Alenquer, soil shear strength in each test area was also sampled using a Torvane.

The tests in Portel were performed in three different areas over a common Ie soil: experimental pine and oak forest (5 tests), grazed "montado" (4 tests) and recently abandoned "montado" with a significant part of the undergrowth composed by Mediterranean shrubs (3 tests). The tests in Alenquer were performed in six sites with different combinations of land use and soil type; the selected land uses were cropland, vineyard and forest, over the Bkc, Bkv, Lrk and Je soil types. The runoff and erosion relationships for these experiments are shown in Figure 4.22.

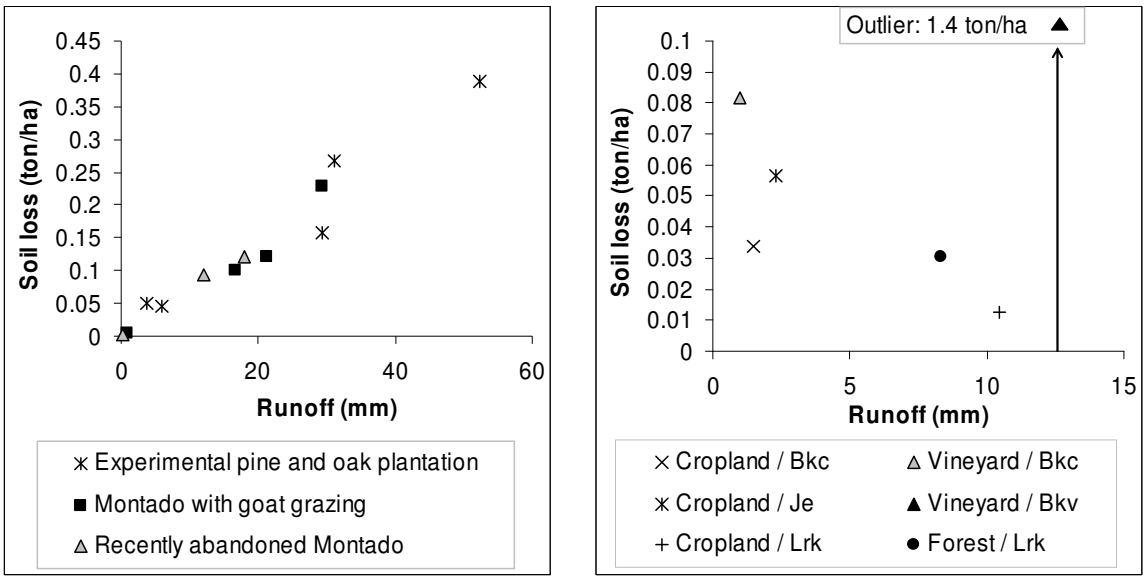

Figure 4.22 – Runoff and erosion results from the rainfall simulation experiments performed in Portel (left) and Alenquer (right).

In Portel, the results allow model parameterization of multiple land covers for a single soil type; they also show that the soil loss per runoff is similar for all land covers, but that the forest sites tend to produce more runoff than the abandoned "montado" / shrubland fields, with the grazed "montado" producing intermediate results. In Alenquer, the results do not

allow the drawing of meaningful conclusions, except perhaps the indication of significantly greater soil loss per runoff in Bkc and Bkv soils when compared with Lrk soils; however, these results are useful to test the robustness of model parameterization for single soils with two land covers, as well as for single land covers with two soils. Model parameterization focused on the differences in land covers and soil types more likely to cause these differences; this issue is further discussed in section 4.4.

4.3 SWAT application and evaluation

The datasets used to parameterize the SWAT model for the Guadiana and Tejo were described in the previous sections. This includes meteorological data (section 4.2.1), topography (section 4.2.3), soil data (section 4.2.4) and land use data (section 4.2.5). The topographic data (Figure 4.14) was used to delineate watersheds and extract channel network characteristics for both study areas. In global terms, watersheds and sub-basins were delineated using a flow direction map, calculated from the DEM following the steepest slope towards each cell's 8 neighbors (commonly called the d8 method; Xu and Lathrop, 1995). In both systems, a 5 Km^2 threshold was considered for sub-basin delineation. This resulted in 248 sub-basins for the Guadiana, with an average area of 11.2 Km^2; and 144 sub-basins for the Tejo, with an average area of 8.7 Km^2. The sub-basin structure formed the basis for spatial discretization in the SWAT model application (see section 3.4 for details).

These sub-basins were combined with the soil maps (Figure 4.18) and land use maps (Figure 4.20) to divide the study areas into Hydrological Response Units (HRUs), consisting on unique combinations of land cover and soil type within a sub-basin, where hydrological response is assumed to be homogenous (see section 3.4 for a further discussion of the role of HRUs in the SWAT modeling structure). The Guadiana area was subdivided into 735 HRUs, each with an average area of 3.8 Km^2. In contrast, the Tejo study area was subdivided into 874 HRUs, each with an average area of 1.4 Km^2, owing to the greater heterogeneity of soils and land covers found in this area. Table 4.26 compares the SWAT application with the work done by Booij (2003), in terms of appropriate scales for parameter representation and model application in regional hydrological modeling; the author estimated the appropriate scale of input parameters weighted against their importance in terms of output. The data used in this study is either close to or below the appropriate scales; this could indicate an excess of spatial detail, but also shows that the resolution of both the model spatial structure and the datasets used for parameterization is sufficient to support the model application.

Table 4.26 – Comparison between the scales used in the SWAT model application for different parameters with the appropriate scales determined by Booij (2003).

Parameter type	Scale used in the SWAT model application (Km)	Appropriate scale for hydrological modeling (Km)
Meteorology	10 to 20	20
Topography	0.09	0.1
Soil	1	5.3
Land cover	0.1	3.3
Modeling units[a]	1.2 to 1.9	10

a – average values; represented by HRUs in the SWAT model.

The model evaluation, consisting of a calibration step and a validation step, used the data collected in the hydrological and sediment network shown in Figure 4.9 (see section 4.2.2). This was coupled with ancillary data, particularly the data collected in the Vale Formoso center (see section 4.2.6) to evaluate model performance within watersheds. This exercise was performed to assess the model's ability to predict the response of hydrological, erosion and vegetation growth processes to changes in climate parameters, taking into consideration the goals of model application in this thesis as described in section 3.1.

4.3.1 Calibration and validation strategy

The SWAT model was calibrated and validated for the study areas for a 10 year period from October 1980 to September 1990. This period was selected to test the model under a wide range of climate conditions, including a severe drought from 1979 to 83; in this 10-year period, annual rainfall ranged from 244 to 808 mm in the driest parts of the Guadiana, and from 387 to 995 mm in the mid-Tejo watersheds (Figure 4.6). The model was forced using daily rainfall data from SNIRH (2006), with 24 stations in the Tejo and 25 in the Guadiana; and daily climate data from the IM network, with 2 stations in the Guadiana and 3 in the Tejo (Figure 4.4). Climate data from 1976 to 1980 was used to stabilize the model. Section 4.2.1 discusses this dataset in detail.

Available data for calibration and validation consisted of daily river flow and sediment yield data for 1980-90, provided by SNIRH (2006); see section 4.2.2 for more details on this dataset. A number of stations represented in Table 4.5 and Table 4.4 were excluded from this analysis for a number of motives:

- station 29M/01 – Tenência (Porto Areias) was excluded from the analysis due to only being operational during very low flow periods, as can be inferred by comparing average annual runoff values with those of neighboring stations (Table 4.4);

- station 19C/03 – Ponte Alenquer was also excluded due to existing modifications to the river immediately upstream (de Macedo, 1996) and their probable impact on hydrological characteristics, as can be inferred when comparing average values with station 19C/02 – Ponte Barnabé, located immediately upstream (Table 4.5);

- stations 21B/05 – Ponte Lido (Amadora) and 21C/02 – Ponte Resinga were also excluded due to extensive urbanization inside these watersheds (see Figure 4.20), which changed significantly during the analysis period;

- sediment samples from station 30L/04 – Atalisca were excluded from the analysis due to the dominance of small sediment measurements in the sediment rating curve;

- sediment samples from station 19D/04 – Ponte Ota were excluded due to the dominance of one single event over the entire sampling period (Table 4.5);

- sediment samples from station 19D/05 – Ponte Couraça were excluded due to the small number of data points used to build the sediment rating curve (Table 4.3).

Remaining hydrometric sampling stations after these exclusions consisted of 8 stations in the Guadiana and 12 in the Tejo (Figure 4.9), representing watersheds with drainage areas from 6 to 709 km^2 and with different combinations of land use and soil type. The evaluation also used data from 4 sediment sampling stations in each study area.

The calibration and validation process followed a differential split-sample approach using proxy basins (Beven, 2000; Xu and Singh, 2004). About half of the stations in each study area were used for validation only, aiming to have a pair of calibration and validation stations for each major type of land cover and climate, as shown in Figure 4.23. Furthermore, two 5-years sets from the calibration stations were considered, one for calibration and the other for validation: about half of the stations were calibrated for 1980-85 and validated for 1985-90, with these periods being inverted for the remaining stations. This approach aims to provide a robust set of calibrated parameters for the study area, thus enhancing model robustness and reducing the possibility of over-calibration, as shown by Refsgaard (1997); these are two essential conditions when applying a hydrological model for climate change research (Beven,

2000). Another advantage relies on the possibility of calibrating and validating the model for a wide range of conditions, since model performance usually diminishes when conditions fall outside the calibration interval (Favis-Mortlock et al., 2001).

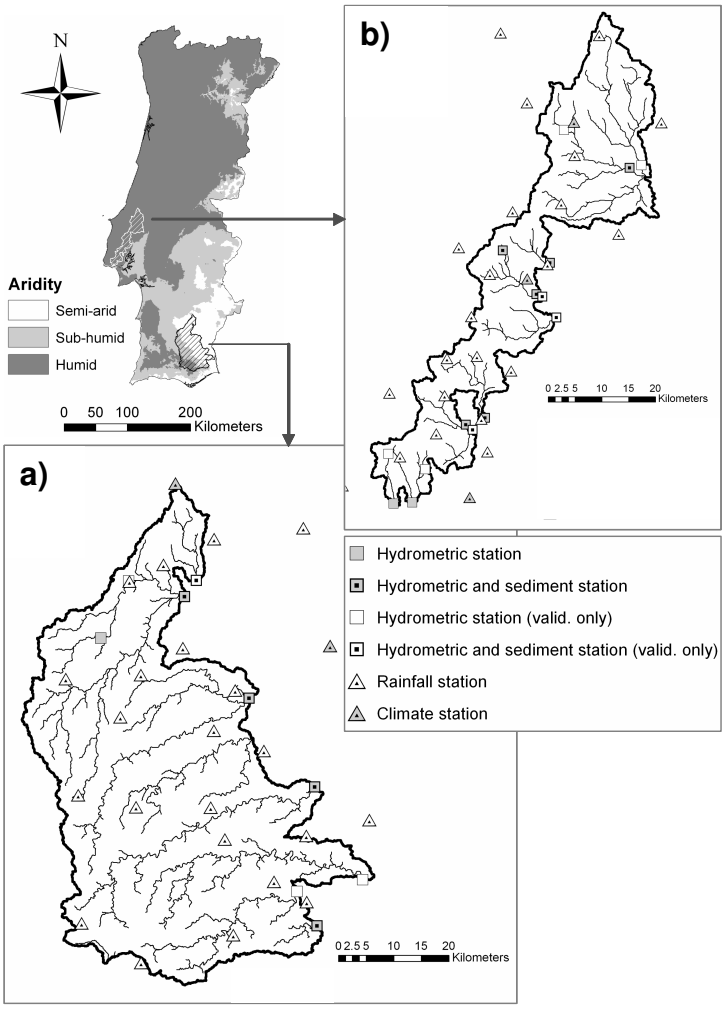

Figure 4.23 – Location of meteorological and river sampling stations in the study areas; the upper left corner shows the UNEP aridity index (UNEP, 1992) for Portugal, calculated using the data provided via SNIRH (2006), while the inserts show the sampling stations for the Guadiana (a) and Tejo (b) areas used for SWAT evaluation.

4.3.2 Model evaluation

The evaluation of the SWAT model, including calibration and validation was performed by comparing river flow and sediment yield simulations with the data described above. Four types of result were evaluated in the framework of climate change impact prediction:

- annual results, to assess the model's ability to predict long-term changes to hydrological, erosion and vegetation productivity variables;

- monthly results, to assess model performance in predicting seasonal changes to these variables;

- results for each sampling station, to assess the model performance variability between watersheds and evaluate its applicability to ungauged basins in the study areas;

- model performance using a stochastic weather generation, to assess the model's capacity in estimating sensitivity to climate change (see section 5.1 for this analysis).

Average annual results

The model performance statistics for mean annual river flows in the Guadiana and Tejo regions, presented in Table 4.27, show good results, following the thresholds of model performance set by Motovilov et al. (1999) and Morgan and Quinton (2001) of r^2 above 0.75 and model efficiency index above 0.5, respectively. It should be noticed that the bias is small when compared with the average unsigned error or the observation range, resulting in a small rate of under- or over-prediction of river flow rates. Furthermore, the differences of model performance between calibration and validation are small in terms of r^2, and in model efficiency, indicating a small level of over-calibration.

Table 4.27 – Calibration and validation statistics for mean annual river flow.

	Guadiana			**Tejo**		
Parameter	**Calibration**	**Validation**	**All Data**	**Calibration**	**Validation**	**All Data**
r^2	0.89 ($p < 0.01$)	0.91 ($p < 0.01$)	0.86 ($p < 0.01$)	0.86 ($p < 0.01$)	0.83 ($p < 0.01$)	0.83 ($p < 0.01$)
Bias ($m^3.s^{-1}$)	-0.17	0.15	0.05	0.05	-0.05	-0.01
Average unsigned error ($m^3.s^{-1}$)	0.49	0.40	0.43	0.16	0.21	0.19
Observed average and range ($m^3.s^{-1}$)	1.4 (0.1 – 7.1)	1.4 (0.05 – 6.6)	1.4 (0.05 – 7.1)	0.6 (0.03 – 2.4)	0.7 (0.004 – 3.3)	0.6 (0.004 – 3.3)
Model efficiency[a]	0.85	0.85	0.85	0.85	0.82	0.83

a – Nash-Sutcliffe model efficiency index (Beven, 2000).

Figure 4.24 compares observed with simulated values; the dispersion of observed vs. simulated values around the 1:1 agreement line in both cases shows a good performance when predicting extreme annual flows, but a less satisfactory for low flow prediction. In fact, the average unsigned error is about 30 % of the average flow for both systems; however, this error is small compared with the range of observed inter-annual variability (Table 4.27). The model also performs well in terms of baseflow separation; the simulated baseflow fraction is 0.31 in the Guadiana and 0.60 in the Tejo, which compares well with the measured values of 0.28 and 0.64 respectively, showing that SWAT is capable of distinguish the different river flow regimes operating in both systems.

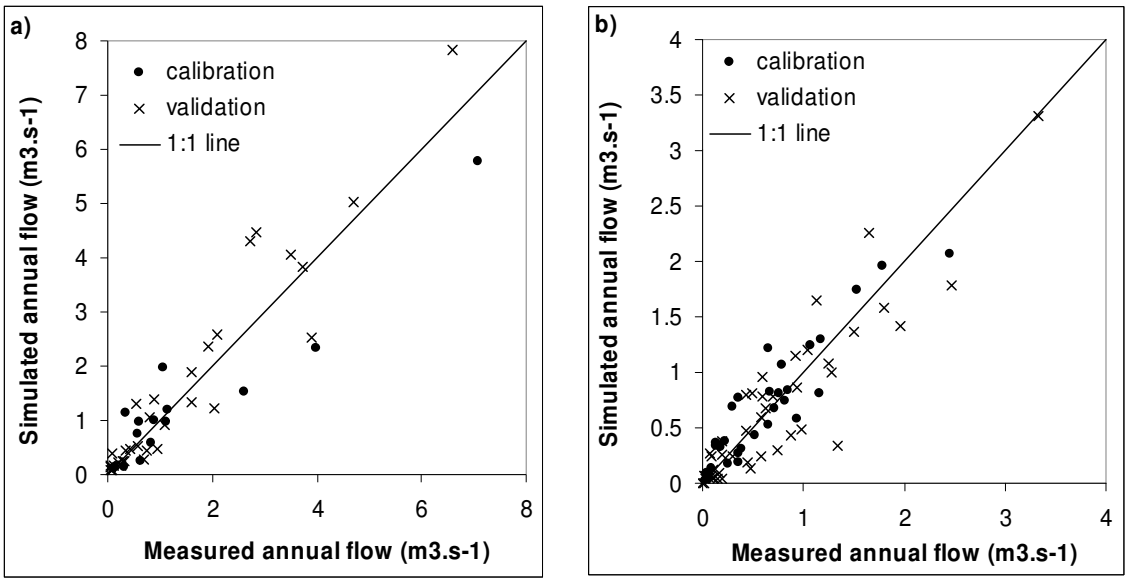

Figure 4.24 – Observed and simulated average annual river flow in the Guadiana (a; r^2 = 0.86, $p < 0.01$) and Tejo (b; $r^2 = 0.83$, $p < 0.01$) catchments.

Model performance statistics for annual watershed sediment yield, shown in Table 4.28, indicate the results can generally be considered good for both systems, taking into account the high significance for the correlations. However, the model underestimates sediment yield in the Guadiana, although this is not significant when compared with the average unsigned error. The decrease of model performance between river flow and sediment yield, as seen in the model efficiency index, is consistent with results presented in other erosion models, partly because of the dependence of soil erosion simulation on model performance for surface runoff; for an example, see the erosion model comparison results by Jetten et al. (1999 and

2003). This decrease in model performance is also reflected in the higher average unsigned error in the Guadiana, 45 % of the average annual sediment yield, although it is still satisfactory when considering the very large range of observations in the systems.

Table 4.28 – Calibration and validation statistics for mean annual sediment yield.

	Guadiana			**Tejo**		
Parameter	**Calibration**	**Validation**	**All Data**	**Calibration**	**Validation**	**All Data**
r^2	0.91 ($p < 0.01$)	0.96 ($p < 0.01$)	0.93 ($p < 0.01$)	0.82 ($p < 0.01$)	0.73 ($p < 0.01$)	0.76 ($p < 0.01$)
Bias (10^3 ton)	-2.8	-6.1	-4.3	0.2	-0.2	0.2
Average unsigned error (10^3 ton)	5.1	8.3	6.6	0.6	1.0	0.6
Observed average and range (10^3 ton)	11.6 (0.02 – 70.5)	18.1 (0.09 – 114.9)	14.6 (0.02 – 114.9)	1.9 (0.2 – 7.8)	2.8 (0.03 – 8.0)	2.3 (0.03 – 8.0)
Model efficiency[a]	0.81	0.71	0.74	0.79	0.71	0.84

a – Nash-Sutcliffe model efficiency index (Beven, 2000).

Figure 4.25 compares observed with simulated values; the underestimation of sediment yield in the Guadiana is discernible from the figure. This underestimation appears to be particularly severe for high levels of sediment yield, which could indicate that only relative model results could be valid at this scale. However, this observation is based on only two measured values, which could also be considered as outliers or as part of a set of evenly dispersed values around the mean, as a comparison with the results for Ribatejo shows. It is therefore not possible to conclude from this data that the SWAT model has a systematic error in the Alentejo; nevertheless, the model results for high sediment yield rates should be taken with care due to the lack of available data to evaluate their accuracy. The figure also shows that the dispersion of model results increases slightly with the amount of exported sediment, resulting in a decrease of percentual errors. A wide range of unsigned errors should always be expected from erosion models, especially for small sediment yield rates, due to the quality of net erosion estimates and to the existence of surface condition factors which greatly affect soil erosion but are difficult to estimate with precision using currently available methods (Nearing et al., 1999). In conclusion, the results presented in Table 4.27 and Table 4.28 show that the model performs satisfactorily when compared with the validation datasets, so it can be said to adequately represent the variability found in annual river flows and sediment yield for these systems.

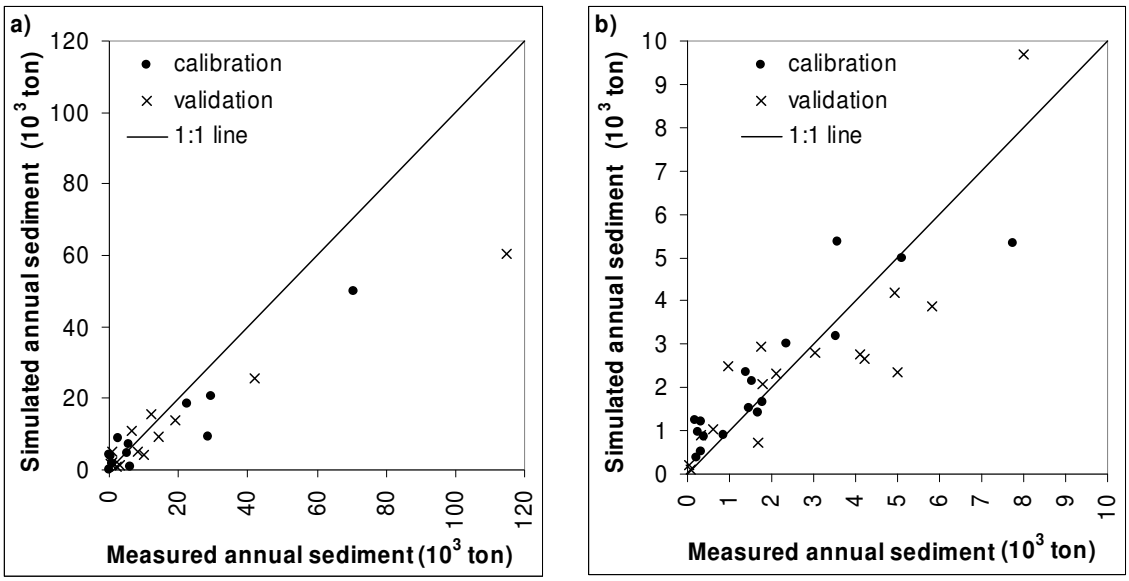

Figure 4.25 – Observed and simulated annual sediment yield in the Guadiana (a; r^2 = 0.93, $p < 0.01$) and Tejo (b; $r^2 = 0.76$, $p < 0.01$) catchments.

The model evaluation was completed with an assessment of vegetation productivity and upslope soil erosion. The data for vegetation productivity was provided by INE (2006; see section 4.2.6). A comparison with model simulation results is shown in Table 4.29. Generally, simulated yields for the most important crops compared well with observations for both regions, although the productivity of grapes can be considered overestimated. It should be noted that the simulated wheat productivity follows the climate constraints in the two study areas, which indicates that the model can assess relative vegetation productivity responses to changes in climate conditions (Favis-Mortlock et al., 2001; Morgan and Quinton, 2001).

Table 4.29 – Observed (INE, 2006) and predicted results for average annual yields for the major crops in the two study areas.

	Guadiana		**Tejo**	
Agricultural yield	**Wheat**	**Olives**	**Wheat**	**Grapes**
Estimated ($ton.ha^{-1}.y^{-1}$)	1.56	0.25	2.06	1.98
Observed ($ton.ha^{-1}.y^{-1}$)	1.39	0.33	1.96	1.39

Average annual upslope erosion rates under different land covers were compared with erosion plot measurements for different Mediterranean regions, including the Guadiana basin,

compiled by Poesen and Hooke (1997) and Wainwright and Thornes (2004). Comparisons were made only for landcovers representing more than 10 % of each study area, in order to insure a distribution over different rainfall rates, soil types and slope gradients. The results are shown in Table 4.30; average simulated values fall into the range of observations in most cases, and the average values for the Guadiana are similar to observed averages in terms of order of magnitude. SWAT also performs well when considering plot values taken in the Guadiana, described in section 4.2.6; model results for HRUs matching the characteristics of the plots – wheat cultivation over rhodo-chromic luvisols – have a good match with observed values: 0.64 vs. 0.79 ton.ha^{-1}.y^{-1}, respectively.

Table 4.30 – Observed and simulated results for average annual erosion rates for the most important land cover types in the two study areas; observed average and range are taken from standard plot measurements in several northern Mediterranean regions from the review published by Poesen and Hooke (1997) and Wainwright and Thornes (2004).

Land cover	**Observed erosion (ton.ha^{-1}.y^{-1})**	**Simulated erosion (ton.ha^{-1}.y^{-1})**	
		Guadiana	**Tejo**
Wheat cultivation	3.6 (0.2 to 19.8)	2.0 (0.1 to 7.5)	7.7 (0.4 to 15.7)
Vineyards	13.5 (0.3 to 70.2)	-	17.2 (0.7 to 35.1)
Forests	1.1 (0.2 to 2.0)	-	5.0 (0.7 to 15.3)
Cork oak forests[a]	1.5 (0.2 to 6.6)	1.2 (0.01 to 13.3)	-
Shrublands	0.5 (0.005 to 2.2)	1.0 (0.01 to 9.3)	-

a – Measured values for natural vegetation, representing the typical soil cover in sparse woodlands.

Values for the Tejo are generally higher than observed averages, particularly for forests; this difference could represent the influence of the rugged topography of this study area on soil erosion, especially when considering that forests tend to occupy the largest slope gradients. While this comparison is insufficient to estimate the difference between simulated and observed erosion rates, SWAT appears to match observations in terms of order of magnitude, and be able to represent the higher rates usually found in agricultural fields, particularly in vineyards, when compared with natural regions.

Overall, the SWAT model performance can be considered satisfactory for every tested parameter. It is capable of simulating the response of river flow and sediment yield to changes in climate and physical conditions throughout the two study areas and, while existing data on vegetation productivity and upslope soil erosion does not permit a full assessment of model results, it is sufficient to indicate that the model results agree with observations in terms of the order of magnitude, and that vegetation productivity simulation responds to changes in climate conditions. It should be noted, however, that gully erosion processes – which can represent a significant part of soil erosion in Mediterranean regions (Vandaele et al., 1997) – are not explicitly simulated by the SWAT model, and were therefore not included in the evaluation procedure. Therefore, the SWAT model can be expected to underestimate soil erosion at scales above the erosion plot and small agricultural field; this factor should be taken into account when analyzing model results.

Monthly results

The model performance statistics for monthly river flows in the Guadiana and Tejo regions, presented in Table 4.31, also show good results following the thresholds of model performance described above. The model overestimates flow in both cases, but this bias is small when compared with the average unsigned error.

Table 4.31 – Calibration and validation statistics for mean monthly river flow.

	Guadiana			**Tejo**		
Parameter	**Calibration**	**Validation**	**All Data**	**Calibration**	**Validation**	**All Data**
r^2	0.74 ($p < 0.01$)	0.77 ($p < 0.01$)	0.76 ($p < 0.01$)	0.82 ($p < 0.01$)	0.81 ($p < 0.01$)	0.81 ($p < 0.01$)
Bias ($m^3.s^{-1}$)	-0.01	0.22	0.13	0.05	0.14	0.11
Average unsigned error ($m^3.s^{-1}$)	0.78	0.84	0.82	0.27	0.50	0.41
Observed average and range ($m^3.s^{-1}$)	1.3 (0 – 44.6)	1.5 (0 – 60.4)	1.4 (0 – 60.4)	0.6 (0 – 9.4)	0.9 (0 – 19.4)	0.8 (0 – 19.4)
Model efficiency[a]	0.74	0.77	0.76	0.79	0.62	0.66

a – Nash-Sutcliffe model efficiency index (Beven, 2000).

Figure 4.26 compares observed with simulated values, normalized through the square root due to the large range between the averaged and maximum observations (see Table 4.31; Jetten et

al., 2003). The dispersion of observed vs. simulated values around the 1:1 agreement line in both cases shows a good performance when predicting extreme monthly flows, but is less satisfactory for low flow prediction. In fact, the average unsigned error is 58.6 % of the average flow for Guadiana and 51.2 % for Tejo. However, this error is small compared with the range of observed values in both systems (Table 4.31), and since the wet season months dominate surface water balance in Mediterranean watersheds (Palutikof et al., 1996), the fact that SWAT is capable of predicting extreme flows adds further confidence to model results.

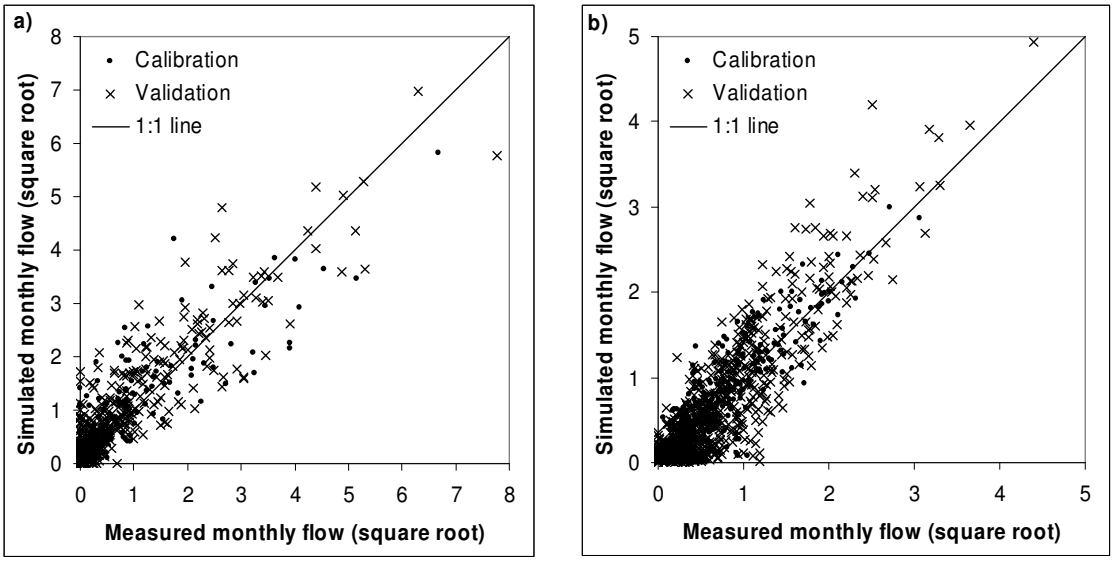

Figure 4.26 – Observed and simulated average monthly river flow in the Guadiana (a; $r^2 = 0.76$, $p < 0.01$) and Tejo (b; $r^2 = 0.81$, $p < 0.01$) catchments (square root of values).

Furthermore, the differences of model performance between calibration and validation are small in terms of r^2, and in model efficiency, particularly in the case of Guadiana, indicating a small level of over-calibration. The differences of model efficiency for Tejo could indicate some degree of over-calibration, perhaps due to the larger range of observed values present for validation. However, the model efficiency still indicates good model performance.

Model performance statistics for monthly sediment export rates, shown in Table 4.32, indicate the results can generally be considered good for the Guadiana and satisfactory for Tejo (r^2 above 0.36; Motovilov et al., 1999). This conclusion is supported by the high significance for the correlations. In this case, the model underestimates soil erosion, although this is not significant when compared with the average unsigned error. The decrease of model

performance between river flow and sediment export is consistent with results presented in other erosion models (as described above). As for average annual values, the decrease in model performance also leads to an increase in higher average unsigned error, 66 % of the average monthly soil erosion for Guadiana and 69 % for Tejo, values which can still be considered satisfactory due to the very large range of observations.

Table 4.32 – Calibration and validation statistics for monthly sediment yield.

	Guadiana			**Tejo**		
Parameter	**Calibration**	**Validation**	**All Data**	**Calibration**	**Validation**	**All Data**
r^2	0.80 ($p < 0.01$)	0.78 ($p < 0.01$)	0.78 ($p < 0.01$)	0.67 ($p < 0.01$)	0.51 ($p < 0.01$)	0.58 ($p < 0.01$)
Bias (10^3 ton)	-0.3	-0.4	-0.3	0.01	-0.02	-0.001
Average unsigned error (10^3 ton)	0.8	0.9	0.8	0.1	0.1	0.1
Observed average and range (10^3 ton)	1.2 (0 – 40.0)	1.3 (0 – 72.3)	1.2 (0 – 72.3)	0.2 (0 – 5.6)	0.2 (0 – 3.7)	0.2 (0 – 5.6)
Model efficiency[a]	0.71	0.51	0.64	0.66	0.42	0.54

a – Nash-Sutcliffe model efficiency index (Beven, 2000).

Figure 4.27 compares observed with simulated values, again normalized using the square root. It shows that the dispersion of model results is similar for small and extreme erosion events, leading to smaller percentual errors in the latter case. This factor, considering the importance of these events for overall soil erosion budgets (see section 2.2.3), increases the confidence in model results.

The poorer results (Table 4.32) for model performance for validation could indicate some level of over-calibration; for the Tejo area, model efficiency falls below the 0.5 threshold for good model performance. This highlights the difficulty in obtaining robust calibrated parameter sets when using a small number of samples for calibration (Favis-Mortlock et al., 2001). It should be noticed that the number of available stations used for sediment export was significantly smaller than that used for river flow. Nevertheless, the model still performs satisfactorily for the validation datasets, so the model adequately represents sediment export for these systems.

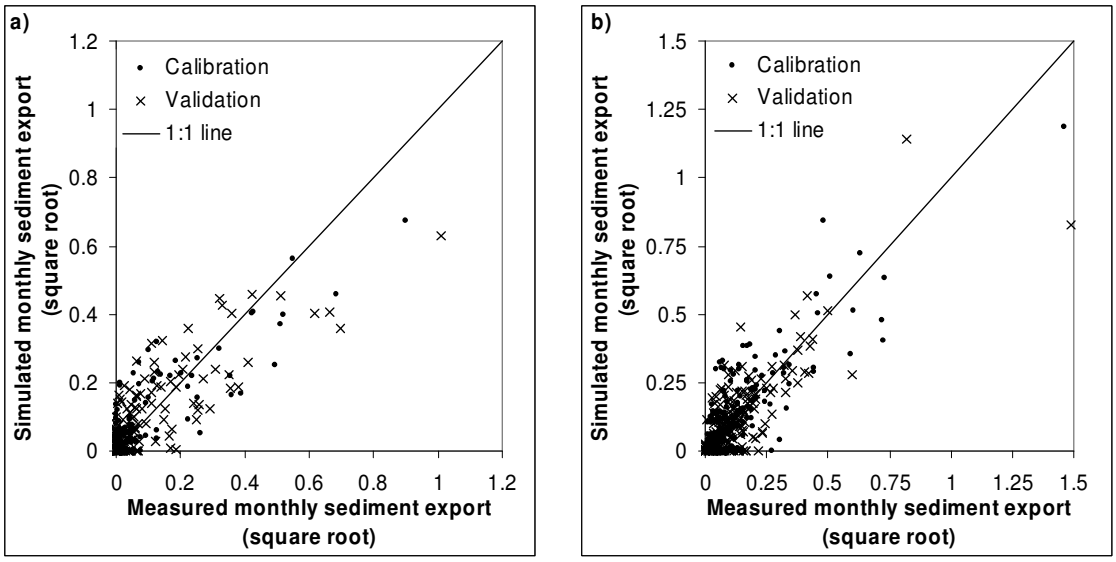

Figure 4.27 – Observed and simulated monthly sediment yield per unit area in the Guadiana (a; $r^2 = 0.78$, $p < 0.01$) and Tejo (b; $r^2 = 0.58$, $p < 0.01$) catchments (square root of values).

Overall, the model performance for monthly results is worse than for annual results, particularly for sediment yield estimates and in the Tejo study area; Jetten et al. (1999) report that this decrease in performance is common in most continuous soil erosion models. However, the results can still be considered good for all tested parameters except for sediment yield in the Tejo, where they can only be considered satisfactory. This indicates that the model is capable of simulating the response of river flow and sediment yield to seasonal changes in climate, including years with different rainfall and temperature conditions.

Performance for individual sampling stations

The model performance statistics broken down by sampling station are shown in Table 4.33 for the Guadiana study area, and in Table 4.34 for the Tejo study area. Overall, the correlation coefficient and model efficiency values range around those calculated for all values within the study area (shown in Table 4.31 and Table 4.32); however, there is a significant dispersion, with the model showing a significant decrease in performance for some stations. In particular, the overall low model efficiency index for sediment yield prediction in the Tejo study area appears to be linked to poor performance in two stations, 18E/01 – Ponte Freiria and 19C/02 – Ponte Barnabé; in the latter case, model efficiency is only 0.07, which is close to the threshold below which models should not be applied (Beven, 2000).

Table 4.33 – Model performance statistics for monthly river flow and sediment export, for selected sampling stations in the Guadiana study area.

			Mean monthly river flow		Mean monthly sediment yield	
	Calibration period	**Validation period**	**r^2**	**Model efficiency[a]**	**r^2**	**Model efficiency[a]**
26K/01 – Monte da Arregota	–	80/81 to 89/90	0.58	0.56	0.45	0.39
27I/01 – Entradas	85/86 to 89/90	80/81 to 84/85	0.48	0.43	–	–
27J/01 – Monte da Ponte	80/81 to 84/85	85/86 to 89/90	0.71	0.67	0.79	0.59
28K/02 – Oeiras	85/86 to 89/90	80/81 to 84/85	0.78	0.76	0.90	0.78
28L/02 – Vascão	80/81 to 84/85	85/86 to 89/90	0.85	0.78	0.57	0.28
29L/01 – Monte dos Fortes	–	80/81 to 89/90	0.91	0.86	–	–
30L/04 – Atalisca	85/86 to 89/90	80/81 to 84/85	0.85	0.84	–	–
26J/01 – Albernoa	–	80/81 to 89/90	0.63	0.58	–	–

a – Nash-Sutcliffe model efficiency index (Beven, 2000).

Table 4.34 – Model performance statistics for monthly river flow and sediment export, for selected sampling stations in the Tejo study area.

			Mean monthly river flow		Mean monthly sediment yield	
	Calibration period	**Validation period**	**r^2**	**Model efficiency[a]**	**r^2**	**Model efficiency[a]**
17D/01 – Rio Maior	–	80/81 to 89/90	0.67	0.30	–	–
18E/01 – Ponte Freiria	80/81 to 84/85	85/86 to 89/90	0.90	0.89	0.59	0.15
18E/06 – Ponte Barbancho	–	80/81 to 89/90	0.87	0.29	–	–
19C/01 – Penedos de Alenquer	85/86 to 89/90	80/81 to 84/85	0.72	0.68	0.62	0.61
19C/02 – Ponte Barnabé	80/81 to 84/85	85/86 to 89/90	0.85	0.78	0.53	0.07
19D/04 – Ponte Ota	85/86 to 89/90	80/81 to 84/85	0.74	0.36	–	–
19D/05 – Ponte Couraça	–	80/81 to 89/90	0.88	0.68	–	–
20C/01 – Ponte Canas	80/81 to 84/85	85/86 to 89/90	0.80	0.78	0.82	0.67
21B/01 – Mercês	–	80/81 to 89/90	0.55	0.21	–	–
21B/02 – Estação Agronómica Nacional	85/86 to 89/90	80/81 to 84/85	0.86	0.77	–	–
21B/03 – Laveiras	85/86 to 89/90	80/81 to 84/85	0.94	0.91	–	–
21C/01 – Ponte Pinhal	85/86 to 89/90	80/81 to 84/85	0.81	0.80	0.65	0.77

a – Nash-Sutcliffe model efficiency index (Beven, 2000).

On the other hand, correlation coefficients for all stations indicate good or satisfactory model performance following the criteria set by Motovilov et al. (1999), even where model efficiency is below 0.5. This indicates that the SWAT model is able to provide satisfactory results, in relative terms, for both river flow and sediment yield in ungauged basins. Absolute results for ungauged basins, however, present a high level of uncertainty, particularly in the Tejo study area.

Weather generator performance

The performance of the SWAT model using a stochastic weather generator was also assessed, aiming to assess its use in the climate scenario simulations. Long-term statistics for rainfall and climate were taken from the sources referred above, for the 1961 – 1990 period. The model was then ran for 1961 to 1990 using the weather generator for current conditions, and the average monthly results were compared with measured monthly results for the same period. Due to the long time-frame involved, only 5 hydrometric stations in Guadiana and 8 in Tejo had sufficient data for analysis; from these, 2 in the Guadiana and 4 in the Tejo had valid sediment-discharge curves.

Model performance varies slightly when comparing with previous results, as observed in Table 4.35 when compared with Table 4.31 and Table 4.32. For river flow, correlation and model efficiency values increase for the Guadiana and decrease for the Tejo, probably due to the removal of several hydrometric stations from this comparison. However, the model can still be considered satisfactory using the criteria set by Motovilov et al. (1999). For sediment yield, model performance significantly decreases for the Guadiana, but it must be noticed that only two sediment-discharge stations were used in this assessment. However, it can still be considered as satisfactory. Finally, it should be noticed that the use of SWAT's weather-generator data results in a significantly smaller inter-annual variability of both parameters when compared with observed values, indicating that inter-annual differences will be attenuated when the SWAT model is forced with synthetic climate data.

The comparison of agricultural yields generated by the model using stochastic climate series with the observed values referred in section 4.2.6 shows that model performance for crop productivity was not significantly affected, as presented in Table 4.36. Concerning upslope erosion, simulated values compare well with observations by Tomás and Coutinho (1993): 0.49 vs. 0.79 $ton.ha^{-1}.y^{-1}$, respectively. Although model performance decreased slightly, simulations are still within the same order of magnitude of observed values.

Overall, it can be concluded that SWAT's weather generator model can be used with a reasonable degree of confidence for climate change scenario analysis.

Table 4.35 – Model performance statistics for average monthly river flow and sediment yield when using a stochastic weather generator.

	Guadiana		**Tejo**	
Parameter	**River flow**	**Sediment yield**	**River flow**	**Sediment yield**
r^2	0.89 ($p < 0.01$)	0.39 ($p < 0.05$)	0.66 ($p < 0.01$)	0.72 ($p < 0.01$)
Model efficiency[a]	0.89	0.39	0.45	0.64

a – Nash-Sutcliffe model efficiency index (Beven, 2000)

Table 4.36 – Observed and predicted results for average annual yields for the major crops in the two study areas when using a stochastic weather generator.

	Guadiana		**Tejo**	
Agricultural yield	**Wheat**	**Olives**	**Wheat**	**Grapes**
Estimated ($ton.ha^{-1}.y^{-1}$)	1.45	0.21	2.11	1.57
Observed ($ton.ha^{-1}.y^{-1}$)	1.39	0.33	1.96	1.39

Discussion and assessment

The validity of the model calibration presented in this work for scenarios of climate change is difficult to assess. An effort has been made to address this issue by calibrating and validating the SWAT model for different watersheds and time periods with significantly different climate conditions, thus providing a calibrated parameter set which is valid under a large range of annual temperatures and rainfall amounts. However, the time period of available measurements did not include the full range of temperature conditions simulated in the climate change scenarios, and therefore the validity of the calibration under these scenarios cannot be fully assessed, which constitutes a limitation of this methodology. Moreover, the effects of CO_2 concentration changes cannot be assessed with the data currently available. Finally, Raclot and Albergel (2006) have shown that erosion models which are not developed for Mediterranean conditions can fail to represent important processes, therefore leading to errors based on the model structure itself which were not corrected in this exercise.

Nevertheless, the statistical indicators of model performance show that the application of SWAT to the Guadiana and Tejo study areas is robust, meaning that model results are either good or satisfactory in a variety of different climatic conditions (Toy et al., 2002). Therefore, it can be used to assess the impacts of climate change on hydrological and soil erosion processes with a reasonable degree of confidence, particularly when considering relative results, both at the annual and seasonal scales. The model is also capable of differentiating streamflow regimes in terms of baseflow and surface flow. Furthermore, the results indicate that the model is capable of simulating the impact of different climate conditions on vegetation productivity, and therefore changes to this parameter can be assessed with a reasonable degree of confidence.

4.4 MEFIDIS application and evaluation

MEFIDIS was parameterized for the Odeleite and Alenquer watersheds using the meteorological data (section 4.2.1), topography (section 4.2.3), soil data (section 4.2.4) and land use data (section 4.2.5) described in the previous sections. Model evaluation used the hydrological and sediment data described in section 4.2.2, coupled with the rainfall experiment results described in section 4.2.6, and was performed both for the patch and watershed scale. The goal of the exercise was to assess the model's ability to predict the response of hydrological and erosion processes to changes in storm patterns and antecedent storm conditions, following the objectives of the modeling exercise in this thesis as described in section 3.1.

4.4.1 Calibration and validation strategy

As referred previously (section 2.3.2), model calibration and validation should focus on the greatest possible number of variables, in order to insure that all processes are being simulated satisfactorily. For erosion patterns in particular, a good model performance when compared with outlet sediment measurements is not sufficient to insure that sediment sources and sinks are being correctly simulated (Jetten et al., 2003). Unfortunately, currently available data on runoff and erosion patterns is scarce and uncertain due to measurement errors; faced with this fact, several authors (e.g. Beven, 2000; Morgan and Quinton, 2001) have stated that the meaningful validation of spatially-distributed process-based models is unfeasible.

Jetten et al. (2003) report that most current erosion models are not very good at predicting spatial patterns of erosion; since precise estimates of these values is highly dependent on difficult to measure initial conditions, Imeson and Lavee (1998) suggest that spatially-

distributed models should be evaluated in terms of pattern description. The quality of simulated erosion patterns can be evaluated qualitatively; according to Morgan and Quinton (2001) and Favis-Mortlock et al. (2001), this approach consists in comparing model outputs with expected results to assert the rationality of model behavior, and therefore the accuracy of response to changes in environmental conditions.

In light of these facts, and given the lack of significant data on spatially-distributed hydrological and erosion patterns in Odeleite and Alenquer, the calibration and validation of the MEFIDIS model was performed in three steps:

- calibration of the spatially distributed parameters at the patch / field scale for the major land cover and soil combinations present in each catchment, in order to insure that MEFIDIS provides reasonable results at this scale;

- calibration of the watershed-scale parameters and model validation using outlet measurements, in order to insure that this calibration does not change the results obtained at the patch / field scale;

- evaluation of model rationality in simulating within-watershed erosion patterns, focusing on ephemeral gullies and sediment delivery from hillslopes to the watershed outlet.

The objective of this strategy is to insure that the model provides reasonable results at different scales. It also follows the procedure described by Wagener (2003) and Refsgaard and Henriksen (2004) for model evaluation, which combines model validation – the comparison of simulated and observed data, with model confirmation – the comparison of model results with the perceptual model for catchment processes.

The most complete model evaluation was performed for catchment outlets since this is where most data was collected. Data for 13 and 15 storms were collected for Odeleite and Alenquer, respectively, representing a large number of different conditions in terms of rainfall intensity and duration, and antecedent baseflow (an indicator of pre-storm soil moisture conditions). The storms are represented in Figure 4.8 and the hydrological and sediment yield data is shown in Table 4.6 and Table 4.7. The processed used a differential split-sample approach (Beven, 2000; Xu and Singh, 2004); about half of the storms were used for calibration, and the remainder for validation. This approach allowed the calibration and evaluation of

MEFIDIS for a wide range of conditions, thus enhancing model robustness and reducing over-calibration (Beven, 2000; Favis-Mortlock et al., 2001).

In contrast, the lack of data for within-watershed erosion patterns caused the analysis to rely on a comparison between model results and the current knowledge on sediment generation and deposition processes for Mediterranean watersheds. First, simulated sediment delivery ratios were compared with those calculated from catchment topographic and morphologic characteristics (see section 4.2.3). The data published by Vandaele et al. (1997) on ephemeral gully erosion characteristics for the Guadiana was compared with the simulated erosion patterns to verify if MEFIDIS is capable of simulating the high spatial heterogeneity of soil erosion which is typically present in these watersheds. Finally, the discrimination of within-watershed sediment sources by MEFIDIS per land use type was also evaluated and compared with current knowledge.

4.4.2 Model evaluation

MEFIDIS was calibrated at the patch / field scale using the rainfall experiment results described in section 4.2.6; only the spatially distributed parameters (Table 3.1, except for channel properties) were changed during this exercise. Afterwards, the model was calibrated and validated using hydrological measurements and sediment estimates at the outlet (see section 4.2.2), changing only watershed-scale parameters (channel properties in Table 3.1 and m in equation 3.18). This exercise was followed by qualitative evaluation of simulated erosion patterns inside each watershed.

Calibration at the patch scale

MEFIDIS was calibrated for the rainfall experiments using a single-cell version of the model; Table 4.37 shows the calibration statistics. For Portel, the calibration statistics can be considered satisfactory following the thresholds of model performance set by Motovilov et al. (1999) and Morgan and Quinton (2001) of r^2 above 0.36 and model efficiency index above 0.5, respectively. The low correlation coefficient can be attributed to the high dispersion of model results for both runoff and erosion, as can be seen in Figure 4.28; it was only possible to adjust model parameters to simulating extreme values. However, the fact that multiple experiments were available for the same land use and soil type combination increases the confidence in the model robustness, while underlining the uncertainty – and the lack of precision in particular – which surrounds model results at the patch / field scale. In contrast, the results for Alenquer are quite good (see Table 4.37), especially when considering the

maximum threshold for model efficiency as 0.7 proposed by Morgan and Quinton (2001) to take into account the natural variability in measurements and the lack of detailed process representation common to most hydrological and erosion models. In fact, these good results (which are illustrated in Figure 4.29) can be explained by the non-existence of replicate samples for each land use and soil type combination; they could indicate that these results are not as robust as those obtained for Portel, even if the model was better adjusted to Alenquer.

Table 4.37 – Model calibration statistics for the rainfall simulation experiments.

	Portel		**Alenquer**	
Parameter	**Runoff (mm)**	**Erosion (ton.ha^{-1})**	**Runoff (mm)**	**Erosion (ton.ha^{-1})**
r^2	0.59 ($p < 0.05$)	0.56 ($p < 0.1$)	0.99 ($p < 0.01$)	0.999 ($p < 0.01$)
Bias	-0.9	-0.006	-0.2	0.02
Average unsigned error	8.9	0.05	0.4	0.02
Observed average and range	18.4 (0.3 – 52.4)	0.1 (0.01 – 0.4)	6.0 (1.0 – 12.8)	0.2 (0.01 – 1.2)
Model efficiency[a]	0.50	0.55	0.98	0.99

a – Nash-Sutcliffe model efficiency index (Beven, 2000).

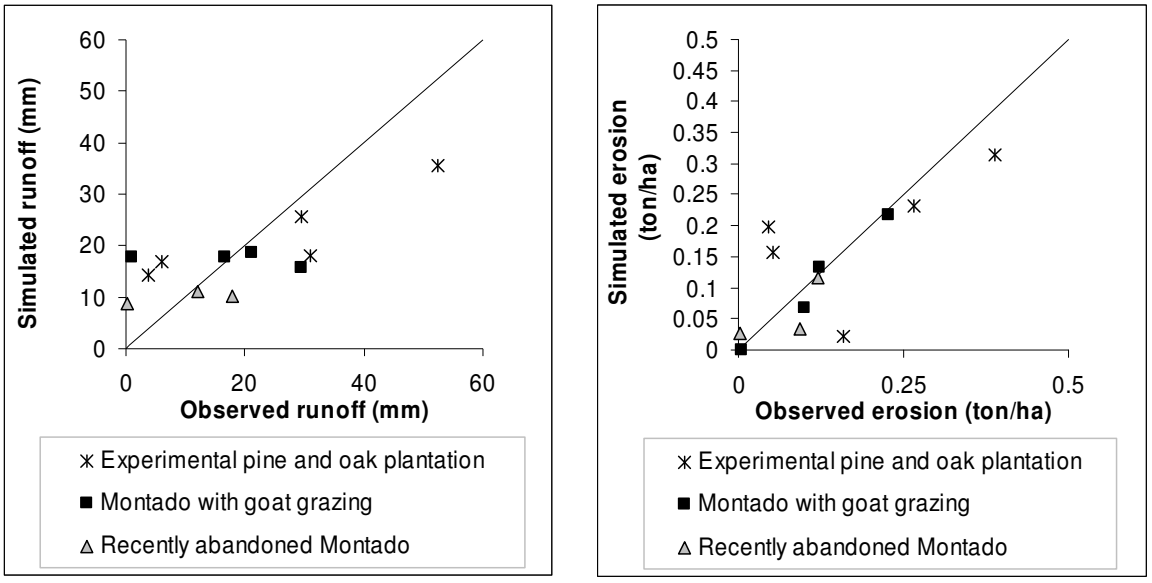

Figure 4.28 – Observed and simulated runoff (left) and soil erosion (right) for the rainfall simulation experiments in Portel.

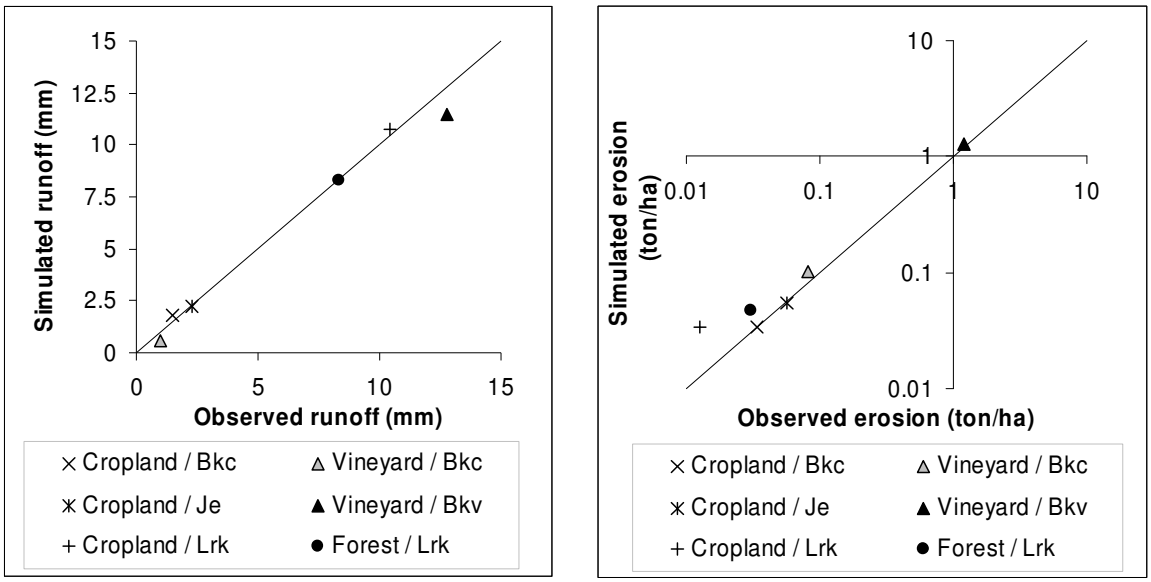

Figure 4.29 – Observed and simulated runoff (left) and soil erosion (right) for the rainfall simulation experiments in Alenquer.

The MEFIDIS calibrated soil hydraulic and texture parameters are shown in Table 4.38, with the Portel calibration applied for the Odeleite watershed as detailed above. All calibrated values are within the parameter ranges shown in Table 4.14 and Table 4.15, or fall outside by a short margin. The same is true for calibrated land use parameters, shown in Table 4.39 (see Table 4.24 for parameter ranges). Note that forests suffered different parameterizations for each watershed, highlighting the model dependency of parameterization scheme. Also, the low canopy cover value for wheat is applicable in autumn and winter conditions only, although several of the test storms occurred in autumn and spring; this illustrates the typical compromises made when deriving parameter sets for hydrological and erosion models (Jetten et al., 1999). Nevertheless, the satisfactory calibration evaluation, coupled with the fact that the model parameters were reasonably close to observed parameter ranges, indicates that MEFIDIS is rationally simulating hydrological and erosion responses at the patch scale for the major land use and soil type combinations in both the Odeleite and Alenquer watersheds.

Table 4.38 – Calibrated soil hydraulic and texture parameters for the Odeleite and Alenquer watersheds; parameters are identified in Table 3.1.

	FAO code	S_{depth} (mm)	θ	Ψ (mm)	K_{sat} (mm.h^{-1})	d_{50} (mm)	σ_{oc} (kPa)	S_{clay}
Odeleite	Ie	93	0.442	250	10.3	0.1635	21.4	0.083
Alenquer	Je	1300	0.407	230	19.5	0.020	11.02	0.144
	Bkc	800	0.469	800	13.7	0.033	17.0	0.245
	Bkv	525	0.478	200	6.0	0.016	17.0	0.295
	Lrk	500	0.374	160	7.0	0.018	37.0	0.257

Table 4.39 – Calibrated land use parameters for the Odeleite and Alenquer watersheds; parameters are identified in Table 3.1.

	Land cover	Manning's roughness coefficient n	Vegetation canopy cover V_{cv}	Pavement cover P_{cv}	Depression storage capacity D_{max} (mm)	Interception capacity I_{max} (mm)
Odeleite	Mediterranean Shrubland[a]	0.51	0.5	0.25	7.0	5
	Forest[a]	0.6	0.8	10.00	5.0	2.5
	Schlerophyllous oak forest[a]	0.5	0.5	15.00	5.0	2.5
Alenquer	Forest[b]	0.8	0.8	0.00	11.0	4.5
	Vineyard[b]	0.07	0.5	0.00	11.0	2.0
	Winter wheat croplands[b]	0.1	0.12	0.00	11.0	1.5

Calibration and validation at the watershed scale

The application of MEFIDIS to the Odeleite and Alenquer watersheds was performed using the storms detailed in Table 4.1 and Table 4.2, using the outlet measurements shown in Table 4.6 and Table 4.7 respectively; in each case, the model was calibrated for around half of the selected storms and validated for the remainder. The average soil moisture deficit at the beginning of each storm was estimated based on baseflow at the beginning of the storm, using the equation described by Beven (2000):

$$Q_b = A_c \cdot e^{-\gamma} \cdot e^{-\frac{D}{m}} \qquad 4.2$$

Where:
Q_b – baseflow before storm ($m^3.h^{-1}$)
A_c – catchment area (m^2)
γ – average topographic wetness index value for the watershed
D – soil moisture deficit for the watershed (m)
m – transmissivity decay with soil profile (m)

The *m* parameter was calibrated iteratively in order to calibrate total storm runoff. The calibration and validation statistics for this parameter are shown in Table 4.40; MEFIDIS has a good performance according to the criteria defined above (including an r^2 above 0.75; Motovilov et al., 1999). The model efficiency values above 0.7 for Odeleite do not indicate overcalibration in this case, as they increase for the validation dataset; an alternative explanation is that this index is biased towards model performance for high magnitude events (Beven, 2000), which in this case is good. One exception for good model performance is the validation dataset for Alenquer, where model efficiency is below the 0.5 threshold; while this can be an indicator of over-calibration, the overall results (shown in Figure 4.30, right) show the calibration and validation values with similar deviations from the 1:1 agreement line. The comparison between measured and simulated values, shown in Figure 4.30, indicates that the model provides reasonable estimates of total runoff for both watersheds although with some lack of precision, a result also indicated by comparing the correlation coefficient with the average unsigned error (c. 27 – 28 % in both cases).

Table 4.40 – Calibration and validation statistics for total storm runoff.

	Odeleite			**Alenquer**		
Parameter	**Calibration**	**Validation**	**All Data**	**Calibration**	**Validation**	**All Data**
r^2	0.88 ($p < 0.01$)	0.99 ($p < 0.01$)	0.89 ($p < 0.01$)	0.90 ($p < 0.01$)	0.76 ($p < 0.05$)	0.83 ($p < 0.01$)
Bias (mm)	1.8	-1.0	0.5	1.1	1.0	1.0
Average unsigned error (mm)	3.7	1.1	2.5	1.37	1.77	1.56
Observed average and range (mm)	11.8 (2.9 – 25.8)	6.4 (0.8 – 18.0)	9.3 (0.8 – 25.8)	3.8 (0.1 – 12.8)	3.1 (0.1 – 8.8)	3.5 (0.1 – 12.8)
Model efficiency[a]	0.76	0.94	0.84	0.82	0.46	0.69

a – Nash-Sutcliffe model efficiency index (Beven, 2000).

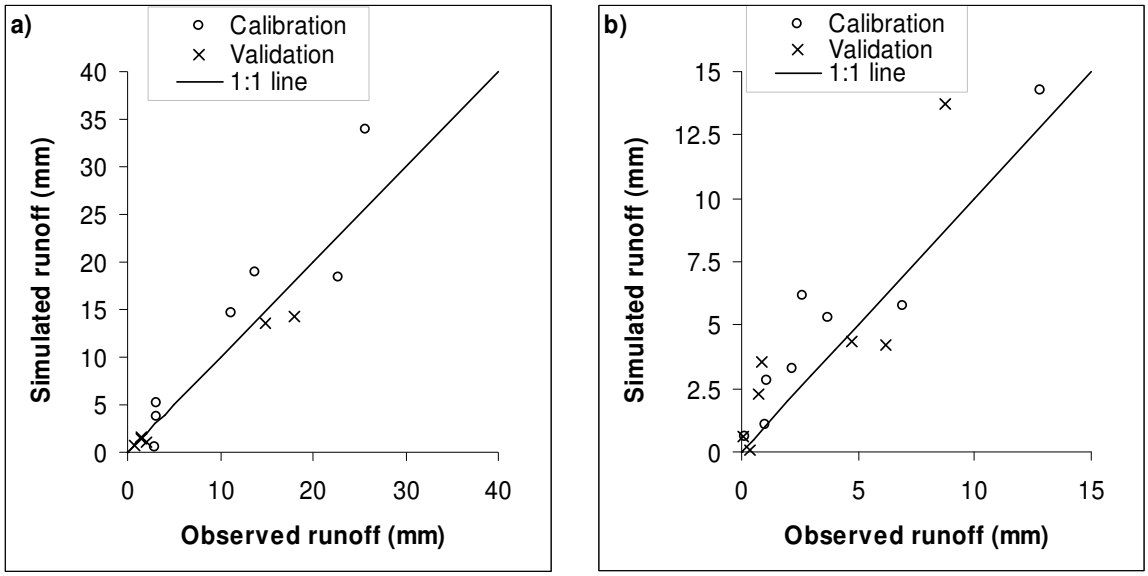

Figure 4.30 – Observed and simulated runoff at the catchment outlet for Odeleite (a, left) and Alenquer (b, right).

After total runoff was calibrated, hydrograph characteristics – peak runoff and time to peak – and sediment yield were calibrated by adjusting the channel roughness coefficient (Manning's *n* in Table 3.1). The calibration and validation statistics are shown in Table 4.41 for peak runoff rate and Table 4.42 for time to hydrograph peak. All fulfill the conditions for good model results defined above, except peak runoff rates in Alenquer which can only be classified as satisfactory. This can be attributed to the dispersion of model results for large magnitude storms (Figure 4.31, right). One explanation for this dispersion could be the fact that MEFIDIS does not consider soil crusting, a phenomena which would be more important in the finer soils of the Alenquer watershed than in the coarser soils of Odeleite and could lead to worse estimates for larger magnitude storms (Jetten et al., 2003; see also section 3.3.1). Another explanation could be the water repellency usually found in pine and eucalyptus forests in central Portugal, a parameter which is usually not taken into account by rainfall-runoff models (Doerr et al., 2003). Overall, MEFIDIS shows a satisfactory performance in estimating hydrograph characteristics, although with some lack of precision, a conclusion which is also supported by the comparison between measured and simulated values shown in Figure 4.31.

Table 4.41 – Calibration and validation statistics for peak runoff rate.

	Odeleite			Alenquer		
Parameter	**Calibration**	**Validation**	**All Data**	**Calibration**	**Validation**	**All Data**
r^2	0.79 ($p < 0.05$)	0.98 ($p < 0.01$)	0.85 ($p < 0.01$)	0.72 ($p < 0.05$)	0.63 ($p > 0.1$)	0.67 ($p < 0.01$)
Bias ($mm.h^{-1}$)	-0.08	-0.14	-0.11	-0.03	0.03	0.0008
Average unsigned error ($mm.h^{-1}$)	0.15	0.15	0.15	0.21	0.28	0.24
Observed average and range ($mm\ h^{-1}$)	0.6 (0.1 – 1.5)	0.4 (0.03 – 1.6)	0.5 (0.03 – 1.6)	0.7 (0.02 – 1.5)	0.5 (0.03 – 1.2)	0.6 (0.03 – 1.5)
Model efficiency[a]	0.75	0.79	0.78	0.71	0.60	0.67

a – Nash-Sutcliffe model efficiency index (Beven, 2000).

Table 4.42 – Calibration and validation statistics for time to hydrograph peak.

	Odeleite			Alenquer		
Parameter	**Calibration**	**Validation**	**All Data**	**Calibration**	**Validation**	**All Data**
r^2	0.89 ($p < 0.01$)	0.84 ($p < 0.05$)	0.84 ($p < 0.05$)	0.80 ($p < 0.02$)	0.96 ($p < 0.01$)	0.87 ($p < 0.01$)
Bias (hr)	-2.5	-7.5	-4.8	-0.2	0.5	0.1
Average unsigned error (hr)	3.5	9.9	6.5	1.3	0.8	1.1
Observed average and range (hr)	39 (27 – 57)	46 (18 – 110)	42 (18 – 110)	8 (2 – 16)	8 (3 – 14)	8 (2 – 16)
Model efficiency[a]	0.82	0.77	0.78	0.77	0.95	0.86

a – Nash-Sutcliffe model efficiency index (Beven, 2000).

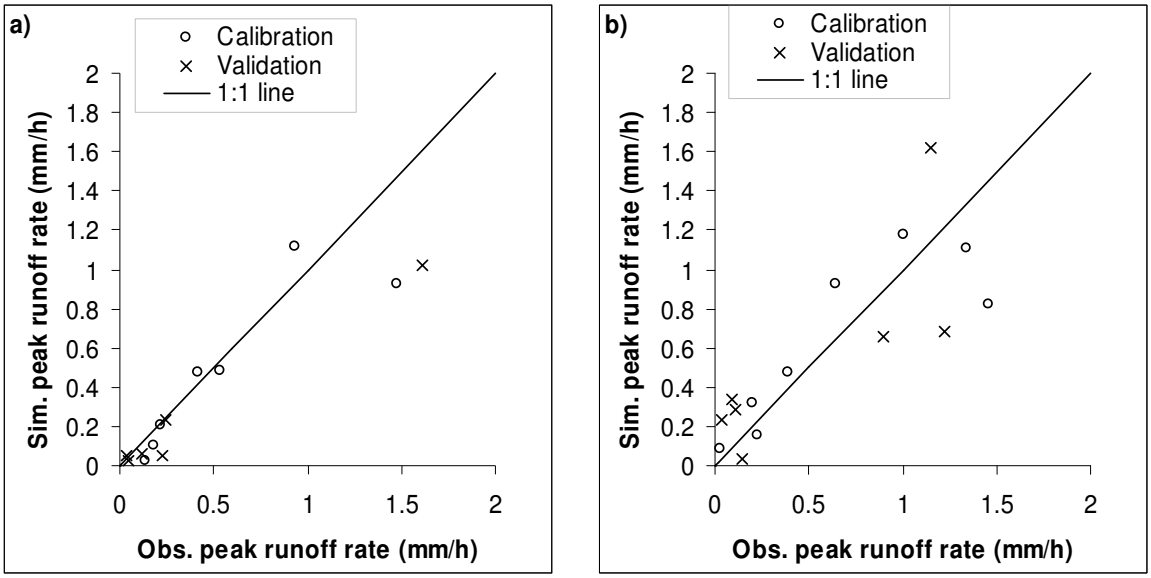

Figure 4.31 – Observed and simulated peak runoff rate at the catchment outlet for Odeleite (a, left) and Alenquer (b, right).

Table 4.43 shows the calibration and validation statistics for sediment yield. The results are good using the criteria defined above, except for the overall application to the Odeleite watershed and for the calibration in Alenquer. In Odeleite, it is interesting to note that the very high correlation coefficients found during calibration and validation are not reflected in the overall model application. This can be explained by observing Figure 4.32 (left), which compares observed and simulated sediment yield values; not only were there few events with higher (relatively speaking) sediment yield rates, but the validated result is significantly different from the calibration values. This fact does not necessarily indicate a poor model performance, as can be seen by the high model efficiency values shown in Table 4.43. Furthermore, estimated sediment yield values for Odeleite are all extremely small – all significantly below 0.01 ton.ha^{-1}. Nearing et al. (1999) report that, for an erosion magnitude of around 0.1 ton.ha^{-1}, soil erosion measurements in replicated plots usually vary c. 150 %; while extrapolation of plot values for watersheds is difficult, this implies that a good simulation of sediment yield with this magnitude should not be expected from MEFIDIS. Overall, MEFIDIS can be said to provide a satisfactory estimate of sediment yield for both basins, although with a significant lack of precision (Figure 4.32); results for Odeleite should be analyzed in light of the very low sediment yield measurements in this watershed.

Table 4.43 – Calibration and validation statistics for sediment yield.

Parameter	Odeleite			Alenquer		
	Calibration	**Validation**	**All Data**	**Calibration**	**Validation**	**All Data**
r^2	0.98 ($p < 0.01$)	0.998 ($p < 0.01$)	0.69 ($p < 0.01$)	0.67 ($p < 0.1$)	0.85 ($p < 0.02$)	0.74 ($p < 0.01$)
Bias ($ton.ha^{-1}$)	0.0003	-0.0011	-0.0004	0.003	0.001	0.002
Average unsigned error ($ton.ha^{-1}$)	0.0004	0.0011	0.0007	0.050	0.037	0.044
Observed average and range ($ton.ha^{-1}$)	0.002 (0.00004 – 0.007)	0.002 (0.00001 – 0.01)	0.002 (0.00001 – 0.01)	0.1 (0.001 – 0.4)	0.1 (0.0003 – 0.3)	0.1 (0.0003 – 0.4)
Model efficiency[a]	0.94	0.53	0.67	0.67	0.75	0.71

a – Nash-Sutcliffe model efficiency index (Beven, 2000).

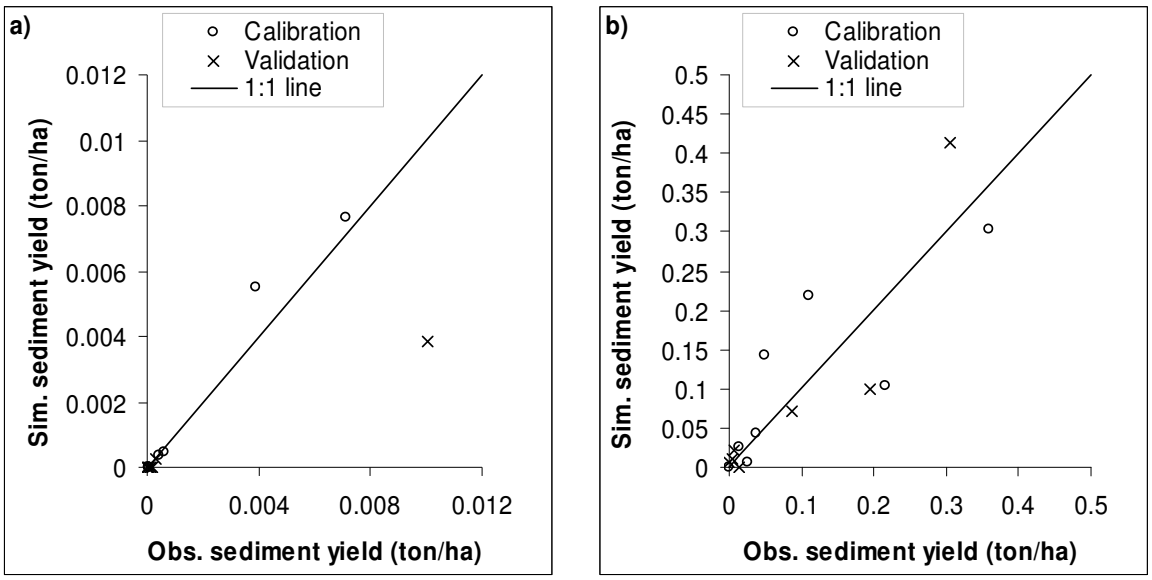

Figure 4.32 – Observed and estimated catchment sediment yield for Odeleite (a, left) and Alenquer (b, right).

Evaluation at the upslope scale

The evaluation of MEFIDIS for within-watershed values was based on a comparison with Sediment Delivery Ratios (SDRs; Lane et al., 1997) and ephemeral gully erosion patterns. Table 4.44 compares estimated and simulated SDRs for Odeleite and Alenquer. The values are similar, but this in itself does not indicate good model performance. While SDR has been shown to be strongly correlated with catchment area and morphology, decreasing with

increasing drainage area above a threshold of c. 10 Km^2, there are usually large differences between catchments due to additional conditions such as vegetation cover and lithology which is difficult to assess using current basin-scale SDR estimation methods (de Vente and Poesen, 2005). However, MEFIDIS appears to capture the impact of different basin area and morphological conditions on sediment yield; these results indicate that the very significant difference between simulated SDRs for Odeleite and Alenquer is similar to the one found using independent estimate methods, and can therefore be assumed to have some basis in reality. Furthermore, simulated SDRs greatly increase with increasing storm magnitude; this process has been described by Favis-Mortlock et al. (2001) as deriving from the increased connectivity caused by greater storm flows, thereby preventing eroded sediment to deposit in regions with lower slope gradients. The relationship between storm runoff and SDR simulated for Odeleite and Alenquer is consistent with observations for semi-arid catchments (Puigdefabregas et al., 1998: Kirkby et al., 2002).

Table 4.44 – Comparison between estimated and simulated sediment delivery ratio and ephemeral gully to rill / interill erosion ratio for Odeleite and Alenquer.

Parameter		**Odeleite**	**Alenquer**
Sediment delivery ratio	Estimated[a]	0.04	0.18
	Simulated	0.04 (0.002 – 0.18)	0.20 (0.09 – 0.28)
Gully to rill / interrill erosion ratio	Estimated[b]	4.5 – 5.2	4.5 – 5.2
	Simulated	3.5 (1.4 – 4.9)	3.1 (0.7 – 6.5)

a – Estimated using the Roehl method (Ponce Álvares and Pimenta, 1998).
b – Vandaele et al. (1997).

The assessment of model performance in locating ephemeral gullies was made by comparison with a gully location index developed by Vandaele et al. (1997) for southern Portugal. The authors found that the wetness index (as described in equation 3.17) and streampower index (the product of accumulated drainage area and local slope) are good indicators of gully location, indicating the importance of flow concentration and subsurface saturation in gully formation. The thresholds of gully initiation are wetness index > 9.8 and streampower index > 40. The relationship between slope, drainage area and the location of ephemeral gullies in semi-arid environments has also been reported by other authors (e.g. Vandekerckhove et al., 1998, 2001; Oostwoud Wijdenes et al., 1999).

Since MEFIDIS does not explicitly simulate gully erosion, model estimates for soil erosion in the gully-prone regions, as estimated by the index, were assumed to represent mostly gully erosion; estimates for the remaining catchment were assumed to represent mostly rill / interill erosion. The ratio between gully and rill / interill erosion rates calculated using this method is shown in Table 4.44, compared with the estimates by Vandaele et al. (1997) for southern Portugal. While the values do not match, they are significantly different from the rates reported by the authors for other environments: 0.25 to 2.3, with most of the regions presenting more erosion from rill / interill regions than from ephemeral gullies. Therefore, these results indicate that MEFIDIS is able to simulate the dominance of gully erosion over rill / interill erosion in both watersheds, which is in agreement with typical erosion processes under Mediterranean climates (Boix-Fayos et al., 2006; see also section 2.2.3).

Finally, an evaluation of the contribution of each land cover for the total upslope erosion was performed and compared with both their fraction of the catchment area and average annual erosion values observed in Mediterranean regions (shown in Table 4.30). The model results, shown in Table 4.45, point to wheat croplands and vineyards as the major sediment sources in Alenquer when compared with their presence, which concurs with the high erosion rates usually observed under these landcovers. In Odeleite, the results indicate wheat croplands as the major sediment source areas when compared with their relatively small distribution over the catchments, which compares well with the high erosion rates observed in these landcovers when compared with shrublands or cork oak forests. These results show that the MEFIDIS model is capable of assessing the relative importance of soil erosion under different vegetation cover types, although there is insufficient data to assess model performance in terms of measured erosion rates per storm.

Table 4.45 – Comparison between model results for sediment sources (in terms of fraction of total upslope erosion) for each landcover in both study areas, and their distribution over the catchments.

Alenquer			**Odeleite**		
Landcover	**Fraction of total erosion (%)**	**Catchment area (%)**	**Landcover**	**Fraction of total erosion (%)**	**Catchment area (%)**
Wheat	84.8	66.6	Wheat	74.2	8.6
Vine	13.3	14.4	Shrub	15.2	52.8
Forest	0.04	6.7	Cork oak	9.7	32.9

Discussion and assessment

The main objective of this evaluation exercise was to validate and confirm the appropriateness of the MEFIDIS application for the Odeleite and Alenquer watersheds, in order to answer the following question: is the model capable of reproducing observed data and patterns at several scales?

Overall, MEFIDIS has been shown to provide reliable estimates of storm hydrographs and total runoff and sediment delivery for the Odeleite and Alenquer watersheds in different rainfall conditions; while precision is not very good, model efficiency still falls above the threshold for good model performance. The representation of sediment detachment and transport processes appears to be consistent with common observations for other Mediterranean watersheds, particularly in terms of gully erosion dominance; gully erosion patterns also appear to follow topographic controls at the hillslope scale. These results, coupled with the fact that spatially-distributed parameters were calibrated to provide good results at the patch / field scale, also give a promising indication that within-watershed erosion rates have a good degree of accuracy; however, more data would be needed to validate this statement. Therefore, MEFIDIS appears to reliably reproduce erosion processes at the patch / field, hillslope and watershed scale.

It should also be noted that MEFIDIS was assessed under a wide range of storm intensities, durations and antecedent baseflow rates, covering the main controls on runoff generation in Mediterranean catchments (Castillo et al., 2003; see also section 2.2.2). The actual error of spatially-distributed erosion rates cannot be assessed due to the lack of data; however, the positive evaluation of erosion patterns performed above indicates the usefulness of MEFIDIS to assess relative erosion risks and to analyze the impacts of change in erosive factors (Favis-Mortlock et al., 2001). The present lack of spatially-distributed data for Alenquer and Odeleite, as well as the difficulties associated in collecting this data (Jetten et al., 2003) limits the capacity to further validate the spatial results of the model in the near future. However, they are sufficient to provide an insight in the effects of change in storm intensity on soil erosion patterns due to climate change.

4.5 Scale issues in storm rainfall representation

The spatial and temporal scales at which models are parameterized and implemented can have an impact on model results. This issue has been studied by several authors in recent years, in terms of appropriate levels of spatial and temporal discretization (e.g. Booij, 2003; Jetten et

al., 2003; Hessel, 2005). However, storm patterns, especially in terms of movement, can also have a significant impact on model results, at least in laboratory conditions (e.g. Singh, 1998, 2002a and b; de Lima and Singh, 2002), although few studies have been conducted using catchment-scale models. Given the expected impacts of climate change on storm rainfall (see section 2.2), an exercise was performed to evaluate the significance of representing small-scale changes to storm movement patterns in the modeling framework of this thesis.

The studies performed with the LISEM model can provide some indications about the response of MEFIDIS to changes in the level of spatial and temporal discretization, since LISEM possesses a similar grid-based discretization scheme and both models share the basic structural principles. Both Jetten et al. (2003) and Hessel (2005) report a reduction of model results for surface runoff, peak runoff rates, flow detachment and deposition with increasing spatial resolution used in the model; changes to soil erosion rates depend on changes to the balance between detachment and deposition. Changes can be as high as -50 % for an increase in spatial resolution from 10 × 10 m to 100 × 100 m. Hessel (2005) links these changes to a reduction of the average slope gradient with coarser resolutions, coupled with an increase of the numerical dispersion of the kinematic wave equation. The author found a similar impact of increasing time-step size, linking this with increased dispersion of the kinematic wave equation coupled with numerical errors in water balance calculations. However, he also suggests that a model can be calibrated for an appropriate resolution, and that the best resolution might be catchment-dependent. The scales presented by Booij (2003), shown in Table 4.26, can be taken as maximum values at which models can represent hydrological and erosion processes; it can be assumed that, below these scales, the model can be calibrated to take into account the impacts of grid resolution; temporal resolution can be linked to spatial scale using e.g. the Courant condition as a guideline (Chapra, 1997).

Rainfall is also highly variable in both time and space, with storms moving across watersheds during extreme events. Many authors have studied this problem (e.g., Eagleson, 1978; Sharon, 1980; Foufoula-Georgiou and Georgakakos, 1991; Ladoy et al., 1991; de Lima, 1998), but the majority of hydrological and erosion studies in Mediterranean regions do not take into account the effect on the hydrologic response caused by the movement of storms across drainage areas. However, the problem of how storm movement affects flows (shape of the hydrograph and peak discharge) has been recognized for some time, normally based on laboratory or numerical simulations; studies on this problem include e.g. Maksimov (1964), Yen and Chow (1968), Wilson et al. (1979), Jensen (1984), Singh (1998, 2002a and b) and de

Lima and Singh (2002). These studies show that ignoring the storm movement can result in (considerable) over- or under-estimation of the runoff peak; when compared with storms moving downstream, storms moving upstream are characterized by hydrographs with: (1) earlier rise, (2) lower peak discharge, (3) less steep rising limb, and (4) longer base time. These results for one-dimensional flows have been obtained theoretically on planar surfaces (e.g. Singh, 1998, 2002a and b; de Lima and Singh, 2002) and experimentally, in the laboratory, for overland flow on impermeable surfaces (de Lima and Singh, 2003) and soil flumes (de Lima et al., 2003). Because of the relation between runoff and water erosion, the movement of storms (direction, velocity, etc.) is also expected to affect the associated soil loss (de Lima et al., 2003). Furthermore, the raindrop splash transport process is affected by wind-driven rains (e.g. de Lima et al., 1992; Dijk et al., 1996; Erpul et al., 2002). However, most of the studies reported in the literature have quantified soil loss in time only in controlled laboratory conditions. Thus, there is also a lack of studies on estimation of erosion under moving storms on natural basins.

This work investigated the variability of runoff and erosion processes caused by the movement of rainstorms over a drainage basin. The MEFIDIS numerical model was used to simulate the response of a basin to rainstorms moving up or down the basin area at a range of speeds, simulating a single dry-wet-dry cycle. Controlled laboratory experiments using a soil flume and a movable sprinkling-type rainfall simulator were used to test the model's capability to adequately simulate slope responses to changes in the storm movement direction. However, the main objective of this study was to quantify the influence of the storm movement on water erosion at the basin scale. The model was applied to the Alenquer drainage basin. The results presented in this section were published by Nunes et al. (2006).

4.5.1 Model application to a laboratory experimental setup

MEFIDIS was used to simulate the processes of runoff and sediment loss involved in laboratory experiments using moving rainfall simulators, reported by de Lima et al. (2003). The objective was to determine the model's ability in simulating the effect of storm movement over conditions analogous to a single hill slope. The laboratory experiments were conducted on a 3 × 0.3 m soil flume with a 10 % slope, using a movable sprinkling-type rainfall simulator (Figure 4.33). Further details on the experiment are given by de Lima et al. (2003). This experiment was used to simulate rainstorms moving upstream and downstream with a constant speed. The storm movement was obtained by moving, on wheels, the support structure of the nozzles over the flume. The average storm intensity was 3.24 mm/min and the

total length of the storm (length of water application) was 5.3 m. Overland flow and sediment loss caused by each rainfall event were measured by collecting samples every 10 seconds in metal containers placed at the bottom end of the soil flume. Hortonian overland flow occurred on the flume when the rain intensity exceeded the infiltration rate; the transport of fine erodible soil material was mainly due to overland flow.

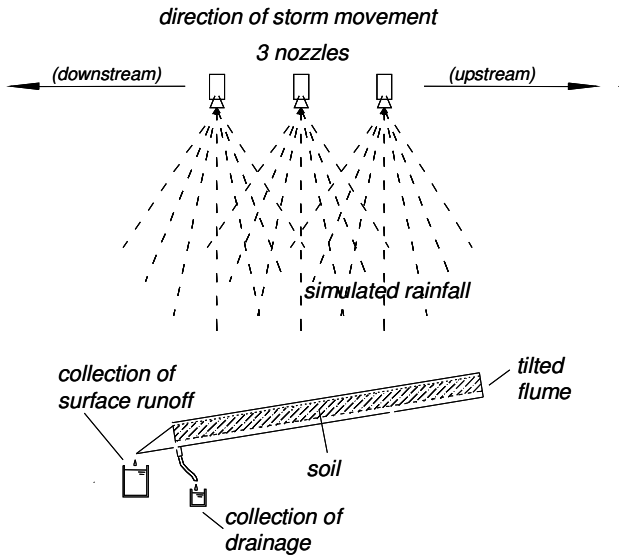

Figure 4.33 – Schematic representation (side view) of soil flume and the nozzles; storm movement was obtained by moving the support structure of the rainfall simulator at a constant speed, with surface runoff collected at the end of the flume.

The analysis of the overland flow hydrographs and of the evolution of sediment transport during the runoff events showed distinct hydrologic responses for storms moving in different directions. Figure 4.34 presents runoff hydrographs and the respective evolution of soil loss obtained for a storm speed of 0.12 m/s, both for downstream and upstream moving rainstorms. These results show significant differences in runoff and soil loss between identical simulated rainstorms moving downstream and upstream. Downstream moving storms yielded higher soil loss than did upstream moving storms. Further analysis of the results can be found in de Lima et al. (2003).

MEFIDIS was applied to this laboratory experimental setup. It was simulated by the model as a one-dimensional slope, divided into ten 0.3 × 0.3 m^2 cells. Figure 4.34 show the model

performance for both runoff and accumulated soil loss. Although there were problems in simulating the beginning of sediment discharge, the results do show that MEFIDIS was able to adequately simulate the differences between storms moving upslope and downslope over the soil flume. While the experimental set-up is considerably less complex than an actual drainage basin, this comparison demonstrated the model's ability to simulate the consequences of storm movement over smaller-scale components such as single hillslopes.

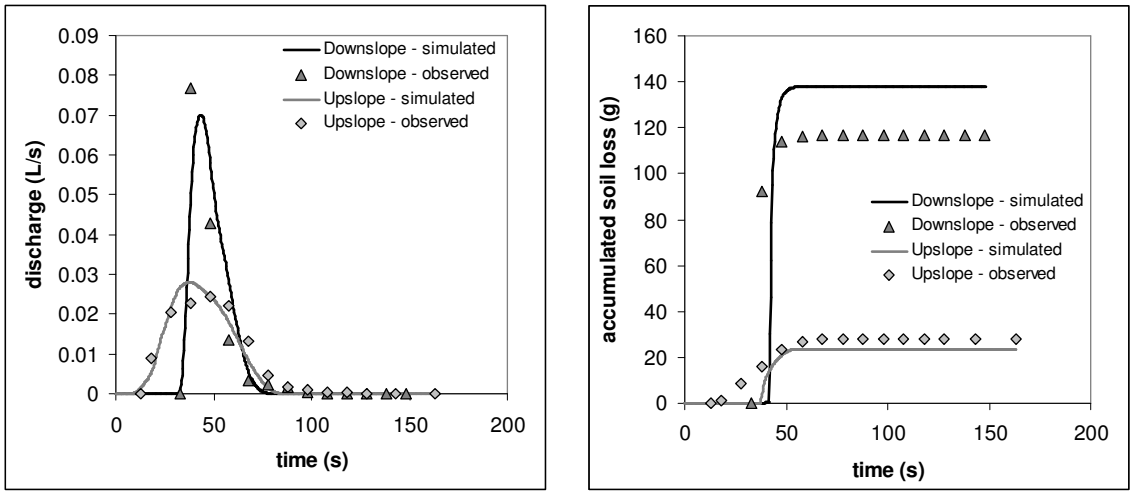

Figure 4.34 – Numerical simulation (continuous line) and observed (laboratory data measured in soil flume) runoff hydrographs (left) and accumulated sediment loss (right) for downstream and upstream moving storms, for a storm with 0.12 m/s speed, and rainfall intensity of c. 4 mm/h.

4.5.2 Experimental setup for the Alenquer drainage basin

The MEFIDIS model was applied to the Alenquer basin; the calibration and validation is described in section 4.4, above. The simulation of storm movement involved nine storms combining different areal extents (diameters) and movement speeds (Table 4.46). The selection of the storm diameters (circular shaped storms) took into consideration the axial length of the Alenquer drainage basin (15.2 Km; Figure 4.35 and Table 4.46). Within the areal extent and for the duration of each storm, rainfall intensity was maintained constant at the rates shown in Table 4.46. Three storm speeds were selected (0.5, 1 and 2 $m.s^{-1}$). In order to make the storms comparable, the total rainfall depth over the basin was maintained constant at 50 mm by varying the storm intensity according to storm area and speed (de Lima and Singh, 2002). MEFIDIS was run for each storm type, with the storm's centre moving both downstream and upstream along the basin's axis (Figure 4.35).

Table 4.46 – Characteristics of the 9 test storms simulated for the Alenquer drainage basin study.

	Description (Size/Speed)	**Diameter (Km)**	**Speed (m/s)**	**Intensity (mm/h)**
LF	**L**arge/**F**ast	30.4[a]	2	12.1
LM	**L**arge/**M**edium		1	6.1
LS	**L**arge/**S**low		0.5	3.0
MF	**M**edium/**F**ast	15.2	2	26.1
MM	**M**edium/**M**edium		1	13.0
MS	**M**edium/**S**low		0.5	6.5
SF	**S**mall/**F**ast	7.6[b]	2	74.1
SM	**S**mall/**M**edium		1	37.1
SS	**S**mall/**S**low		0.5	18.5

a – Doubles the basin axial length.
b – Halves the basin axial length.

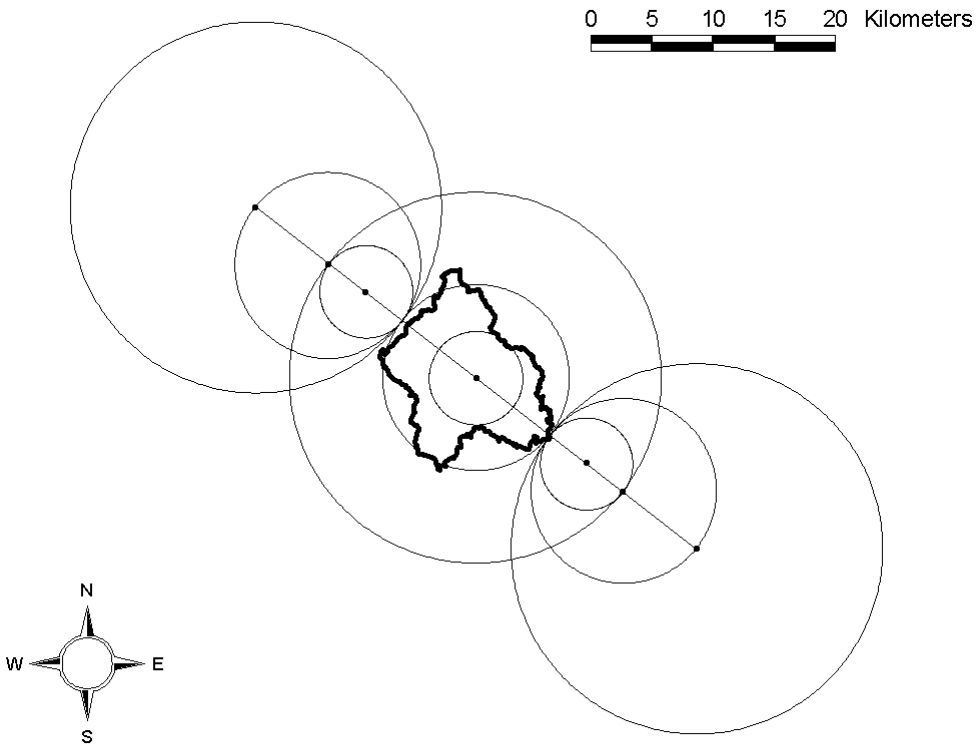

Figure 4.35 – Spatial extent of test storms (0.5, 1 and 2 times the basin axial length). Circumferences in the upper left and lower right show the beginning and the end of storm movement over the basin axis which is represented by the diagonal line.

For each case, the storm intensity was determined from the basin area under rainfall and from the storm duration (dependent on the storm movement speed and storm diameter). The test storms can be considered as representative of a number of possible atmospheric and hydrologic conditions over the Alenquer drainage basin, associated with various return periods. Figure 4.36 presents the Intensity-Duration-Frequency curves available for the Alenquer drainage basin; most storms used (also represented in Figure 4.36) fall between the 2-year and the 50-year return period range.

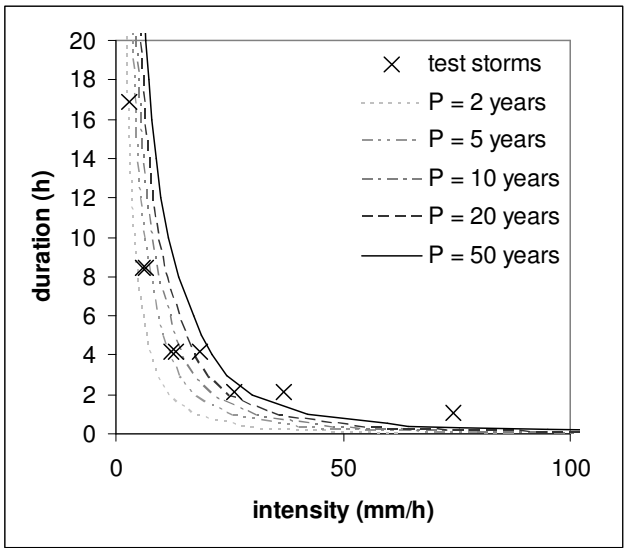

Figure 4.36 – Frequency of test storms; IDF curves for S. Julião do Tojal, near Alenquer, determined by Brandão et al. (2001), where P is the return period.

4.5.3 Results and discussion

MEFIDIS was used to simulate the test storms, described in Table 4.46, moving over the Alenquer drainage basin. The storms were simulated in pairs: one storm moving downstream and another upstream, along the basin's axis. In total, 18 model runs were undertaken. Table 4.47 summarizes the results; "gross erosion" should be understood as the amount of soil detached by rain splash and overland flow, without deposition (Foster, 1982), while "net erosion" should be understood as the basin's sediment export, equaling the gross erosion minus deposition. Overall, the downstream storm movement generated greater peak runoff rates and more net erosion than did the upstream storm movement (Figure 4.37). When comparing the consequences of upstream- and downstream-moving storms by peak runoff

rates increased on average by 56.5 % (16.8 to 78.3 %) and the net erosion rates increased on average by 9.1 % (0 to 21.7 %, with significant increases in smaller and faster storms only).

Table 4.47 – Summary of all simulation results for all tests conducted in the Alenquer drainage basin; runoff and net erosion are for the basin's outlet (see also Table 4.46 for nomenclature).

Test	Direction	Runoff (mm)	Peak runoff ($mm.h^{-1}$)	Net erosion ($ton.ha^{-1}$)	Gross erosion ($ton.ha^{-1}$)
LF	Downstream	5.1	1.92	0.21	0.49
	Upstream	4.9	1.20	0.19	0.50
LM	Downstream	2.1	0.35	0.017	0.056
	Upstream	2.0	0.25	0.016	0.057
LS	Downstream	1.54	0.11	0.004	0.009
	Upstream	1.49	0.09	0.003	0.009
MF	Downstream	8.5	4.9	0.8	1.4
	Upstream	8.4	2.8	0.7	1.4
MM	Downstream	5.9	2.0	0.29	0.59
	Upstream	5.7	1.1	0.25	0.60
MS	Downstream	2.4	0.39	0.027	0.079
	Upstream	2.3	0.26	0.027	0.079
SF	Downstream	20.9	14.4	2.0	2.4
	Upstream	20.7	8.1	1.9	2.4
SM	Downstream	17.3	6.4	1.2	1.5
	Upstream	17.1	4.0	1.1	1.5
SS	Downstream	12.0	2.4	0.5	0.6
	Upstream	11.8	1.6	0.4	0.6

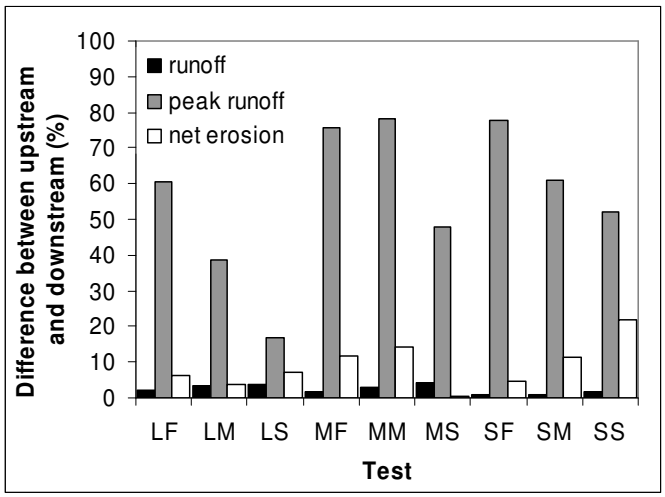

Figure 4.37 – Relative difference between the results for upstream and downstream storm movements shown in Table 4.47; positive values indicate that the results increase with downstream movement.

The results were less significant for total runoff, which increased on average by 2.4 % (0.8 to 5.1 %). Gross erosion was in most cases not significantly affected by storm movement, and in some cases increased slightly with upstream-moving storms (0.5 %). occurred These results contrast with those found in laboratory experiments (Figure 4.34). One possible explanation stems from the fact that runoff generation and gross erosion, as defined above, are processes that occur on hill slopes. In a spatially complex basin, such as Alenquer, hillslope direction is not uniform; hillslopes face all possible directions, and the water lines (where most of the concentrated flow erosion occurs) change directions several times, therefore reducing or even cancelling the effects of storm movement. Furthermore, several other factors affect the spatial variability of total runoff and gross erosion inside a basin, such as the spatial distribution of vegetation and soil properties (Foster, 1982), and their importance could be much more significant than the relationship between hill slope orientation and storm movement direction.

One possible explanation for the difference between the impact of storm movement on slope processes (runoff generation and gross erosion) and basin-scale processes (peak runoff rate and net erosion) is the scale difference itself. At the basin scale, the positioning of different tributary basins along the main channel appears to be more important than slope orientation. This statement can be exemplified with an analysis of Figure 4.38, which shows the simulated hydrographs for the Medium/Medium test (as defined in Table 4.46) calculated for several cross-sections of the drainage network. Some conclusions can be taken from the figure:

- There is a clear delay of the starting time of the hydrograph, especially in the upstream water courses of the basin as expected; downstream moving storms are associated with faster hydrological responses than are upstream moving storms.

- Peak flows in the main river and in the tributaries are higher for downstream moving storms than are for upstream moving storms. This can be partly explained by the layout of the drainage network: the water courses are all positioned approximately in the direction of the movement of the storms.

- In the main river and in the tributaries, the rising limb of the hydrograph is steeper for downstream moving storms.

- At the outlet of the main stream, upstream moving storm hydrographs have an earlier rise than do corresponding downstream moving storm hydrographs as expected. The different behavior observed for some upstream sub-basins is due to the relative position of these basins with respect to the outlet (it should be noted that for upstream moving storms, time starts when the storm enters the Alenquer basin near the outlet).

- The difference between peak flows for upstream and downstream moving storms increases along the river's length. This indicates that when storms move downstream, a "cascade effect" of tributaries discharging runoff in the main river could be responsible for these differences in peak flows.

The "cascade" effect of runoff discharging from tributaries was observed in all other tests and therefore appears to be the most likely reason for the differences in peak runoff rates shown in Table 4.47 and Figure 4.37. Also, in all tests the outlet hydrographs showed larger flow peaks with a steeper rising limb for downstream moving storms, although the storm size and speed influenced the magnitude of the differences; Figure 4.39 (left) exemplifies these differences for the medium-sized storms (tests MF, MM and MS). The hydrologic behavior is similar to the ones observed in the laboratory tests (Figure 4.34), although less pronounced, and follows the theoretical expectations (e.g., Singh, 1998, de Lima and Singh, 2002). Figure 4.37 shows some consequences of storm size and movement speed on the peak runoff rate difference, which increases both with increasing storm speed and decreasing storm size. Since the smaller and faster storms used in the tests had larger intensities (Table 4.46), this result points to a correlation between storm intensity and the difference in peak runoff rates; this correlation can also be seen in Figure 4.39 (right).

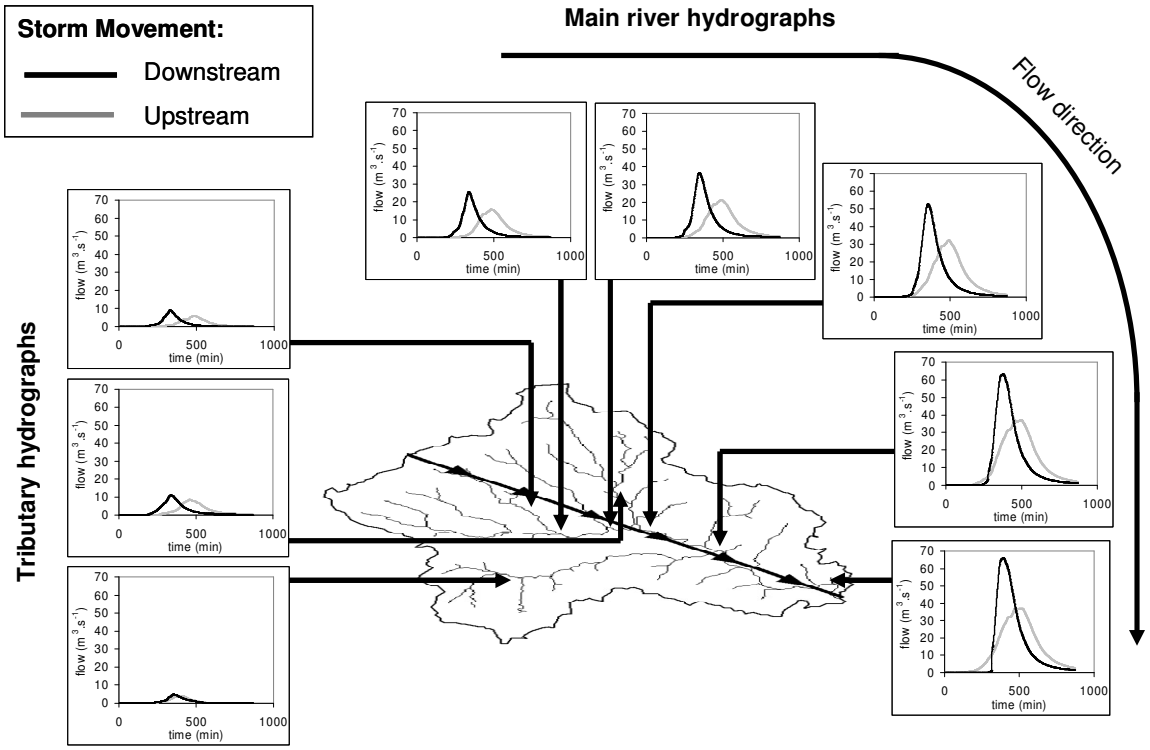

Figure 4.38 – Simulated hydrographs for several sections in the Alenquer river (right) and its tributaries (left) for test Medium/Medium, for both downstream and upstream storm movements (see also Table 4.46).

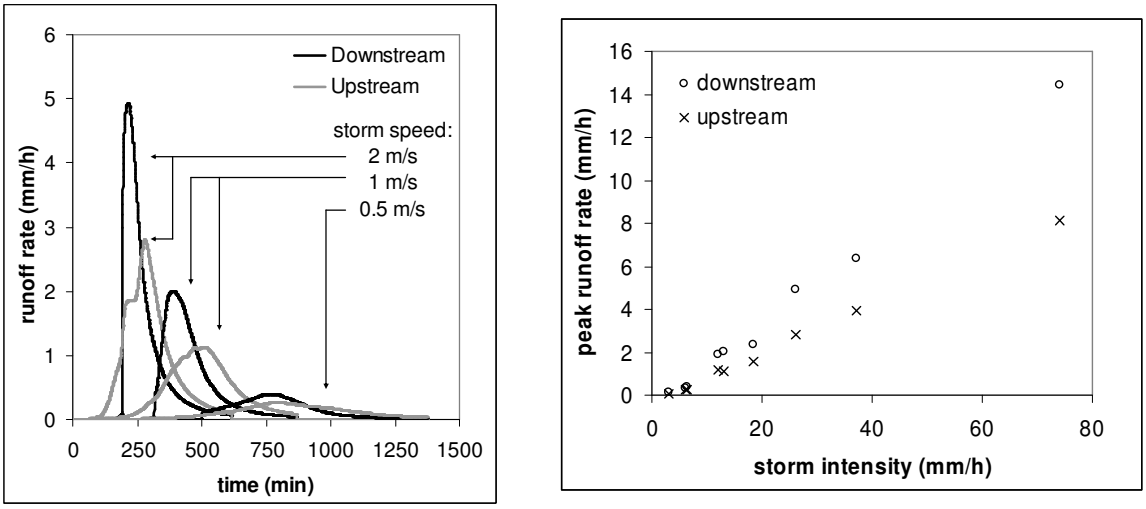

Figure 4.39 – Left: simulated hydrographs at the Alenquer basin's outlet for tests Medium/Fast (left), Medium/Medium (center) and Medium/Slow (right), for both downstream and upstream movements (see Table 4.46); Right: simulated peak runoff rate at the Alenquer basin's outlet as a function of storm intensity, for all 18 tests.

The impact of storm movement direction on net erosion appears to be a direct consequence of the impact in peak flow rates, through an increase of the sediment yield ratio (defined as net erosion / gross erosion); Figure 4.40 (left) shows that the sediment yield increases with downstream movement for every test. One possible explanation is the fact that the larger peak runoff rates in downstream-moving storms increase the sediment transport capacity of the main river and its tributaries (Govers, 1990), thereby reducing sedimentation in the channel bed. In other words, more of the sediment eroded in the upland is exported from the basin. Another possible explanation is the increase in total runoff for downstream-moving storms; albeit it is small (as referred to above), the flow generated upslope travels towards the basin outlet, reducing the likelihood of soil eroded in upslope areas depositing in the lower bottom of the slopes (Favis-Mortlock et al., 2001). Figure 4.40 (right) shows that both these processes appear to contribute to the increase in the net erosion.

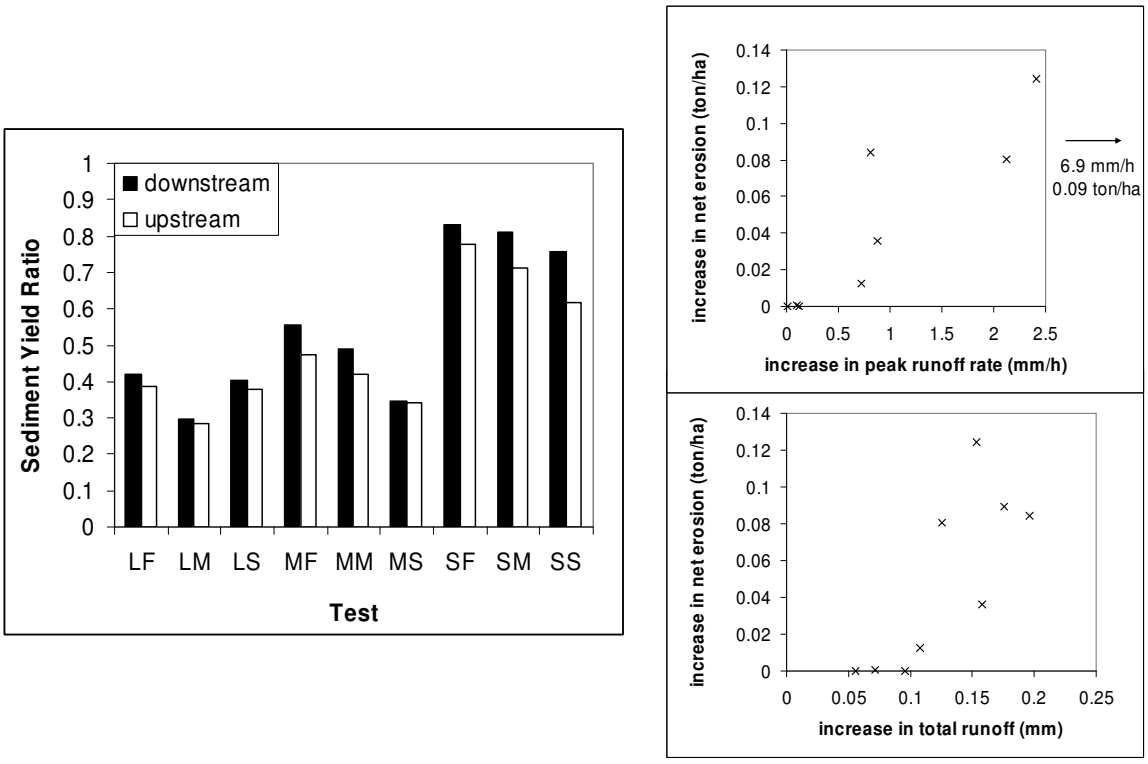

Figure 4.40 – Left: Sediment Yield Ratio (net erosion / gross erosion) for downstream and upstream storm movements (see Table 4.46); right: net erosion increase with downstream storm movement, in the Alenquer basin, for all 18 tests, correlated with the increase in peak runoff rates (above) and total runoff (below), with the arrow in the upper figure indicating the position of one outlier.

4.5.4 Conclusions

The results of the present study show that the storm movement significantly affects runoff and water erosion processes at both small (laboratory plot) scale and basin scale, although through different processes. Both the laboratory experiments and the numerical modeling with MEFIDIS at the small-scale basin of Alenquer show that the soil loss is clearly linked with the characteristics of runoff hydrographs resulting from rainstorms moving in the upstream and downstream directions.

The following main conclusions can be drawn:

- Rainfall intensity patterns induced by moving storms, whatever their direction, influence the characteristics of runoff and soil erosion. Downstream storm movement is potentially more hazardous in terms of peak flow discharge and sediment yield.

- Storm movement is more likely to affect peak flow than the total surface runoff production. The effect of storm movement on peak flow increases with storm intensity. This may have serious repercussions on the impact of extreme flood events.

- During downstream moving storms, river flow rates rise at a faster pace and peak flow occurs earlier than during storms moving in other directions.

- For the same speed and approximately the same runoff volume, downstream moving storms yield larger quantities of net erosion than do upstream moving storms. This is not due to an increase in upland erosion; rather, it is due to a decrease of sedimentation rates within the main channels.

In the context of this thesis, these results show that changes to storm movement patterns caused by climate change could have significant impacts in watershed peak runoff rates and sediment yield; however, the spatial resolution of current RCM scenarios is still too coarse to indicate impacts in these patterns at the watershed scale, although the uncertainty associated with this problem should be taken into account. Further investigation of these processes will require detailed monitoring of the movement of storms (e.g. wind direction, rain patterns) which, combined with data on flow rates and sediment transport on water courses, could allow a better view of the complex interactions involved between movement direction and the spatial variability within the drainage basin. It would also allow a better quantification of the uncertainty associated with this process for hydrological modeling, as well as an assessment of possible methods to better incorporate this information in numerical simulations.

4.6 References

Almeida AC, Landsberg JJ, Sands PJ, 2004. Parameterisation of 3-PG model for fast-growing Eucalyptus grandis plantations. For. Ecol. Manage. 193: 179-195.

Arnold JG, Allen PM, Muttiah R, Bernhardt G, 1995. Automated base flow separation and recession analysis techniques. Ground Water 33 (6): 1010-1018.

Arnold JG, Allen PM, 1999. Automated methods for estimating baseflow and ground water recharge from streamflow records. Journal of the American Water Resources Association 35 (2): 411-424.

Batjes NH, 2002. Soil parameter estimates for the soil types of the world for use in global and regional modelling (version 2.1; July 2002). ISRIC report 2002/02c, International Food Policy Research Institute (IFPRI) and International Soil Reference and Information Centre (ISRIC), Wageningen.

Beasley DB, Huggins LF, 1981. ANSWERS User's Manual. USDA Report No. EPA-905/9-82-01, United States Department of Agriculture.

Beven K, 1997. TOPMODEL: a critique. Hydrol. Process. 11 (9): 1069–1086.

Beven K, 2000. Rainfall-Runoff Modelling – The Primer. John Wiley & Sons, Chichester.

Bittelli M, Campbell GS, Flury M, 1999. Characterization of Particle-Size Distribution in Soils with a Fragmentation Model. Soil Sci. Soc. Am. J. 63(4): 782-788.

Boix-Fayos C, Martínez-Mena M, Calvo-Cases A, Castillo V, Albaladejo J, 2005. Concise review of interrill erosion studies in SE Spain (Alicante and Murcia): erosion rates and progress of knowledge from the 1980s. Land Degrad. Develop. 16: 517–528.

Boix-Fayos C, Martínez-Mena M, Arnau-Rosalén E, Calvo-Cases A, Castillo V, Albaladejo J, 2006. Measuring soil erosion by field plots: Understanding the sources of variation. Earth-Science Reviews 78: 267-285.

Bombelli A, Gratani L, 2003. Interspecific differences of leaf gas exchange and water relations of three evergreen Mediterranean shrub species. Photosynthetica 41 (4): 619-625.

Booij MJ, 2003. Determination and integration of appropriate spatial scales for river basin modelling. Hydrol. Process. 17: 2581-2598.

Botelho da Costa J, 1995. Caracterização e constituição do solo (soil characterization and constitution), 5th ed. Calouste Gulbenkian Foundation, Lisbon.

Brandão C, Rodrigues R, Pinto da Costa J, 2001. Análise de fenómenos extremos: precipitações intensas em Portugal continental (extreme phenomena analysis: intense precipitations in continental Portugal). Water Institute (INAG), Lisbon.

Brandt CJ, Thornes JB (Eds.), 1996. Mediterranean desertification and land use. John Wiley and sons, Chichester.

Bussotti F, Borghini F, Celesti C, Leonzio C, 2003. Leaf shedding, crown condition and element return in two mixed holm oak forests in Tuscany, central Italy. For. Ecol. Manage. 176: 273-285.

Cardoso JVJC, 1965. Os solos de Portugal, sua classificação, caracterização e génese: 1- a sul do rio Tejo (Portuguese soils, their classification, characterization and genesis: 1- south from the Tagus river). General-Directorate for Agricultural Services, Lisbon.

Cardoso JC, Bessa MT, Marado MB, 1973. Carta dos solos de Portugal – 1:1.000.000 (Portuguese soil map – 1:1,000,000). Agronomia Lusitana 33 (1-4): 481-602.

Castelan-Estrada M, 2001. Répartition de la Biomasse chez Vitis vinifera L.; Rendement de Conversion du Rayonnement Solaire Global et Coûts Energétiques (biomass partitioning for Vitis vinifera L.; outputs of global solar radiation conversion and energetic costs). PhD Thesis, Institut National Agronomique Paris-Grignon, Paris.

Castillo VM, Gómez-Plaza A, Martínez-Mena M. 2003. The role of antecedent soil water content in the runoff response of semiarid catchments: a simulation approach. J. Hydrol. 284:114–130.

Cerdà A, 1998. The influence of geomorphological position and vegetation cover on the erosional and hydrological processes on a Mediterranean hillslope. Hydrol. Process. 12: 661-671.

Chapra SC, 1997. Surface Water-Quality Modeling. McGraw-Hill, New York.

Chow VT, Maidment DR, Mays LW, 1988. Applied Hydrology. McGraw-Hill, New York.

Cook JA, Ward WR, Wicks AS, 1983. Phosphorus deficiency in California vineyards. Calif. Agric. 37: 16-18.

Correia MJ, Pereira JS, Chaves MM, Rodrigues ML, Pacheco CA, 1995. ABA xylem concentrations determine maximum daily leaf conductance of field-grown Vitis vinifera L. plants. Plant Cell Environ. 18: 511-521.

Coutinho MA, Tomás PP, 1995. Characterization of raindrop size distributions at the Vale-Formoso-Experimental-Erosion-Center. Catena 25 (1-4): 187-197.

David TS, Ferreira MI, David JS, Pereira JS, 1997. Transpiration from a mature Eucalyptus globulus plantation in Portugal during a spring-summer period of progressively higher water deficit. Oecologia 110: 153-159.

David TS, Ferreira MI, Cohen S, Pereira JS, David JS, 2004. Constraints on transpiration from an evergreen oak tree in southern Portugal. Agric. For. Meteorol. 122: 193-205.

de Lima JLMP, van Dijk PM, Spaan WP, 1992. Splash - saltation transport under wind - driven rain. Journal of Soil Technology 5: 151 - 166.

de Lima JLMP, Singh VP, 2002. The influence of the pattern of moving rainstorms on overland flow. Advances on Water Resources 25 (7): 817-828.

de Lima JLMP, Torfs PJJF, Singh VP, 2002. A mathematical model for evaluating the effect of wind on downward-spraying rainfall simulators. CATENA 46: 221-241.

de Lima JLMP, Singh VP, 2003. Laboratory experiments on the influence of storm movement on overland flow. Journal Physics and Chemistry of the Earth 28 (6-7): 277-282.

de Lima JLMP, Singh VP, de Lima MIP, 2003. The influence of storm movement on water erosion: Storm direction and velocity effects. CATENA 52: 39-56.

de Lima MIP, 1998. Multifractals and the temporal structure of rainfall. PhD thesis, Wageningen University, Wageningen.

de Macedo MERZ, 1996. Aplicação do radar meteorológico na previsão de cheias (meteorological radar application for flood prediction). MSc thesis in Geophysical Sciences, Faculty of Sciences, University of Lisbon, Lisbon.

de Melo-Abreu JP, Barranco D, Cordeiro AM, Tous J, Rogado BM, Villalobos FJ, 2004. Modelling olive flowering date using chilling for dormancy release and thermal time. Agric. For. Meteorol. 125: 117-127.

de Vente J, Poesen J, 2005. Predicting soil erosion and sediment yield at the basin scale: Scale issues and semi-quantitative models. Earth-Science Reviews 71: 95–125.

Deguchi A, Hattori S, Park H-T, 2006. The influence of seasonal changes in canopy structure on interception loss: Application of the revised Gash model. Journal of Hydrology 318: 80–102.

Dijk PM van, de Lima JLMP, Stroosnijder L, 1996. The influence of rainfall on transport of beach sand by wind. Earth Surface Processes and Landforms 21: 341-352.

Doerr SH, Ferreira AJD, Walsh RPD, Shakesby RA, Leighton-Boyce G, Coelho COA, 2003. Soil water repellency as a potential parameter in rainfall-runoff modelling: experimental evidence at point to catchment scales from Portugal. Hydrol. Process. 17 (2): 363-377.

dos Santos TAG, 2003. Actualização de cartografia temática com imagens de satélite (actualizing tematic cartography using satellite images). MSc Thesis in Geographical Information Systems, Technical Superior Institute, Technical University of Lisbon, Lisbon.

Driessen P, Deckers J, Spaargaren O, Nachtergaele F, 2001. Lecture notes on the major soils of the world. World soil resources report no. 94, United Nations Food and Agriculture Organization (FAO), Rome.

Eagleson PS, 1978. Climate, soil and vegetation: The distribution of annual precipitation derived from observed storm sequences. Water Resources Research 14 (5): 713-721.

EEA: European Environmental Agency, 1995. CORINE Land Cover. European Environmental Agency, Commission of the European Communities, Copenhagen.

Erpul G, Norton LD, Gabriels D, 2002. Raindrop-induced and wind-driven soil particle transport. Catena 47 (3): 227-243.

Foster GR, 1982. Modeling the erosion process. In: Haan CT, Johnson HP, Brakensiek DL (Eds.), Hydrologic Modeling of Small Watersheds. American Society of Agricultural Engineers, St. Joseph: 295-380.

Foufoula-Georgiou E, Georgakakos KP, 1991. Hydrologic advances in space time precipitation modeling and forecasting. In: Bowles DS, O'Connell PE (Eds.), Recent advances in the modeling of hydrologic systems. NATO ASI Series, Serie C: mathematical and physical sciences, vol. 345, Kluwer Academic Publishers, Dordrecht: 47-65.

Favis-Mortlock D, Boardman J, MacMillan V, 2001. The limits of erosion modeling: why we should proceed with care. In: Harmon RS, Doe WW (Eds.), Landscape Erosion and Evolution Modeling. Kluwer Academic/Plenum Publishers, New York: 477-516.

Ferrer-Julià M, Estrela-Monreal T, Sánchez del Corral Jiménez A, García-Meléndez E, 2004. Constructing a saturated hydraulic conductivity map of Spain using pedotransfer functions and spatial prediction. Geoderma 123 (3 and 4): 257-277.

Filella I, Peñuelas J, Llorens L, Estiarte M, 2004. Reflectance assessment of seasonal and annual changes in biomass and CO2 uptake of a Mediterranean shrubland submitted to experimental warming and drought. Remote Sens. Environ. 90: 308-318.

Flanagan DC, Nearing MA, 1995. USDA Water Erosion Prediction Project – Hillslope Profile and Watershed Model Documentation. NSERL Report no. 10, National Soil Erosion Research Laboratory, United States Department of Agriculture – Agricultural Research Service (USDA-ARS), West Laffayette.

García-Mozo H, Galán C, Aira MJ, Belmonte J, Díaz de la Guardia C, Fernández D, Gutierrez AM, Rodriguez FJ, Trigo MM, Dominguez-Vilches E, 2002. Modelling start of oak pollen season in different climatic zones in Spain. Agric. For. Meteorol. 110: 247-257.

García-Ruiz JM, Arnaéz J, Beguería S, Seeger M, Martí-Bono C, Regüés D, Lana-Renault N, White S, 2005. Runoff generation in an intensively disturbed, abandoned farmland catchment, Central Spanish Pyrenees. Catena 59: 79–92.

Gardea AA, Martinez-Tellez MA, Sanchez A, Baez M, Siller JH, Gonzalez G, Baez R, Crisosto CH, Criddle RS, 1994. Post-Harvest Weight Loss of Flame Seedless Clusters. Proceedings of the International Symposium on Table Grape Production 1994: 203-206.

Giorio P, Sorrentino G, d'Andria R, 1999. Stomatal behaviour, leaf water status and photosynthetic response in field-grown olive trees under water deficit. Environ. Exp. Bot. 42: 95-104.

Gómez-Plaza A, Alvarez-Rogel J, Albaladejo J, Castillo VM, 2000. Spatial patterns and temporal stability of soil moisture across a range of scales in a semi-arid environment. Hydrol. Process. 14: 1261-1277.

Gonçalves MC, Reis LCL, Pereira MV, 2005. Progress of soil survey in Portugal. In: Jones RJA, Houšková B, Bullock P, Montanarella L (Eds.), Soil Resources of Europe, 2nd ed. Research report no. 9 (EUR 20559 EN), European Soil Bureau, European Commission Joint Research Centre, Ispra: 275-279.

Govers G, 1990. Empirical relationships for the transporting capacity of overland flow. International Association of Hydrological Sciences Publication 189: 45-63.

Hessel R, 2005. Effects of grid cell size and time step length on simulation results of the Limburg soil erosion model (LISEM). Hydrol. Process. 19 (15): 3037-3049.

Hoff C, Rambal S, Joffre R, 2002. Simulating carbon and water flows and growth in a Mediterranean evergreen Quercus ilex coppice using the FOREST-BGC model. For. Ecol. Manage. 164: 121-136.

Hoyningen-Huene Jv, 1983. Die Interzeption des Niederschlages in landwirtschaftlichen Pflanzenbeständen (rainfall interception in agricultural plants). DVWK-Schrift Nr. 57, Verlag Paul Parey, Hamburg / Berlin.

IGP: Instituto Geográfico Português, 1990. Carta de ocupação do solo COS 90 (COS 90 land occupation map). Portuguese Geographical Institute, Lisbon.

Imeson AC, Lavee H, 1998. Soil erosion and climate change: the transect approach and the influence of scale. Geomorphology 23: 219–227.

INE: Instituto Nacional de Estatística. 2006. INFOLINE – servíço de informação online do INE (INFOLINE – INE online information system). Available online in www.ine.pt (accessed in June 2006). National Statistics Institute, Lisbon.

Infante JM, Damesin C, Rambal S, Fernández-Alés R, 1999. Modelling leaf gas exchange in holm-oak trees in southern Spain. Agric. For. Meteorol. 95: 203-223.

Infante JM, Domingo F, Férnandez-Alés R, Joffre E, Rambal S, 2003. Quercus ilex transpiration as affected by a prolonged drought period. Biol. Plant. 46 (1): 49-55.

INIA-LQARS: Instituto Nacional de Investigação Agrária – Laboratório Químico Agrícola Rebelo da Silva, 2000. Manual de fertilização das culturas (culture fertilization manual). Ministry for Agriculture, Rural Development and Fisheries, Lisbon.

Jacobs CMJ, van den Hurk BJJM, de Bruin HAR, 1996. Stomatal behaviour and photosynthetic rate of unstressed grapevines in semi-arid conditions. Agric. For. Meteorol. 80: 111-134.

Jarvis A, Reuter HI, Nelson A, Guevara E, 2006. Hole-filled seamless SRTM data V3. Available online in srtm.csi.cgiar.org (accessed in December 2006). International Centre for Tropical Agriculture (CIAT), Cali.

Jensen M, 1984. Runoff pattern and peak flows from moving block rains based on linear time-area curve. Nordic Hydrology 15: 155-168.

Jetten V, de Roo A, Favis-Mortlock D, 1999. Evaluation of field-scale and catchment-scale soil erosion models. Catena 37 (4): 521-541.

Jetten V, Govers G, Hessel R, 2003. Erosion models: quality of spatial predictions. Hydrol. Process. 17: 887-900.

Johnson LF, 2003. Temporal stability of an NDVI-LAI relationship in a Napa Valley vineyard. Aust. J. Grape Wine Res. 9: 96-101.

Kamphorst EC, Jetten V, Guerif J, Pitkanen J, Iversen BV, Douglas JT, Paz A, 2000. Predicting depressional storage from soil surface roughness. Soil Sci. Soc. Am. J. 64 (5): 1749-1758.

Kirkby M, Bracken L, Reaney S, 2002. The influence of land use, soils and topography on the delivery of hillslope runoff to channels in SE Spain. Earth Surf. Process. Landforms 27: 1459–1473.

Kirkby MJ, Bracken LJ, Shannon J, 2005. The influence of rainfall distribution and morphological factors on runoff delivery from dryland catchments in SE Spain. Catena 62: 136–156.

Klein I, Strime M, Fanberstein L, Mani Y, 2000. Irrigation and fertigation effects on phosphorus and potassium nutrition of wine grapes. Vitis 39 (2): 55-62.

Korner C, 1994. Leaf diffusive conductances in the major vegetation types of the globe. In: Schulze E-D, Caldwell MM (Eds.), Ecophysiology of Photosynthesis, Springer-Verlag, Berlin: 463-485.

Ladoy P, Lovejoy S, Schertzer D, 1991. Extreme variability of climatological data: scaling and intermittency. In: Schertzer D, Lovejoy S (Eds.), Non linear variability in Geophysics: scaling and fractals. Kluwer Academic Publishers, Dordrecht: 241 250.

Landsberg JJ, Hingston FJ, 1996. Evaluating a simple radiation/dry matter conversion model using data from Eucalyptus globulus plantations in Western Australia. Tree Physiol. 16: 801-808.

Lane LJ, Hernandez M, Nichols M, 1997. Processes controlling sediment yield from watersheds as functions of spatial scale. Environmental Modelling & Software 12 (4): 355-369.

Lebon E, Dumas V, Pieri P, Schultz HR, 2003. Modelling the seasonal dynamics of the soil water balance in vineyards. Funct. Plant Biol. 30: 699-710.

Lencastre A, Franco FM, 1992. Lições de hidrologia (lessons in hydrology), 2nd ed. New University of Lisbon Editorial Services, Lisbon.

Lhomme JP, Rocheteau A, Ourcival JM, Rambal S, 2001. Non-steady-state modelling of water transfer in a Mediterranean evergreen canopy. Agric. For. Meteorol. 108: 67-83.

Llorens i Guasch, L, 2003. Plant ecophysiological responses to experimentally drier and warmer conditions in European shrublands. PhD Thesis, Centre de Recerca Ecològica i Aplicacions Florestals, Universitat Autònoma de Barcelona, Barcelona.

Lillesand TM, Kiefer RW, 2000. Remote sensing and image interpretation, 4th ed. John Wiley and Sons, Chichester.

Lu P, Yunusa IAM, Walker RR, Müller WJ, 2003. Regulation of canopy conductance and transpiration and their modelling in irrigated grapevines. Funct. Plant Biol. 30(6): 689-698.

Mairota P, Thornes JB, Geeson N (Eds.), 1998. Atlas of Mediterranean environments in Europe. John Wiley and Sons, Chichester.

Maksimov VA, 1964. Computing runoff produced by a heavy rainstorm with a moving center. Sov. Hydrol. 5: 510-513.

Mariscal MJ, Orgaz F, Villalobos FJ, 2000a. Modelling and measurement of radiation interception by olive canopies. Agric. For. Meteorol. 100: 183-197.

Mariscal MJ, Orgaz F, Villalobos FJ, 2000b. Radiation-use efficiency and dry matter partitioning of a young olive (Olea europaea) orchard. Tree Physiol. 20: 65-72.

Maroco JP, Breia E, Faria T, Pereira JS, Chaves MM, 2002. Effects of long-term exposure to elevated CO2 and N fertilization on the development of photosynthetic capacity and biomass accumulation in Quercus suber L. Plant Cell Environ. 25 (1): 105-113.

Martínez-Vilalta J, Piñol J, Beven K, 2002. A hydraulic model to predict drought-induced mortality in woody plants: an application to climate change in the Mediterranean. Ecol. Model. 155 (2-3): 127-147.

Medlyn BE, Barton CVM, Broadmeadow MSJ, Ceulemans R, De Angelis P, Forstreuter M, Freeman M, Jackson SB, Kellomäki S, Laitat E, Rey A, Roberntz P, Sigurdsson BD, Strassemeyer J, Wang K, Curtis PS, Jarvis PG, 2001. Stomatal conductance of forest species after long-term exposure to elevated CO2 concentration: a synthesis. New Phytol. 149: 247-264.

Morgan RPC, Quinton JN, 2001. Erosion Modeling. In: Harmon RS, Doe WW (Eds.), Landscape Erosion and Evolution Modeling. Kluwer Academic/Plenum Publishers, New York: 117-143.

Motovilov YG, Gottschalk L, Engeland K, Rodhe A, 1999. Validation of a distributed hydrological model against spatial observations. Agricultural and Forest Meteorology 98-99: 257-277.

Moutinho-Pereira JM, Correia CM, Gonçalves BM, Bacelar EA, Torres-Pereira JM, 2004. Leaf gas exchange and water relations of grapevines grown in three different conditions. Photosynthetica 42 (1): 81-86.

Nearing MA, Govers G, Norton LD, 1999. Variability in soil erosion data from replicated plots. Soil Sci. Soc. Am. J. 63: 1829-1835.

Neitsch SL, Arnold JG, Kiniry JR, Srinivasan R, Williams JR, 2002. Soil and Water Assessment Tool user's manual. TWRI report TR-192, Texas Water Resources Institute, College Station.

Nelson RL, 2003. CropSyst: Cropping Systems Simulation Model. Available online in bsyse.wsu.edu/cropsyst (accessed in August 2004). Washington State University, Pullman.

Nielsen DC, Vigil MF, Anderson RL, Bowman RA, Benjamin JG, Halvorson AD, 2002. Cropping System Influence on Planting Water Content and Yield of Winter Wheat. Agron. J. 94: 962-967.

Nunes JP, de Lima JLMP, Singh VP, de Lima MIP, Vieira GN, 2006. Numerical modelling of surface runoff and erosion due to moving rainstorms at the drainage basin scale. J. Hydrol. 330 (3-4): 709-720.

Oostwoud Wijdenes DJ, Poesen J, Vandekerckhove L, Nachtergaele J, de Baerdemaeker J, 1999. Gully-head morphology and implications for gully development on abandoned fields in a semi-arid environment, Sierra de Gata, Southeast Spain. Earth Surf. Process. Landforms 24: 585-603.

Palutikof JP, Conte M, Casimiro Mendes J, Goodess CM, Espirito Santo F, 1996. Climate and climate change. In: Brandt CJ, Thornes JB (Eds.), Mediterranean desertification and land use. John Wiley and sons, Chichester: 43-86.

Peñuelas J, Llusia J, Piñol J, Filella I, 1997. Photochemical reflectance index and leaf photosynthetic radiation-use-efficiency assessment in Mediterranean trees. Int. J. Remote Sens. 18 (13): 2863-2868.

Pérez-Latorre AV, Cabezudo B, 2002. Use of monocharacteristic growth forms and phenological phases to describe and differentiate plant communities in Mediterranean-type ecosystems. Plant Ecol. 161: 231-249.

Pimenta MT, 1998. Directrizes para a aplicação da Equação Universal de Perda dos Solos em SIG – factor de cultura C e factor de erodibilidade do solo K (directions for the application of the Universal Soil Loss Equation in GIS – culture factor C and soil erodibility factor K. Water Institute (INAG), Lisbon.

Poesen JWA, Hooke JM, 1997. Erosion, flooding and channel management in Mediterranean environments of southern Europe. Progress in Physical Geography 21: 157–199.

Ponce Álvares MT, Pimenta MT, 1998. Erosão e transporte sólido em pequenas bacias hidrográficas (erosion and soil transport in small watersheds). Water Institute (INAG), Lisbon.

Proietti P, Antognozzi E, 1996. Effect of irrigation on fruit quality of table olives (Olea europaea), cultivar "Ascolana tenera". New Zealand Journal of Crop and Horticultural Science 24: 175-181.

Puigdefabregas J, del Barrio G, Boer MM, Gutiérrez L, Solé B, 1998. Differential responses of hillslope and channel elements to rainfall events in a semi-arid area. Geomorphology 23: 337-351.

Rachman A, Anderson SH, Gantzer CJ, Thompson AL, 2003. Influence of Long-term Cropping Systems on Soil Physical Properties Related to Soil Erodibility. Soil Sci. Soc. Am. J. 67: 637-644.

Raclot D, Albergel J, 2006. Runoff and water erosion modelling using WEPP on a Mediterranean cultivated catchment. Physics and Chemistry of the Earth 31: 1038–1047.

Rapp M, Regina IS, Rico M, Gallego HA, 1999. Biomass, nutrient content, litterfall and nutrient return to the soil in Mediterranean oak forests. For. Ecol. Manage. 119: 39-49.

Rawls WJ, Brakensiek DL, Miller N, 1983. Green-ampt infiltration parameters from soils data. Journal of Hydraulic Engineering-ASCE 109 (1): 62-70.

Refsgaard JC, 1997. Parameterisation, calibration and validation of distributed hydrological models. J. Hydrol. 198: 69-97.

Refsgaard JC, Henriksen HJ, 2004. Modelling guidelines—terminology and guiding principles. Advances in Water Resources 27: 71–82.

Romero-Díaz A, Cammeraat LH, Vacca A, Kosmas C, 1999. Soil erosion at three experimental sites in the Mediterranean. Earth Surf. Process. Landforms 24: 1243-1256.

Roxo MJ, 1994. A acção antrópica no processo de degradação de solos: a serra de Serpa e Mértola (anthropic activity in the soil degradation process: the Serpa and Mértola mountain range). PhD thesis in Geography and Regional Planning, Faculty of Social and Human Sciences, New University of Lisbon, Lisbon.

Roxo MJ, Cortesão Casimiro P, Soeiro de Brito R, 1996. Inner lower Alentejo field site: cereal cropping, soil degradation and desertification. In: Brandt CJ, Thornes JB (Eds.), Mediterranean desertification and land use. John Wiley and sons, Chichester: 111-135.

Roxo MJ, Cortesão Casimiro P, 1998. Human impact on land degradation in the inner Alentejo, Mértola, Portugal. In: Mairota P, Thornes JB, Geeson N (Eds.), Atlas of Mediterranean environments in Europe. John Wiley and Sons, Chichester: 106-109.

Sala A, Tenhunen JD, 1996. Simulations of canopy net photosynthesis and transpiration in Quercus ilex L. under the influence of seasonal drought. Agric. For. Meteorol. 78: 203-222.

Salisbury FW, Ross CW, 1991. Plant Physiology, 2nd ed. Wadsworth Inc., Belmont.

Saxton KE, Rawls WJ, Romberger JS, Papendick RL, 1986. Estimating generalized soil-water characteristics from texture. Soil Sci. Soc. Am. J. 50(4): 1031-1036.

Schulze ED, Kelliher FM, Korner C, Lloyd C, Leuning R, 1994. Relationships among maximum stomatal conductance, ecosystem surface conductance, carbon assimilation rate, and plant nitrogen nutrition: a global ecology scaling exercise. Annu. Rev. Ecol. Syst. 25: 629-660.

Scurlock JMO, Asner GP, Gower ST, 2001. Global Leaf Area Index from Field Measurements, 1932-2000. Available online in www.daac.ornl.gov (accessed in August 2004). Oak Ridge National Laboratory Distributed Active Archive Center, Oak Ridge.

Seixas J, 2000. Assessing heterogeneity from remote sensing images: the case of desertification in southern Portugal. Int. J. Remote Sensing 21 (13 and 14): 2645–2663.

Sharon D, 1980. The distribution of hydrologically effective rainfall incident on sloping ground. Journal of Hydrology 46: 165-188.

Singh VP, 1998. Effect of the direction of storm movement on planar flow. Hydrological Processes 12: 147-170.

Singh VP, 2002a. Effect of the duration and direction of storm movement on infiltrating planar flow with full areal coverage. Hydrological Processes 16: 1479-1511.

Singh VP, 2002b. Effect of the duration and direction of storm movement on planar flow with full and partial areal coverage. Hydrological Processes 16: 3437-3466.

Silva JRM, Ferreira AG, Tomás PMPP, 1998. Rainfall Characteristics and Soil Erosion in Alentejo. Geoökodynamik XIX: 249-255.

Skaggs TH, Arya LM, Shouse PJ, Mohanty BP, 2001. Estimating Particle-Size Distribution from Limited Soil Texture Data. Soil Sci. Soc. Am. J. 65: 1038-1044.

SNIRH: Sistema Nacional de Informação de Recursos Hídricos, 2006. Sistema Nacional de Informação de Recursos Hídricos (National Hydrological Resources Information System). Avaliable online in snirh.pt (accessed in December 2006). Water Institute (INAG), Lisbon.

Tognetti R, Johnson JD, Michelozzi M, Raschi A, 1998. Response of foliar metabolism in mature trees of Quercus pubescens and Quercus ilex to long-term elevated CO2. Environ. Exp. Bot. 39: 233-245.

Tognetti R, Minnocci A, Peñuelas J, Raschi A, Jones MB, 2000. Comparative field water relations of three Mediterranean shrub species co-occuring at a natural CO2 vent. J. Exp. Bot. 51 (347): 1135-1146.

Tognetti R, Sebastiani L, Vitagliano C, Raschi A, Minnocci A, 2001. Responses of two olive tree (Olea europaea L.) cultivars to elevated CO2 concentration in the field. Photosynthetica 39 (3): 403-410.

Tomás PMPP, Coutinho MMJA, 1993. Estudo da erosão hídrica em solos agrícolas: comparação da perda de solo observada e calculada pela Equação Universal de Perda de Solo (studying soil erosion in agricultural soils: comparing observed soil loss with calculations using the Universal Soil Loss Equation). Recursos Hídricos 15 (3): 3-17.

Toy TJ, Foster GR, Renard KG, 2002. Soil erosion: processes, prediction, measurement, and control. John Wiley and Sons, New York.

UNEP: United Nations Environment Program, 1997. World Atlas of Desertification, 2nd ed. Middleton N, Thomas D (Eds.), UNEP, London.

USDA: United States Department of Agriculture, 1986. Urban Hydrology for Small Watersheds. Natural Resources Conservation Service, Conservation Engineering Division, Technical Release 55.

Vandaele K, Poesen J, Marques de Silva JR, Govers G, Desmet P, 1997. Assessment of factors controlling ephemeral gully erosion in Southern Portugal and Central Belgium using aerial photographs. Zeitschrift fur Geomorphologie 41 (3): 273-287.

Vandekerckhove L, Poesen J, Wijdenes DO, de Figueiredo T, 1998. Topographical thresholds for ephemeral gully initiation in intensively cultivated areas of the Mediterranean. Catena 33 (3-4): 271-292.

Vandekerckhove L, Poesen J, Wijdenes DO, Gyssels G, 2001. Short-term bank gully retreat rates in Mediterranean environments. Catena 44 (2): 133-161.

Veitzer SA, Gupta VK, 2001. Statistical self-similarity of width function maxima with implications to floods. Advances in Water Resources 24: 955-965.

Villalobos FJ, Orgaz F, Mateos L, 1995. Non-destructive measurement of leaf area in olive (Olea europaea L.) trees using a gap inversion method. Agric. For. Meteorol. 73: 29-42.

Wagener T, 2003. Evaluation of catchment models. Hydrol. Process. 17: 3375–3378.

Wainwright J, Thornes JB, 2004. Environmental Issues in the Mediterranean. Routledge, London.

Whitehead D, Beadle CL, 2004. Physiological regulation of productivity and water use in Eucalyptus: a review. For. Ecol. Manage. 193 (1-2): 113-140.

Williams DW, Andris HL, Beede RH, Luvisi DA, Norton MVK, Williams LE, 1985. Validation of a model for the growth and development of the Thompson Seedless grapevine. II. Phenology. American Journal of Enology and Viticulture 36: 283-289.

Williams JR, 1995. Chapter 25: The EPIC model. In: Singh VP (Ed.), Computer models of watershed hydrology. Water Resources Publications, Highlands Ranch: 909-1000.

Wilson CB, Valdes JB, Rodrigues-Iturbe I, 1979. On the influence of the spatial distribution of rainfall on storm runoff. Water Resources Research 15 (2): 321-328.

Xu J, Lathrop RG, 1995. Improving Simulation Accuracy of Spread Phenomena in a Raster-based Geographic Information System. Int. J. Geographical Information Systems 9 (2): 153-168.

Xu C-Y, Singh VP, 2004. Review on Regional Water Resources Assessment Models under Stationary and Changing Climate. Water Resources Management 18: 591-612.

Yen BC, Chow VT, 1968. A study of surface runoff due to moving rainstorms. Hydraulic Engineering Series No. 17, Department of Civil Engineering, University of Illinois, Urbana.

5. Impacts of climate change on the biophysical drivers for desertification

The previous chapter described the study areas, and described and evaluated the application of both the SWAT and MEFIDIS models. This chapter presents the main results of this thesis, following the objectives and methods described in chapter 3. The chapter begins with the analysis of the **Sensitivity to changes in climate at the seasonal scale**, using the SWAT model, followed by an analysis of the **Sensitivity to changes in climate at the extreme event scale**, using the MEFIDIS model. Finally, the section presents the **Watershed response to climate change scenarios**, a test combining the PROMES regional climate model with both the SWAT and MEFIDIS catchment models. Section 3.1 describes the rationale behind these analyses, and the framework which supports them; a graphical illustration of the results presented in this chapter and their overall place in the vulnerability assessment methodology used in this thesis is shown in Figure 5.1

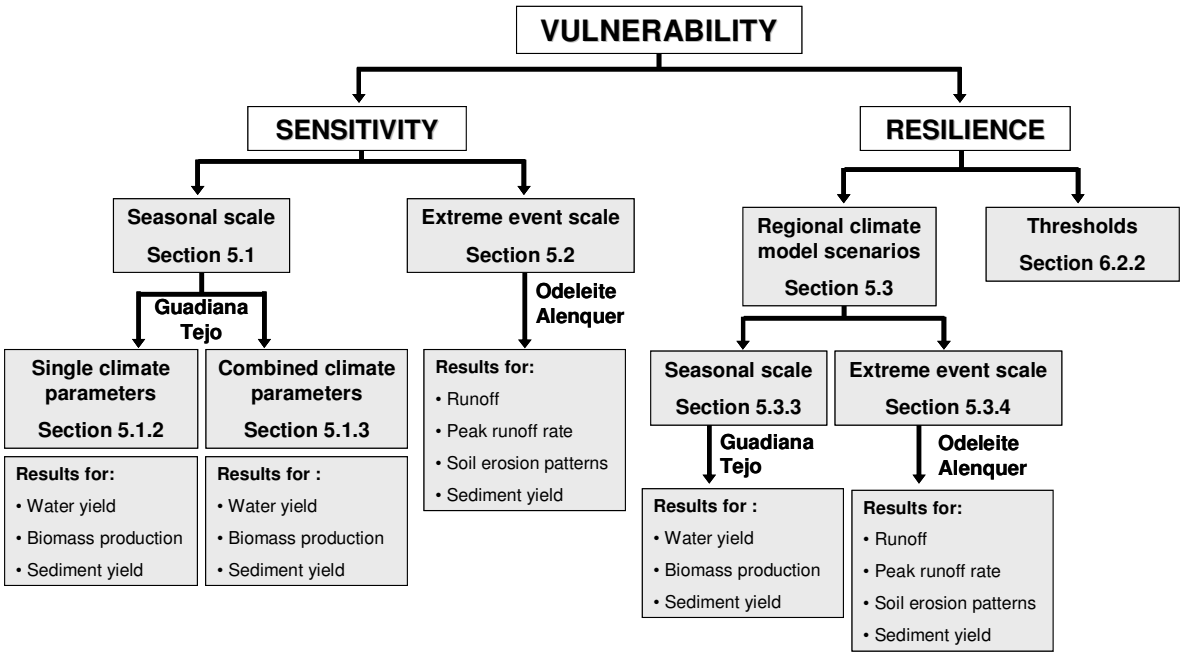

Figure 5.1 – Roadmap for the results shown in this chapter, following the vulnerability analysis framework described in section 3.1.

5.1 Sensitivity to changes in climate at the seasonal scale

The first part of this section analyses the response of hydrology, soil erosion and vegetation productivity to changes in temperature, rainfall and atmospheric CO_2 concentration in an integrated framework; the simulations are performed at the seasonal scale, with a resolution of one month and an extent of three decades, aiming to evaluate long-term responses to climate change. The analysis was performed for two contrasting Mediterranean regions located in Portugal, one humid and one semi-arid (see section 4), using the Soil and Water Assessment Tool (SWAT) watershed model (Neitsch et al., 2002; see section 3.4). It adapted the method applied by Pruski and Nearing (2002), extending the simulations to the watershed scale and to climate parameters beyond rainfall. This work combines incremental temperature, rainfall and CO_2 change scenarios (based on the range of predictions reported by Cunha et al., 2002, and PRUDENCE, 2007) to circumvent the uncertainty of climate change estimates. The results provide an assessment of the sensitivity of water runoff, biomass productivity and soil erosion to changes in climate, from which a trend can be extracted for policy design purposes. The work presented in this section has been accepted for publication (Nunes et al., in press).

5.1.1 Rationale and test description

The scenarios of climate change which include the Portuguese territory have a high variability, as shown in Figure 5.2. The Figure shows a compilation of 27 General Circulation Model (GCM) and Regional Climate Model (RCM) results for scenarios of change to current (1961-1990 normal) annual mean temperatures and rainfall values, for two scenarios of increased atmospheric CO_2 concentrations; the results were compiled from those reported by Cunha et al. (2002) and those reported in the PRUDENCE project (PRUDENCE, 2007; the project is described by Déqué et al., 2005). The authors reported results varying from +2 to +6 ºC increase in annual mean temperature, as well as annual rainfall changes from -36 % to +6 %, which do not appear to be correlated with temperature changes, although there is a slightly higher tendency for rainfall decrease for the double CO_2 scenarios.

The framework for this exercise is described in section 3.1. It adapted the approach from Pruski and Nearing (2002) for single slope scenarios to assess the response to climate changes, by (a) including temperature, CO_2 concentration and rainfall changes, and (b) upscaling the simulations to the watershed scale. The SWAT model was ran with several changes in rainfall, temperature and CO_2 concentration, using the model's in-built weather generator to generate 30-year weather series with changed average values. The analysis of the results included correlating changes in precipitation, temperature and CO_2 to changes in

evapotranspiration, water runoff and upslope soil erosion. Runoff was further decomposed into surface runoff (i.e. direct runoff) and subsurface runoff.

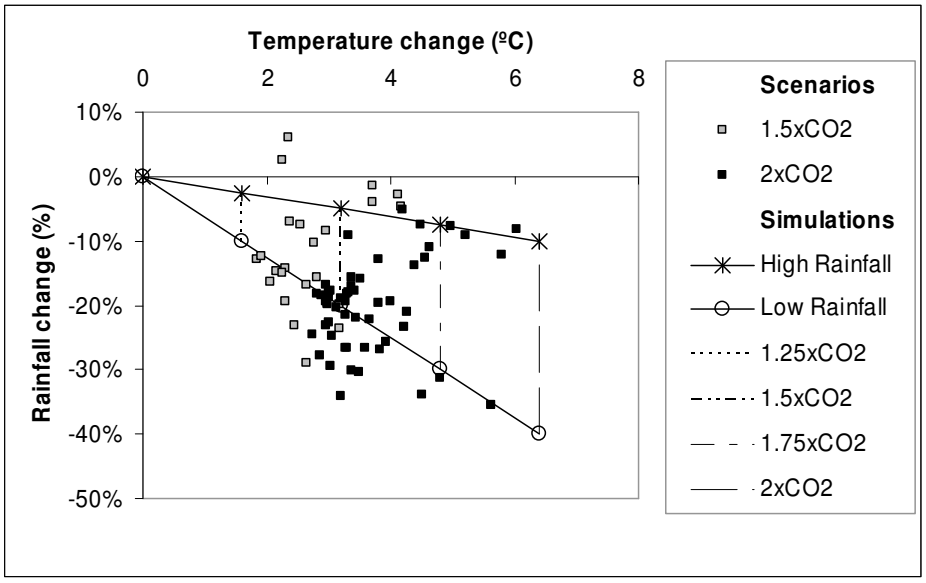

Figure 5.2 – Relation between climate change scenarios for temperature and rainfall, for central and southern Portugal, following Cunha et al. (2002) and the PRUDENCE (2007) project results (with approximate CO_2 concentrations); the lines represent the coupled simulation sets used in this work.

Two simulation sets were performed to assess the sensitivity of hydrological parameters, soil erosion and productivity: (1) sensitivity analysis to changes in single climate parameters, to assess responses to systematic changes in climate variables to detect meaningful trends; and (2) sensitivity analysis to simultaneous changes to all climate parameters, with the combination of changes chosen from within the GCM and RCM prediction range, to verify possible interactions of the effects of simultaneously changing several climate variables. The results focus on annual averages; spatial distribution was assessed for different vegetation covers, as the differences between watersheds and soil types did not appear significant. The results from the two simulation sets are presented in the following sections.

5.1.2 Sensitivity analysis to changes in single climatic parameters

The sensitivity of runoff, vegetation productivity and soil erosion to changes in temperature, rainfall and CO_2 concentrations was examined independently. The tests proceeded in steps of

1.6 ºC increase to current average annual temperature, -10 % decrease to current average annual rainfall, and 25 % increase to current average CO2 concentrations. Current climate refers to the 1961-1990 climate normals referred in section 4, while a current CO_2 concentration of 330 ppm was used. The maximum change was of +6.4 ºC to temperature, -40 % to rainfall and +100 % to CO_2 concentrations. Three scenarios of change to precipitation were considered: changes to rainfall intensity only, changes to rainfall frequency (keeping intensity unchanged), and changes evenly distributed between the two parameters. Changes to rainfall intensity were made by reducing total rainfall while keeping the number of rain days constant; changes to rainfall frequency were simulated by reducing both total rainfall and the number of rain days in a proportional amount. When changing rainfall intensity, the maximum possible 30-min rainfall rate value was also changed proportionally.

Water runoff response

The responses of evapotranspiration and runoff (surface and subsurface) to climate parameter changes are shown in Table 5.1, and illustrated in Figure 5.3. In both study areas, water yield decreased with increasing temperatures – as rainwater was diverted for evapotranspiration – and decreasing rainfall. Changes to CO_2 concentrations had negligible impacts on runoff.

Changes to temperature affected mostly subsurface runoff due to the diversion of soil water to evapotranspiration. The impacts were greater in the Guadiana, where it changed by down to -50 %, compared with down to -38 % in the Tejo. Changes to rainfall affected both surface and subsurface runoff equally in the Tejo, which decreased down to -76 % and -82 %, respectively. In the Guadiana, however, rainfall changes had a significantly greater impact in subsurface runoff, with a decrease down to -85 % (compared with -62 % for surface runoff). This effect can be explained by the extremely shallow Lithosols which dominate the region, as described in section 4.2.4; the low water holding capacity of these soils would be quickly exceeded by the autumn, winter and spring storms where most rainfall is concentrated, resulting in a constant rainfall excess regardless of evapotranspiration deficits, a process which has also been observed in other Mediterranean regions by Ramos and Mulligan (2005). Moreover, changes to rainfall had a much greater effect over runoff than over evapotranspiration, which only decreased down to -16 to -18 % in both regions. The response to decreased rainfall was to channel an increasing percentage of water towards plant water use at the expense of runoff.

Table 5.1 – Response of evapotranspiration, surface runoff and subsurface runoff to changes in climatic parameters, in mm per year.

	Guadiana			**Tejo**		
	Evapotranspiration ($mm.y^{-1}$)	**Surface runoff ($mm.y^{-1}$)**	**Subsurface runoff ($mm.y^{-1}$)**	**Evapotranspiration ($mm.y^{-1}$)**	**Surface runoff ($mm.y^{-1}$)**	**Subsurface runoff ($mm.y^{-1}$)**
Control	*277*	*105*	*111*	*438*	*69*	*186*
T + 1.6ºC	290	103	92	455	67	169
T + 3.2ºC	301	100	77	475	66	151
T + 4.8ºC	313	98	65	497	64	132
T + 6.4ºC	324	96	56	517	62	115
PP - 10%	268	92	85	420	55	147
PP - 20%	262	71	58	406	38	104
PP - 30%	246	50	34	392	26	67
PP - 40%	228	37	20	369	17	34
CO_2 + 25%	274	106	113	433	69	190
CO_2 + 50%	273	106	114	431	70	192
CO_2 + 75%	272	106	114	429	70	193
CO_2 + 100%	272	106	115	428	70	194

These results compare well with those obtained by Pruski and Nearing (2002), who analyzed the effects of changing rainfall from -20% to +20 % in agricultural slopes using the WEPP model for different regions in the US. They found runoff changing on average -1.97 % per % decrease in rainfall (with rainfall intensity changing by half this amount), which compares well with the slope of the surface and subsurface runoff curves shown in Figure 5.3: -1.9 % per % decrease in rainfall for the Guadiana and -2.1 % per % decrease in the Tejo.

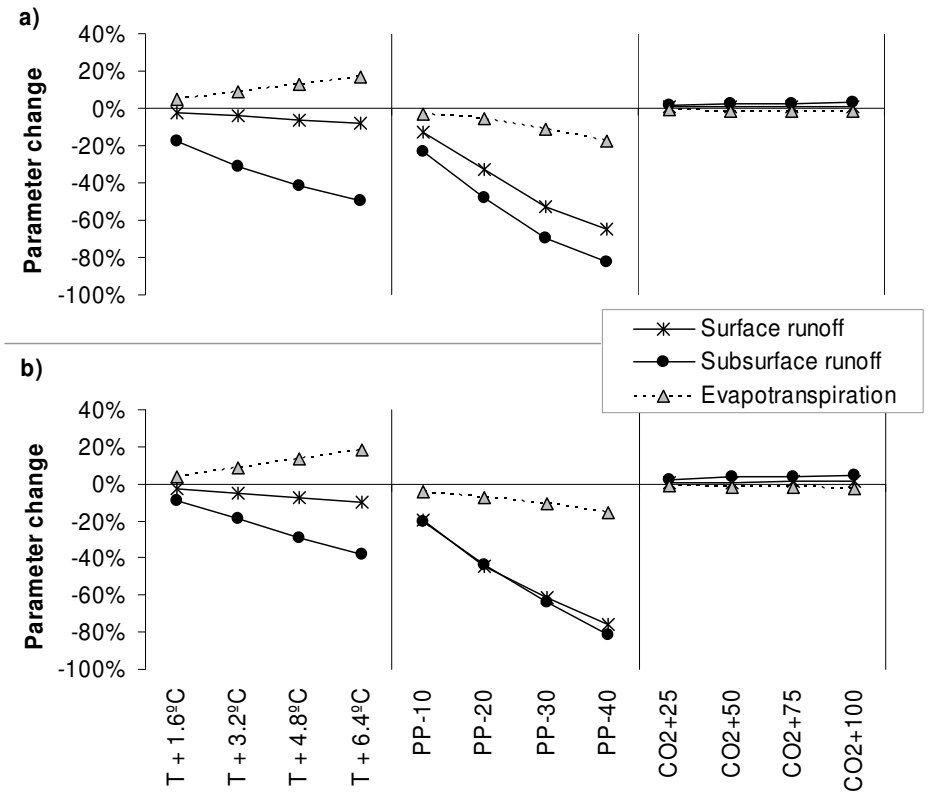

Figure 5.3 – Simulated responses of evapotranspiration, surface runoff and subsurface runoff to changes in temperature (T – left), rainfall (PP – center) and atmospheric CO_2 concentration (CO2 – right) for the Guadiana (a) and the Tejo (b).

The mode by which rainfall is changed – decreased rainfall intensity only, or decreased rainfall frequency while keeping intensity constant – led to different hydrological changes in the Guadiana region, as shown in Figure 5.4. A decrease in rainfall intensity (Figure 5.4 – right) leads to more significant changes in surface runoff than when intensity is kept constant (Figure 5.4 – left), a result also reported by Pruski and Nearing (2002) in the study referred above. This result can again be explained by the dominance of very shallow soils in the Guadiana, especially when comparing with the Tejo where this effect is much less pronounced.

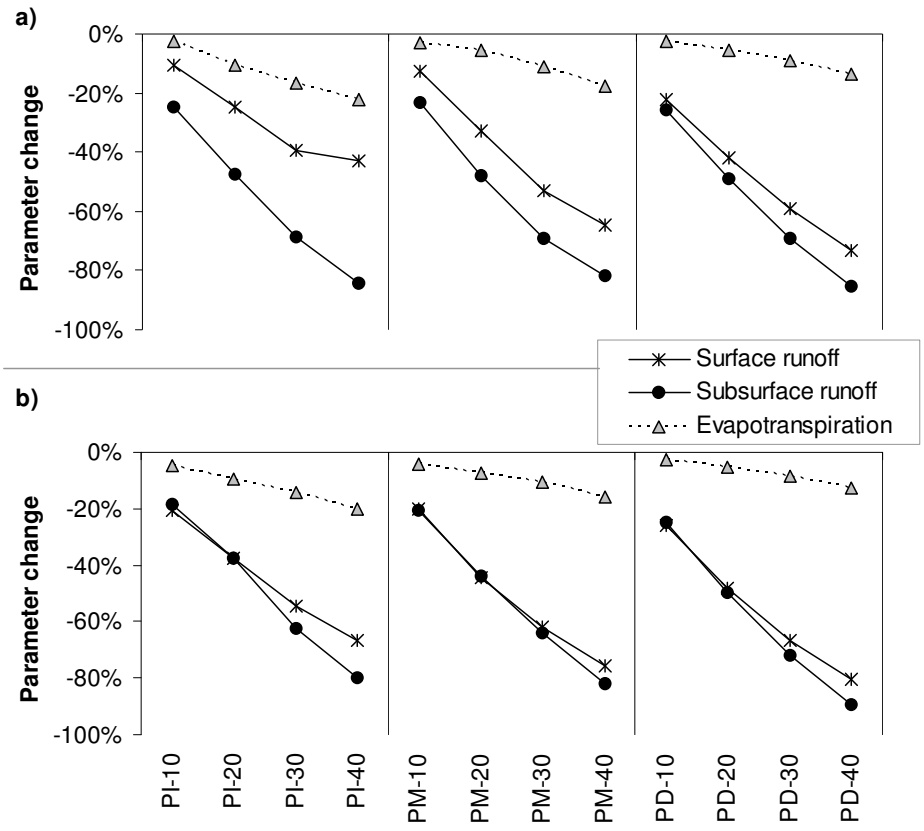

Figure 5.4 – Simulated responses of evapotranspiration, surface runoff and subsurface runoff to changes in rainfall, considering constant rainfall intensity (PI – left), intensity decreasing at half the decrease in rainfall rate (PM – center), and intensity decreasing at the same rate as rainfall (PD – right) for the Guadiana (a) and Tejo (b) watersheds.

Biomass growth response

The responses of the biomass growth of dominant vegetation types to climate parameter changes are shown in Figure 5.5, representing 98 % of the Guadiana area and 78 % of the Tejo area; in the latter case, the remainder is occupied by multiple vegetation covers, each representing less than 10 % of the total surface area. On average, biomass growth decreased with temperature increases, increased with larger CO_2 concentrations and appears to be insensitive to changes in rainfall; however, there was a significant difference between both the different vegetation types and the two test regions.

Increases in temperature led to systematic decreases of wheat biomass production in both regions, up to more than 40 %. In the Tejo, the production of vines (decreases down to -46 %) appears more sensitive than pine forests (down to -27 %). In the Guadiana, however, cork oak

productivity only started to significantly decrease (down to -15 %) after a 5 ºC increase in temperature. Mediterranean shrub productivity increased by 27 % with a 1.6 ºC temperature increase and appears to be insensitive to further increases. These results suggest different adaptation strategies of vegetation types; cork oaks appear to have some tolerance for temperature increases (up to 30 % according to Figure 5.5) and Mediterranean shrubs actually appear to benefit from warmer conditions.

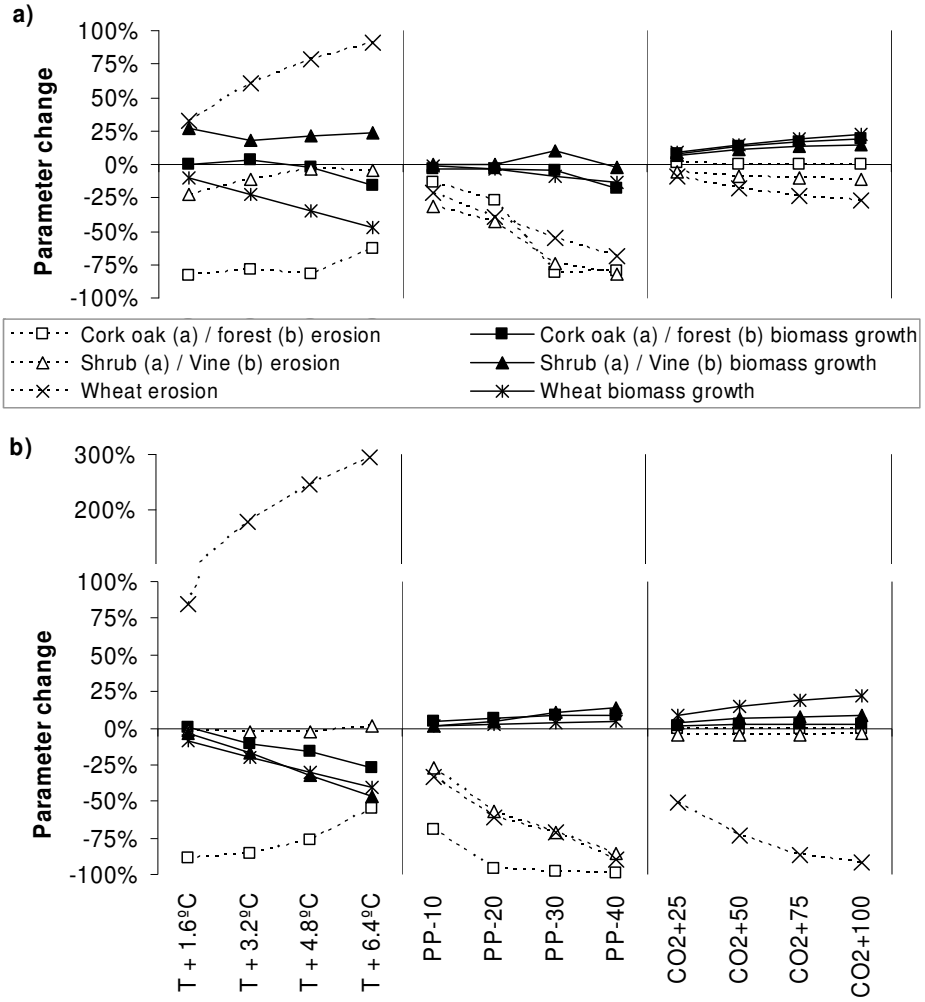

Figure 5.5 – Simulated responses of total biomass growth and soil erosion of different vegetation covers to changes in temperature (T – left), rainfall (PP – center) and atmospheric CO_2 concentration (CO2 – right) for the Guadiana (a) and Tejo (b) watersheds; the vegetation cover types are cork oaks, mediterranean shrubs and wheat for the Guadiana, and pine forest, vines and wheat for the Tejo.

Rainfall decreases led to negligible changes in vegetation biomass production, mainly in the Tejo, possibly due to the currently available rain water surpassing vegetation water requirements. In the Guadiana, however, rainfall decreases beyond -20 % led to decreases of down to -18 % in cork oak productivity, and down to -14 % in wheat productivity; the more arid conditions currently existing in this region could imply that wheat and cork oaks are growing close to their minimum water requirements, and are therefore more vulnerable to decreases in available rainwater.

Finally, increases in atmospheric CO_2 concentrations led to increases in vegetation biomass production for most species, with wheat productivity increasing up to 22 % in both regions, followed by cork oak (up to 19 % increase), Mediterranean shrubs (up to 14 %), and vines (up to 9 %); pine forests showed little response. The response of wheat, however, became smaller for greater changes to CO_2, with changes over 75 % having little additional consequences for biomass growth (Figure 5.5), implying a response threshold above which wheat stops responding to this parameter.

Soil erosion response

The percent changes of soil erosion to current conditions are shown in Figure 5.5. These values must be analyzed taking into consideration the current importance of soil erosion problems. Table 4.30 shows that current soil erosion rates are more significant in vineyards and wheat regions, especially when compared with the threshold of 2 to 12 $ton.ha^{-1}.y^{-1}$, below which normal soil regeneration is sufficient to compensate for soil losses (Romero-Díaz et al., 1999). Soil erosion decreases under cork oaks and pine forests have smaller impacts since current soil losses are already small; however, changes to soil erosion rates in vineyards and wheat regions can have significant potential impacts, either alleviating current soil loss problems or significantly increasing their severity. Therefore, the absolute erosion values should be kept in mind when analyzing the results of these tests.

The sensitivity of soil erosion to temperature, rainfall and CO_2 changes depended mainly on the combination of surface water yield and biomass growth responses, as can be seen by comparing Figure 5.3 with Figure 5.5 and therefore showed significant differences between vegetation types and regions. Thus, the results are presented for each vegetation type.

With increased temperatures, the decrease in wheat growth was more significant than the decrease in surface runoff (Figure 5.3), leading to an increase in erosion of up to almost 100 % in the Guadiana and up to almost 300 % in the Tejo. Inversely, the decrease in the growth

of cork oak (in Guadiana) and pine forest (in Tejo) was less significant that of surface runoff, and erosion decreased by more than 80 % for both species. However, after a 5 ºC increase in temperature, the growth of cork oak and pine started to decline and this is noticeable in the smaller rate of decrease of soil erosion, although corresponding to very small changes in absolute erosion rates as previously mentioned. Erosion under Mediterranean shrubs (in the Guadiana) and vines (in the Tejo) had little response to vegetation growth.

This type of erosion response was also observed to changed rainfall and CO_2 concentrations, although with less differences between vegetation types. When rainfall was decreased, surface runoff suffered the most significant reductions and erosion decreased for every vegetation type and region (Figure 5.3 and Figure 5.5), with maximum decreases in the range of -70 to -80 % in the Guadiana, and -90 to -100 % in the Tejo. Similarly, when CO_2 concentrations were increased, vegetation growth increased without significant changes to surface runoff, and erosion decreased slightly in most cases (Figure 5.3 and Figure 5.5), with exception for wheat areas with a decrease of about -30 % in the Guadiana and -100 % in the Tejo.

Finally, it should also be noticed in Figure 5.5 that soil erosion under wheat cultivation has a much higher response to changes in all climate parameters in the Tejo region, both for positive and negative responses. This could be explained by the median terrain slope, which is 42 % higher than the Guadiana, making soil loss more sensitive to changes to other erosive factors – in this case, surface runoff and vegetation cover – as can be deducted from the MUSLE formulation used by SWAT (see section 3.4).

The average slope of the soil erosion response curves to decreasing rainfall, shown in Figure 5.5, compares well with the results obtained by Pruski and Nearing (2002): -2 % per % decrease in rainfall for the Guadiana and -2.6 % per % decrease in the Tejo obtained in this study versus -1.66 % per % decrease obtained by the authors, with the higher sensitivity in the Tejo likely to be explained due to high slopes as suggested above.

Comparison of sensitivity to changes in climate parameters

The sensitivity analysis to single climate parameters can be summarized as follows:

- the most vulnerable parameter to changes in temperature, rainfall and CO_2 is soil erosion, particularly under wheat fields;
- runoff is also significantly vulnerable to changes in temperature and rainfall, particularly subsurface runoff;

- increased temperature led to increased evapotranspiration and a correspondent decrease in subsurface runoff, with erosion in wheat fields increasing, due to reduced vegetation cover;

- reduced rainfall led to significant decreases in both runoff and erosion, with a significantly greater impact for subsurface runoff in the Guadiana;

- increased CO_2 concentrations led to significant increases in biomass growth for all vegetation types, with corresponding decreases in soil erosion, particularly in wheat fields.

Overall, the interactions between surface runoff and biomass growth appeared to play an important role in the impacts of climate changes on soil erosion. Increases in biomass growth led to negative changes to erosion, but the inverse was only verified for wheat regions (Figure 5.5); in other vegetation types, particularly pine forests, soil erosion was more sensitive to decreases in surface runoff.

5.1.3 Sensitivity analysis to combined changes in climate parameters

The sensitivity of runoff, vegetation productivity and soil erosion to combined changes in temperature, rainfall and CO_2 concentrations was also examined. Two different combinations between these parameters were tested. Both tests proceeded in steps of 1.6 ºC increase from current average annual temperature up to a maximum of +6.4 ºC, and 25 % increase from current average CO_2 concentrations up to a maximum of +100 %. The difference between the two tests relied on rainfall: the "high rainfall" test proceeded in steps of -2.5 % changes from current average annual rainfall down to -10 %, while the "low rainfall" test proceeded in steps of -10 % changes down to -40 %. Changes to rainfall were evenly distributed between intensity and number of rainfall days, considered by Pruski and Nearing (2002) to be a realistic scenario to represent precipitation changes. The characteristics of both tests are shown in Table 5.2.

Figure 5.2 compares the tests, marked as high rainfall and low rainfall, with the GCM and RCM predictions described above. The figure shows how increased CO_2 are related with increased temperatures, and also how temperature relates with rainfall changes, from very slow to very high rates of change. The tests were selected to follow the trends shown in Figure 5.2, but also to be comparable with the sensitivity analysis for individual parameters described in the previous section. They were not intended to represent any coherent and

concrete climate change scenarios, but rather to determine the presence of interactions and synergistic impacts on hydrology, vegetation growth and soil erosion.

Table 5.2 – Characteristics of simulation sets to explore the consequences of combined changes in climate parameters; changes are shown as percentage over current average annual values.

Test	Temperature changes	Rainfall changes		Atmospheric CO_2 concentration changes
		"high rainfall"	"low rainfall"	
1	+1.6 ºC	-2.5 %	-10 %	+25 %
2	+3.2 ºC	-5 %	-20 %	+50 %
3	+4.8 ºC	-7.5 %	-30 %	+75 %
4	+6.4 ºC	-10 %	-40 %	+100 %

Water runoff response

The responses for evapotranspiration and runoff (surface and subsurface) to coupled climate parameter changes are shown in Table 5.3; Figure 5.6 shows the percent changes from current conditions, with the "low rainfall" test on the left and the "high rainfall" on the right. The response of runoff follows the results obtained above for its sensitivity to rainfall changes, including a large decrease when compared with evapotranspiration; temperature changes appear to have caused more significant changes in subsurface runoff, particularly in the Guadiana.

The "low rainfall" simulations showed a larger response than the ones for "high rainfall". The former generate a decrease in subsurface runoff greater than -90 % in both regions, which is larger than the one observed for the single parameter changes in temperature or rainfall, pointing to a synergistic combination of the effects of both, while the later generates a lesser impact, namely a decrease of -50 to -60 %, in the Tejo and the Guadiana, respectively. Similarly, surface runoff decreased down to -70 % and -80 % in the Guadiana and Tejo, respectively, under the low rainfall test, while under the high rainfall test, it decreased down to -20 and -28 % in the Guadiana and Tejo.

Table 5.3 – Response of evapotranspiration, surface runoff and subsurface runoff to changes in multiple climatic parameters, in mm per year.

			Guadiana			Tejo		
			Evapo-transpiration ($mm.y^{-1}$)	**Surface runoff ($mm.y^{-1}$)**	**Subsurface runoff ($mm.y^{-1}$)**	**Evapo-transpiration ($mm.y^{-1}$)**	**Surface runoff ($mm.y^{-1}$)**	**Subsurface runoff ($mm.y^{-1}$)**
Control			*277*	*105*	*111*	*438*	*69*	*186*
T+1.6ºC	PP-10%	CO_2+25%	277	90	70	431	54	136
T+3.2ºC	PP-20%	CO_2+50%	280	68	38	433	36	81
T+4.8ºC	PP-30%	CO_2+75%	271	46	16	430	24	40
T+6.4ºC	PP-40%	CO_2+100%	254	33	10	413	14	12
T+1.6ºC	PP-2.5%	CO_2+25%	286	94	89	445	64	166
T+3.2ºC	PP-5%	CO_2+50%	292	89	68	457	60	137
T+4.8ºC	PP-7.5%	CO_2+75%	306	85	54	472	53	111
T+6.4ºC	PP-10%	CO_2+100%	307	85	43	484	50	92

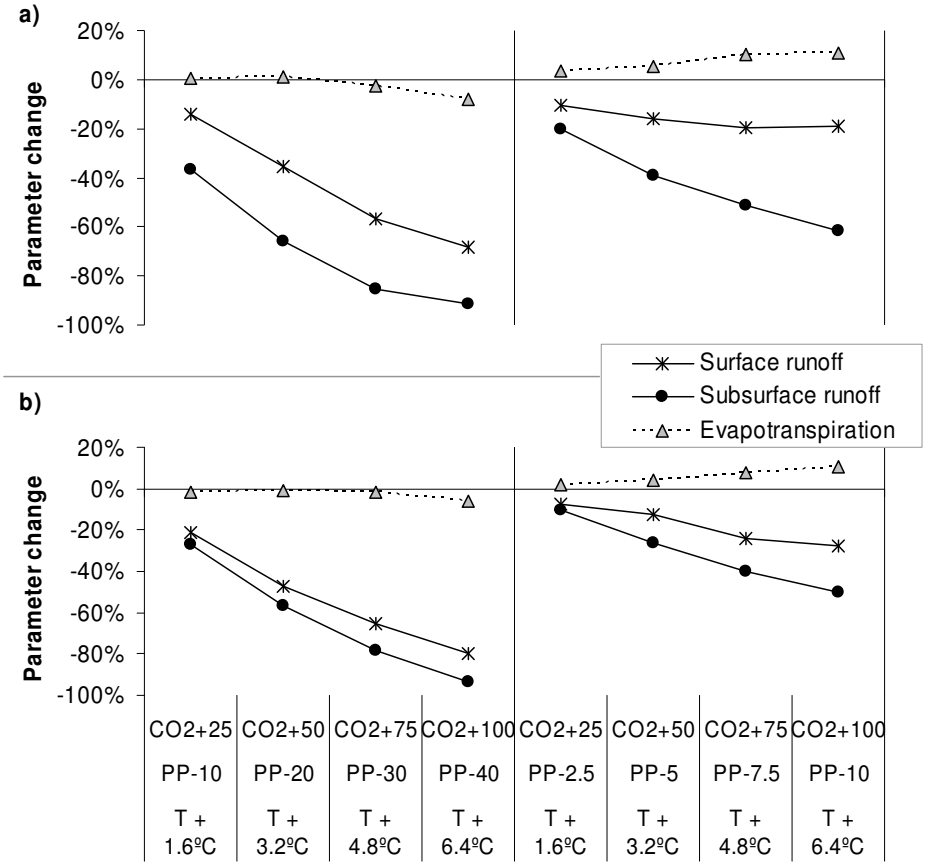

Figure 5.6 – Simulated responses of evapotranspiration, surface runoff and subsurface runoff to the combined changes in climate described in Table 5.2 for the Guadiana (a) and the Tejo (b), with the "low rainfall" test on the left and the "high rainfall" on the right.

The trend of larger decreases to subsurface runoff can be attributed to the diversion of soil water for plant evapotranspiration. In the "high rainfall" simulations, the available rainfall was sufficient to allow an increase of evapotranspiration at the expense of runoff: up to 11 % in both regions. In the "low rainfall" simulations, however, the available rainfall was only enough to allow for the maintenance of evapotranspiration at current rates, at least with smaller climate changes; these results agree with the predictions reported by Wetherald and Manabe (2002) and Nohara et al. (2006) for dryland regions. In Figure 5.6, a shift of impacts from runoff to evapotranspiration can be observed as climate changes increase for both regions, with evapotranspiration decreasing -6 % to -8 % with larger climate changes. These results point to different consequences of climate changes in a first stage – essentially affecting water runoff – and at a second stage – essentially affecting vegetation water availability. Figure 5.6 (left) indicates that the threshold between the first stage and the second is a change of c. 5 ºC in temperature coupled with a c. -30 % decrease in rainfall.

Furthermore, it was again observed that the difference between the response of subsurface and surface runoff was larger in the Guadiana. As discussed in detail above, this effect can be attributed to the low water storage capacity of soils in this region, leading to a smaller recharge in the rainiest months.

These results agree with those obtained by Cunha et al. (2002), who analyzed one climate change scenario (using the HadCM3 GCM for 2100, assuming double CO_2 concentration) for surface runoff in Portugal. For the Guadiana, the authors considered a temperature increase of c. 3.9 ºC coupled with a rainfall decrease of -25.8 %, which led to a decrease of river flows by -40 % to -60 %; for the Tejo, a temperature increase of c. 4.4 ºC coupled with a rainfall decrease of -12.7 % was considered, leading to a decrease of river flows by -15 % to -30 %. These results compare well with those obtained in this work for similar changes to rainfall and temperature (Figure 5.6).

Bathurst et al. (1996) also analyzed the consequences of one climate change scenario (using the CCCM GCM with double CO_2 concentrations) for the Cobres watershed in the Guadiana study area, with a temperature increase of c. 2.9 ºC and a rainfall decrease of -17 %. Their results point to a -55 % decrease of annual runoff, which agrees with the c. -50 % decrease found in this study for a similar degree of climate change (Figure 5.6).

Biomass growth response

The responses of the biomass growth of the main vegetation types to coupled climate parameter changes are shown in Figure 5.7. The response of biomass growth generally follows the results obtained above for its sensitivity to changes to temperature; the positive response to temperature of certain vegetation types was amplified by higher rainfall and CO_2 rates, while a negative responses were attenuated.

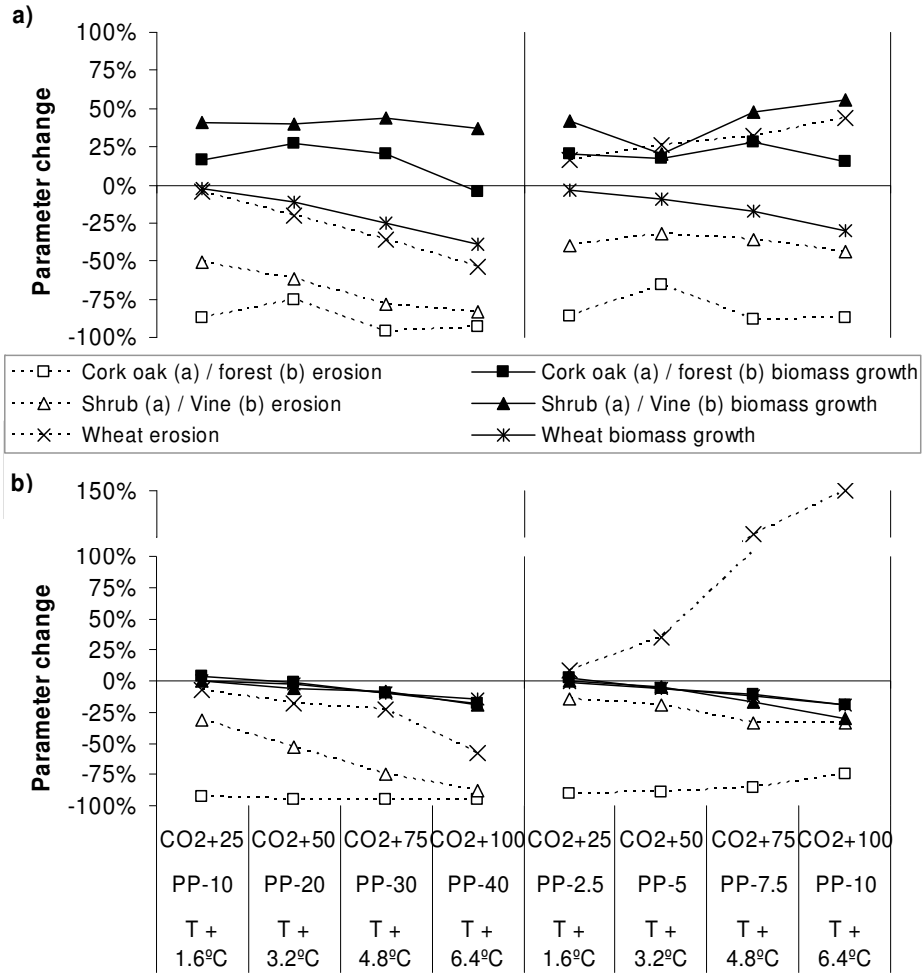

Figure 5.7 – Simulated responses of total biomass growth and erosion of different vegetation covers to the combined changes in climate described in Table 7 for the Guadiana (a) and Tejo (b) watersheds; the vegetation cover types are cork oaks, mediterranean shrubs and wheat for the Guadiana, and pine forest, vines and wheat for the Tejo.

In the "low rainfall" simulations, increased changes in climate led to a significant decrease of wheat biomass production: down to -39 % in the Guadiana and -15 % in the Tejo. These results are less severe than those obtained when changing temperature alone, especially in the Tejo, pointing to a mitigating effect of increased CO_2 concentrations. The "high rainfall" simulations led to less severe decreases in the Guadiana, of down to -30 %, without significant differences in the Tejo, pointing to the higher dependence of wheat production on available water in the semi-arid region.

As in the previous simulations, other species had different responses to climate changes. In the Tejo, there was a decrease in the productivity of vines (down to -20 to -30 %) and pine forests (down to -19 %) in both rainfall scenarios, also showing the mitigating effect of increased CO_2 concentrations. In the Guadiana, Mediterranean shrub productivity increased between 21 % and 57 %, showing a combination of the beneficial effects of higher temperatures and CO_2 concentrations, coupled with a low sensitivity to rainfall decreases. Cork oak productivity increased up to 27 % in both scenarios, also due to the a combination of higher temperature and CO_2 concentrations, but these beneficial effects diminished with temperature increases above 3 ºC, and in the "low rainfall" simulations the highest rate of climate changes led to a small decrease of cork oak productivity. Again, these results point to a cork oak tolerance to temperature increases of up to 5 ºC, and a beneficial effect of higher temperatures on Mediterranean shrubs.

These results agree with those obtained by Pinto and Brandão (2002), who simulated the consequences of one climate change scenario (using the HadRM2 RCM for 2100, with double CO_2 concentration), proposing a c. 5.8 ºC increase in temperature and a -12.2 % decrease in rainfall, for wheat productivity in the Guadiana. They found that, if no changes were made to agricultural practices and without an increase in irrigation, wheat productivity would drop by -25 %, while in this study, wheat productivity in the Guadiana under similar changes dropped by -30 % (Figure 5.7).

Soil erosion response

The results showed clear decreasing trends both for surface runoff and biomass growth (Figure 5.6 and Figure 5.7) in most climate change simulations and, as described above, these changes have opposite consequences for soil erosion, which is decreased by the former and increased by the latter. Therefore the balance between both changes appears to determine the increasing or decreasing trend for soil erosion. The responses of erosion under the main vegetation types to coupled climate parameter changes are shown in Figure 5.7. As discussed

in the previous section, these values must take into consideration current soil erosion rates, as changes to soil erosion in vineyards and wheat producing regions have more significant impacts than those under most other vegetation types due to the high erosion rates currently experienced there.

Soil erosion rates under wheat fields decreased in the "low rainfall" simulations, falling down to -53 % in the Guadiana and -58 % in the Tejo. These decreases were smaller than the ones found due to changes to rainfall or CO_2 concentrations only, probably due to the decrease in wheat biomass growth occurring at the same time. Nevertheless, the large decrease in surface runoff determined a similar downward trend for soil erosion rates. In the "high rainfall" simulations, however, soil erosion rates increased up to 44 % in the Guadiana and 149 % in the Tejo. In this case, it is the large decrease in wheat biomass growth determining an upward trend for soil erosion rates, which is not as marked as the one found during the sensitivity to temperature tests (Figure 5.5), probably due to the mitigating effects of both the rainfall decrease and the increase in CO_2 concentrations. It should again be noted the higher response of soil erosion under wheat fields in the Guadiana.

In the case of cork oaks (in the Guadiana) and pine forests (in the Tejo), soil erosion rates showed a marked tendency to decrease with increased changes in climate, dropping by -87 to -94 % in the former case and by -74 to -95 % in the latter; smaller decreases occurred in the "high rainfall" scenario, probably due to smaller changes in surface runoff. For Mediterranean shrubs (in the Guadiana) and vines (in the Tejo), responses were very similar to those found in the rainfall change tests described in the previous section, particularly in the "low rainfall" simulations; the changes to biomass growth for these vegetation types appear to have little impact in soil erosion rates.

These results can be compared with those obtained under the Pan-European Soil Erosion Assessment (PESERA) project (Mantel et al., 2003) which, for the HADRM3-A2B scenario (which shows a 4 ºC temperature increase and an -18 % rainfall decrease for the Guadiana), predicted a decrease in soil erosion rates in most of southern Portugal. The climate change scenario is similar to the one used in the "low rainfall" simulations, which also shows a trend of decreasing erosion. They are also comparable with the results of Bathurst et al. (1996) for the Cobres watershed (Guadiana), occupied with wheat agriculture; for the tests described above, they found a decrease in erosion of -27 %, comparable with the -20 % decrease found in the "low rainfall" scenarios for a similar degree of climate change (Figure 5.7).

Compared response to both combinations of climate changes

The results of the combined changes to climate parameters can be summarized as follows:

- the combination of increased temperature and reduced rainfall had a synergistic effect for water runoff, leading to an increased vulnerability to change when compared with the results for individual changes to each parameter;

- therefore, there was a trend for declining runoff in all simulation sets, with a maximum decrease of c. -40 to -45 % for the "high rainfall" simulations and of c. -81 to -90 % for the "low rainfall" simulations, in both regions;

- the impacts in subsurface runoff were more severe than in surface runoff, with the Guadiana region more vulnerable (26 % difference between impacts), followed by the Tejo (12 % difference between impacts);

- for biomass growth, the increase in CO_2 concentrations had a dampening effect on the consequences of higher temperatures, leading to a reduced vulnerability to change;

- however, a trend for declining vegetation growth in most species was still observed, particularly wheat, with a maximum decrease of c. -30 to -39 % in the Guadiana (depending on the rate of rainfall decrease) and -15 % in the Tejo (with little influence of rainfall rates);

- the trend for soil erosion under wheat fields, which currently experience the highest erosion rates, is not detectable as the results are very sensitive to changes in rainfall: soil erosion changes from -53 % to 44 % in the Guadiana, and -58 % to 149 % in the Tejo, respectively for the "low rainfall" and "high rainfall" simulations.

Once more, trends in erosion change appeared to result from the interactions between changes to surface runoff and vegetation biomass growth, particularly under wheat fields. For a similar rate of decrease in biomass growth, soil erosion increased with small changes to surface runoff, and decreased with large changes to surface runoff (Figure 5.7).

5.1.4 Sensitivity analysis at the seasonal scale – conclusions

This work has shown how a modeling tool can be used to study the response of hydrology, vegetation productivity and soil erosion to changes in climate factors, and how these results can be used to study the range of plausible impacts for different changes in climate variables,

by studying the gradual response of watershed systems to increasing degrees of change. The results indicate that, in the Portuguese Mediterranean regions, the watershed's water and sediment yield are highly sensitive to changes in rainfall and temperature, which affect the processes underlying these variables; changes to atmospheric CO_2 concentration appear to have smaller consequences for these parameters. The results point to a maximum decrease of runoff of c. -81 to -90 % in both study areas, particularly of the subsurface runoff component; soil erosion show a decreasing trend in most vegetation types, driven by lower surface runoff rates coupled with increased biomass production in some cases. However, erosion trends in regions with wheat cultivation, which currently suffer the largest erosion rates, are uncertain; predictions range from a -58 % decrease to a 149 % increase. Erosion predictions appear to depend on the combination of changes to surface runoff and vegetation biomass; the latter parameter appeared to be very significant in determining the response of soil erosion, despite its smaller sensitivity to climate change. Finally, changes to atmospheric CO_2 concentration appear to have a mitigating effect on the negative impacts of increasing temperatures and decreasing rainfall. These concussions are further discussed in section 6.1, below.

5.2 Sensitivity to changes in climate at the extreme event scale

The second part of this section analyses the response of hydrology and soil erosion parameters to changes in the main runoff and erosion drivers in Mediterranean watersheds: storm rainfall characteristics, soil moisture patterns and vegetation cover. The tests were performed over two Mediterranean watersheds with contrasting characteristics: Odeleite (semi-arid climate, natural vegetation landcover) and Alenquer (humid climate, agricultural landcover), described in section 4. Storm rainfall and intensity, pre-storm soil moisture patterns and several vegetation cover parameters were changed by several degrees of severity; these changes were introduced in the MEFIDIS storm erosion model (Nunes et al., 2005; see section 3.2 for a full description) which was then used to do a comparative analysis of the effects of these changes on storm runoff and erosion for three storms in each watershed. The results provide an assessment of the sensitivity of surface runoff and soil erosion patterns to changes in climate, with a focus on the importance of different changes to overall water and sediment budgets. This approach was developed in conjunction with the Soil Erosion Network team for application in the Tucson model intercomparison exercise, as described in section 3.3, the results of which were published by Nearing et al. (2005). A preliminary version of the results presented in this section, for Alenquer only, was published by Nunes et al. (2006).

5.2.1 Rationale and test description

Climate change is likely to impact runoff generation and soil erosion during extreme events, not only due to direct changes on rainfall intensity (e.g. Räisänen et al., 2004), but also due to changes in vegetation cover protection (e.g. Gitay et al., 2002) or soil moisture patterns (e.g. Wetherald and Manabe, 2002); these changes and their potential impacts are discussed in section 2.2. This exercise involved a comparative analysis of the sensitivity of storm runoff and erosion patterns to changes in these parameters, using the framework described in section 3.1. It used a similar approach to the one employed by Nearing et al. (2005), who studied the impacts of changes to rainfall amount and intensity, as well as vegetation canopy and ground cover, on watershed runoff, peak runoff rate and sediment yield. In this study, a new climate change factor is added: soil moisture at the beginning of the storm. Furthermore, changes to within-watershed soil erosion patterns, runoff generation ratio and sediment delivery ratio were also analyzed, to evaluate potential changes to water and sediment connectivity and to gully erosion rates; however, and taking into account the limitations of MEFIDIS described in section 4.4, result analysis focused on averaged soil erosion rates and the statistical properties of erosion patterns, rather than their actual location in space. Model results were measured in sensitivity to change, following Nearing et al. (2005), meaning the % change of each variable per % change in storm rainfall and intensity, initial soil moisture or vegetation cover.

The approach is schematized in Table 5.4 for the different variables under study; it is comparable with the one adopted by Nearing et al. (2005), described in section 3.3.2 and shown in Table 3.9. The MEFIDIS model was ran by changing the variables shown in the Table for three selected storms in both watersheds, with different rainfall, intensity and soil moisture conditions; these variables were varied from -20 % to +20 % in 10 % steps. The storms are described in Table 4.1 and Table 4.6 for Odeleite, and for Alenquer in Table 4.2 and Table 4.7, referring to rainfall characteristics and storm runoff and sediment yield, respectively. The selected storms for Odeleite occurred from 10 to 13-Dec-2001, 3 to 5-Mar-2002 and 12 to 15-Mar-2002; the selected storms for Alenquer occurred from 1 to 2-Feb-1998, 28-Apr to 1-May-2000 and 1 to 2-Mar-2001.

Table 5.4 – Approach used in the sensitivity analysis, describing the different variables and tests.

Designation	Description
IC, PPch	Changes to total rainfall amount from -20 to +20 %, keeping intensity constant by increasing storm duration
Ich, PPch	Changes to rainfall intensity from -20 to +20 %, by varying rainfall amount in the same way, keeping duration constant
Ich, PPC	Changes to rainfall intensity from -20 to +20 % while keeping rainfall constant, reducing storm duration
Ich0.5, PPch	Changes to total rainfall amount from -20 to +20 %, increasing intensity by half (-10 to +10 %)
SWDch	Changes to the catchments' average soil water deficit before storm from -20 to +20 %
LCch	Changes to land cover, changing standing vegetation biomass from -20 to +20 %, and estimating resulting changes to vegetation canopy cover and interception capacity

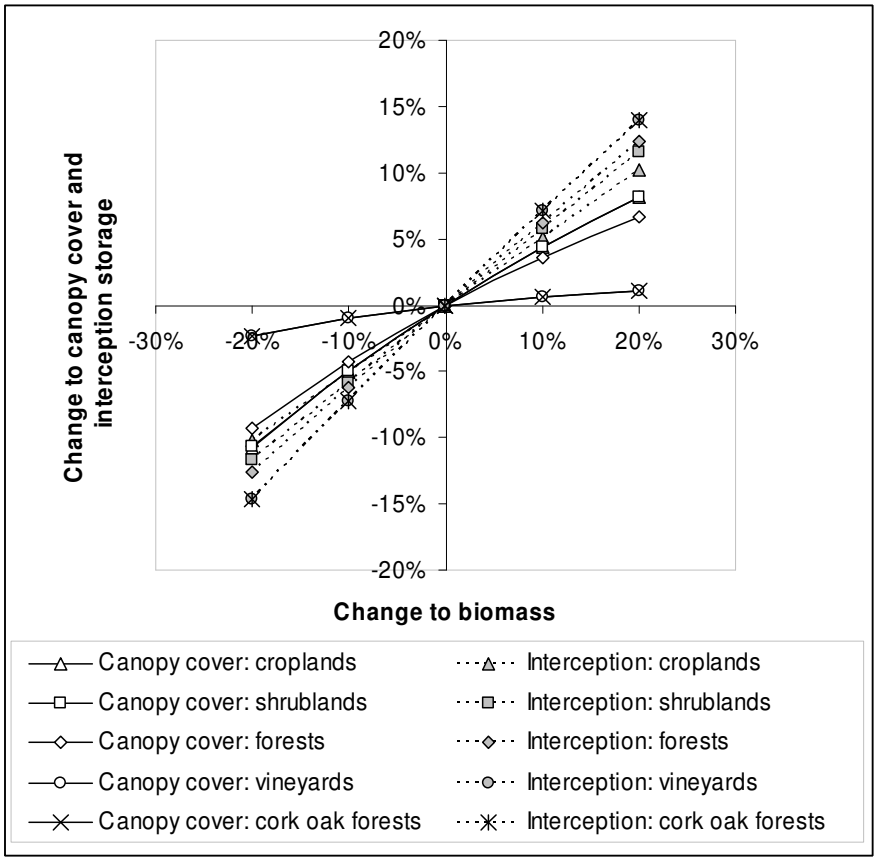

Figure 5.8 – Impact of biomass changes on canopy cover and interception storage for the most important vegetation types in the Alenquer and Odeleite watersheds.

One important change was made in the way that changes to vegetation biomass are represented in the tests. Nearing et al. (2005) analyzed changes to vegetation cover and ground cover, the latter represented as direct changes to runoff roughness (Manning's n). This approach took into account morphological differences between vegetation types. Changes to biomass were applied directly as changes to runoff roughness; but they were also applied as changes to canopy cover using the equations published by Flanagan and Nearing (1995), taking into account both currently observed values (together with current typical values, shown in Table 4.24) and different shape coefficients for each vegetation type. Biomass changes were also transformed into changes to leaf area index using the light extinction coefficient approach published by Deguchi et al. (2006); these were used to calculate changes to interception storage capacity following Hoyningen-Huene (1983). The results from the application of these methods to the main vegetation cover types in Alenquer and Odeleite are shown in Figure 5.8. It should be noted that changes to canopy cover of vineyards and cork oak forests are significantly smaller than those of other vegetation cover types. Furthermore, changes to interception storage are higher than those to canopy cover, but both fall significantly below changes to vegetation biomass.

5.2.2 Results and discussion

The overall results for all tests for aggregated catchment parameters measured at the outlet, in terms of sensitivity to change, are shown in Table 5.5. In general, all parameters show a significant sensitivity to change (above 1 % per % change in parameter) except to changes in rainfall intensity only and land cover. The model shows a positive sensitivity to changes in storm pattern scenarios, which is consistent with an increase in the driving force for runoff generation and soil detachment. Conversely, the model shows a negative sensitivity to changes in soil water deficit, which is consistent with a decrease in the amount of rainfall diverted for surface runoff and therefore available for sediment detachment and transport. The model also shows a negative sensitivity to changes in vegetation cover, which is consistent with an increase in the interception capacity and soil protection provided by the plant canopy and ground cover. The results also indicate that:

- runoff, peak runoff rate and sediment yield show more sensitivity to changes to storm pattern than to changes in soil water deficit and vegetation cover, with the exception of changes to rainfall intensity alone;

- the parameters show more sensitivity to changes in both rainfall amount and intensity than changes in rainfall amount alone, but the impact of intensity changes appears to be smaller than that of changes to rainfall amount;

- sediment yield shows more sensitivity to changes in climate than peak runoff rates or total runoff, particularly in the Odeleite catchment;

- the response of the Odeleite catchment shows more sensitivity to changes in climate patterns than that of the Alenquer catchment, with the exception of changes to rainfall intensity.

Sediment yield appears to be more sensitive to climate changes than runoff; this can be explained since runoff is dependent on the external changes alone, while sediment yield is dependent on changes to both external factors and surface runoff, indicating that these changes are cumulative and influence dependent processes in a non-linear fashion. These results concur with the high variability usually observed in soil erosion processes due to small changes in climate and other factors (Nearing et al., 1999; Tucker and Bras, 2000). It should be noted that catchment response is more sensitive to changes in storm patterns than to vegetation cover. These results agree, in relative terms, with those published by Nearing et al. (2005), and discussed in section 3.3.2; they are shown in Figure 3.17, Figure 3.18, Figure 3.19 and Figure 3.20. This agreement between the results obtained in both tests indicates that they could represent a hierarchy of sensitivity found in most watersheds, although further modeling work and observations are needed to substantiate this claim.

Table 5.5 – Average sensitivity to change (in % per % change) of runoff, peak runoff rate and sediment yield for both study areas, for the tests described in Table 5.4.

Parameter		**IC, PPch**	**Ich, PPch**	**Ich, PPC**	**Ich0.5, PPch**	**SWDch**	**LCch**
Runoff	Odeleite	2.3	2.7	0.4	2.5	-1.5	-0.3
	Alenquer	1.4	2.1	0.7	1.8	-1.0	-0.3
Peak runoff rate	Odeleite	2.7	3.2	0.5	2.9	-1.7	-0.5
	Alenquer	2.1	2.5	0.4	2.3	-1.2	-0.4
Sediment yield	Odeleite	10.8	12.6	1.1	11.7	-7.6	-2.0
	Alenquer	3.3	4.4	0.9	4.0	-2.2	-0.6

However, the sensitivity values for runoff in this study are significantly lower than those found by Nearing et al. (2005). The response of runoff to storms is expected to vary between catchments due to differences in factors such as the structure of the hydrological network or the spatial distribution of soil hydrological properties (Woods and Sivapalan, 1999); but in this case, the large difference in catchment area between both studies should be taken into account. The catchments used by Nearing et al. (2005) have areas of 0.04 and 1.1 Km^2, while the catchments used in this study have areas of 115 and 290 Km^2. Kavvas (1999) has proposed that hydrological response variability is dampened with increasing catchment scale; see section 2.2.2 for further debate on this issue. Therefore, the lower sensitivity of runoff to changes in climate found in this study could be attributed to the larger catchment area.

This is not the case for the sensitivity for sediment yield; the results in this study are similar to those reported by Nearing et al. (2005). The relationship between sediment yield variability and spatial scale appears to be non-linear, with increasing scale leading to different responses depending on the importance of hillslope and channel erosion processes (Lane et al., 1997; de Vente and Poesen, 2005); these issues are further discussed in section 2.2.3. Furthermore, the importance of gully erosion for Mediterranean watersheds (Vandaele et al., 1997) and its sensitivity to changes in storm patterns (Vandekerckhove et al., 2003) can be a significant factor for a high sensitivity of erosion to changes in climate, even at larger spatial scales; in fact, the higher sensitivity of erosion to storm patterns in Mediterranean watersheds was already noticed by Puigdefabregas et al. (1999). It is difficult to evaluate if these processes are taken into account by the model due to the lack of available data for erosion patterns (see section 4.4); however, the fact that model results agree with observed erosion processes indicates that this issue merits further investigation.

The sensitivity of peak runoff rate (Table 5.5) shows an intermediate value between that of runoff and erosion, which can be due to the fact that peak runoff rates are dependent both on changes to external parameters and to runoff, increasing the non-linearity of its response. This reinforces the indication that sensitivity to climate change increases with the number of processes involved, as previously mentioned. The sensitivity to changes in soil water deficit (Table 5.5) is lower than the one found for changes to storm runoff, but still significant when compared with the one found for changes in rainfall intensity; this can be attributed to the importance of saturation-excess runoff generation processes in Mediterranean watersheds, when compared with infiltration-excess processes (Castillo et al., 2003; see also section

2.2.2). This sensitivity value could be lower for more humid watersheds, such as the ones used in the study by Nearing et al. (2005).

Finally, Table 5.5 also shows a greater sensitivity to change of runoff in Odeleite, when compared with Alenquer. This can be attributed to the low soil water storage capacity of the former (as discussed in section 4.2.4). Skøien and Blöschl (2003) note that soil storage acts as a dampener on the temporal variability of hydrological processes; therefore a low water storage capacity can be expected to increase their sensitivity to changes in climate patterns. A similar impact of soil storage has also been noticed by van den Hurk et al. (2005). The exception to this case is when event intensity is changed; in this case, runoff in Alenquer is more sensitive than in Odeleite. This can also be explained by the soil properties of both watersheds; as shown in section 4.2.4, soils in Alenquer have lower hydraulic conductivity than those in Odeleite and therefore changes to rainfall intensity should have larger impacts in runoff generation. As for sediment yield, it should be noted that it also appears to be significantly more sensitive to land cover changes in Odeleite. This can be attributed to the greater canopy cover estimated for shrublands, the dominant vegetation type in this watershed, when compared with the canopy cover for the dominant vegetation type in Alenquer, wheat (see section 4.4 for details), leading to greater climate change impacts on splash erosion.

Response variability

The results also showed a considerable variability, both between different magnitudes of change to parameters, and between storms. Figure 5.9 shows the impact of each degree of change on runoff and peak runoff rate for three tests; from the changes to storm patterns, only test Ich0.5, PPC is shown following the suggestion by the Pruski and Nearing (2002) of dividing rainfall changes evenly into changes to intensity and amount when representing changes to rainfall patterns. The results agree with those shown in Table 5.5. Furthermore, they also show a non-linearity of response with the magnitude of changes to storm patterns and soil water deficit. In the case of storm patterns, greater increases lead to greater changes of runoff and peak runoff rate; for example, while the range of change for a -20 % decrease in rainfall ranges from -30 to -50 % for both watersheds and parameters, a 20 % increase in rainfall leads to changes ranging from 40 to 80 %. This effect was also observed for absolute values in each storm. In the case of soil water deficits, greater increases have the opposite effect but the non-linearity is also observable.

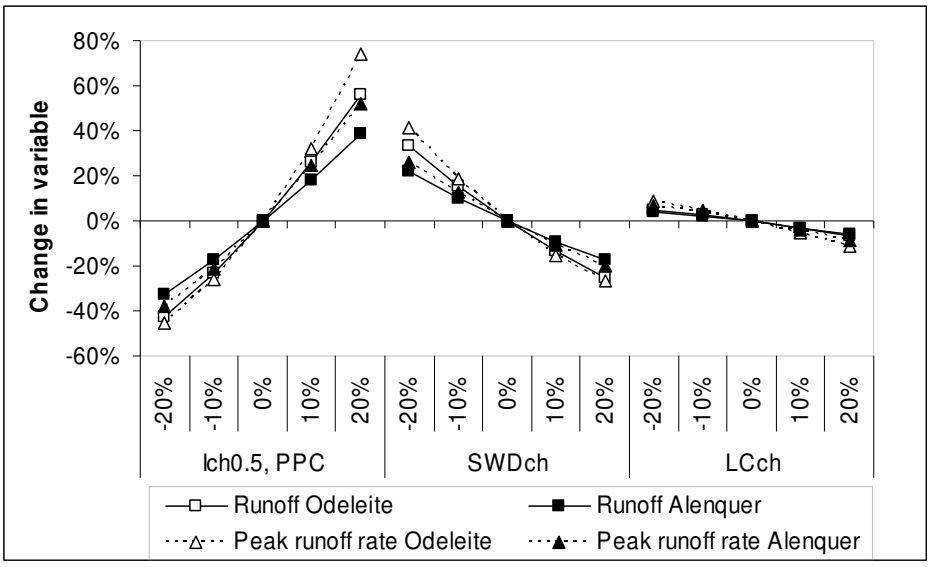

Figure 5.9 – Averaged changes to runoff and peak runoff rates in both study areas for changes to rainfall (left), soil water deficit (center) and land cover (right); test designations are explained in Table 5.4.

This non-linearity of response is due to the fact that changes to changes in storm rainfall and soil water deficit impact not only the amount of available water for runoff (by increasing rainfall in the former case and increasing soil water retention in the latter), but also the runoff generation ratio. The impacts on runoff generation ratio are shown on Figure 5.10, for changes to storm patterns; a similar impact was found for changes to soil moisture deficit. It should be noted that, in the Alenquer watershed, changes to runoff generation increase when it is already large, which can be attributed to the lower hydraulic conductivity of the soils as described previously, leading to greater impacts when storm intensity is already large. Overall, these results indicate that impacts on runoff and peak runoff rates depend on the magnitude of change on storm patterns and soil moisture deficit; note that, in Figure 5.9, this non-linearity is not apparent for changes to land cover.

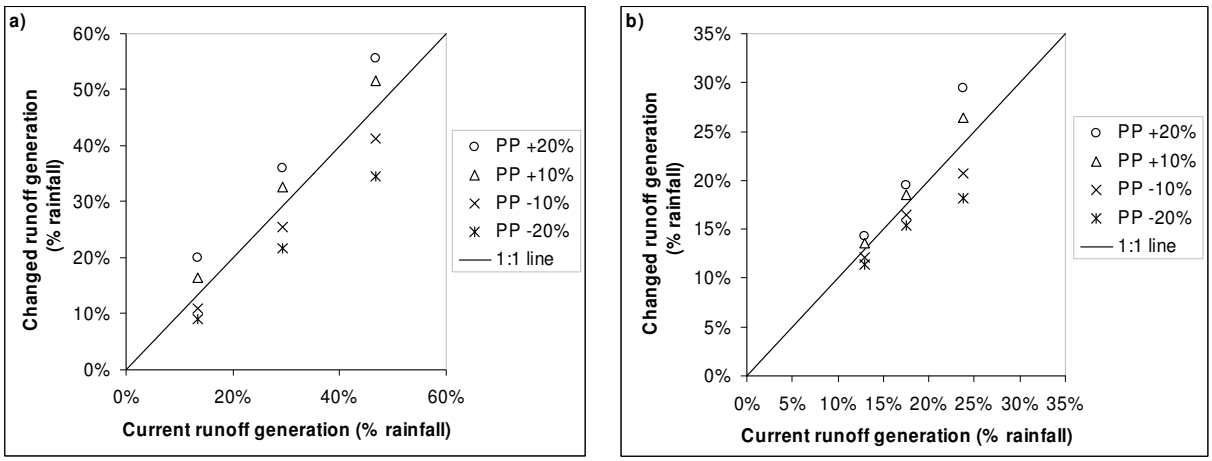

Figure 5.10 – Current and changed runoff generation per storm, for Odeleite (a) and Alenquer (b), for test Ich0.5, PPch (as defined in Table 5.4).

This non-linearity of response was also apparent for sediment yield, as shown in Figure 5.11, for changes to storm patterns and soil water deficit. In this case, the non-linearity of responses is significantly higher for the Odeleite watershed. This result can be partly explained due to changes in runoff generation, as impacts on runoff and peak runoff rates will propagate to sediment yield. However, a further explanation resides in changes to the Sediment Delivery Ratio (SDR), i.e. the relationship between field / hillslope erosion and catchment sediment yield (Lane et al., 1997). These results indicate that part of the impacts on sediment yield are due to an increase in sediment connectivity within the watershed, as defined by Favis-Mortlock et al. (2001); changes to storm patterns and soil water deficit can impact the rate of sediment deposition in the channel network, leading to changes in sediment yield that are not reflected in erosion rates on fields and hillslopes. This issue is further explored below.

The variability of results between different storms was also examined. Figure 5.12 shows the sensitivity of change for runoff, for all tests, according to current runoff. The results show no significant differences between storms for the Alenquer watershed; in Odeleite, however, it is noticeable that the smaller storm is more sensitive to changes to storm rainfall (whether changing rainfall only or changing rainfall and intensity) or to soil water deficit. No significant differences were found for changes to rainfall intensity only or vegetation cover. These results are also apparent for peak runoff rates (shown in Figure 5.13) and sediment yield (Figure 5.14); in the latter case, the differences in sensitivity between storms in Odeleite are much higher.

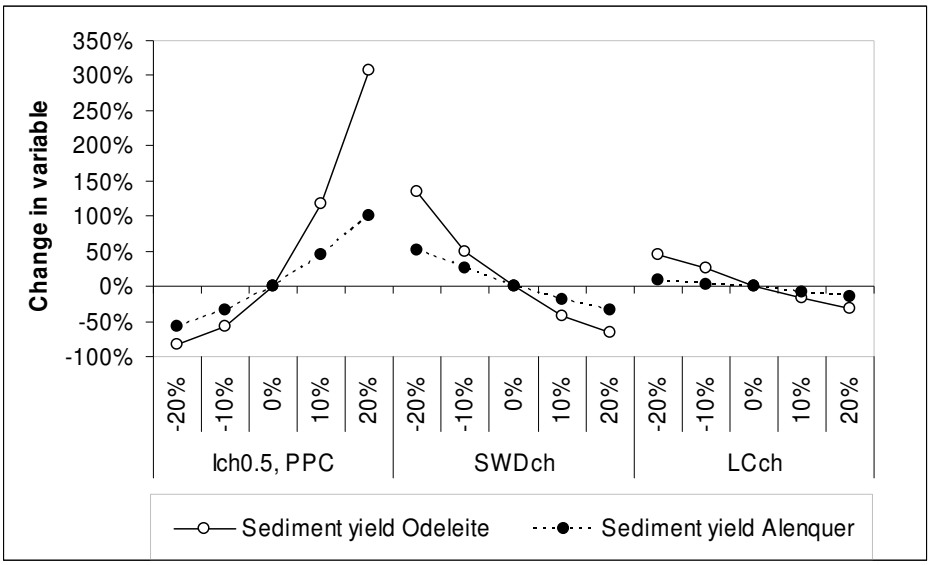

Figure 5.11 – Averaged changes to sediment yield in both study areas for changes to rainfall (left), soil water deficit (center) and land cover (right); test designations are explained in Table 5.4.

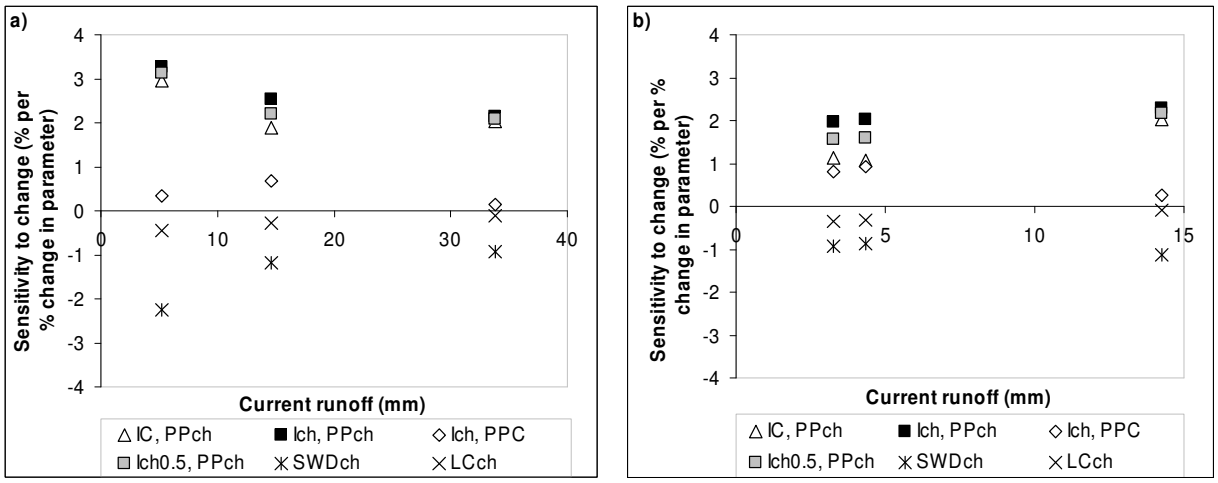

Figure 5.12 – Sensitivity to change (in % per % change) of runoff to changes to rainfall, soil water deficit and land cover, per storm, for Odeleite (a) and Alenquer (b); test designations are explained in Table 5.4.

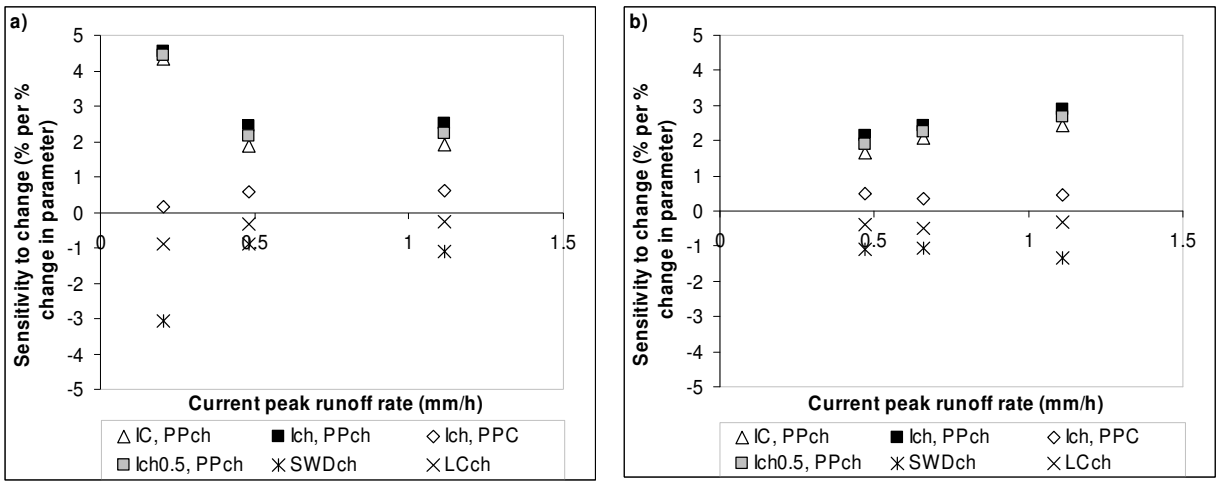

Figure 5.13 – Sensitivity to change (in % per % change) of peak runoff rate to changes to rainfall, soil water deficit and land cover, per storm, for Odeleite (a) and Alenquer (b); test designations are explained in Table 5.4.

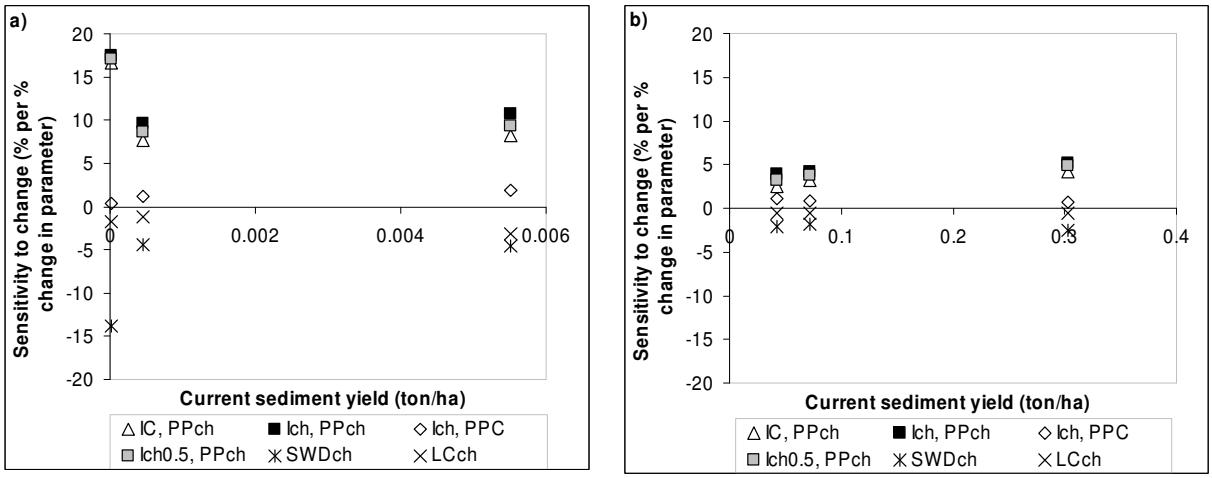

Figure 5.14 – Sensitivity to change (in % per % change) of sediment yield to changes to rainfall, soil water deficit and land cover, per storm, for Odeleite (a) and Alenquer (b); test designations are explained in Table 5.4.

While these results are difficult to explain, it should be noted that Nearing et al. (2005) found similar results in his study: runoff and soil erosion were found to be more sensitive in smaller storms for the Lucky Hills catchment, but this was not apparent in the Ganspoel catchment. It is interesting to note that both Lucky Hills and Odeleite are dryland catchments covered by natural vegetation, while both Ganspoel and Alenquer are humid agricultural catchments, and dryland catchments have been shown to be highly sensitive to small changes in storm patterns

(Puigdefabregas et al., 1999; see also sections 2.2.2 and 2.2.3 for a more detailed discussion of this issue). Despite this, the model results are insufficient to allow any conclusions to be drawn from the differences in sensitivity between storms.

Sediment delivery ratio and soil erosion patterns

As discussed above, the high sensitivity of sediment yield for both catchments shown in Table 5.5 could be attributed in part to the impacts on the SDR and on gully erosion rates. These issues were further explored by analyzing model results for SDR, and the sensitivity in regions experiencing significant erosion rates (above 1 ton.ha^{-1} in each storm), where erosion can be attributed to concentrated flow and therefore where model results more closely approach the processes involved in gully erosion. Table 5.6 shows the results, in terms of sensitivity to change; all parameters other than Alenquer's SDR show a significant sensitivity to change (above 1 % per % change in parameter) except to changes in rainfall intensity only and land cover. Upslope erosion should be understood as the amount of soil detached at the model cell scale (90 × 90m), representing erosion at the field / hillslope scale.

Overall, the results indicate that:

- upslope erosion shows less sensitivity than watershed sediment yield to changes in climate, while SDRs show also a significant sensitivity to change in most cases;
- the amount of erosion in areas with significant rates shows as much sensitivity as overall upslope erosion, but the area where this rates occur shows smaller changes;
- all parameters show similar responses to changes in storm patterns, soil water deficit and vegetation cover as those shown in Table 5.5;
- as in the previous case, the response of the Odeleite catchment appears to be more sensitive to changes in climate patterns than that of the Alenquer catchment, with the exception of changes to rainfall intensity.

A comparison between Table 5.5 and Table 5.6 shows that the sensitivity to change of upslope erosion is significantly smaller than that of sediment yield, since sediment yield changes also due to an increase in the SDR. These results show that changes to sediment yield are also due to changes to catchment hydrological sediment connectivity, as proposed above; Favis-Mortlock et al. (2001) describe changes in sediment connectivity as dependent on changes to storm flow, which can increase or decrease the deposition of eroded sediment in

regions with lower slope gradients. This indicates that part of the non-linearity associated with sediment yield, as shown in Figure 5.11, is due to changes in the SDR compounded with changes to upslope erosion. Furthermore, changes to upslope erosion and SDR in response to changing storm patterns are themselves non-linear, as shown in Figure 5.15, explaining the high response of sediment yield to this parameter shown in Figure 5.11.

Table 5.6 – Average sensitivity to change (in % per % change) of upslope erosion, sediment delivery ratio, and both total erosion and catchment area in regions with significant erosion rates, for both study areas; significant erosion rate is defined as being above 1 ton.ha^{-1}, and the tests are described in Table 5.4.

Parameter		**IC, PPch**	**Ich, PPch**	**Ich, PPC**	**Ich0.5, PPch**	**SWDch**	**LCch**
Upslope erosion	Odeleite	4.3	5.0	0.5	4.7	-2.8	-1.5
	Alenquer	2.8	3.5	0.7	3.2	-1.8	-0.6
Sediment delivery ratio	Odeleite	2.9	2.0	0.005	2.1	-0.9	0.5
	Alenquer	0.7	0.7	0.002	0.7	-0.3	0.03
Amount of erosion in areas with significant rates (> 1 ton.ha^{-1})	Odeleite	4.5	5.0	0.5	4.7	-2.9	-1.5
	Alenquer	2.9	3.6	0.7	3.3	-1.8	-0.6
Area with significant rates of erosion (> 1 ton.ha^{-1})	Odeleite	3.2	3.5	0.3	3.3	-2.1	-1.3
	Alenquer	1.9	2.3	0.5	2.2	-1.3	-0.8

Two points should be noted in these results. First, the SDR shows a much greater response to changes in all parameters for the Odeleite watershed. This can be attributed to the significant difference between SDRs in both catchments, as discussed in section 4.5 and shown in Table 4.44. The high SDR calculated for Alenquer could indicate that there is a smaller scope for changes than in Odeleite, whose shape and topographic characteristics indicate a much lower SDR. As previously referred, no measurements of SDR were made for either watershed and therefore these results are only indicative; however, they merit further research as the current SDR could potentially be used as an indicator of the sensitivity of sediment yield to changes in climate for a given watershed. Second, the results in Table 5.6 show that an increase in vegetation cover leads to a decrease in upslope erosion rates but to an increase in SDR. Therefore, for this test, sediment yield shows a smaller sensitivity to change than upslope erosion. This result can be attributed to the fact that vegetation cover affects erosion mostly at the upslope scale, while channel processes governing channel deposition are not changed; in

other words, the sediment detachment rates are affected but not the sediment transport capacity of the channel flows, leading to a relative increase of SDR.

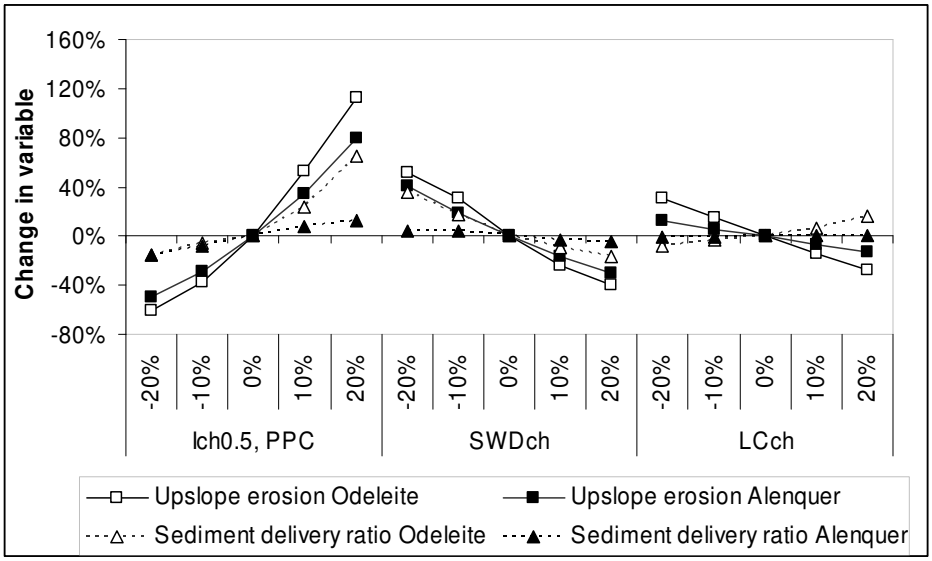

Figure 5.15 – Averaged changes to upslope erosion and sediment delivery ratio in both study areas for changes to rainfall (left), soil water deficit (center) and land cover (right); test designations are explained in Table 5.4.

In regions with significant erosion rates, the results in Table 5.6 show a similar sensitivity to change between erosion in these areas and overall upslope erosion. However, the area affected by significant erosion shows a smaller sensitivity that the changes to total erosion. This indicates that a part of changes to significant erosion is due to the spread of the problem to new areas within the watershed, while another part is due to changes in erosion rates in areas already experiencing the problem; according to Table 5.6, roughly one third of the changes can be attributed to the latter cause. This indicates that erosion in areas with significant problems is more sensitive to changes in storm patterns and soil water deficit than in the remaining areas. Furthermore, this difference increases with the magnitude of storm and water deficit changes, as can be seen in Figure 5.16, indicating that the sensitivity of erosion rates in these areas increases with the magnitude of change. If the areas with significant erosion rates are taken as an indicator for the occurrence of ephemeral gully erosion, as proposed above, then these results concur with the observations by Kirkby et al. (2003) and Vandekerckhove et al. (2003) of a high sensitivity of gully erosion rates to changes in storm patterns. It should be

noted that, for changes to vegetation cover, total erosion shows approximately the same sensitivity as area in Table 5.6.

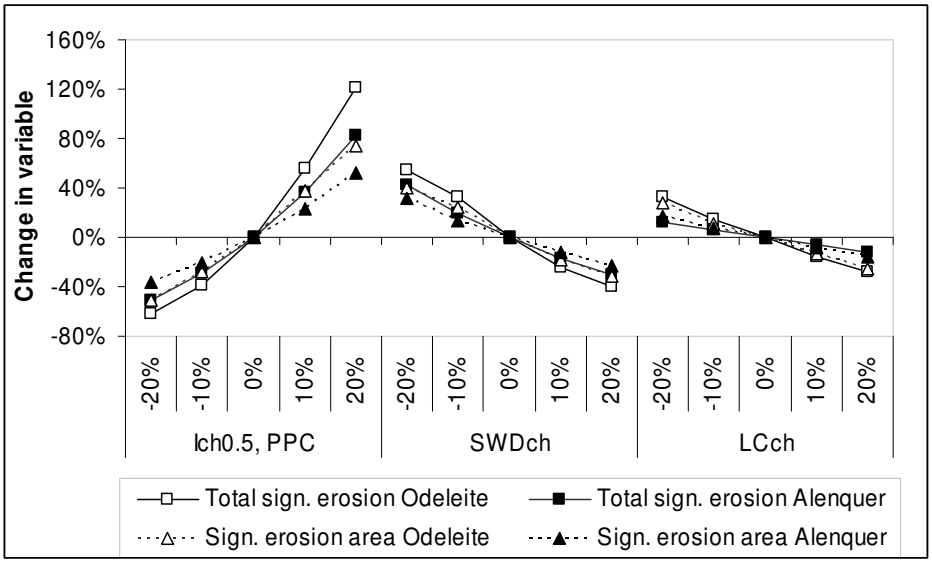

Figure 5.16 – Averaged changes to erosion in areas with significant erosion rates and to catchment area suffering significant erosion rates, in both study areas, for changes to rainfall (left), soil water deficit (center) and land cover (right); significant erosion rate is defined as being above 1 ton.ha^{-1}, and test designations are explained in Table 5.4.

5.2.3 Sensitivity analysis at the extreme event scale – conclusions

The results of this modeling study indicate that catchment runoff, peak runoff rates and sediment yield are highly sensitive to changes in storm patterns and soil moisture conditions, with a smaller sensitivity to changes in vegetation cover. Furthermore, sediment yield appears to be more sensitive to changes than peak runoff and soil erosion. These parameters are also affected by changes to the hydrological and sediment connectivity of watersheds, leading to different rates of change according to the magnitude of changes to storm patterns and soil water deficit, and to different sensitivities when considering erosion at the field/hillslope scale and at the watershed scale. Finally, erosion appears to be more sensitive to changes in regions already suffering from significant rates of soil loss. These results are further discussed in section 6.1, below.

5.3 Watershed response to climate change scenarios

This section analyses the response of hydrology, soil erosion and vegetation biomass productivity to climate change at multiple spatial and temporal scales in Mediterranean watersheds, as part of the resilience analysis described in section 3.1. This test was performed for the Guadiana and Tejo study areas. Analysis at the extreme event scale and for within-watershed patterns was performed for the Odeleite and Alenquer catchments, located within each study area respectively. The study areas are fully described in section 4.

The test considered two CO_2 emission scenarios, A2 and B2 (IPCC, 2000; see section 2.2.1 for a further discussion), assuming a CO_2 atmospheric concentration of 760 and 575 ppm between 2071 and 2100 for each scenario, respectively, which represents an approximate increase of 56 and 107 % above levels in 2000 (c. 370 ppm). Daily climate scenarios for the period from 2070 to 2100 were generated using the PROMES RCM (Gallardo et al., 2001). The daily data was used as a direct input by the SWAT watershed model (Neitsch et al., 2002; see section 3.4) to estimate average, interannual and seasonal changes to evapotranspiration, streamflow and vegetation biomass productivity.

The PROMES results for changes to extreme event patterns were combined with the SWAT results to provide inputs for the MEFIDIS storm erosion model (Nunes et al., 2005; see section 3.2 for a full description). A comparative analysis on how seasonal changes could impact storm runoff and soil erosion, especially when they acted to mitigate the effects of increased event intensity, was performed. The results provide a basis to assess the resilience of the catchments to climate change, i.e. to evaluate if the estimated impacts of climate change are (or are not) likely to change fundamental hydrological and erosion processes at multiple scales.

5.3.1 Rationale and test description

Scenarios of climate change for extreme rainfall event conditions are difficult to predict, because of the many uncertainties inherent to GCM predictions (Giori, 2005; see Figure 5.2 for an example), and also due to contrasts between predicted long-term trends and extreme weather events. For example, while the total rainfall amount is expected to decrease, rainfall intensity in extreme events is expected to increase (Räisänen et al., 2004; see also section 2.2.1). Furthermore, a decrease in total rainfall can lead to a decrease in soil moisture and baseflow, as described in the previous sections, which could counteract the effects of increased event intensity, as pre-storm soil moisture conditions play an important role for

runoff generation in Mediterranean catchments (Boix-Fayos et al., 2006; see section 2.2.2 for a further discussion of this issue). For soil erosion assessment, this problem becomes more complex due to the impacts of climate change on vegetation cover; as shown in the previous section, climate change could increase the cover of some plant types while decreasing others. This is compounded with the impact of storm patterns on the spatial distribution of soil erosion, especially in the case of ephemeral gullies (Vandekerckhove et al., 2003; see section 2.2.3 for a further discussion of this issue).

The objective of this exercise was to evaluate the resilience of catchment hydrological and erosion processes to likely changes in climate parameters, using the framework described in section 3.1. This approach uses a coupled model simulation at both the seasonal and extreme event scales, which constitutes a novelty over previous studies focusing only on the seasonal scale (e.g. Pruski and Nearing, 2002; Zhang and Nearing, 2005) or on the storm scale (e.g. Michael et al, 2005). In this exercise, changes to watershed runoff, peak runoff rate and sediment yield, as well as within-watershed soil erosion patterns, runoff generation ratio and sediment delivery ratio, were considered. The latter were used as indicators of potential changes to water and sediment connectivity and to gully erosion rates, focusing mostly on average properties of erosion patterns due to the limitations of MEFIDIS (described in section 4.4). The tests were performed for all storms described in Table 4.1 and Table 4.6 for Odeleite, and in Table 4.2 and Table 4.7 for Alenquer, referring to rainfall characteristics and storm runoff and sediment yield, respectively.

5.3.2 Climate change scenario description

The climate change scenarios selected for this study were daily time-series for maximum and minimum values of temperature, rainfall, wins speed, solar radiation and relative humidity, generated by using the PROMES RCM (Gallardo et al., 2001). The datasets were built within the framework of the PRUDENCE project (PRUDENCE, 2007), described in detail by Déqué et al. (2005). The RCM seasonal averages for every parameter were compared with the measured data for the 1961-1990 climate normals in both study areas, as described in section 4.2.1. PROMES was able to replicate the main observed patterns, although with some significant biases. As an example, Figure 5.17 shows a comparison between simulated and measured values for monthly maximum and minimum temperature in both study areas; while simulated maximum temperature values were close to observations, minimum temperature values were significantly above measurements in both study areas. A similar case occurred for rainfall, with monthly measured and observed values shown in Figure 5.18. In this case,

PROMES provided a reasonable estimation of dry season rainfall, but significantly underestimated wet season rainfall. These biases were corrected using regression methods based on the relations between measurements and uncorrected simulations (Wilby and Wigley, 1997). Table 5.7 shows the average correction factors applied in both study areas, for all five simulated climate parameters. The most significant corrections were applied to minimum temperature, rainfall and wind speed. Despite the significant differences for rainfall, the correlation between simulated and observed values is good for all climate parameters except wind speed (Table 5.7).

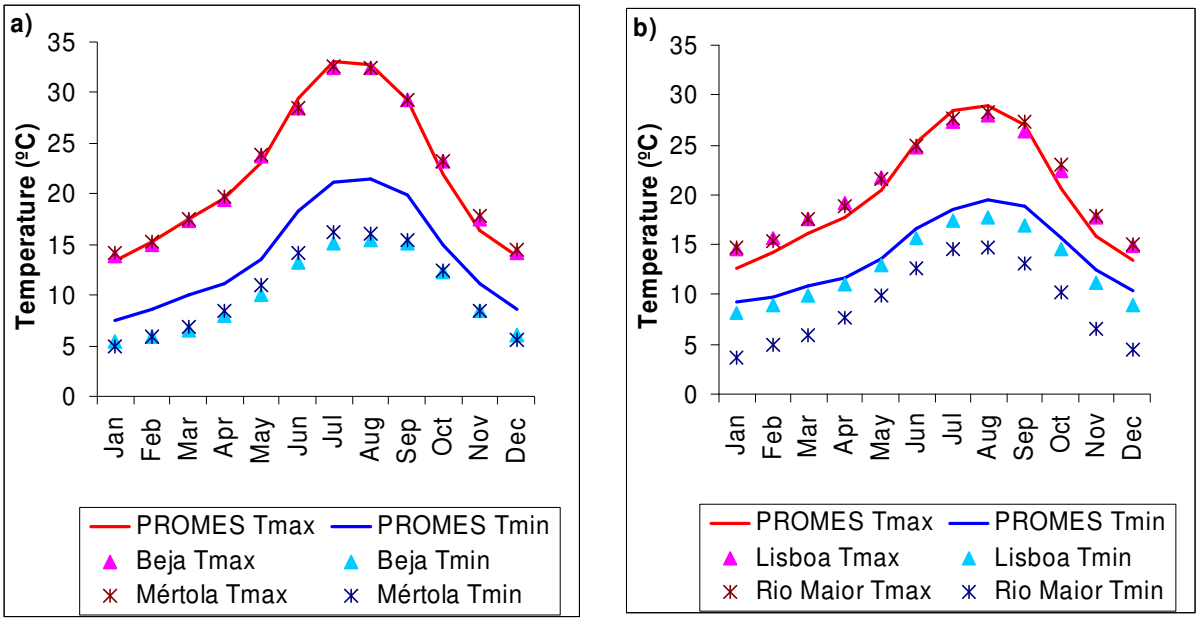

Figure 5.17 – Comparison between PROMES results and measured values for monthly maximum and minimum temperatures in the Guadiana (a, left) and the Tejo (b, right) study areas; climate stations are identified in Figure 4.5.

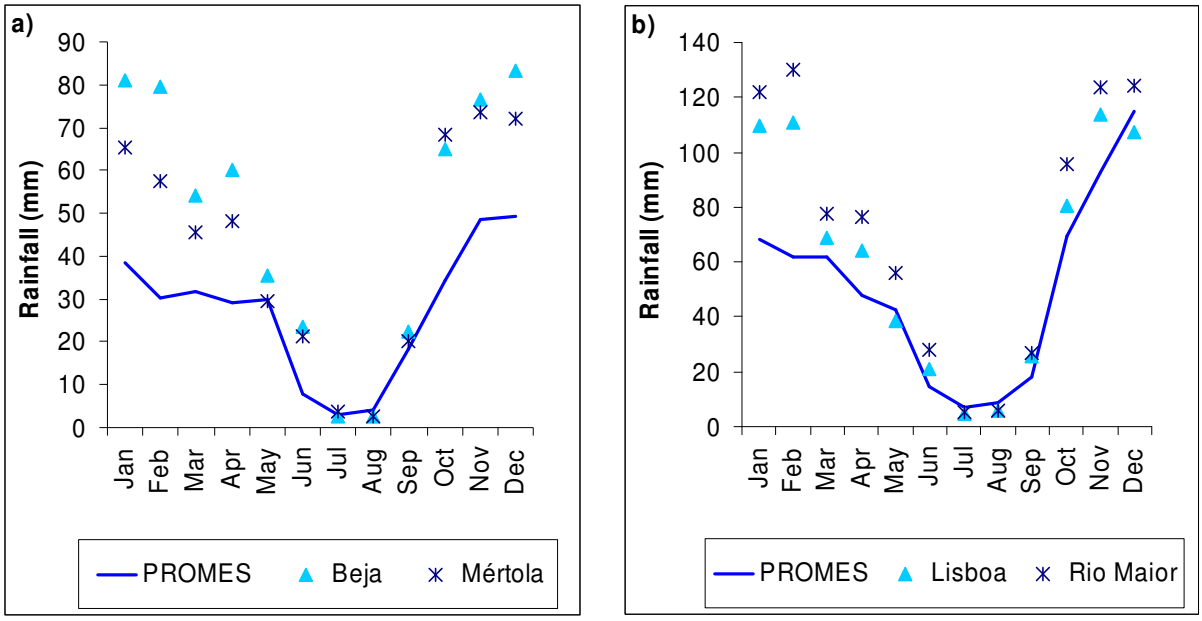

Figure 5.18 – Comparison between PROMES results and measured values for monthly rainfall in the Guadiana (a, left) and the Tejo (b, right) study areas; climate stations are identified in Figure 4.5.

Table 5.7 – Average correction applied to the PROMES climate parameters in both study areas, and the correlation between the uncorrected climate model results and observations.

	Guadiana		Tejo	
Parameter	**Correction**	**r^2**	**Correction**	**r^2**
Maximum temperature (ºC)	0.2	0.99	0.9	0.99
Minimum temperature (ºC)	-3.6	0.98	-3.0	0.97
Rainfall (%)	68.2	0.86	33.3	0.83
Wind speed (%)	-21.4	0.49	-47.5	0.37
Solar radiation (%)	4.4	0.99	17.6	0.99
Relative humidity (%)	14.4	0.94	7.5	0.86

Average and inter-annual changes

Table 5.8 shows the expected average annual changes for the climate parameters referred above, as predicted by the PROMES model for the two emission scenarios. When comparing with the multiple climate change scenarios shown in Figure 2.6 and Figure 5.2, the PROMES scenarios are among those which predict the largest decrease in rainfall. In comparison with the sensitivity tests described in section 6.1, these climate change scenarios follow the line used in the "low rainfall" simulations (see also Figure 5.2), although with a greater

atmospheric CO_2 concentration increase . Overall, the predicted average values shown in Table 5.8 follow the expected trends of increasing temperatures and decreasing rainfall rates predicted for the Mediterranean rim of Europe (Räisänen et al., 2004; see also section 2.2.1). The increase in solar radiation and decrease in relative humidity can also be linked with the reduction of rainfall days (and hence nebulosity) and the increase in temperature associated with the presence of less water vapor in the atmosphere, respectively. The greater increase of maximum temperatures when compared with the increase in minimum temperatures should also be noted.

Table 5.8 – Predicted average annual changes in climate parameters for the PROMES A2 and B2 scenarios, compared with the control run.

	Guadiana		**Tejo**	
Parameter	**A2**	**B2**	**A2**	**B2**
Maximum temperature (ºC)	4.5	3.3	4.3	3.1
Minimum temperature (ºC)	2.8	2.0	2.2	1.4
Average temperature (ºC)	3.7	2.7	3.2	2.2
Rainfall (%)	-29.0	-24.0	-24.7	-20.5
Windspeed (%)	-2.1	-2.4	-2.1	-3.8
Solar radiation (%)	8.4	6.8	8.8	8.0
Relative humidity (%)	-7.7	-6.6	-6.0	-3.0

Overall, the increase in temperature coupled with the decrease in rainfall is expected to lead to changes in the aridity of both study areas. These changes can be assessed using the ratio of rainfall to potential evapotranspiration developed by the UNEP (1997), shown in Figure 5.19. In the Guadiana study area, the ratio falls from 0.5 to 0.3 in both scenarios, which shifts the local climate from the upper end of the semi-arid classification (close to sub-humid) to the lower end (close to arid). In the Tejo study area, the ratio falls from 0.7 to 0.45 in the A2 scenario and 0.5 in the B2 scenario, shifting the local climate from a humid classification (although close to sub-humid) to semi-arid (although close to sub-humid) in both cases. Therefore, these scenarios point to a shift in climate regime, at least when considering a climate-based assessment. Furthermore, it is interesting to note that the aridity in the Tejo area is expected to shift to the values currently found in the Guadiana area; this could lead to future hydrological and vegetation conditions in the Tejo comparable to the ones currently found in

the Guadiana, assuming that the aridity index can be used as an indicator of the hydrological characteristics of a certain area, as suggested by Arora (2002).

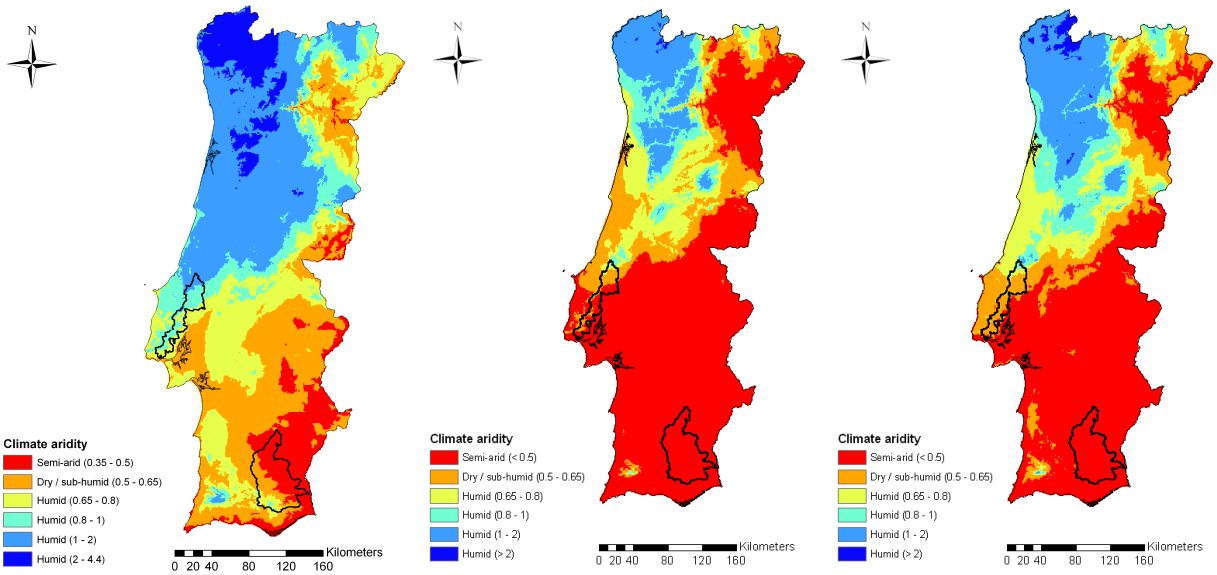

Figure 5.19 – Map of Portugal showing the location of the study areas superimposed over the climate aridity index (UNEP, 1997), for current conditions (left), the A2 PROMES scenario (center) and the B2 scenario (right); the Guadiana area is located in southeastern Portugal, while the Tejo area is located in the west.

Average annual values, however, can mask predicted changes to inter-annual variability in climate parameters. The cumulative histogram for current and predicted climate is shown in Figure 5.20 for average annual temperature, and in Figure 5.21 for annual rainfall. The lower and upper extreme values are shown in Table 5.9 for temperature, and Table 5.10 for rainfall. For temperature, it appears to be no significant difference in the relative distribution of temperature above the average between the control conditions and the B2 scenario; for the A2 scenario however, Table 5.9 shows a small increase of the frequency of occurrence of high temperature extremes, even after discounting the overall average temperature increase. These results agree with other scenarios published for southern Europe (e.g. Räisänen et al., 2004; see also section 2.2.1). For rainfall, the only significant differences appear to be a slight trend in the increase of the frequency of wet years when compared with average annual values in both scenarios (Table 5.10), which is however insufficient to lead to extreme rainfall years with a similar magnitude to the ones found in the current climate, particularly in the Tejo area.

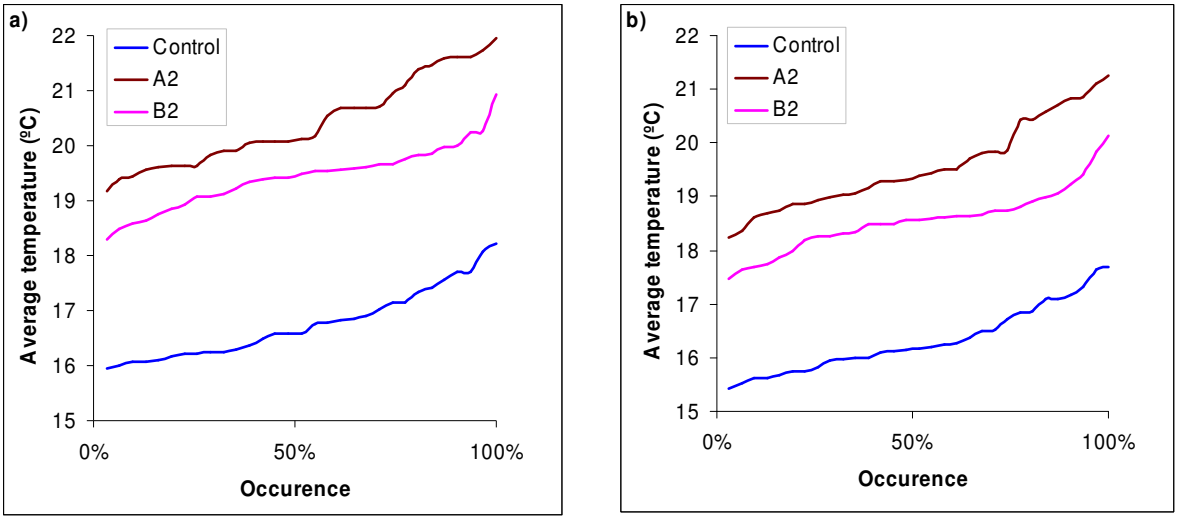

Figure 5.20 – PROMES results for the control conditions (1961-90) and climate change scenarios A2 and B2 (2071-2100) showing the cumulative histogram for average annual temperature in the Guadiana (a, left) and Tejo (b, right) study areas.

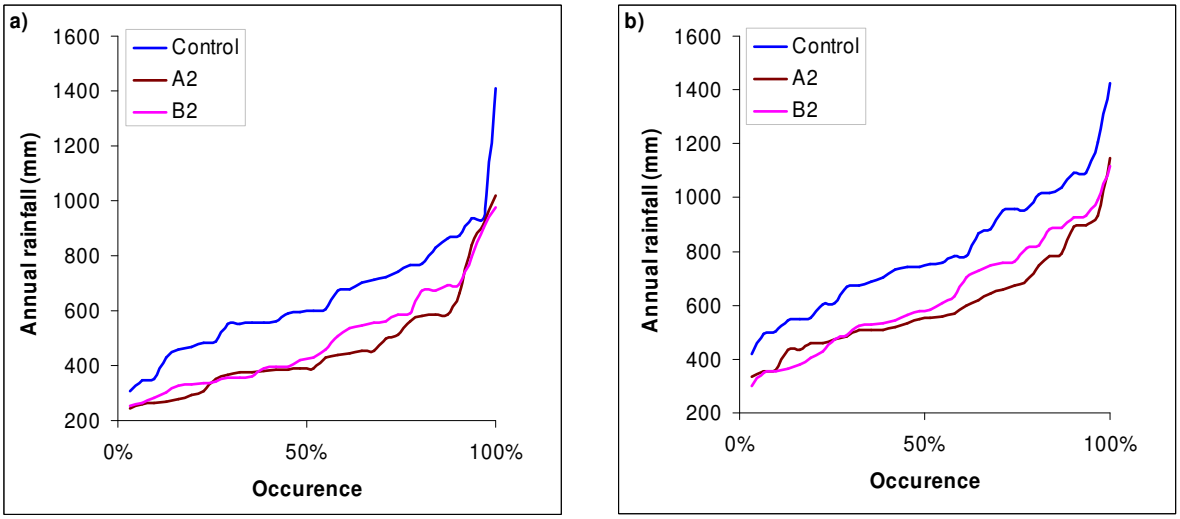

Figure 5.21 – PROMES results for the control conditions (1961-90) and climate change scenarios A2 and B2 (2071-2100) showing the cumulative histogram for annual rainfall in the Guadiana (a, left) and Tejo (b, right) study areas.

Table 5.9 – Lower and upper percentile annual temperature values, measured in ºC above or below long-term annual average, for the PROMES control, A2 and B2 scenarios.

	Guadiana			Tejo		
	Control	**A2**	**B2**	**Control**	**A2**	**B2**
Percentile 10 (ºC from average)	-0.7	-0.9	-0.8	-0.7	-0.9	-0.8
Percentile 25 (ºC from average)	-0.5	-0.7	-0.3	-0.4	-0.6	-0.3
Percentile 75 (ºC from average)	0.4	0.6	0.3	0.4	0.6	0.2
Percentile 90 (ºC from average)	0.9	1.2	0.6	0.8	1.3	0.7

Table 5.10 – Lower and upper percentile rainfall values, measured in % above or below long-term annual average, for the PROMES control, A2 and B2 scenarios.

	Guadiana			Tejo		
	Control	**A2**	**B2**	**Control**	**A2**	**B2**
Percentile 10 (% from average)	-34	-42	-38	-32	-28	-42
Percentile 25 (% from average)	-20	-22	-29	-20	-20	-24
Percentile 75 (% from average)	16	16	19	19	13	24
Percentile 90 (% from average)	35	44	41	37	48	45

The aridity index described above is used to perform a first evaluation of the impacts of these climate change scenarios on the inter-annual variability of climatic conditions, particularly on the frequency of extreme droughts. The cumulative histogram for current and predicted annual aridity is shown in Figure 5.22. In the Guadiana area, current conditions are (as referred above) semi-arid but close to sub-humid, with conditions above the sub-humid threshold c. 40 % of the years, and above the humid threshold c. 10 % of the years; conversely, extreme droughts would be expected when conditions are closer to arid. In contrast, both climate change scenarios present most years with semi-arid conditions, and a number of them (10 – 20 %) fall below the arid threshold.

In the Tejo area, current conditions are humid but close to sub-humid (as referred above). Figure 5.22 shows that in current conditions, about half of the years can be considered dry, with about 20 % presenting semi-arid conditions. In both climate change scenarios, conditions are semi-arid most of the time (c. 60 % for the B2 scenario and 75 % for the A2 scenario), and in some cases they approach the arid threshold. Similarly, the frequency of humid years falls to around 10-15 %. In both study areas, these changes in climate aridity indicate an increase

in the frequency and severity of droughts, when considering current average and extreme conditions. Furthermore, the similarity between both the A2 and B2 scenarios should be noted, particularly in terms of extreme values; the major difference in both study areas appears to be the relatively more frequent occurrence of wetter years in the B2 scenario, which could somewhat offset the more extreme drought years.

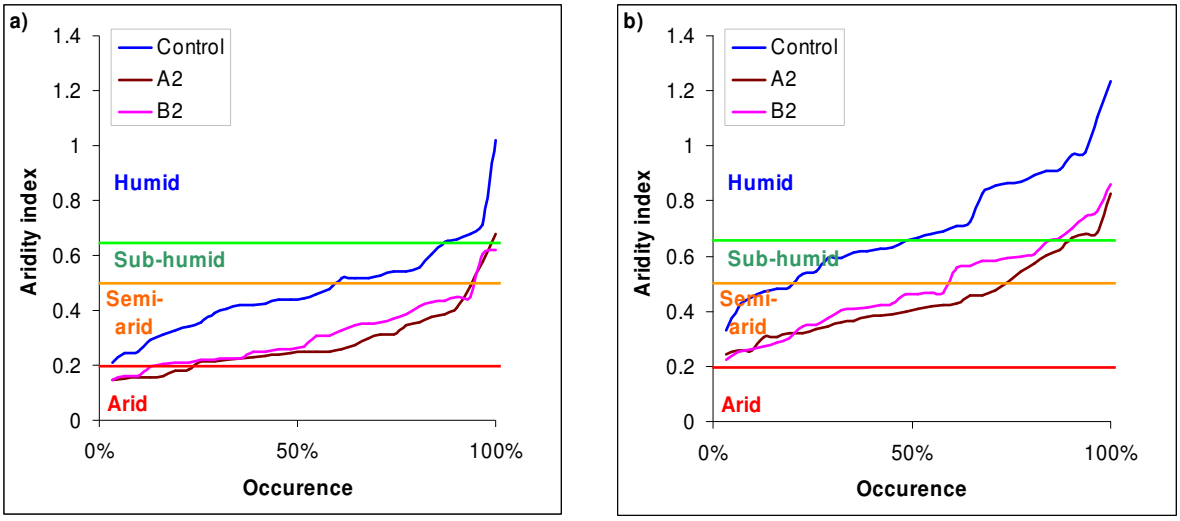

Figure 5.22 – PROMES results for the control conditions (1961-90) and climate change scenarios A2 and B2 (2071-2100) showing the cumulative histogram for annual aridity in the Guadiana (a, left) and Tejo (b, right) study areas; aridity is measured using the aridity index developed by UNEP (1997).

Seasonal and extreme event changes

Climate change scenarios for the Mediterranean rim of Europe (e.g. Cunha et al., 2002; Räisänen et al., 2004; see also section 2.2.1) also predict that temperature increases and rainfall decreases will be greater during the dry season, pointing to an increase in the seasonal variability of climate. The PROMES results follow these scenarios, as can be seen in Figure 5.23 for maximum and minimum temperatures, and in Figure 5.24 for rainfall. The latter case shows that changes in rainfall patterns are expected to increase the duration of the dry season in both study areas, bringing its onset forward from June to May in both scenarios. The major difference between both scenarios lies in the rainfall predictions for the wet season, particularly from February to April, which decrease significantly more in the A2 scenario. This change is also shown in Table 5.11, which shows the distribution of annual rainfall

throughout four seasons in terms of percentage; while the B2 scenario is similar to control conditions, the A2 scenario shows a marked trend for the concentration of rainfall in the DJF (December, January and February) season at the expense of the MAM (March, April and May) season in both study areas, further increasing the existing seasonal contrast.

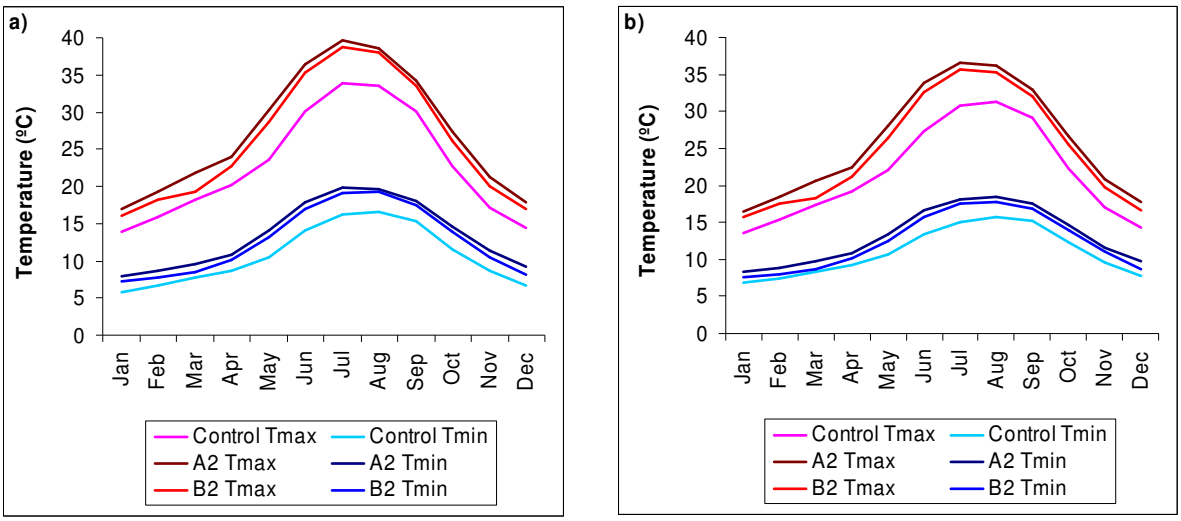

Figure 5.23 – PROMES results for average monthly maximum and minimum temperature in the control situation (1961-90) and climate change scenarios A2 and B2 (2071-2100), for the Guadiana (a, left) and Tejo (b, right) study areas.

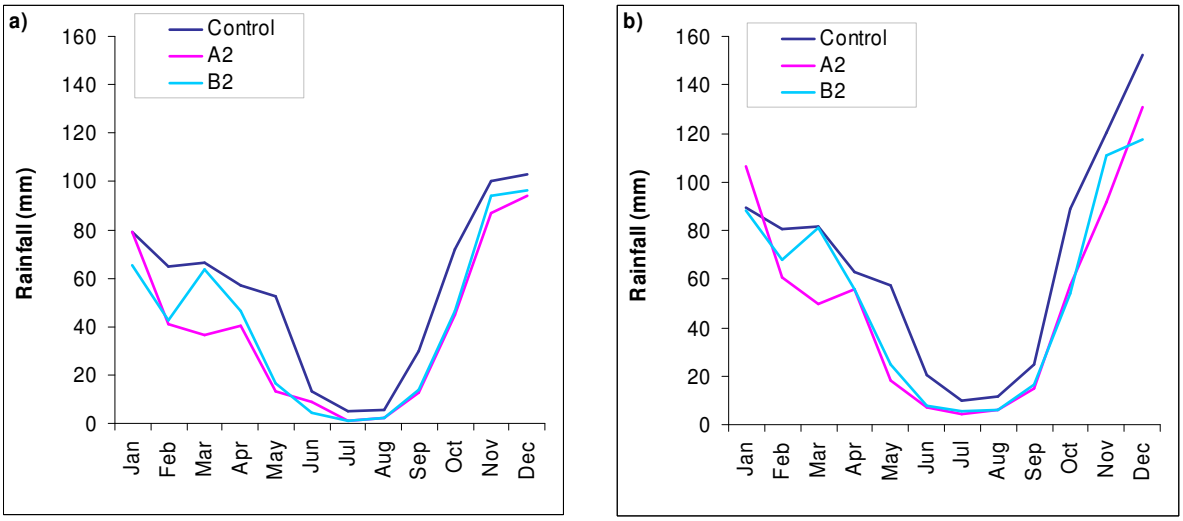

Figure 5.24 – PROMES results for average monthly rainfall in the control situation (1961-90) and climate change scenarios A2 and B2 (2071-2100), for the Guadiana (a, left) and Tejo (b, right) study areas.

Table 5.11 - Percentage of annual rainfall falling on each season for the PROMES control, A2 and B2 scenarios; SON is September, October and November, DJF is December, January and February, MAM is March, April and May, and JJA is June, July and August.

	Guadiana			Tejo		
Season	**Control**	**A2**	**B2**	**Control**	**A2**	**B2**
SON	31	31	31	29	27	29
DJF	38	46	41	40	49	43
MAM	27	20	26	25	20	25
JJA	4	3	2	5	3	3

The predicted decreases in rainfall are not followed by a decrease in extreme event intensity. Overall, the rainfall per day decreases only c. 8 to 12 % in both areas and scenarios, which is significantly smaller than the total rainfall decreases of 20 to 30 % shown in Table 5.8; this is due to a significant decrease in the number of days. In particular, when taking only "storm days" into account – considered as those with rainfall above 10 mm, following the range of values used by e.g. Santos et al. (2005) – the rainfall per day does not change significantly in any case in the Tejo, and only changes significantly for the B2 scenario (-10.4 %) in the Guadiana. When separating these results in two "storm seasons" – an early season during October, November and December (OND) and a late season during January, February, March and April (JFMA) – the changes become more significant, as can be seen in Figure 5.25. While in most cases rainfall intensity per storm day does no change in the OND season, in the JFMA it increases significantly, reaching an increase of 18.8 % for the A2 scenario in the Tejo; the exception is once again the B2 scenario for the Guadiana. It should be noted that the total rainfall arriving during storm days is evenly divided between both seasons for both study areas and in all scenarios. These results are also in agreement with those found in other studies for this region (e.g. Miranda et al., 2002; Räisänen et al., 2004; see section 2.2.1 for a further discussion).

One interesting result shown in Figure 5.25 is that the increase in storm day rainfall intensity is more noticeable for the A2 scenario, where rainfall is expected to suffer a stronger decrease (JFMA), pointing to a greater rise in climatic instability. This can also be seen in the standard deviation between years, which increases for the A2 scenario, indicating greater changes in the most extreme events (those with low return periods). In this work, the changes in days with intermediate or strong rainfall (above 10 mm) have been used to represent changes in extreme event rainfall.

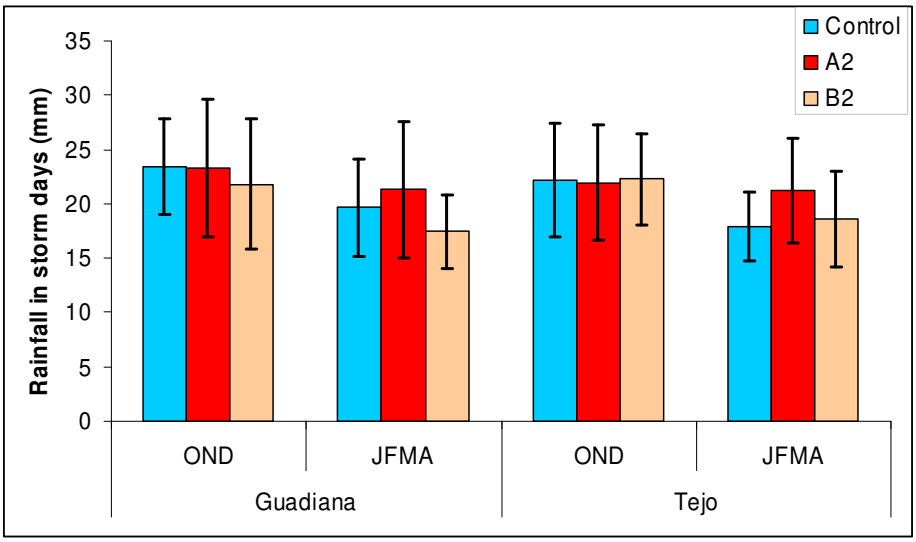

Figure 5.25 – PROMES results for average daily rainfall in storm days (with rainfall above 10 mm), for the OND and JFMA seasons, in the control situation (1961-90) and climate change scenarios A2 and B2 (2071-2100), for the Guadiana (a, left) and Tejo (b, right) study areas; the black lines represent the standard deviation between years.

5.3.3 Results and discussion – seasonal scale

The SWAT model was run for 30 years using the control and climate change scenarios generated by the PROMES model, referred above. This section presents the results for hydrology and vegetation growth; as in section 5.1, results were only spatially discretized by vegetation cover. The average changes predicted by the model for the main hydrological parameters are presented in Table 5.12. Overall, the patterns are similar to those found in the sensitivity analysis described in section 5.1: total runoff is more affected than evapotranspiration in both scenarios, and subsurface runoff is more affected than surface runoff. Furthermore, the results compare well with those shown for a similar magnitude in Figure 5.6, except for evapotranspiration, which suffers a greater reduction. However, it should be noted that the rainfall decreases in the scenarios are larger than the ones considered in the "low rainfall" sensitivity tests above, for a similar degree of temperature increases. Furthermore, the shift in rainfall towards winter, which could lead to less available rainfall and evapotranspiration in summer periods, was not so pronounced in the sensitivity tests.

Table 5.12 – SWAT results for average annual changes in hydrological parameters, in comparison with a control run, using the PROMES A2 and B2 scenarios shown in Table 5.8.

	Guadiana		Tejo	
Parameter	**A2**	**B2**	**A2**	**B2**
Rainfall (%)	-29.0	-24.0	-24.7	-20.5
Evapotranspiration (%)	-21.6	-17.4	-13.5	-10.2
Surface runoff (%)	-30.7	-28.6	-31.7	-27.9
Subsurface runoff (%)	-70.4	-64.5	-46.9	-41.5
Total runoff (%)	-44.0	-40.5	-41.0	-36.2

The reasons behind these changes are similar to those found in the sensitivity tests. The trend of larger decreases to runoff, particularly subsurface, indicates a diversion of soil water towards vegetation water use; the large differences between changes to surface and subsurface runoff in the Guadiana study area can be attributed to the low water storage capacity of soils in this region, reducing their ability to recharge during rainfall episodes. Overall, the results show a trend of an amplification of rainfall decreases in runoff rates, since there is less water inputted into the hydrological system, and also more of the available rain water (in relative terms) is used in evapotranspiration.

This shift towards evapotranspiration appears to be non-linear and vary significantly between years. Arora (2002) describes how the diversion of rain water towards evapotranspiration increases with lower aridity index values, as the available energy increasingly exceeds the amount required to evaporate annual precipitation; at very low values, annual evapotranspiration tends to approach annual precipitation. These results show that, despite the small changes to the inter-annual distribution of temperature and rainfall caused by climate change scenarios (Figure 5.20 and Figure 5.21), there is a significant shift in the frequency of occurrence of hydrological extremes, as shown by the steepest slope of the histograms in Figure 5.26. The model results suggest that extreme runoff will show greater variability around average values, as shown in Table 5.13, particularly in the B2 scenario. It should be noted that both the A2 and B2 scenarios present a similar number of low runoff years, but the latter also presents a greater frequency of higher runoff years which increases the average annual runoff values. These non-linear changes can be attributed to a variation of both the available rain water supply and the rainfall to evapotranspiration ratio, with less water available for runoff in the drier years, especially when considering the expected increase in the frequency of semi-arid years in both study areas (shown in Figure 5.22).

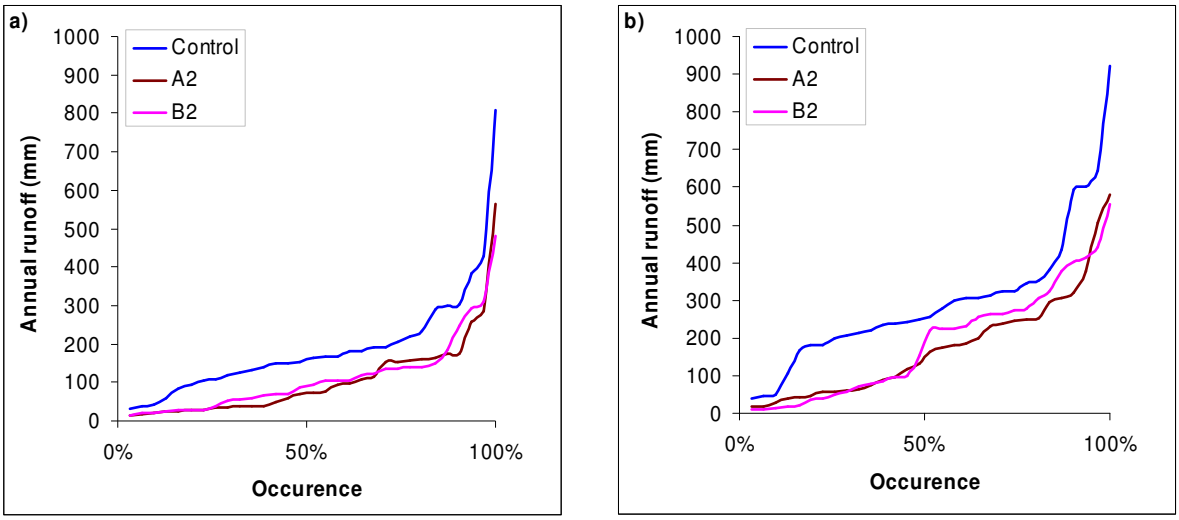

Figure 5.26 – SWAT results for the control run (1961-90) and climate change scenarios A2 and B2 (2071-2100), using the PROMES A2 and B2 scenarios shown in Table 5.8, showing the cumulative histogram for annual runoff in the Guadiana (a) and Tejo (b) study areas.

Table 5.13 – SWAT results for lower and upper percentile annual runoff values, measured in % above or below long-term average, using the PROMES control, A2 and B2 scenarios.

	Guadiana			**Tejo**		
	Control	**A2**	**B2**	**Control**	**A2**	**B2**
Percentile 10 (% from average)	31	22	22	36	22	9
Percentile 25 (% from average)	59	33	40	68	34	28
Percentile 75 (% from average)	110	144	121	112	141	145
Percentile 90 (% from average)	159	163	217	199	181	212

The results also indicate significant shifts to seasonal runoff patterns, a consequence of the decrease in rainfall coupled with the increase in the seasonal variability of rainfall rates. Figure 5.27 shows the simulated results for average monthly surface and subsurface runoff rates, for both the control conditions and climate change scenarios, during a hydrological year as defined by Palutikof et al. (1996). The decrease in total runoff, as well as the greater impacts on subsurface runoff rates (particularly in the Guadiana) are visible in the figure. Another important difference from the control condition is an extension of the very low flow period; from the current low flows during July and August, SWAT predicts a very low flow period beginning in June and lasting until September for both scenarios and study areas. For the A2 scenario in the Tejo, this change is sufficient to lead to negligible flow during August,

in effect turning them into ephemeral rivers, a situation which is currently only observed in the Guadiana study area. This increase in the summer low flow period is associated with a significant delay in the soil water recharge period. Currently, subsurface flow starts to increase significantly in December for the Guadiana and November for the Tejo; this situation is not expected to change in the B2 scenario, but in the A2 scenario subsurface flow increase is delayed one month in both systems. Both these results can be attributed to the smaller duration of the rainy season predicted by the PROMES model for both scenarios, as previously shown in Figure 5.24.

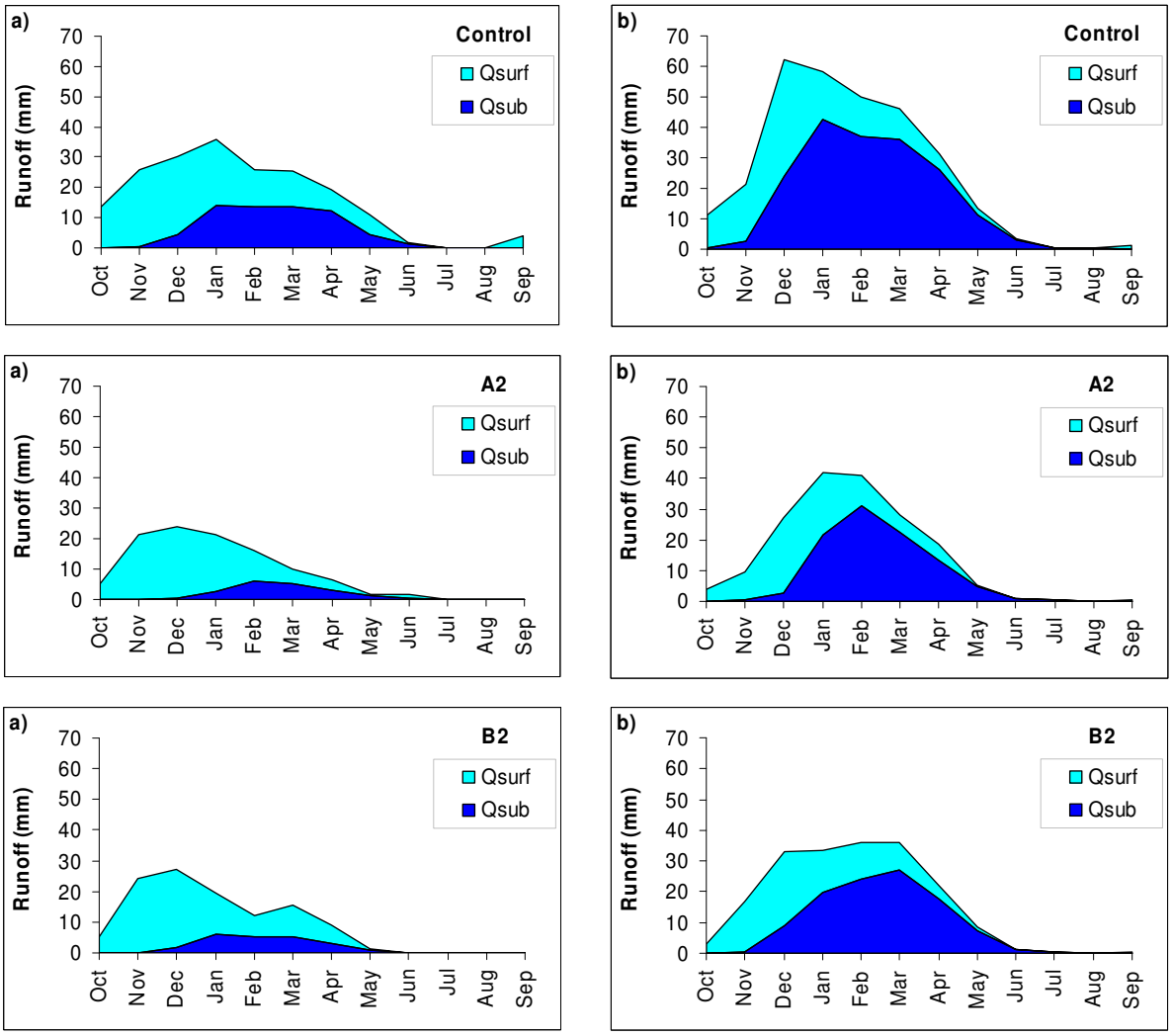

Figure 5.27 – SWAT results for average monthly surface runoff (Qsurf) and subsurface runoff (Qsub) in the control conditions (top, 1961-90) and climate change scenarios A2 (center, 2071-2100) and B2 (bottom, 2071-2100), using the PROMES A2 and B2 scenarios shown in Table 5.8, for the Guadiana (a, left) and Tejo (b, right) study areas.

Finally, SWAT results for changes in vegetation biomass growth were also analyzed since, as previously referred, these changes could further impact soil erosion rates. Table 5.14 shows the model results for this parameter; the model predicts a moderate to significant increase in the biomass for all vegetation types for both scenarios, except cork oak and forest in the Guadiana and Tejo study areas respectively, for the B2 scenario. It should also be noted that several vegetation types – shrub, cork oak, vine and forests – present much more significant responses to the A2 scenario, indicating a significant impact of CO_2 fertilization. In the B2 scenario, this impact can be mitigated by higher temperature rates and lower rainfall. In contrast, wheat presents a more significant response to the B2 scenario in both areas, indicating that this is the only case where CO_2 fertilization is sufficient to counteract the negative impacts of growing temperatures. It should be noted that the fact that a rise in CO2 would be sufficient to offset the adverse effects of a temperature increase on winter wheat growth concurs with the results obtained by Zhang and Nearing (2005).

Table 5.14 – SWAT results for average annual changes in vegetation biomass growth, using the PROMES A2 and B2 scenarios shown in Table 5.8.

	Guadiana			**Tejo**	
Parameter	**A2**	**B2**	**Parameter**	**A2**	**B2**
Wheat biomass growth (%)	5.3	15.5	Wheat biomass growth (%)	9.9	11.7
Shrub biomass growth (%)	58.0	11.7	Vine biomass growth (%)	9.4	1.2
Cork Oak biomass growth (%)	34.8	-3.2	Forest biomass growth (%)	3.8	-1.8

The results present significant differences with the biomass growth estimated for the sensitivity analysis, described in section 5.1.3 and shown in Figure 5.7. For the result closest to both the PROMES A2 and B2 scenarios (increase of 3.2 ºC in temperature, 20 % rainfall decrease and double CO_2 concentrations), the sensitivity results predicted a small decrease in wheat biomass (c. -10 %) in the Guadiana, coupled with significant increases in cork oak and shrub biomass (c. +25 and +40 %, respectively); in the Tejo, the sensitivity results showed a small decrease (c. -5 %) of biomass for all vegetation types. The differences in the results for these tests could be attributed to several factors, the most important being that CO_2 fertilization is significantly greater in both the A2 and B2 scenarios (107 and 56 % increase, respectively, as referred above) than in the sensitivity tests. Another factor is that, in the PROMES scenarios, the magnitude of changes is smaller during the vegetation growth period

(spring), while they were considered evenly distributed throughout the year in the sensitivity tests; a similar impact of the seasonal distribution of changes was observed by Zhang and Nearing (2005).

While these differences highlight the limitations of the method used for the sensitivity analysis, especially in respect to the relation between changes to temperature, rainfall and atmospheric CO_2 concentrations, they should also be analyzed in light of the small sensitivity of storm runoff and sediment yield to vegetation cover changes when examining the response of catchments to extreme rainfall events (see section 5.2). However, they do indicate that the "combined tests" presented in the sensitivity analysis are constrained by the assumptions taken while designing them, which is further discussed in section 6.4 (below).

The results also show that, despite the increased frequency of occurrence of arid years (Figure 5.22), there are no significant shifts in the interannual distribution of vegetation biomass productivity values, as shown in Figure 5.28. In most cases, shifts in productivity appear to be evenly distributed between average and extreme values, pointing to the impact of a constant factor such as atmospheric CO_2 concentration (as suggested above); in most cases there is a similar degree of variability around average values, as shown in Table 5.15 for the Guadiana and Table 5.16 for the Tejo. When compared with the changes to the inter-annual frequency of runoff values described above (Figure 5.26), these results indicate that changes to the frequency of climatic droughts have greater impacts over hydrological processes than over vegetation growth. This reinforces the indications for the greater impacts of climate change on runoff when compared with vegetation water use, described above (Table 5.12).

Overall, the SWAT results show significant impacts of the climate change scenarios for runoff patterns, including a decrease in overall runoff (particularly subsurface runoff), an increase in inter-annual runoff variability, and a lengthening of the summer low flow season, with a possibility for rivers in the Tejo watersheds becoming ephemeral. However, the results also show a slight increase in vegetation biomass, particularly for the Mediterranean species (shrubs and cork oak) present in the Guadiana study area. When combined, these results indicate that the impacts of increasing rainfall rates (shown in Figure 5.25) on storm runoff could be mitigated by the lower soil moisture values throughout the wet season; as for sediment yield, these impacts could be further mitigated by an increase in vegetation cover.

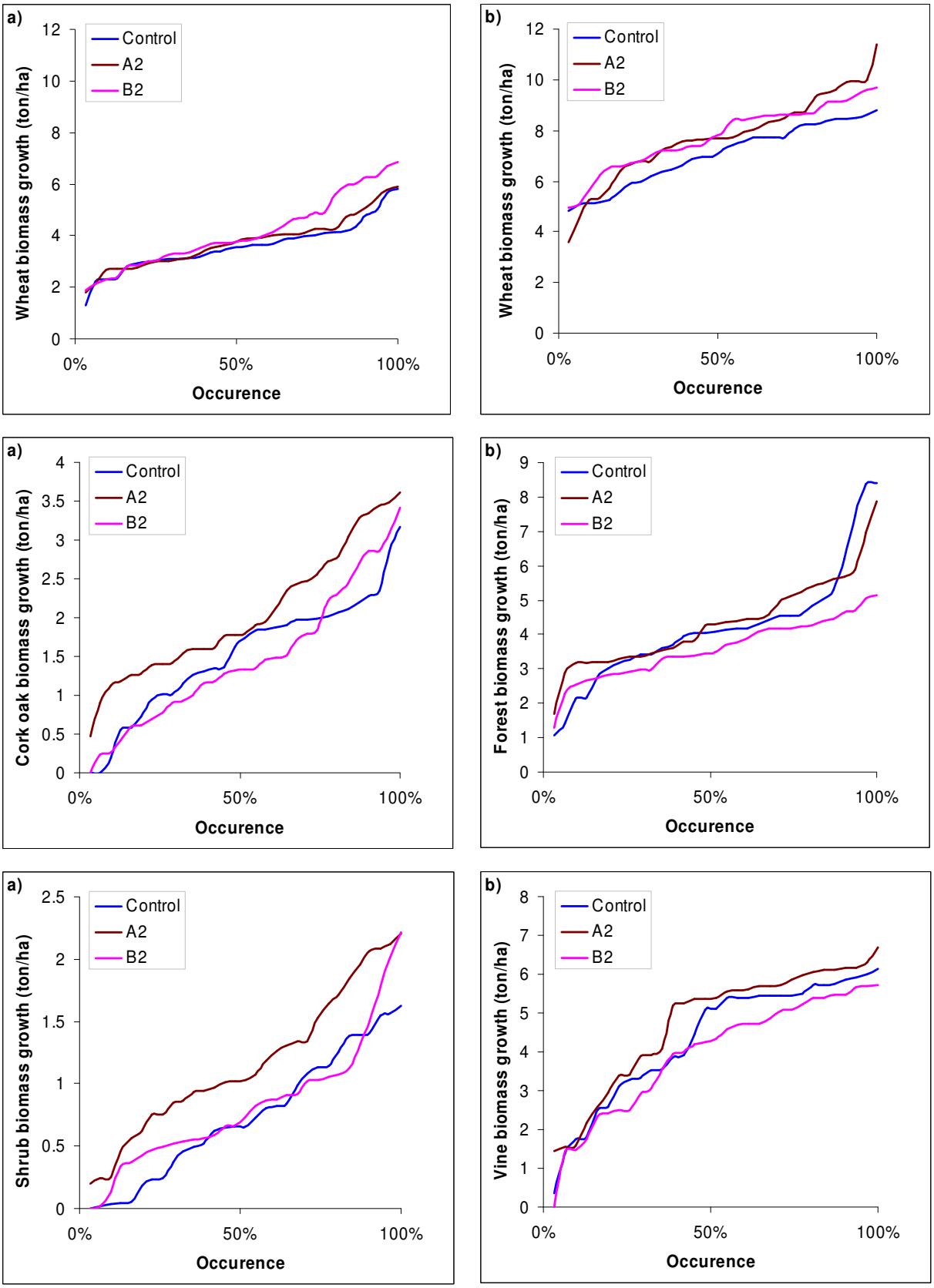

Figure 5.28 – SWAT results for average annual biomass growth for wheat (top), cork oak and forest (center) and shrub and vine (bottom) using the PROMES A2 and B2 scenarios shown in Table 5.8, for the Guadiana (a, left) and Tejo (b, right) study areas.

Table 5.15 – SWAT results for lower and upper extreme biomass production values in the Guadiana, measured in % above or below long-term annual average, using the PROMES control, A2 and B2 scenarios.

	Wheat			**Cork oak**			**Shrub**		
	Control	**A2**	**B2**	**Control**	**A2**	**B2**	**Control**	**A2**	**B2**
Percentile 10 (% from average)	66	72	58	37	57	28	6	39	41
Percentile 25 (% from average)	85	80	77	66	69	57	41	69	61
Percentile 75 (% from average)	113	113	118	131	129	137	153	136	126
Percentile 90 (% from average)	134	135	152	149	163	194	190	177	183

Table 5.16 – SWAT results for lower and upper extreme biomass production values in the Tejo, measured in % above or below long-term annual average, using the PROMES control, A2 and B2 scenarios.

	Wheat			**Forest**			**Vine**		
	Control	**A2**	**B2**	**Control**	**A2**	**B2**	**Control**	**A2**	**B2**
Percentile 10 (% from average)	73	69	80	52	73	74	42	46	44
Percentile 25 (% from average)	86	88	89	80	77	82	76	77	69
Percentile 75 (% from average)	116	113	111	109	119	117	127	125	130
Percentile 90 (% from average)	120	128	118	149	130	129	135	130	139

5.3.4 Results and discussion – extreme event scale

As described earlier, the SWAT results detailed above were combined with the PROMES scenario results to build a number of extreme event scenarios, which were then inputted in the MEFIDIS model to perform simulations for the Odeleite and Alenquer watersheds. The SWAT and PROMES results indicate different changes to storm runoff generation in the OND and JFMA seasons, given the different predictions for storm intensity (Figure 5.25) and soil moisture (as implied by changes to baseflow, shown in Figure 5.27), the two main factors governing runoff generation in Mediterranean watersheds (Boix-Fayos et al., 2006; see also section 2.2.2). The model results imply more favorable conditions for storm runoff generation

in the JFMA season due to an increase in storm intensity and a smaller decrease in soil water storage, with the reverse happening in the OND season. Therefore, two seasonal simulations using MEFIDIS were conducted (in OND and JFMA) for both the A2 and B2 climate change scenarios.

The MEFIDIS scenarios used three parameters from the PROMES and SWAT results: changes to storm rainfall intensity, subsurface runoff (to estimate changes in pre-storm soil water deficit) and vegetation biomass production (to estimate changes in vegetation cover). Results for the Guadiana and Tejo study areas were used to provide input values for the Odeleite and Alenquer simulations, respectively. Table 5.17 shows the changes in subsurface runoff and storm rainfall predicted by the SWAT and PROMES model, respectively, for each season, climate change scenario, and study area.

Table 5.17 – SWAT results for average changes in subsurface runoff during the OND and JFMA seasons, using the PROMES A2 and B2 scenarios shown in Table 5.8, compared with the changes in storm rainfall shown in Figure 5.25.

		Guadiana		**Tejo**	
		A2	**B2**	**A2**	**B2**
Subsurface runoff change (%)	OND	-89.3	-65.4	-89.1	-64.2
	JFMA	-68.3	-62.9	-37.6	-37.7
Storm rainfall change (%)	OND	-0.7	-6.7	-1.2	0.3
	JFMA	8.3	-11.2	18.8	3.8

Changes to subsurface runoff were applied directly to pre-storm baseflow values, shown in Table 4.6 for Odeleite and Table 4.7 for Alenquer. The changed values were then used to calculate new values for the spatial distribution of pre-storm soil water deficits using the wetness index-based method described by Beven (2000) and discussed in sections 3.2 and 4.2.3. The logarithmic nature of the equations used resulted in each change to subsurface runoff causing a similar change to soil water deficit in every storm, regardless of the different values of sub-surface pre-storm values; the changes to soil water deficit (in terms of spatial averages) are shown in Table 5.18. The high degree of changes to subsurface runoff for the OND season in the A2 scenario are mostly due to the shift of rainfall towards winter, delaying soil water recharge, as discussed in the previous section.

Table 5.18 – Impacts of changes to subsurface runoff (shown in Table 5.17) on soil water deficit during the OND and JFMA seasons, using the PROMES A2 and B2 scenarios, for the Odeleite and Alenquer study areas.

		Odeleite		Alenquer	
Scenario		**Changes to subsurface runoff (%)**	**Changes to soil water deficit (mm)**	**Changes to subsurface runoff (%)**	**Changes to soil water deficit (mm)**
A2	OND	-89.3	14.5	-89.1	24.4
	JFMA	-68.3	7.5	-37.6	5.2
B2	OND	-65.4	6.9	-64.2	11.3
	JFMA	-62.9	6.4	-37.7	5.2

The storm rainfall changes shown in Table 5.17 were applied directly to the rainfall totals for the storms described in Table 4.1 (for Odeleite) and Table 4.2 (for Alenquer). Due to the lack of any information on changes to storm intensity and duration, rainfall changes were evenly divided between these two parameters, following suggestion by the Pruski and Nearing (2002). In other words, storm intensity was considered to increase by half the amount shown for storm rainfall in Table 5.17.

Finally, vegetation biomass changes were represented by a single situation for both the OND and JFMA seasons, per climate change scenario. The changes predicted by the SWAT model (shown in Table 5.14) were considered to directly represent changes to runoff roughness (Manning's n). These were used to calculate changes to canopy cover using the equations published by Flanagan and Nearing (1995), taking into account both currently observed values and different shape coefficients for each vegetation type; and changes to interception storage capacity following Hoyningen-Huene (1983), using changes to leaf area index (following the light extinction coefficient approach by Deguchi et al., 2006) as an intermediate step in the calculations. This morphological approach is similar to the one applied in the previous exercise, described in section 5.2. The results for different vegetation parameters are shown in Figure 5.29; vegetation parameters are predicted to experience much more significant changes in the Guadiana study area. These changes were applied directly to the MEFIDIS land use parameters (Table 4.39), using the Guadiana results to simulate changes to the Odeleite watershed, and the Tejo results to simulate changes to the Alenquer watershed.

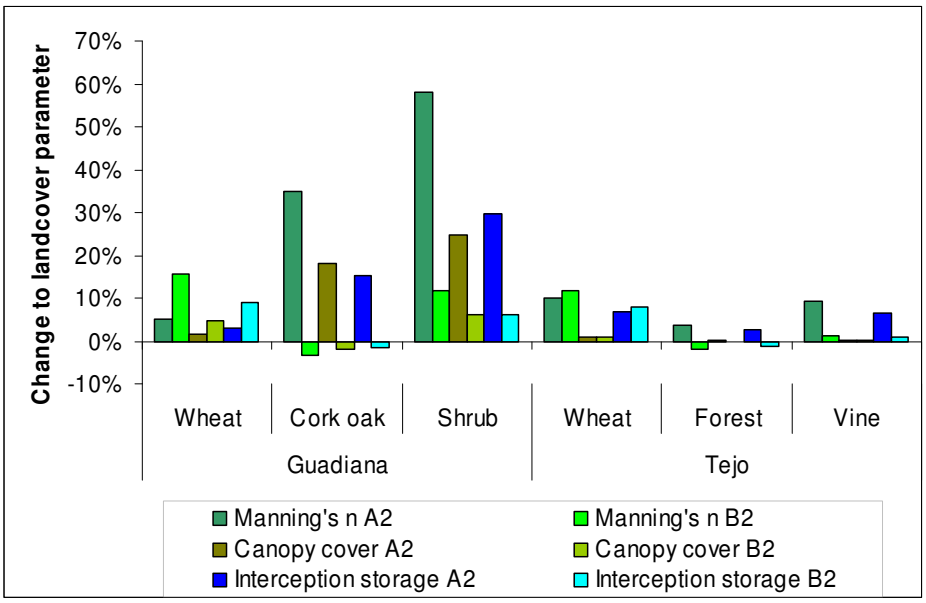

Figure 5.29 – Changes to the Manning's n, canopy cover and interception storage of different vegetation types in the Guadiana (left) and Tejo (right) study areas, calculated from the SWAT results for biomass changes for the PROMES A2 and B2 climate change scenarios.

Impacts on storm runoff and peak runoff rates

The overall results for catchment runoff and peak runoff rates, in both climate change scenarios, are shown in Table 5.19. Generally, there is a trend for the reduction of these parameters in both seasons, for the two sites, except for the A2 scenario in Alenquer during the JFMA season. The results also indicate that:

- the impacts of scenario B2 are evenly distributed between both seasons, but the impacts of scenario A2 are concentrated in the OND season, with lesser magnitude impacts in JFMA and, in one case, impacts with a different trend than those found for OND;
- in general, peak runoff rates show a similar behavior to that of storm runoff;
- the Odeleite watershed suffers larger negative impacts than the Alenquer watershed, which can mostly be attributed to the greater reduction in storm rainfall and baseflow (Table 5.17).

Table 5.19 – Average change (in %) of runoff and peak runoff rate for both study areas, for the scenarios described in Table 5.17.

		A2		B2	
Parameter		**OND**	**JFMA**	**OND**	**JFMA**
Runoff	Odeleite	-57.5	-30.9	-40.2	-45.5
	Alenquer	-46.6	13.9	-27.2	-9.1
Peak runoff rate	Odeleite	-51.5	-30.0	-37.8	-43.2
	Alenquer	-44.0	15.7	-26.7	-9.2

Overall, the extreme event results for hydrological parameters agree with the trends detected at the seasonal scale (Table 5.12), with both scenarios pointing to a significant reduction in runoff. The results also indicate that increased storm rainfall is insufficient to compensate the impacts of reduced baseflow, as could also be inferred by a comparative analysis of these changes in Table 5.17. It should be noted that the reduction in surface runoff is greater than that predicted at the seasonal scale, which can be attributed to the fact that the results in Table 5.17 refer to average values across a range of storms with different magnitudes while the results in Table 5.12 represent average annual values which integrate storm magnitude-frequency relations.

The results in table Table 5.19 also agree with the sensitivity tests described in section 6.1.2. First, storm runoff and peak runoff rates appear to be more sensitive to changes in storm rainfall than to changes in soil water deficit, as shown by the positive balance for the A2 JFMA scenario in Alenquer, and by the fact that in every other test the decrease in these parameters is smaller than the decrease in soil water deficit in percentual terms. However, the impact of larger soil water deficits is still sufficiently important to lead to a reduction in storm runoff, even in cases where storm rainfall increases. Second, peak runoff rates appear to be more sensitive to increases in storm rainfall than decreases in baseflow, as they show smaller reductions that storm runoff in most cases and, when storm runoff increases, peak runoff also increases by a wider margin. As debated above, peak runoff rates are dependent on changes to storm rainfall, soil water deficit and surface runoff, increasing the non-linearity of its response.

Furthermore, it should be noted that the Alenquer watershed actually shows an increase in storm runoff and peak runoff rates for the JFMA season, although smaller than the decrease predicted for OND. Even in this case, however, an increase in average storm rainfall of 18.8

% (Table 5.17) only results in an increase of 13.9 % for runoff and 15.7 % for peak runoff rates, which represents a significantly lower impact than the one expected for changes to storm intensity only (as inferred from the sensitivity analysis results shown in section 5.2). In the B2 scenario, the results show an increase of variability only in Alenquer, although the trend is still negative. These results are in agreement with the prediction for increased storm rainfall variability in the A2 scenario (shown in Figure 5.25).

Finally, the Odeleite watershed shows significantly larger reductions of storm runoff and peak runoff rates than the Alenquer watershed (Table 5.19). This can be partly attributed to the greater changes to storm rainfall and soil water deficit predicted for this watershed by the PROMES and SWAT models, particularly in the JFMA season (Table 5.17). However, there are also cases such as the A2 scenario for the OND season, where runoff parameters suffer a greater reduction in Odeleite even though changes to storm rainfall and soil water deficit are significantly larger in Alenquer. Furthermore, changes to baseflow result in greater increases to soil water deficit in the Alenquer watershed when compared with Odeleite (Table 5.18), which could have otherwise indicated that Alenquer would suffer greater reductions in runoff parameters. As discussed in section 6.1.2, this can be attributed to the low soil water storage capacity in Odeleite, which prevents the soil system from dampening changes to storm patterns (Skøien and Blöschl, 2003; van den Hurk et al., 2005). Another contributing factor is the significant increase of the interception storage capacity of shrubs and cork oaks in the A2 scenario (Figure 5.29), which constitute the majority of the vegetation cover in Odeleite.

The results also reveal some variability of the impacts between storms, particularly in the Alenquer watershed. Figure 5.30 shows the impact of each climate change scenario for each storm. In terms of storm runoff, and for the scenarios which greater runoff decrease, there appears to be greater impacts for the larger storms in Alenquer; in contrast, the scenario with runoff increase shows no significant variability between storms. As for peak runoff rates, the results show a similar variability in Alenquer. In Odeleite, however, a similar pattern is visible only up to a certain storm magnitude (peak runoff rate of c. 1 $mm.h^{-1}$ in Figure 5.30); above this level, the relative importance of impacts appears not to change with storm magnitude.

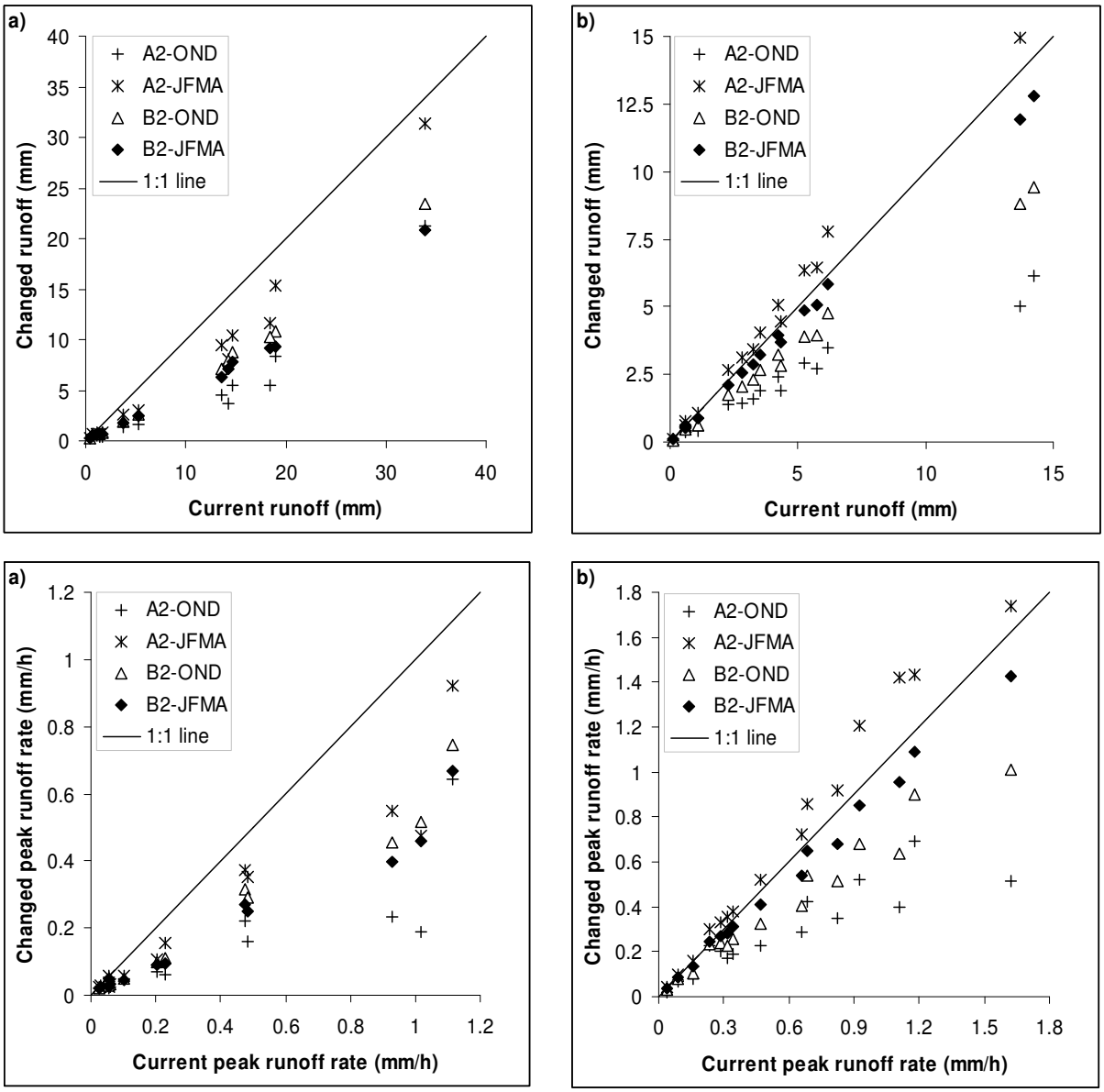

Figure 5.30 – Current and changed runoff (top) and peak runoff rates (bottom) in the Odeleite (a, left) and Alenquer (b, right) watersheds, for the scenarios described in Table 5.17.

This non-linearity can be attributed to the impact that changes in storm rainfall and soil water deficit have on the runoff generation ratio, shown in Figure 5.31. In Alenquer, the figure shows two cases: (1) when storm rainfall increases together with soil water deficit (e.g. in the A2 JFMA scenario), the positive effect of the former on the rainfall generation ratio appears to cancel the negative effect of the latter and rainfall generation suffers practically no changes; (2) when storm rainfall decreases and soil water deficit increases (e.g. in the A2 OND scenario), the effect of the two parameters leads to a reduction of the rainfall generation ratio, therefore explaining the non-linearity found in this case (Figure 5.30). The processes in

Odeleite appear to be more complex. There appears to be a trend for a decrease in the runoff generation ratio for lower values, but this response shows a considerable variability for higher values. This can again be attributed to the low soil water holding capacity found in Odeleite, coupled with the importance of saturation-excess and infiltration-excess runoff generation processes in Mediterranean watersheds (Castillo et al., 2003; see also section 2.2.2). Runoff generation in smaller storms can usually be attributed to saturation-excess processes, more sensitive to soil water deficit; in the larger storms, both processes can be important, and runoff generation can become independent of soil saturation when storm rainfall largely exceeds the soil water holding capacity. In Odeleite, the threshold for exceeding this limit is significantly lower than in Alenquer, and runoff generation is independent of soil saturation in a significant part of the larger storms (see section 4.2 for a further discussion). These storms will be significantly more affected by changes to storm rainfall, which are smaller than changes to soil water deficit (Table 5.17), leading to lesser changes to the runoff generation ratio as shown in Figure 5.31. These results also imply that the impacts of the climate change scenarios will decrease for storms with a very high magnitude. They also agree with the results shown in section 6.1.2 for the variability of sensitivity to change with storm magnitude in Odeleite.

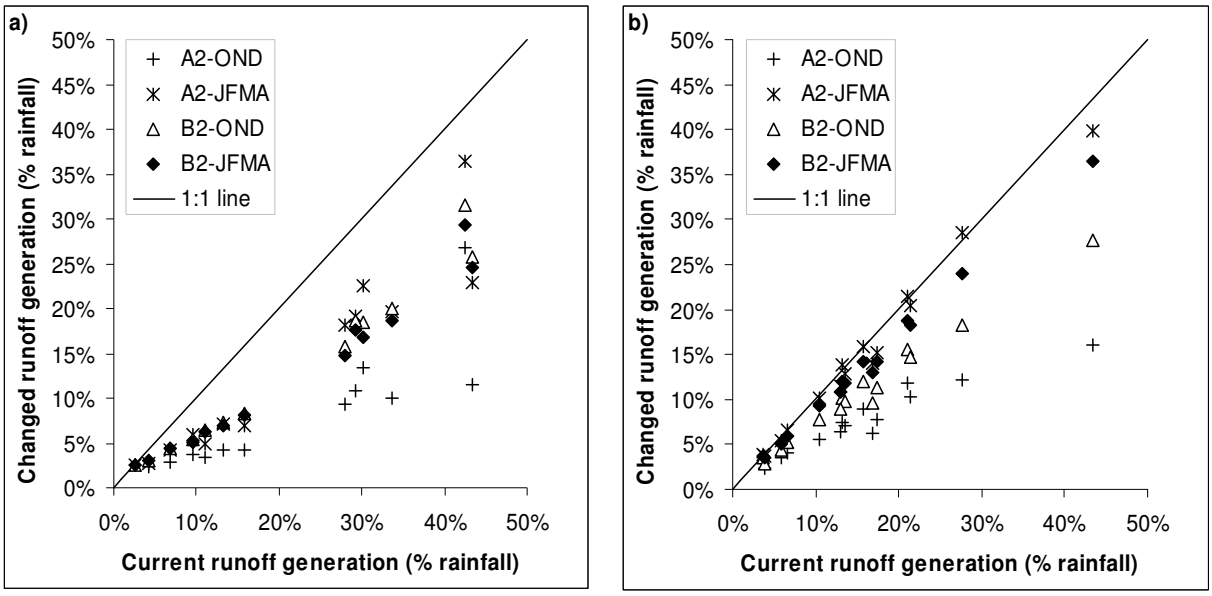

Figure 5.31 – Current and changed runoff generation ratio in the Odeleite (a, left) and Alenquer (b, right) watersheds, for the scenarios described in Table 5.17.

Impacts on sediment yield and soil erosion patterns

Table 5.20 shows the impacts of the climate change scenarios for sediment yield, upslope erosion (soil detached at the field / hillslope scale) and the Sediment Delivery Ratio (SDR – the relationship between field / hillslope erosion and catchment sediment yield as defined by Lane et al., 1997). The results follow the trend for runoff parameters shown in Table 5.19: a reduction of soil erosion in both seasons, although by a much greater rate than runoff changes. The exception is again the A2 scenario in Alenquer during the JFMA season. The results for erosion follow those for runoff in terms of the different seasonal impacts for the A2 scenarios, and the larger erosion reductions in Odeleite. Furthermore, they indicate that:

- upslope erosion shows less reductions than watershed sediment yield in Odeleite, leading to a very significant decrease of the SDR;
- in contrast, the SDR for Alenquer shows a very slight change and therefore the impacts on upslope erosion and sediment yield are similar.

Table 5.20 – Average change (in %) of sediment yield, upslope erosion and sediment delivery ratio for both study areas, for the scenarios described in Table 5.17.

		A2		**B2**	
Parameter		**OND**	**JFMA**	**OND**	**JFMA**
Sediment yield	Odeleite	-95.8	-76.2	-83.4	-89.0
	Alenquer	-77.0	29.4	-51.6	-17.8
Upslope erosion	Odeleite	-74.6	-44.6	-54.7	-62.5
	Alenquer	-69.7	20.0	-44.5	-16.6
Sediment delivery ratio	Odeleite	-86.7	-65.6	-70.7	-76.5
	Alenquer	-0.7	7.5	-4.5	-0.2

The greater response of soil erosion to the climate change scenarios, when compared with runoff parameters, follows the results obtained in the sensitivity tests discussed in section 6.1.2. The motives for this result follow the same reasoning in both cases: runoff is dependent on the external changes alone, while soil erosion shows a non-linear dependency on cumulative changes to both external factors and surface runoff; this non-linearity concurs with field observations of erosion response variability (e.g. Nearing et al., 1999; Puigdefabregas et al., 1999). Furthermore, in Odeleite the impacts of changes to rainfall and runoff are

compounded by changes to vegetation cover (Figure 5.29) which, in most cases, tend to increase soil surface protection from erosive forces, leading to a large decrease in upslope erosion. In contrast, most scenarios for Alenquer present small changes to vegetation cover.

The results also show that, in the Odeleite watershed, the impact of climate change scenarios is larger for sediment yield when compared with upslope erosion. Figure 5.32 shows the variability of impacts between storms for both parameters. For Odeleite, not only are the impacts significantly greater for sediment yield, but they also tend to increase with storm magnitude, pointing to a coupling of two effects: a decrease of available sediment (following a decrease in upslope erosion) coupled with a decrease in the SDR. This indicates that the results can be explained in part by a decrease in sediment connectivity within the watershed, since changes to runoff patterns can impact the rate of sediment deposition in the channel network, leading to changes in sediment yield that are not reflected in erosion rates on fields and hillslopes (Favis-Mortlock et al., 2001). However, the high degrees of change shown in Table 5.20 for sediment yield should be analyzed in light of the very low sediment yield estimates for this watershed in the control run (section 4.2.2), resulting in a small change in terms of absolute values.

In contrast, the impacts of climate change on Alenquer are similar for both sediment yield and upslope erosion; while they increase with storm magnitude for the OND scenarios, this is probably due in a large measure to the same process occurring for peak runoff changes (Figure 5.30). These results can partly be explained by the greater reductions experienced by peak runoff rates in Odeleite when compared with Alenquer (Table 5.17), which could result in greater relative impacts to sediment yield. Another possible explanation is that the higher SDR in Alenquer leaves a smaller scope for changes than in Odeleite, where a much slower SDR was calculated; this explanation concurs with the results found for the sensitivity tests (as discussed in section 6.1.2).

A discrimination of the upslope erosion results per dominant land use, shown in Table 5.21, also indicates that climate change could have different impacts for soil erosion under different vegetation types. When compared with the overall results (shown in Table 5.20), wheat croplands suffer either smaller reductions or larger increases than the catchment averaged values in the Odeleite watershed, particularly for the A2 climate change scenario. This result is particularly significant as wheat croplands are the watershed's main sediment sources despite their relatively small area, as discussed in section 4.4.2 (Table 4.45). This indicates that soil erosion problems will continue to be concentrated in croplands. The significant

increase of soil erosion in forests for Alenquer under the B2 climate change scenario does not indicate an important increase of soil erosion rates in forested areas; in fact, they result from the very small erosion rates estimated for the current conditions (Table 4.45).

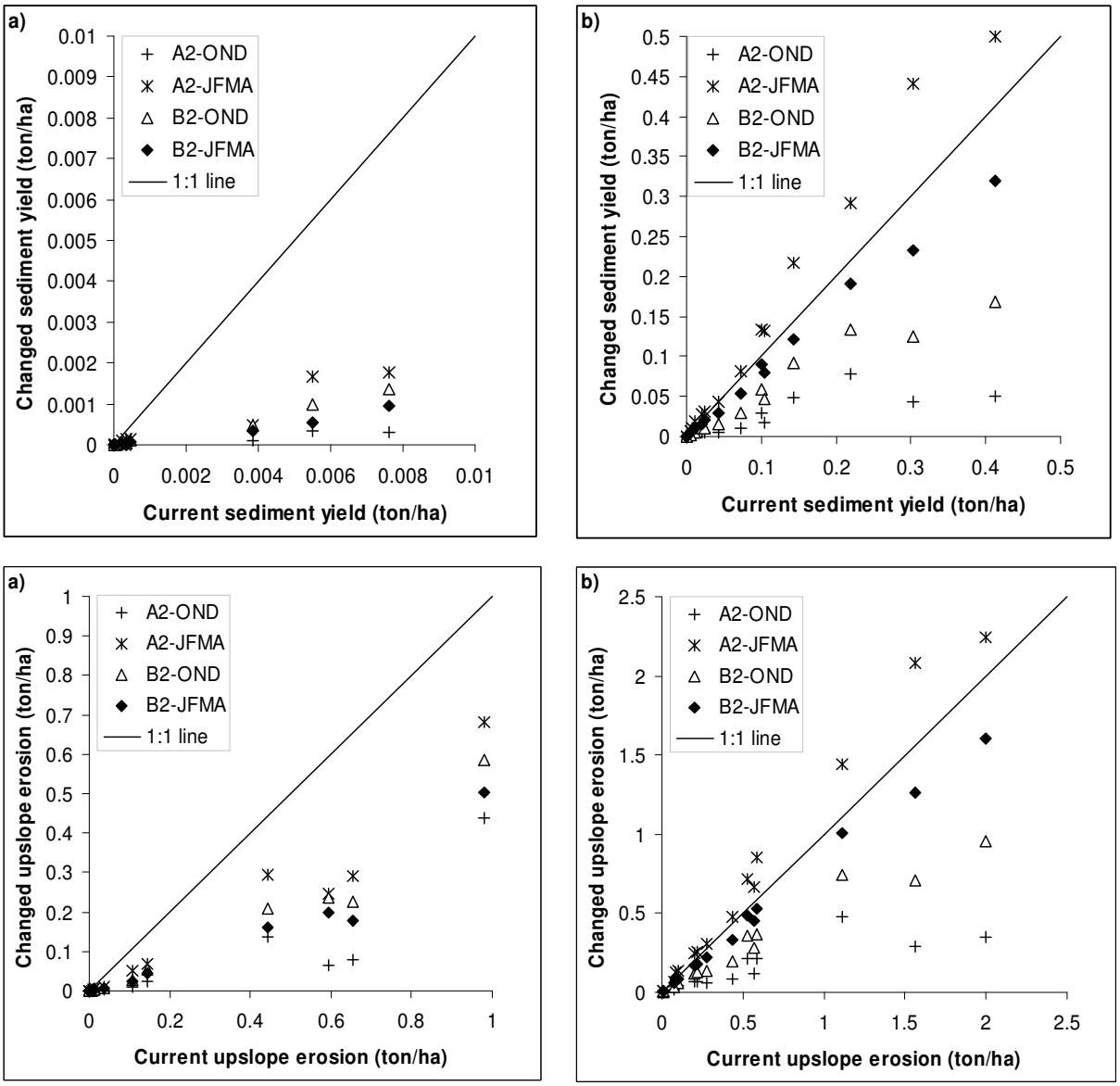

Figure 5.32 – Current and changed sediment yield (top) and upslope erosion (bottom) in the Odeleite (a, left) and Alenquer (b, right) watersheds, for the scenarios described in Table 5.17.

Table 5.21 – Average change (in %) of upslope erosion under different land uses for both study areas, for the scenarios described in Table 5.17.

		A2		B2	
Landcover		**OND**	**JFMA**	**OND**	**JFMA**
Odeleite	Wheat	-68.1	-32.1	-51.6	-59.3
	Cork oak	-90.8	-72.0	-62.0	-70.7
	Shrub	-96.3	-90.2	-64.8	-72.4
Alenquer	Wheat	-69.6	22.8	-45.3	-17.7
	Forest	-64.7	34.4	107.7	233.4
	Vine	-70.9	3.5	-41.0	-12.9

Table 5.22 shows the impacts of climate change scenarios for the total erosion in regions experiencing significant erosion rates (above 1 ton.ha^{-1} in each storm), where erosion can be attributed to concentrated flow and therefore where model results more closely approach the processes involved in gully erosion. The impact to the watershed area covered by this type of erosion is also presented in the table. The results follow the trend for runoff parameters (Table 5.19) and overall soil erosion parameters (Table 5.20): a reduction of erosion and affected areas in both seasons, with an exception for the JFMA season in the Alenquer A2 scenario. Furthermore, they also indicate that:

- the amount of erosion in areas with significant rates shows a similar response to that predicted for overall upslope erosion, implying a similarity of underlying processes;

- however, in both watersheds the impacts over total erosion and affected area are very similar, implying a spread or reduction of the extent of these areas rather than changes to the erosion rates experienced within them.

Figure 5.33 illustrates this phenomenon by comparing the affected area and total erosion in these regions for every storm, in the control and climate change scenarios. In general, both the control and climate change area/erosion ratios remain in roughly the same region, with changes in total erosion compensated with changes in affected area, although there appears to be some differences in this ratio between storms, and in the impacts of climate change scenarios for this parameter If these results are taken as an indicator of the impacts on the occurrence of ephemeral gully erosion, as proposed above, then they indicate that the area covered by ephemeral gullies is more affected by the climate change scenarios than the erosion rate within gullies. Furthermore, it should be noted that most climate change scenarios

do not significantly impact the gully-to-rill/interill erosion ratio, which is kept similar to the rates shown in Table 4.44; gully erosion is therefore expected to continue to be the most important erosion process in these watersheds, regardless of the climate change scenario.

Table 5.22 – Average change (in %) of total erosion and catchment area in regions with significant erosion rates, for both study areas; significant erosion rate is defined as being above 1 ton.ha^{-1}, and the scenarios are described in Table 5.17.

		A2		B2	
Parameter		**OND**	**JFMA**	**OND**	**JFMA**
Amount of erosion in areas with significant rates (> 1 ton.ha^{-1})	Odeleite	-75.0	-44.4	-55.5	-63.4
	Alenquer	-76.4	25.2	-48.0	-16.9
Area with significant rates of erosion (> 1 ton.ha^{-1})	Odeleite	-69.4	-36.1	-50.6	-57.0
	Alenquer	-63.2	16.7	-38.1	-15.0

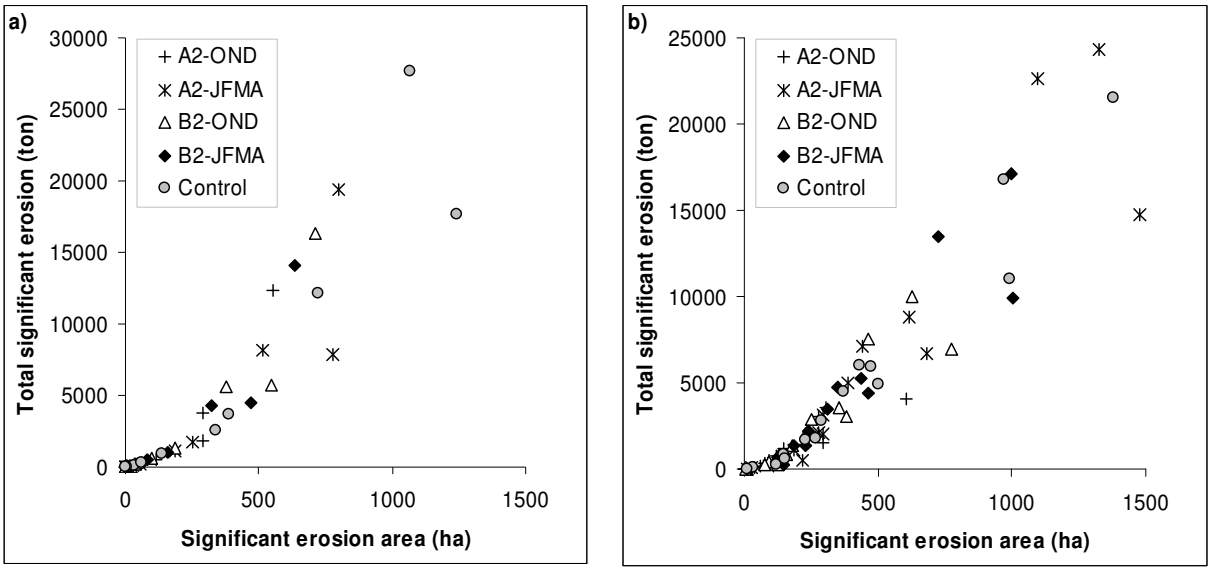

Figure 5.33 – Relationship between catchment area and total erosion in regions with significant erosion rates, in the Odeleite (a, left) and Alenquer (b, right) watersheds; significant erosion rate is defined as being above 1 ton.ha^{-1}, and the scenarios are described in Table 5.17.

5.3.5 Watershed response to climate change scenarios – conclusions

The work presented in this section demonstrates how a coupling of modeling tools can be used to study the impacts of climate change scenarios on hydrology and vegetation productivity at the seasonal scale, and how these results can be used to estimate impacts at the extreme event scale. The main findings are that, for the PROMES climate change scenarios A2 and B2 and in Portuguese Mediterranean watersheds, a large impact over surface water resources appears to be likely, with a decrease of water runoff by c. 35 to 40 %. An increase in the variability of runoff is also likely to occur, with a decrease of the baseflow fraction when compared with surface runoff and an increase of seasonal and inter-annual variability. The results also point to an increase of the differences of storm runoff between autumn (OND) and winter (JFMA); in Alenquer and for the A2 scenario, an increase in storm runoff is predicted despite the average decrease in all runoff parameters.

Vegetation productivity is expected to experience a small increase due mostly to the increased concentration of atmospheric CO_2. This factor, combined with the general reduction of rainfall and surface runoff, is expected to lead to a significant decrease of soil erosion rates (c. 60 % in the Guadiana and c. 25 to 35 % in the Tejo), with a smaller expression in wheat croplands for the Guadiana study area. However, ephemeral gully erosion rates are expected to remain sensibly the same, although the area affected by this phenomena is expected to decrease; and in the Tejo (represented by the Alenquer watershed), soil erosion rates for the A2 scenario are expected to increase during winter storms by c. 20 %. These results are further discussed in section 6.2, below, and compared with desertification threshold estimates for a full qualitative analysis (as described in section 3.1) of the resilience of the study areas to climate change.

5.4 References

Arora VK, 2002. The use of the aridity index to assess climate change effect on annual runoff. J. Hydrol. 265 (1-4): 164-177.

Bathurst JC, Kilsby C, White S, 1996. Modeling the impacts of climate and land-use change on basin hydrology and soil erosion in Mediterranean Europe. In: Brandt CJ, Thornes JB (Eds.), Mediterranean desertification and land use. John Wiley and sons, Chichester: 355-388.

Beven K, 2000. Rainfall-Runoff Modelling – The Primer. John Wiley & Sons, Chichester.

Boix-Fayos C, Martínez-Mena M, Arnau-Rosalén E, Calvo-Cases A, Castillo V, Albaladejo J, 2006. Measuring soil erosion by field plots: Understanding the sources of variation. Earth-Science Reviews 78: 267-285.

Castillo VM, Gómez-Plaza A, Martínez-Mena M, 2003. The role of antecedent soil water content in the runoff response of semiarid catchments: a simulation approach. J. Hydrol. 284:114–130.

Cunha LV, Oliveira R, Nunes V, 2002. Water Resources. In: Santos FD, Forbes K, Moita R (Eds.), Climate change in Portugal: scenarios, impacts and adaptation measures. Gradiva – Publicações, Lisbon: 23-83.

de Vente J, Poesen J, 2005. Predicting soil erosion and sediment yield at the basin scale: scale issues and semi-quantitative models. Earth-Science Reviews 71: 95–125.

Deguchi A, Hattori S, Park H-T, 2006. The influence of seasonal changes in canopy structure on interception loss: application of the revised Gash model. Journal of Hydrology 318: 80–102.

Déqué M, Jones RG, Wild M, Giorgi F, Christensen JH, Hassell DC, Vidale PL, Rockel B, Jacob D, Kjellström E, de Castro M, Kucharski F, van den Hurk B, 2005. Global high resolution versus Limited Area Model climate change projections over Europe: quantifying confidence level from PRUDENCE results. Climate Dynamics 25: 653–670.

Favis-Mortlock D, Boardman J, MacMillan V, 2001. The limits of erosion modeling: why we should proceed with care. In: Harmon RS, Doe WW (Eds.), Landscape Erosion and Evolution Modeling. Kluwer Academic/Plenum Publishers, New York: 477-516.

Flanagan DC, Nearing MA, 1995. USDA Water Erosion Prediction Project – Hillslope Profile and Watershed Model Documentation. NSERL Report no. 10, National Soil Erosion Research Laboratory, United States Department of Agriculture – Agricultural Research Service (USDA-ARS), West Laffayette.

Gallardo C, Arribas A, Prego JA, Gaertner MA, de Castro M, 2001. Multi-year simulations using a regional-climate model over the Iberian Peninsula: current climate and doubled CO_2 scenario. Quarterly Journal of the Royal Meteorological Society 127: 2740-2756.

Giorgi F. 2005. Climate change prediction. Climatic Change 73 (3): 239-265.

Gitay H, Brown S, Easterling W, Jallow B, 2002. Ecosystems and their goods and services. In: McCarthy J, Canziani O, Leary N, Dokken D, White K (Eds.), Climate Change 2001: Impacts, Adaptation, and Vulnerability. Cambridge University Press, Cambridge: 235-342.

Hoyningen-Huene Jv, 1983. Die Interzeption des Niederschlages in landwirtschaftlichen Pflanzenbeständen (rainfall interception in agricultural plants). DVWK-Schrift Nr. 57, Verlag Paul Parey, Hamburg / Berlin.

IPCC: Intergovernmental Panel on Climate Change, 2000. Special Report on Emissions Scenarios. A Special Report of Working Group III of the Intergovernmental Panel on Climate Change. Nakićenović N, Swart R (Eds.). Cambridge University Press, Cambridge.

Kavvas ML, 1999. On the coarse-graining of hydrologic processes with increasing scales. J. Hydrol. 217 (3-4): 191-202.

Kirkby MJ, Bull LJ, Poesen J, Nachtergaele J, Vandekerckhove L, 2003. Observed and modelled distributions of channel and gully heads – with examples from SE Spain and Belgium. Catena 50 (2-4): 415-434.

Lane LJ, Hernandez M, Nichols M, 1997. Processes controlling sediment yield from watersheds as functions of spatial scale. Environmental Modelling & Software 12 (4): 355-369.

Mantel S, Van Lynden GJ, Huting J, 2003. PESERA, Work package 6: Scenario analysis. In: PESERA final report: April 2003 - September 2003. ISRIC - World Soil Information, Wageningen.

Michael A, Schmidt J, Enke W, Deutschländer Th, Malitz G, 2005. Impact of expected increase in precipitation intensities on soil loss – results of comparative model simulations. Catena 61: 155-164.

Miranda P, Coelho FES, Tomé AR, Valente MA, 2002. 20th century Portuguese climate and climate scenarios. In: Santos FD, Forbes K, Moita R (Eds.), Climate change in Portugal: scenarios, impacts and adaptation measures – project SIAM. Gradiva – Publicações, Lisbon: 23-83.

Nearing MA, Govers G, Norton LD, 1999. Variability in soil erosion data from replicated plots. Soil Sci. Soc. Am. J. 63: 1829-1835.

Nearing MA, Jetten V, Baffaut C, Cerdan O, Couturier A, Hernandez M, Le Bissonnais Y, Nichols MH, Nunes JP, Renschler CS, Souchère V, van Oost K, 2005. Modeling response of soil erosion and runoff to changes in precipitation and cover. CATENA 61 (2-3): 131-154.

Neitsch SL, Arnold JG, Kiniry JR, Williams JR, Kiniry KW. 2002. Soil and Water Assessment Tool theoretical documentation. TWRI report TR-191, Texas Water Resources Institute, College Station.

Nohara D, Kitoh A, Hosaka M, Oki T, 2006. Impact of Climate Change on River Discharge Projected by Multimodel Ensemble. Journal of Hydrometeorology 7 (5): 1076-1089.

Nunes JP, Vieira G, Seixas J, Gonçalves P, Carvalhais N, 2005. Evaluating the MEFIDIS model for runoff and soil erosion prediction during rainfall events. Catena 61 (2-3): 210-228.

Nunes JP, Vieira GN, Seixas J, 2006. MEFIDIS - A Physically-based, Spatially-Distributed Runoff and Erosion Model for Extreme Rainfall Events. In: Singh VP, Frevert DK (Eds.), Watershed Models. CRC press, Boca Raton: 291-314.

Nunes JP, Seixas J, Pacheco NR, in press. Vulnerability of water resources, vegetation productivity and soil erosion to climate change in Mediterranean watersheds. Accepted for publication by Hydrol. Process. (2007).

Palutikof JP, Conte M, Casimiro Mendes J, Goodess CM, Espirito Santo F, 1996. Climate and climate change. In: Brandt CJ, Thornes JB (Eds.), Mediterranean desertification and land use. John Wiley and sons, Chichester: 43-86.

Pinto PA, Brandão AP, 2001. Agriculture. In: Santos FD, Forbes K, Moita R (Eds.), Climate change in Portugal: scenarios, impacts and adaptation measures. Gradiva – Publicações, Lisbon: 133-171.

PRUDENCE: Prediction of Regional scenarios and Uncertainties for Defining EuropeaN Climate change risks and Effects, 2007. PRUDENCE data archive. Available online in prudence.dmi.dk (accessed in January 2007). The PRUDENCE project (EU contract EVK2-CT2001-00132).

Pruski FF, Nearing MA, 2002. Runoff and Soil-Loss Responses to Changes in Precipitation: A Computer Simulation Study. J. Soil Water Conserv. 57 (1): 7-16.

Puigdefabregas J, Solé A, Gutiérrez L, del Barrio G, Boer M, 1999. Scales and processes of water redistribution in drylands: results from the Rambla Honda field site in Southeast Spain. Earth-Science Reviews 48: 39-70.

Räisänen J, Hansson U, Ullerstig A, Döscher R, Graham LP, Jones C, Meier HEM, Samuelsson P, Willén U, 2004. European climate in the late twenty-first century: regional simulations with two driving global models and two forcing scenarios. Climate Dynamics 22: 13–31.

Ramos MC, Mulligan M, 2005. Spatial modelling of the impact of climate variability on the annual soil moisture regime in a mechanized Mediterranean vineyard. J. Hydrol. 306: 207-301.

Romero-Díaz A, Cammeraat LH, Vacca A, Kosmas C, 1999. Soil erosion at three experimental sites in the Mediterranean. Earth Surf. Process. Landforms 24: 1243-1256.

Santos JA, Corte-Real J, Leite SM, 2005. Weather regimes and their connection to the winter rainfall in Portugal. Int. J. Climatol. 25: 33–50.

Skøien JO, Blöschl G, 2003. Characteristic space scales and timescales in hydrology. Water Resources Research 39 (10): 1304.

Tucker GE, Bras RL, 2000. A stochastic approach to modeling the role of rainfall variability in drainage basin evolution. Water Resour. Res. 36 (7): 1953-1964.

UNEP: United Nations Environment Program, 1997. World Atlas of Desertification, 2nd ed. Middleton N, Thomas D (Eds.), UNEP, London.

van den Hurk B, Hirscho M, Schär C, Lenderink G, van Meijgaard E, van Ulden A, Rockel B, Hagemann S, Graham P, Kjellström E, Jones R, 2005. Soil control on runoff response to climate change in regional climate model simulations. Journal of Climate 18 (17): 3536-3551.

Vandaele K, Poesen J, Marques de Silva JR, Govers G, Desmet P, 1997. Assessment of factors controlling ephemeral gully erosion in Southern Portugal and Central Belgium using aerial photographs. Zeitschrift fur Geomorphologie 41 (3): 273-287.

Vandekerckhove L, Poesen J, Govers G, 2003. Medium-term gully headcut retreat rates in Southeast Spain determined from aerial photographs and ground measurements. Catena 50 (2-4): 329-352.

Wetherald RT, Manabe S, 2002. Simulation of hydrologic changes associated with global warming. J. Geophys. Res. 107 (D19): 4379-4393.

Wilby RL, Wigley TML, 1997. Downscaling general circulation model output: a review of methods and limitations. Progress in Physical Geography 21 (4): 530-548.

Woods R, Sivapalan M, 1999. A synthesis of space-time variability in storm response: rainfall, runoff generation, and routing. Water Resour. Res. 35 (8): 2469-2485.

Zhang XC, Nearing MA, 2005. Impact of climate change on soil erosion, runoff and wheat productivity in central Oklahoma. Catena 61 (2-3): 185-195.

6. Vulnerability of Mediterranean watersheds to climate change and desertification

The previous chapter presented the main results of this thesis, focusing on the modeling framework application. This chapter discusses the results in light of the main objective of this thesis: assessing the vulnerability of the biophysical component of Mediterranean socio-ecologic systems to climate change, as a result of enhanced desertification processes. Therefore, the discussion focuses on the main biophysical drivers for desertification: hydrological processes, vegetation productivity and soil erosion.

Following the vulnerability assessment framework discussed in 3.1, this chapter begins by discussing the results in order to assess the **Sensitivity to climate change** of Mediterranean watersheds, followed by a discussion on their **Resilience to climate change**. Sensitivity and resilience are coupled to assess the overall **Vulnerability to climate change** of Mediterranean watersheds, including a proposal of the main issues requiring adaptation. Finally, the chapter concludes by framing the uncertainties surrounding these results by exposing the most important **Methodological limitations**.

6.1 Sensitivity to climate change

According to the vulnerability assessment framework exposed in section 3.1 (following Adger, 2006), sensitivity is defined as the response of watershed biophysical processes to perturbations, i.e. changes in climate. This section performs a sensitivity analysis for watersheds in the Guadiana and Tejo study areas (described in section 4.2), based on modeling results for the entire study areas at the seasonal scale (section 5.1) and for two subset watersheds, Odeleite and Alenquer, at the extreme event scale (section 5.2).

6.1.1 Seasonal scale

The SWAT model was applied to the Guadiana and Tejo study areas using a range of temperature increases up to 6.4 ºC, coupled with an increase of atmospheric CO_2 concentration of up to 100 %. Two rainfall change scenarios were simulated: "low rainfall" establishes a -6 % decrease in rainfall per 1 ºC increase in temperature, and "high rainfall" establishes a -1.5 % decrease in rainfall per 1 ºC increase in temperature. Model results for the study areas indicate that, in Mediterranean regions, the watersheds' water and sediment yield are highly sensitive to changes in rainfall and temperature, which affect the processes underlying these variables. Changes to atmospheric CO_2 concentration appear to have smaller

consequences for these parameters. When looking at the response to combined climate change scenarios for the region – rising temperatures and CO_2 concentrations, decreasing rainfall rates – the results point to a trend of decreasing water runoff and, for most vegetation types, biomass production. There is a high variability in the response of soil erosion, however, ranging from significant decreases to significant increases depending on rainfall changes. These trends appear to be driven mostly by the interaction between changes to surface runoff and vegetation biomass growth. Furthermore, while vegetation biomass growth shows a smaller sensitivity to climate change, it appears to be very significant in determining the response of soil erosion, particularly when considering different vegetation types.

For **hydrological processes**, the results for the sensitivity to combined changes in rainfall, temperature and CO_2 point to different responses in a first stage, where water runoff (and therefore river flow) is mostly affected, but evapotranspiration shows a smaller response since a greater percentage of rainwater tends to be shifted towards this parameter; and a second stage, where the response shifts gradually from runoff to evapotranspiration. The threshold between the first and second stages appears to be an increase of c. 5 ºC in temperature coupled with a c. -30 % decrease in rainfall.

Runoff responds mostly to decreases in available rainwater, with a smaller response due to increased evapotranspiration rates caused by rising temperatures. These impacts affect mostly subsurface runoff, especially in the Guadiana, while surface runoff shows a smaller response. The difference in response between these two variables indicates that the river flow regime in both regions is also sensitive to changes in climate, since regular river flows are mostly fed by subsurface runoff, while extreme flow events are, in these conditions (semi-arid to sub-humid catchments with thin soils), mostly fed by surface runoff (Beven, 2000). Therefore, river flow is expected to tend towards increased irregularity with climate changes, with this response being more marked in the Guadiana study area and in watersheds with similarly shallow soils.

The response of **vegetation biomass production** to the combined changes shows a decreasing trend for most species, particularly wheat, although with a lesser response (in percentual terms) than that of water yield. CO_2 concentration increases showed a mitigating effect on the negative impact of rising temperatures. Furthermore, sclerophyllous cork oaks and Mediterranean shrubs in the Guadiana study area benefit from increased temperatures, although the former only appeared to tolerate increases of up to 20%. Nevertheless, it should be noted that cork oaks currently grow essentially on the less arid hillslopes in the southwest of the study area, and could potentially suffer more negative impacts if located in the more

arid regions of the Guadiana, as it is more sensitive to drought conditions than shrubs (Martínez-Vilalta et al., 2002). Mediterranean shrubs appear to benefit from increased temperatures in all the study area; these results coincide with the trend of increased shrub productivity with desertification found by Seixas (2000) for this region.

Finally, the results indicate a decreasing trend for **soil erosion** under most vegetation types, driven by lower surface runoff rates coupled with increased biomass production in some cases. However, the results in regions with wheat cultivation, which currently suffer significant erosion rates, are uncertain and showed a large sensitivity to rainfall trends. For the "low rainfall" scenario, soil erosion shows a very significant reduction in both regions, while for the "high rainfall" it shows a significant increase, particularly in the Tejo study area where the higher slopes appear to play a role in soil erosion response. The differences between both scenarios are mainly due to the balance between the response to decreasing surface runoff rates, acting to reduce erosion; and lower biomass productivity, increasing erosion rates, concurring with the results obtained by Pruski and Nearing (2002).

6.1.2 Extreme event scale

The MEFIDIS model was applied to the Odeleite and Alenquer watersheds using 3 storms in each site, comparing control conditions with a range of changes to storm rainfall and intensity, soil water deficit and vegetation cover ranging from -20 % to 20 %. Overall, the results of the modeling study indicate that:

- catchment runoff, peak runoff rates and sediment yield are highly sensitive to changes in storm patterns and soil moisture conditions, with a sensitivity to change above 1 % per % change in input parameter in most cases, while the sensitivity appears to be smaller for changes to vegetation cover;

- sediment yield appears to be more sensitive to changes than peak runoff, which itself is more sensitive than total runoff, indicating that sensitivity increases as the direct impacts of changes to storm patterns, soil water deficit and vegetation cover accumulate with the changes to first-order processes such as total runoff;

- storm pattern and soil water changes also affect the hydrological and sediment connectivity of watersheds, impacting the runoff generation and sediment delivery ratios as well as the amount of available water and sediment detached upslope;

- upslope erosion is less sensitive to storm pattern and soil water changes than sediment yield, since the latter accumulates changes to sediment detachment and transport with changes to the sediment delivery ratio;

- erosion in regions suffering the most significant problems is more sensitive to changes than erosion in the remaining areas of the watershed.

The sensitivity values obtained in this study are affected by the model calibration and validation procedure (discussed in section 4.4) and are therefore subject to the uncertainties found during model evaluation; in particular, the absolute results for within-watershed erosion patterns and sediment delivery ratio were not evaluated and therefore no assessment can be made on their validity. However, runoff and erosion models have been found to perform better in relative terms than in absolute terms (Jetten et al., 1999; see also section 2.3), and therefore the relative results present an additional level of confidence. Furthermore, these results are comparable with the ones found in the study conducted by Nearing et al. (2005), indicating that the pattern for the sensitivity of different watershed parameters to different consequences of climate change presented above is consistent across watersheds. Further work is necessary to support this conclusion, however.

As already noted by Nearing et al. (2005), the sensitivities found in this study do not imply that changes in storm patterns will dominate over changes in soil water deficit or vegetation cover. A full assessment of this problem must analyze coupled scenarios of changes to storm rainfall and intensity, soil moisture conditions and vegetation cover (including land use changes) to estimate the impact of the different changes on runoff and soil erosion; one example is given by the work of Michael et al. (2005), who analyzed the impact of combined changes to storm intensity patterns and wheat cultivation practices on soil erosion for a small humid catchment. The results do indicate, however, that:

- the increases in storm rainfall and intensity for the Mediterranean predicted by Räisänen et al. (2004) and others (see section 2.2.1) could lead to a significant increase of runoff, peak runoff rates and sediment yield in Mediterranean watersheds, especially when considering areas which already experience erosion problems;

- changes to vegetation biomass productivity could add to this impact if it is reduced due to an increase in climate aridity, as reported by Morales et al. (2007), although

these impacts could vary significantly with vegetation type and region (see the sensitivity results at the seasonal scale, above);

- conversely, a decrease in soil moisture values in the Mediterranean, as predicted by Wetherald and Manabe (2002) and shown by the sensitivity analysis at the seasonal scale could act to mitigate the impact of these changes.

6.1.3 Sensitivity assessment

It is difficult to analyze the interactions between sensitivity at the seasonal and extreme event scales, due in a large degree to the different climate change impacts expected for annual rainfall rates and storm intensity patterns. However, the results still allow for a qualitative assessment of sensitivity at both scales. Overall, the general response of **hydrological processes** at the seasonal scale indicates a reduction of the saturated fraction of a watershed in most scenarios, indicated by a significant decrease in subsurface flow (Beven, 2000). This implies that the overall trend for storm runoff will depend on the balance between changes to storm intensity patterns and to subsurface flow, leading to a number of implications:

- climate change scenarios with a significant rainfall reduction could lead to a reduction in storm runoff, although smaller than the overall reduction in river baseflow, since the increase in storm intensity would not compensate the very large decrease in soil moisture and saturated areas;

- conversely, scenarios with a small rainfall reduction coupled with an increase in storm intensity could lead to an increase in storm runoff, regardless of a negative runoff trend at the seasonal scale;

- large storms would still occasionally coincide with more saturated watersheds and, in this case, an increase in storm intensity could lead to a greater variability in the rainfall/runoff relationship, an effect which could be enhanced by changes to the runoff generation ratio;

- the decrease of saturated catchment areas in all scenarios could lead to a decrease in hydrological connectivity, regardless of the overall storm runoff trend, with the possibility of more runoff being generated over a smaller part of the catchment area.

It must also be noted that, according to the results, storm runoff in the Odeleite watershed is more sensitive to changes in storm patterns and soil water saturation than in the Alenquer

watershed, due mostly to the shallower Lithosols. This implies that the variability between storm runoff responses to different scenarios of climate change would be greater in Odeleite and in the Guadiana study area, increasing the uncertainty in predicting storm runoff trends for this region. In terms of sensitivity, it can be said that runoff – particularly subsurface runoff – appears to be highly responsive to changes in climate at the annual and seasonal scales and shows a strongly negative trend, especially in the Guadiana study area. At the extreme event scales, however, the decrease in soil saturation patterns is expected to mitigate the impacts of increased storm intensity; the sensitivity of storm runoff is expected to be significantly lower than that of overall runoff, with positive or negative trends depending on the magnitude of rainfall changes. The response of peak runoff rates is expected to follow the one for storm runoff, although with a slightly larger sensitivity to change.

Concerning **soil erosion**, the results indicate that upslope erosion responds more strongly to storm intensity patterns than to soil water deficit or vegetation cover. However, both upslope erosion and sediment yield were shown to respond in a similar manner to storm runoff patterns. Furthermore, changes to vegetation cover could also change the response of soil erosion. The points made in the discussion for storm runoff patterns imply that:

- soil erosion rates could be expected to respond differently according to the overall change in rainfall rates, with a significant rainfall reduction leading to a negative trend and a small rainfall reduction coupled with an increase in storm intensity leading to a positive trend;

- the direction of this trend could be more sensitive to changes in storm intensity than changes in vegetation cover;

- nevertheless, the increase in the cover of Mediterranean vegetation would be expected to mitigate the effects of increased storm intensity, while the impacts on wheat cover would either mitigate or enhance these effects;

- sediment yield would show a significantly stronger response than upslope erosion, regardless of the direction of the trend, due to changes in sediment connectivity (Favis-Mortlock et al., 2001).

As in the case of hydrological processes, soil erosion in the Odeleite watershed appears to be more sensitive to changes in storm patterns than in the Alenquer watershed, implying that the same would be true for the Guadiana study area. It should be noted that the low sensitivity to

changes to vegetation cover does not imply a contradiction between the seasonal and extreme event scale model estimates, since MEFIDIS applied similar changes to all vegetation cover types while SWAT estimated different magnitudes and directions of change between different vegetation types (see section 5.1), increasing the complexity of the relationships between vegetation cover and soil erosion for similar changes to rainfall. In this case it should be noted, however, that the importance of gully erosion in Mediterranean watersheds would give more credibility to the responses predicted by the MEFIDIS model, as the SWAT model in not capable of simulated concentrated flow erosion processes (Jetten et al., 1999).

In terms of sensitivity, it can be said that soil erosion processes appear to be responsive to changes in climate at all scales, with a lesser sensitivity than seasonal-scale runoff but a larger sensitivity than storm runoff, particularly in the case of sediment yield. The direction of storm runoff response is expected to govern the direction of soil erosion response, particularly for sediment yield. A decrease of vegetation cover in wheat croplands is expected to enhance positive trends or mitigate negative trends; the inverse is expected for Mediterranean species – e.g. shrublands and cork oak forests – due to an increase in vegetation cover. Finally, it should be noted that, regardless of the response direction of soil erosion, ephemeral gullies are expected to remain an important factor in watershed erosion processes; and that a reduction in soil erosion is more likely to imply a reduction in the area affected by gullies, with small changes to the severity of the problem where they remain.

Overall, the watersheds in the study areas appear to be sensitive to climate change due to an enhancement of desertification processes, particularly in the case of agricultural regions. The modeling results indicate that the response of hydrological processes contributes the most to this sensitivity, particularly due to the trend of an exposure of socio-economic systems to a significant reduction in surface water resources. The response of vegetation productivity also contributes to this trend in wheat croplands, with a reduction of overall vegetation cover, but not in regions covered by natural Mediterranean vegetation where vegetation cover is expected to increase. This points to an increase in the differences between the intensity of desertification processes occurring in agricultural regions and natural areas, already present in Mediterranean semi-arid regions (Martínez-Fernández and Esteve, 2005).

Finally, the degree of changes to rainfall rates is expected to affect desertification drivers differently. A small reduction would have less impact on surface water resources but could increase soil erosion rates in croplands; conversely, a large reduction could lead to a decrease of soil erosion rates at the expense of more significant impacts on water resource availability.

Furthermore, continuing erosion rates could have long-term impacts on ecosystem sustainability by reducing vegetation productivity (Bakker, 2004), particularly in the case of ephemeral gully processes (Avni, 2005). These issues are explored in the following section.

6.2 Resilience to climate change

According to the vulnerability assessment framework exposed in section 3.1 (and following Gallopín, 2006), and in the context of this thesis, resilience can be assessed by determining the current position of the Guadiana and Tejo study areas (described in section 4.2) to thresholds of desertification, and by evaluating whether the expected climate changes could move the system beyond them. The analysis focuses on establishing whether the impacts of climate change on biophysical systems are sufficient to affect their capacity to provide services to socio-economic systems and to sustain current agricultural practices and natural ecosystems functioning. Many of the results rely on extrapolations, which are assumed to be significantly less reliable than the results obtained for sensitivity using the modeling framework.

6.2.1 Impacts of climate change scenarios at multiple scales

The coupled seasonal and extreme event scale modeling framework was applied to the study areas with two RCM climate change scenarios based on the A2 and B2 emission scenarios (PRUDENCE, 2007), with the results described in section 5.3. The climate change scenarios were derived from the PROMES RCM (Gallardo et al., 2001), and fall into the range of the "low rainfall" simulations described in section 5.1, which establishes a -6 % decrease in rainfall per 1 ºC increase in temperature. This range was selected since a significant part of the available RCM results for the study areas fall into the "low rainfall" range, as shown in Figure 6.1. This range also indicates a greater degree of change from current climate patterns than the "high rainfall" scenarios (-1.5 % decrease in rainfall per 1 ºC increase in temperature). Additionally, the RCM predicts a decrease in storm intensity in the early part of the wet season, from October to December (OND), coupled with a significant increase in the later part of this season, from January to April (JFMA), in all cases except the B2 scenario for the Guadiana study area.

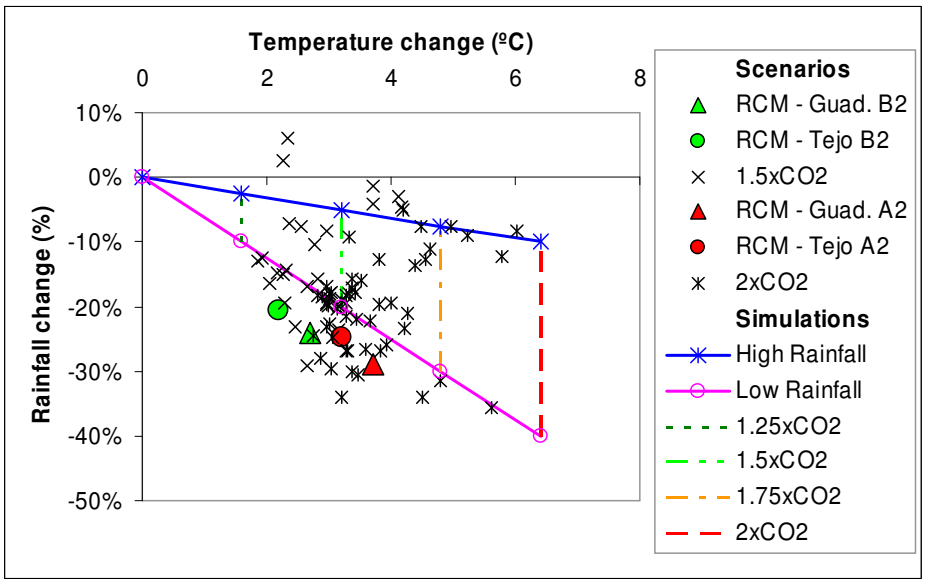

Figure 6.1 – Relation between changes to temperature and rainfall for the low and high rainfall simulations used in the sensitivity analysis (section 5.1), the PROMES RCM climate change scenarios (section 5.3), and published scenarios for central and southern Portugal (Cunha et al., 2002; PRUDENCE, 2007; approximated CO_2 concentrations).

Seasonal scale

This section summarizes the results shown in detail in section 5.3.3. The SWAT model was applied to the Guadiana and Tejo study areas using control and changed climate series from the RCM. Overall, model results for hydrological processes follow the general trends obtained in the sensitivity analysis, with a strong decrease in water runoff. Results for vegetation productivity show an increase for most vegetation types due to higher atmospheric CO_2 concentrations (an increase of c. 20 % per 1 ºC increase in temperature) when compared with the ones used to analyze sensitivity (c. 15 % per 1 ºC). Nevertheless, these results are still in agreement with vegetation response for independent increases to temperature and CO_2.

For **hydrological processes**, the results follow the overall trends obtained in the sensitivity analysis, with a decrease in evapotranspiration coupled with a significantly larger decrease in water runoff, as rainfall shifts towards the former. The decrease in evapotranspiration is more pronounced than the one previously verified, which is partly explained with the shift of rainfall to the wet season predicted by the RCM, leading to less water availability and therefore less evapotranspiration in summer. Model results for runoff indicate a decrease by c. 35 to 40 % in both scenarios and study areas, associated with an increase in streamflow

variability due to a larger decrease in baseflow. Furthermore, the results they point to a significant increase in the frequency of occurrence of hydrological extremes at the interannual scale, particularly hydrological drought years. At the seasonal scale, they indicate a concentration of runoff during winter, associated with a delay in the soil water recharge period at the start of the wet season; the decrease in runoff is more pronounced in the OND period, with less significant changes occurring in the JFMA period.

Concerning **vegetation productivity**, the results indicate no changes or small increases in agricultural vegetation and forests, as the negative impacts of higher temperatures are compensated by the beneficial effects of increased atmospheric CO_2 concentration. For Mediterranean vegetation, the model predicts in most cases a significant increase in productivity due to the cumulative effects of higher temperatures and CO_2 concentrations. These results concur with the assessment performed under the sensitivity analysis which indicates that the balance between the impacts of temperature and CO_2 changes governs the response to climate change of most species. Furthermore, while the results show a continuing trend of agricultural and ecosystem drought years with significant reductions in biomass production, they do not indicate significant changes to the frequency of this phenomena, possibly due to the constant mitigating effect of increased CO_2 concentrations.

Extreme event scale

This section summarizes the results shown in detail in section 5.3.3 The seasonal scale model provided a range of changes to seasonal hydrological and vegetation patterns which were inputted in the event scale model, together with the storm intensity changes predicted by the RCM. As a result, this combined methodology was able to generate scenarios for the balance between changes to storm patterns, soil moisture saturation and vegetation cover, which as previously discussed dominate catchment response to climate changes at this scale.

The MEFIDIS model was applied to the Odeleite and Alenquer watersheds using about a dozen storms per site, applying both the changes to storm intensity predicted by the RCM, and the SWAT results to soil water deficit (calculated from baseflow) and vegetation cover (calculated from biomass productivity). The OND and JFMA show a different balance between changes to storm rainfall intensity and soil water saturation, with OND showing a clear trend towards decreasing conditions for storm runoff generation and JFMA showing a greater equilibrium between changes. Therefore, MEFIDIS simulations were conducted for both seasons.

For **hydrological processes**, model results point to an overall decrease in storm runoff rates. These results indicate that, in the "low rainfall" climate change predictions, an increase in storm intensity will not be able to compensate the negative impacts caused by a reduction in soil water saturation patterns with a consequential decrease in hydrological connectivity. Peak runoff rates show a similar trend, although with a smaller decrease than storm runoff. The results also indicate greater impacts for the Odeleite watershed, following a similar pattern to the ones observed for RCM and seasonal scale model results.

However, the results for the A2 scenario also point to a significant increase of seasonal storm runoff variability, as the negative impacts occur mostly in the first half of the wet season (OND). For the JFMA season, the Odeleite and Alenquer watersheds show a different response. In Odeleite, the results show a decrease in storm runoff, although smaller than in OND, but this impact is reduced for larger storms due to the watershed's shallow soils (as discussed in section 5.3); these impacts might not be felt during more extreme rainfall events. The magnitude of infrequent winter floods could therefore remain unchanged despite an average decrease in storm runoff. In Alenquer, the results indicate an increase in storm runoff for this season, mostly as a response to a very significant increase in storm intensity. These changes could modify the frequency distribution of flood events in the watershed, with a decrease in the magnitude of the most frequent floods coupled with an increased severity of the more infrequent floods.

Concerning **soil erosion**, the results follow the response of storm runoff rates, with a general negative trend. This trend, however, is significantly more marked due to the cumulative impacts of lower storm runoff rates and higher vegetation cover, particularly in the Odeleite watershed. It should be noted that wheat croplands in Odeleite suffer significantly smaller impacts than other vegetation types. The different seasonal impacts for the A2 scenario are also reproduced; in Odeleite, the decrease in soil erosion is smaller in the JFMA season, and the impacts on upslope erosion are reduced for larger storms, indicating that these impacts might not be felt during more extreme rainfall events, while soil erosion in Alenquer follows the trend for storm runoff with an increase in the JFMA season. Gully erosion is expected to remain the most important process in both study areas and, while the results indicate a reduction in the extension of this phenomenon, the remaining affected areas are likely to keep experiencing significant problems

The overall impacts of these changes indicate, for the B2 scenario, a decrease of soil erosion of c. -60 % in Odeleite and c. -30 % in Alenquer. The overall impacts for the A2 scenario are

more difficult to estimate due to the expected seasonal differences. Average results indicate a decrease of soil erosion of c. -60 % in Odeleite and c. -25 % in Alenquer, although the impacts in Odeleite are unevenly distributed between croplands (c. -50 %) and Mediterranean vegetation types (c. -85 %). During winter (JFMA), however, soil erosion in Odeleite could suffer a significantly smaller decrease, of c. -30 % in croplands; and soil erosion in Alenquer could increase by c. 20 %. These changes could signal a dominance of winter storms for soil erosion in the A2 scenario, since the large magnitude storms that dominate soil erosion in Mediterranean regions (Silva et al., 1998) and which have greater impacts on ephemeral gully formation (Kirkby et al., 2002) would be more likely to fall in winter; however, the modeling results are not sufficient to confirm this hypothesis.

Long-term impacts of soil erosion on vegetation productivity

Soil erosion diminishes soil fertility in the long-term by reducing soil organic matter, nutrient content, water holding capacity and rooting depth (Toy et al., 2002; Bakker et al., 2004). While the modeling framework described above is not capable of addressing this problem, a simple estimate can be made based on the available literature. A recent review by Bakker et al. (2004) estimates an average crop productivity loss of c. 0.4 % per cm of soil loss, based on published results for compared experimental plots using different crop varieties grown over different soil conditions and under different climates. These losses, however, are non-linear and generally become more severe with progressing erosion, with some observations of up to 20 % per cm in very shallow soils. The authors attribute this process to the available soil depth above bedrock or an impermeable soil layer; as soil erosion reduces this depth, the capacity for water storage decreases and vegetation root growth becomes hindered. The soil loss / productivity curves generally have a convex shape when soil depth is reduced below a critical threshold, where soil water storage capacity is insufficient to meet vegetation water demands or where root growth is hampered by increased soil density. The authors suggest the depth at which most of the vegetation roots are concentrated as a possible threshold estimate.

This highlights one important difference between both study areas when considering the long-term impacts of erosion on soil fertility. While soil erosion in wheat fields is currently higher in the Tejo study area, particularly when considering an erosion tolerance threshold of 2 to 12 $ton.ha^{-1}.y^{-1}$ (Romero-Díaz et al., 1999), the soil depth is also considerably higher. In fact, the low soil depths in many croplands in the Guadiana study area, averaging 10 to 24 cm (Cardoso, 1965; Batjes, 2002; see also section 4), are significantly shallower than the depth at which winter wheat roots have their greatest density, c. 40 cm (Zhang et al., 2004); this makes

them more likely to experience fertility losses due to erosion than soils in the Tejo area (average depth of c. 90 cm; see section 4). This indicates that even low erosion rates in the Guadiana could have very significant impacts on wheat productivity, continuing a trend which has been observed in this study area since intensive cereal cultivation was introduced at the beginning of the XXth century (Roxo et al., 1996; Roxo and Cortesão Casimiro, 1998).

A simple estimate for soil fertility loss can be performed using the current upslope erosion rates occurring in wheat fields (section 4.3) and the climate change impact estimates for 2100, based on the PROMES RCM scenarios (section 5.3). For the Tejo study area, a productivity loss of 0.4 %.cm^{-1} is assumed (Bakker et al., 2004) due to the fact that current soil depths greatly exceed the depth of maximum concentration for wheat roots. For the Guadiana study area, an estimate was made taking into account the current soil depth. Bakker et al. (2004) report that the relationship between soil fertility loss and depth to bedrock is often logarithmic or exponential in nature. Figure 6.2 shows the shape of these two curves when assuming that soil fertility loss increases from the average rate of 0.4 %.cm^{-1} when depth to bedrock decreases below a threshold of 40 cm (for wheat rooting systems; Zhang et al., 2004), and reaches a maximum of 100 %.cm^{-1} when depth to bedrock is under 1 cm. Considering the soil depths observed in the Guadiana, soil productivity losses are estimated to fall between 4 and 29 %.cm^{-1} for the exponential curve, and between 14 and 48 %.cm^{-1} for the logarithmic curve. The average of these values is c. 24 %.cm^{-1}; the final estimate of soil fertility loss for the Guadiana study area was c. 20 %.cm^{-1}, selected both to avoid overestimating this parameter and since this value is within the range of observations reported by Bakker et al. (2004).

The results for the RCM soil fertility loss estimates are shown in

Table 6.1 Table 6.1; a similar estimate, using the model results for the seasonal-scale sensitivity analysis (section 5.1), is shown in Figure 6.3. While the uncertainties involved in the estimate method result in a low degree of confidence for these results, they do indicate that, in the Guadiana, the impacts of continuing upslope erosion in croplands could be as important as the impacts of climate change. For the PROMES scenarios, the results indicate that the negative consequences of upslope erosion could to offset the beneficial impacts of an increase in CO_2 fertilization.

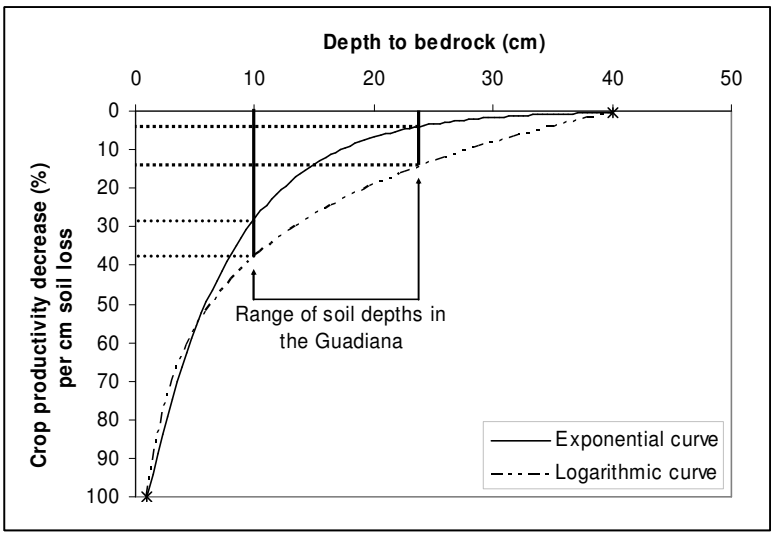

Figure 6.2 – Estimated relationship between soil fertility loss due to erosion and depth to bedrock, following the thresholds and curve shapes proposed by Bakker et al. (2004), with the range of soil depth and fertility loss estimates for the Guadiana study area superimposed.

Table 6.1 – Impacts of climate change and soil erosion on wheat productivity for the PROMES climate change scenarios described in section 5.3; the Guadiana results refers to lithosols.

	Guadiana		**Tejo**	
Parameter	**A2**	**B2**	**A2**	**B2**
Changes to wheat productivity due to climate change (%)	5.3	15.5	9.9	11.7
Changes to wheat productivity due to soil erosion (%)	-14.8	-13.2	-1.7	-1.5

For the sensitivity analysis, the results indicate that the "high rainfall" and "low rainfall" scenarios could have similar impacts on wheat productivity in the Guadiana, the former due to an increase on soil erosion rates and the latter due to a decrease of climatic suitability for wheat cultivation; the range in both cases is a decrease of c. -30 to -60 % with increasing climate change magnitude. It should be noted that this loss in productivity could in turn increase soil erosion in wheat croplands due to a positive feedback effect. Furthermore, these impacts are likely to be highly variable in space, due to localized differences in soil depth and exposure to soil erosion processes. However, these results indicate an intensification of the cropland abandonment trend verified today in the Guadiana, due to the already low yields currently experienced. It should be noted that this approach does not take into account other

long-term phenomena such as the impact of changes on soil moisture and temperature on aggregate stability, which could further impact soil erodibility (Imeson and Lavee, 1998), or the long-term maintenance of soil erosion rates over tolerance thresholds in the Tejo study area which could present problems beyond the temporal horizon of this study. However, the overall results indicate that soil erosion could cause significantly greater fertility losses in the Guadiana lithosols, even where erosion rates in the Tejo study area are significantly larger.

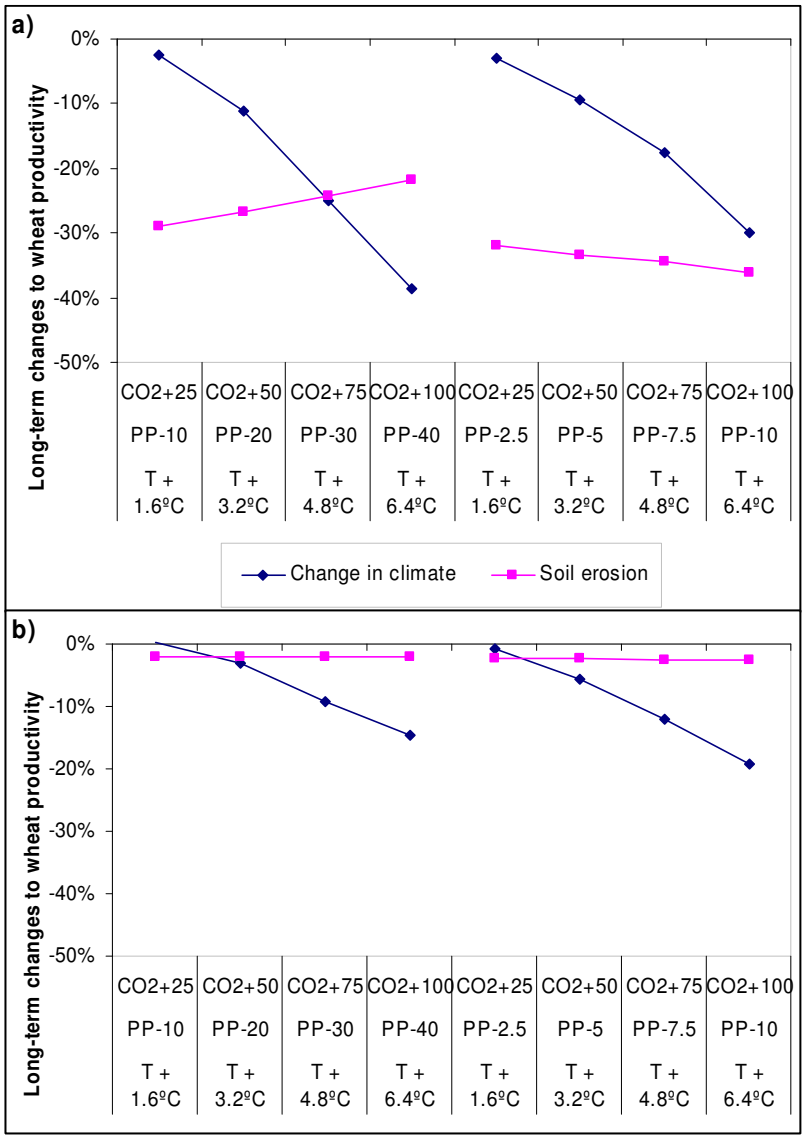

Figure 6.3 – Impacts of climate change and soil erosion on wheat productivity for the climate change scenarios used in the sensitivity analysis (section 5.1) for the Guadiana lithosols (a) and Tejo (b) study areas.

A final remark should be made on the long-term impacts of gully erosion processes, considering that they are estimated to represent c. 80 % of the total soil erosion in Mediterranean semi-arid systems (Vandaele et al, 1997; see also section 2.2.3). Regions of concentrated flow where deposition occurs can be preferential locations for agriculture due to the local increase in soil moisture (Pachepsky et al., 2001) and fertility (e.g. Gessler et al., 2000; Li and Lindstrom, 2001). Farming activities could increase the hydrological and sediment connectivity in these regions (Favis-Mortlock et al., 2001), changing them from depositional to erosional regions. According to Avni (2005), in these regions ephemeral gullies can act as a major driver for desertification as they slowly extend throughout the landscape, leading to a reduction of the agricultural potential of the region due both to a drop in soil fertility around the gullies and to the development of a dissected topography which hampers cultural practices; agriculture is transferred upstream to less eroded regions and increases the local erosive processes, leading to an expansion of the gully system upstream in an escalating process. Examples of the agricultural impacts of gully erosion and cropland movement towards less eroded landscapes were also reported for sub-humid and semi-arid Mediterranean regions (e.g. Bakker et al., 2005; Martínez-Casasnovas et al., 2005; in abandoned croplands, gully expansion can intensify in an initial phase and continue for several years until the gully system stabilizes (Oostwoud Wijdenes et al., 1999).

In the study areas, the Odeleite watershed is representative of a region where agriculture was recently abandoned in most of the watershed but retained over deeper soils along the main channel, which could indicate the start of a similar process (see section 4.2.5). It is difficult to estimate regions in particular risk of this process due to the limitations of the modeling framework in simulating gully erosion processes (see section 4.4). However, the results detailed above indicate that gully erosion would continue under most climate change scenarios, leading to the potential for a slow but continuing desertification process driven by gully erosion in croplands. The potential for cropland abandonment, particularly in the Guadiana where the process is already occurring due to low crop yields, could lead to a temporary intensification of this phenomenon in recently abandoned agricultural fields.

Discussion

Overall, the combined results at the seasonal and extreme event scales allow an estimate for the most likely impacts of climate change on hydrological, vegetation and erosion processes in the study areas. The results indicate:

- a decrease of water runoff in both the Tejo and Guadiana study areas of c. -35 to -40 %, coupled with higher streamflow variability, an increase in the length of the low flow season and a higher frequency of hydrological drought years;

- less significant impacts on storm runoff rates, with the possibility of a change to the frequency distribution of flood events in both study areas, leading to an increase in the frequency of winter floods for the Tejo area;

- moderate increases in agricultural biomass productivity of up to 10 %, with no significant changes to the frequency of agricultural drought years, which in the Guadiana could be negated by the long-term impacts of soil erosion on cropland fertility;

- very significant increases in the productivity of Mediterranean vegetation types (cork oaks and shrubs) of up to 50 % in the Guadiana;

- a very significant decrease in soil erosion rates for the Guadiana, ranging from -85 % in regions with Mediterranean vegetation to -50 % in croplands, although ephemeral gully erosion is expected to remain a problem;

- a more moderate soil erosion decrease in the Tejo of c. -25 to -30 %, coupled with the possibility of an increase in erosion and ephemeral gully formation during the most severe winter storms.

These results follow the sensitivity analysis responses found for the "low rainfall" scenario. The modeling framework was not applied for RCM results representative of the "high rainfall" scenario (shown in Figure 6.1). However, the results found in the sensitivity analysis at the seasonal and watershed scales indicate that, for rainfall decreases down to -5 %, the balance between storm intensity and soil moisture saturation could favor runoff generation in the Tejo; this assumption is based on a baseflow decrease of down to -25 % (see section 5.1), coupled with a possible increase in storm intensity. This scenario could lead to an increase in hydrological connectivity, storm runoff rates and flood frequency; consequentially, the increase in sediment connectivity could lead to a significant increase in soil erosion rates, particularly in terms of ephemeral gully erosion. Still for the "high rainfall" scenario, an increase of temperature above +3 to +4 ºC could lead to a significant increase in erosion rates in wheat fields (see section 5.1) which according to the sensitivity results would manifest itself mostly in the form of increased gully erosion.

Finally, these results only indicate significant changes to surface water resource availability and Mediterranean vegetation productivity, with the former acting as an enhanced driver for desertification and the latter mitigating this process. As found in the sensitivity analysis, the relationship between temperature and rainfall changes is expected to have different impacts on soil erosion, depending on the occurrence of a "high rainfall" or "low rainfall" scenario; however, these results also indicate that even in the latter case, an increase in the variability of seasonal storm patterns could lead to only a moderate reduction of soil erosion in croplands, with significant areas still affected by ephemeral gullies. Furthermore, it is estimated that the long-term impacts of upslope erosion for soil fertility in the Tejo study area could be small even with significant erosion increases, while in the Guadiana they could be significant in all scenarios, offsetting the potential benefic effects of climate change on crop productivity.

This indicates that the significant enhancement of soil erosion as a driver for desertification is only likely in a "high rainfall" scenario and mostly in highly localized regions due to an expansion of ephemeral gully systems. However, the "low rainfall" scenarios are not expected to eliminate soil erosion as a desertification driver from the study areas, although processes linked with gully erosion could see a decrease in extension.

6.2.2 Desertification thresholds

The consequences of the changes described above for desertification processes can only be assessed by evaluating their impact on the overall functioning of Mediterranean biophysical systems. Significant shifts to system functions usually occur when external changes rise above a certain threshold that forces the system to shift into a different state (Puigdefábregas, 1998). However, there is a lack of research on these thresholds due to low availability of long-term data for desertification drivers in drylands (Herrmann and Hutchinson, 2005). Considering the definition of desertification as the degradation of biophysical and socio-economic conditions in dry regions (Thornes, 1998), this section contributes to overcome this problem by using two different approaches to threshold quantification: (i) water stress thresholds, used to evaluate the natural system's capacity to sustain water requirements by socio-economic systems; and (ii) aridity thresholds for vegetation, used to evaluate the system's capacity to support current agroforestry activities and natural ecosystems.

Water resources

In a study on the impacts of climate change on the vulnerability of human populations to water scarcity, Arnell (2004) discusses the establishment of thresholds for the socio-economic

requirements of water systems in climate change studies. The total runoff production in a watershed, including upstream contributions which are often harvested and used for downstream consumptions, can be compared with water withdrawals to indicate stress level. Alcamo et al. (2003) indicate that higher withdrawal ratios indicate a more severe level of water stress, leading to higher frequency of water resource depletion and degradation with potential water conflicts between users; a ratio of 0.4 serves as a threshold for severe stress. The authors also note that the effects of severe water stress are different in developing and industrialized countries, where water resources can be used in a more intensive fashion due to e.g. the general treatment of wastewater before reintroduction in the system to be re-used further downstream. Nevertheless, a severe level of stress could still lead to a strong competition between different users leading to periodic disruptions of water supplies, and to a degradation of water quality which could prevent some uses requiring higher quality levels.

However, Arnell (2004) refers that this index is limited in climate change studies since it requires future estimates of water withdrawal, including eventual adaptation measures; he proposes the use of alternative thresholds in terms of runoff available per watershed inhabitant per year. These empirical thresholds were derived by comparing current water availability with the presence of water conflicts, and are shown in Table 6.2; it should be noted that they underestimate water stress in watersheds where water withdrawal for irrigation is high.

Table 6.2 – Water stress thresholds, following Arnell (2004).

Threshold for water stress	**Water runoff per watershed inhabitant ($m^3.y^{-1}$)**
No stress	> 1700
Moderate stress	1000-1700
Severe stress	500-1000
Extreme stress	< 500

These thresholds can first be compared with the current water resources availability in the study areas. Information for this purpose was taken for the entire Guadiana and Tejo river basins in Portugal, since runoff collected in the study watersheds is mostly used outside; it should be noted, however, that runoff rates in the study areas are representative of those occurring in the remainder of the watershed. Information for the Portuguese part of the basins

is available in a recent assessment conducted the Portuguese Water Institute (Instituto da Água – INAG) as a first step to build and implement watershed management plans for both systems (INAG, 1999a and b). The most relevant water availability and consumption data for the basins is shown in Table 6.3.

Table 6.3 – Annual average water availability and consumption for the Guadiana and Tejo river basins (INAG, 1999a and b).

	Guadiana river basin			**Tejo river basin**
	Current	**Alqueva dam[b]**	**Total**	
Population (thousands)[a]	760	+32	792	2 999
Runoff (million $m^3.y^{-1}$)[c]	1 818	+2 135	3 953	6 715
Water consumption (million $m^3.y^{-1}$)[c]	361	+890	1 251	2 398
Withdrawal ratio	0.20	0.42	0.32	0.36
Runoff per inhabitant ($m^3.y^{-1}$)	2 391	66 615	4 989	2 239

a – Data for 1997 and 1998.
b – Estimated for 2030.
c – Average annual values for 1961-1990.

Data for the Guadiana river basin was divided into two situations. The current situation only takes into account runoff produced in the Portuguese part of the watershed; this water is currently collected mostly for irrigation (c. 83 %). About half of the collected water is exported outside the watershed, to supply irrigation and domestic demands in the eastern Algarve, including tourism domestic consumptions equivalent to c. 330 permanent inhabitants (c. 43 % of the total population supported by the system). Overall, the withdrawal ratio and runoff per inhabitant are well below the water stress thresholds shown above. However, the recent completion of the Alqueva dam will significantly alter the water resource situation in the near future. The Alqueva is Europe's largest dam, and represents a fourfold increase of the Guadiana reservoir capacity. It is designed to collect additional water coming from the Spanish part of the watershed, more than doubling available runoff for catchment uses. The water collected by the dam is expected to irrigate an area of c. 110 000 ha, representing a threefold increase in irrigation water use, with c. 95 % of water resources in the basin diverted for agriculture (GPAa, 2005). While the dam is expected to double the available runoff per inhabitant, the withdrawal ratio is also expected to increase to levels closer to the severe stress threshold (Table 6.3) due mostly to the intensive irrigation uses.

The Tejo river basin presents a contrast with the Guadiana. While the available runoff is almost double, even when considering the Alqueva reservoir scenario, the water consumption is also much greater. About 80 % of the water is used in agriculture; of the remainder, c. 14 % is consumed by the urban population of c. 3 million inhabitants, concentrated around the city of Lisbon close to the basin's estuary. Most of the river runoff is collected either in reservoirs or by direct extraction to irrigate low-lying croplands near the river mouth, leading to a withdrawal ratio close to the severe water stress threshold; however, the importance of irrigation in this basin leaves the runoff withdrawal per inhabitant well above the stress threshold. Finally, it should be noted that a significant part of the water used in the Lisbon municipality is currently discharged in the ocean, preventing its reutilization downstream.

The estimation of the watershed resilience to climate change, in terms of water resource availability, was performed using the modeling results for the seasonal-scale sensitivity analysis (section 5.1) and RCM climate change scenarios (section 5.3). The predicted changes to water runoff were used in conjunction with current runoff estimates (Table 6.3) in order to estimate future runoff availability for the Guadiana and Tejo basins under several climate scenarios. Both the Guadiana and the Tejo study areas represent subsets of the wider basins, but the similarity between measured runoff in the study areas (respectively 159 and 257 $mm.y^{-1}$; see section 4.2.2) and the basins (157 and 280 $mm.y^{-1}$; INAG, 1999a and b) indicates that the results presented in section 5 can be extrapolated for the wider areas.

The estimated impacts of climate changes on withdrawal ratios are shown in Table 6.4. For the Guadiana basin, the estimate for current conditions does not consider the added runoff and withdrawals caused by the Alqueva dam; in this case, only the "low rainfall" scenarios are estimated to cause severe water stress, and only for a drop in rainfall below -20 %. With the Alqueva dam, however, all climate change scenarios with a rainfall drop below -5 % are estimated to cause severe water stress; and for the "low rainfall" scenarios, a rainfall drop below -20 % is expected to reduce runoff below the total withdrawal requirements. These results indicate that the Alqueva dam will bring the Guadiana basin closer to water stress thresholds, despite the added runoff collection, mostly due to the irrigation network built to take advantage of the water in this reservoir. In contrast, for the Tejo basin, all scenarios are expected to cause severe water stress, and for the "low rainfall" scenarios, a decrease in rainfall below -20 % is expected to reduce runoff below current water requirements.

Table 6.4 – Current and estimated runoff changes and water withdrawal ratios for the climate change scenarios presented in section 5 and shown in Figure 6.1; for withdrawal ratios, numbers in bold indicate severe water stress, while underline numbers indicate water shortfalls (withdrawals above runoff rates).

Scenario					Guadiana			Tejo	
					Runoff change (%)	Withdrawal ratio		Runoff change (%)	Withdrawal ratio
						Current conditions	With Alqueva dam		
Control					–	0.20	0.32	–	0.36
Sensitivity analysis	Low rainfall	T+1.6ºC	PP-10	CO2+25	-25.8	0.27	**0.43**	-25.2	**0.48**
		T+3.2ºC	PP-20	CO2+50	-51.3	**0.41**	**0.65**	-54.1	**0.78**
		T+4.8ºC	PP-30	CO2+75	-71.3	**0.69**	**1.10**	-75.0	**1.43**
		T+6.4ºC	PP-40	CO2+100	-80.1	**1.00**	**1.59**	-89.9	**3.52**
	High rainfall	T+1.6ºC	PP-2.5	CO2+25	-15.6	0.24	0.37	-9.7	**0.40**
		T+3.2ºC	PP-5	CO2+50	-27.7	0.27	**0.44**	-22.5	**0.46**
		T+4.8ºC	PP-7.5	CO2+75	-35.8	0.31	**0.49**	-35.6	**0.55**
		T+6.4ºC	PP-10	CO2+100	-40.9	0.34	**0.54**	-44.0	**0.64**
RCM		A2			-44.0	0.35	**0.56**	-41.0	**0.61**
		B2			-40.5	0.33	**0.53**	-36.2	**0.56**

The thresholds shown in Table 6.4 assume no changes to water withdrawal from present conditions to the climate change scenario horizon (2070-2100). However, a significant number of changes could act to increase or decrease water requirements, such as:

- the increase in potential evapotranspiration caused by climate change (Kundzewicz et al., 2007; see also section 2.2.2), which is likely to increase irrigation water requirements above current levels;
- water conservation using precision agriculture technologies, which can increase irrigation efficiency by an average of 8 to 20 % (Sadler et al., 2005);
- increased water use efficiency in industry and urban uses (Arnell, 2004) due e.g. to technological improvements or water conservation awareness;
- socio-economic changes altering water demands (Arnell, 2004).

Furthermore, withdrawals would have to be forcibly reduced where they exceed runoff availability (Table 6.4). Therefore, the changes in runoff shown in Table 6.4 were also used to

estimate changes to water availability per capita, which were then compared with the water thresholds shown in Table 6.2. The results are shown in Figure 6.4.

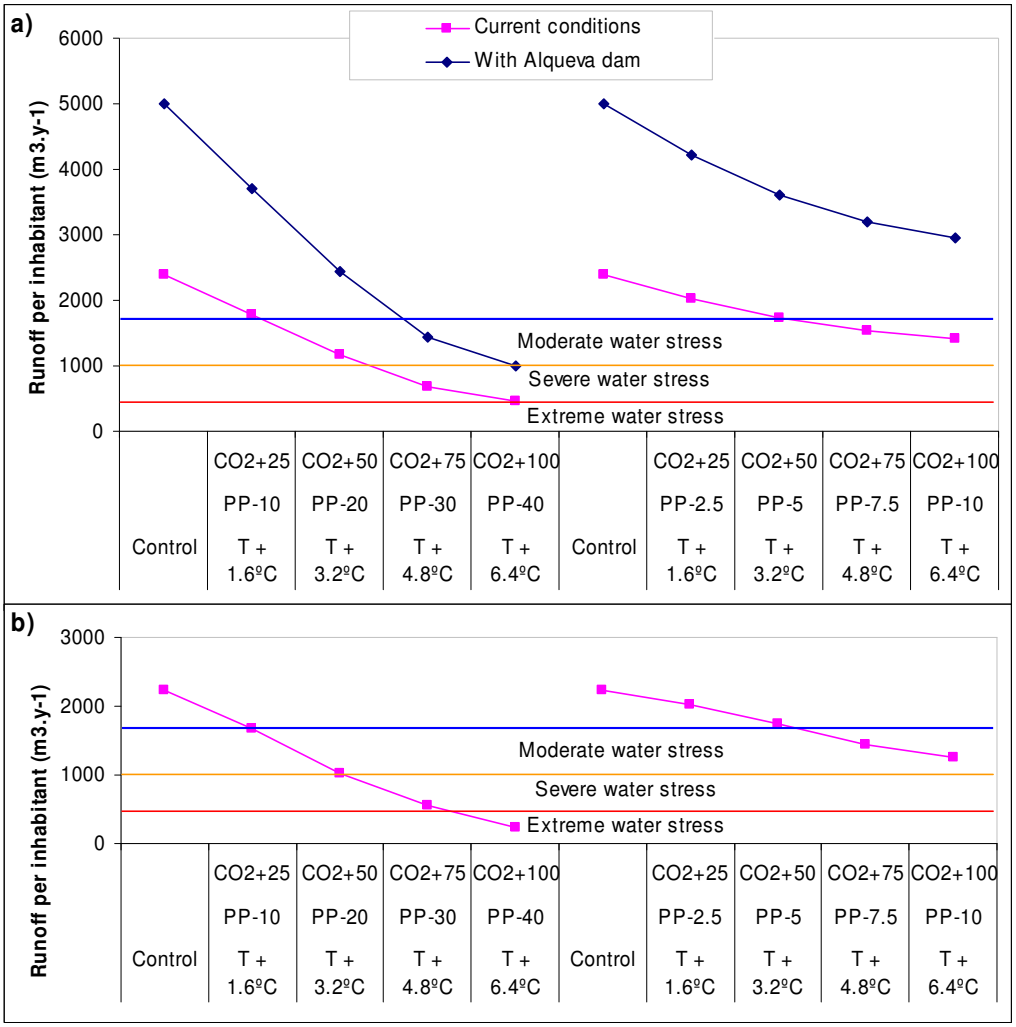

Figure 6.4 – Current and estimated runoff per inhabitant for the Guadiana (a) and Tejo (b) basins, under the climate change scenarios presented in section 5.1 and shown in Figure 6.1; horizontal lines indicate the stress thresholds shown in Table 6.2.

For the Guadiana basin, the results for current conditions are similar to those shown in Table 6.4, with severe water stress occurring only in the "low rainfall" scenario, for a rainfall drop under -30 %. The results for conditions with the Alqueva dam show a very significant difference, however, since these thresholds do not take into account the existence of extensive irrigation systems (Arnell, 2004). Therefore, the stress thresholds for the Alqueva dam should be interpreted as a scenario where the water stored in the reservoir is used to support only

moderate irrigation schemes; in this case, the Guadiana river basin is not expected to suffer from severe water stress except in the "low rainfall" scenario with rainfall dropping below -40 %. A similar case occurs in the Tejo basin, where the results should be interpreted as stress levels with moderate irrigation consumptions. This basin is expected to suffer from severe water stress only in the "low rainfall" scenario, with rainfall dropping below -20 %; however, stress levels could reach extreme cases for rainfall reductions below -30 %.

The results indicated above are for annual average values. However, Arnell (2004) also recommends an analysis of water stress thresholds for drought years (in this case, the lowest 10-year runoff values), which result in disruptions to water supply, also an indicator of water stress. The interannual results from the PROMES RCM, described in section 5.3.3, were used to estimate changes to water availability per capita; the results are shown in Figure 6.5. The RCM climate change estimates fall into the "low rainfall" sensitivity scenarios (Figure 6.1) and therefore the average annual water stress results are similar to those shown above, with water levels remaining above the severe water stress threshold in all scenarios.

However, an analysis of changes to drought years shows a significant increase in water stress frequency. In both basins, severe water stress levels are currently only reached once in ten years on average; and in the Guadiana basin, the additional runoff collected in the Alqueva dam is expected to further improve this situation. With the climate change scenarios, however, the increased frequency of hydrological droughts is expected to lead to the occurrence of extreme water stress levels in the Guadiana basin once every 2.5 years; the Alqueva dam can mitigate these conditions, leading to the occurrence of severe water stress once every 2.5 years for the A2 scenario (-29 % drop in rainfall) and once every 10 years for the B2 scenario (-24 % drop in rainfall). In the Tejo basin, climate change is expected to lead to extreme water stress every 2.5 years (-20 to -25 % drop in rainfall).

It should be noted that human management of water systems can significantly mitigate the impacts of droughts by improving the reliability of water reserves even under drought years (Kundzewicz et al., 2007). In the Guadiana basin, the reservoir system (including the Alqueva dam) is capable of storing 5 140 million m^3 (INAG, 1999a), which represents the average amount of runoff generated in c. 1.4 years in current conditions. For the scenarios shown in Figure 6.1, the reservoir is capable of storing the average runoff generated in c. 2.4 years which is probably sufficient to maintain water supplies during severe water stress years (provided, as discussed above, that extensive irrigation practices are not conducted). In the Tejo basin, however, the reservoir system is only capable of storing c. 1 590 million m^3

(INAG, 1999b), representing c. 0.25 years of average runoff in current conditions. With the decrease in annual runoff shown in Figure 6.1, the reservoir system is capable of storing c. 0.4 years of average runoff, which is probably insufficient to insure water supply reliability in years of extreme water stress. Furthermore, a large part of the existing irrigation systems rely on direct water extraction from the Tejo river (INAG, 1999b) and therefore possess little capacity to maintain water supply during drought years.

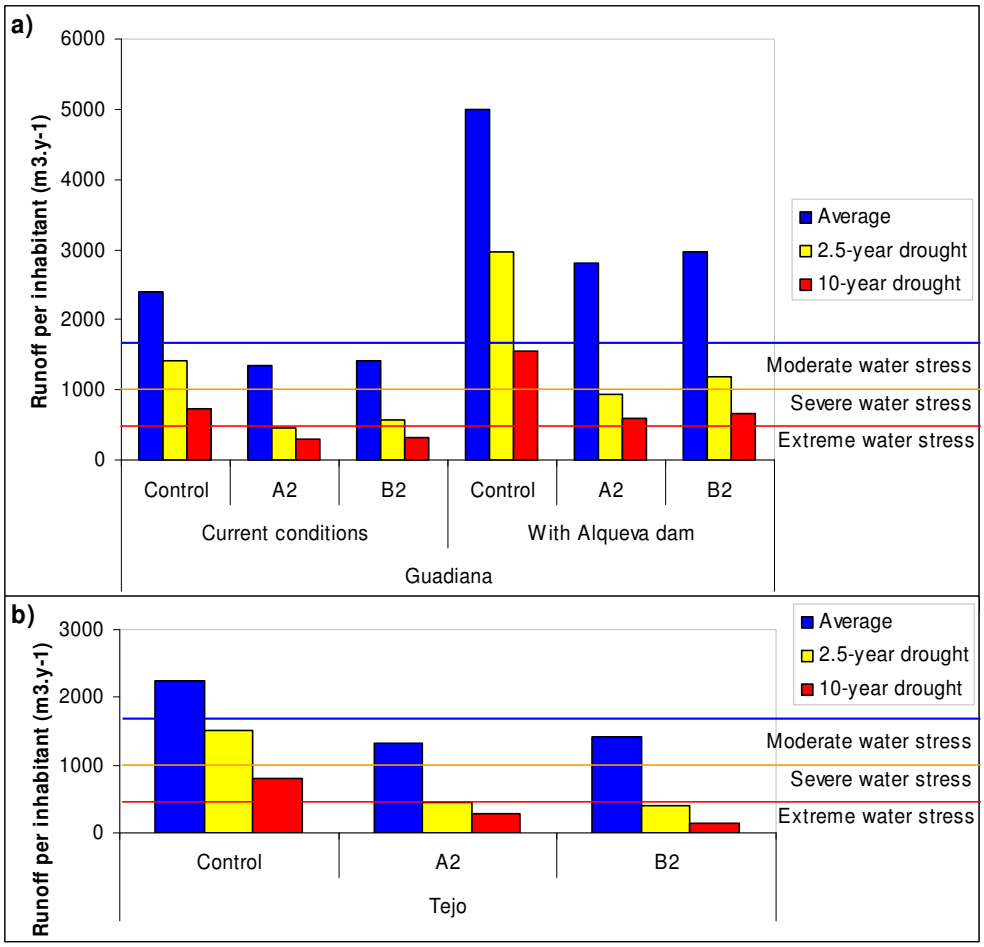

Figure 6.5 – Current and estimated runoff per inhabitant for the Guadiana (a) and Tejo (b) basins, under the climate change scenarios presented in section 5.3 and shown in Figure 6.1, for average and drought conditions; horizontal lines indicate the stress thresholds shown in Table 6.2.

Overall, the results presented in this section indicate that:

- virtually all climate change scenarios are likely to lead to severe water stress in both basins when considering current water withdrawals (which for the Guadiana river includes water used in irrigation networks currently under construction);

- a rainfall decrease below -20 % (in the "low rainfall scenario") is likely to lead to insufficient runoff to meet all water demands;

- considering a more moderate use of water for irrigation, the Guadiana basin is not expected to experience severe water stress except under the most extreme climate change scenarios (rainfall decrease below -40 %);

- in similar conditions, the Tejo basin is only expected to experience severe water stress with a rainfall decrease below -20 % ("low rainfall scenario");

- however, the increase in hydrological drought frequency is expected to lead to the frequent occurrence of years with severe or extreme levels of water stress – in the Tejo basin, a rainfall decrease below -20 % is expected to lead to extreme water stress in 1 year out of 4.

The results also indicate that the reservoir system in the Guadiana basin is more likely to be able to maintain water supplies at regular levels during drought years than in the Tejo basin, although this capacity could be hampered by the concentration of runoff in a shorter wet season, coupled with increased river flow irregularity (as discussed in section 6.2.1) and the probable increase in irrigation water requirements during drier years. Furthermore, the additional runoff generated in Spain and stored by the Alqueva dam is the greatest contributor to the relatively lower water stress risk expected for the Guadiana basin. An increase in water uptakes in the Spanish side of the basin, due to e.g. increased irrigation requirements, could increase this risk to a level similar to the one estimated for the Tejo basin.

The main conclusion that can be taken from these results is that **the capacity of the Guadiana and Tejo river basins for sustaining current water requirements shows low resilience to climate change, with severe stress occurring even with low magnitude changes and shortfalls occurring with rainfall decreasing below -20 %**. This capacity shows considerably more resilience when considering a moderation in agricultural water usage, with stress levels unlikely to be achieved in the Guadiana for the most likely climate

change scenarios, and only occurring with rainfall decreasing below -20 % in the Tejo basin. Even in the case of low magnitude climate changes, however, the basins' capacity for water supply during drought years shows a low resilience, with moderate to extreme stress levels occurring on average twice every 5 years. The similarity of these results for both basins despite the significantly drier conditions in the Guadiana can be attributed to the higher pressure on the Tejo basin's water resources, mostly as a function of the higher population.

Finally, it should be noted that, while these conclusions apply mainly to the Guadiana and Tejo basins as a whole, they are also apply in the watersheds within the study areas analyzed in this thesis since a significant part of the water supplies originate in basin-wide reservoir systems. Therefore, basin-wide water stress levels are likely to affect the study areas as well. Furthermore, the basin-scale water use conflicts caused by stress conditions may difficult water uptake within these watersheds for e.g. domestic consumption and small-scale irrigation due to water requirements further downstream.

Vegetation support

The overall results for the impacts of climate change on vegetation biomass growth (discussed in section 5) point to a decreasing trend for agricultural species (in this test, wheat and vines) and forest species, mostly due to the increase in climatic aridity. They also indicate a possible mitigating effect of the increase in CO_2 atmospheric concentrations in the lesser magnitude climate change scenarios (temperature increasing up to 4 ºC). In contrast, Mediterranean species (in this test, shrubs and sclerophyllous trees) appear to benefit from most of the simulated climate change scenarios, although the tree species only appear to tolerate rainfall decreases down to -20 %. However, the results alone do not indicate if these changes are sufficient to surpass thresholds for agricultural production or the overall system's capacity to support biomass. In particular, farmers can usually adapt to changes in climate as long as new options for cultivation are available (Berry et al., 2006), and the species composition of ecosystems can adapt to different climates to a certain degree without significant changes to productivity (Clark, 1996; Pereira et al., 2006).

However, a number of thresholds for agricultural productivity and natural vegetation support can be derived from an analysis of the current distribution of agricultural and natural vegetation patterns along climatic gradients, in what is usually termed a "space-for-time" study (e.g. Fleischer and Sternberg, 2006). Considering the dryland characteristics of many Mediterranean regions, including the two study areas (section 4.2), and the increasingly drier conditions expected under climate change, a suitable climatic gradients is the ratio of annual

evapotranspiration to precipitation, which is commonly used as an aridity index (UNEP, 1997). Arora (2002) reports that this ratio represents the relationship between the primary controls on hydrological processes: available water and available energy for evapotranspiration. When the index is below unity, there is a transition from energy-limited to water-limited evapotranspiration, and a shift of rainfall partitioning from runoff to evapotranspiration. In dry climates with little seasonal variability, the trend is for all rainfall to be used in evapotranspiration, leading to little runoff; in Mediterranean dry climates, runoff mostly occurs because the seasonal cycles of rainfall and evapotranspiration are out of phase with each other. Furthermore, since the interannual variability of evapotranspiration is generally smaller than that of rainfall, there is a trend for increasing drought frequency and severity with decreasing values of the rainfall to evapotranspiration ratio. The aridity index levels proposed by the UNEP (1997) – humid, dry/sub-humid, semi-arid and arid – reflect increasing degrees of evapotranspiration potential shortfalls.

The changes to climatic aridity can also impact agriculture by increasing vegetation water demands and/or water stress levels; while farmers can usually choose between a range of cultivation options adapted to different temperature and drought ranges, choices in the Mediterranean are already constrained by high temperatures and low water availability (Olesen and Bindi, 2002). Furthermore, increased aridity can constrain intensive farming due to higher irrigation needs coupled with less available water to meet those needs, and some forms of extensive farming may become unprofitable due to increased yield variability induced by droughts (Berry et al., 2006). Natural vegetation is also constrained by climatic aridity, which plays an important role in determining canopy cover and leaf density (Puigdefabregas et al., 1998). Clark (1996) reports that Mediterranean communities are usually composed of a mix of evergreen trees, evergreen and deciduous shrubs and annual grasses, but the relative composition of each vegetation type changes to better take advantage of climate conditions. An example is the dominance of sclerophyllous oaks in sub-humid areas, becoming increasingly sparser with climate aridity and replaced by drought-adapted shrublands in semi-arid areas (FAO, 2001). This indicates that the different levels of the climatic aridity index may be used as thresholds for changes to agriculture and natural vegetation support capacity caused by climate change.

The vegetation support threshold analysis was in part based on the Guadiana study area as a reference site for Portuguese conditions, since the current climate aridity ranges from humid to semi-arid, being quite close to arid in some regions (see section 4.2.1). The distribution of

agriculture and natural vegetation in the Guadiana, calculated using the physical data described in section 4.2, is shown in Figure 6.6; for this analysis, annual crops were divided between those that are occupied only by cereals, and those that contain important patches of natural vegetation (referred in the figure as "mixed agriculture"). Mixed agriculture, in the Guadiana context, usually consists of winter wheat associated with permanent crops or forestry in the more humid climates, and a mosaic of cultivated and abandoned crop fields with important patches of natural shrublands in more arid regions which indicates an ongoing process of land abandonment.

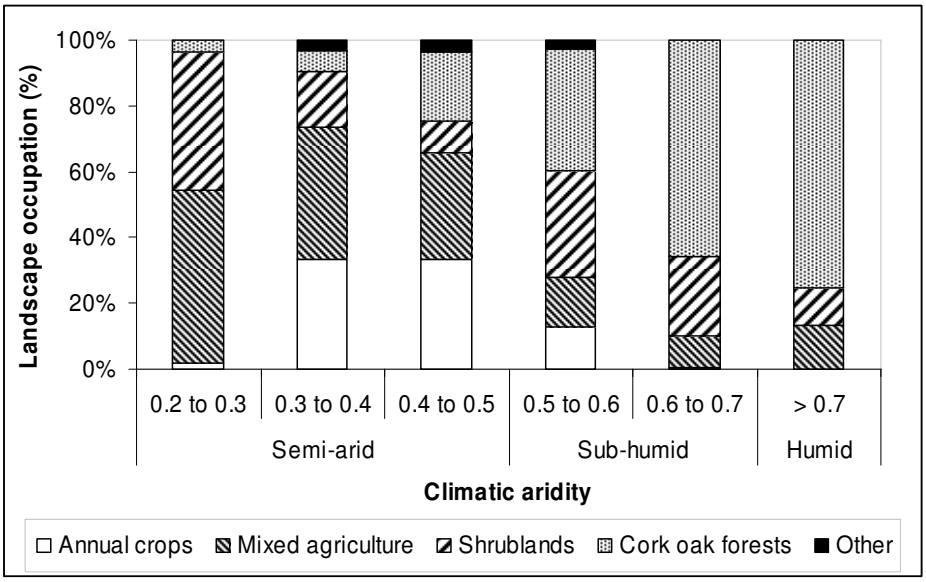

Figure 6.6 – Agriculture and natural vegetation distribution in the Guadiana study area broken down by climatic aridity classes (UNEP, 1997).

The figure shows that sclerophyllous cork oak forests, often associated with annual croplands, dominate humid and transitional sub-humid regions, gradually declining in more arid regions to be replaced by winter wheat croplands and mixed agriculture. The presence of annual croplands in semi-arid regions can be explained by past policies encouraging intensive wheat cultivation in the Guadiana basin (Roxo et al., 1996). The regions of more extreme aridity show a mixed dominance of shrublands and mixed agricultural, with the latter class referring mostly to active and abandoned fields. It should be noted that the presence of shrublands in sub-humid areas is also associated with the extensive land degradation and abandonment in the hillslopes where these climates occur, as exemplified by the Odeleite watershed (see

section 4.2.5 for further details). The low presence of land uses which are important in the Tejo study area, such as vineyards and commercial forestry, should also be noted.

The data shown in Figure 6.6 was compared with published data to estimate climatic aridity thresholds for different agricultural and natural vegetation types in Mediterranean and other drylands; the results are shown in Table 6.5. It should be noted that this data refers to rainfed agriculture only, as irrigated agriculture can exist at much lower aridity thresholds (e.g. Vincente-Serrano et al., 2006). The aridity gradient found in the Guadiana appears to be present in other Mediterranean regions, with forestry occupying at best sub-humid areas, sclerophyllous oaks and permanent crops surviving in the transitional area between sub-humid and semi-arid climates, and shrublands and steppelands occupying semi-arid and arid climates. Croplands are a special case; although rainfed cereal agriculture can be conducted under most semi-arid climates (FAO, 1989), the yield variability increases significantly when climatic aridity drops below 0.5 (Puigdefábregas and Mendizabal, 1998). In this case, the socio-economic conditions of farmers can limit the profitability of wheat cultivation (e.g. Berry et al., 2006); judging by the current trend for marginal agriculture abandonment in Mediterranean semi-arid regions (Puigdefábregas and Mendizabal, 1998), aridity levels ranging between 0.5 and 0.3 can be seen as a risk interval where annual croplands are still viable but probably not economically sustainable in current conditions.

The natural vegetation estimates in this table also coincide with reports of theoretical climax of deciduous forests in the more humid regions, transitioning to sclerophyllous forests, dense shrublands and sparse shrublands with the increase in climate aridity (e.g. Clark, 1996; FAO, 2001). However, it should be noted that these climate-vegetation relationships rely on extrapolations which possess a relatively low reliability when compared with e.g. the modeling framework results presented earlier, as they leave into account factors such as soil type and winter temperatures which also play a determinant role in the suitability of a given region for different vegetation types (Clark, 1996; Barboni et al., 2004).

The aridity thresholds shown in Table 6.5 were compared with the estimates for aridity in the Guadiana and Tejo under the climate change scenarios shown in Figure 6.1. The results for both study areas are shown in Figure 6.7. For comparison purposes, the RCM scenarios discussed in section 5.3 predict aridity values of 0.3 for the Guadiana in both scenarios, and 0.45 to 0.5 in the Tejo for the A2 and B2 scenario (respectively).

Table 6.5 – Estimated aridity thresholds for different vegetation types in the study areas, compared with other dryland estimates.

Vegetation type		Aridity threshold: Adopted in this work	Guadiana[a]	NE Spain[b]	Lesvos, Greece[c]	Mediterranean drylands[d]	Global drylands[e, f]
Forests		0.50		0.60	Sub-humid	0.40	
Permanent crops		0.45		0.45	Transient[g]		
Sclerophyllous forests		0.40	0.40		Transient[g]	0.30	
Annual crops		0.30	0.30	<0.40	Semi-arid		Semi-arid
Shrublands	Dense	0.20	<0.20		Semi-arid	0.20	Semi-arid
	Sparse	0.10	<0.20		Semi-arid	0.10	Arid
Steppelands		0.10		<0.40		0.10	Arid

a – Figure 6.6.
b – Vincente-Serrano et al. (2006).
c – Kosmas et al. (1999).
d – Barboni et al. (2004).
e – FAO (1989).
f – von Hardenberg et al. (2001).
g – Transition between semi-arid and sub-humid.

For **agricultural production**, the results indicate that current agricultural suitability would be maintained in the "high rainfall" scenario for both study areas. For the "low rainfall" scenarios, however, the results indicate the existence of one important threshold for both study areas. An increase of temperature above c. 4 ºC (coupled with a rainfall decrease below -20 %) could lead to the total unsuitability of the Guadiana for rainfed wheat cultivation, while in the Tejo wine production could be impossible without irrigation and the reliability of annual crops would decline significantly. In the Tejo, a temperature increase of c. 6.5 ºC (with rainfall decreasing by -40 %) would also put crop cultivation close to the limit of sustainability. The RCM results indicate do not indicate changes to any significant thresholds in both study areas.

For **natural vegetation**, including forestry, the results for the Guadiana indicate a threshold for cork oak growth in the "high rainfall" and "low rainfall" scenarios of c. 4 ºC increase in temperature, below which the maintenance of these trees could become unsustainable; this threshold is also surpassed in the RCM A2 and B2 scenarios. Dense shrublands remain above the threshold in all scenarios except in the most extreme (temperature increase of c. 6.5 ºC, rainfall decrease of -40 %) where conditions are close to the sustainability threshold. In the Tejo, the "low rainfall" scenario shows a threshold of c. 4 ºC increase in temperature (coupled with a rainfall decrease below -20 %), beyond which forestry activities could become

unsustainable. It should be noted that these results present only general trends for the study areas; there is some degree of spatial variability in aridity conditions, particularly in the Guadiana study area (see Figure 4.1, section 4), and climate change could lead to more moderate levels of aridity in the southwestern hillslopes and more severe levels in the eastern part of the study area. It should also be noted that these results coincide with the agricultural land use trends under climate change reported by several authors (e.g. Metzger et al., 2005; Berry et al., 2006) for these regions.

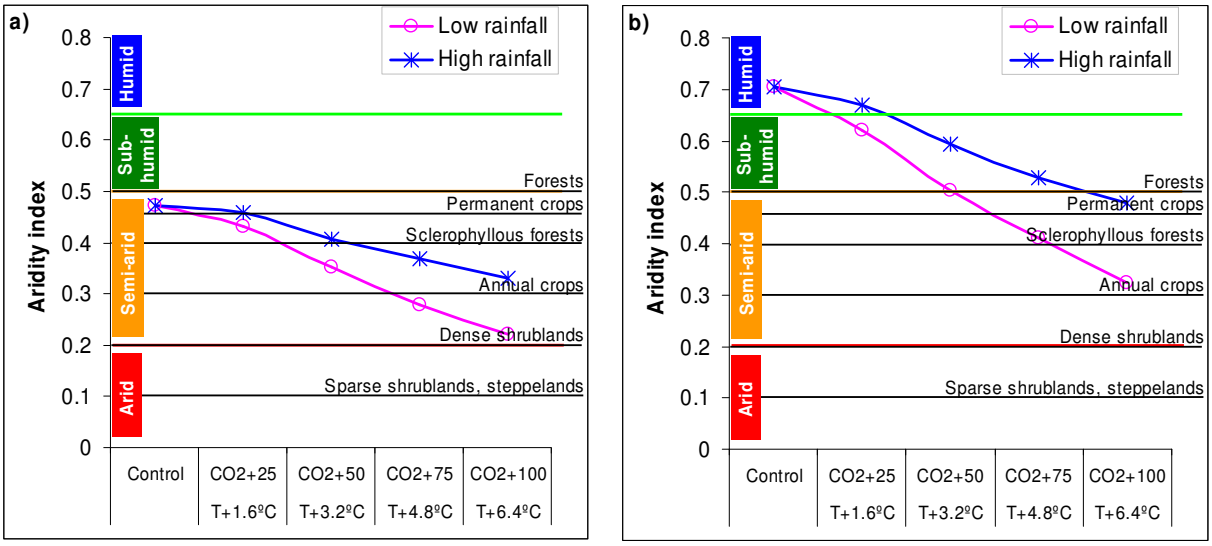

Figure 6.7 – Comparison between changes to aridity for the climate change scenarios shown in Figure 6.1 and the vegetation thresholds shown in Table 6.5, for the Guadiana (a) and Tejo (b) study areas.

These results can also be compared with the model estimates for vegetation biomass changes, shown in section 5.1 (Figure 5.7) and section 5.3 (Figure 5.28). Model results do not indicate clear thresholds, but they do indicate a trend for decreasing wheat productivity in the Guadiana starting from a temperature increase of c. 2 ºC, coupled with an increase in shrub biomass for all scenarios. However, for scenarios beyond the threshold for sclerophyllous oak shown in Figure 6.7, the model results indicate productivity values above current levels, although with a declining trend in the "low rainfall" scenario. The discrepancy between model results and the aridity index estimates may be due to drought-induced mortality in woody plants, which is not taken into account by the SWAT model; however, evergreen oaks can experience significant mortality rates if summer drought periods last longer than three

months, particularly if associated with high temperatures, while evergreen shrubs are able to withstand significantly longer drought periods (Martínez-Vilalta et al., 2002). Furthermore, the aridity index does not take into account possible mitigating effects of the increase in atmospheric CO_2 concentration both in vegetation biomass productivity and drought resistance, which could increase their tolerance to climatic aridity (Cheddadi at al., 2001). The RCM results indicate that this factor could play a significant role in mitigating the effects of climate change on vegetation productivity. For the Tejo study area, model results indicate a decreasing trend for the productivity of all vegetation but without clear thresholds, and a possible mitigating effect of increased CO_2 concentrations; however, the impacts of more extended summer droughts for woody plant mortality could indicate that, beyond the aridity threshold, this problem could also affect forests and rainfed vineyards.

One result from Figure 6.7 requires further analysis. As referred above, climate aridity in the Guadiana could reach the threshold between semi-arid and arid with the more extreme climate scenario. The transition between these two climate aridity types is non-linear and often quite abrupt due to significant transformations to soil structural properties (Lavee et al., 1998). These changes significantly reduce the water that vegetated species can capture with their root systems; Puigdefábregas (1998) reports that vegetation adapts its spatial structure in order to create a patchwork of bare areas and vegetation clumps, with runoff generated in the former and infiltrating in the latter, significantly increasing the water and nutrients harvested by the plants but with significant erosion in bare areas. Vegetation productivity becomes dependent on the existence and size of the bare areas, and beyond this threshold vegetation patchiness increases with greater climatic aridity, leading to the fragmentation of the landscape and possibly to a disruption of existing ecosystems. If this threshold is surpassed in the Guadiana study area, this could lead to a significant reduction of overall vegetation cover. In fact, the beginnings of this process have already been observed by Seixas (2000) in the most arid regions of the study area.

The probability the Guadiana and Tejo study areas surpassing this fragmentation threshold was estimated using a method proposed by Boer and Puigdefábregas (2003 and 2005) which assessed the maximum vegetation density in a given area according to climatic aridity, estimated using potential evapotranspiration. The authors used a simple monthly water balance calculation to estimate the optimal canopy conductance of vegetation cover, allowing for maximized monthly evapotranspiration rates while keeping soil water storage positive at all times. Optimal conductance estimates were performed for a study area in southern Spain

and compared with remote sensing observations of the Normalized Differential Vegetation Index (NDVI), taken as a linear estimator of vegetation Leaf Area Index (LAI); the upper 95 % were taken as indicating optimal LAI values for a given optimal conductance. The authors observed a conductance threshold of 0.0038 mm^{-1}, below which optimal LAI steadily declines due to an increase in vegetation patchiness; above this threshold, optimal LAI remains constant indicating homogenous vegetation cover.

This method was applied to the study areas using monthly evapotranspiration rates predicted for the climate change scenarios shown in Figure 6.1, assuming the validity of the conductance-LAI relationships published by Boer and Puigdefábregas (2003). The results are shown in Table 6.6; they indicate that there is a threshold of c. +4 ºC above which maximum LAI starts to severely decline in the Guadiana; no threshold was found in the Tejo for the simulated degrees of climate change. The results concur with the threshold assessment discussed above, although this method does not take into account the rainfall differences between the "low rainfall" and "high rainfall scenarios; this reinforces the indications that the capacity of the Guadiana study area to support vegetation cover will be significantly affected by an increase in temperature over +4 to +6 ºC. Again, the results for shrubland cover do not agree with the modeling estimates for increased shrub biomass productivity in all scenarios (section 5.1, Figure 5.7). This can be attributed to simulation of vegetation shrub density in the SWAT model as a constant, area-averaged value which could be significantly below the optimal density, coupled with the fact that the method proposed by Boer and Puigdefábregas (2003 and 2005) is based on current data, not taking into account the potential impacts of increased CO_2 concentration in vegetation drought resistance (Cheddadi at al., 2001).

Overall, and despite the uncertainties associated with the extrapolation methods used to obtain these results, the following conclusions can be drawn:

- most scenarios with moderate rainfall decreases ("high rainfall" scenarios) do not indicate significant changes to the sustainability of current agricultural practices and natural vegetation, although in the Guadiana temperature rises over +3.5 to +4.5 ºC could significantly decrease the suitability for wheat cultivation and cork oaks;

- for severe rainfall decrease scenarios ("low rainfall" scenarios), an increase in temperature above c. +3.5 to +4.5 ºC (coupled with a rainfall decrease below -20 %) appears to be a significant threshold for the Guadiana, beyond which the

unsustainability of wheat cultivation and the disappearance of cork oaks could be expected;

- beyond this temperature level, the total vegetation support capacity of the Guadiana could also begin to decrease, leading to a shift toward sparser vegetation patterns;
- in the Tejo, a similar threshold exists beyond which wheat yield variability is expected to increase (Figure 6.7), and wine production and forestry activities become unsustainable;
- these results are expected to present a high degree of spatial variability in the Guadiana study area, with more severe impacts in the eastern part of the study area;
- the increase in atmospheric CO_2 concentrations could increase the system's tolerance to aridity for moderate rainfall decreases.

Table 6.6 – Estimated optimal canopy conductance and changes to maximum potential LAI for the Guadiana and Tejo study areas, for the climate change scenarios shown in Figure 6.1.

	Guadiana		**Tejo**	
Scenario	**Opt. canopy conductance (mm^{-1})**	**Change to max. potential LAI (%)**	**Opt. canopy conductance (mm^{-1})**	**Change to max. potential LAI (%)**
Control	0.0048	–	0.0056	–
RCM B2: T+2.5 ºC[a]	0.0040	-1.5	0.0044	-0.1
RCM A2: T+3.5 ºC[b]	0.0039	-2.8	0.0043	-0.2
Sensitivity: T+1.6 ºC	0.0044	-0.1	0.0055	0.0
Sensitivity: T+3.2 ºC	0.0039	-2.8	0.0050	0.0
Sensitivity: T+4.8 ºC	**0.0036**	**-20.6**	0.0046	0.0
Sensitivity: T+6.4 ºC	**0.0033**	**-58.3**	0.0042	-0.4

a – T +2.7 ºC in the Guadiana, +2.2 ºC in the Tejo.
b – T +3.7 ºC in the Guadiana, +3.2 ºC in the Tejo.

The most important implication from these results is that the resilience of agriculture and natural vegetation in the Guadiana and Tejo study areas depends on the expected magnitude of climate change; however, **some of the scenarios predicted for the study areas are sufficient to lead the systems beyond vegetation support thresholds** (Figure 6.1). The biophysical systems appear to be resilient to high degrees of temperature increases if they are

accompanied by a low degree of changes to rainfall. However, the systems do not appear to be resilient to high increases in temperature if coupled with high decreases in rainfall. An increase in temperature above c. +3.5 to +4.5 ºC, coupled with a rainfall decrease below -20 %, is expected to lead to significant changes for agricultural practices and natural vegetation in both study areas. This threshold corresponds to a decrease of the aridity index below 0.3 in the Guadiana, leading to the appearance of arid conditions such as the lack of significant agricultural productivity and sparse natural vegetation patterns. In the Tejo, the threshold leads to a decrease of the aridity index below 0.5, leading to the appearance of semi-arid conditions similar to the ones occurring in the Guadiana today, marked by irregular wheat yields and little presence of permanent crops or commercial forestry. Finally, the impacts of increased CO_2 concentrations could be sufficient to mitigate the effects of moderate levels of climate change and possibly lead to increased vegetation productivity.

The consequence of these changes is likely to be an overall transition towards drought-tolerant vegetation types in both study areas, with the degree of transition determined by the magnitude of climate change under the constraints referred above. Agricultural transitions can be planned by farmers, but in many cases they result from the sum of individual decisions due to changes to yield or profitability, and are often induced due to extreme perturbations such as severe droughts (Puigdefábregas and Mendizabal, 1998; Berry et al., 2006). Similarly, natural ecosystems usually change due to extreme perturbations, such as severe droughts and wildfires, that push systems beyond their resilience thresholds and drives them to qualitatively different states; recovery can be prevented by the pressures exerted by the normal climatic variability of dryland climates and self-reinforcing mechanisms of land degradation (Imeson and Lavee, 1998; Puigdefábregas, 1998; Pereira et al., 2006). The long regrowth period of arboreal vegetation makes it particularly vulnerable to the frequent occurrence of disturbances (Clark, 1996).

Furthermore, ecosystems show a certain degree of resilience to perturbations due to natural mechanisms such as changes in species composition to adapt to climate shifts (as described by Clark; 1996). Transition trigger events are usually the result of a synergistic combination of anthropogenic and climatic factors; Puigdefábregas (1998) describes the alternation of humid and dry periods as a common example of these events, with the former leading to increased pressure on resources while the latter leading to irreversible degradation if pressure is not released before resilience thresholds are exceeded. The results shown above underestimate the importance of trigger events, mostly due to limitations in the modeling framework (section

5.3), particularly the fact that the impacts of wildfires, drought-induced mortality, arboreal vegetation regrowth and changes to agricultural and grazing pressures during severe droughts are not taken into account.

A final note should be made on the possibility of natural vegetation recovery in abandoned croplands. As discussed above, an increase in yield variability or a decrease in productivity due to loss of fertility could lead to an increased trend of agricultural land abandonment with climate change magnitude, particularly in the Guadiana study area; this would continue a trend which has occurred in recent decades (Roxo et al., 1996; Roxo and Cortesão Casimiro, 1998). In Mediterranean drylands, many of these abandoned areas are expected to revert to dense shrublands (Puigdefábregas and Mendizabal, 1998; Bakker et al., 2005). Vincente-Serrano et al. (2004) have reported an increase in vegetation density in recently abandoned Mediterranean farmlands due to regeneration processes, leading to a significant decrease in runoff, especially of high flow rates, in these regions (López-Moreno et al., 2006). The abandonment of marginal agricultural areas has also been linked with a reduction in land degradation processes (Roxo and Cortesão Casimiro, 1998; Martínez-Fernández and Esteve, 2005). A similar process could occur in fields set aside for vegetation recovery following the European Union's common agricultural policy.

However, stopping annual agriculture in drylands does not necessarily lead to vegetation recovery, which is linked with other factors such as the state of soil degradation and rainfall instability (Puigdefábregas, 1998). The relationship between climatic aridity and maximum vegetation cover implies that the soil is able to store available water to meet evapotranspiration demands; in degraded soils, the decrease in soil water holding capacity is therefore expected to lead to significantly lower vegetation cover (Arora, 2002; Bakker et al., 2004; Boer and Puigdefábregas, 2005). In the Tejo study area, the current soil status and expected loss of fertility through soil erosion (as discussed earlier) indicates that natural vegetation would not be impeded by soil conditions. However, this problem could arise in the degraded Lithosols of the Guadiana study area. An example of the different suitability of this soil type when compared with a less shallow Luvisol in the same region is given Figure 6.8 (calculated in a similar way as Figure 6.6). For similar aridity classes, the prevalence of shrublands and mixed wheat / natural vegetation is greater in the Lithosol; furthermore, the Luvisol show a significant proportion of permanent agriculture (classified as "other" in the figure) in sub-humid regions, which uncommon throughout the study area (Figure 6.6).

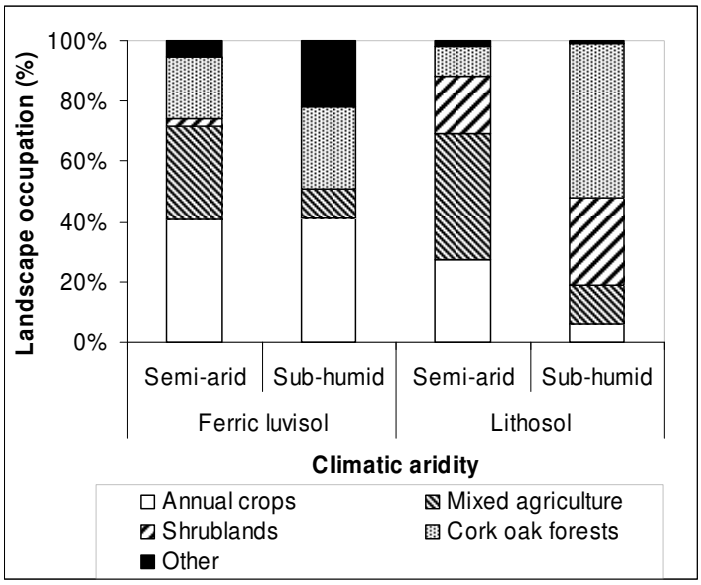

Figure 6.8 – Agriculture and natural vegetation distribution in the Guadiana study area over different soil types, broken down by climatic aridity classes (UNEP, 1997).

A further example for the northern part of the study area is given by Casimiro (2003), who reports that, in croplands abandoned or set aside from 1985 to 2001, 57 % kept a continuous herbaceous cover, 38 % suffered a vegetation reduction to steppelands or sparse shrublands, and only 6 % transitioned to dense shrublands or cork oak forests. Furthermore, the resulting sparse shrublands were not necessarily a first step in vegetation recovery, with 20 % changing to dense shrublands or cork oak forests and 24 % reverting to grasslands or steppelands. This phenomenon was also reported for this region by Seixas (2000), who observed an increase in the spatial heterogeneity of vegetation cover in shrublands and abandoned farmlands.

These observations indicate that degradation of Lithosols in the Guadiana study area could have already surpassed the threshold required to support dense vegetation patterns. In these situations, land abandonment can lead to an increase in soil erosion and land degradation, as observed by Oostwoud Wijdenes et al. (1999) who note the development of a permanent gully system in the first years after abandonment as farmers cease to refill ephemeral gullies. Furthermore, human intervention in abandoned farmlands through afforestation can lead to greater soil erosion rates than under the sparse shrublands, due to the inadaptation of tree cover to the low rainfall regimes (Martínez-Fernández and Esteve, 2005). A further in-depth study of the vegetation recovery potential in this region is required to further assess the impacts of land abandonment and suggest appropriate measures of human intervention;

however, this factor indicates that the vegetation support capacity of Lithosols in the Guadiana study area have a significantly lower resilience to climate change than indicated by the results discussed in this section.

6.2.3 Resilience assessment

The results discussed in the previous section indicate that climate change can cause significant impacts in the hydrological and vegetation components of Mediterranean biophysical systems. In both study areas, the hydrological system's capacity for water resources provisioning shows a low resilience to climate change where considering current water extractions; a more moderate use of water for irrigation could decrease stress levels, but even in this situation, water supplies are expected to experience severe stress in drought years. The Guadiana appears to be more resilient than the Tejo in this situation, mostly due to the storage of water collected from Spain in the Alqueva dam, coupled with a significantly lower pressure on available resources.

The system's capacity to support vegetation appears to be more resilient, in part due to the mitigating effect of an increase in CO_2 concentrations for vegetation productivity; however, a large magnitude change in climate could still lead to a significant shift in agricultural and natural vegetation patterns towards more arid characteristics. The Guadiana appears to be less resilient than the Tejo, since (i) the long-term impacts of soil erosion on soil fertility could counteract the impacts of higher CO_2 concentrations; and (ii) soil degradation levels are already high in most of the study area, preventing vegetation from taking full advantage of rainwater in the more arid regions (Arora, 2002).

While a quantitative assessment of resilience is difficult due to the uncertainty associated with the threshold estimation performed in this work, it can be hypothesized that a decrease in rainfall under -20 % is sufficient to cause moderate water stress in the Guadiana, and severe water stress in the Tejo. If this change is coupled with an increase in temperature above +3.5 to +4.5 ºC, this could be sufficient to significantly change agriculture practices and natural vegetation patterns in both study areas. One indicative conclusion is that, above this threshold, the Guadiana could shift towards an arid system with agriculture present only in irrigated areas; and the Tejo could acquire the semi-arid characteristics which characterize the Guadiana today. These shifts are expected to occur mostly due to extreme events, particularly droughts. The thresholds could be higher, particularly for Mediterranean vegetation species, due to the mitigating effect of an increase in CO_2 atmospheric concentration on vegetation

productivity; and they could be significantly lower in the shallow Lithosols of the Guadiana watersheds.

Overall, the watersheds in the study areas do not appear to be resilient to climate change. Even low magnitude climate changes could take them beyond water provisioning and vegetation support thresholds, leading to an enhancement of desertification processes in these watersheds. The results concur with the sensitivity assessment described earlier, and the lower thresholds for water provisioning can be attributed to the higher sensitivity of hydrological processes to climate change. Finally, it should be noted that soil fertility thresholds are not expected to be surpassed due to the action of soil erosion, particularly in the Guadiana where Lithosols appear to already be beyond them. However, the action of ephemeral gullies could continue to destroy soil productive capacity in localized regions.

6.3 Vulnerability to climate change

According to the vulnerability assessment framework exposed in section 3.1 (and following Adger, 2006), the final vulnerability analysis couples the results for the sensitivity and resilience of biophysical processes to climate change with an analysis of the systems' adaptive capacity. This analysis is focused on desertification drivers, and summarizes the results presented above; the results are also used to propose and discuss adaptation methods to reduce the vulnerabilities exposed in the analysis (following the approach proposed by Smit and Wandel, 2006).

6.3.1 Overall vulnerability assessment

As the previous sections show, there is a significant uncertainty in the magnitude of climate change which propagates into all the impacts estimated in this work. In the resilience analysis, the surpassment of a set of thresholds depends in a large degree on the expected magnitude of climate change. However, the results indicate that most of the temperature thresholds are located at around +3.5 to +4.5 ºC. They also indicate a significant difference between the "low rainfall" and "high rainfall" scenarios, leading to a rough threshold of c. -10 to -20 % decrease in rainfall. Therefore, the vulnerability assessment took into account four scenarios with different combinations of moderate (below threshold) and severe (above threshold) changes to temperature and rainfall, presented in Table 6.7. It should be noted that the threshold for the rainfall scenarios was arbitrarily set between the rainfall changes used in the sensitivity analysis, and should therefore be taken mostly as an indicative reference. The temperature change thresholds, however, are supported by the results described previously.

Table 6.7 – Climate change scenarios used for vulnerability assessment.

	Temperature change		Rainfall change	
Scenario	**Threshold (ºC)**	**Classification**	**Treshold (%.ºC^{-1})**	**Classification**
MM	<4	Moderate	>-3.8	Moderate
MS	<4	Moderate	<-3.8	Severe
SM	>4	Severe	>-3.8	Moderate
SS	>4	Severe	<-3.8	Severe

These thresholds encompass a number of published scenarios of climate change, as can be seen in Figure 6.9. However, two things should be noted in terms of scenario distribution. First, a significant part of Global Circulation Model (GCM) and Regional Climate Model (RCM) climate change scenarios fall into the MS (moderate temperature and severe rainfall change) vulnerability scenario, which could indicate a higher likelihood of occurrence if taking a scenario ensemble approach to climate change estimation (Giorgi, 2005). A more detailed analysis can be made by comparing the results for the two study areas which fall inside each vulnerability assessment scenario, as shown in Table 6.8. This comparison indicates that, for the B2 emission scenario, most climate change model results fall inside the MS vulnerability scenario in both watersheds, with a significant number also falling inside the MM scenario. For the A2 emission scenario, most climate change model results still fall inside the MS scenario; in the Guadiana, a significant number also fall inside the SS scenario. Therefore, there is a difference in the magnitude of climate change impacts for different emission scenarios that should be taken into account, although these results are only indicative since the performance of the different models shown in Figure 6.9 for the Guadiana and Tejo study areas was not evaluated.

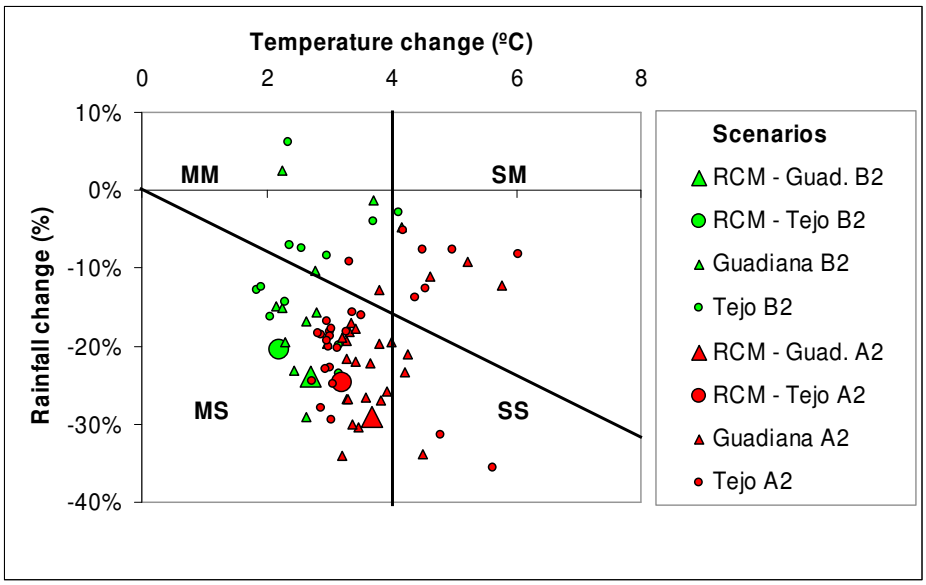

Figure 6.9 – Relation between changes to temperature and rainfall for the vulnerability assessment scenarios (Table 6.7), the PROMES RCM scenarios (section 5.3), and published scenarios for central and southern Portugal (Cunha et al., 2002; PRUDENCE, 2007).

Table 6.8 – Frequency of occurrence of each climate change scenario (Figure 6.9) within each vulnerability assessment scenario (Table 6.7); CO_2 concentration values are approximate.

	Guadiana (%)		**Tejo (%)**	
Scenario	**B2 (c. 1.5×CO_2)**	**A2 (c. 2×CO_2)**	**B2 (c. 1.5×CO_2)**	**A2 (c. 2×CO_2)**
MM	41.7	3.8	41.7	3.7
MS	50.0	73.1	50.0	66.7
SM	8.3	11.5	8.3	22.2
SS	0.0	11.5	0.0	7.4

Table 6.9 summarizes the results presented throughout this thesis, focusing on the most important vulnerabilities to climate change in the context of desertification processes. The results are based on the sensitivity and resilience analysis discussed previously. It should again be noted that the thresholds used in the resilience assessment possess a low degree of reliability and therefore these results should be taken as being indicative. In particular, an increase in irrigation requirements needs would lead to an increased vulnerability, while the positive impacts of higher CO_2 concentrations could mitigate the vulnerabilities identified for vegetation productivity.

Table 6.9 – Main vulnerabilities of the Guadiana and Tejo study areas to climate change, in terms of impacts on hydrological processes, vegetation productivity and soil erosion capable of enhancing desertification.

	Scenario	Hydrological processes	Vegetation productivity	Soil erosion
Guadiana	MM	Current water withdrawals[a]: severe water stress.	–	–
	MS	Current water withdrawals[a]: severe water stress. Reduced irrigation water use: severe water stress during droughts (1 in 4 years).	–	–
	SM	Current water withdrawals[a]: severe water stress.	Agricultural yield reduction. Low sustainability for cork oak growth.	Increased upslope and gully erosion in croplands.
	SS	Current water withdrawals[a]: water resource shortfall. Reduced irrigation water use: severe water stress during droughts (1 in 4 years)[b]. Increased storm runoff in arid regions[c].	Agricultural yield reduction. Low sustainability for wheat and cork oak growth. Arid vegetation cover.	Increased upslope and gully erosion in arid regions[c].
Tejo	MM	Current water withdrawal: severe water stress. Increased magnitude of all floods.	–	Increased upslope and gully erosion[b].
	MS	Current water withdrawals: severe water stress. Reduced irrigation water use: severe water stress. during droughts (1 in 4 years). Increased magnitude of extreme floods.	–	Increase in gully erosion.
	SM	Current water withdrawals: severe water stress.	Reduction in vegetation productivity.	Increased upslope and gully erosion in croplands.
	SS	Current water withdrawals: water resource shortfall. Reduced irrigation water use: severe water stress.	Reduction in vegetation productivity. Wheat yield variability. Low sustainability for wine production and forestry.	–

a – includes planned irrigation networks draining from the Alqueva dam.
b – extrapolated from model results for different scenarios.
c – due to the transition from semi-arid to arid vegetation patterns, as discussed by Lavee et al. (1998).

The **MM vulnerability scenario** (moderate changes to temperature and rainfall) appears to be the one with less consequences for desertification processes. Table 6.9 shows that the major vulnerability is in terms of the system's capacity to sustain water demands; both study areas are expected to suffer from severe water stress if current water abstractions for irrigation at the basin scale are maintained, but a more rational use of water could be sufficient to mitigate this problem. This is the only case where an increase in magnitude for floods is expectable,

but only for the Tejo study area and depending on the magnitude of changes to storm intensity; this could also lead to increased soil erosion, particularly by ephemeral gullies. This vulnerability scenario appears to result mostly from the more moderate increase in atmospheric CO_2 concentrations expected for the B2 emission scenario (Table 6.8).

The **MS vulnerability scenario** (moderate changes to temperature, severe changes to rainfall) appears to have more significant consequences for desertification, but still mostly in terms of water resources availability. Table 6.9 indicates that both study areas could suffer severe water stress if current irrigation practices at the basin scale are maintained, as in the previous scenario. However, even a more rational water use could lead to severe water stress during hydrological droughts, which could occur once every four years in both study areas and would be more extreme in the Tejo. This study area could also experience an increase in magnitude for the most severe floods while lowering the magnitude of the average storm runoff, which could essentially lead to the increase of ephemeral gully erosion process; this change would depend on the degree of climatic instability caused by climate change. This vulnerability scenario appears to be the most likely, resulting from the atmospheric CO_2 increases predicted by both the A2 and B2 emission scenarios (Table 6.8).

The **SM vulnerability scenario** (severe changes to temperature, moderate changes to rainfall) shows a significant increase in consequences for desertification processes over the previous scenarios, as impacts on water resource availability are coupled with impacts on vegetation productivity and soil erosion rates. As indicated in Table 6.9, the maintenance of current irrigation practices at the basin scale could lead to severe water stress in both study areas, but this problem could be mitigated by some moderation in water use. Both study areas could experience reduced wheat yields due to higher temperatures, and this phenomena could also affect the vineyards and forests of the Tejo area. Furthermore, both study areas could experience a significant increase in upslope and gully erosion processes due to lower wheat yields, with an increase of localized desertification problems driven by gully expansion; however, upslope erosion is only expected to have long-term effects on Lithosols over the Guadiana. Finally, the increased aridity in the Guadiana is expected to decrease the overall suitability for wheat and cork oak growth, increasing the areas where these vegetation types are not expected to thrive. This vulnerability scenario appears to be possible under the atmospheric CO_2 increases predicted by both the A2 and B2 emission scenarios, put more probable for the Tejo study area (Table 6.8).

The **SS vulnerability scenario** (severe changes to temperature and rainfall) shows the most significant increases in desertification processes, and both the Tejo and the Guadiana study areas could suffer significant shifts in overall aridity conditions. Table 6.9 indicates that, for this scenario, the watersheds in both study areas will be unable to supply enough water to meet current demands at the basin scale; even with a more moderate use of water, the Guadiana is expected to experience severe water stress conditions once every four years, while regular water stress conditions are expected for the Tejo. Furthermore, both study areas could experience significant shifts in vegetation patterns. A significant part of the Guadiana study area could exhibit arid conditions, including a low sustainability of rainfed agriculture and sparse vegetation cover in non-cultivated areas. In the Tejo study area, forestry and wine production could become unsustainable while wheat production could experience significant yield variability between years. This vulnerability scenario only appears to be possible under the A2 CO_2 emission scenario, particularly for the Guadiana study area (Table 6.8).

This latter scenario merits a further exploration of the consequences of a transition of the Guadiana study are towards arid climate and vegetation patterns. This transition appears to be abrupt, as described by Lavee et al. (1998); beyond a threshold level of low soil moisture and organic matter content caused by increased aridity, the stability of the soil begins to decrease, leading to low permeability and the development of surface crusts. The consequence is the initiation of a self reinforcing process, where decreased infiltration rates reduce soil moisture, and increased overland flow leads to significantly higher erosion rates and lower soil organic matter contents. This would lead not only to sparser vegetation patterns, as vegetation adjusts to collect rainfall from neighboring bare areas (as discussed previously); but could also imply a significant increase in storm flow and soil erosion rates for this region, despite the low rainfall and high temperatures. An example of these land cover types could be found in the badlands systems currently found in arid regions of SE Spain, as described by Cantón et al. (2001). Once this threshold is surpassed, it would be extremely difficult for the local ecosystems to revert to more homogenous conditions, even with extensive human intervention (Puigdefábregas, 1998).

Overall, the vulnerability assessment shown in Table 6.9 indicates an increase in desertification drivers with increase magnitude of climate change. Low magnitude changes appear to impact mostly the provisioning of water resources for use by socio-economic systems, particularly for irrigation which is currently the most important water use in both basins. It should be noted that most of these impacts are not expected to occur inside the study

areas themselves, since irrigation is mostly practiced elsewhere in the Guadiana and Tejo river basins; however, they are expected to impact the availability of water supplies for within-watershed use as this could compete with demands elsewhere in the basins, particularly if an overall condition of water resource scarcity exists. Larger magnitude changes appear to also impact the biophysical system's capacity to support current agricultural and vegetation patterns, and a significant number of expected climate change scenarios might be sufficient to move both systems further in the climatic aridity threshold. Furthermore, all the scenarios detailed above are expected to lead to a significant increase in streamflow irregularity at the seasonal and daily scales, which could pose further difficulties for water resource collection.

Finally, the results indicate that the Guadiana study area also suffers from two additional vulnerabilities not shown in Table 6.9 and which are expected to be present in all vulnerability scenarios. First, water resource provisioning in the Guadiana takes into account the Alqueva dam, built to collect runoff coming mostly from the Spanish part of the Guadiana river basin. Without these additional resources, the results point to a more significant level of vulnerability, approaching that of the Tejo study area. Consequentially, the resilience of the Guadiana's ability to support water demands of the socio-economic systems could be significantly affected by an increase in water resource abstraction in the Spanish basin, resulting e.g. from increased irrigation needs caused by climate change.

Second, the shallow Lithosols appear to be determinant for many of this system's response to changes in climate. The low soil water holding capacity can lead to a greater sensitivity of runoff and soil erosion to changes in climate, and to a low resilience of soil fertility even to small soil erosion rates. Furthermore, regions with this type of soil could present a much reduced capacity for natural vegetation to recover if croplands are abandoned, leading to a much sparser vegetation cover than could be expected due to climate changes alone. The accelerated soil erosion rates due to intensive agriculture in this region have significantly contributed to this current state of soil degradation (Roxo et al., 1996; Roxo and Cortesão Casimiro, 1998), even if they currently present very low values; therefore, soil erosion appears to be a fundamental driving force behind the vulnerability of the Guadiana study area to desertification, particularly under climate change conditions. These results also highlight the necessity of controlling soil erosion rates in the Tejo study area, even if a significant loss of agricultural productivity due to erosion is not expected during the next century.

6.3.2 Adaptation requirements

To complete the vulnerability assessment described in this section, an assessment of the system's adaptive capacity (Gallopín, 2006) should be developed. While it is possible to evaluate this capacity using subjective indexes (Smit and Wandel, 2006), the dynamic nature of socio-ecological systems and the long-term timeframe for the impacts of climate change described in this thesis make this evaluation a complex task. In alternative, this work uses the results from the vulnerability assessment described in Table 6.9 to evaluate and suggest appropriate adaptation measures from a number of possible options (taken from a survey of the current scientific literature), following the method proposed by Smit and Wandel (2006) and described in section 3.1. These will focus on the most important vulnerabilities indicated by the previous section: water resource provisioning, vegetation support and soil erosion.

Water resources

As discussed previously, an assessment of water resource availability must contemplate both the study areas and the wider Guadiana and Tejo river basins. Table 6.9 lists two different water resource vulnerabilities, one considering current water uses (which are mostly for agricultural purposes, as previously described) and another considering modifications to water use with a moderate approach to irrigation. Adaptation to the first vulnerability would require a reduction in irrigation water demand; Sadler et al. (2005) point to the effectiveness of precision irrigation to achieve this objective. In a review of this subject, the authors indicate a number of measures which can be taken for water conservation, such as optimizing the spatial and temporal distribution of water according to soil water content and vegetation productivity. Based on a number of case-studies, they estimate that these measures can lead to an average reduction of irrigation water demand of c. -8 to -20 %, going down to -50 % in single years (depending on the effectiveness of previous irrigation systems). Precision irrigation would be a measure to be adapted at the basin scale, focusing on irrigated areas. Table 6.10 shows the impact of an average reduction in irrigation of -14 % on water withdrawal ratios and water stresses; this estimate indicates that this measure might only be effective for the most moderate scenario (MM), and other scenarios must contemplate either a reduction of irrigation water use, or measures to adapt to severe water stress levels. In the most severe scenario (SS) a reduction in irrigation appears to be a requirement due to expected water resource shortfalls.

Table 6.10 – Current and estimated water withdrawal ratios for the vulnerability scenarios described in Table 6.7, for current irrigation (based on the calculations presented in section 6.2.2) and precision irrigation (Sadler et al., 2005); numbers in bold indicate severe water stress, while underline numbers indicate withdrawals above runoff rates.

	Guadiana withdrawal ratio				**Tejo withdrawal ratio**	
	Current irrigation		**Precision irrigation**			
Scenario	**Current conditions**	**With Alqueva dam**	**Current conditions**	**With Alqueva dam**	**Current irrigation**	**Precision irrigation**
Control	0.20	0.32	0.18	0.27	0.36	0.32
MM	0.25	**0.41**	0.23	0.35	**0.43**	0.38
MS	0.34	**0.54**	0.30	**0.47**	**0.63**	**0.56**
SM	0.32	**0.51**	0.28	**0.45**	**0.60**	**0.53**
SS	**0.84**	**1.35**	**0.75**	**1.17**	**2.48**	**2.20**

A reduction of irrigation can imply either a reduction in irrigated area, or a change in crops for less water-demanding varieties; in the Tejo river basin, this could entail e.g. the substitution of rice cultivation for less water-demanding crops. This would also be a measure to be adopted at the larger river basin scale. Table 6.9 shows the vulnerability of water resource provisioning under this assumption (labeled "changed water uses"); an adoption of this measure could lead to a significant decrease in water stress, in most cases only during drought years (c. 1 in every 4) for the severe rainfall change vulnerability scenarios (MS and SS). The downside of this option would be a significant decrease in irrigation-dependent agricultural productivity.

The main impacts of severe water stress include an increase in water competition by different users and a decrease in water quality; the existence of infrastructure for e.g. water recycling and wastewater treatment can allow for a more intensive water use without scarcity (Alcamo et al., 2003). Ragab and Prudhomme (2002) review a number of solutions which can be used when adapting to severe water stress:

- conventional solutions, designed to collect the maximum possible runoff and transfer water from non-stressed to stressed river basins, which usually involve a significant investment in financial resources and could lead to a number of severe environmental problems;

- search for new water sources, such as desalination of seawater or rainfall generation with precipitation enhancement technologies, both of which are currently costly options with intensive energy demands;

- reduce water demand by increasing efficiency in water use.

Considering the current importance of agricultural water use, a number of practical adaptation measures can be considered for application at the basin scale. One adaptation measure which could be explored for the Tejo basin refers to the use of salt-tolerant crops in some areas, which could be irrigated with a mixture of fresh water and seawater which is readily available in the nearby Tejo estuary, with potential negative consequences for soil quality in the long-term (Ragab and Prudhomme, 2002). Another example for this basin could be the use of recycled wastewater from the Lisbon municipality in irrigation (as reviewed by e.g. Kennedy and Tsuchihashi, 2005, and da Fonseca et al., 2007), although it is unlikely that this would have a large impact given the low importance of industrial and domestic consumption in the overall water budget (20 %). These and other practical options have received a significant attention in the recent years. For example, a number of tools have been developed and explored to increase water use efficiency using e.g. economic-based approaches or non-cooperative negotiation methods (see the reviews by e.g. Carraro et al., 2007, and Ward, 2007); these measures can be adopted both at the basin scale and inside the Guadiana and Tejo study areas.

Another vulnerability indicated by Table 6.9 in an increase in the frequency of hydrological drought, which for severe changes in rainfall (MS and SS vulnerability scenarios) is expected to increase from the current values (1 year out 10) to 1 year out of 4 (although for the SS scenario in the Tejo, these conditions are expected to be a regular feature). This problem could be enhanced due to the increased daily and seasonal variability of streamflow expected for all scenarios. The variability in the recharge of water resources has important implications for water management, since it introduces a level of risk in water resource planning which requires the adoption of expensive storage reservoir systems and the use of contingency plans to mitigate the consequences (Ragab and Prudhomme, 2002). In the Guadiana river basin, the existing reservoir system appears to be sufficient to provide storage capacity for drought periods, mainly due to the capacity of the Alqueva dam. In the Tejo basin, however, existing storage capacity is designed for humid conditions and might require a significant increase in order to adapt to the increased drought conditions caused by climate change.

Finally, and regardless of the actual strategies used to adapt to the impacts of climate change on water resources, there is also a need to implement selected adaptation measures using effective planning tools. In particular, water resource planning must be able to take into account the impacts of climate change on normal climate conditions (Ragab and Prudhomme, 2002). Watershed plans for the Guadiana and Tejo river basins are already being implemented (INAG, 1999a and b), which can be considered a significant improvement in the adaptive capacity of these areas to changes in water resource availability; future plans should consider the likely impacts of climate change on hydrological processes at the basin scale, and take into account recent planning developments (e.g. Hedelin, 2007; Woltjer and Al, 2007) which could further improve the adaptability of these basins.

Vegetation cover

Table 6.9 lists a number of vegetation cover vulnerabilities, related with the negative effects of higher temperatures on biomass productivity, and with climate aridity surpassing thresholds for different agricultural and natural vegetation types. The first vulnerability could occur mainly in severe temperature change scenarios (MS and SS). Agricultural adaptation could be achieved through the use of agricultural management options, such as adapting crops to the new climate regime, or changing the scheduling of cultivation practices such as sowing, irrigation, fertilization and harvesting, so they are better suited to changed climatic conditions (e.g. Maracchi et al., 2005; Kalra et al., 2007). For example, Pinto and Brandão (2002) suggest that, in the Guadiana study area, an anticipation of the wheat planting date could offset decreases in productivity caused by higher temperatures. Maracchi et al. (2005) also suggest that earlier planting dates could reduce irrigation requirements in southern Europe.

The second vulnerability could occur mainly in the severe climate changes scenario (SS) and, as described in the resilience assessment, may lead to agriculture and natural ecosystem change through the action of transition trigger events (as previously described). One possible adaptation measure could be a reduction of the impact of these events. In agricultural lands, the increase in water scarcity described for this scenario (Table 6.9) could make an extension of irrigated farmland difficult; as an alternative, Sadler et al. (2005) suggests the selective irrigation of rainfed agriculture during drought periods, although this option would compete with existing irrigation water demands and could be difficult to implement in a context of water scarcity adaptations. Drought risks in commercial forests could be reduced with shorter rotations, regular thinnings and wider spacings (Maracchi et al., 2005), although it must be noted that the cork oak forests in the Guadiana are already managed in this way. Another

adaptation measure would be to reduce the pressure over agricultural lands by promoting extensive agriculture, coupled with an increased recognition and rewarding of the environmental and social functions of agricultural systems (Olesen and Bindi, 2002; Berry et al., 2006). In this case, Nair (2007) suggests that some attention should be paid to modern agroforestry practices due to the added benefits of soil improvement, greater biodiversity, carbon storage and control of diffuse pollution. Puigdefábregas (1998) also suggests an extensive approach to grazing by an adaptation of traditional practices such as nomadism and transhumance to current economic conditions.

These measures would be more difficult to adopt for natural ecosystems due to the lack of intensive management. In this case, Puigdefábregas (1998) recommends preventive measures that allow for the reduction of human pressures in the most vulnerable systems. Furthermore, as described above, the degraded Lithosols of the Guadiana study area are particularly vulnerable to a decrease in vegetation cover due to arid conditions, and rehabilitation or restoration options could be implemented in the most degraded areas (Puigdefábregas, 1998).

The implementation of adaptation measures in all scenarios would require policy support; Olesen and Bindi (2002) suggest an encouragement of the flexibility of land use, crop production and farming systems as a way to improve adaptation capacity. An adaptation strategy for the Guadiana and Tejo study areas would also be linked with the European Union's Common Agricultural Policy, and therefore these issues would have to be discussed at the European level. Finally, it should be noted that possible reductions in overall agricultural yield and increased yield variability in the severe temperature scenarios (SM and SS) is not expected to affect food security, as societies with credit, access to global markets and storage and shipping infrastructures can usually accommodate these changes (e.g. Milesia et al., 2005). However, the compensation of food production shortfalls might require an adaptation to a more irregular food market caused by e.g. higher demand variability from other dryland regions negatively affected by climate change, global population growth and competition with biofuel production, as exemplified in the work of e.g. Yang and Zehnder (2002) or Jolly (2006).

Soil erosion

The vulnerabilities to soil erosion listed in Table 6.9 can be divided into upslope and gully erosion enhancement. The first vulnerability could occur mostly for the scenario considering severe temperature changes associated with moderate rainfall changes (SM), particularly over croplands due to a reduction in wheat cover; in the Tejo study area, this problem could also

occur due to an increase in storm intensity in the more moderate scenario (MM). There are a number of existing conservation agriculture practices, such as no tillage and conservation tillage, permanent soil cover and grazing management (Toy et al., 2002); Zhang and Nearing (2005) have suggested that the adoption of these practices could be sufficient to reduce this impact in croplands. Therefore, a possible adaptation measure could be a generalization of conservation agriculture throughout the study area. Furthermore, the adaptation practices to increase wheat yield suggested above would also have a positive effect in this situation. In more vulnerable locations, the adoption of agroforestry practices or the abandonment of croplands could be effective if done before resilience thresholds are surpassed and an increase of vegetation cover can be achieved (Puigdefábregas, 1998; Nair, 2007).

The second vulnerability could occur for the same scenarios, plus the moderate temperature and severe rainfall change (MS) in the Tejo study area. Terracing is a traditional practice used in both study areas which has shown a capacity for combating gully erosion processes in the long-term, if properly maintained (Avni, 2005). A potential adaptation measure could be the repair and maintenance of existing terraces, coupled with the adoption of other techniques such as plugging existing gullies and provide protected paths to channelize surface runoff (Toy et al., 2002). The collection of sediment in retention basins and re-distribution over ephemeral gullies could be used where other adaptation options are unfeasible (Martínez-Casanovas et al., 2005). A special attention should be given to abandoned farmlands, as gully expansion could intensify after abandonment (Oostwoud Wijdenes et al., 1999); post-abandoned monitoring and occasional intervention could mitigate this problem.

Finally, a third vulnerability is shown in Table 6.9 for the Guadiana study area in the most severe vulnerability scenario (SS), with an increase in upslope and gully erosion rates in regions where shrub cover becomes sparser. Adaptation to these processes appears to be more complex, as they could represent part of the natural adaptation process of ecosystems to arid climates leading to a redistribution of soil resources under vegetated patches (Lavee et al., 1998; Cantón et al., 2001; Martínez-Fernández and Esteve, 2005). Martínez-Fernández and Esteve (2005) point in particular to the unsuitability of reforestation attempts in these cases, leading to higher soil erosion rates in the long-term due to the low arboreal growth.

An effective way of implementing the adaptation measures described above could be the adoption of large-scale spatial planning in drylands. Puigdefábregas (1998) suggests the early prevention of land degradation through soft management techniques such as a restriction of agriculture to areas capable of sustaining it, coupled with policies to increase local economic

complexity in order to alleviate human pressure on natural resources. This issue can be a significant concert in the Guadiana study area and the overall river basin, since the implementation of irrigation networks connected to the Alqueva dam are presently under study, opening a window of opportunity for taking climate change and desertification processes into account.

6.4 Methodological limitations

Assessing vulnerability to climate change is dependent on both the assumptions of the climate change scenarios used and the validity of the methods used to estimate their impacts (for a discussion of this issue for hydrological assessment see Beven, 2000). This work aimed to analyze a number of climate change scenarios for two study areas, Guadiana and Tejo, combining different magnitudes of change of three main climatic variables: temperature, rainfall and atmospheric CO_2 concentrations. The methodology used in this analysis, described in section 3, combined two models working at different scales for impact assessment on hydrology, erosion and vegetation productivity; the significance of these impacts was estimated using indicative thresholds as described in this section. However, the uncertainties associated with this methodology impose a number of constraints on the conclusions that can be made from these results.

First, there are a significant number of uncertainties in the estimation of **exposure to climate change**. Part of these uncertainties lie in the number of different climate change scenarios for similar levels of CO_2 emissions, as shown in Figure 6.1; this appears to be an intrinsic problem for climate change prediction, due to the large number of variables and processes involved (Giorgi, 2005). Furthermore, GCMs still present some significant uncertainties due the misrepresentation of potentially important processes. For example, current climate modeling capability is not sufficient to analyze future abrupt climate changes which could greatly amplify the impacts of long-term climate change (Overpeck and Cole, 2006). Furthermore, current GCMs fail to properly represent feedbacks between climate and surface hydrology (Huntingford et al., 2006) or vegetation processes (Lashof and DeAngelo, 1997; Field et al., 2007). Field et al. (2007) refer that the feedbacks between terrestrial ecosystems and climate change are likely to be negative for low magnitude changes in climate, and positive for higher magnitude changes; for the Iberian Peninsula, Arribas et al (2003) estimate that positive feedbacks between climate aridity and vegetation productivity decreases could reinforce arid conditions. Kleidon (2006) also points to specific feedbacks between agricultural systems and climate change, leading to less favorable conditions for vegetation

growth where agroforestry is present. These results suggest that the this work could be overestimating the impacts of the most moderate climate change scenarios (MM in Figure 6.9) while underestimating them for the most severe scenarios (SS in Figure 6.9).

Furthermore, the method used to represent climate change in this work also suffers from a number of limitations. The sensitivity analysis represented increasing magnitudes of changes to temperature, rainfall and CO_2 concentration (Figure 6.1); however, these parameters are not clearly related. For example, Figure 6.9 shows that the MS vulnerability scenario contains GCM and RCM results with CO_2 increases ranging from 50 to 100 %, while the sensitivity analysis for this case estimated CO_2 increases between 25 and 50 %. One consequence can be observed in a comparison of the biomass predictions for wheat in the MS scenario: -5 to -10 % in the sensitivity analysis compared with +5 to +15 % in the PROMES RCM results, which considered significantly higher CO_2 concentrations (see section 5.3 for a further discussion of these differences). These results indicate that the positive impacts of CO_2 concentrations for vegetation growth could be under-represented in the MS scenario (Figure 6.9), where several changes in CO_2 atmospheric concentrations lead to these magnitudes of climate change.

Moreover, climate change is expected to affect the inter-annual, seasonal and daily variability of temperature and rainfall in Mediterranean regions (e.g. Trigo and Palutikof, 2001; Giorgi, 2006; Good et al., 2006; see also section 2.2). However, climate change representation in the sensitivity scenario assessment focused only on long-term average changes to climate, due to the complex data analysis processes required to properly represent inter-annual, seasonal and extreme event changes in the stochastic weather generator used by the SWAT model (Yu, 2005). A detailed assessment of the impacts of variability increase was only performed for the MS vulnerability scenario using the PROMES RCM results; for other vulnerability scenarios, the impacts of these changes were not taken into account in detail, which could have led to e.g. an overestimation of changes to water distribution between evapotranspiration and runoff during the wet season.

The second main source of uncertainty is the **methodology** itself. The validity of the model framework calibration for scenarios of climate change is difficult to assess. For the SWAT model, an effort has been made to address this issue by calibrating and validating it for different watersheds and time periods with significantly different rainfall and temperature combinations, thus providing a calibrated parameter set which is valid under a large range of climatic conditions. However, the time period of available measurements did not include the full range of rainfall and temperature values simulated in the climate change scenarios, and

therefore the validity of the calibration for climate change cannot be fully assessed. Also, the effects of CO_2 concentration changes on vegetation cannot be assessed due to the lack of observed data. The MEFIDIS model was evaluated using a range of storm data with different initial moisture conditions, intensity and duration, but none had a return period over 5 years, excluding from this analysis the most extreme events. These facts indicate that the evaluation assessment could overestimate the performance of the SWAT and MEFIDIS erosion models for future climates, particularly for those representing more severe changes (MS, SM and SS; Beven, 2000).

A further problem in model calibration and validation is that the available data on spatial erosion patterns was insufficient to adequately assess the results of both models for upslope and gully erosion. In particular, ephemeral gully simulation using the MEFIDIS model was assessed in a way which only allowed examining if the results coincided with current knowledge of gully distributions in Mediterranean watersheds. In these conditions, all erosion predictions should be taken as indicative only (Favis-Mortlock et al., 2001). Furthermore, the estimate of the long-term consequences of soil erosion for fertility should be taken as indicative, as it fails to account for interactions and feedbacks between soil erosion and vegetation growth processes, which are still not well understood (Boardman, 2006).

The model framework also fails to take into account several disturbances in biophysical systems. One important uncertainty for the SWAT model is that it does not take into account the impacts of drought-induced mortality in Mediterranean woody plants, which could increase due to higher temperatures even with small changes in drought frequency (Martínez-Vilalta et al., 2002). This uncertainty would impact the long-term predictions for vegetation productivity of cork oaks, vineyards and forests, particularly for scenarios estimating severe temperature changes (SM and SS). Another factor which was not taken into account was a possible increase in wildfire frequency due to a more arid climate, which could impact the suitability of the Tejo study area for forestry and could have significant consequences for storm runoff, soil erosion and land degradation rates in forested areas (see Shakesby and Doerr, 2006, and Meyn et al., 2007, for recent reviews on this subject). This uncertainly also impacts the ability of this methodology to estimate changes to desertification trigger events and their impacts in the transition of the study areas towards more advanced states of desertification (Puigdefábregas, 1998; Olesen and Bindi, 2002).

Finally, the methodology relied on indicative estimates to evaluate existing thresholds of desertification. Thresholds were estimated using process-pattern and space-for-time

approaches, which rely on current observations in regions with more arid climates and fail to take into account changes that are currently not observable, such as the impacts of CO_2 concentrations on vegetation productivity. Not taking into account this and other changes in the processes underlying these thresholds can significantly add to the uncertainty in their estimation (Helmuth et al., 2005). This uncertainty is particularly severe for the SS scenario, where several thresholds for vegetation support could be surpassed.

The third main source of uncertainty is the fact that this methodology does not take into account the **feedbacks between socio-economic and natural systems**, which makes the results valid only if the current socio-economic situation is maintained in the next hundred years, a highly unlikely scenario (e.g. Huntingford et al., 2006; Simonovic and Davies, 2006). This issue is particularly important when studying desertification processes, since desertification is understood as the degradation of both biophysical and socio-economic conditions, where socio-economic driving forces play an important role (e.g. Puigdefábregas, 1998, or Herrmann and Hutchinson, 2005; see section 2.1 for a further discussion). There are several examples of possible interactions in the scientific literature, which could lead to the enhancement of desertification processes, such as:

- soil erosion and land degradation processes are particularly sensitive to land use changes, which are usually driven by socio-economic conditions and could have a significantly greater impact than climate change (Boardman, 2006);

- agricultural yield variability can have a significant negative impact on socio-economic stability, even when a long-term yield growth trend is present, leading to land abandonment (Milesia et al., 2005);

- an increase in the depopulation of rural areas, due to lower agricultural yields, can lead to a more homogenous landscape in which wildfire risks would increase (Puigdefábregas, 1998);

- changes in agricultural management practices as an adaptation to climate change could in some cases lead to a significant increase in soil erosion rates (O'Neal et al., 2005).

In this study, one important interaction is the role of human populations on land degradation in the Guadiana study area through intensive agricultural practices, resulting in a decrease in soil fertility and in land abandonment, with consequences for hydrological processes, soil

erosion and revegetation (Roxo et al., 1996). This uncertainty affects all vulnerability scenarios analyzed in this work.

Overall, it can be stated that the work presented in this thesis has a significant number of limitations and uncertainties which should be taken into account when assessing the results. A significant number of them can be attributed to lack of scientific process knowledge, and can be overcome by further research on the subject of climate change and desertification. Others are methodological limitations, mostly occurring due to the lack of data for the study areas and to the complexity of the subject matter, which is difficult to fully embrace during a single doctoral period. These can be overcome in future studies of climate change and desertification, where the experience presented in this work may allow for a better methodological design and implementation. Finally, and despite these limitations, the results presented in this work still provide a reliable assessment of vulnerability in qualitative terms, and the assessment for hydrological processes and water resources appears to also be reliable in quantitative terms.

6.5 References

Adger WN, 2006. Vulnerability. Global Environmental Change 16: 268–281.

Alcamo J, Doll P, Henrichs T, Kaspar F, Lehner B, Rosch T, Siebert S, 2003. Global estimates of water withdrawals and availability under current and future "business-as-usual" conditions. Hydrological Sciences Journal – Journal Des Sciences Hydrologiques 48 (3): 339-348.

Arnell N. 2004. Climate change and global water resources: SRES emissions and socio-economic scenarios. Global Environmental Change 14: 31–52.

Arora VK, 2002. The use of the aridity index to assess climate change effect on annual runoff. J. Hydrol. 265 (1-4): 164-177.

Arribas A, Gallardo C, Gaertner MA, Castro M, 2003. Sensitivity of the Iberian Peninsula climate to a land degradation. Climate Dynamics 20: 477–489.

Avni Y, 2005. Gully incision as a key factor in desertification in an arid environment, the Negev highlands, Israel. Catena 63: 185–220.

Bakker MM, Govers G, Rounsevell MDA, 2004. The crop productivity–erosion relationship: an analysis based on experimental work. Catena 57: 55–76.

Bakker MM, Govers G, Kosmas C, Vanacker V, van Oost K, Rounsevell M, 2005. Soil erosion as a driver of land-use change. Agriculture, Ecosystems and Environment 105: 467-481.

Barboni D, Harrison SP, Bartlein PJ, Jalut G, New M, Prentice IC, Sanchez-Goñi M-F, Spessa A, Davis B, Stevenson AC, 2004. Relationships between plant traits and climate in the Mediterranean region: a pollen data analysis. Journal of Vegetation Science 15: 635-646.

Batjes NH, 2002. Soil parameter estimates for the soil types of the world for use in global and regional modelling (version 2.1; July 2002). ISRIC report 2002/02c, International Food Policy Research Institute (IFPRI) and International Soil Reference and Information Centre (ISRIC), Wageningen.

Berry PM, Rounsevell MDA, Harrison PA, Audsley E, 2006. Assessing the vulnerability of agricultural land use and species to climate change and the role of policy in facilitating adaptation. Environmental Science and Policy 9: 189-204.

Beven K, 2000. Rainfall-Runoff Modelling – The Primer. John Wiley & Sons, Chichester.

Boardman J, 2006. Soil erosion science: reflections on the limitations of current approaches. Catena 68: 73-86.

Boer MM, Puigdefábregas J, 2003. Predicting potential vegetation index values as a reference for the assessment and monitoring of dryland condition. International Journal of Remote Sensing, 24 (5): 1135-1141.

Boer MM, Puigdefábregas J, 2005. Assessment of dryland condition using spatial anomalies of vegetation index values. International Journal of Remote Sensing 26 (18): 4045-4065.

Cantón Y, Domingo F, Solé-Benet A, Puigdefábregas J, 2001. Hydrological and erosion response of a badlands system in semiarid SE Spain. J. Hydrol. 252: 65-84.

Cardoso JVJC, 1965. Os solos de Portugal, sua classificação, caracterização e génese: 1- a sul do rio Tejo (Portuguese soils, their classification, characterization and genesis: 1- south from the Tagus river). General-Directorate for Agricultural Services, Lisbon.

Carraro C, Marchiori C, Sgobbi A, 2007. Negotiating on water: insights from non-cooperative bargaining theory. Environment and Development Economics 12: 329-349.

Casimiro PC, 2003. Análise quantitativa da paisagem, evolução temporal de padrões espaciais – concelho de Mértola (Quantitative landscape analysis, temporal evolution of spatial patterns – Mértola municipality). Revista GeoInova – Revista do Departamento de Geografia e Planeamento Regional da FCSH – UNL 6: 59-84.

Cheddadi R, Guiot J, Jolly D, 2001. The Mediterranean vegetation: what if the atmospheric CO_2 increased? Landscape Ecol. 16: 667-675.

Clark SC, 1996. Mediterranean ecology and an ecological synthesis of the field sites. In: Brandt CJ, Thornes JB (Eds.), Mediterranean desertification and land use. John Wiley and sons, Chichester: 271-302.

Cunha LV, Oliveira R, Nunes V, 2002. Water Resources. In: Santos FD, Forbes K, Moita R (Eds.), Climate change in Portugal: scenarios, impacts and adaptation measures. Gradiva – Publicações, Lisbon: 23-83.

da Fonseca AF, Herpin U, de Paula AM, Victoria RL, Melfi AJ, 2007. Agricultural use of treated sewage effluents: Agronomic and environmental implications and perspectives for Brazil. Scientia Agricola 64 (2): 194-209.

FAO: Food and Agriculture Organization, 1989. Arid zone forestry: A guide for field technicians. Forestry Department, United Nations Food and Agriculture Organization, Rome.

FAO: Food and Agriculture Organization, 2001. Global ecological zoning for the global forest resources assessment 2000: final report. Forestry Department, United Nations Food and Agriculture Organization, Rome.

Favis-Mortlock D, Boardman J, MacMillan V, 2001. The limits of erosion modeling: why we should proceed with care. In: Harmon RS, Doe WW (Eds.), Landscape Erosion and Evolution Modeling. Kluwer Academic/Plenum Publishers, New York: 477-516.

Field CB, Lobell DB, Peters HA, Chiariello NR, 2007. Feedbacks of terrestrial ecosystems to climate change. Annual Review of Environment and Resources 32: 7.1-7.29.

Fleischer A, Sternberg M, 2006. The economic impact of global climate change on Mediterranean rangeland ecosystems: A Space-for-Time approach. Ecological Economics 59 (3): 287-295.

Gallardo C, Arribas A, Prego JA, Gaertner MA, de Castro M, 2001. Multi-year simulations using a regional-climate model over the Iberian Peninsula: current climate and doubled CO2 scenario. Quarterly Journal of the Royal Meteorological Society 127: 2740-2756.

Gallopín GC, 2006. Linkages between vulnerability, resilience, and adaptive capacity. Global Environmental Change 16: 293–303.

Gessler PE, Chadwick OA, Chamran F, Althouse L, Holmes K, 2000. Modeling soil-landscape and ecosystem properties using terrain attributes. Soil Sci. Soc. Am. J. 64: 2046-2056.

Giorgi F, 2005. Climate change prediction. Climatic Change 73 (3): 239-265.

Giorgi F, 2006. Climate change hot-spots. Geophys. Res. Lett. 33: L08707.

Good P, Barring L, Giannakopoulos C, Holt T, Palutikof J, 2006. Non-linear regional relationships between climate extremes and annual mean temperatures in model projections for 1961-2099 over Europe. Climate Research 31 (1): 19-34.

GPAa: Grupo de Projecto Alqueva Agrícola, 2005. Plano de intervenção para a zona de Alqueva, tomo 3: identificação das potencialidades do regadio de Alqueva (Alqueva region intervention plan, tome 3: identification of the irrigation potentials of Alqueva; revised edition). Ministry for Agriculture, Rural Development and Fisheries, Lisbon

Hedelin B, 2007. Criteria for the assessment of sustainable water management. Environmental Management 39 (2): 151-163.

Helmuth B, Kingsolver JG, Carrington E, 2005. Biophysics, physiological ecology, and climate change: does mechanism matter? Annual Review of Physiology 67: 177-201.

Herrmann SM, Hutchinson CF, 2005. The changing contexts of the desertification debate. J. Arid Environments 63: 538–555.

Huntingford C, Gash J, Giacomello AM, 2006. Climate change and hydrology: next steps for climate models. Hydrol. Process. 20: 2085–2087.

Imeson AC, Lavee H, 1998. Soil erosion and climate change: the transect approach and the influence of scale. Geomorphology 23: 219–227.

INAG: Instituto da Água, 1999a. Plano de bacia hidrográfica do rio Guadiana, 1ª fase: análise e diagnóstico da situação de referência. Volume III: análise (Guadiana river watershed plan, 1st phase: reference situation analysis and diagnostic. Volume III: analysis). Water Insitute (INAG), Lisbon.

INAG: Instituto da Água, 1999b. Plano de bacia hidrográfica do rio Tejo, 1ª fase: análise e diagnóstico da situação de referência. Volume III: análise (Tejo river watershed plan, 1st phase: reference situation analysis and diagnostic. Volume III: analysis). Water Insitute (INAG), Lisbon.

Jetten V, de Roo A, Favis-Mortlock D, 1999. Evaluation of field-scale and catchment-scale soil erosion models. Catena 37 (4): 521-541.

Jolly L, 2006. Will ethanol destabilise the world sugar market? International Sugar Journal 108 (1295): 606.

Kalra N, Chander S, Pathak H, Aggarwal PK, Gupta NC, Sehgal M, Chakraborty D, 2007. Impacts of climate change on agriculture. Outlook on Agriculture 36 (2): 109-118.

Kennedy LA, Tsuchihashi R, 2005. Is water reuse sustainable? Factors affecting its sustainability. Arabian Journal for Science and Engineering 30 (2C): 3-15.

Kirkby M, Bracken L, Reaney S, 2002. The influence of land use, soils and topography on the delivery of hillslope runoff to channels in SE Spain. Earth Surf. Process. Landforms 27: 1459–1473.

Kleidon A, 2006. The climate sensitivity to human appropriation of vegetation productivity and its thermodynamic characterization. Global and Planetary Change 54 (1-2): 109-127.

Kosmas C, Kirkby M, Geeson N (Eds.), 1999. Manual on key indicators of desertification and mapping environmentally sensitive areas to desertification. MEDALUS project report EUR 18882, European Comission, Brussels.

Kundzewicz ZW, Mata LJ, Arnell NW, Döll P, Kabat P, Jiménez B, Miller KA, Oki T, Sen Z, Shiklomanov IA, 2007. Freshwater resources and their management. In: Parry ML, Canziani OF, Palutikof JP, van der Linden PJ, Hanson CE (Eds.), Climate Change 2007: Impacts, Adaptation and Vulnerability. Contribution of Working Group II to the Fourth Assessment Report of the Intergovernmental Panel on Climate Change. Cambridge University Press, Cambridge: 173-210.

Lashof DA, DeAngelo BJ, 1997. Terrestrial ecosystem feedbacks to global climate change. Annual Review of Energy and the Environment 22: 75-118.

Lavee H, Imeson AC, Sarah P, 1998. The impact of climate change on geomorphology and desertification along a Mediterranean-arid transect. Land Degradation & Development 9 (5): 407-422.

Li Y, Lindstrom MJ, 2001. Evaluating soil quality–soil redistribution relationship on terraces and steep hillslope. Soil Sci. Soc. Am. J. 65: 1500-1508.

López-Moreno JI, Beguería S, García-Ruiz JM, 2006. Trends in high flows in the Central Spanish Pyrenees: response to climatic factors or to land-use change? Hydrological Sciences Journal 51 (6): 1039-1050..

Maracchi G, Sirotenko O, Bindi M, 2005. Impacts of Present and Future Climate Variability on Agriculture and Forestry in the Temperate Regions: Europe. Climatic Change 70 (1-2): 117-135.

Martínez-Casasnovas JA, Concepción Ramos M, Ribes-Dasi M, 2005. On-site effects of concentrated flow erosion in vineyard fields: some economic implications. Catena 60: 129-146.

Martínez-Fernández JM, Esteve MA, 2005. A critical view of the desertification debate in southeastern Spain. Land Degrad. Develop. 16: 529-539.

Martínez-Vilalta J, Piñol J, Beven K, 2002. A hydraulic model to predict drought-induced mortality in woody plants: an application to climate change in the Mediterranean. Ecol. Model. 155 (2-3): 127-147.

Metzger MJ, Leemans R, Schröter D. 2005. A multidisciplinary multi-scale framework for assessing vulnerabilities to global change. International Journal of Applied Earth Observation and Geoinformation 7: 253–267.

Meyn A, White PS, Buhk C, Jentsch A, 2007. Environmental drivers of large, infrequent wildfires: the emerging conceptual model. Progress in Physical Geography 31 (3): 287-312.

Michael A, Schmidt J, Enke W, Deutschländer Th, Malitz G, 2005. Impact of expected increase in precipitation intensities on soil loss – results of comparative model simulations. Catena 61: 155-164.

Milesia C, Hashimoto H, Running SW, Nemani RR, 2005. Climate variability, vegetation productivity and people at risk. Global and Planetary Change 47: 221–231.

Morales P, Hickler T, Rowell DP, Smith B, T Sykes M, 2007. Changes in European ecosystem productivity and carbon balance driven by regional climate model output. Global Change Biology 13 (1): 108-122.

Nair PKR, 2007. The coming of age of agroforestry. Journal of the Science of Food and Agriculture 87 (9): 1613-1619.

Nearing MA, Jetten V, Baffaut C, Cerdan O, Couturier A, Hernandez M, Le Bissonnais Y, Nichols MH, Nunes JP, Renschler CS, Souchère V, van Oost K, 2005. Modeling response of soil erosion and runoff to changes in precipitation and cover. CATENA 61 (2-3): 131-154.

O'Neal MR, Nearing MA, Vining RC, Southworth J, Pfeifer RA, 2005. Climate change impacts on soil erosion in Midwest United States with changes in crop management. Catena 61 (2-3): 165-184.

Olesen JE, Bindi M, 2002. Consequences of climate change for European agricultural productivity, land use and policy. European Journal of Agronomy 16: 239–262.

Oostwoud Wijdenes DJ, Poesen J, Vandekerckhove L, Nachtergaele J, De Baerdemaeker J, 1999. Gully-head morphology and implications for gully development on abandoned fields in a semi-arid environment, Sierra de Gata, southeast Spain. Earth Surf. Process. Landforms 24: 585-603.

Overpeck JT, Cole JE, 2006. Abrupt Change in Earth's Climate System. Annual Review of Environment and Resources 31: 1-31.

Pachepsky YaA, Timlin DJ, Rawls WJ, 2001. Soil water retention as related to topographic variables. Soil Sci. Soc. Am. J. 65: 1787-1795.

Pereira JS, Chaves MM, Caldeira MC, Correia AV, 2006. Water availability and productivity. In: Morison JIL, Morecroft MD (Eds.), Plant growth and climate change. Blackwells, London: 118-145.

Pinto PA, Brandão AP, 2002. Agriculture. In: Santos FD, Forbes K, Moita R (Eds.), Climate change in Portugal: scenarios, impacts and adaptation measures – project SIAM. Gradiva – Publicações, Lisbon: 133-171.

PRUDENCE: Prediction of Regional scenarios and Uncertainties for Defining EuropeaN Climate change risks and Effects, 2007. PRUDENCE data archive. Available online in prudence.dmi.dk (accessed in January 2007). The PRUDENCE project (EU contract EVK2-CT2001-00132).

Pruski FF, Nearing MA, 2002. Climate-induced changes in erosion during the 21st century for eight US locations. Water Resources Research 38 (12): Art. No. 1298.

Puigdefábregas J, 1998. Ecological impacts of global change on drylands and their implications for desertification. Land Degrad. Develop. 9: 393-406.

Puigdefábregas J, Mendizabal T, 1998. Perspectives on desertification: western Mediterranean. J. Arid Environments 39: 209-224.

Ragab R, Prudhomme C, 2002. Climate change and water resources management in arid and semi-arid regions: prospective and challenges for the 21st century. Biosystems Engineering 81 (1): 3-34.

Räisänen J, Hansson U, Ullerstig A, Döscher R, Graham LP, Jones C, Meier HEM, Samuelsson P, Willén U, 2004. European climate in the late twenty-first century: regional simulations with two driving global models and two forcing scenarios. Climate Dynamics 22: 13–31.

Romero-Díaz A, Cammeraat LH, Vacca A, Kosmas C. 1999. Soil erosion at three experimental sites in the Mediterranean. Earth Surf. Process. Landforms 24: 1243-1256.

Roxo MJ, Cortesão Casimiro P, Soeiro de Brito R, 1996. Inner lower Alentejo field site: cereal cropping, soil degradation and desertification. In: Brandt CJ, Thornes JB (Eds.), Mediterranean desertification and land use. John Wiley and sons, Chichester: 111-135.

Roxo MJ, Cortesão Casimiro P, 1998. Human impact on land degradation in the inner Alentejo, Mértola, Portugal. In: Mairota P, Thornes JB, Geeson N (Eds.), Atlas of Mediterranean environments in Europe. John Wiley and Sons, Chichester: 106-109.

Sadler EJ, Evans RG, Stone KC, Camp CR, 2005. Opportunities for conservation with precision irrigation. Journal of Soil and Water Conservation 60 (6): 371-379.

Seixas J, 2000. Assessing heterogeneity from remote sensing images: the case of desertification in southern Portugal. Int. J. Remote Sensing 21 (13-14): 2465-2663.

Shakesby RA, Doerr SH, 2006. Wildfire as a hydrological and geomorphological agent. Earth-Science Reviews 74: 269-307.

Silva JRM, Ferreira AG, Tomás PMPP, 1998. Rainfall Characteristics and Soil Erosion in Alentejo. Geoökodynamik XIX: 249-255.

Simonovic SP, Davies EGR. 2006. Are we modelling impacts of climatic change properly? Hydrol. Process. 20: 431-433.

Smit B, Wandel J, 2006. Adaptation, adaptive capacity and vulnerability. Global Environmental Change 16: 282–292.

Thornes JB, 1998. Mediterranean desertification. In: Mairota P, Thornes JB, Geeson N (Eds.), Atlas of Mediterranean environments in Europe. John Wiley and Sons, Chichester: 2-5.

Toy TJ, Foster GR, Renard KG, 2002. Soil erosion: processes, prediction, measurement, and control. John Wiley and Sons, New York.

Trigo RM, Palutikof JP, 2001. Precipitation scenarios over Iberia: A comparison between direct GCM output and different downscaling techniques. Journal of Climate 14 (23): 4422-4446.

UNEP: United Nations Environment Program, 1997. World Atlas of Desertification, 2nd ed. Middleton N, Thomas D (Eds.), UNEP, London.

Vandaele K, Poesen J, Marques de Silva JR, Govers G, Desmet P, 1997. Assessment of factors controlling ephemeral gully erosion in Southern Portugal and Central Belgium using aerial photographs. Zeitschrift fur Geomorphologie 41 (3): 273-287.

Vicente-Serrano SM, Lasanta T, Romo A, 2004. Analysis of spatial and temporal evolution of vegetation cover in the Spanish central Pyrenees: Role of human management. Environmental Management 34 (6): 802-818.

Vicente-Serrano SM, Cuadrat-Prats JM, Romo A, 2006. Aridity influence on vegetation patterns in the middle Ebro Valley (Spain): evaluation by means of AVHRR images and climate interpolation techniques. Journal of Arid Environments 66: 353-375.

von Hardenberg J, Meron E, Shachak M, Zarmi Y, 2001. Diversity of Vegetation Patterns and Desertification. Physical Review Letters 87 (19): art. no. 198101.

Ward FA, 2007. Decision support for water policy: a review of economic concepts and tools. Water Policy 9 (1): 1-31.

Wetherald RT, Manabe S, 2002. Simulation of hydrologic changes associated with global warming. J. Geophys. Res. 107 (D19): 4379-4393.

Woltjer J, Al N, 2007. Integrating water management and spatial planning - Strategies based on the dutch experience. Journal of the American Planning Association 73 (2): 211-222.

Yang H, Zehnder AJB, 2002. Water scarcity and food import: a case study for southern Mediterranean countries. World Development 30 (8): 1413-1430.

Yu B, 2005. Adjustment of CLIGEN parameters to generate precipitation change scenarios in southeastern Australia. Catena 61: 196-209

Zhang XC, Nearing MA, 2005. Impact of climate change on soil erosion, runoff and wheat productivity in central Oklahoma. CATENA 61 (2-3): 185-195.

Zhang X, Pei D, Chen S, 2004. Root growth and soil water utilization of winter wheat in the North China Plain. Hydrological Processes 18 (12): 2275-2287.

7. Conclusions

The overall scope of the work presented in this thesis was to assess the vulnerability of Mediterranean watersheds to climate change. The main focus was on the issue of desertification, since it is already critical for Mediterranean drylands (Brandt and Thornes, 1996; Mairota et al., 1998), and the expected trends of climate change in these regions point to a reinforcement of the biophysical driving forces behind desertification processes (Schroter et al., 2005), indicating an aggravation of its extension and severity. In this context, vulnerability was defined as resulting from the sensitivity of biophysical driving forces to changes in climate, the systems' resilience when faced with the impacts of climate change (which could lead to the surpassment of desertification thresholds), and the availability of adaptation options to these impacts.

The main objective of this thesis was to **assess the vulnerability of Mediterranean watersheds to climate change, as a result of enhanced desertification processes**. The results were obtained by developing a modeling framework capable of analyzing the processes linking climate and the main biophysical drivers for desertification: hydrology, vegetation cover and soil erosion. The framework coupled different modeling tools adapted to different spatial and temporal scales, focusing on the particularities of Mediterranean watershed processes. This methodology was applied to two contrasting study areas: the Guadiana and the Tejo, which currently present a semi-arid and humid climate, respectively.

This work aimed to cover a significant part of the research gaps identified in section 2.4 for two contrasting Mediterranean watersheds, which therefore may serve as exemplificative case-studies for other, similar systems. In particular, the novelty of this work relies both on the proposed methodology and the knowledge gained from the results. Methodological innovations include:

- the development of a framework coupling models operating at two distinct spatial and temporal scales – the SWAT model at the seasonal scale and the MEFIDIS model at the extreme event scale, using coarse-scale model results to frame boundary conditions when applying the fine-scale model;

- the formulation, implementation and assessment of a new event-scale model – MEFIDIS – designed for Mediterranean watersheds, in particular by taking into account the spatial distribution of saturated areas;

- the development of a method to assess the impact of storm movement direction on extreme event runoff and sediment yield rates, which unfortunately could not be applied in this work due to the lack of climate change estimates with an appropriate resolution, but which could prove useful if and when these estimates are developed.

Novel results, particularly for Mediterranean watersheds, include:

- impact assessment for multiple climate change scenarios with increasing degrees of severity, taking into account the uncertainty in CO_2 emission scenarios and climate model predictions (see section 2.4);

- climate change impact estimates for different scales in space (regional, catchment and vegetation / soil type combinations) and time (long-term, interannual, seasonal and extreme event);

- hydrological impact assessment for streamflow partitioning, balance between changes to storm intensities and soil saturation patterns, and storm floods;

- impact assessment for the balance between surface runoff and vegetation cover, and consequences for soil erosion rates;

- erosion impact assessment differentiating between upslope erosion, gully erosion and sediment yield.

These results were integrated in a vulnerability assessment methodology, similar to the one proposed by Adger (2006), which assessed the sensitivity of desertification drivers to climate change, the resilience of watersheds to their impacts, and possible adaptation measures. Overall, the main conclusions for the sensitivity of desertification drivers to climate change, taken from the application of the modeling framework, can be summarized as follows:

- at the seasonal scale, hydrological processes appear to be the most sensitive to changes in climate, with increases in potential evapotranspiration reinforcing the consequences of a decrease in rainfall, leading to a significant decrease in runoff;

- this decrease is expected to be accompanied by an increase in streamflow variability, with significant differences to the interannual and seasonal distribution of runoff;

- at the extreme event scale, increases in storm intensity are expected to be mitigated by decreases in surface saturation, leading to a negative balance for storm runoff in most climate change scenarios;

- vegetation growth processes appear to be less sensitive to changes in climate than hydrological processes, with the negative effects of increasing temperatures over agricultural species and forests mitigating the impacts of rising CO_2 concentrations, leading to small changes or decreases in productivity;

- in contrast, Mediterranean species (sclerophyllous oaks and shrubs) appear to benefit from the positive impacts of temperature and CO_2 concentrations, indicating positive changes to growth up to an aridity threshold;

- soil erosion processes appear to depend on the balance between the positive impacts of lower vegetation cover, and the negative impacts of lower surface runoff generation, with a decrease in storm runoff also contributing to a decrease in soil erosion;

- the overall balance appears to be highly dependent on the predicted magnitudes for changes to rainfall, and for high magnitudes of changes to temperature, soil erosion could either significantly increase or decrease;

- these impacts are expected to present a high variability in space, with cropfields registering the less significant decreases or the most significant increases, and gully erosion processes are expected to remain a problem in all scenarios despite a possible decrease in the extent of this problem.

The resilience of watersheds to the impacts of climate change was assessed by comparing the results from the modeling framework with desertification thresholds estimated for the study areas. Despite the indicative nature of these thresholds, the resilience assessment allowed for an estimation of the vulnerability of the study areas to climate change due to enhanced desertification processes. As expected by the sensitivity analysis, vulnerabilities depend on the magnitude of climate change; as the magnitude of changes to climate increases, thresholds are surpassed in a sequential way, starting with the watersheds' ability to sustain current water demands and followed by the vegetation support capacity. The results indicate the existence of a threshold separating moderate and severe climate changes, which is temperature increases of +3.5 to +4.5 ºC and rainfall decreases of -10 to -20 %; current climate change predictions for the study areas include results surpassing one or both thresholds. Considering these

thresholds, different vulnerability scenarios for moderate and severe changes to temperature and rainfall were estimated. The main vulnerabilities can be summarized as follows:

- for moderate changes to temperature and rainfall, the river basins of the Guadiana and the Tejo (where the study areas are located) might experience severe water stresses if current irrigation practices are maintained;

- for severe changes to rainfall only, severe water stresses could occur during drought years (1 out of 4), even with moderate irrigation – this is the most frequent result from climate change scenarios for the study areas;

- for severe changes to temperature only, agricultural yield may decrease significantly, accompanied by a significant increase in upslope and gully erosion;

- for severe changes to temperature and rainfall, the Guadiana could transition towards an arid system, while the Tejo could shift to a semi-arid system, leading to severe water stresses and significant changes to the support capacity for current agriculture and natural vegetation in both study areas;

- the shallow Lithosols which occupy a significant proportion of the Guadiana study area could lose a significant part of their fertility regardless of the climate change scenario, and leave the cultivated and natural vegetation growing over them significantly more vulnerable to climate change than the climate scenarios might otherwise indicate.

Finally, the vulnerabilities outlined above were used to indicate a number of possible adaptation measures for each climate change scenario. Most of the adaptation options are focused on strategies to reduce water consumption and adapt agriculture to the changes in climate; however, all would require a significant amount of planning to implement which should take into account expected climate change impacts to be successful.

The thesis was able to achieve the objectives that were set above, although with some limitations. These were mostly due to uncertainties associated with the climate change scenarios and the methodology used in this thesis; limitations in the current knowledge of climate prediction (Giorgi, 2005), erosion processes (Boardman, 2006) and desertification thresholds (Herrmann and Hutchinson, 2005) were particularly important for this work.

Furthermore, the interactions and feedbacks between biophysical and socio-economic systems were not assessed.

Despite these limitations, the results presented in this work provide a comprehensive assessment of the main vulnerabilities of Mediterranean watersheds to changes in climate, focusing on the biophysical drivers of desertification processes. The trends identified in this work can serve as the basis for future research, and contribute for wider studies on the response of natural, economic and social systems to climate change. The main challenge for Mediterranean socio-ecological systems continues to be, as referred by Thornes (1998), to adapt to climate change and reduce the risk of desertification while maintaining the socio-economic achievements of recent decades, which depend on a large extent on the support provided by the local biophysical systems.

Finally, this work also leaves a number of open questions, and raises others which could be the focus of future research efforts in the area of climate change and desertification, such as:

- the methodology used in this thesis can be significantly improved, particularly in the field of soil erosion science, where there is a lack of spatially-distributed erosion data and a number of processes related with gully erosion and the impacts of soil loss on vegetation productivity are not well understood (Boardman, 2006);

- the overall impact of processes related with drought-induced disturbances, particularly in terms of drought-induced mortality and vegetation pattern shifts, requires further research and integration within this methodology;

- changes to the frequency of wildfires due to changes in climate should be taken into account, and their impacts on hydrological and soil erosion processes also require further research (Shakesby and Doerr, 2006);

- the climatic thresholds for agricultural and vegetation support require further study, particularly in terms of gathering data on climate-vegetation interactions and understanding the processes underlying these thresholds (Herrmann and Hutchinson, 2005);

- the results obtained for the Guadiana and Tejo study areas should be compared with other Mediterranean systems with different biophysical and socio-economic conditions to derive common processes and trends for Mediterranean watersheds;

- the results from this work can in the future be integrated within a combined framework including socio-economic processes, such as the one described by Adger (2006), in order to present a more complete assessment of the vulnerability of ecological, economic and social systems to climate change in the Mediterranean.

7.1 References

Adger WN, 2006. Vulnerability. Global Environmental Change 16: 268–281.

Boardman J, 2006. Soil erosion science: reflections on the limitations of current approaches. Catena 68: 73-86.

Brandt CJ, Thornes JB (Eds.), 1996. Mediterranean desertification and land use. John Wiley and sons, Chichester.

Giorgi F, 2005. Climate change prediction. Climatic Change 73 (3): 239-265.

Herrmann SM, Hutchinson CF, 2005. The changing contexts of the desertification debate. J. Arid Environments 63: 538–555.

Mairota P, Thornes JB, Geeson N (Eds.), 1998. Atlas of Mediterranean environments in Europe. John Wiley and Sons, Chichester.

Schroter D, Cramer W, Leemans R, Prentice IC, Araujo MB, Arnell NW, Bondeau A, Bugmann H, Carter TR, Gracia CA, de la Vega-Leinert AC, Erhard M, Ewert F, Glendining M, House JI, Kankaanpaa S, Klein RJT, Lavorel S, Lindner M, Metzger MJ, Meyer J, Mitchell TD, Reginster I, Rounsevell M, Sabate S, Sitch S, Smith B, Smith J, Smith P, Sykes MT, Thonicke K, Thuiller W, Tuck G, Zaehle S, Zierl B, 2005. Ecosystem service supply and vulnerability to global change in Europe. Science 310 (5752): 1333-1337.

Shakesby RA, Doerr SH, 2006. Wildfire as a hydrological and geomorphological agent. Earth-Science Reviews 74: 269-307.

Thornes JB, 1998. Mediterranean desertification. In: Mairota P, Thornes JB, Geeson N (Eds.), Atlas of Mediterranean environments in Europe. John Wiley and Sons, Chichester: 2-5.